Partonic structure and small x: TMD PDFs and GPDs

Charlotte Van Hulse
University of Alcalá

AdT

Comunidad de Madrid

GDR QCD "From Hadronic Structure to Heavy Ion Collisions"
10-14 June 2024
IJCLab, Orsay, France

The various dimensions of the nucleon structure

Wigner distributions $W(x, \vec{k}_T, \vec{b}_\perp)$

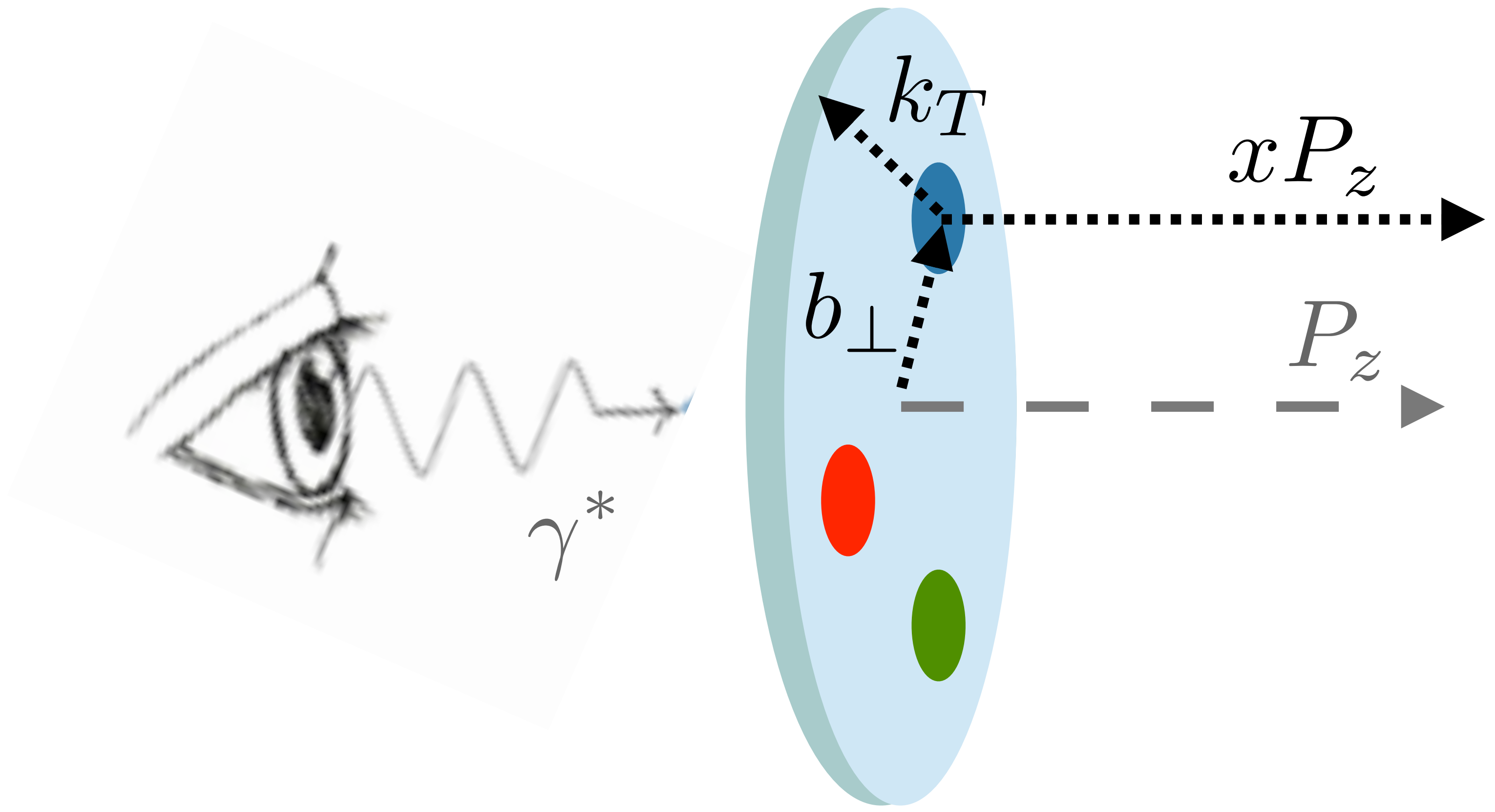

The various dimensions of the nucleon structure

Wigner distributions $W(x, \vec{k}_T, \vec{b}_\perp)$

$\int d^2\vec{b}_\perp$

transverse-momentum
dependent (TMD)
parton distribution functions
(PDFs)

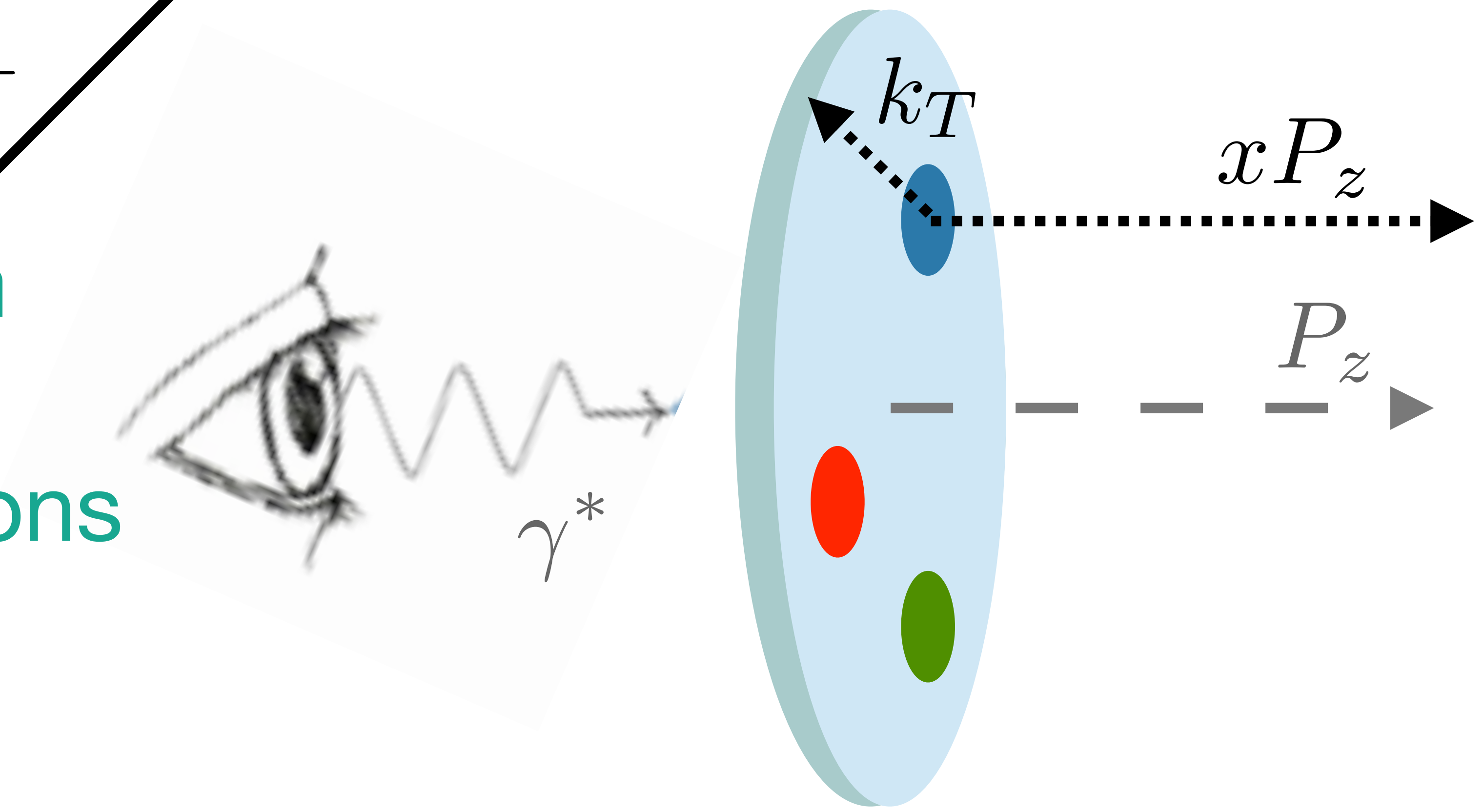

The various dimensions of the nucleon structure

Wigner distributions $W(x, \vec{k}_T, \vec{b}_\perp)$

$\int d^2\vec{b}_\perp$

transverse-momentum
dependent (TMD)
parton distribution functions
(PDFs)

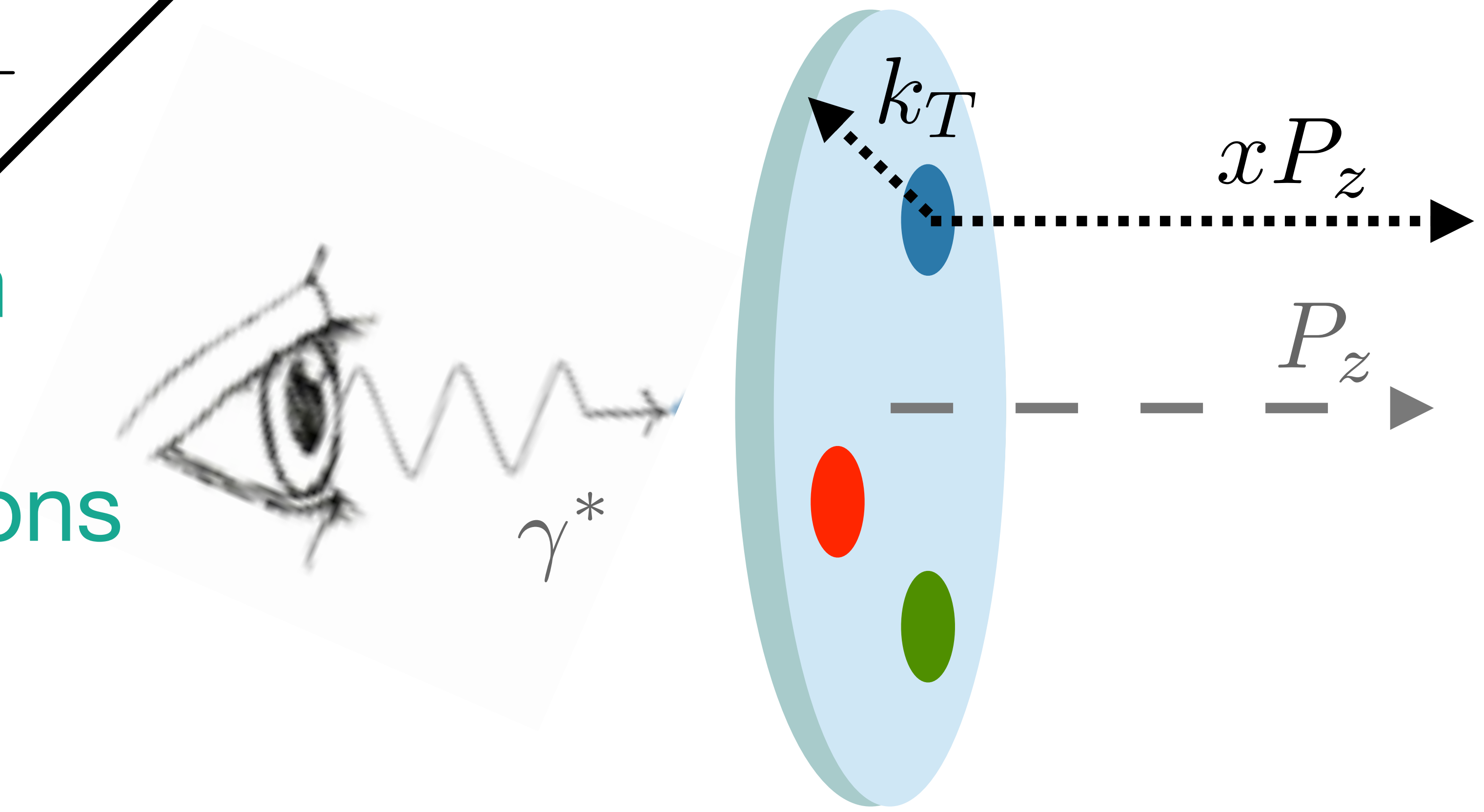

Semi-inclusive production

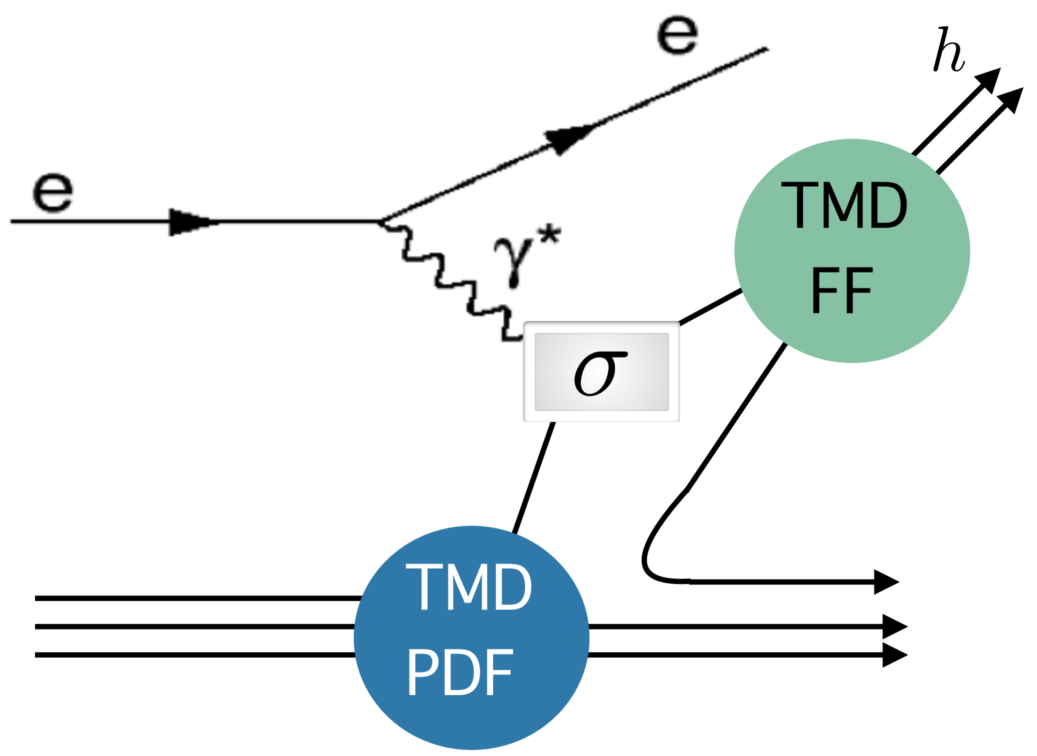

The various dimensions of the nucleon structure

Wigner distributions $W(x, \vec{k}_T, \vec{b}_\perp)$

$\int d^2\vec{b}_\perp$

transverse-momentum dependent (TMD) parton distribution functions (PDFs)

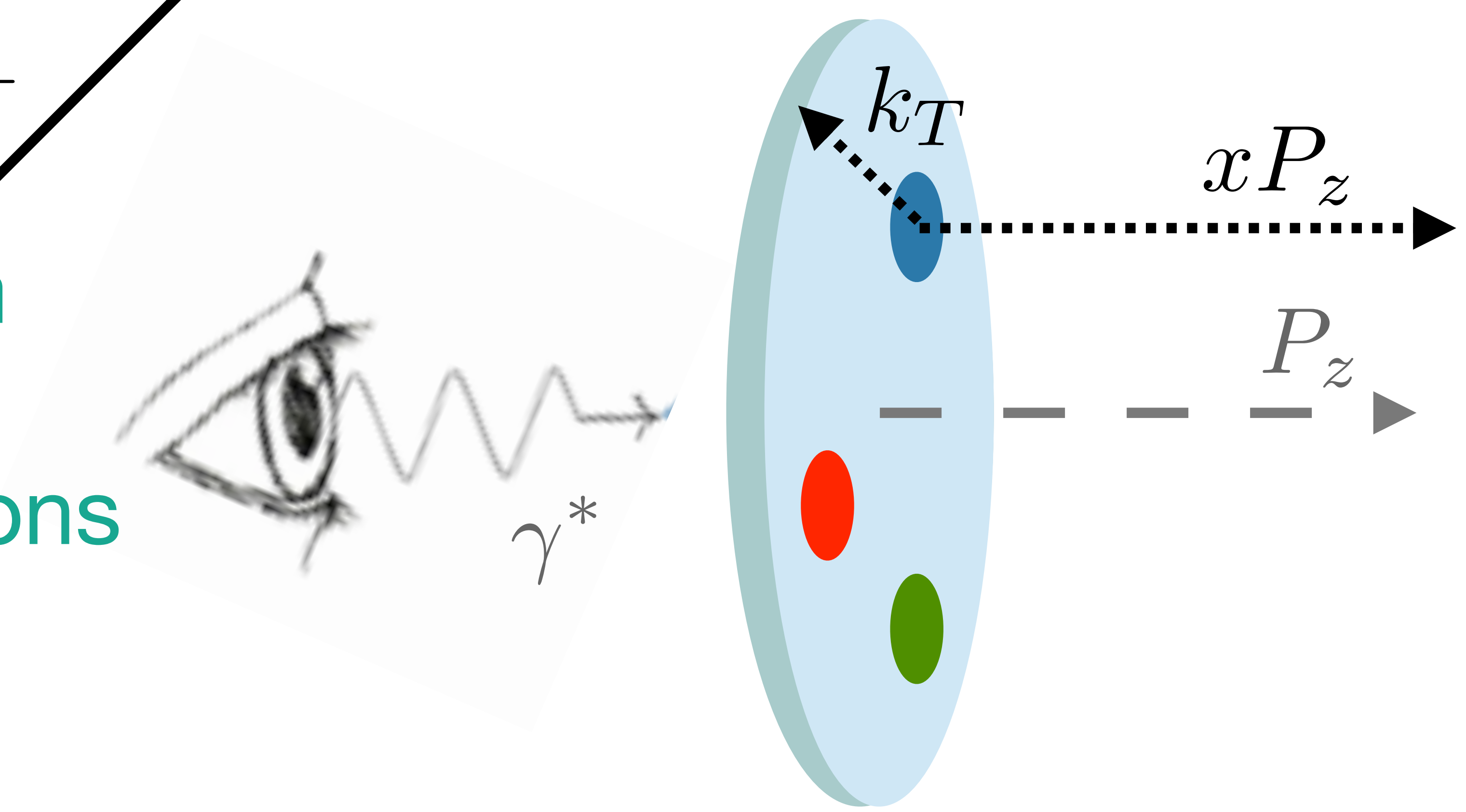

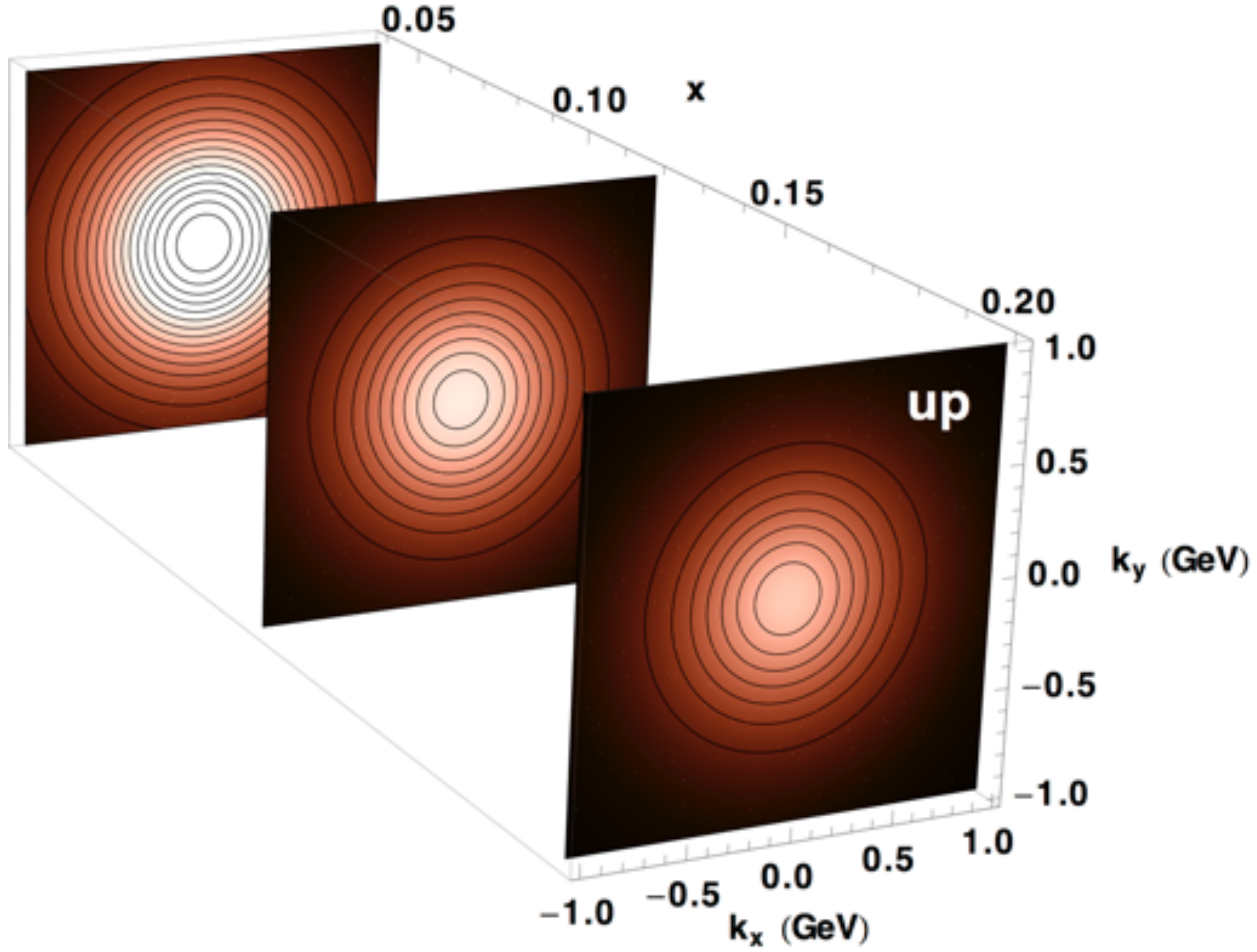

The various dimensions of the nucleon structure

Wigner distributions $W(x, \vec{k}_T, \vec{b}_\perp)$

$\int d^2\vec{b}_\perp$

transverse-momentum
dependent (TMD)
parton distribution functions
(PDFs)

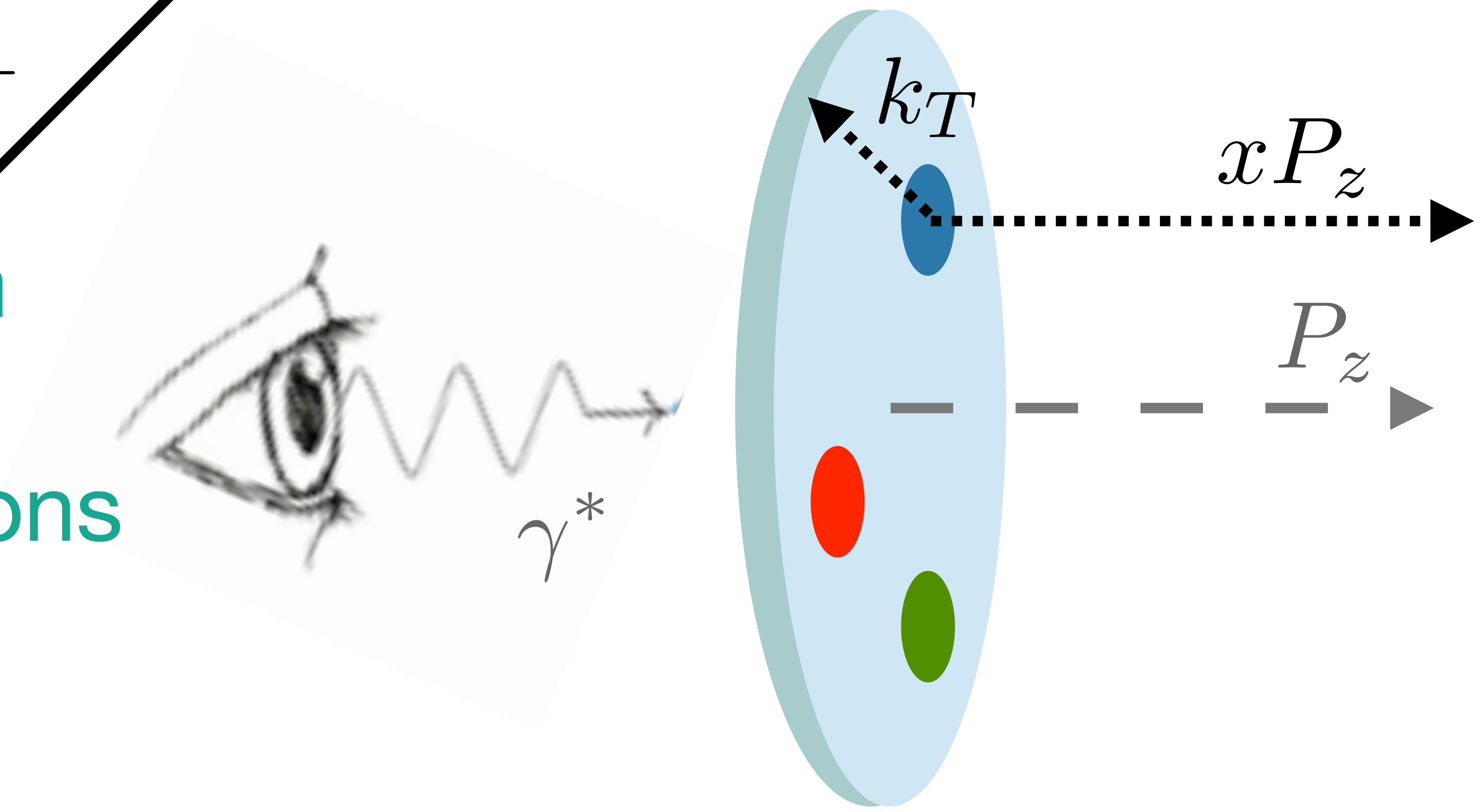

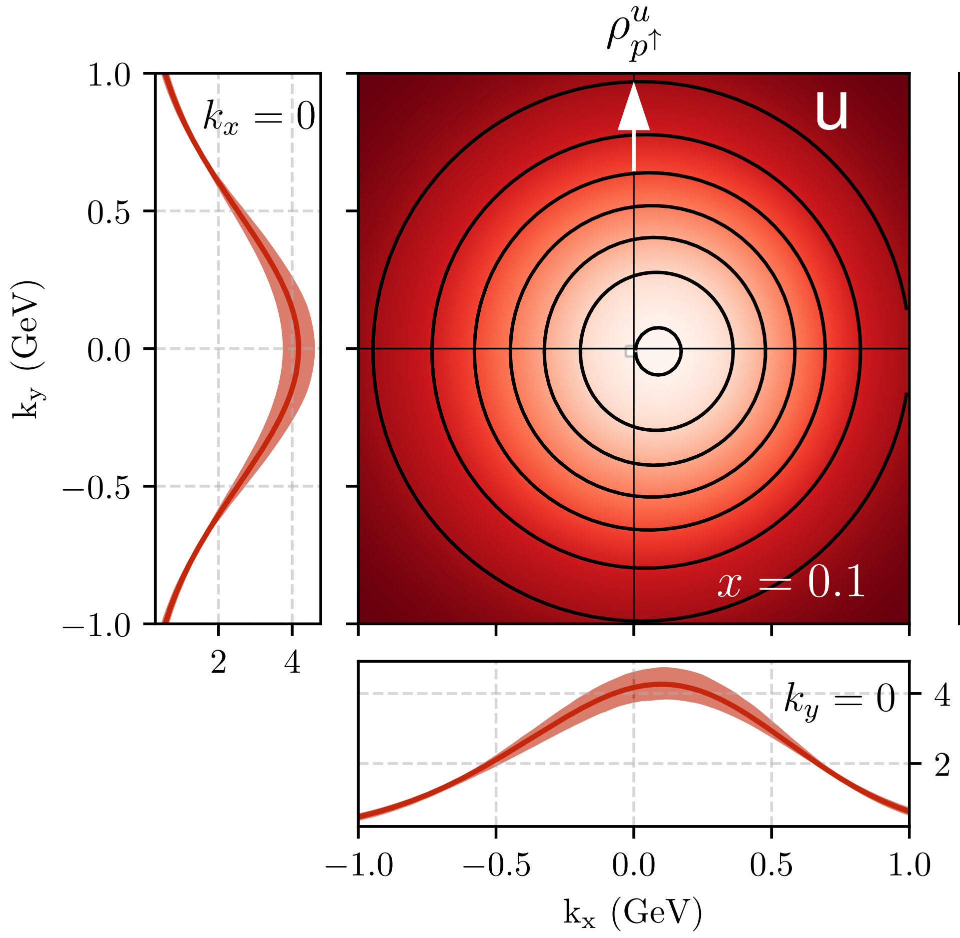

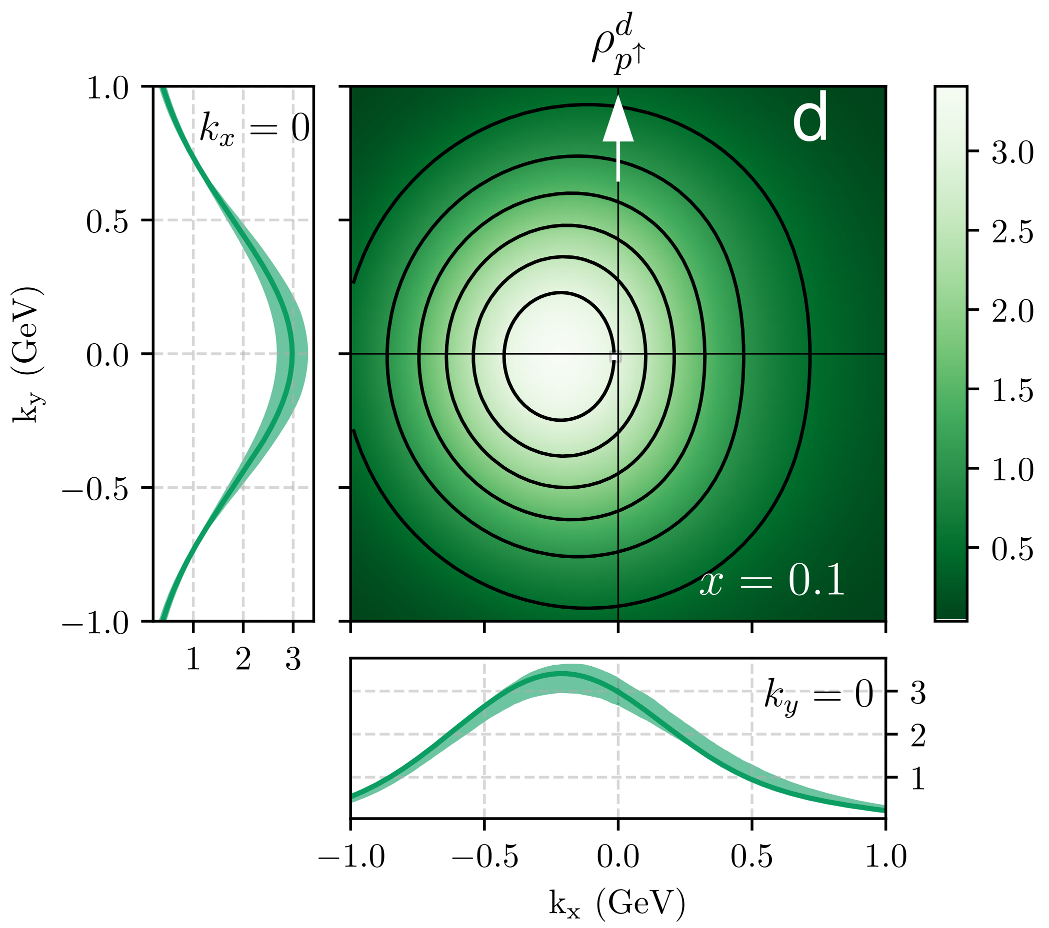

The various dimensions of the nucleon structure

Wigner distributions $W(x, \vec{k}_T, \vec{b}_\perp)$

$\int d^2\vec{b}_\perp$

$\int d^2\vec{k}_T$

transverse-momentum dependent (TMD) parton distribution functions (PDFs)

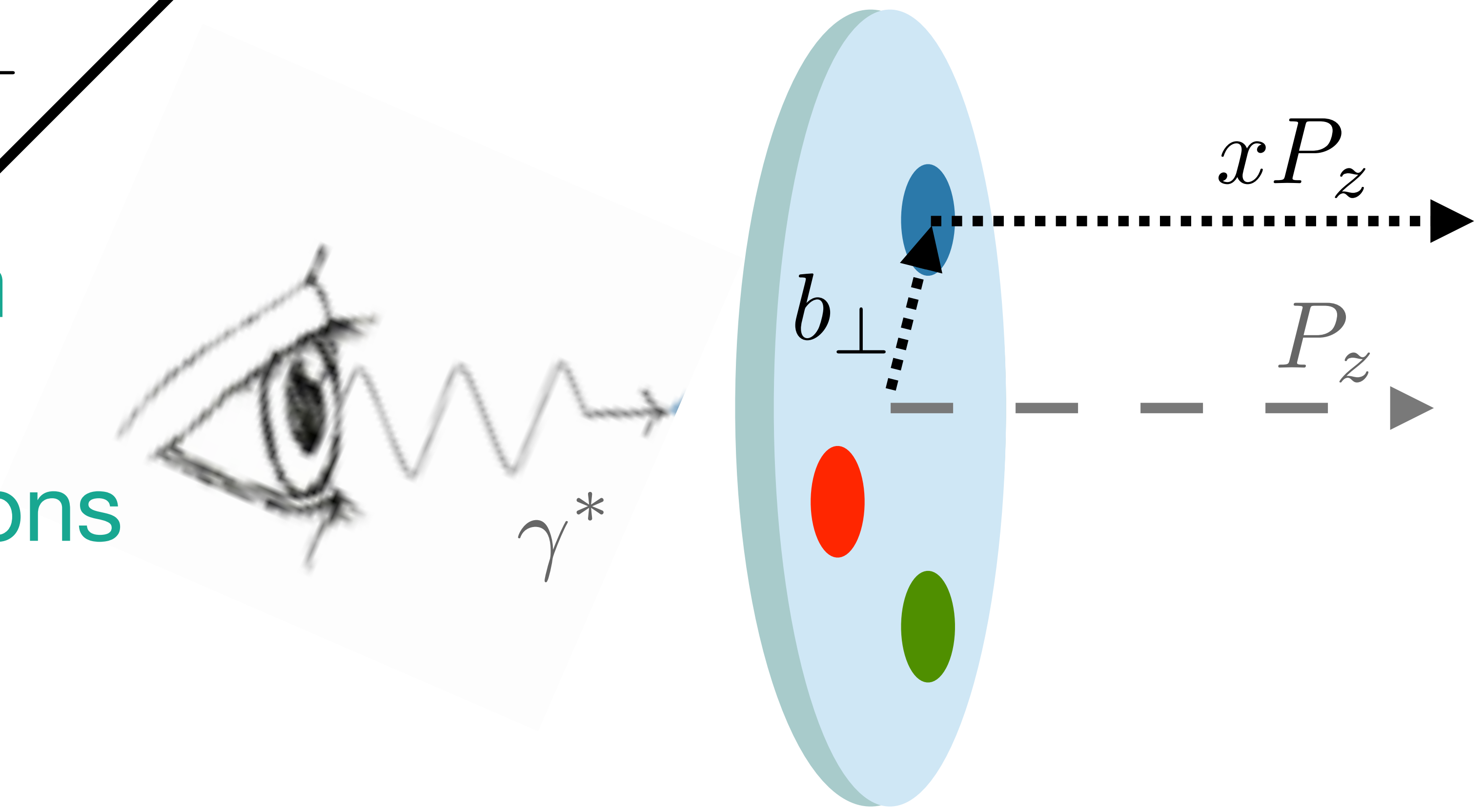

impact-parameter dependent PDFs

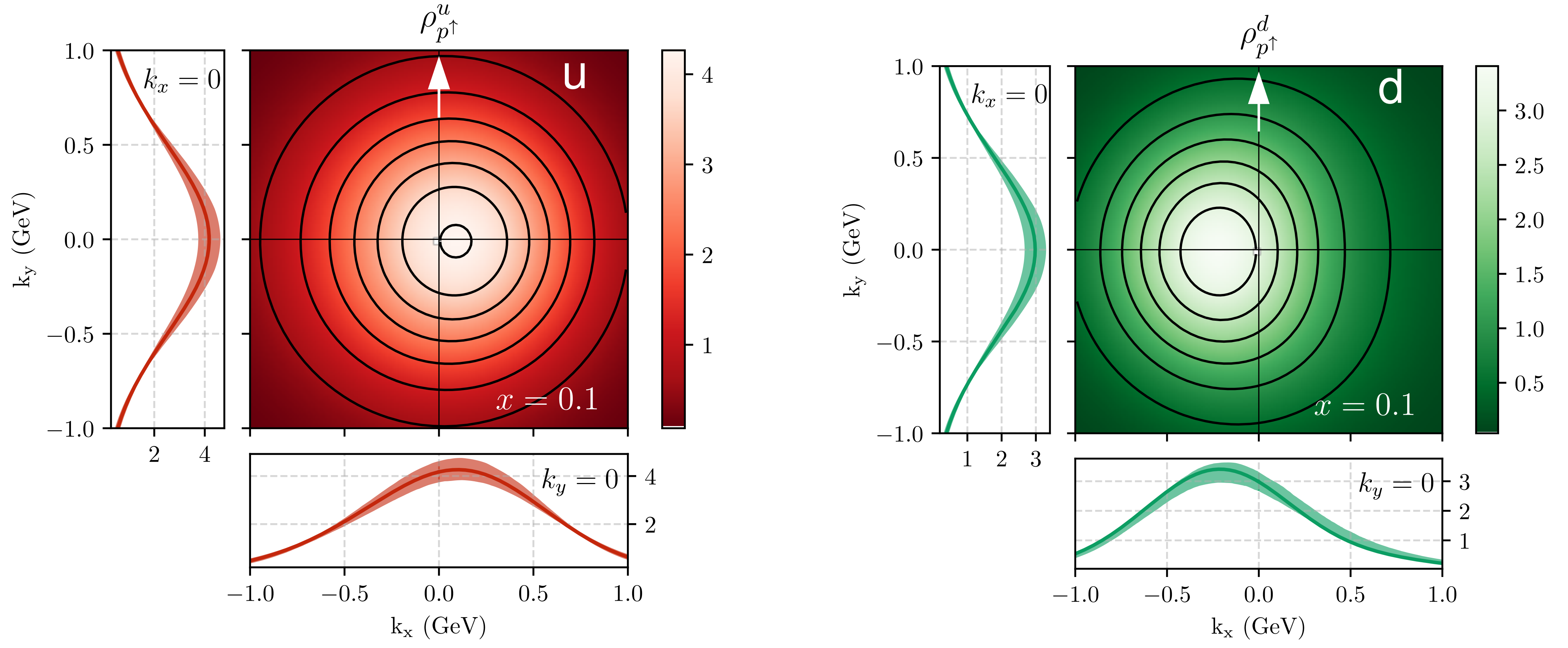

The various dimensions of the nucleon structure

Wigner distributions $W(x, \vec{k}_T, \vec{b}_\perp)$

$\int d^2\vec{b}_\perp$

transverse-momentum
dependent (TMD)
parton distribution functions
(PDFs)

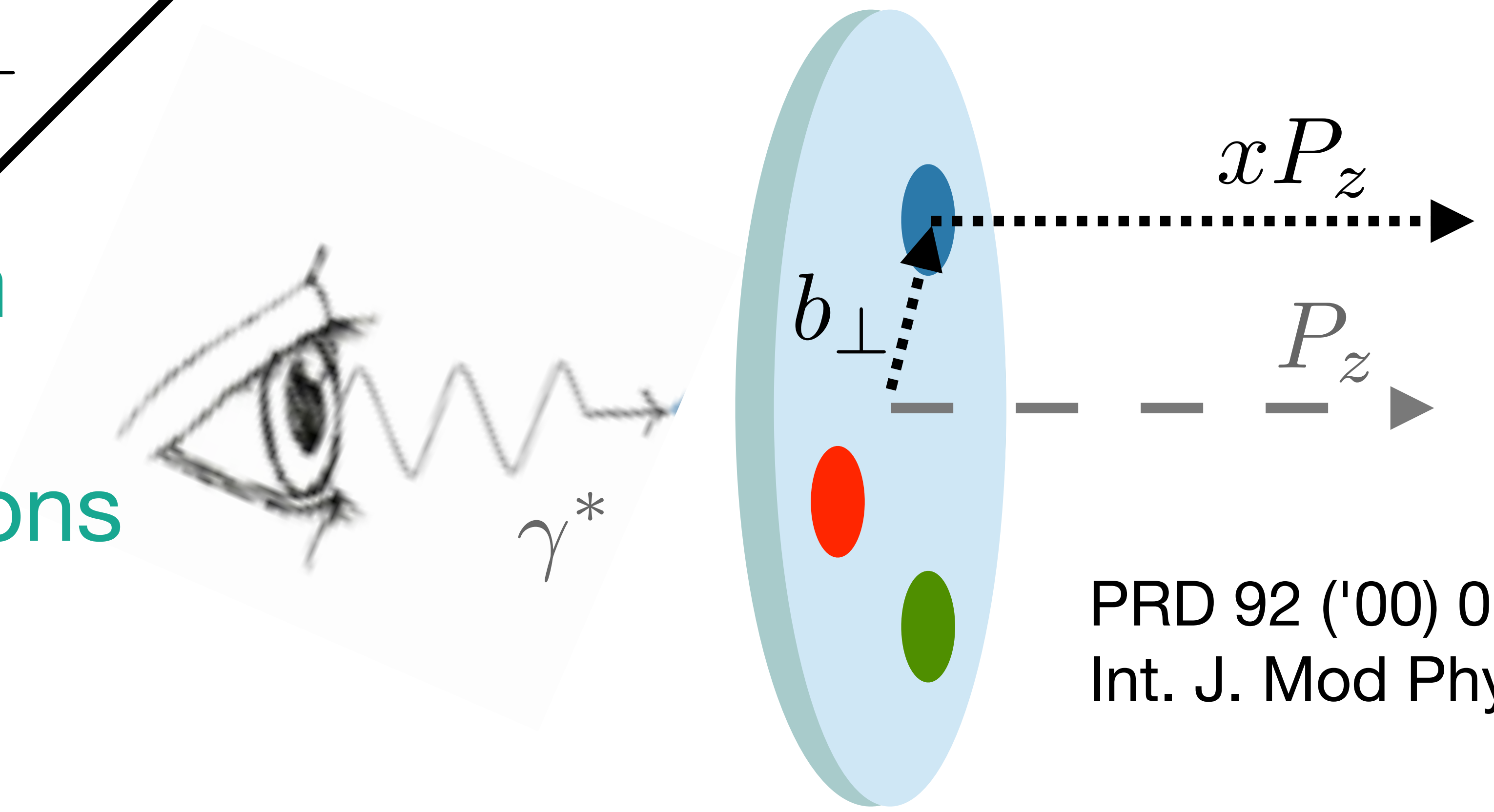

$\int d^2\vec{k}_T$

impact-parameter
dependent PDFs

Fourier transform

generalised parton
distributions (GPDs)

PRD 92 ('00) 071503
Int. J. Mod Phys. A 18 ('03) 173

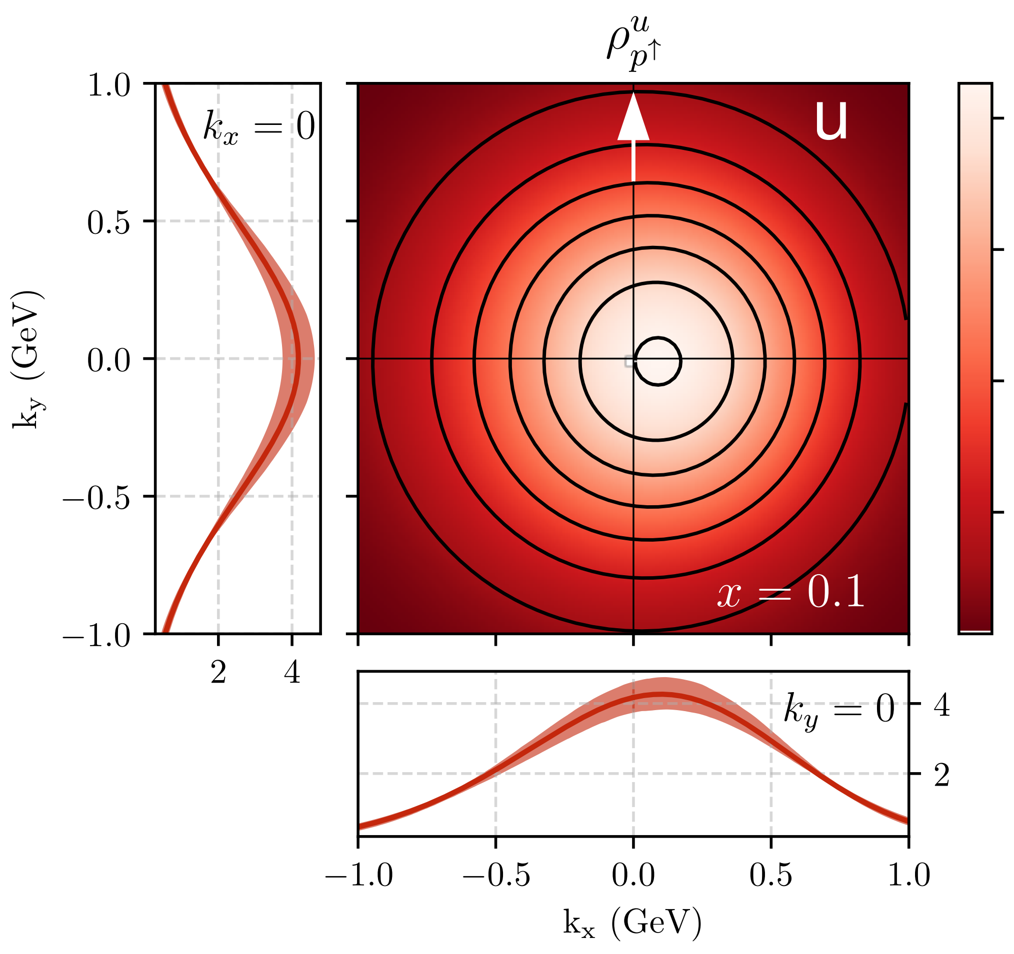

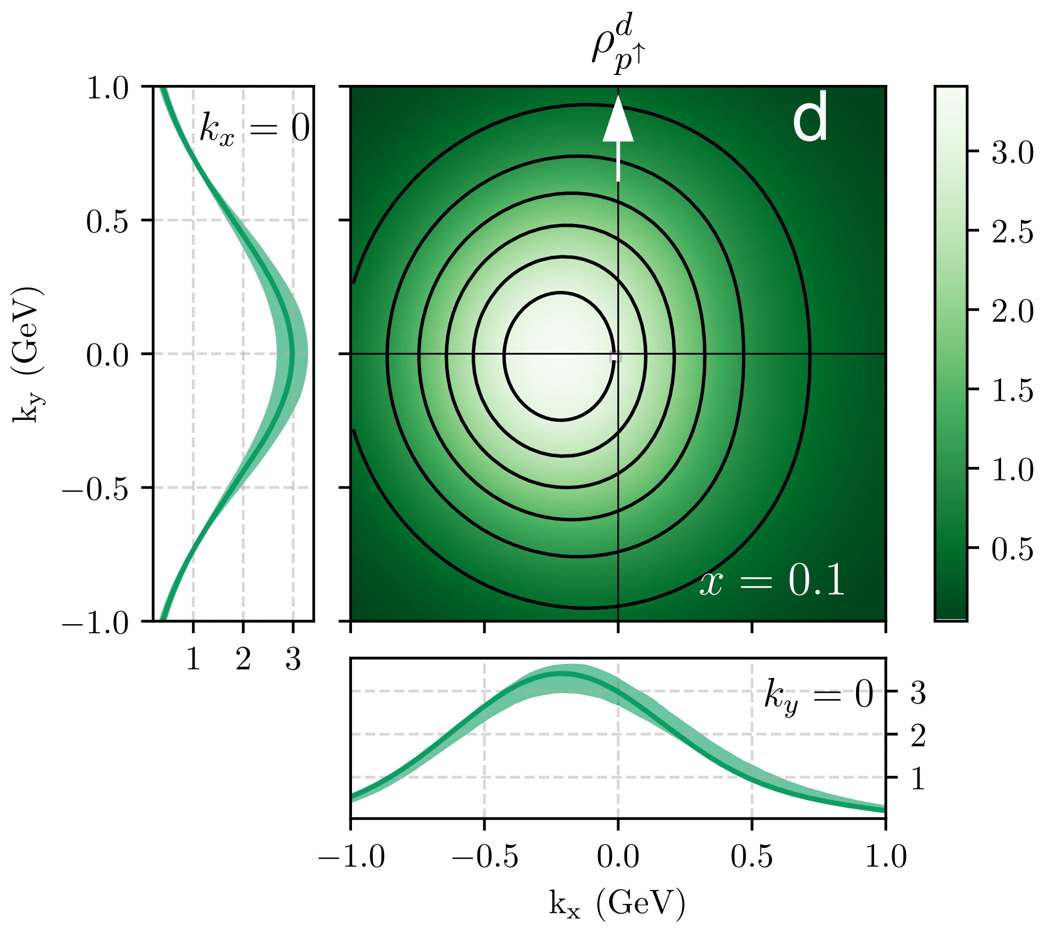

The various dimensions of the nucleon structure

Wigner distributions $W(x, \vec{k}_T, \vec{b}_\perp)$

$\int d^2\vec{b}_\perp$

$\int d^2\vec{k}_T$

transverse-momentum dependent (TMD) parton distribution functions (PDFs)

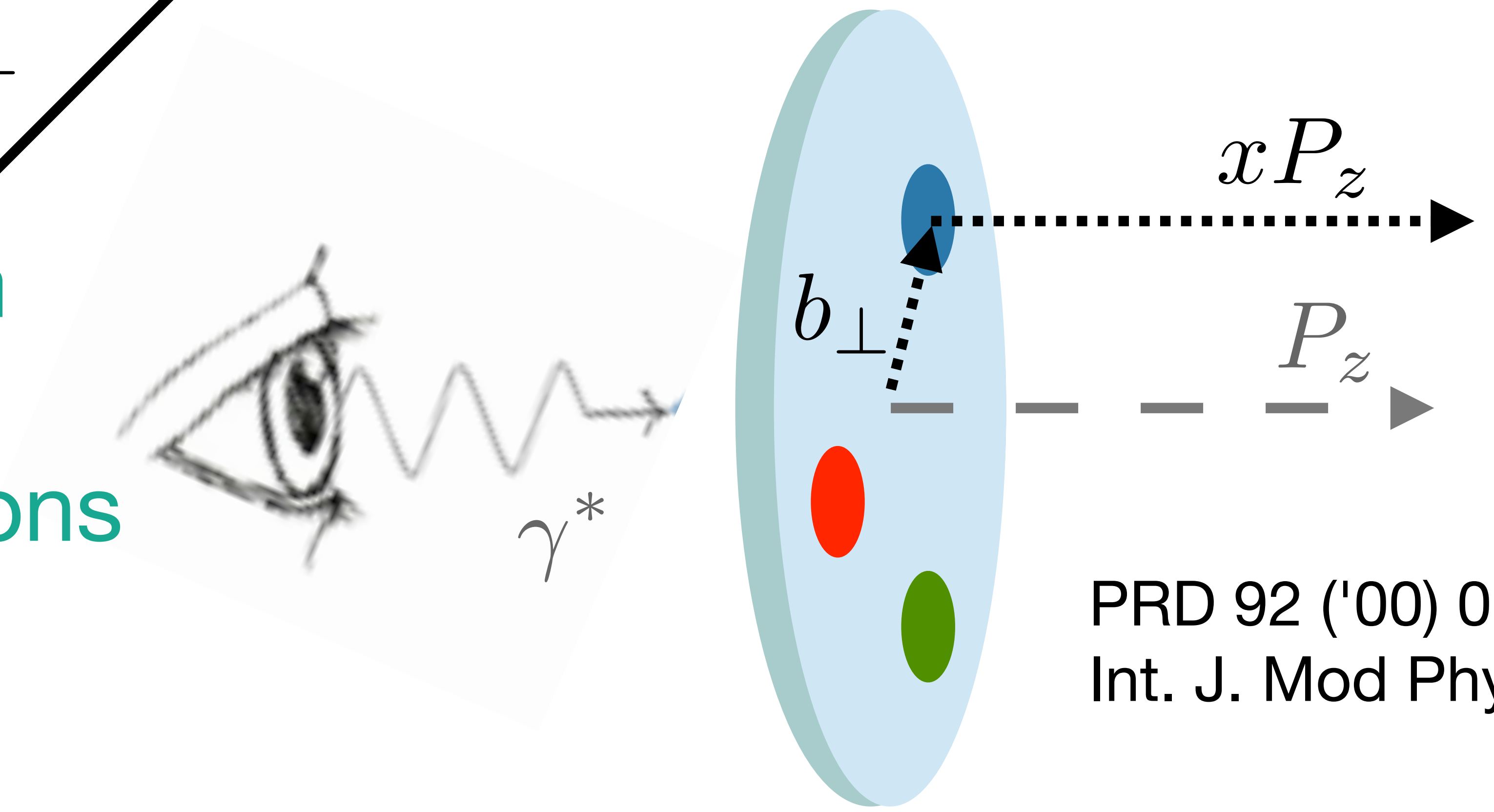

impact-parameter dependent PDFs

PRD 92 ('00) 071503
Int. J. Mod Phys. A 18 ('03) 173

Fourier transform

generalised parton distributions (GPDs)

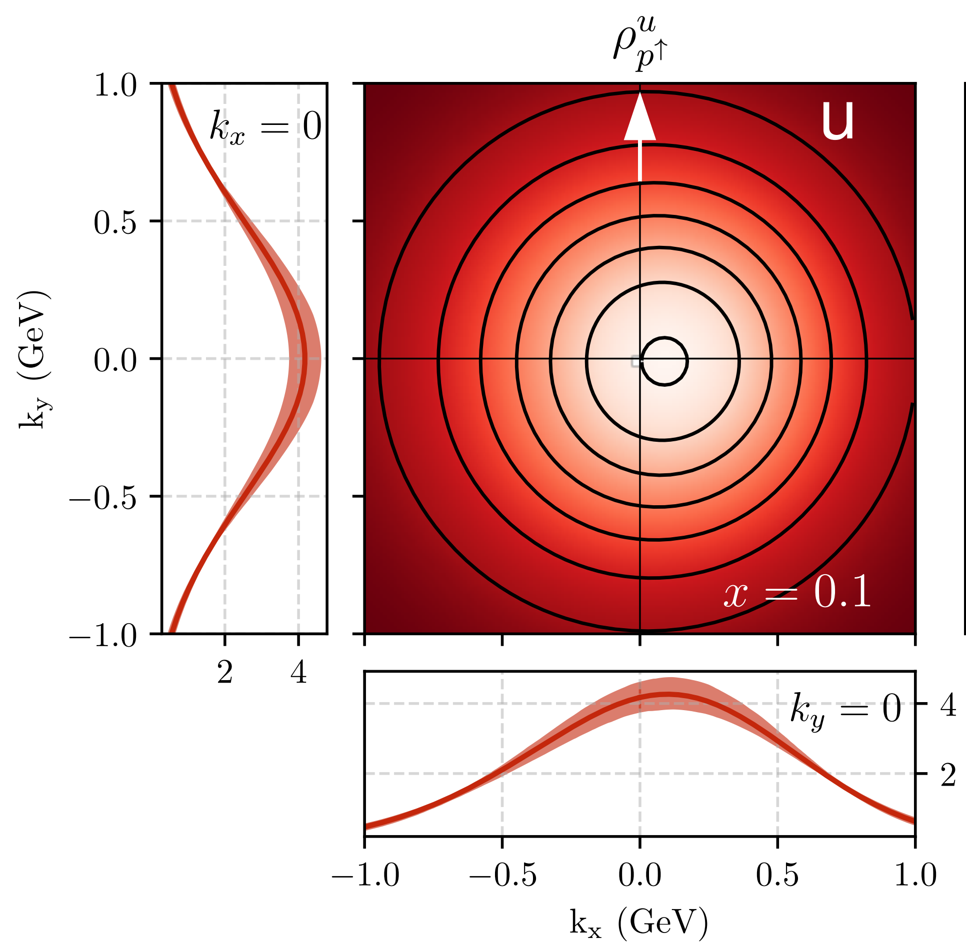

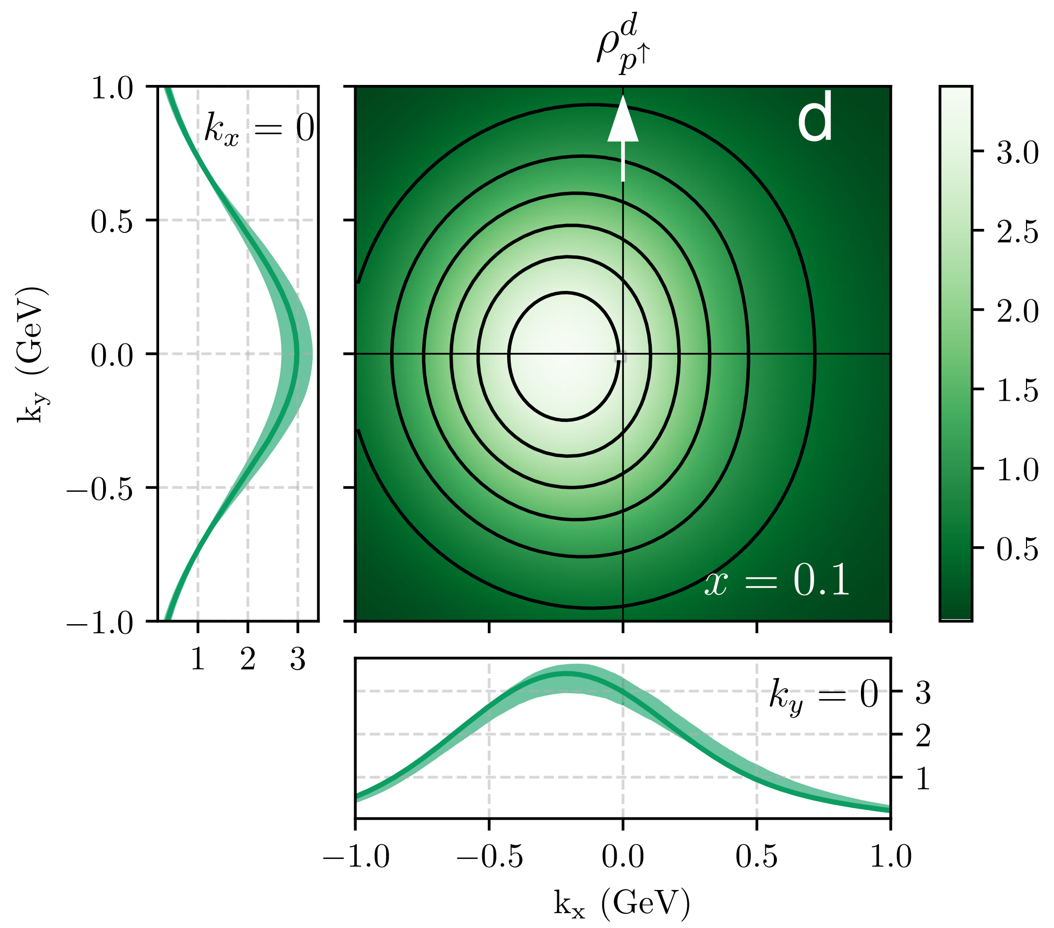

Exclusive production

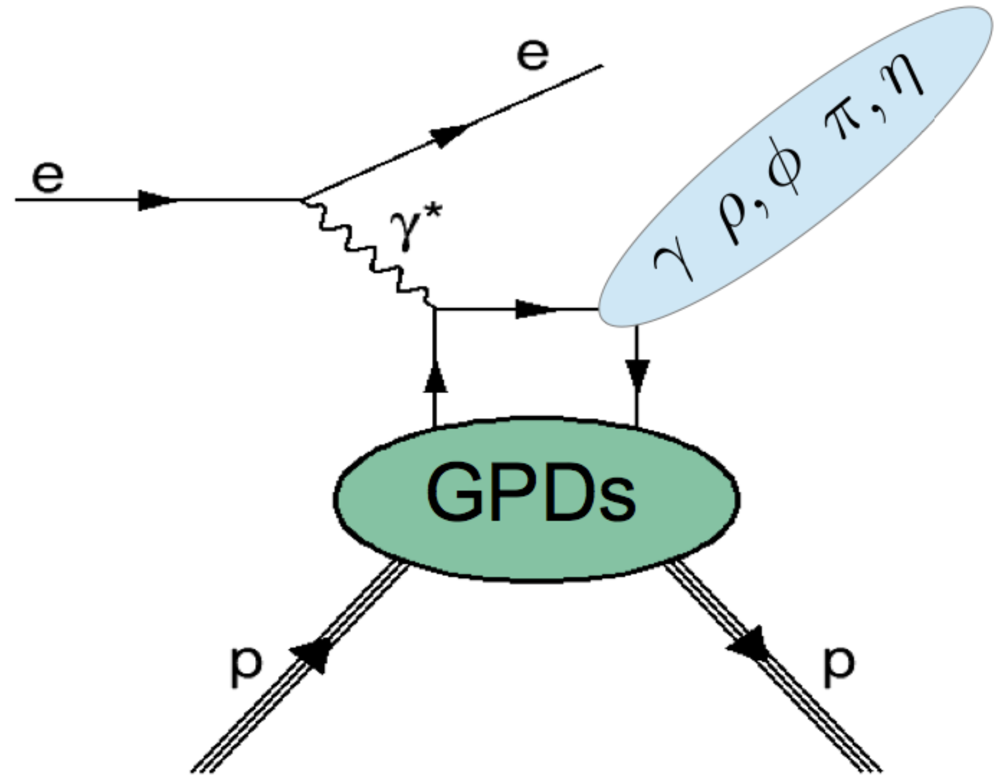

The various dimensions of the nucleon structure

Wigner distributions $W(x, \vec{k}_T, \vec{b}_\perp)$

$\int d^2\vec{b}_\perp$

transverse-momentum dependent (TMD) parton distribution functions (PDFs)

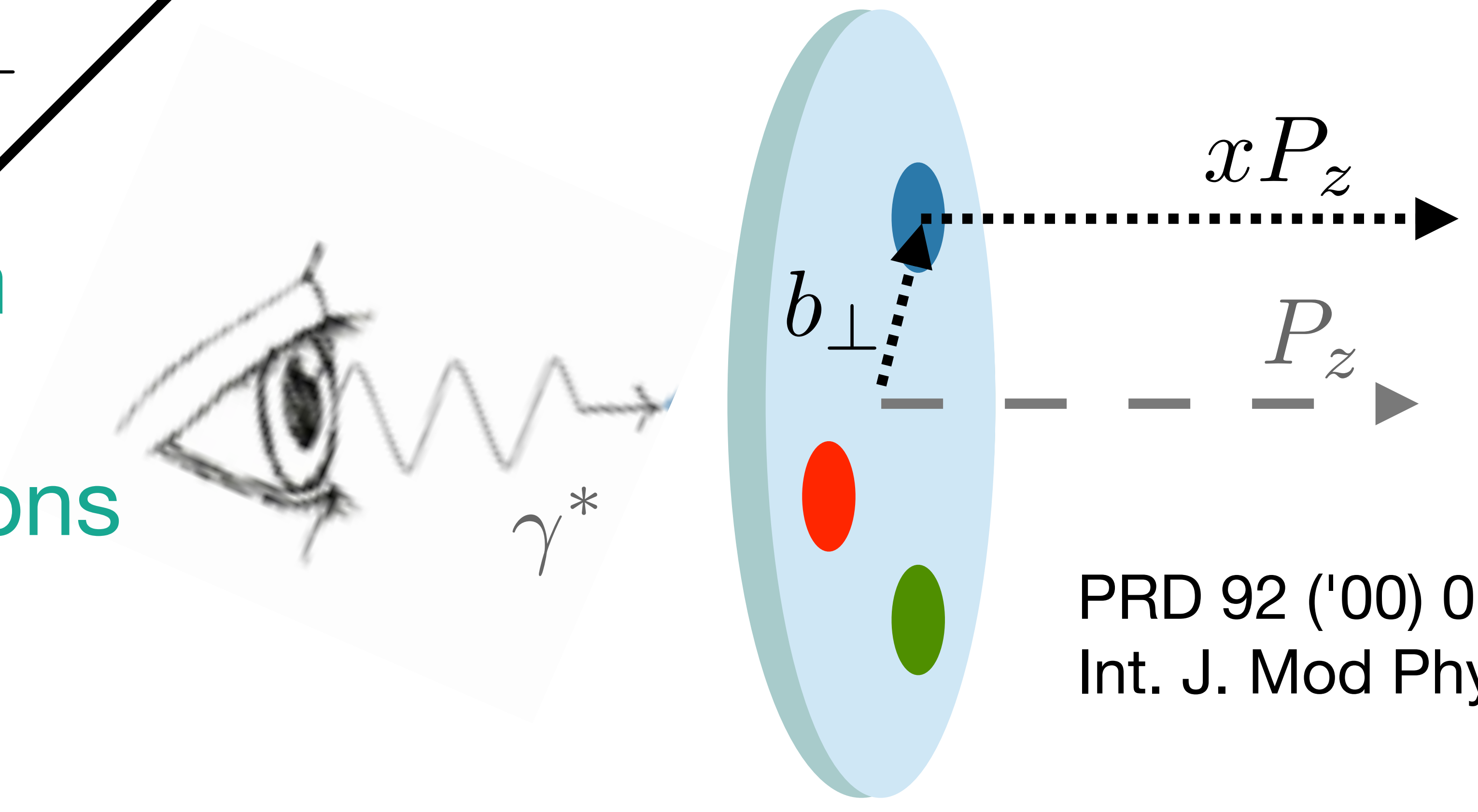

$\int d^2\vec{k}_T$

impact-parameter dependent PDFs

PRD 92 ('00) 071503
Int. J. Mod Phys. A 18 ('03) 173

Fourier transform

generalised parton distributions (GPDs)

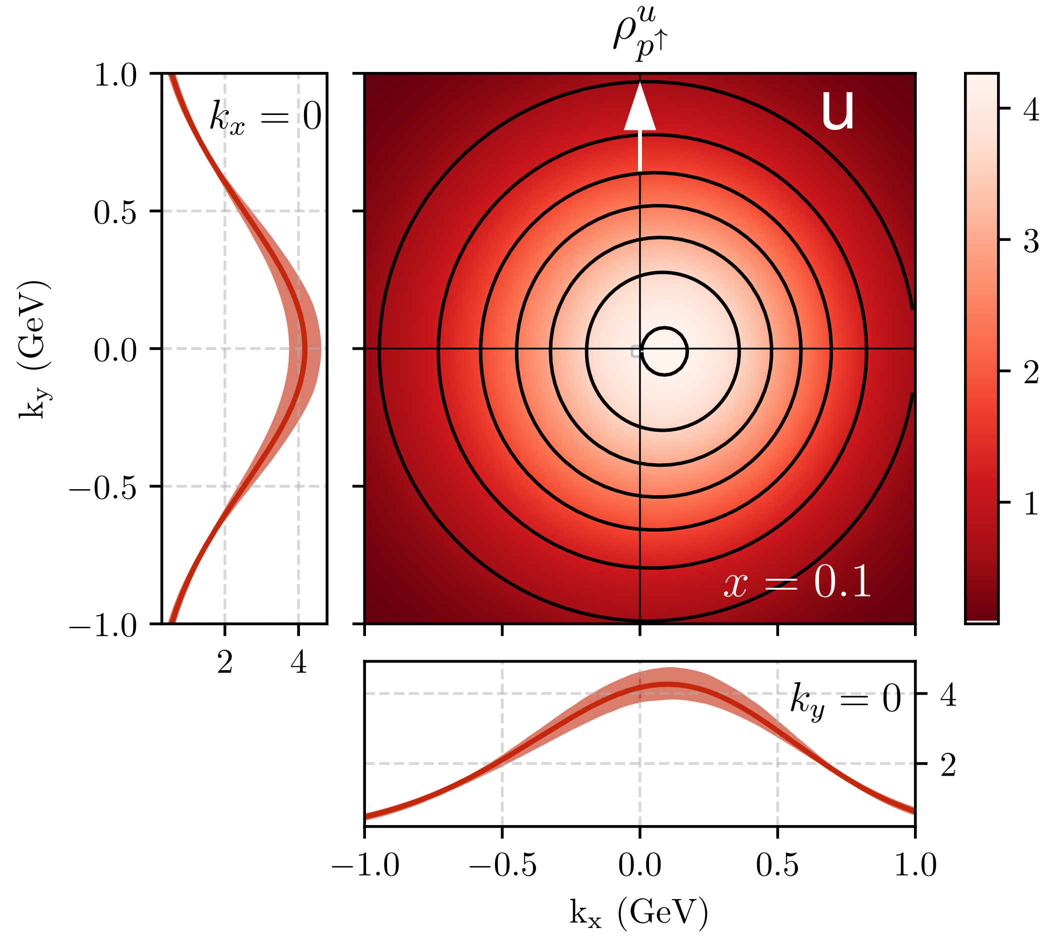

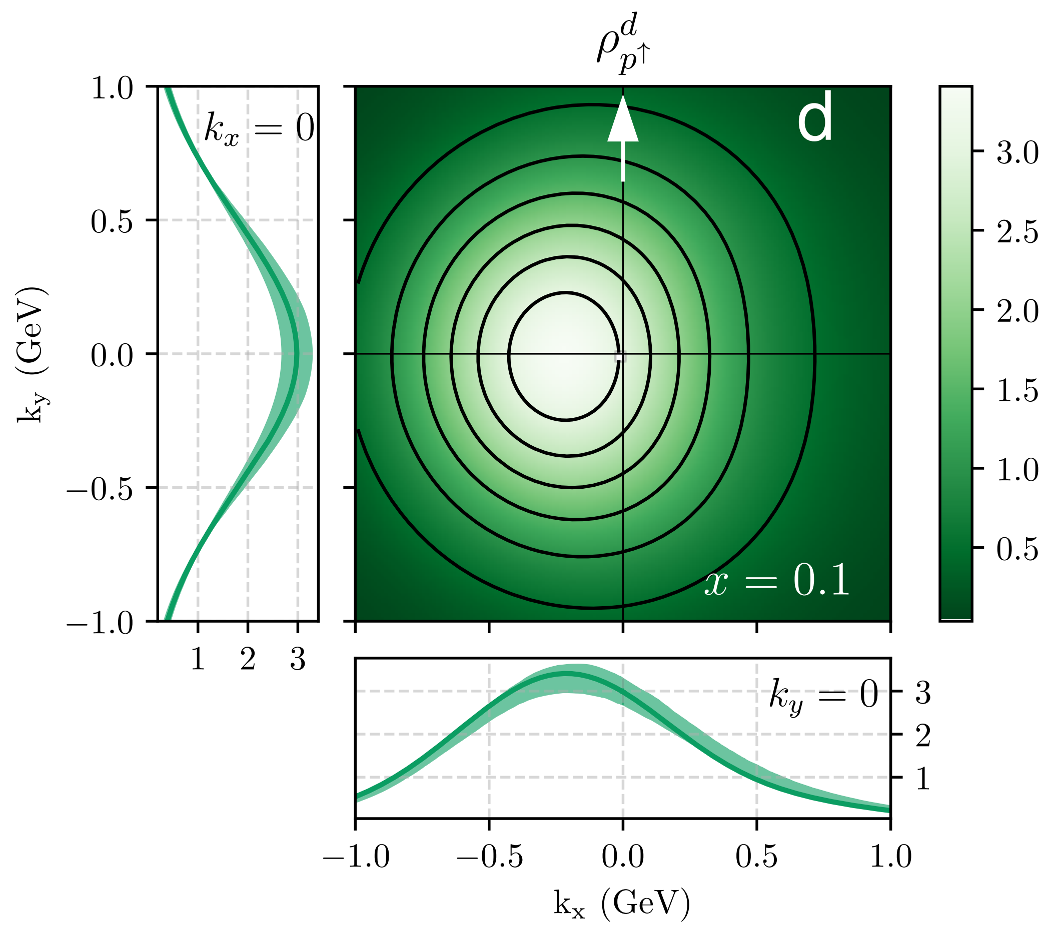

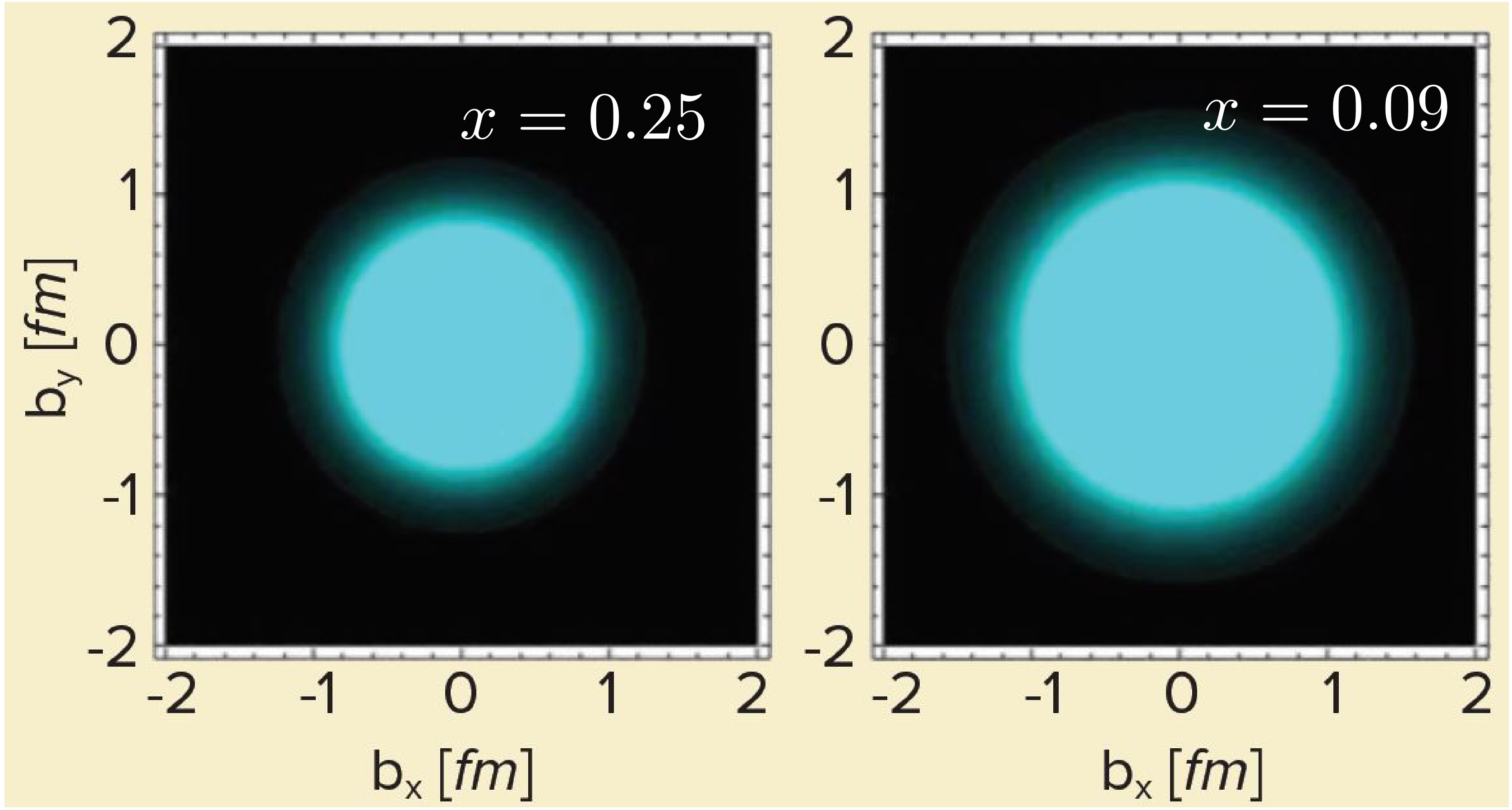

The various dimensions of the nucleon structure

Wigner distributions $W(x, \vec{k}_T, \vec{b}_\perp)$

$\int d^2\vec{b}_\perp$

$\int d^2\vec{k}_T$

transverse-momentum dependent (TMD) parton distribution functions (PDFs)

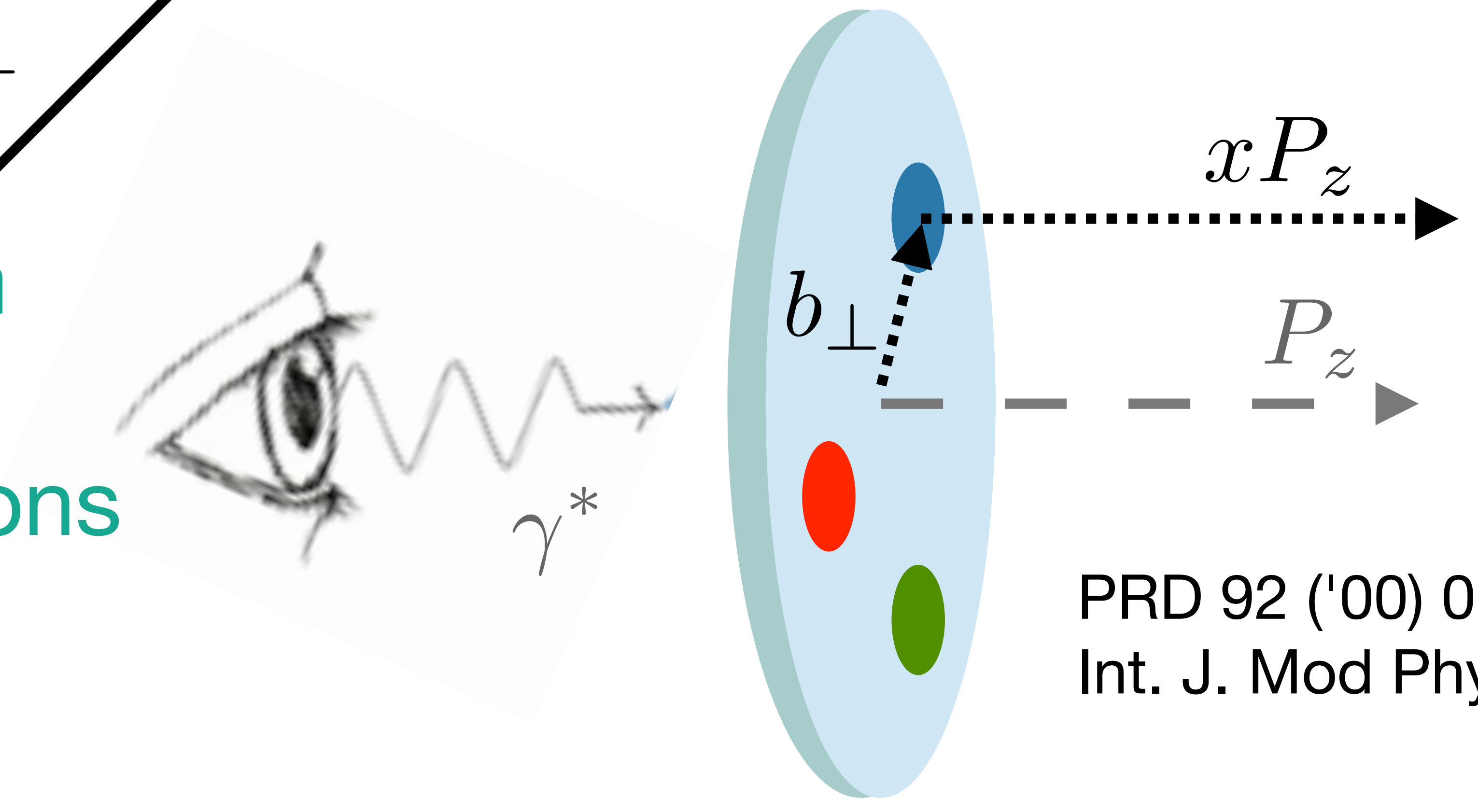

impact-parameter dependent PDFs

PRD 92 ('00) 071503
Int. J. Mod Phys. A 18 ('03) 173

Fourier transform

generalised parton distributions (GPDs)

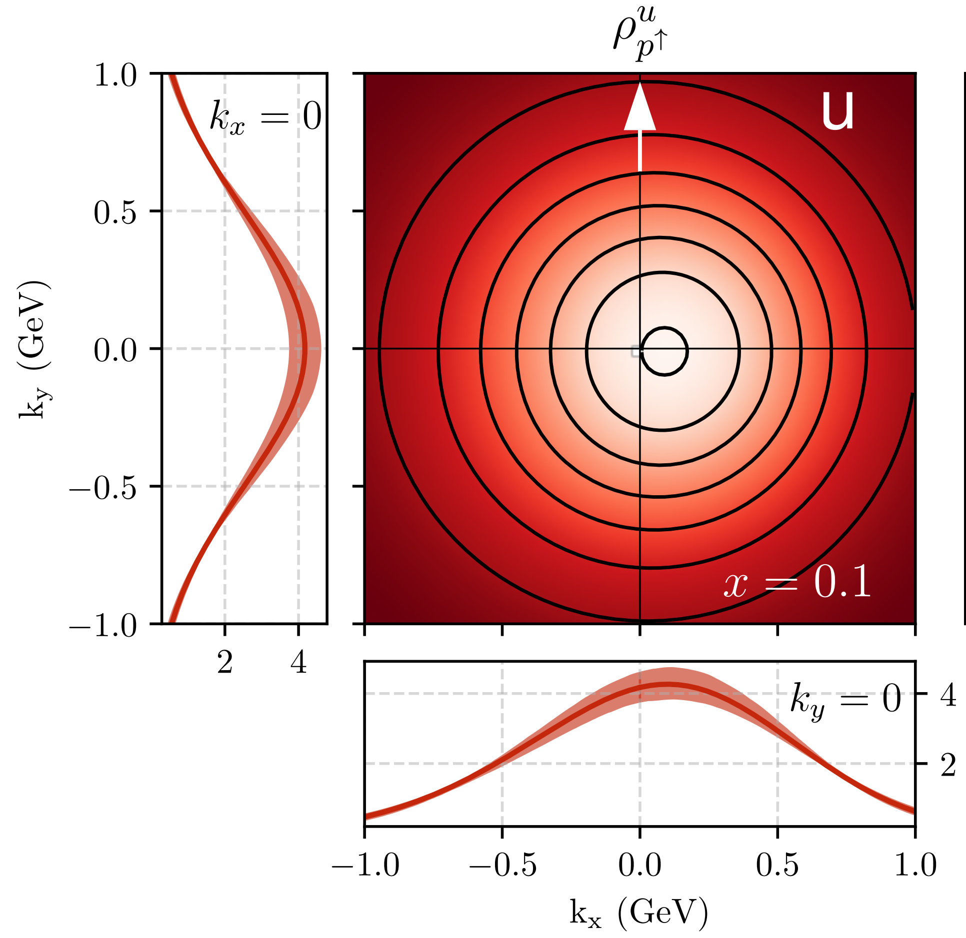

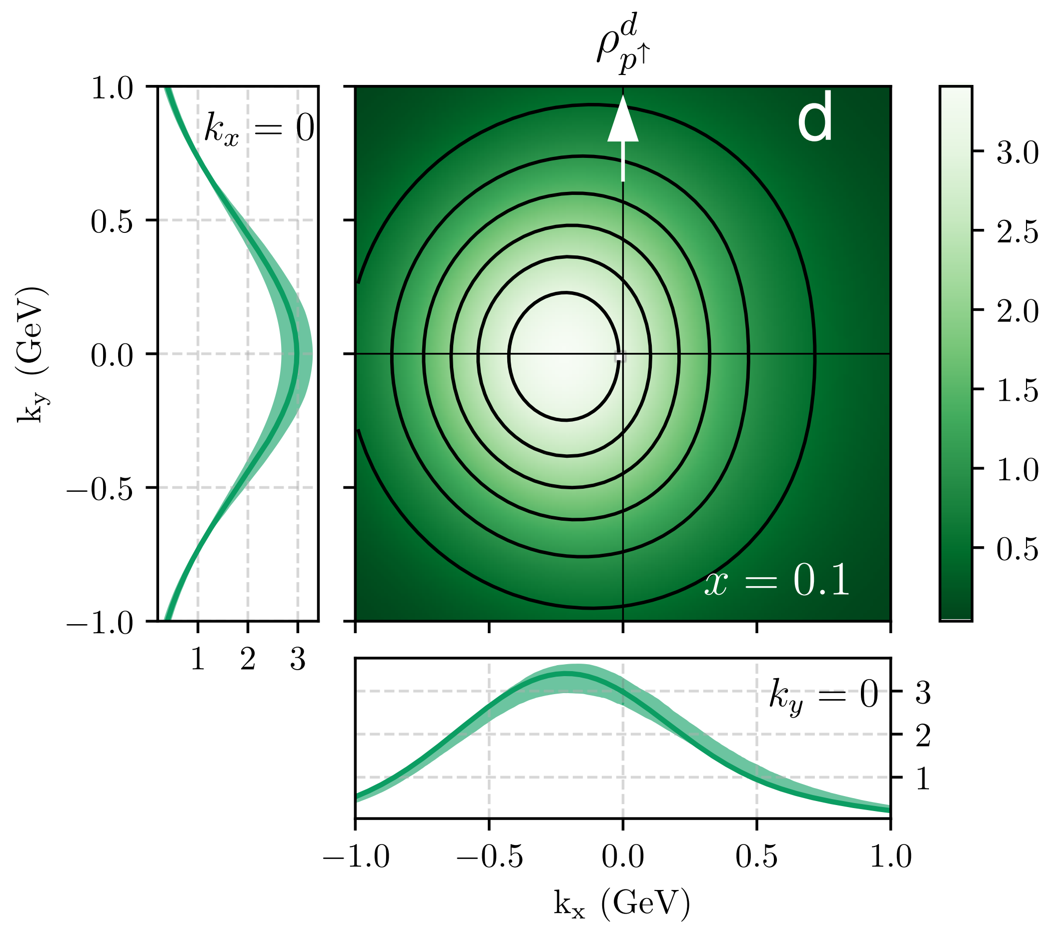

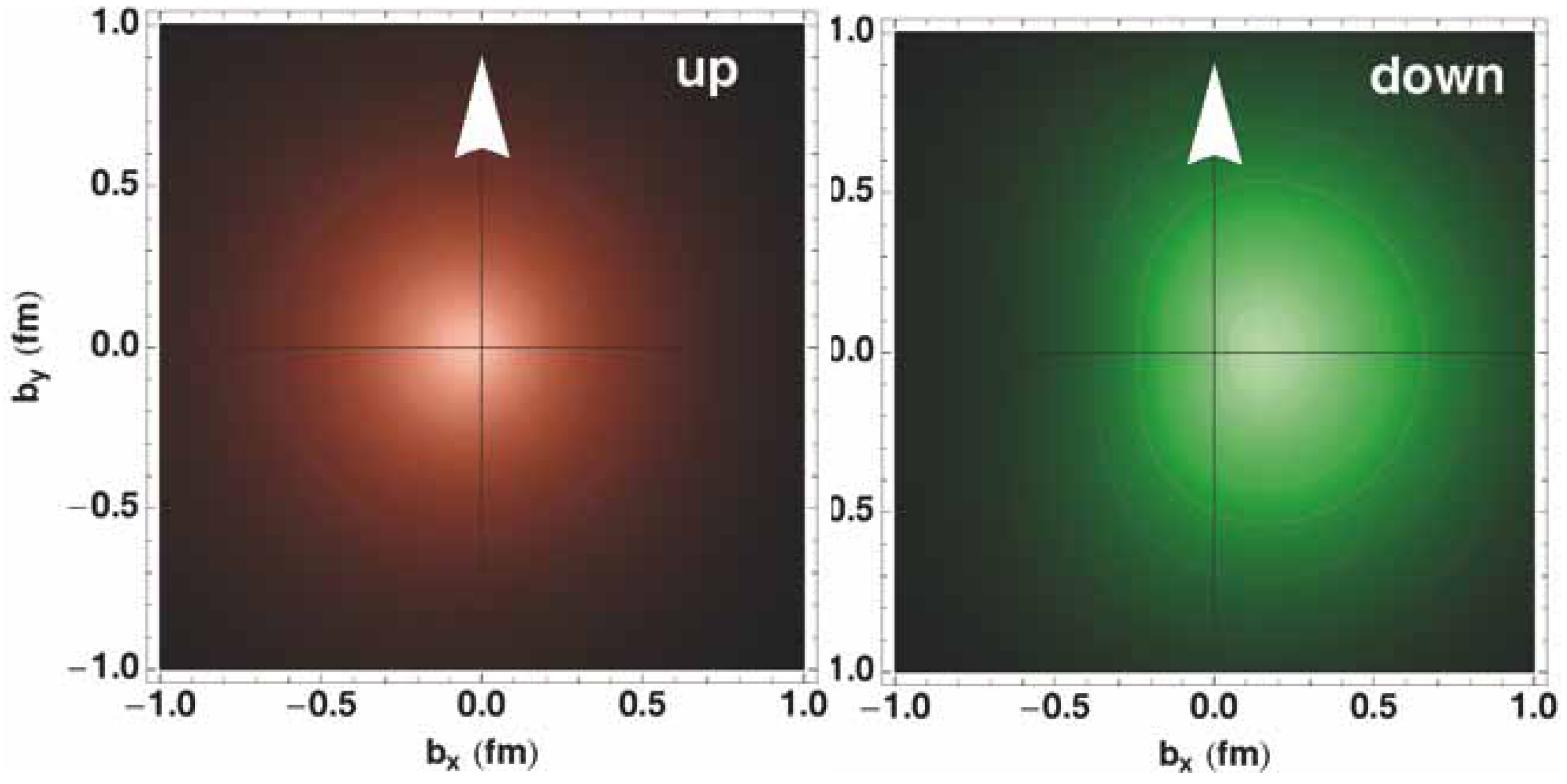

The various dimensions of the nucleon structure

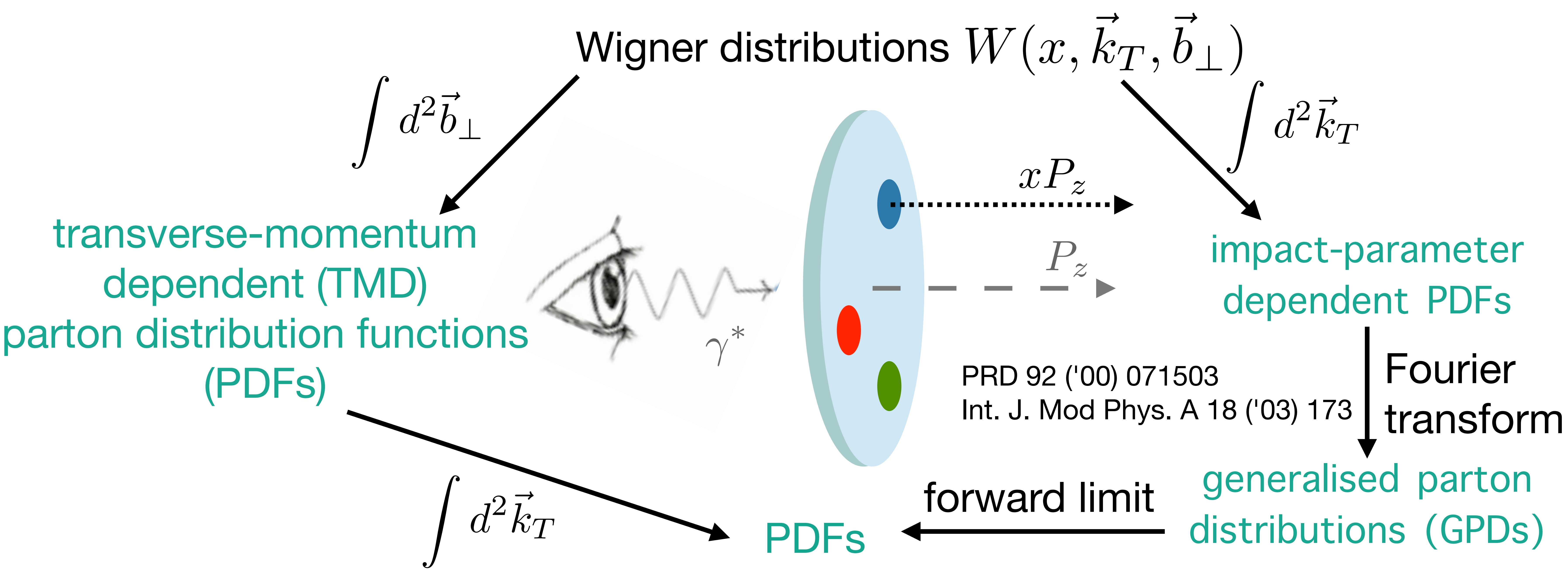

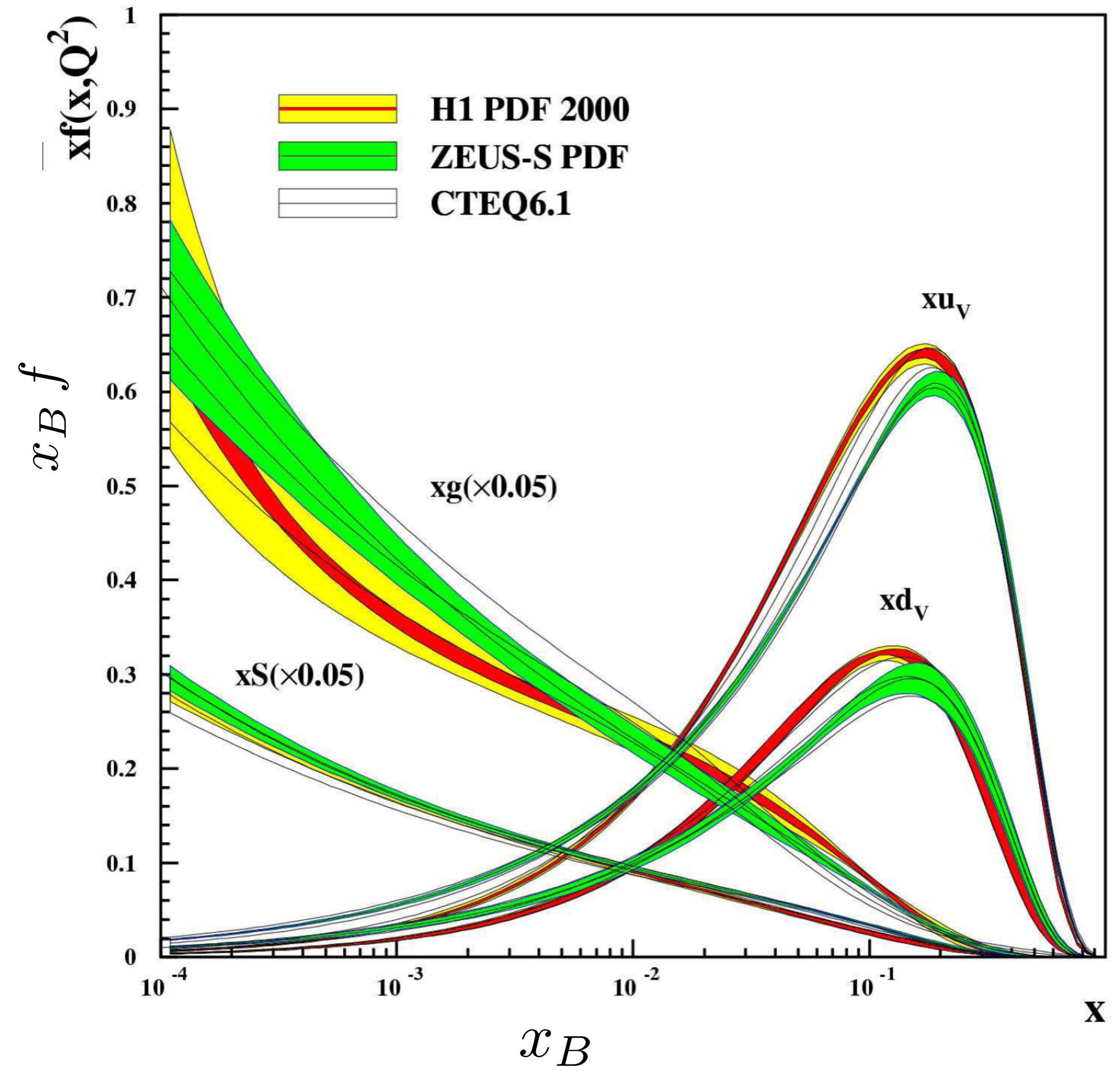

Transverse momentum dependent parton distribution functions

quark polarisation (columns); nucleon polarisation (rows)

	U	L	T
U	f_1		
L		g_{1L}	
T			h_{1T}

survive integration of parton transverse momentum

Transverse momentum dependent parton distribution functions

quark polarisation (columns) / nucleon polarisation (rows)

	U	L	T
U	f_1		$h_1^\perp$
L		g_{1L}	$h_{1L}^\perp$
T	$f_{1T}^\perp$	$g_{1T}^\perp$	$h_{1T}\, h_{1T}^\perp$

Transverse momentum dependent parton distribution functions

quark polarisation

nucleon polarisation

	U	L	T
U	f_1		$h_1^{\perp}$
L		g_{1L}	$h_{1L}^{\perp}$
T	$f_{1T}^{\perp}$	$g_{1T}^{\perp}$	$h_{1T}\, h_{1T}^{\perp}$

Chiral odd

Transverse momentum dependent parton distribution functions

quark polarisation (columns) / nucleon polarisation (rows)

	U	L	T
U	f_1		$h_1^\perp$
L		g_{1L}	$h_{1L}^\perp$
T	$f_{1T}^\perp$	$g_{1T}^\perp$	$h_{1T}\, h_{1T}^\perp$

Chiral odd

Naive T-odd

Transverse momentum dependent parton distribution functions

Unpolarized

Spin-spin correlations

Spin-momentum correlations

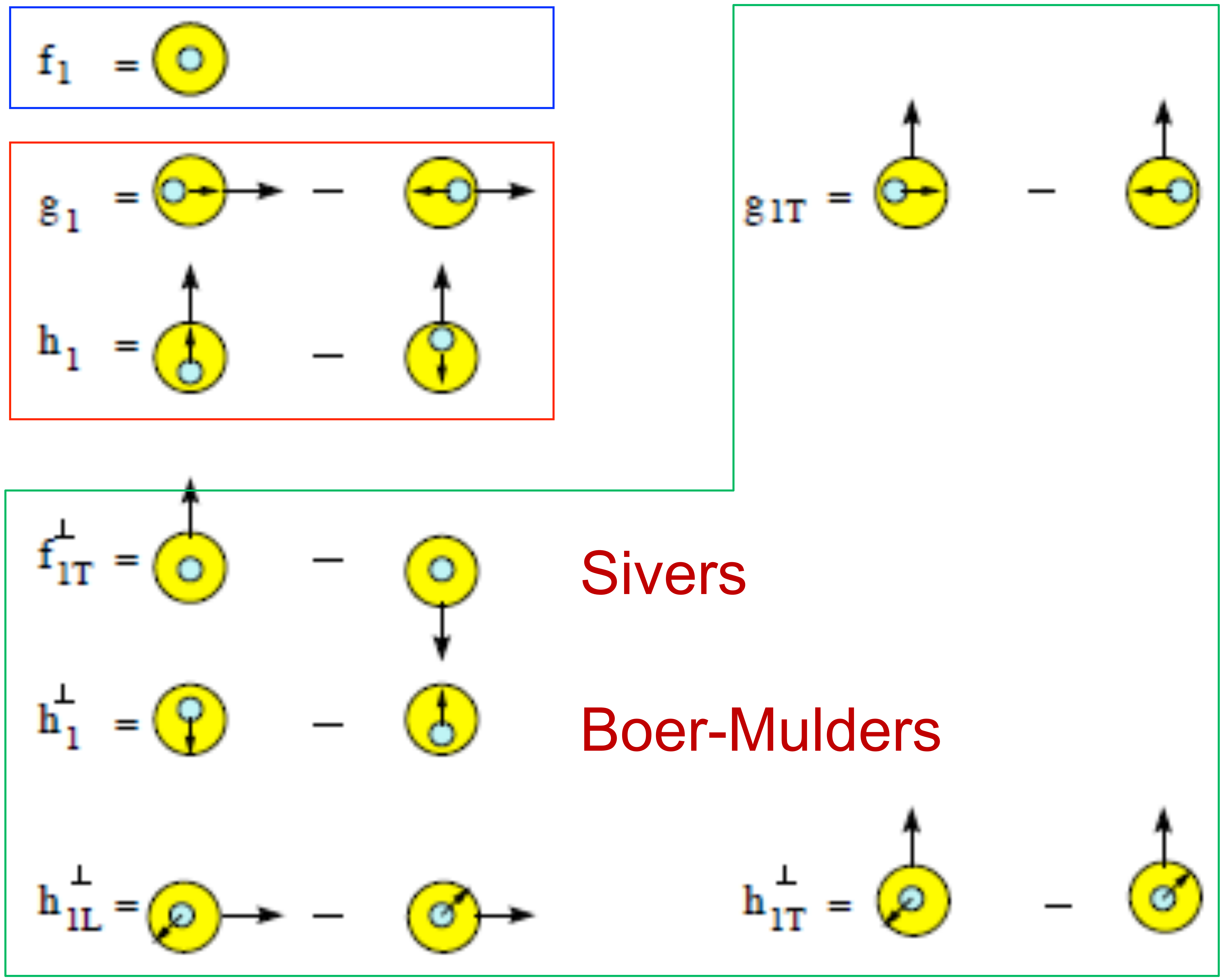

Single-hadron production in semi-inclusive DIS

$$Q^2 = -q^2$$

$$x_B = \frac{Q^2}{2P \cdot q}$$

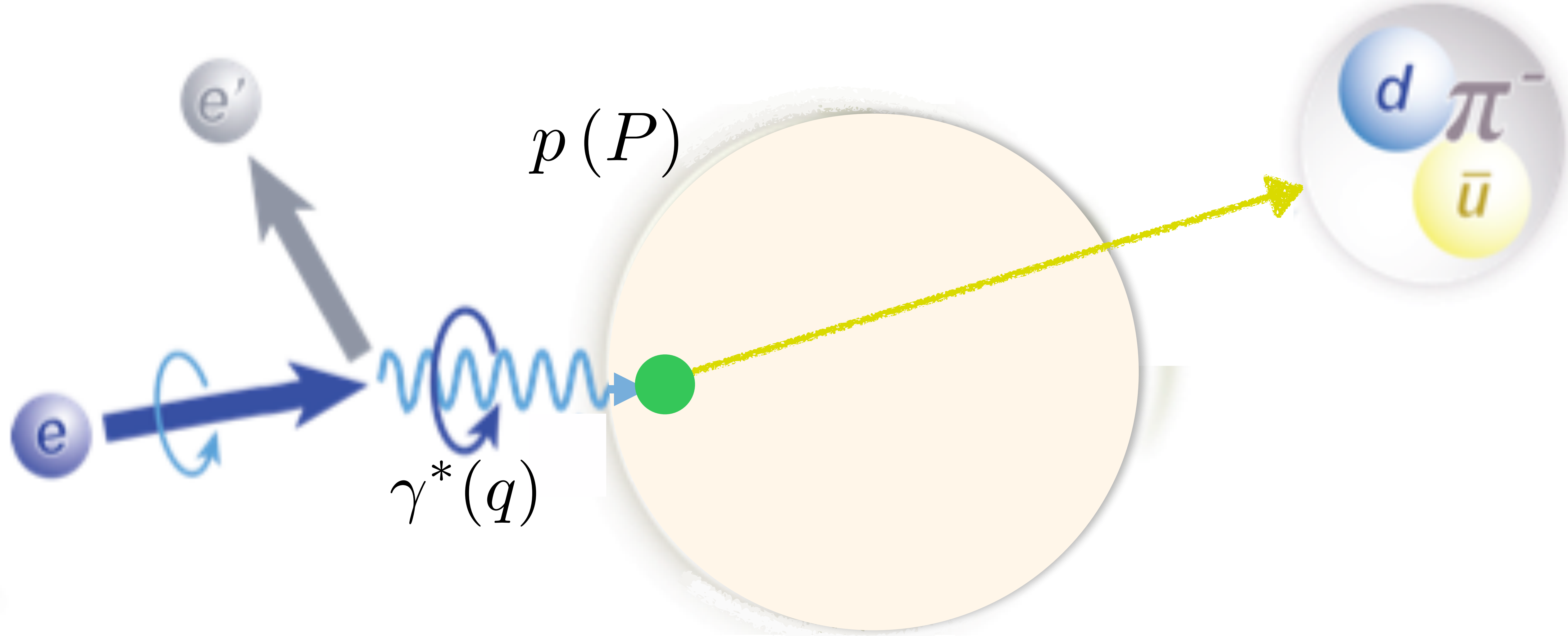

Highly virtual photon:
$Q^2 \gg 1$ GeV^2
provides hard
scale of process

Single-hadron production in semi-inclusive DIS

$$Q^2 = -q^2$$

$$x_B = \frac{Q^2}{2P \cdot q}$$

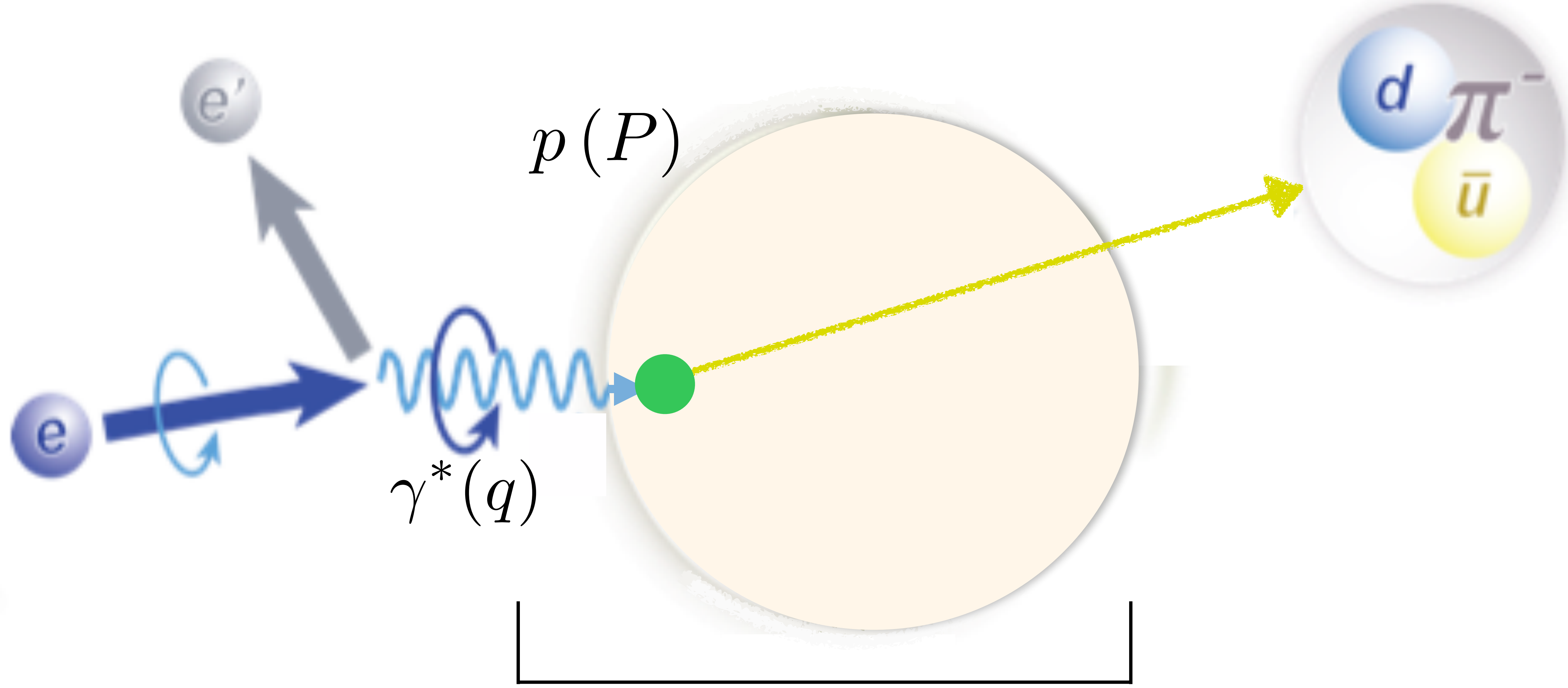

parton distribution function $PDF(x_B)$

Highly virtual photon:
$Q^2 \gg 1$ GeV^2
provides hard
scale of process

Single-hadron production in semi-inclusive DIS

$$Q^2 = -q^2$$

$$x_B = \frac{Q^2}{2P \cdot q}$$

$$z \overset{\text{lab}}{=} \frac{E_h}{E_{\gamma*}}$$

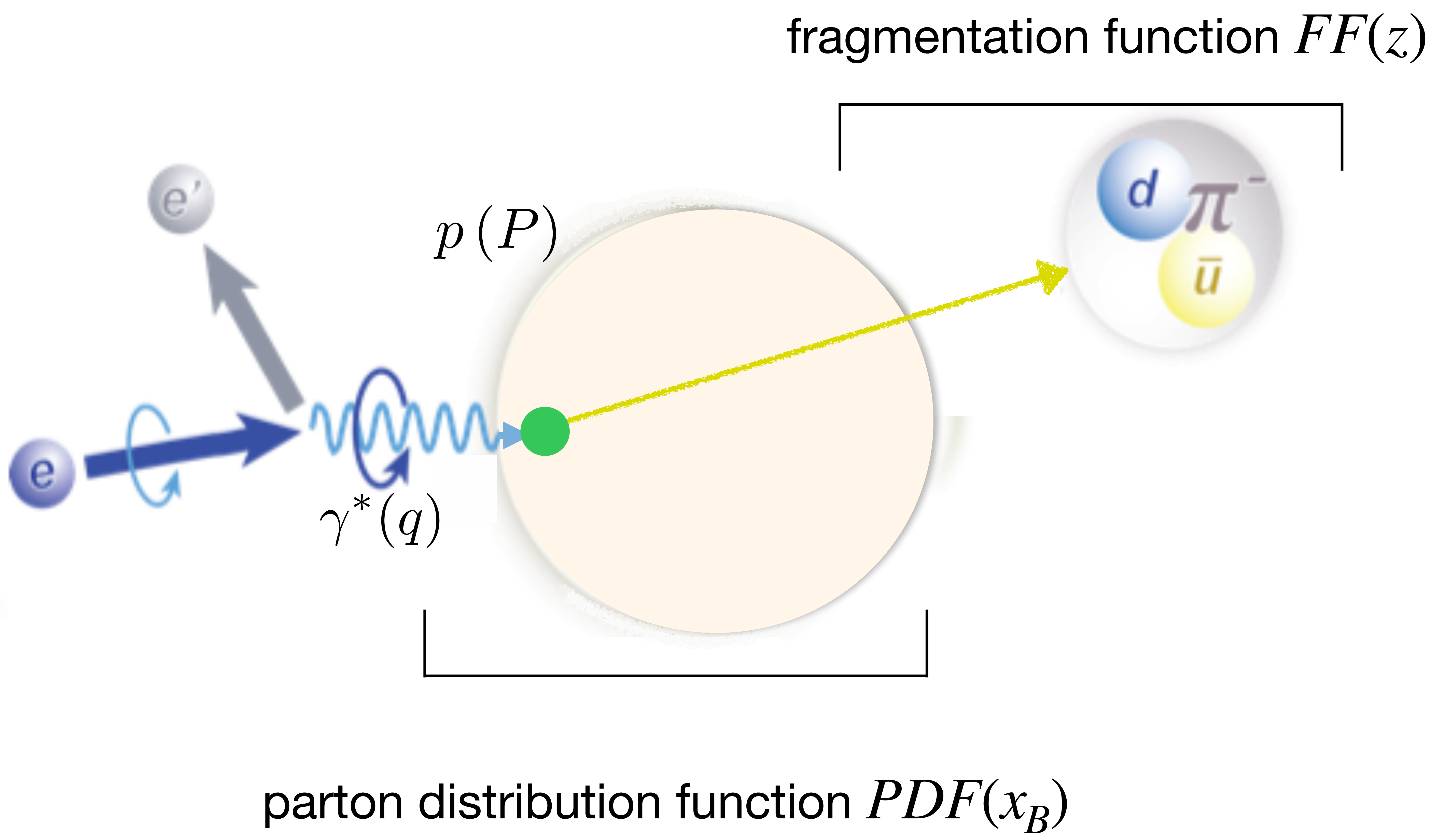

Highly virtual photon:
$Q^2 \gg 1$ GeV^2
provides hard
scale of process

Single-hadron production in semi-inclusive DIS

$Q^2 = -q^2$

$x_B = \frac{Q^2}{2P \cdot q}$

$z \overset{\text{lab}}{=} \frac{E_h}{E_{\gamma *}}$

Transverse-momentum-dependent (TMD) fragmentation function $FF(z, p_\perp)$

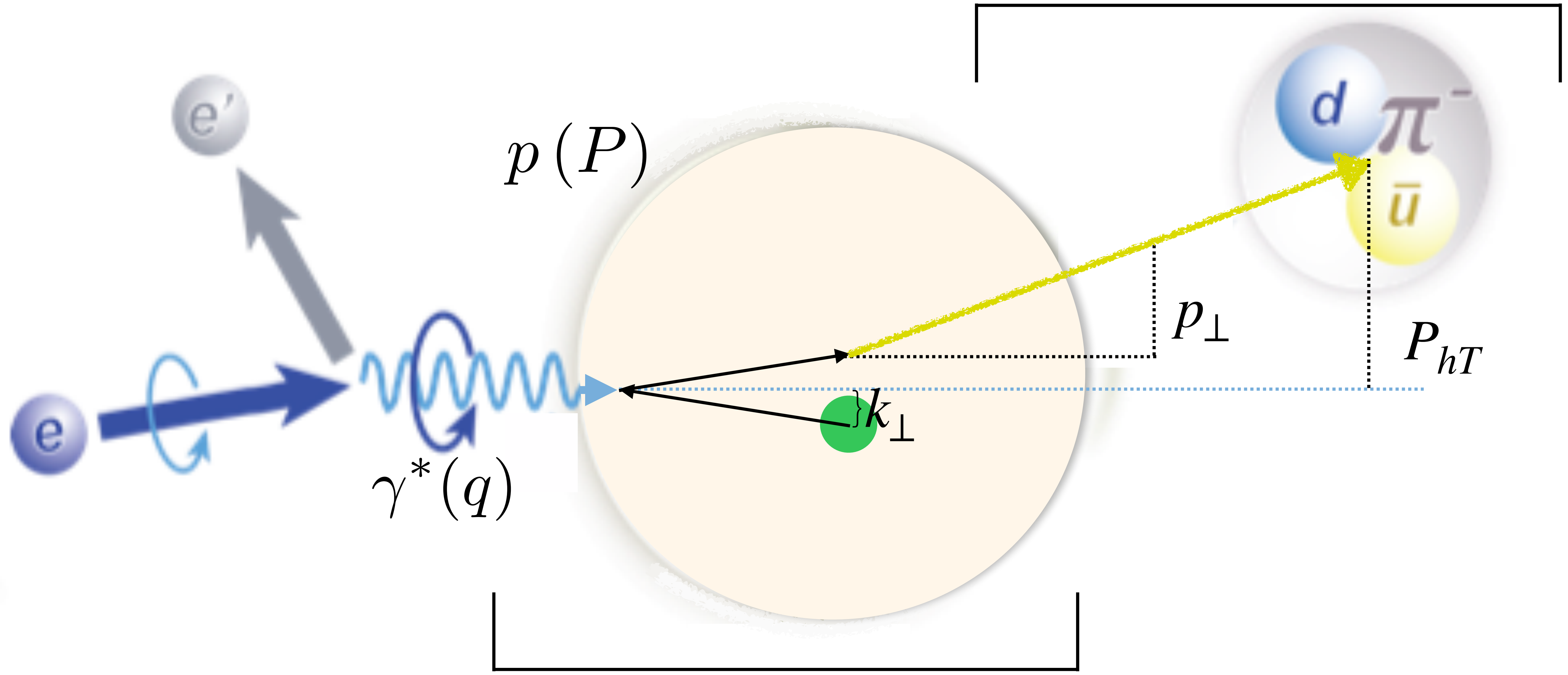

Transverse-momentum-dependent (TMD) parton distribution function $PDF(x_B, k_\perp)$

Highly virtual photon: $Q^2 \gg 1$ GeV^2 provides hard scale of process

Single-hadron production in semi-inclusive DIS

$Q^2 = -q^2$

$x_B = \frac{Q^2}{2P \cdot q}$

$z \overset{\text{lab}}{=} \frac{E_h}{E_{\gamma*}}$

Transverse-momentum-dependent (TMD) fragmentation function $FF(z, p_\perp, Q^2)$

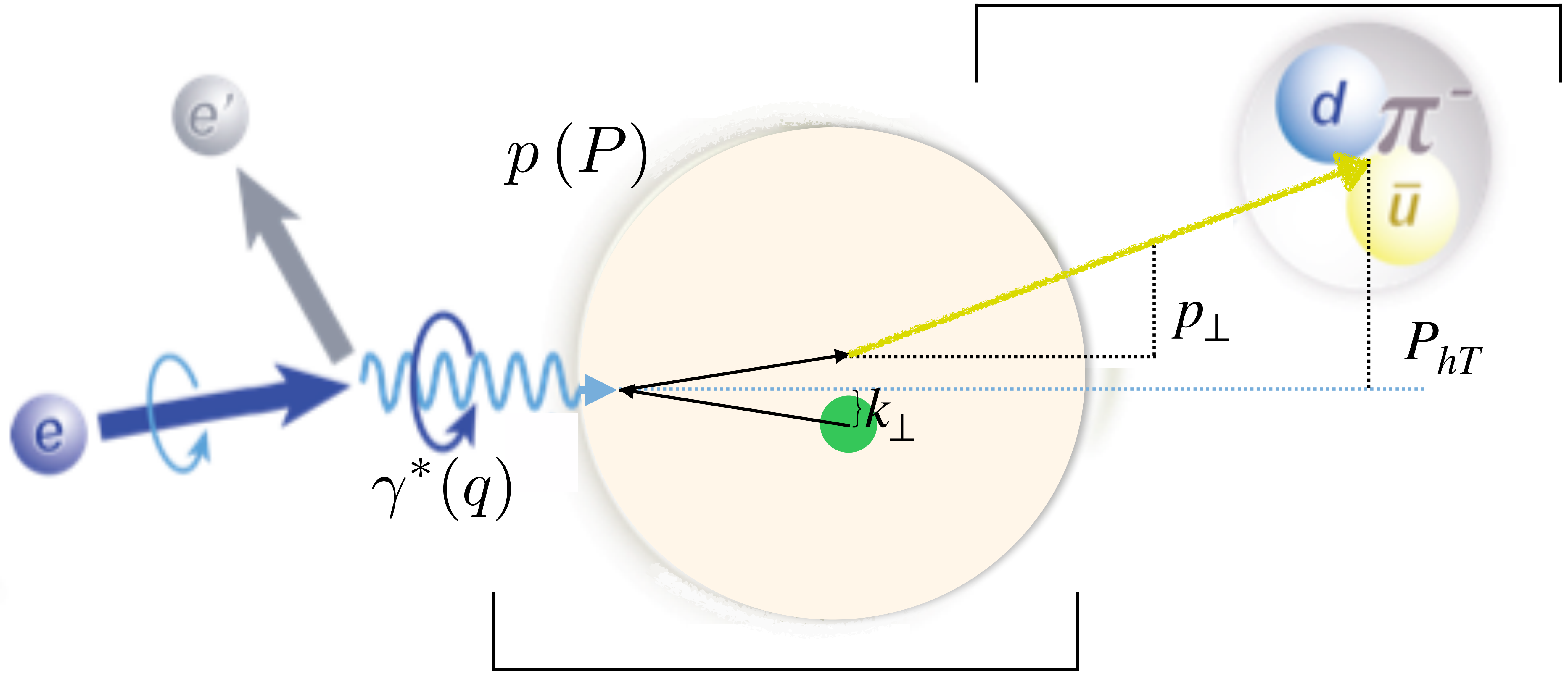

Transverse-momentum-dependent (TMD) parton distribution function $PDF(x_B, k_\perp, Q^2)$

TMD evolution

Highly virtual photon:
$Q^2 \gg 1$ GeV^2
provides hard
scale of process

Single-hadron production in semi-inclusive DIS

$$Q^2 = -q^2$$

$$x_B = \frac{Q^2}{2P\cdot q}$$

$$z \overset{\text{lab}}{=} \frac{E_h}{E_{\gamma*}}$$

Transverse-momentum-dependent (TMD)
fragmentation function $FF(z, p_\perp, Q^2)$

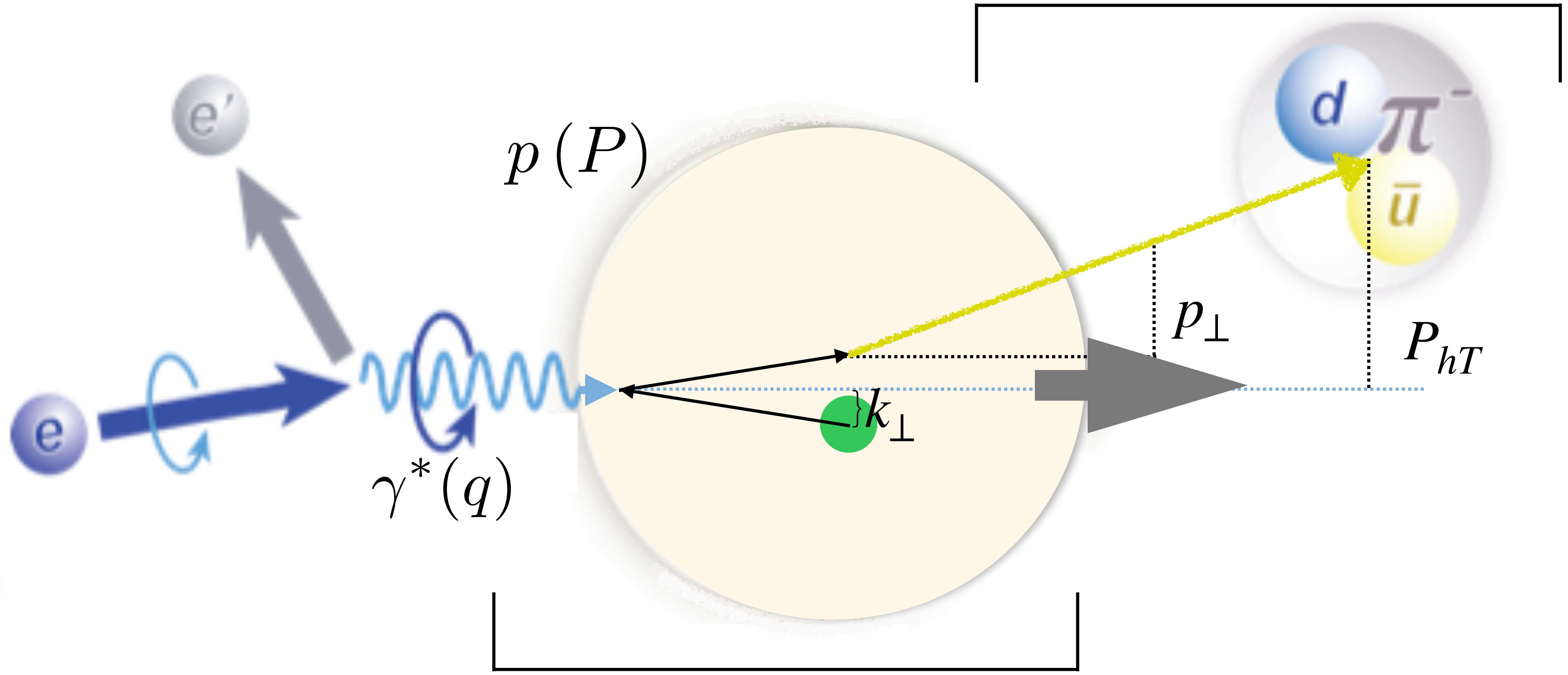

Transverse-momentum-dependent (TMD)
parton distribution function $PDF(x_B, k_\perp, Q^2)$

TMD evolution

Highly virtual photon:
$Q^2 \gg 1$ GeV^2
provides hard
scale of process

Single-hadron production in semi-inclusive DIS

$Q^2 = -q^2$

$x_B = \frac{Q^2}{2P \cdot q}$

$z \overset{\text{lab}}{=} \frac{E_h}{E_{\gamma*}}$

Transverse-momentum-dependent (TMD) fragmentation function $FF(z, p_\perp, Q^2)$

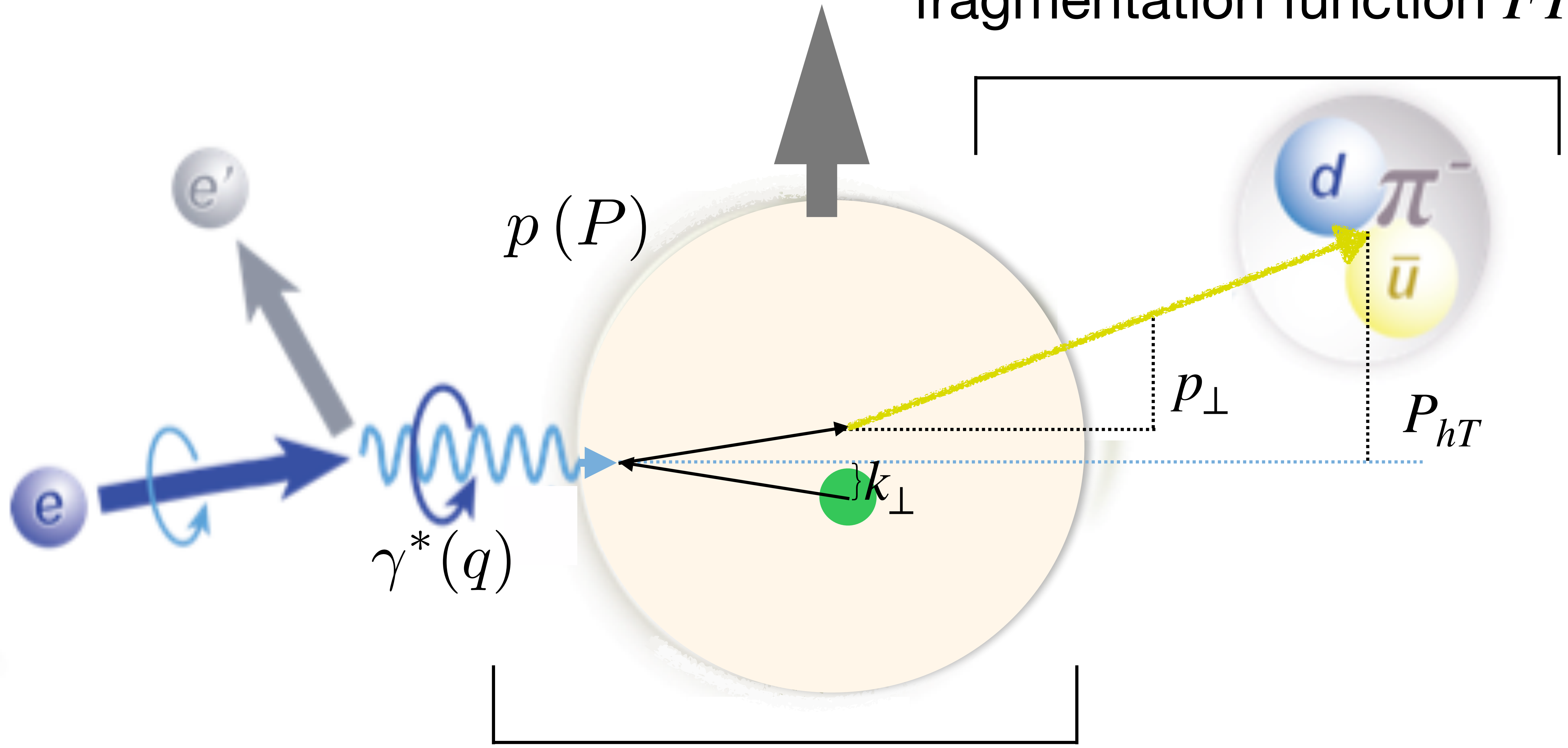

Transverse-momentum-dependent (TMD) parton distribution function $PDF(x_B, k_\perp, Q^2)$

TMD evolution

Highly virtual photon:
$Q^2 \gg 1$ GeV^2
provides hard
scale of process

Single-hadron production in semi-inclusive DIS

Transverse-momentum-dependent (TMD)

fragmentation function $FF(z, p_\perp, Q^2)$

$$Q^2 = -q^2$$

$$x_B = \frac{Q^2}{2P \cdot q}$$

$$z \overset{\text{lab}}{=} \frac{E_h}{E_{\gamma *}}$$

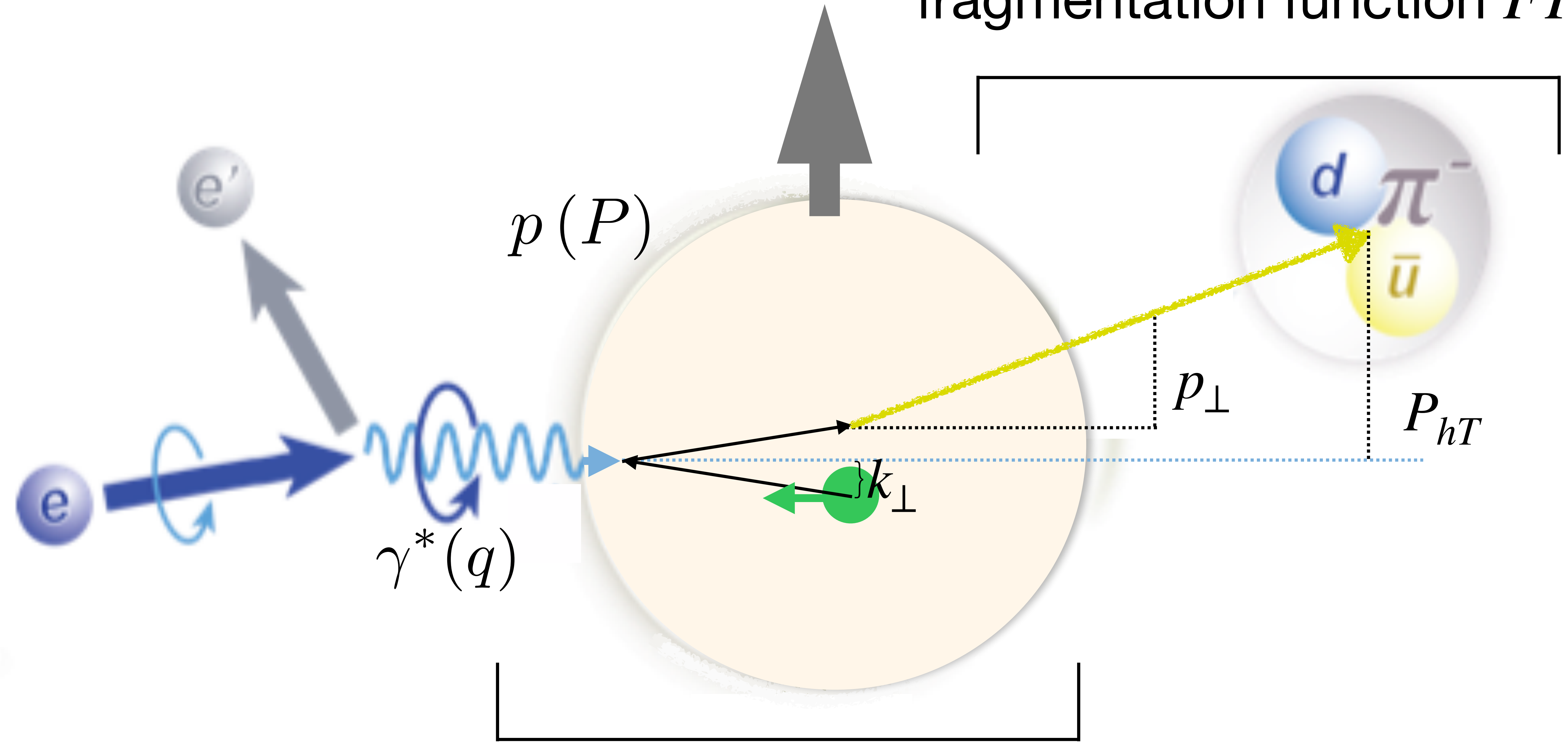

TMD evolution

Transverse-momentum-dependent (TMD)

parton distribution function $PDF(x_B, k_\perp, Q^2)$

Highly virtual photon:
$Q^2 \gg 1$ GeV^2
provides hard
scale of process

Single-hadron production in semi-inclusive DIS

$Q^2 = -q^2$

$x_B = \frac{Q^2}{2P \cdot q}$

$z \overset{\text{lab}}{=} \frac{E_h}{E_{\gamma*}}$

Transverse-momentum-dependent (TMD)

fragmentation function $FF(z, p_\perp, Q^2)$

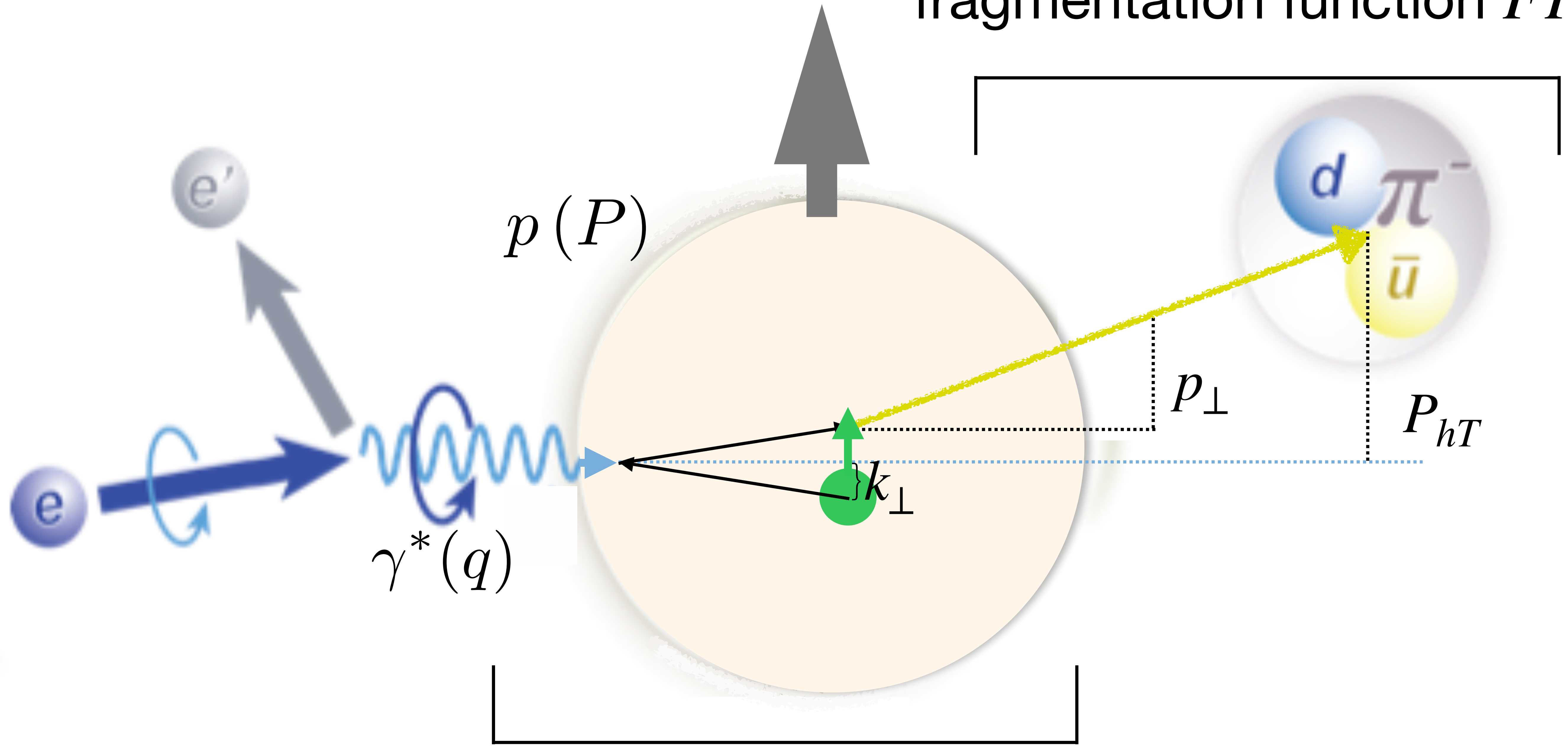

Transverse-momentum-dependent (TMD)

parton distribution function $PDF(x_B, k_\perp, Q^2)$

TMD evolution

Highly virtual photon:
$Q^2 \gg 1$ GeV^2
provides hard
scale of process

Semi-inclusive DIS cross section

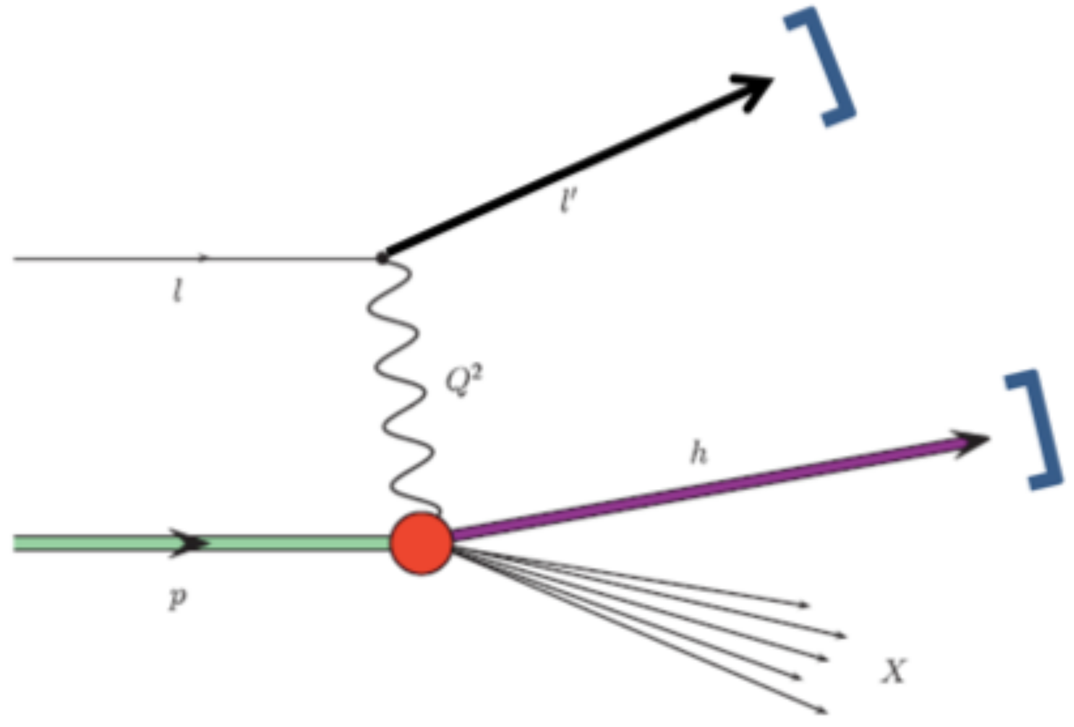

$$
\begin{aligned}
\sigma^h(\phi,\phi_S) &= \sigma^h_{UU}\Big\{1 + 2\langle\cos(\phi)\rangle^h_{UU}\,\cos(\phi) + 2\langle\cos(2\phi)\rangle^h_{UU}\,\cos(2\phi) \\
&+ \lambda_l\, 2\langle\sin(\phi)\rangle^h_{LU}\,\sin(\phi) \\
&+ S_L\Big[2\langle\sin(\phi)\rangle^h_{UL}\,\sin(\phi) + 2\langle\sin(2\phi)\rangle^h_{UL}\,\sin(2\phi) \\
&+ \lambda_l\Big(2\langle\cos(0\phi)\rangle^h_{LL}\,\cos(0\phi) + 2\langle\cos(\phi)\rangle^h_{LL}\,\cos(\phi)\Big)\Big] \\
&+ S_T\Big[2\langle\sin(\phi-\phi_S)\rangle^h_{UT}\,\sin(\phi-\phi_S) + 2\langle\sin(\phi+\phi_S)\rangle^h_{UT}\,\sin(\phi+\phi_S) \\
&+ 2\langle\sin(3\phi-\phi_S)\rangle^h_{UT}\,\sin(3\phi-\phi_S) + 2\langle\sin(\phi_S)\rangle^h_{UT}\,\sin(\phi_S) \\
&+ 2\langle\sin(2\phi-\phi_S)\rangle^h_{UT}\,\sin(2\phi-\phi_S) \\
&+ \lambda_l\Big(2\langle\cos(\phi-\phi_S)\rangle^h_{LT}\,\cos(\phi-\phi_S) \\
&+ 2\langle\cos(\phi_S)\rangle^h_{LT}\,\cos(\phi_S) + 2\langle\cos(2\phi-\phi_S)\rangle^h_{LT}\,\cos(2\phi-\phi_S)\Big)\Big]\Big\}
\end{aligned}
$$

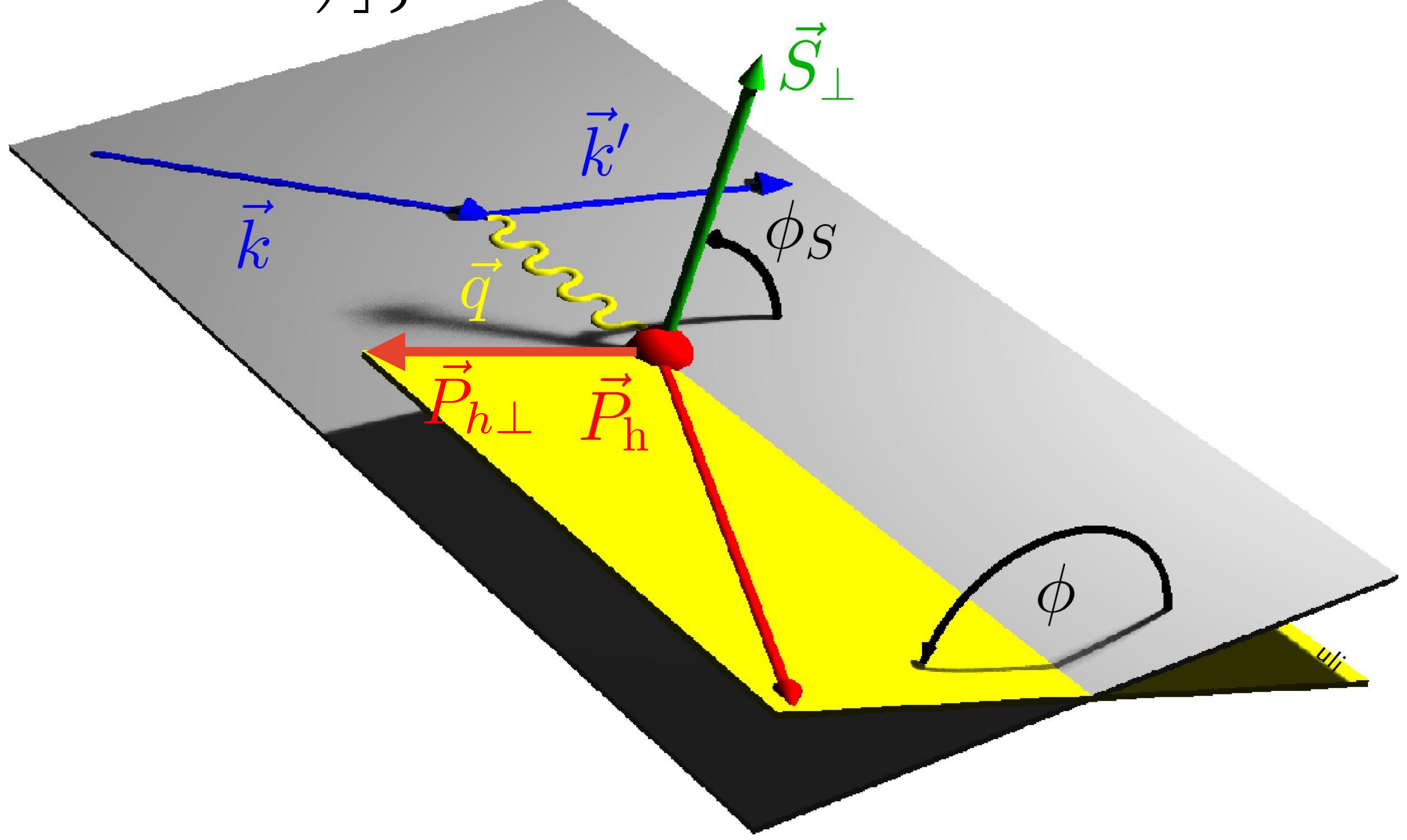

Semi-inclusive DIS cross section

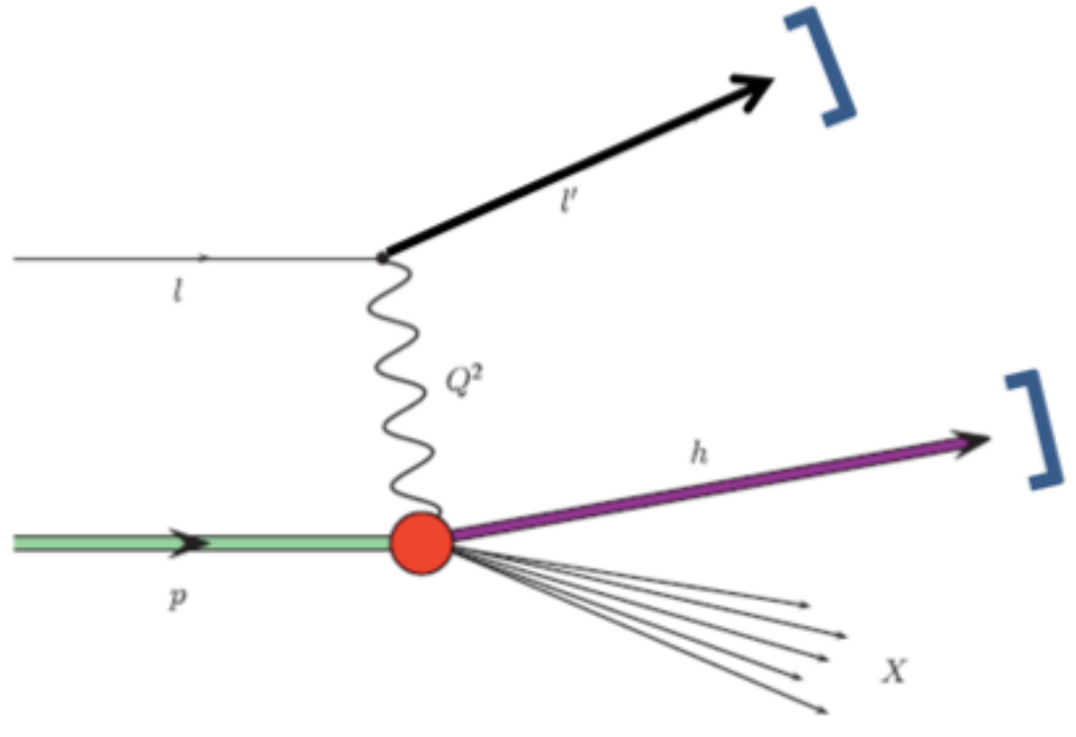

$$
\begin{aligned}
\sigma^h(\phi,\phi_S) \;=\;& \sigma^h_{UU}\Big\{1 + 2\langle\cos(\phi)\rangle^h_{UU}\,\cos(\phi) + 2\langle\cos(2\phi)\rangle^h_{UU}\,\cos(2\phi)\\
&+ \lambda_l\, 2\langle\sin(\phi)\rangle^h_{LU}\,\sin(\phi)\\
&+ S_L\Big[2\langle\sin(\phi)\rangle^h_{UL}\,\sin(\phi) + 2\langle\sin(2\phi)\rangle^h_{UL}\,\sin(2\phi)\\
&+ \lambda_l\Big(2\langle\cos(0\phi)\rangle^h_{LL}\,\cos(0\phi) + 2\langle\cos(\phi)\rangle^h_{LL}\,\cos(\phi)\Big)\Big]\\
&+ S_T\Big[2\langle\sin(\phi-\phi_S)\rangle^h_{UT}\,\sin(\phi-\phi_S) + 2\langle\sin(\phi+\phi_S)\rangle^h_{UT}\,\sin(\phi+\phi_S)\\
&+ 2\langle\sin(3\phi-\phi_S)\rangle^h_{UT}\,\sin(3\phi-\phi_S) + 2\langle\sin(\phi_S)\rangle^h_{UT}\,\sin(\phi_S)\\
&+ 2\langle\sin(2\phi-\phi_S)\rangle^h_{UT}\,\sin(2\phi-\phi_S)\\
&+ \lambda_l\Big(2\langle\cos(\phi-\phi_S)\rangle^h_{LT}\,\cos(\phi-\phi_S)\\
&+ 2\langle\cos(\phi_S)\rangle^h_{LT}\,\cos(\phi_S) + 2\langle\cos(2\phi-\phi_S)\rangle^h_{LT}\,\cos(2\phi-\phi_S)\Big)\Big]\Big\}
\end{aligned}
$$

longitudinal target polarisation (S_L)

transverse target polarisation (S_T)

beam polarisation (λ_l)

LT: beam polarisation, target polarisation

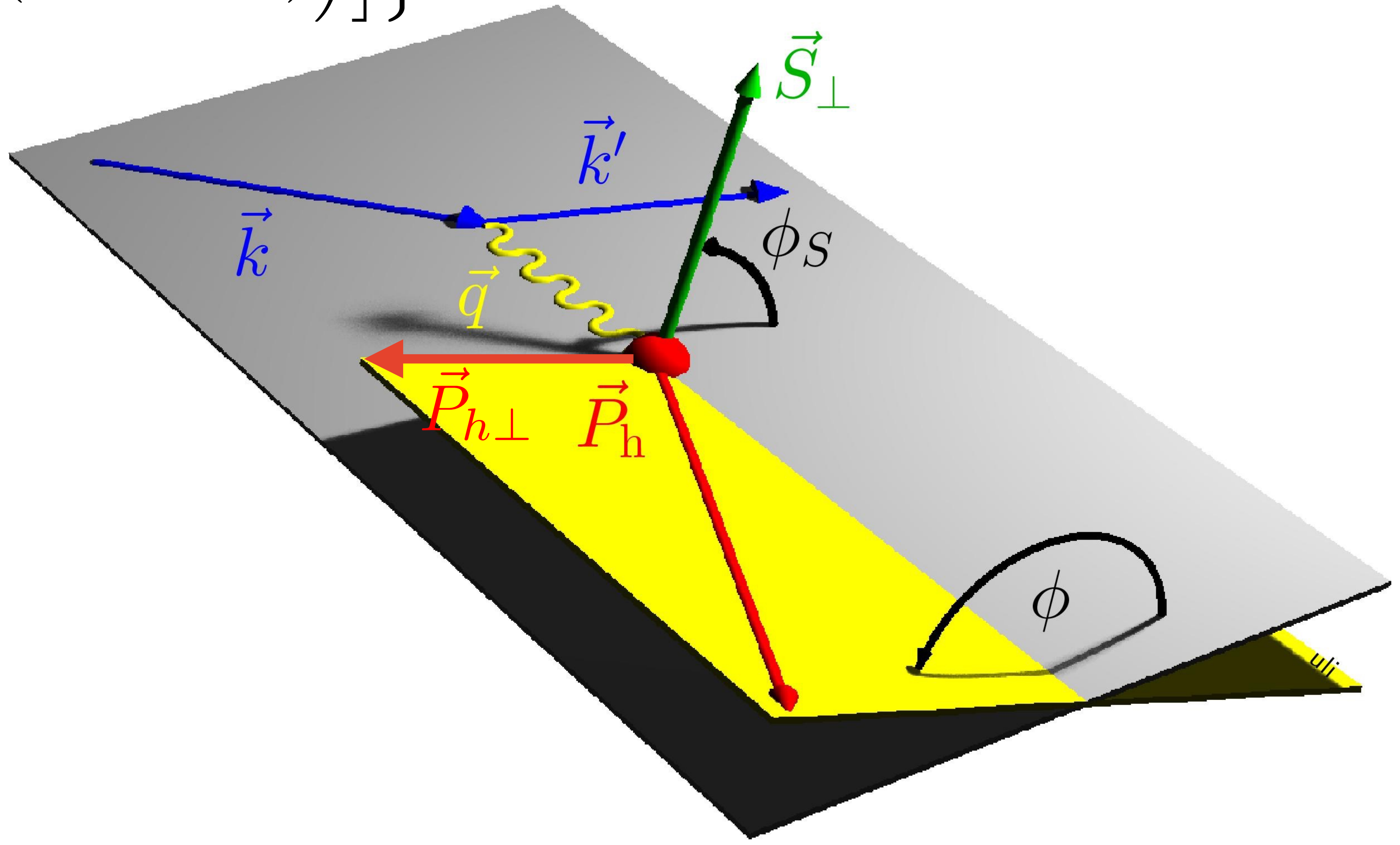

Semi-inclusive DIS cross section

$$
\begin{aligned}
\sigma^h(\phi,\phi_S) \;=\; & \sigma^h_{UU}\Big\{1 + 2\langle\cos(\phi)\rangle^h_{UU}\,\cos(\phi) + 2\langle\cos(2\phi)\rangle^h_{UU}\,\cos(2\phi) \\
& + \lambda_l\, 2\langle\sin(\phi)\rangle^h_{LU}\,\sin(\phi) \\
& + S_L\Big[2\langle\sin(\phi)\rangle^h_{UL}\,\sin(\phi) + 2\langle\sin(2\phi)\rangle^h_{UL}\,\sin(2\phi) \\
& + \lambda_l\Big(2\langle\cos(0\phi)\rangle^h_{LL}\,\cos(0\phi) + 2\langle\cos(\phi)\rangle^h_{LL}\,\cos(\phi)\Big)\Big] \\
& + S_T\Big[2\langle\sin(\phi-\phi_S)\rangle^h_{UT}\,\sin(\phi-\phi_S) + 2\langle\sin(\phi+\phi_S)\rangle^h_{UT}\,\sin(\phi+\phi_S) \\
& + 2\langle\sin(3\phi-\phi_S)\rangle^h_{UT}\,\sin(3\phi-\phi_S) + 2\langle\sin(\phi_S)\rangle^h_{UT}\,\sin(\phi_S) \\
& + 2\langle\sin(2\phi-\phi_S)\rangle^h_{UT}\,\sin(2\phi-\phi_S) \\
& + \lambda_l\Big(2\langle\cos(\phi-\phi_S)\rangle^h_{LT}\,\cos(\phi-\phi_S) \\
& + 2\langle\cos(\phi_S)\rangle^h_{LT}\,\cos(\phi_S) + 2\langle\cos(2\phi-\phi_S)\rangle^h_{LT}\,\cos(2\phi-\phi_S)\Big)\Big]\Big\}
\end{aligned}
$$

longitudinal target polarisation

transverse target polarisation

beam polarisation

beam polarisation

target polarisation

leading twist

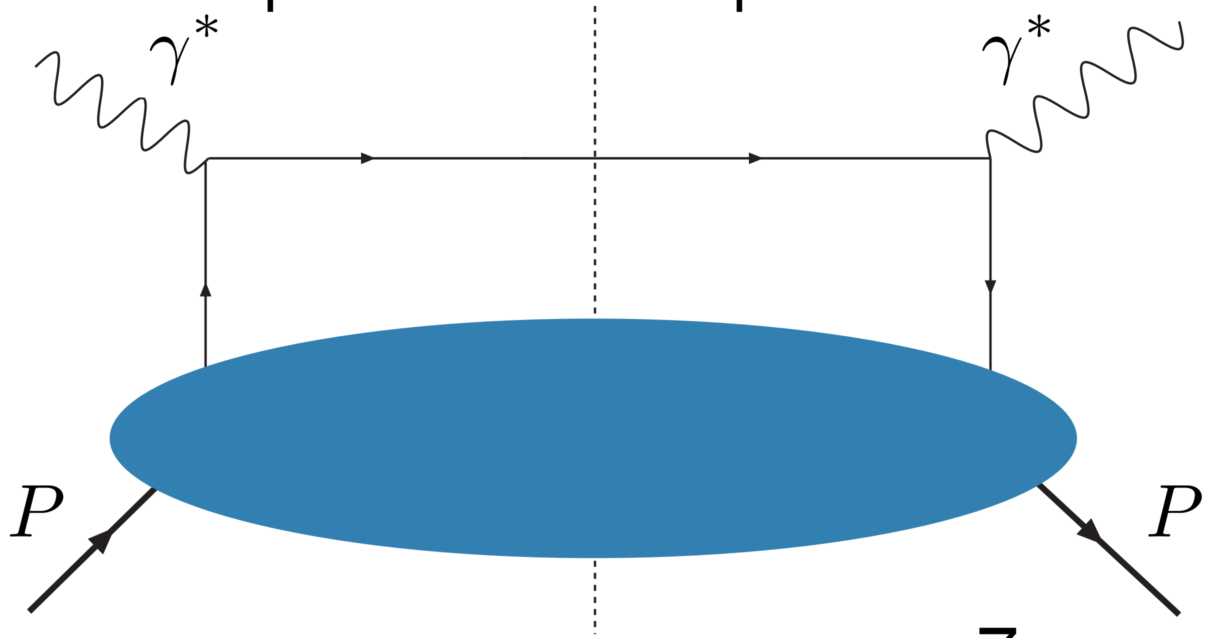

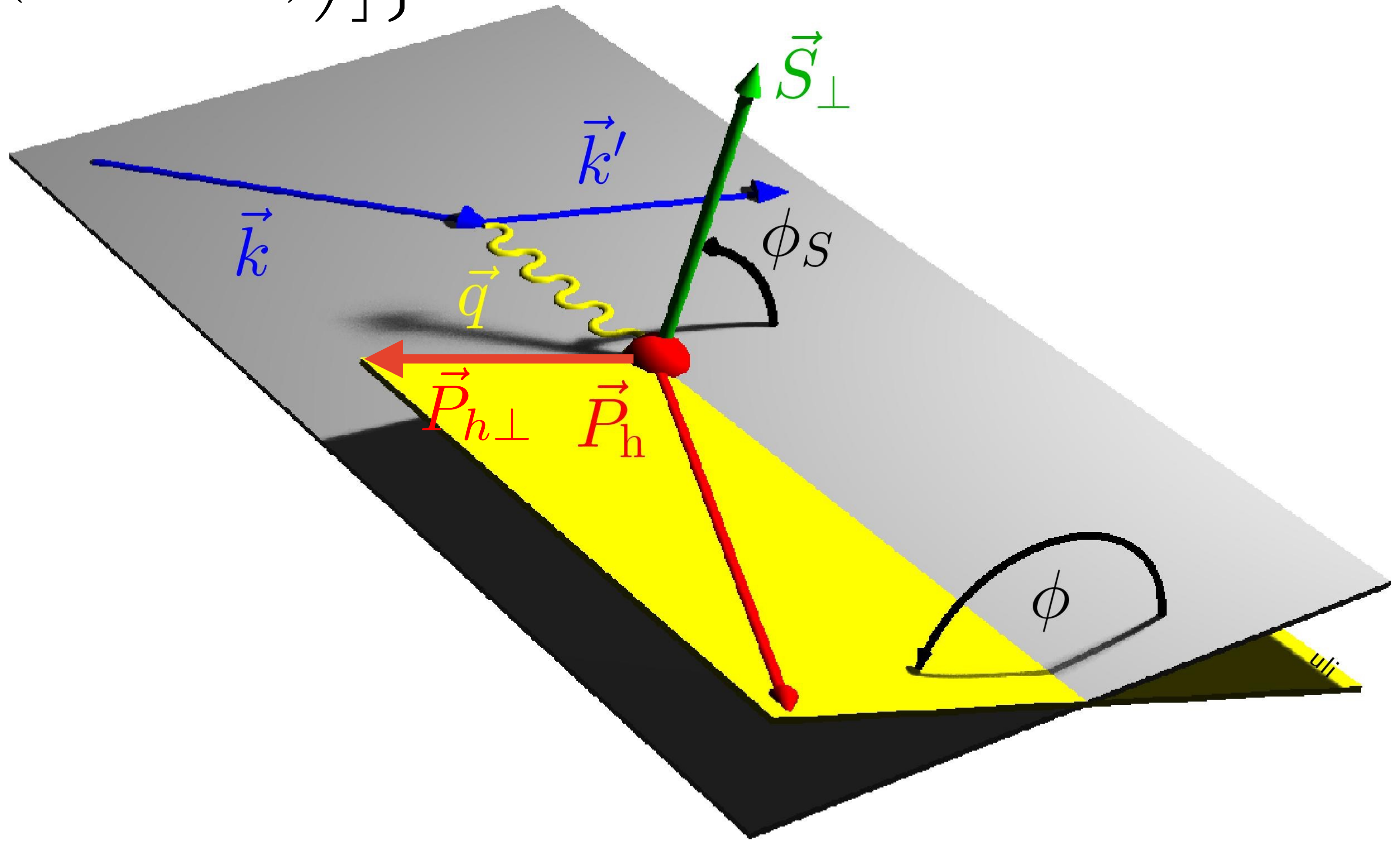

Semi-inclusive DIS cross section

$$
\begin{aligned}
\sigma^h(\phi,\phi_S) \;=\;& \sigma^h_{UU}\Big\{1 + 2\langle\cos(\phi)\rangle^h_{UU}\cos(\phi) + 2\langle\cos(2\phi)\rangle^h_{UU}\cos(2\phi)\\
&+ \lambda_l\, 2\langle\sin(\phi)\rangle^h_{LU}\sin(\phi)\\
&+ S_L\Big[2\langle\sin(\phi)\rangle^h_{UL}\sin(\phi) + 2\langle\sin(2\phi)\rangle^h_{UL}\sin(2\phi)\\
&+ \lambda_l\Big(2\langle\cos(0\phi)\rangle^h_{LL}\cos(0\phi) + 2\langle\cos(\phi)\rangle^h_{LL}\cos(\phi)\Big)\Big]\\
&+ S_T\Big[2\langle\sin(\phi-\phi_S)\rangle^h_{UT}\sin(\phi-\phi_S) + 2\langle\sin(\phi+\phi_S)\rangle^h_{UT}\sin(\phi+\phi_S)\\
&+ 2\langle\sin(3\phi-\phi_S)\rangle^h_{UT}\sin(3\phi-\phi_S) + 2\langle\sin(\phi_S)\rangle^h_{UT}\sin(\phi_S)\\
&+ 2\langle\sin(2\phi-\phi_S)\rangle^h_{UT}\sin(2\phi-\phi_S)\\
&+ \lambda_l\Big(2\langle\cos(\phi-\phi_S)\rangle^h_{LT}\cos(\phi-\phi_S)\\
&+ 2\langle\cos(\phi_S)\rangle^h_{LT}\cos(\phi_S) + 2\langle\cos(2\phi-\phi_S)\rangle^h_{LT}\cos(2\phi-\phi_S)\Big)\Big]\Big\}
\end{aligned}
$$

longitudinal target polarisation

transverse target polarisation

beam polarisation

beam polarisation

target polarisation

sub-leading twist

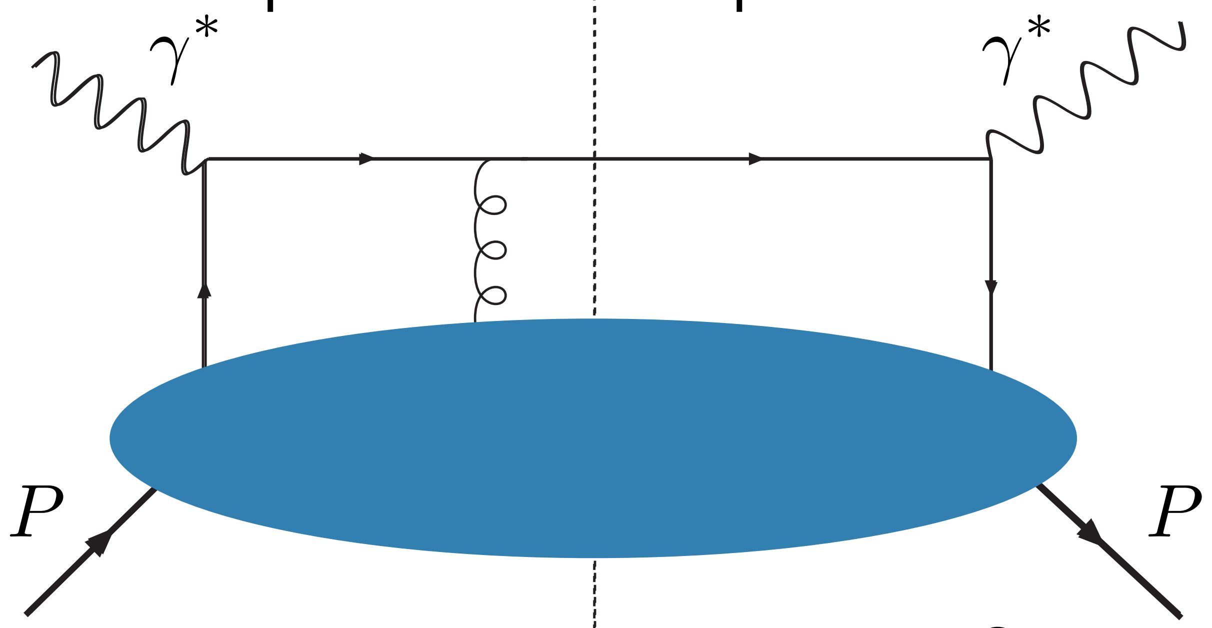

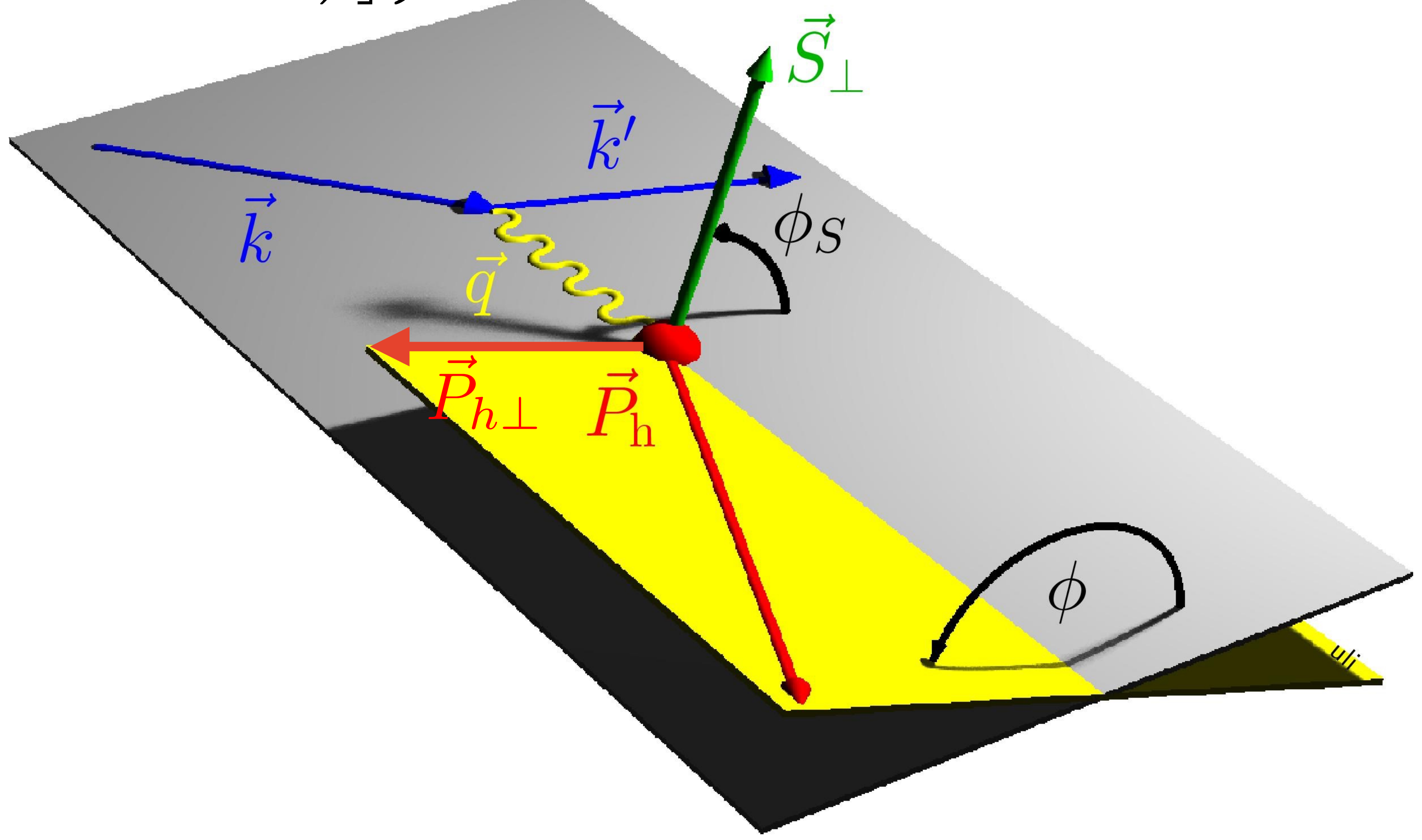

TMD PDFs and fragmentation functions (FFs)

Azimuthal amplitudes related to structure functions F_{XY} :

$$2\langle \sin(\phi + \phi_S)\rangle_{UT}^{h} = \epsilon \, F_{UT}^{\sin(\phi+\phi_S)}$$

TMD PDFs and fragmentation functions (FFs)

Azimuthal amplitudes related to structure functions F_{XY} :

$$2\langle \sin(\phi + \phi_S)\rangle^h_{UT} = \epsilon\, F^{\sin(\phi+\phi_S)}_{UT}$$

$$F_{XY} \propto \mathcal{C}\,[\mathrm{TMD\ PDF}(x, k_\perp) \times\ \mathrm{TMD\ FF}\ (z, p_\perp)]$$

$$z \stackrel{\mathrm{lab}}{=} \frac{E_h}{E_{\gamma*}}$$

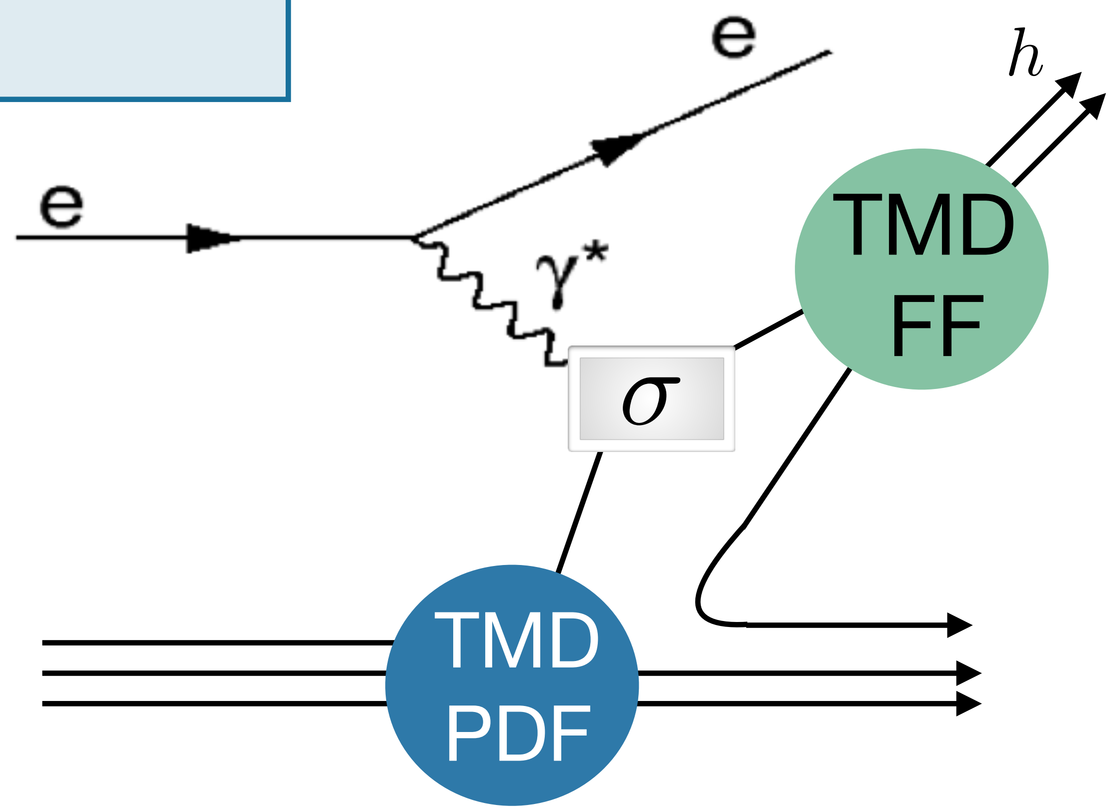

TMD PDFs and fragmentation functions (FFs)

Azimuthal amplitudes related to structure functions F_{XY} :

$$2\langle \sin(\phi + \phi_S)\rangle^h_{UT} = \epsilon\, F_{UT}^{\sin(\phi+\phi_S)}$$

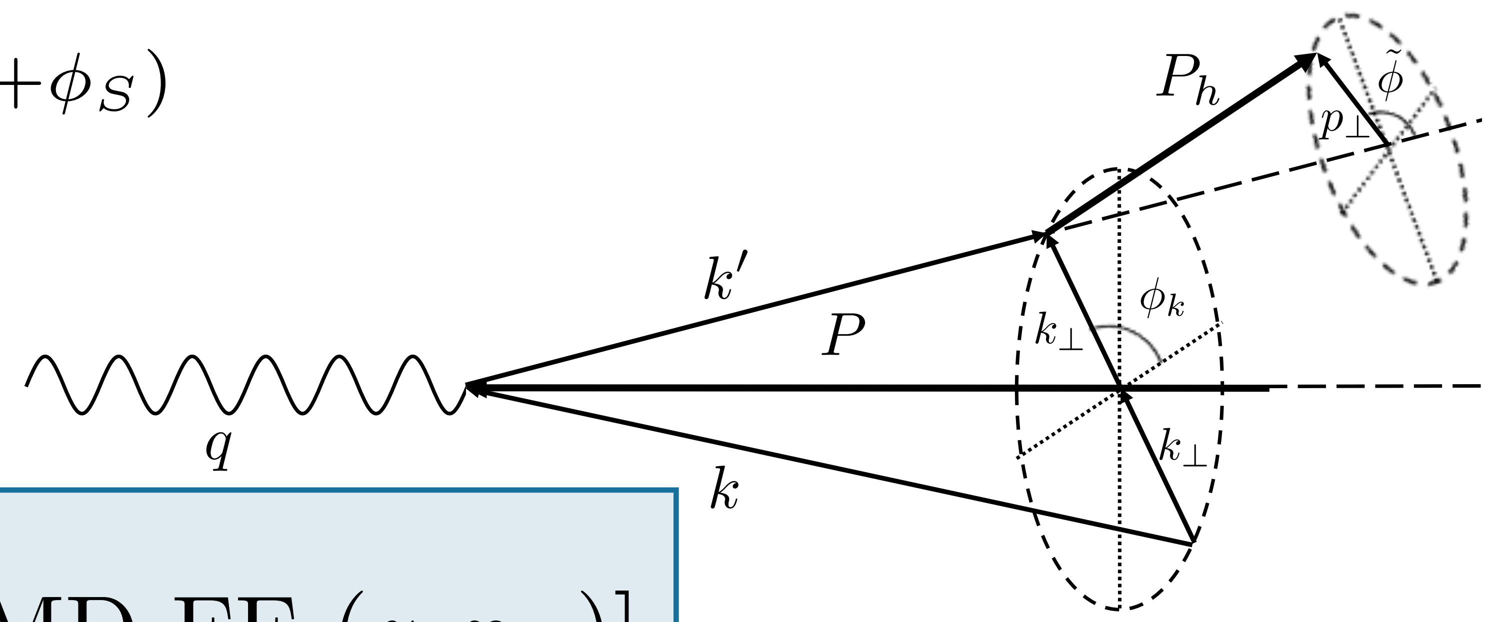

$$F_{XY} \propto \mathcal{C}\,[\mathrm{TMD\ PDF}(x, k_\perp) \times\ \mathrm{TMD\ FF}\ (z, p_\perp)]$$

$$z \overset{\mathrm{lab}}{=} \frac{E_h}{E_{\gamma *}}$$

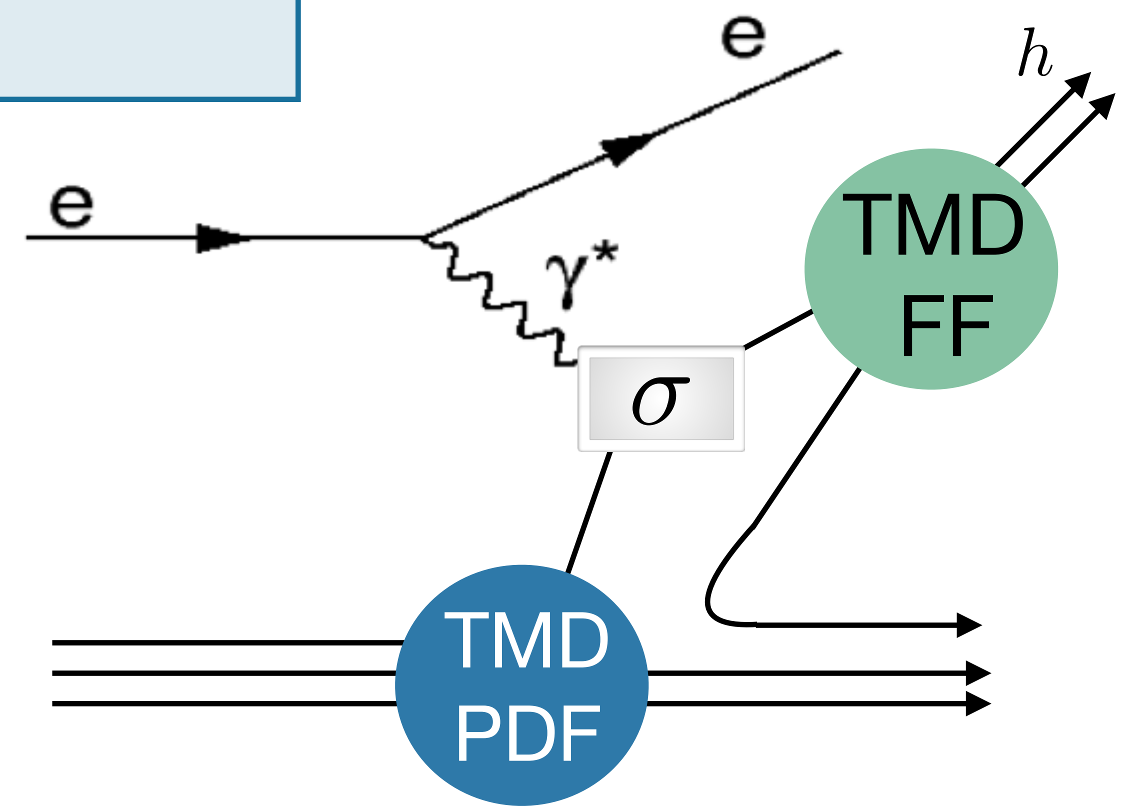

TMD PDFs and fragmentation functions (FFs)

Azimuthal amplitudes related to structure functions F_{XY} :

$$2\langle \sin(\phi + \phi_S)\rangle^h_{UT} = \epsilon \, F_{UT}^{\sin(\phi+\phi_S)}$$

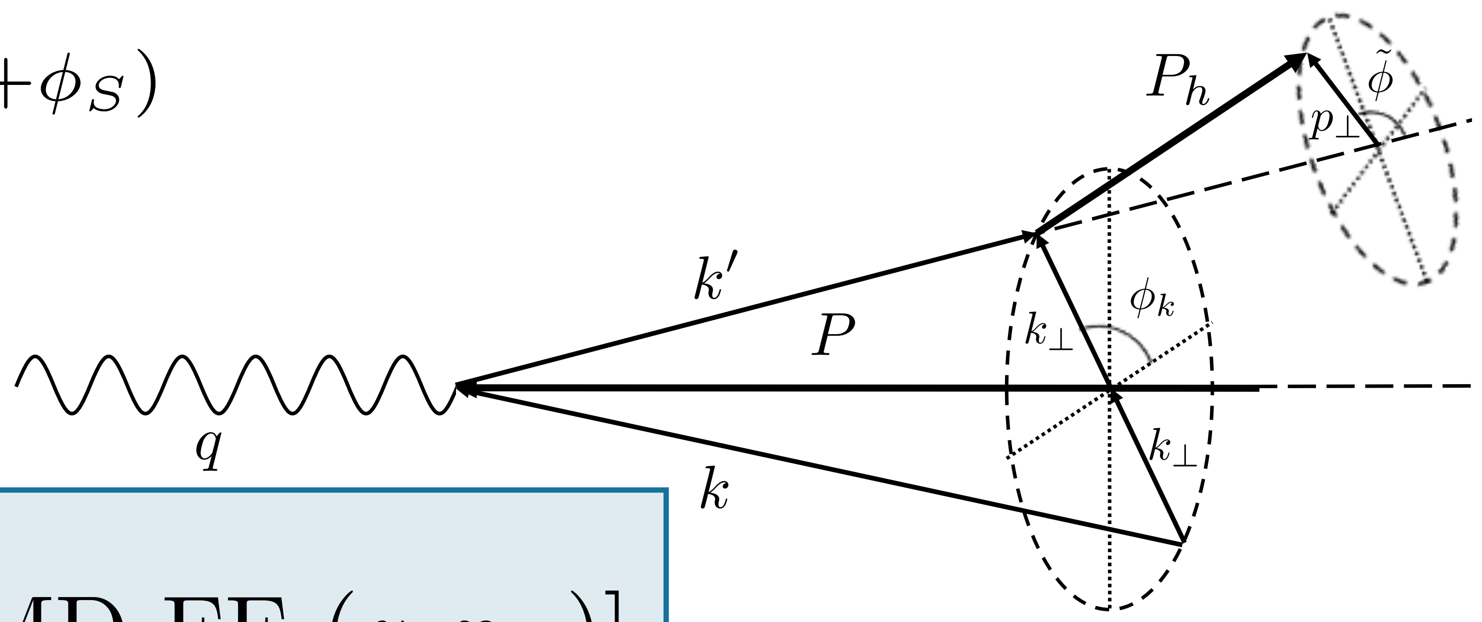

$$F_{XY} \propto \mathcal{C}\,[\text{TMD PDF}(x, k_\perp) \times \text{ TMD FF } (z, p_\perp)]$$

$$z \stackrel{\text{lab}}{=} \frac{E_h}{E_{\gamma *}}$$

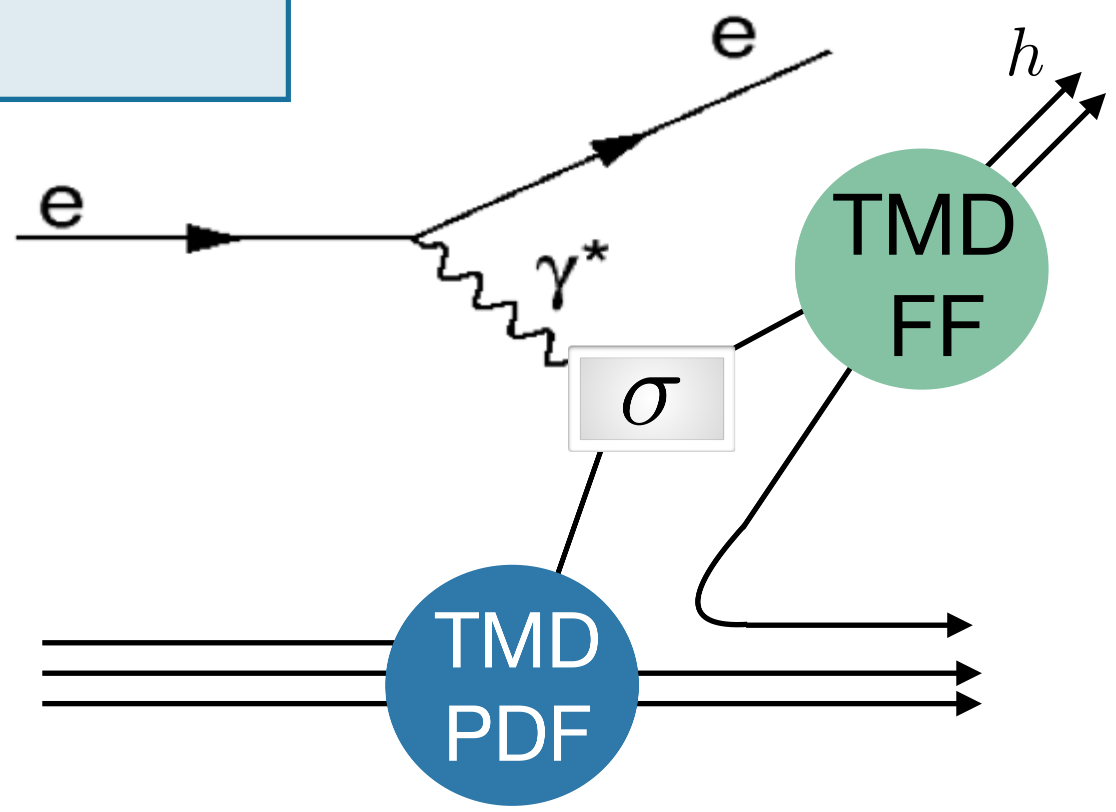

quark polarisation

nucleon polarisation

	U	L	T
U	f_1		$h_1^\perp$
L		g_{1L}	$h_{1L}^\perp$
T	$f_{1T}^\perp$	$g_{1T}^\perp$	$h_{1T}\, h_{1T}^\perp$

TMD PDFs and fragmentation functions (FFs)

Azimuthal amplitudes related to structure functions F_{XY} :

$$2\langle \sin(\phi + \phi_S) \rangle_{UT}^{h} = \epsilon \, F_{UT}^{\sin(\phi+\phi_S)}$$

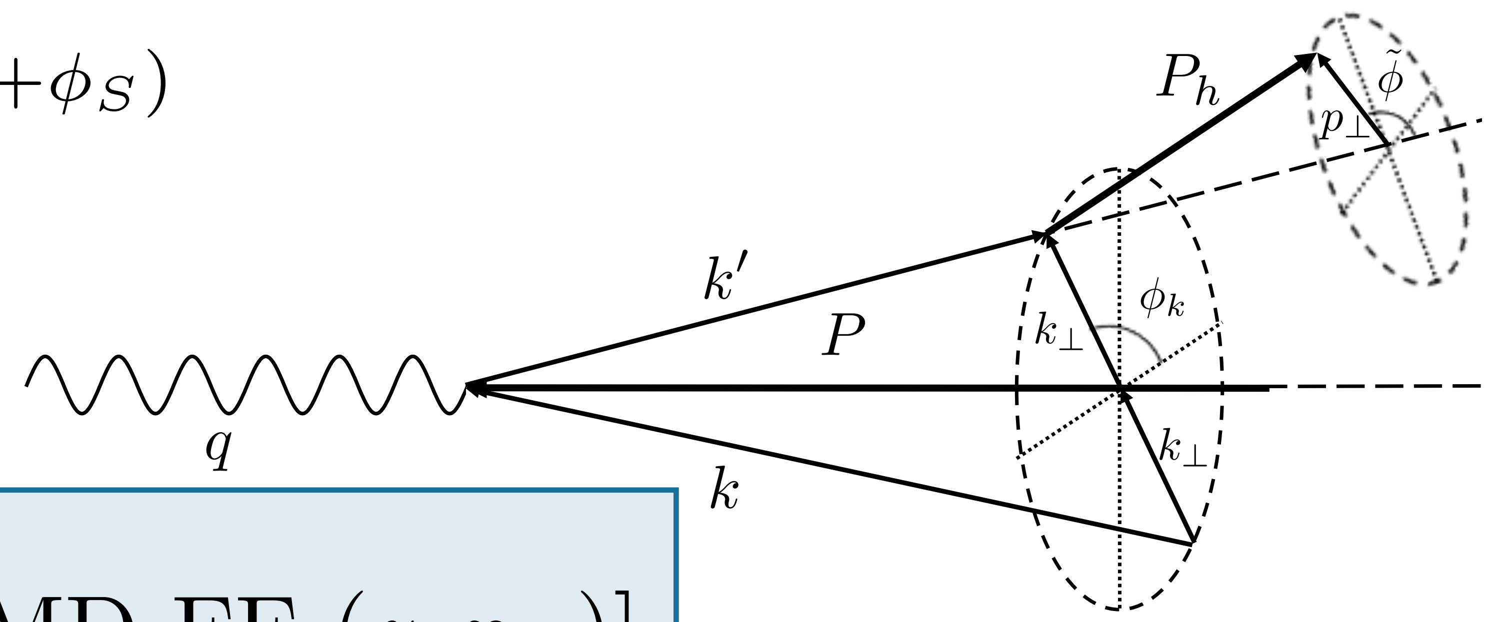

$$F_{XY} \propto \mathcal{C}\,[\text{TMD PDF}(x, k_\perp) \times \; \text{TMD FF } (z, p_\perp)]$$

$$z \overset{\text{lab}}{=} \frac{E_h}{E_{\gamma *}}$$

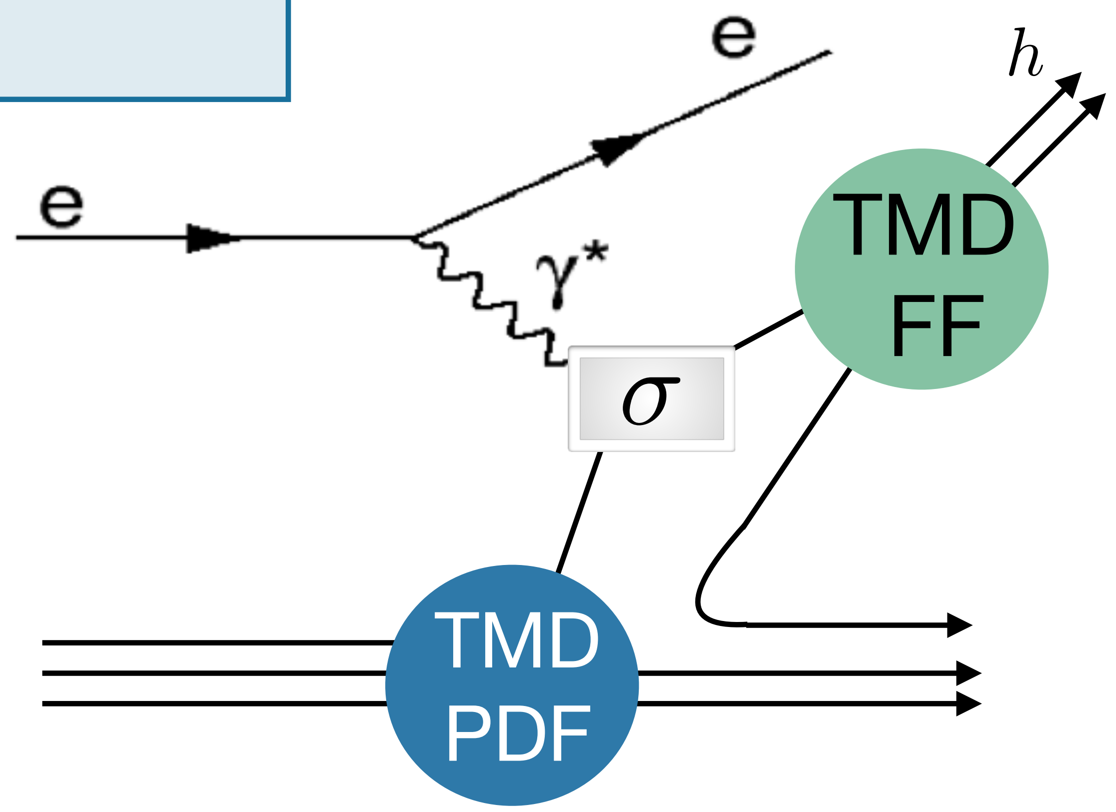

quark polarisation (columns) / nucleon polarisation (rows)

	U	L	T
U	f_1		$h_1^\perp$
L		g_{1L}	$h_{1L}^\perp$
T	$f_{1T}^\perp$	$g_{1T}^\perp$	$h_{1T}\, h_{1T}^\perp$

quark polarisation (columns) / hadron polarisation (rows)

	U	L	T
U	D_1		$H_1^\perp$

TMD PDFs and fragmentation functions (FFs)

Azimuthal amplitudes related to structure functions F_{XY} :

$$2\langle \sin(\phi+\phi_S)\rangle^h_{UT} = \epsilon\, F_{UT}^{\sin(\phi+\phi_S)}$$

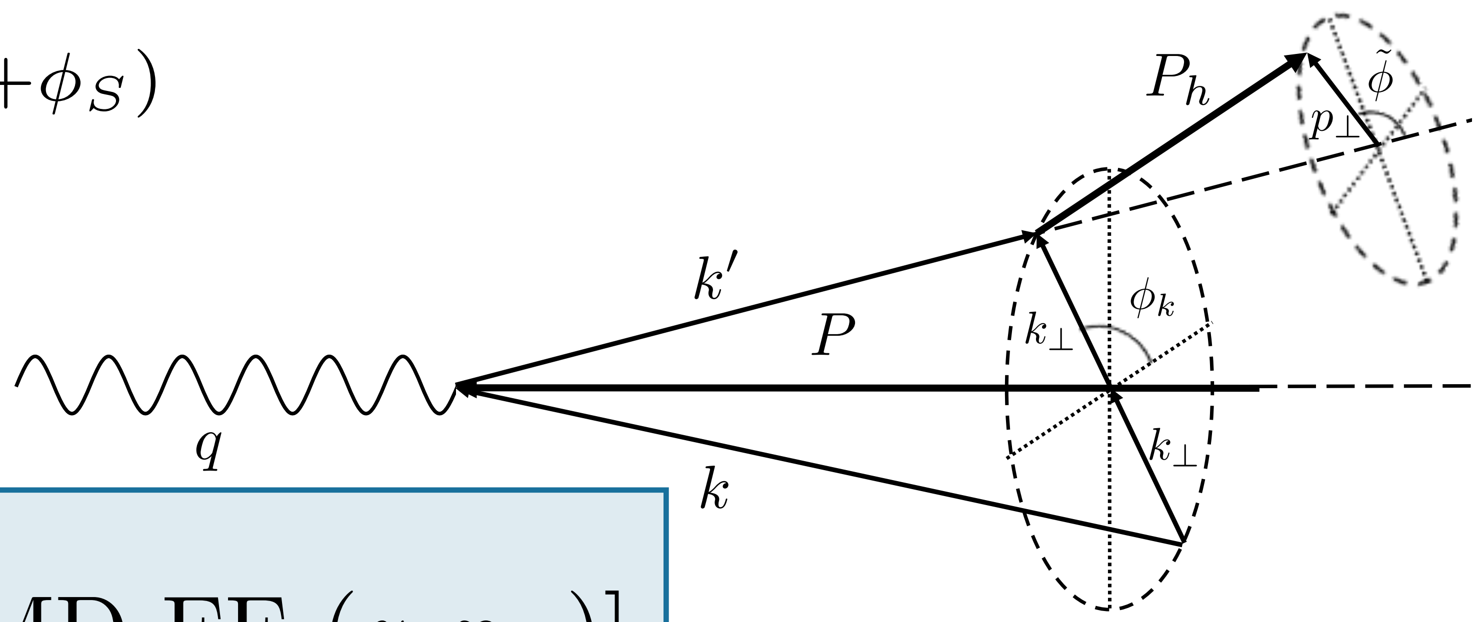

$$F_{XY} \propto \mathcal{C}\,[\text{TMD PDF}(x,k_\perp) \times \ \text{TMD FF}\ (z,p_\perp)]$$

$$z \stackrel{\text{lab}}{=} \frac{E_h}{E_{\gamma*}}$$

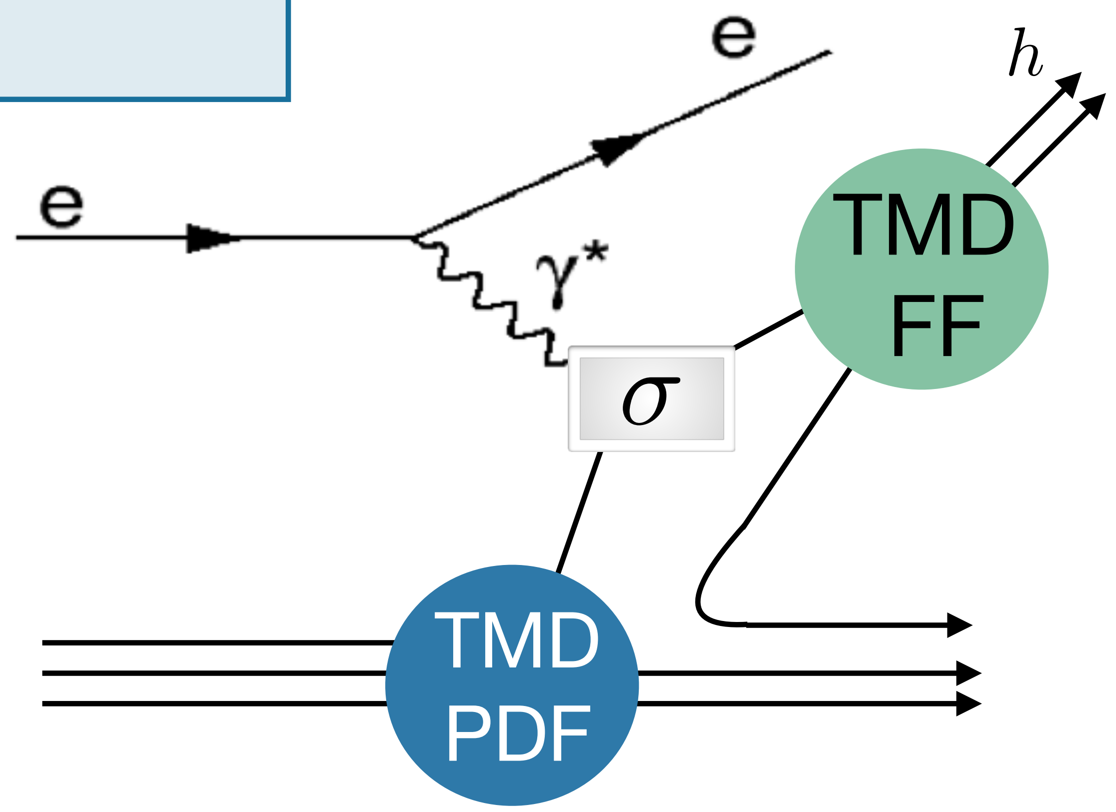

quark polarisation (columns) / nucleon polarisation (rows)

	U	L	T
U	f_1		$h_1^\perp$
L		g_{1L}	$h_{1L}^\perp$
T	$f_{1T}^\perp$	$g_{1T}^\perp$	$h_{1T}\, h_{1T}^\perp$

quark polarisation (columns) / hadron polarisation (rows)

	U	L	T
U	D_1		$H_1^\perp$

Chiral odd

TMD PDFs and fragmentation functions (FFs)

Azimuthal amplitudes related to structure functions F_{XY} :

$$2\langle\sin(\phi+\phi_S)\rangle^h_{UT} = \epsilon\, F_{UT}^{\sin(\phi+\phi_S)}$$

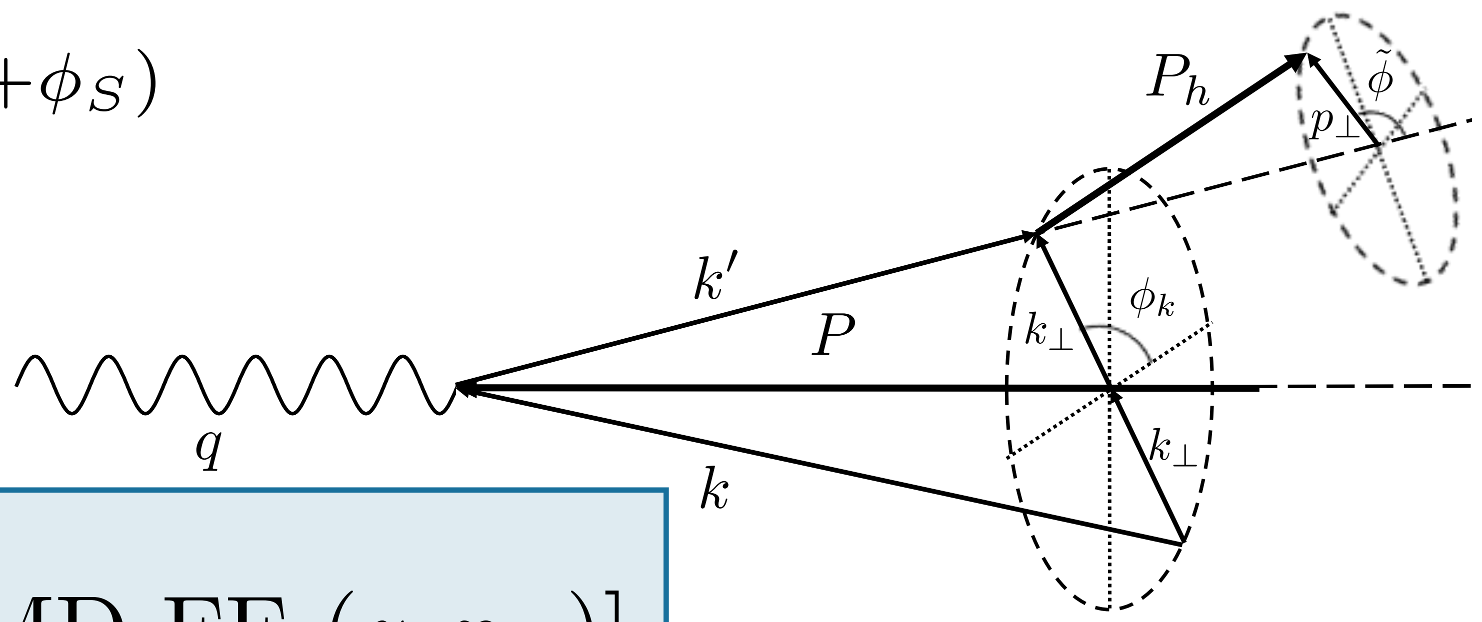

$$F_{XY} \propto \mathcal{C}\,[\text{TMD PDF}(x,k_\perp)\times\ \text{TMD FF}\ (z,p_\perp)]$$

$$z \overset{\text{lab}}{=} \frac{E_h}{E_{\gamma *}}$$

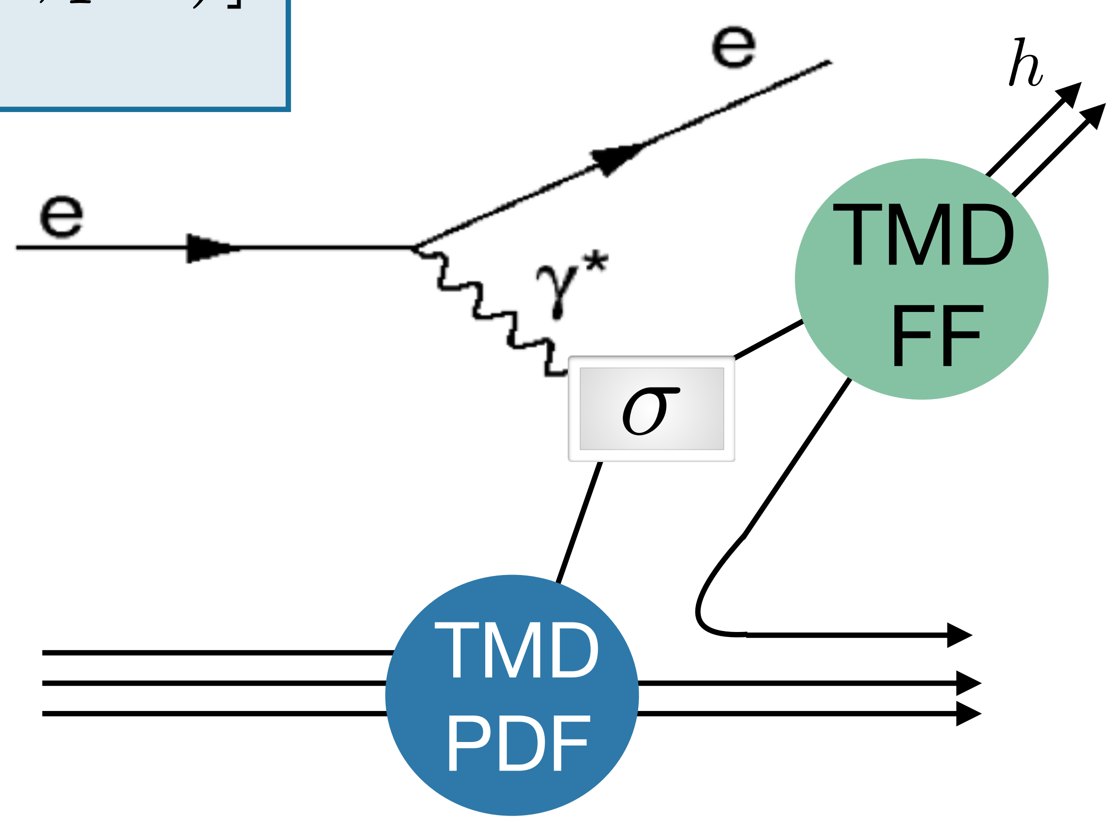

quark polarisation (columns) / nucleon polarisation (rows)

	U	L	T
U	f_1		$h_1^\perp$
L		g_{1L}	$h_{1L}^\perp$
T	$f_{1T}^\perp$	$g_{1T}^\perp$	$h_{1T}\, h_{1T}^\perp$

quark polarisation (columns) / hadron polarisation (rows)

	U	L	T
U	D_1		$H_1^\perp$

Chiral odd

Naive T-odd

TMD PDFs and fragmentation functions (FFs)

Azimuthal amplitudes related to structure functions F_{XY} :

$$2\langle \sin(\phi + \phi_S)\rangle^h_{UT} = \epsilon\, F^{\sin(\phi+\phi_S)}_{UT}$$

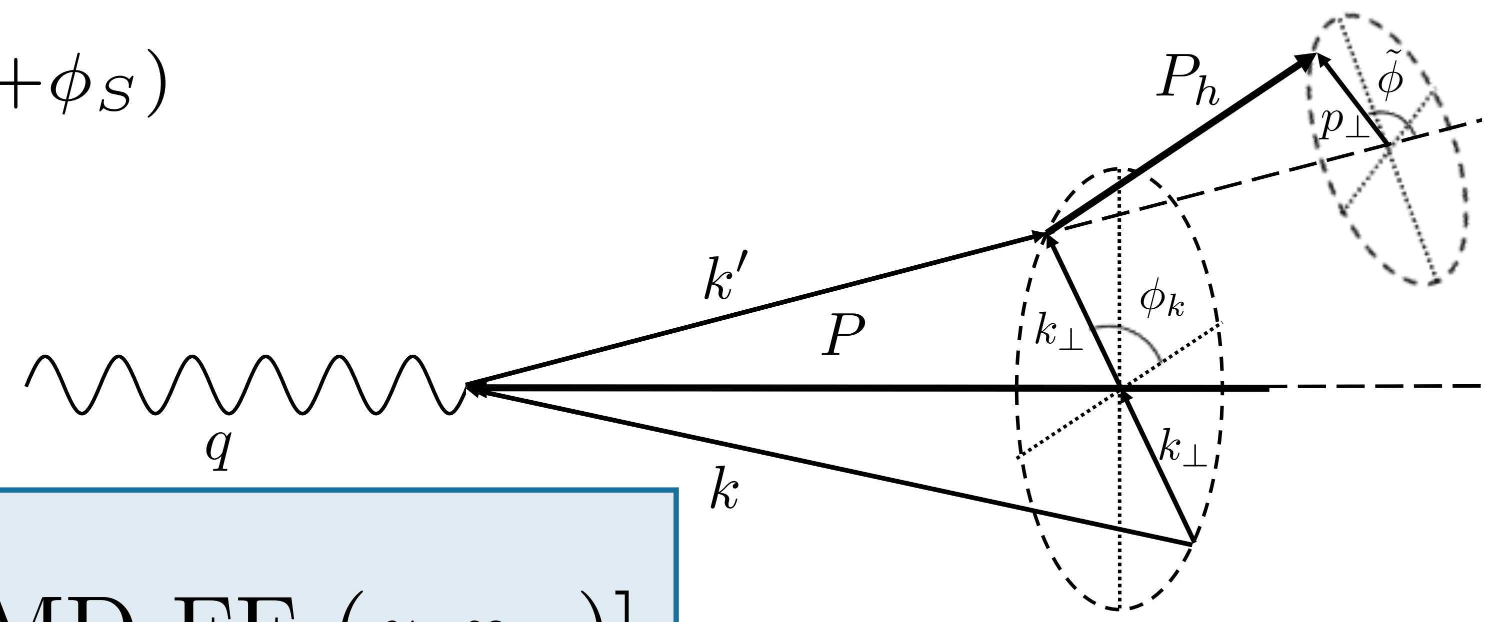

$$F_{XY} \propto \mathcal{C}\,[\text{TMD PDF}(x, k_\perp) \times \ \text{TMD FF}\ (z, p_\perp)]$$

$$z \stackrel{\text{lab}}{=} \frac{E_h}{E_{\gamma *}}$$

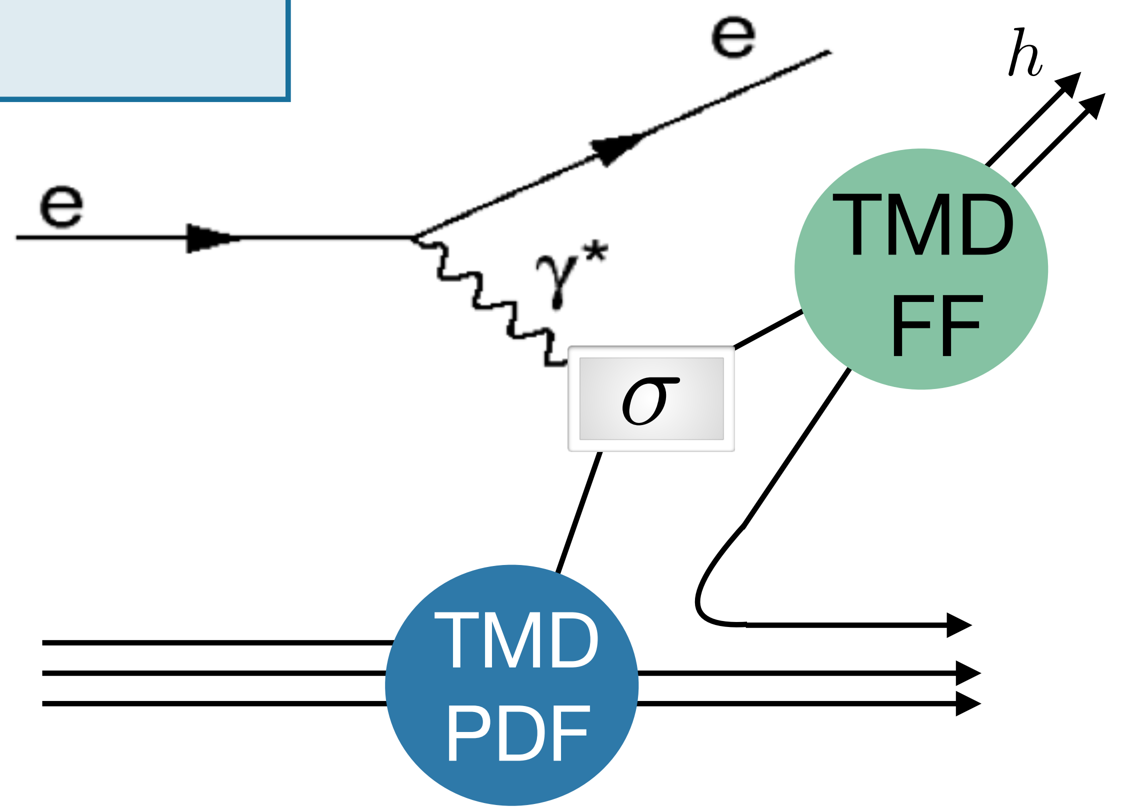

quark polarisation (columns) / nucleon polarisation (rows)

	U	L	T
U	f_1		$h_1^\perp$
L		g_{1L}	$h_{1L}^\perp$
T	$f_{1T}^\perp$	$g_{1T}^\perp$	$h_{1T}\, h_{1T}^\perp$

quark polarisation (columns) / hadron polarisation (rows)

	U	L	T
U	D_1		$H_1^\perp$

Chiral odd

Naive T-odd

TMD PDFs and fragmentation functions (FFs)

Azimuthal amplitudes related to structure functions F_{XY} :

$$2\langle \sin(\phi + \phi_S)\rangle^h_{UT} = \epsilon\, F^{\sin(\phi+\phi_S)}_{UT}$$

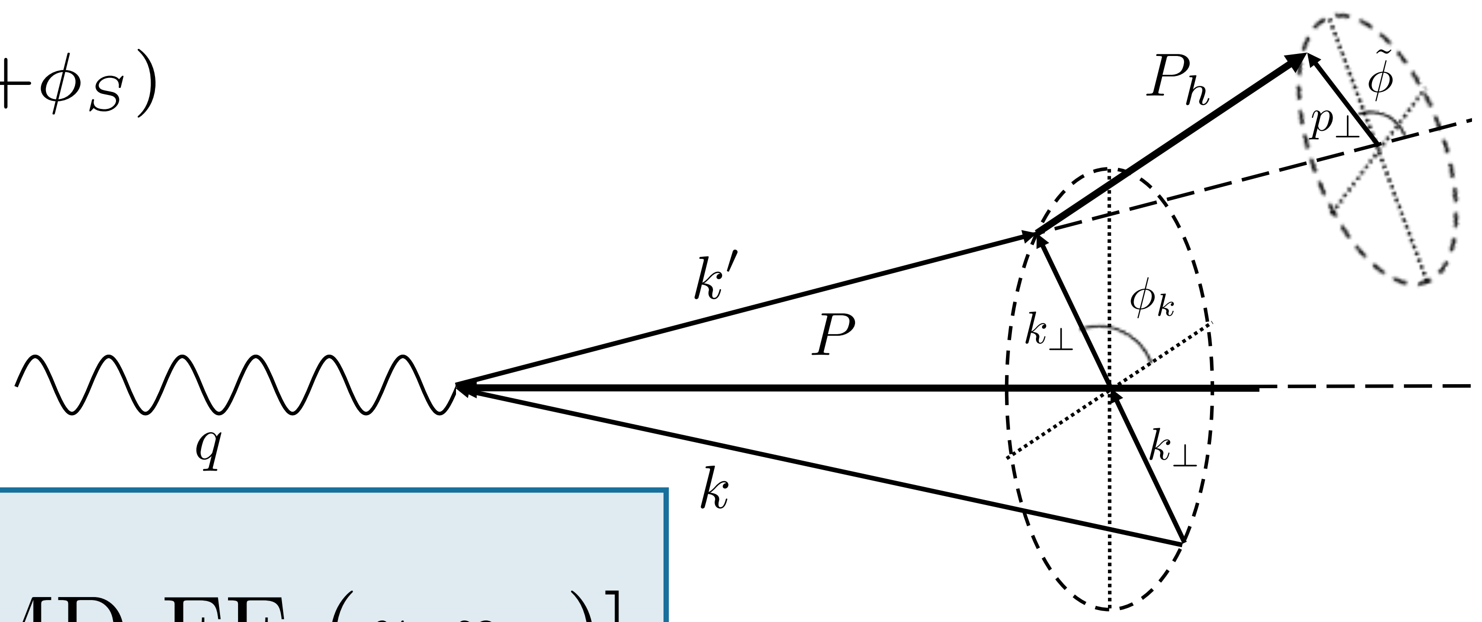

$$F_{XY} \propto \mathcal{C}\,[\text{TMD PDF}(x, k_\perp) \times \text{ TMD FF } (z, p_\perp)]$$

$$z \overset{\text{lab}}{=} \frac{E_h}{E_{\gamma *}}$$

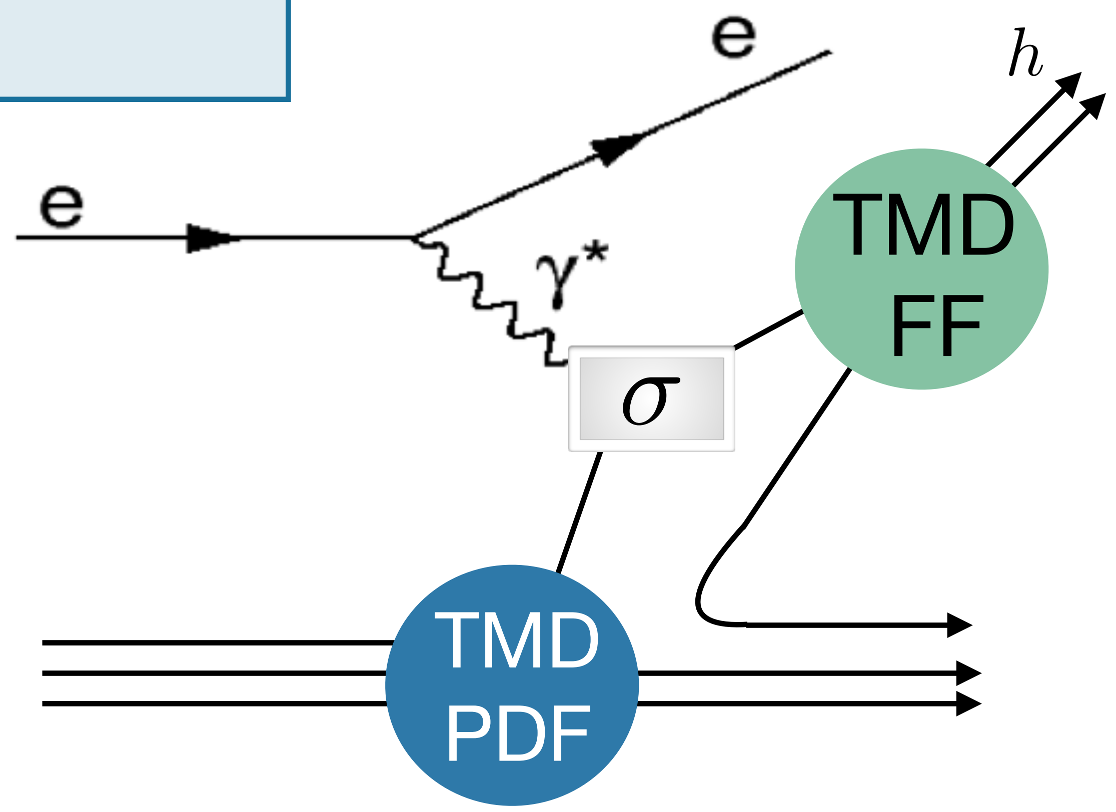

quark polarisation (columns) / nucleon polarisation (rows)

	U	L	T
U	f_1		$h_1^\perp$
L		g_{1L}	$h_{1L}^\perp$
T	$f_{1T}^\perp$	$g_{1T}^\perp$	$h_{1T}\, h_{1T}^\perp$

quark polarisation (columns) / hadron polarisation (rows)

	U	L	T
U	D_1		$H_1^\perp$

Chiral odd

Naive T-odd

Transverse momentum dependent fragmentation functions

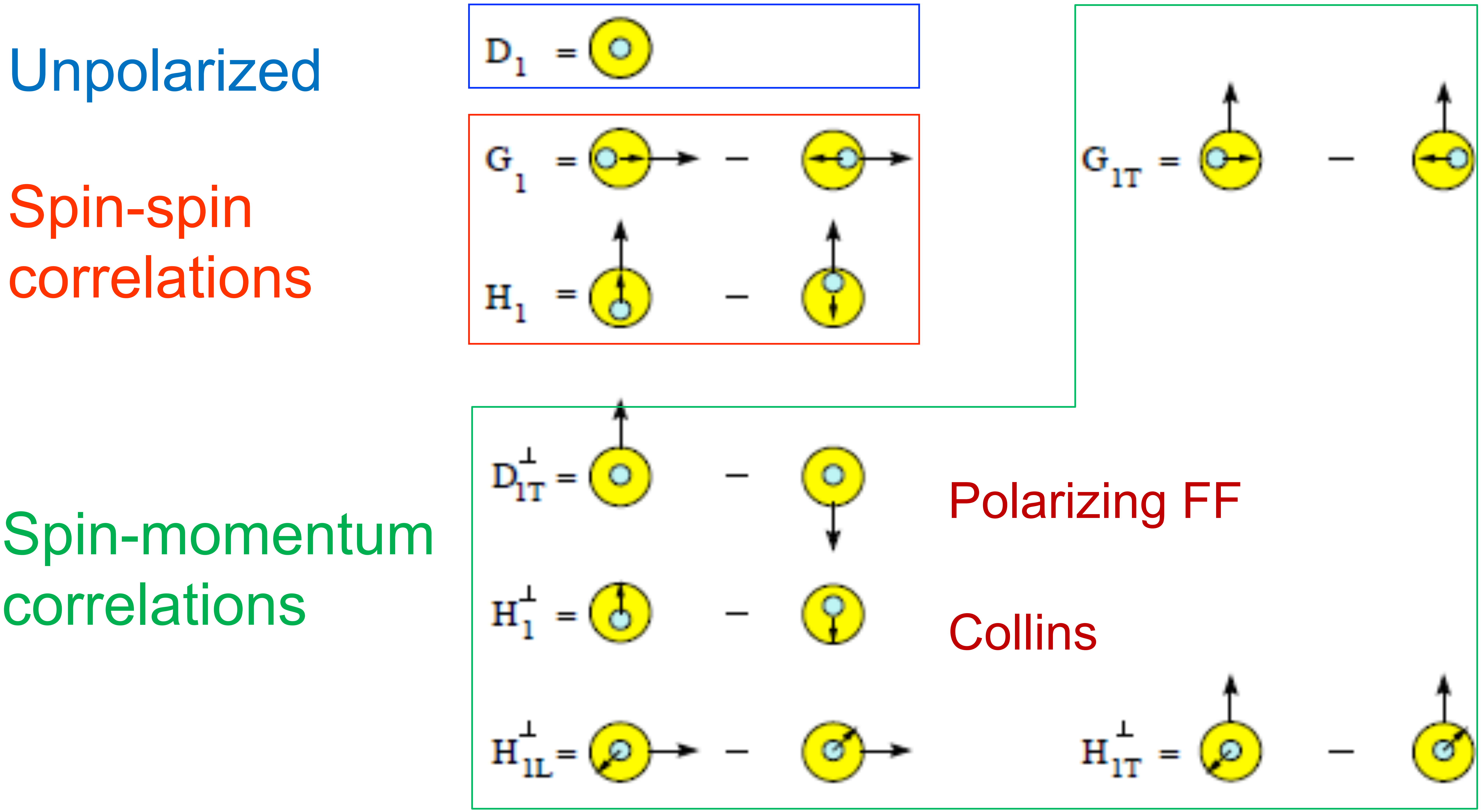

Fragmentation functions (FFs)

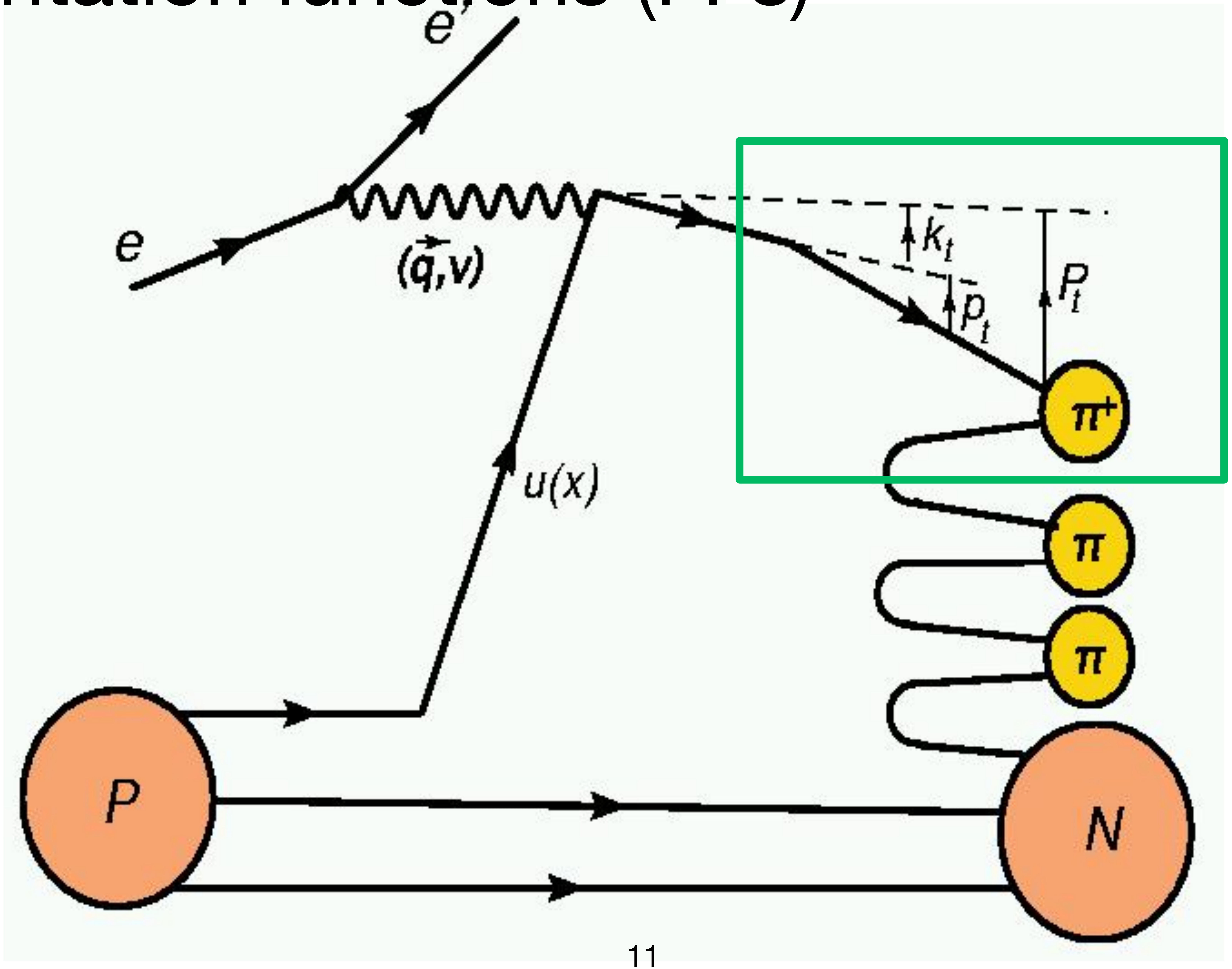

Fragmentation functions

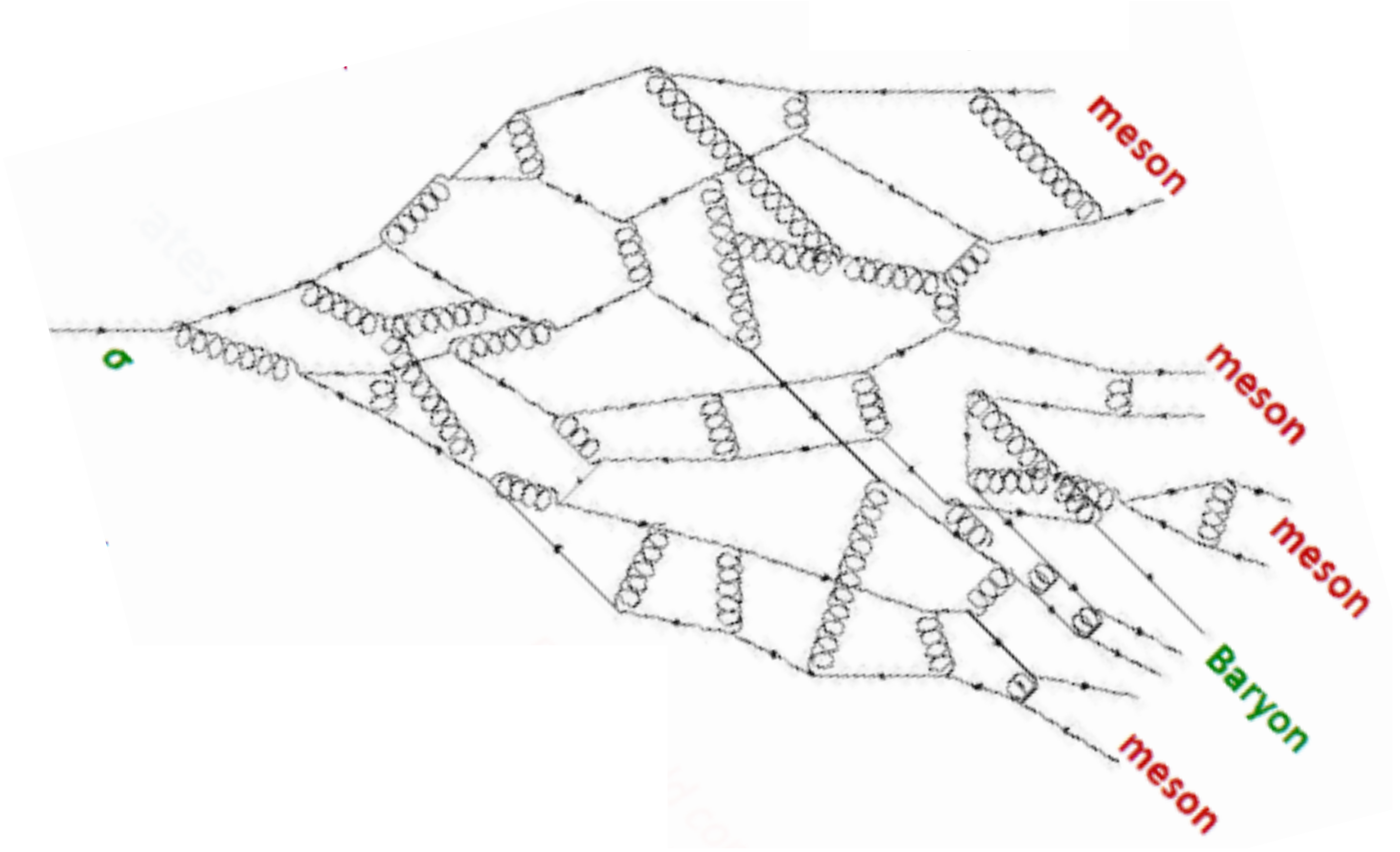

Factorisation and universality

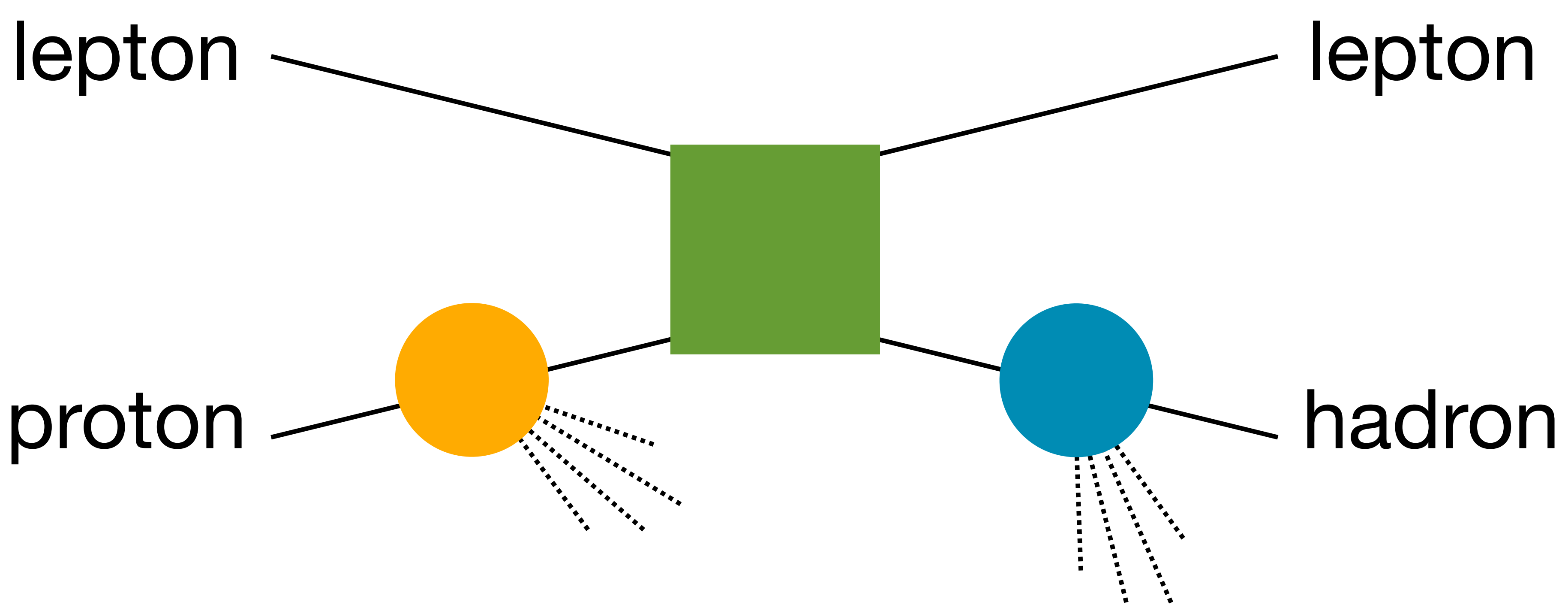

semi-inclusive DIS

Adapted from A. Bacchetta

Factorisation and universality

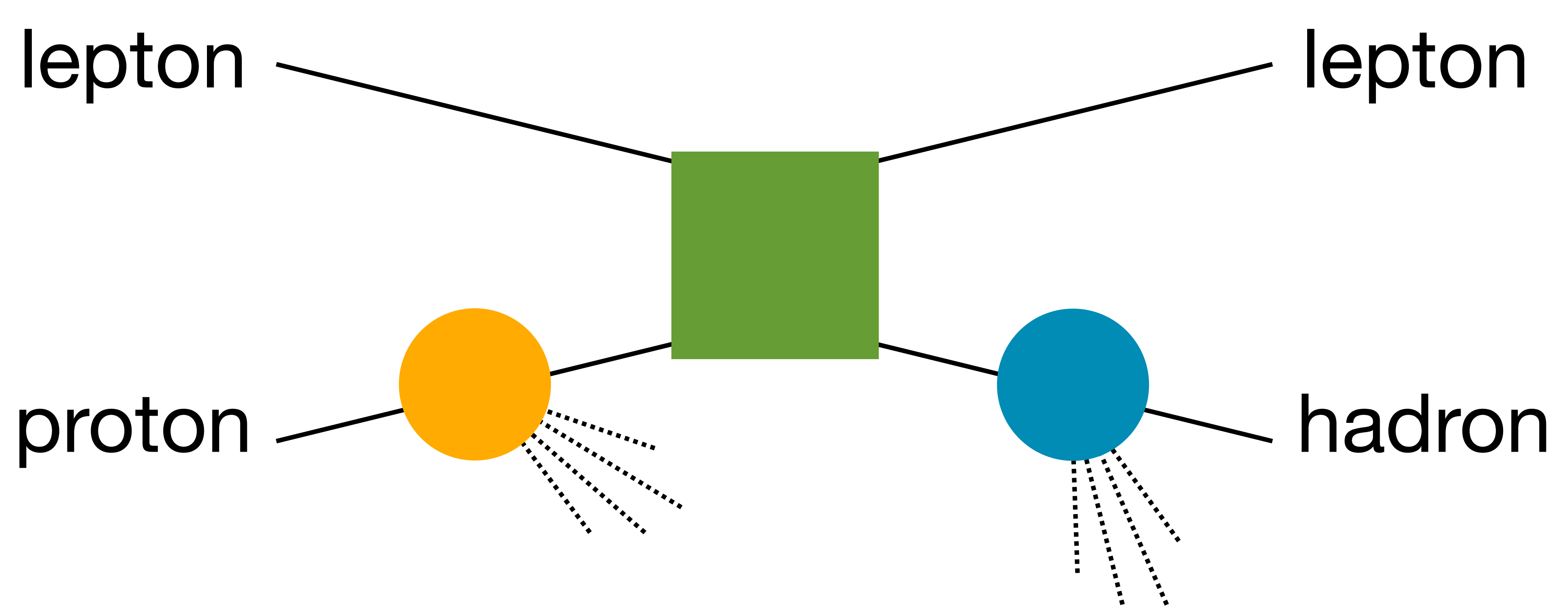

semi-inclusive DIS

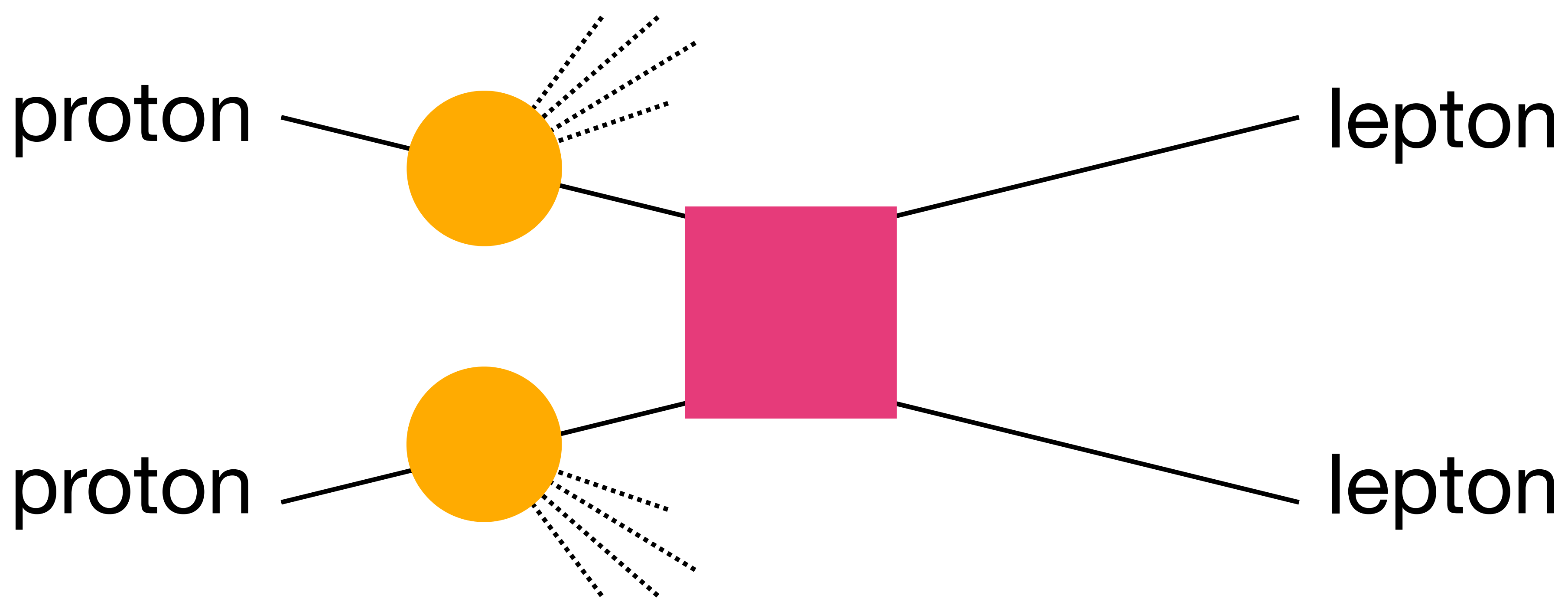

Drell-Yan

Adapted from A. Bacchetta

Factorisation and universality

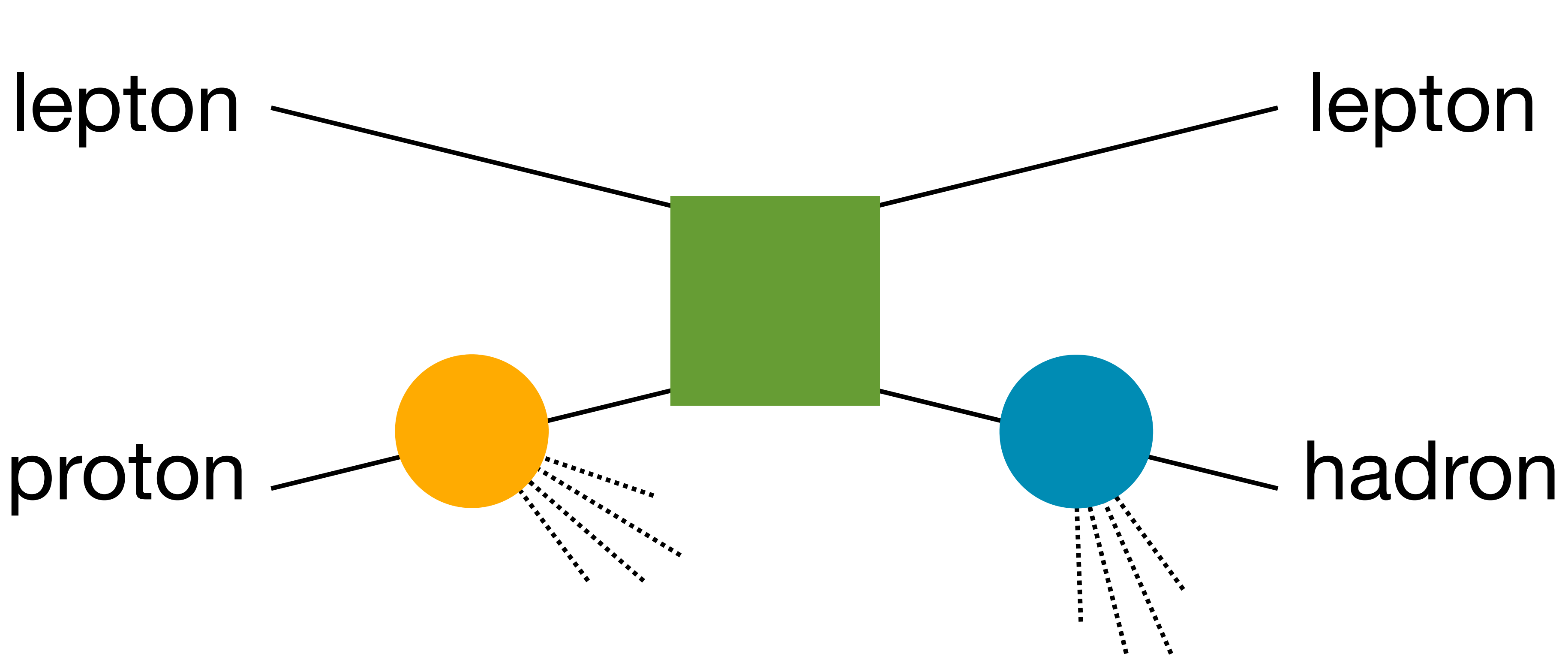

semi-inclusive DIS

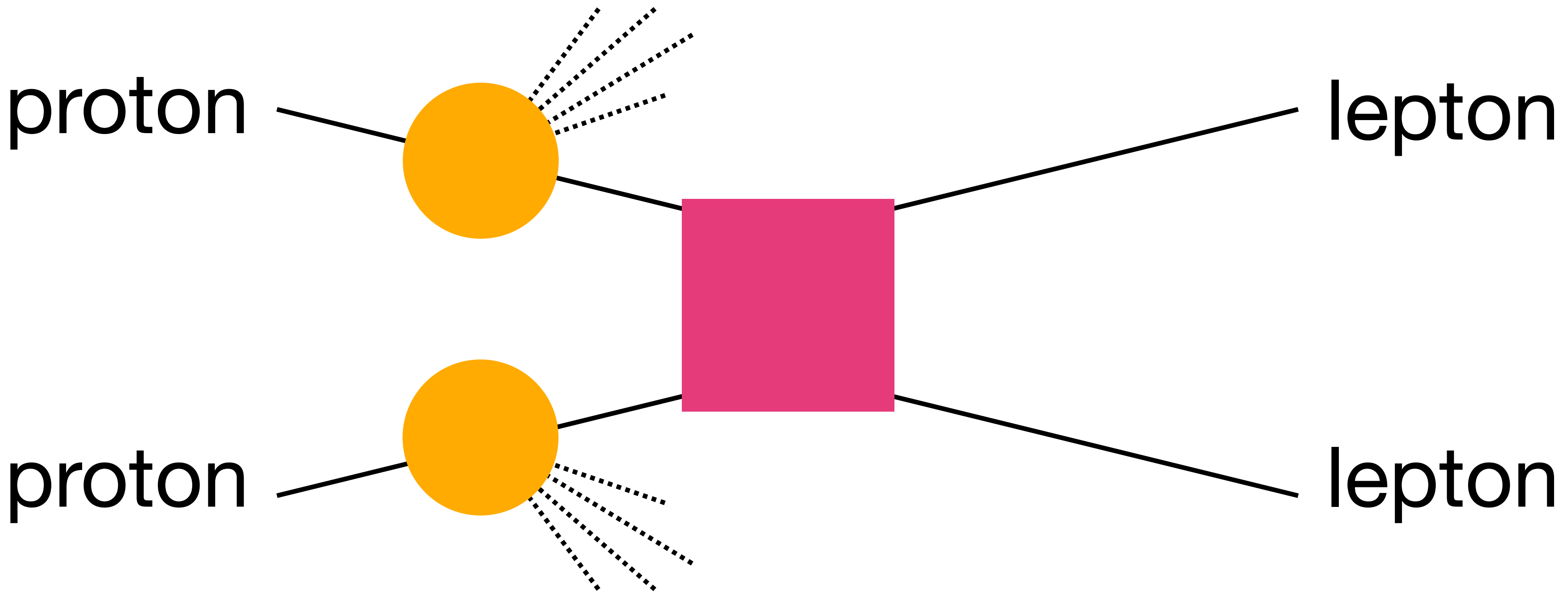

Drell-Yan

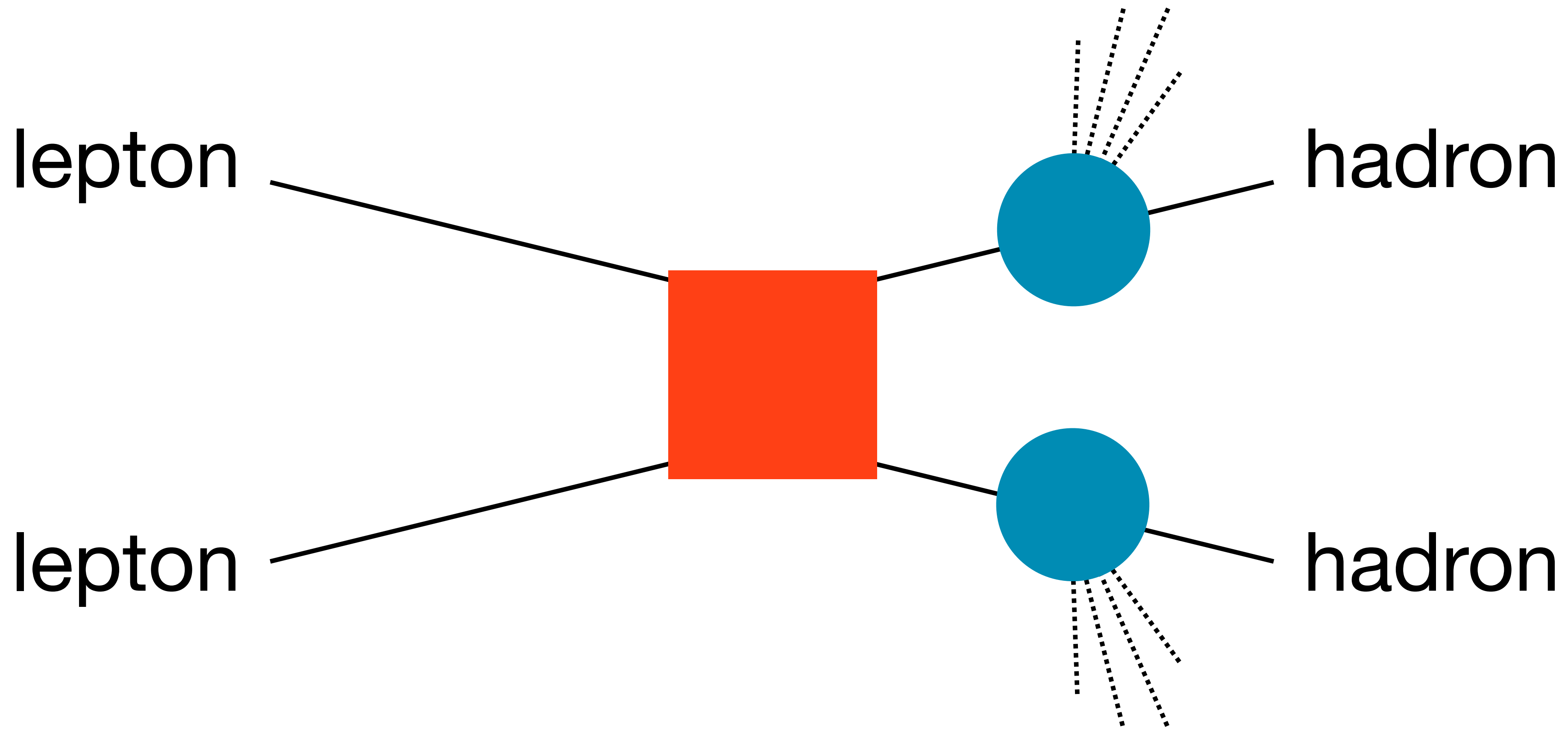

e^+e^- annihilation

Adapted from A. Bacchetta

Factorisation and universality

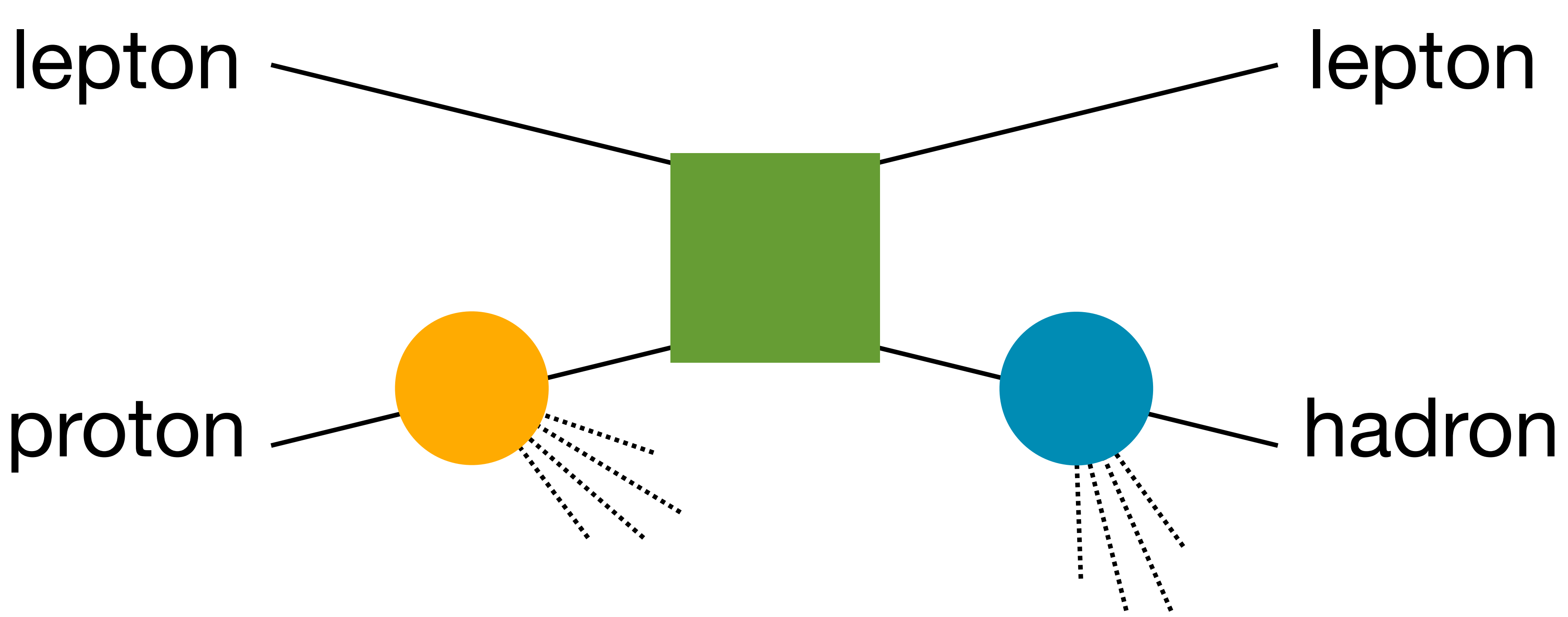

semi-inclusive DIS

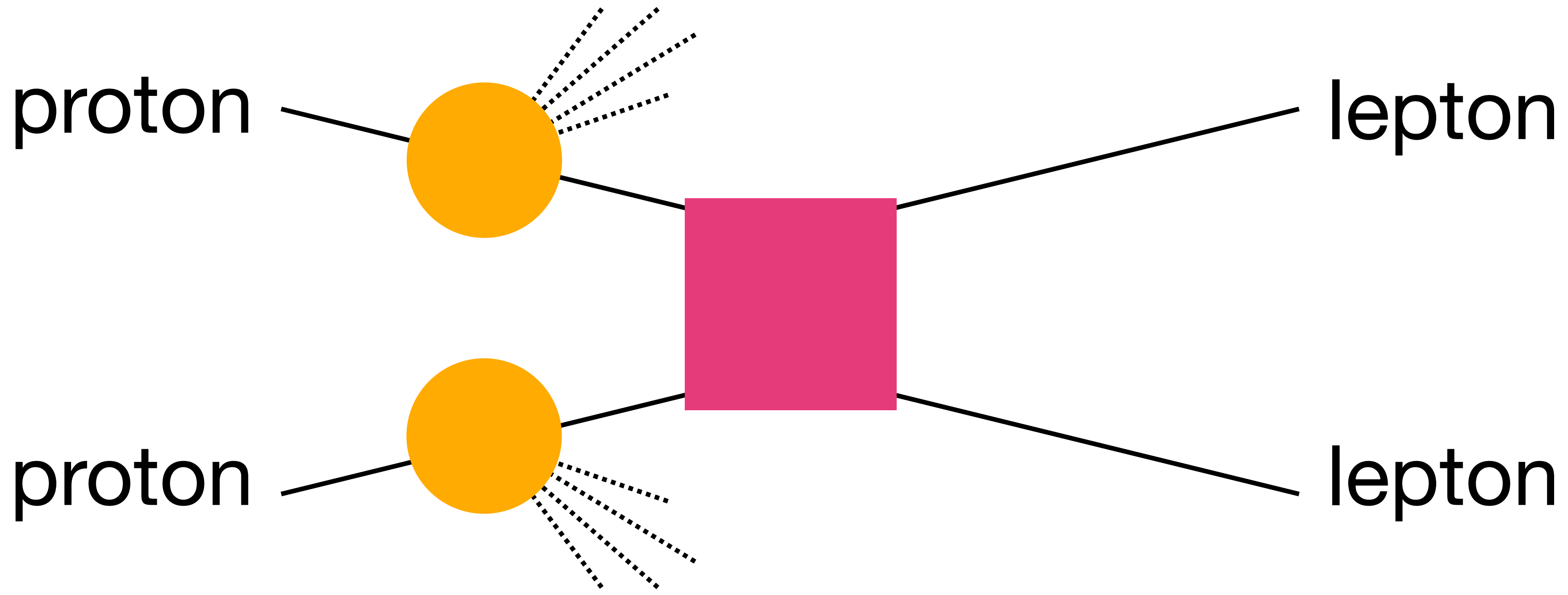

Drell-Yan

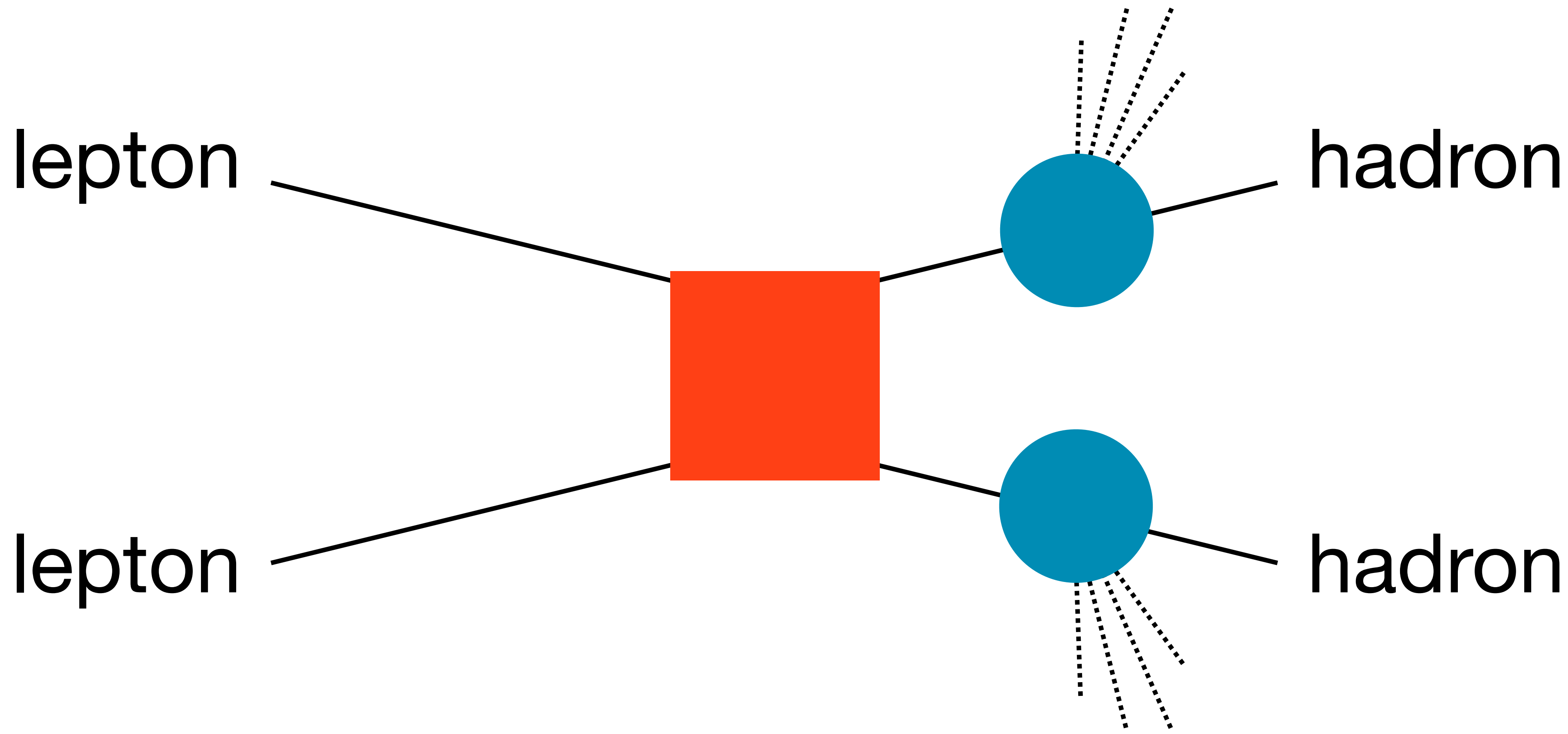

e^+e^- annihilation

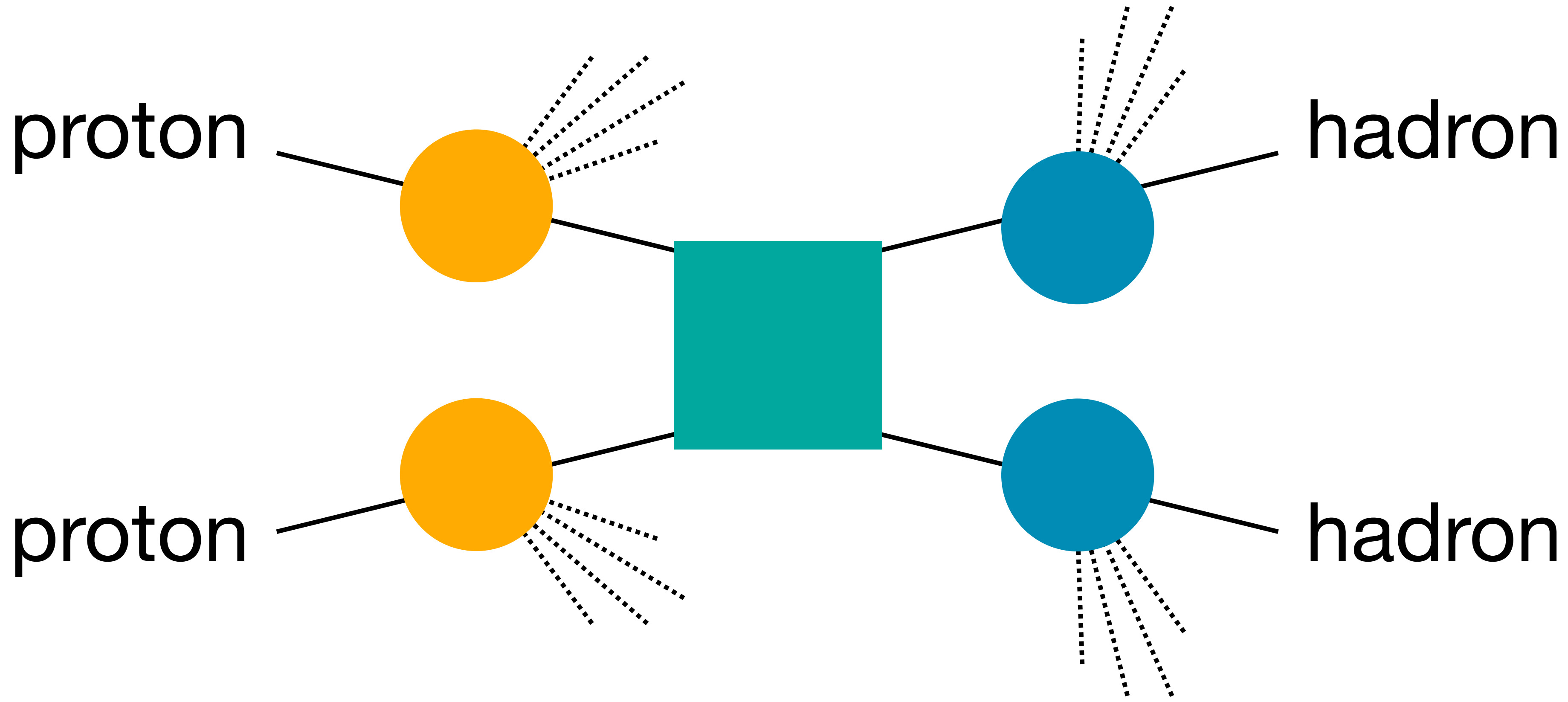

inclusive hadron production in pp collisions

Adapted from A. Bacchetta

Factorisation and universality

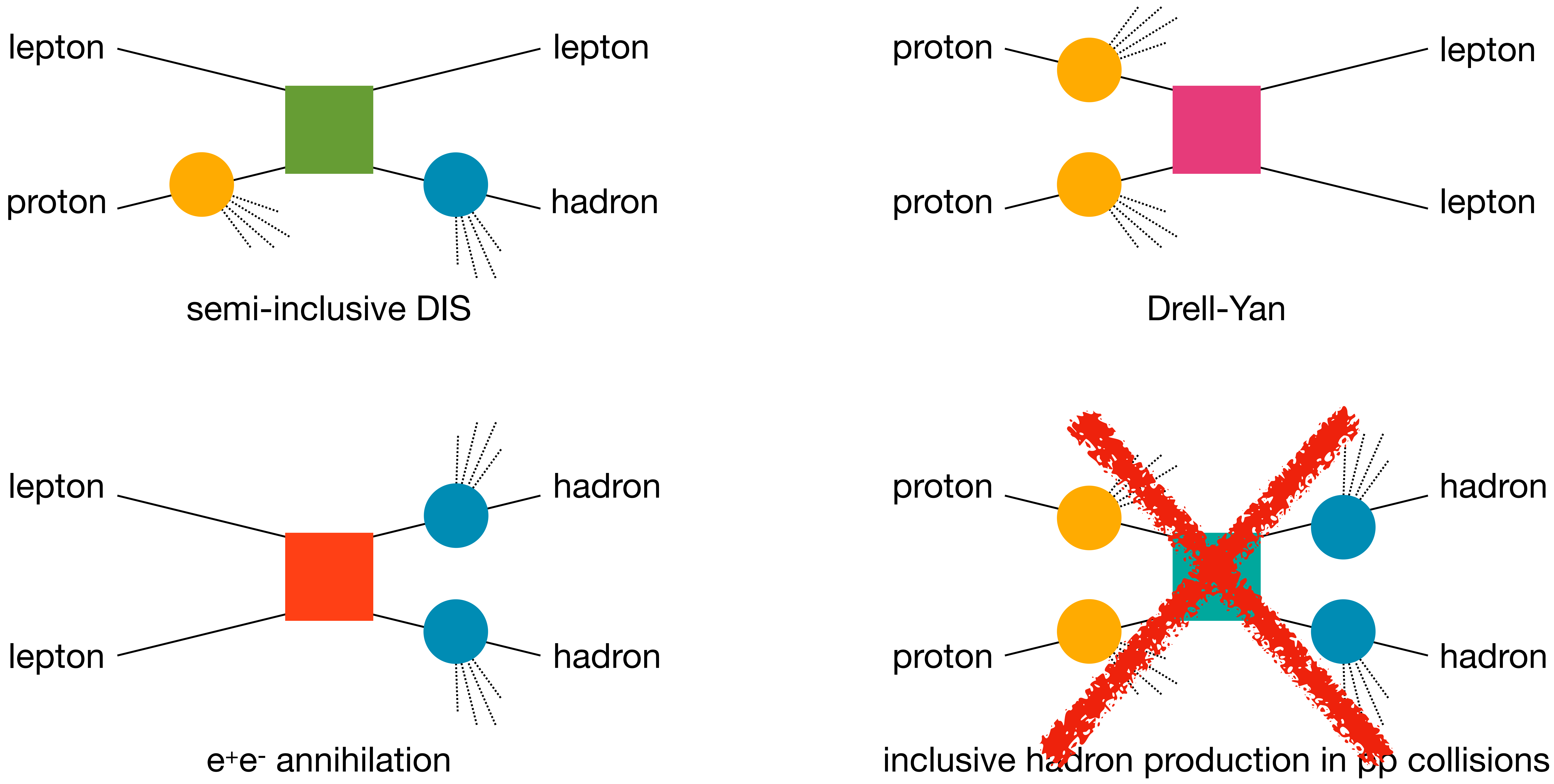

Adapted from A. Bacchetta

Validity of TMD description

2 characteristic scales:
small P_{hT} and large Q^2

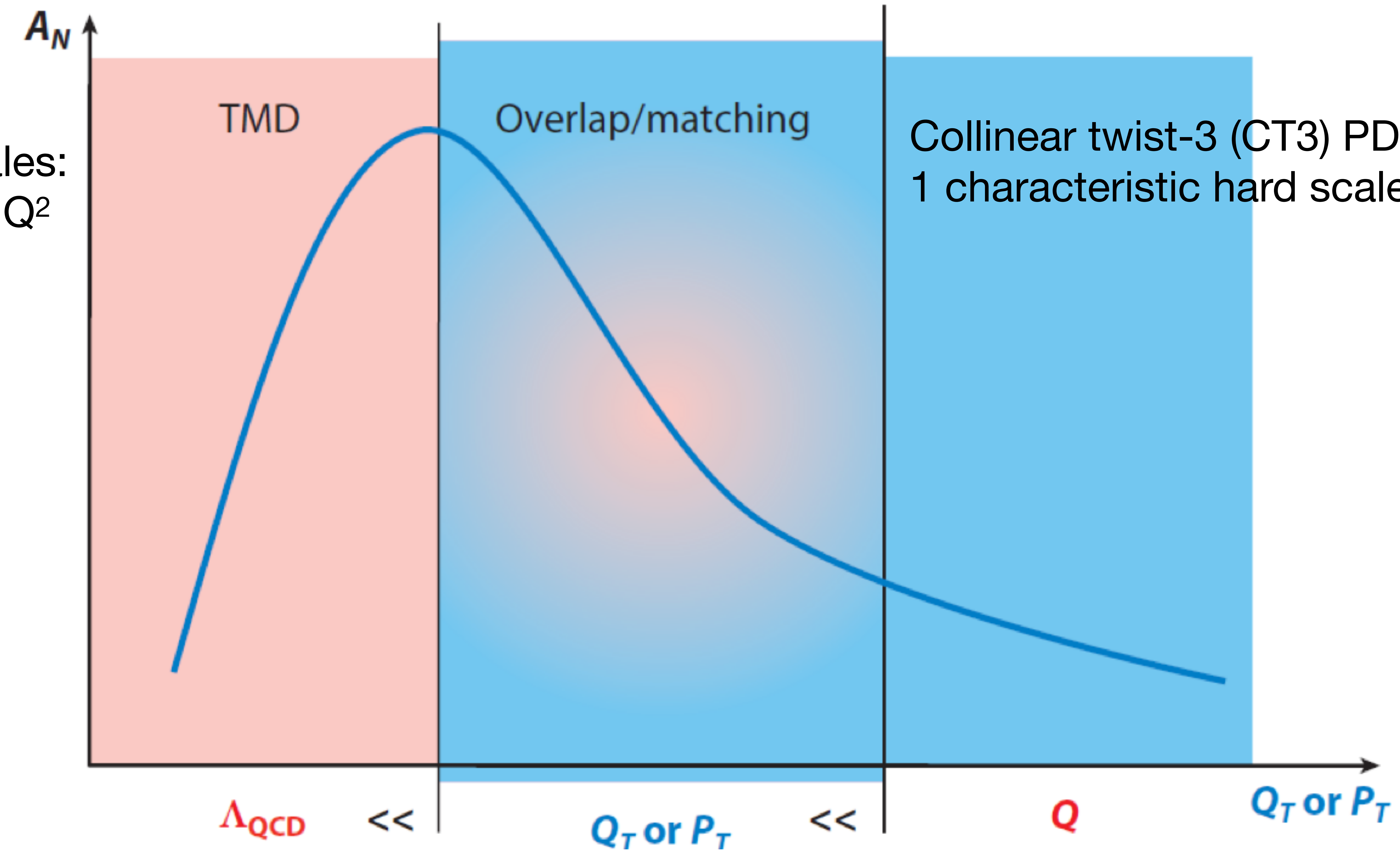

Collinear twist-3 (CT3) PDFs.
1 characteristic hard scale, e.g., P_{hT}

Consistent results for TMD and CT3 in overlap region

Experiments investigating TMD PDFs and TMD FFs

Spin-independent TMD PDFs: global analysis

Spin-independent TMD PDFs: global analysis

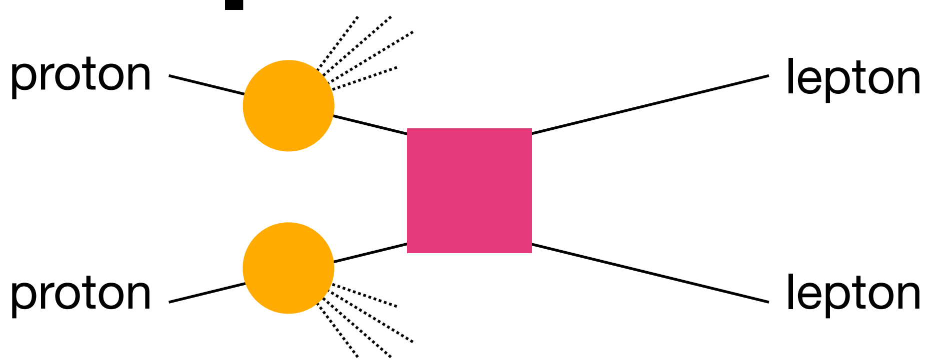

Spin-independent TMD PDFs: global analysis

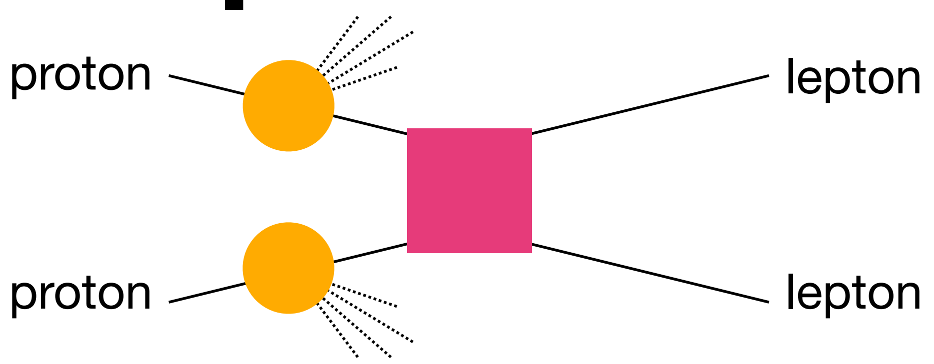

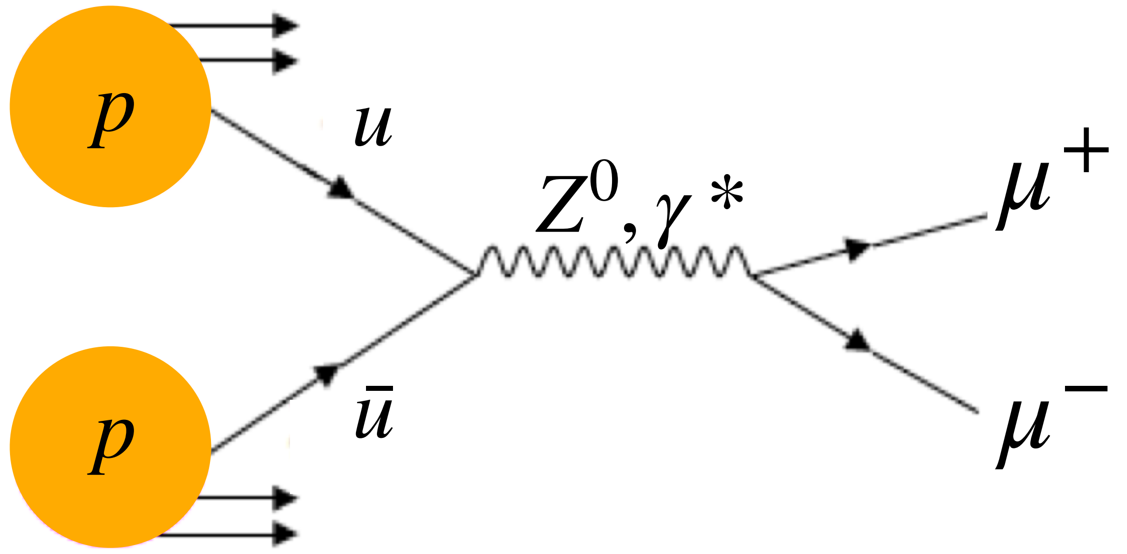

Spin-independent TMD PDFs: global analysis

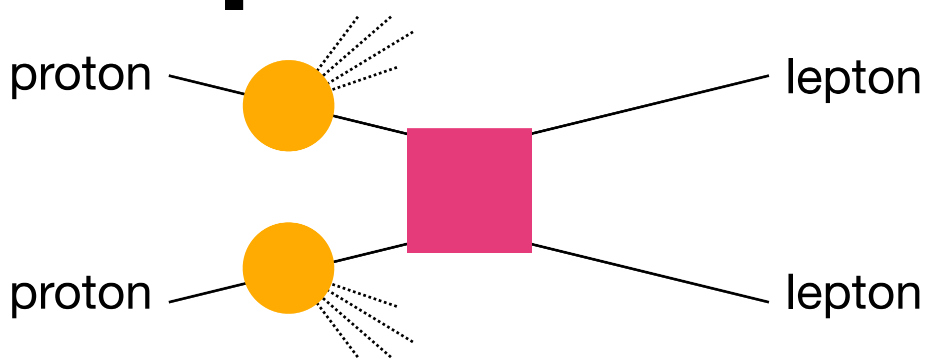

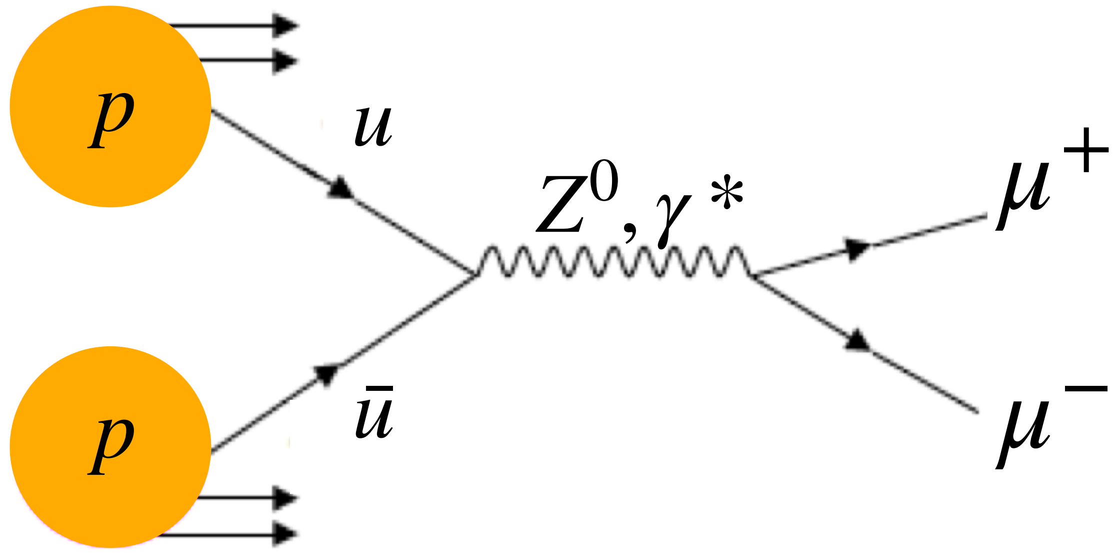

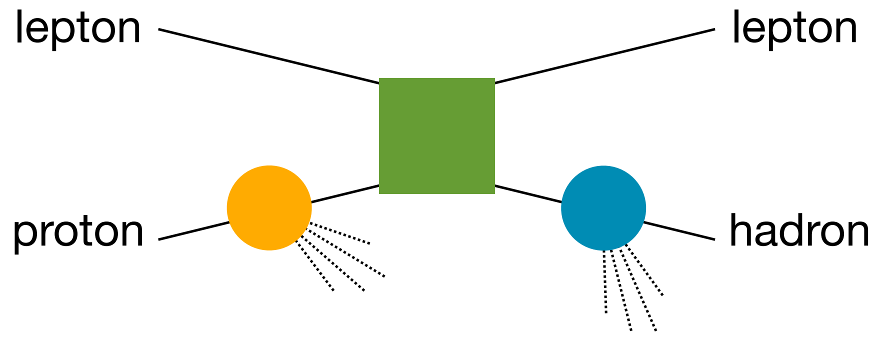

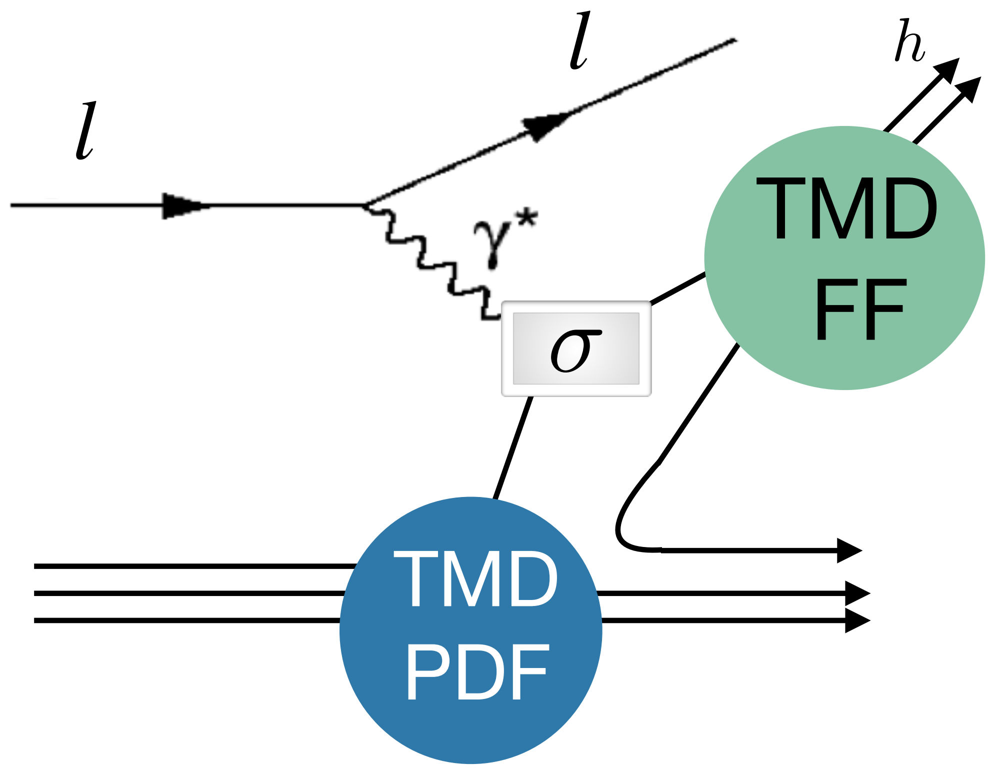

Kinematic coverage

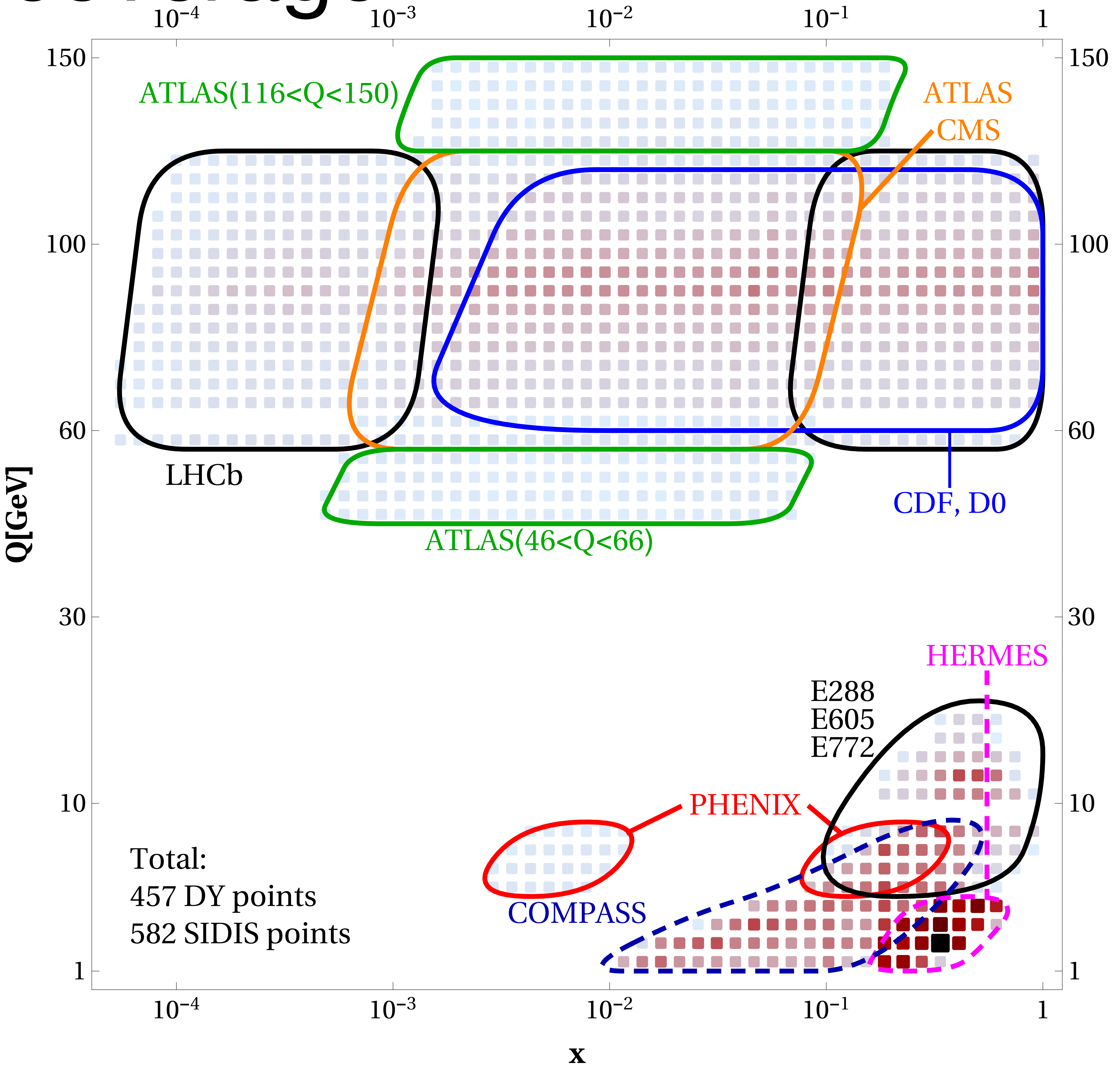

Kinematic coverage

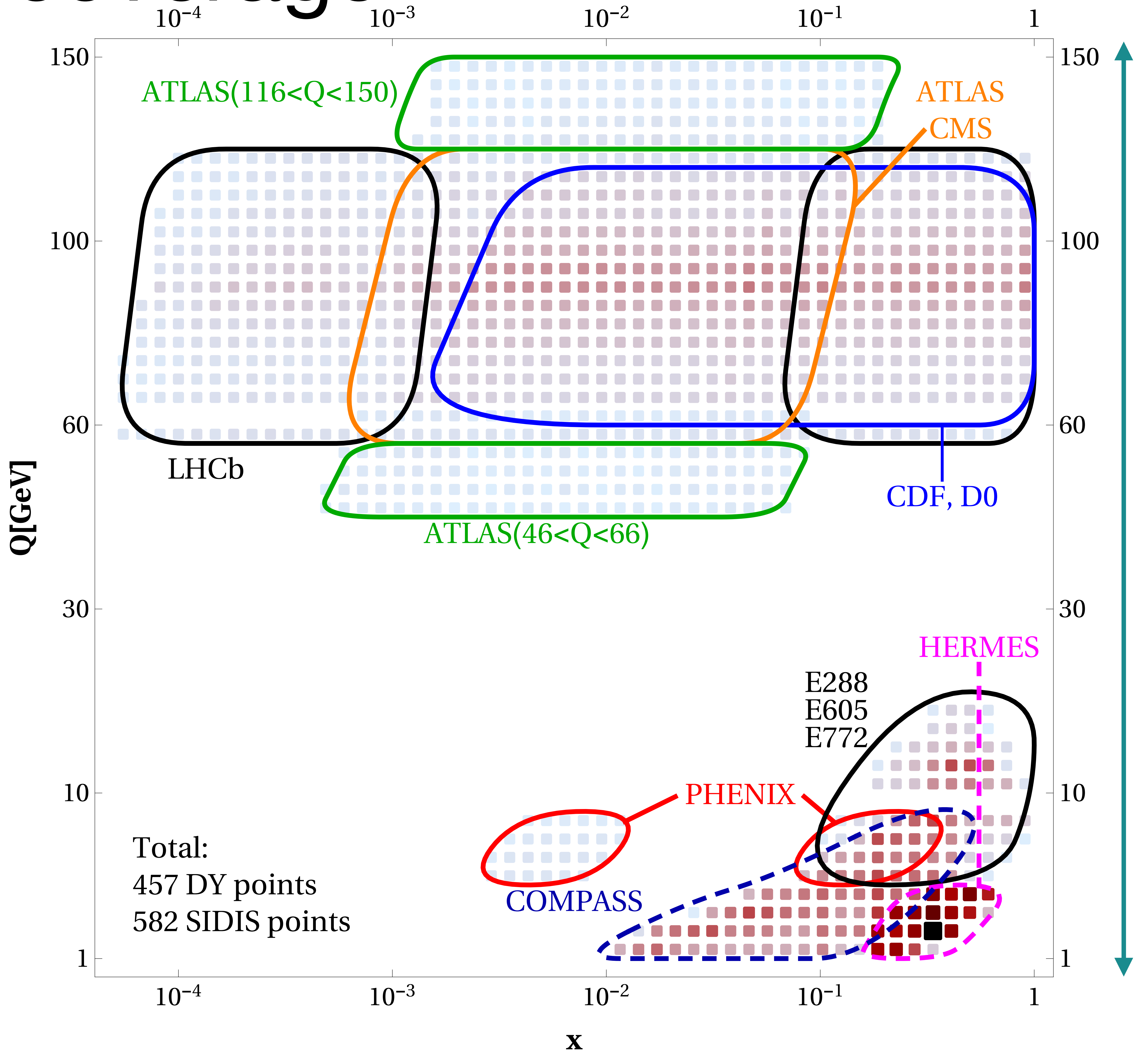

Large lever-arm in Q^2
→ Q^2 evolution of TMD PDF

Spin-independent TMD PDFs: global analysis

I. Scimemi, A. Vladimirov JHEP **06** (2020)137

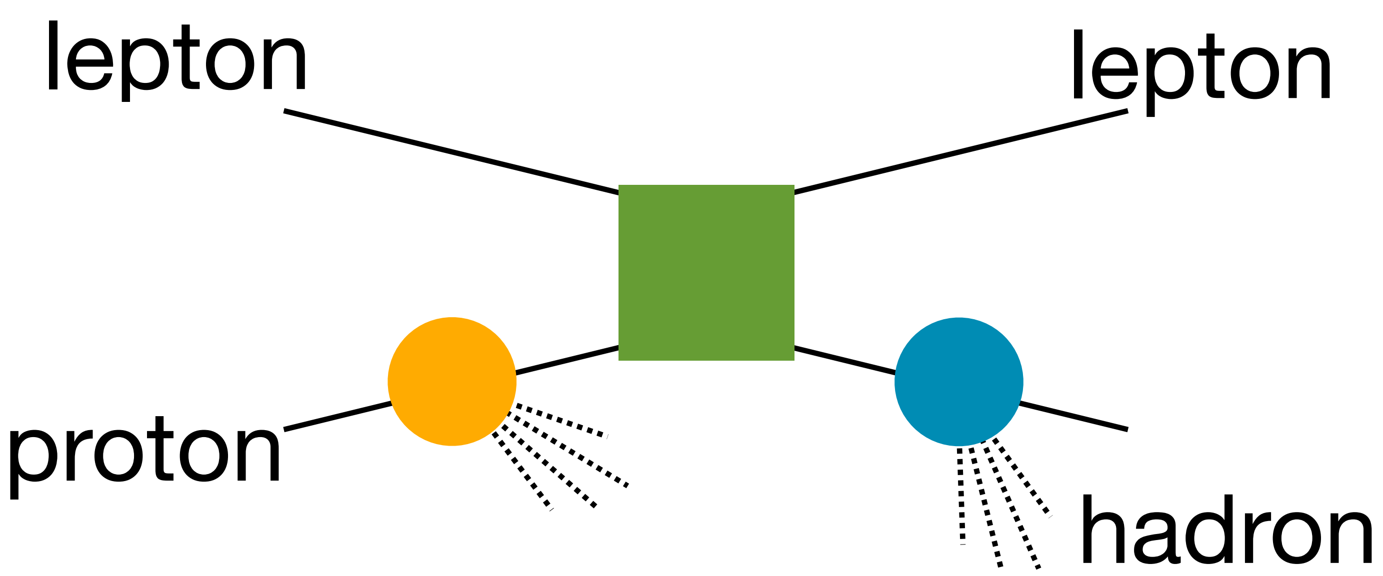

semi-inclusive DIS

Experiment	Reaction	ref.	Kinematics	$N_{\rm pt}$ after cuts
HERMES	$p \to \pi^+$	[67]	$0.023 < x < 0.6$ (6 bins) $0.2 < z < 0.8$ (6 bins) $1.0 < Q < \sqrt{20}\,$GeV $W^2 > 10$GeV^2 $0.1 < y < 0.85$	24
	$p \to \pi^-$			24
	$p \to K^+$			24
	$p \to K^-$			24
	$D \to \pi^+$			24
	$D \to \pi^-$			24
	$D \to K^+$			24
	$D \to K^-$			24
COMPASS	$d \to h^+$	[68]	$0.003 < x < 0.4$ (8 bins) $0.2 < z < 0.8$ (4 bins) $1.0 < Q \simeq 9\,$GeV (5 bins)	195
	$d \to h^-$			195
Total				582

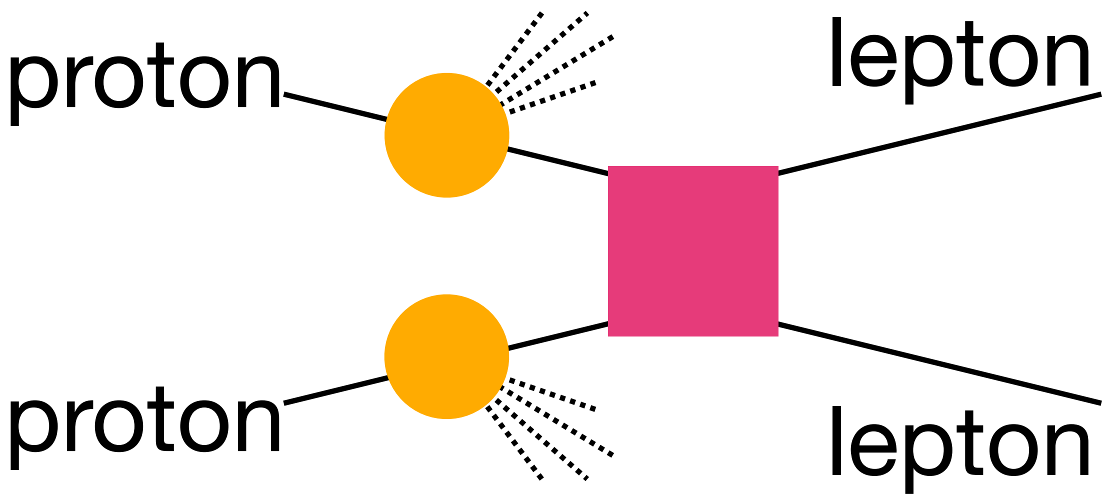

Drell-Yan

Experiment	ref.	$\sqrt{s}$ [GeV]	Q [GeV]	y/x_F	fiducial region	$N_{\rm pt}$ after cuts
E288 (200)	[73]	19.4	4–9 in 1 GeV bins*	$0.1 < x_F < 0.7$	—	43
E288 (300)	[73]	23.8	4–12 in 1 GeV bins*	$-0.09 < x_F < 0.51$	—	53
E288 (400)	[73]	27.4	5–14 in 1 GeV bins*	$-0.27 < x_F < 0.33$	—	76
E605	[74]	38.8	7–18 in 5 bins*	$-0.1 < x_F < 0.2$	—	53
E772	[75]	38.8	5–15 in 8 bins*	$0.1 < x_F < 0.3$	—	35
PHENIX	[76]	200	4.8–8.2	$1.2 < y < 2.2$	—	3
CDF (run1)	[77]	1800	66–116	—	—	33
CDF (run2)	[78]	1960	66–116	—	–	39
D0 (run1)	[79]	1800	75–105	—	—	16
D0 (run2)	[80]	1960	70–110	—	—	8
D0 (run2)$_\mu$	[81]	1960	65–115	$\lvert y\rvert < 1.7$	$p_T > 15$ GeV $\lvert\eta\rvert < 1.7$	3
ATLAS (7 TeV)	[47]	7000	66–116	$\lvert y\rvert < 1$ $1 < \lvert y\rvert < 2$ $2 < \lvert y\rvert < 2.4$	$p_T > 20$ GeV $\lvert\eta\rvert < 2.4$	15
ATLAS (8 TeV)	[48]	8000	66–116	$\lvert y\rvert < 2.4$ in 6 bins	$p_T > 20$ GeV $\lvert\eta\rvert < 2.4$	30
ATLAS (8 TeV)	[48]	8000	46–66	$\lvert y\rvert < 2.4$	$p_T > 20$ GeV $\lvert\eta\rvert < 2.4$	3
ATLAS (8 TeV)	[48]	8000	116–150	$\lvert y\rvert < 2.4$	$p_T > 20$ GeV $\lvert\eta\rvert < 2.4$	7
CMS (7 TeV)	[49]	7000	60–120	$\lvert y\rvert < 2.1$	$p_T > 20$ GeV $\lvert\eta\rvert < 2.1$	8
CMS (8 TeV)	[50]	8000	60–120	$\lvert y\rvert < 2.1$	$p_T > 20$ GeV $\lvert\eta\rvert < 2.1$	8
LHCb (7 TeV)	[82]	7000	60–120	$2 < y < 4.5$	$p_T > 20$ GeV $2 < \eta < 4.5$	8
LHCb (8 TeV)	[83]	8000	60–120	$2 < y < 4.5$	$p_T > 20$ GeV $2 < \eta < 4.5$	7
LHCb (13 TeV)	[84]	13000	60–120	$2 < y < 4.5$	$p_T > 20$ GeV $2 < \eta < 4.5$	9
Total						457

Spin-independent TMD PDFs: global analysis

I. Scimemi, A. Vladimirov JHEP **06** (2020)137

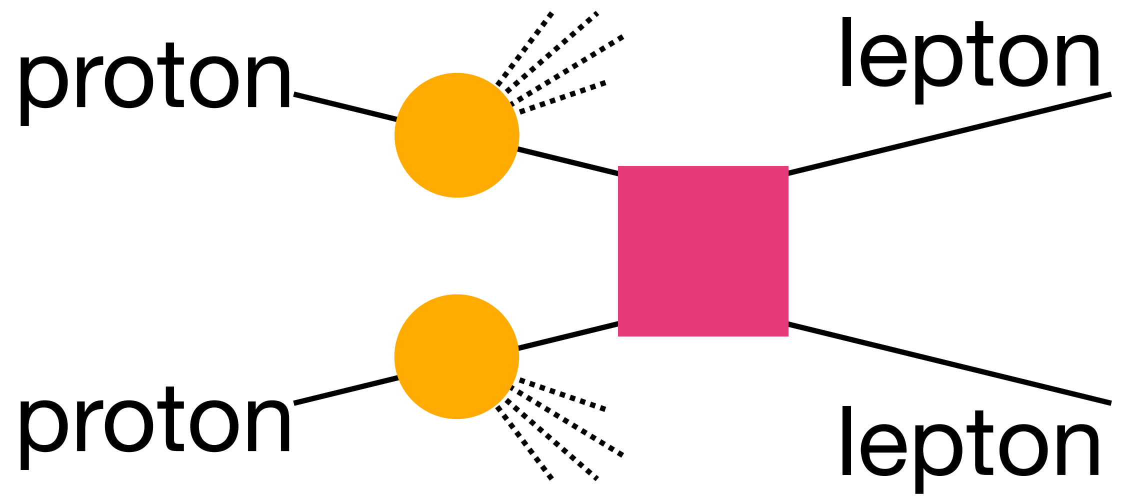

Experiment	ref.	$\sqrt{s}$ [GeV]	Q [GeV]	y/x_F	fiducial region	N_{pt} after cuts
E288 (200)	[73]	19.4	4–9 in 1 GeV bins*	$0.1 < x_F < 0.7$	—	43
E288 (300)	[73]	23.8	4–12 in 1 GeV bins*	$-0.09 < x_F < 0.51$	—	53
E288 (400)	[73]	[illegible]	5–14 in	[illegible]		[illegible]
Total						457

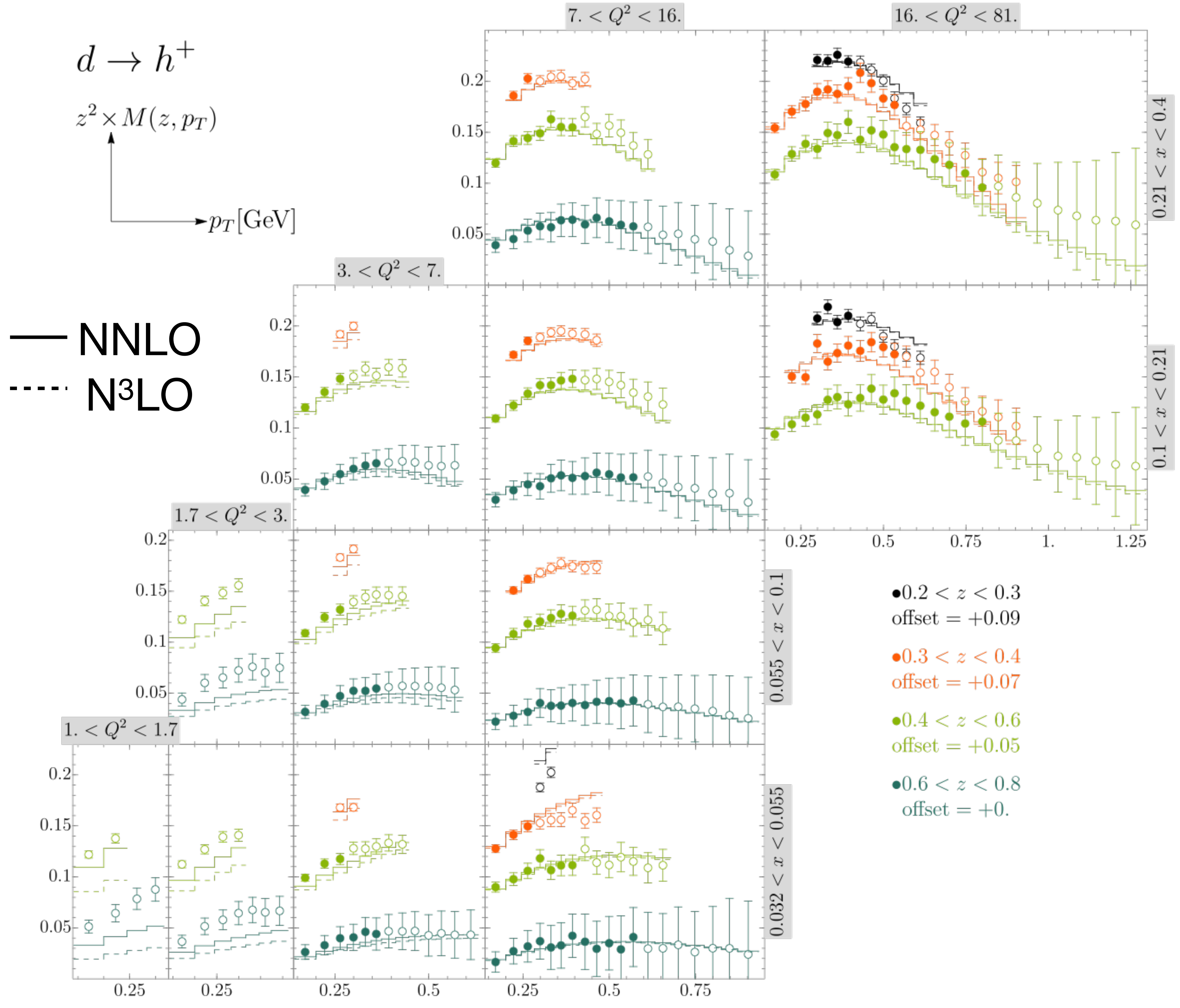

Description of the data

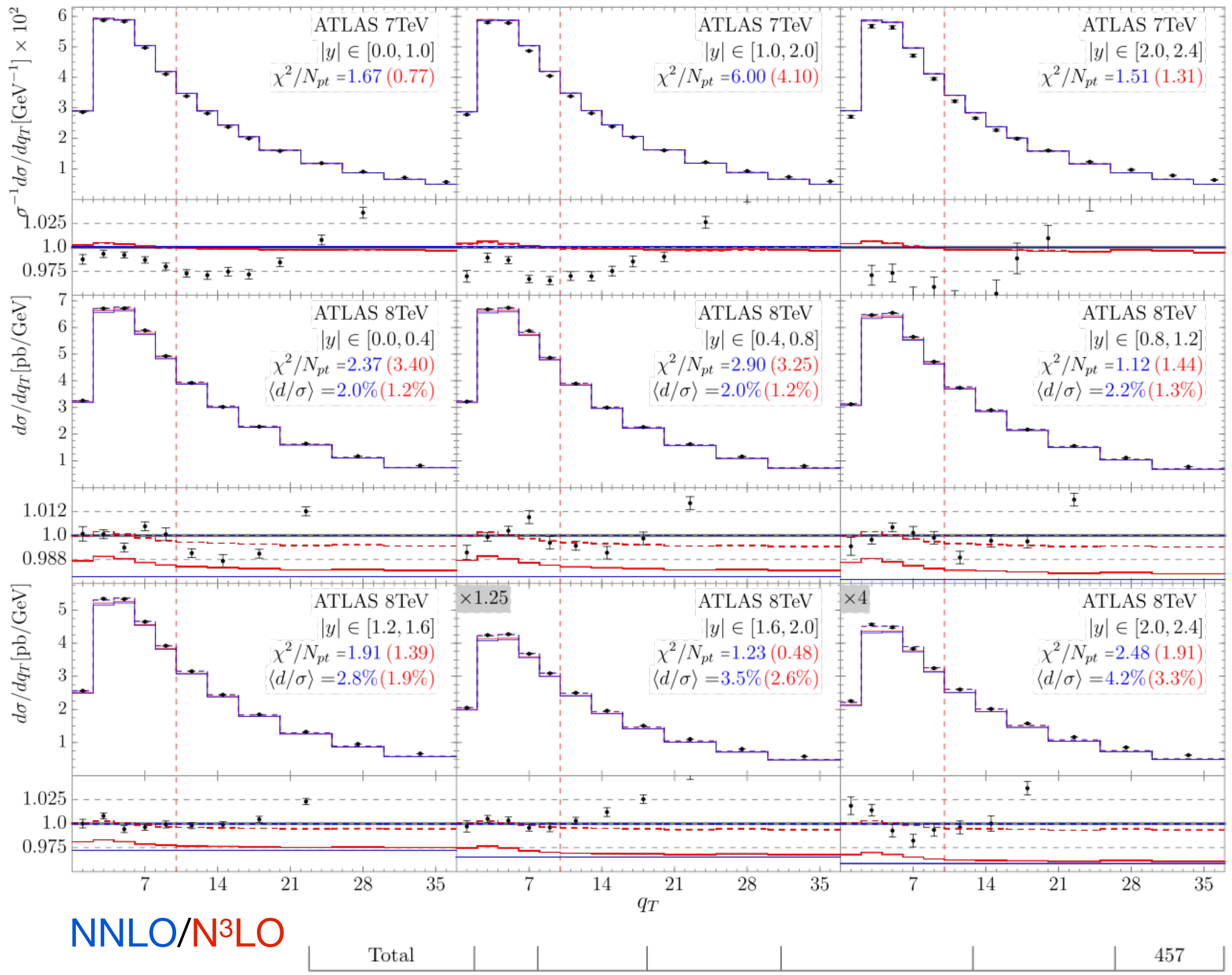

Spin-independent TMD PDFs: global analysis

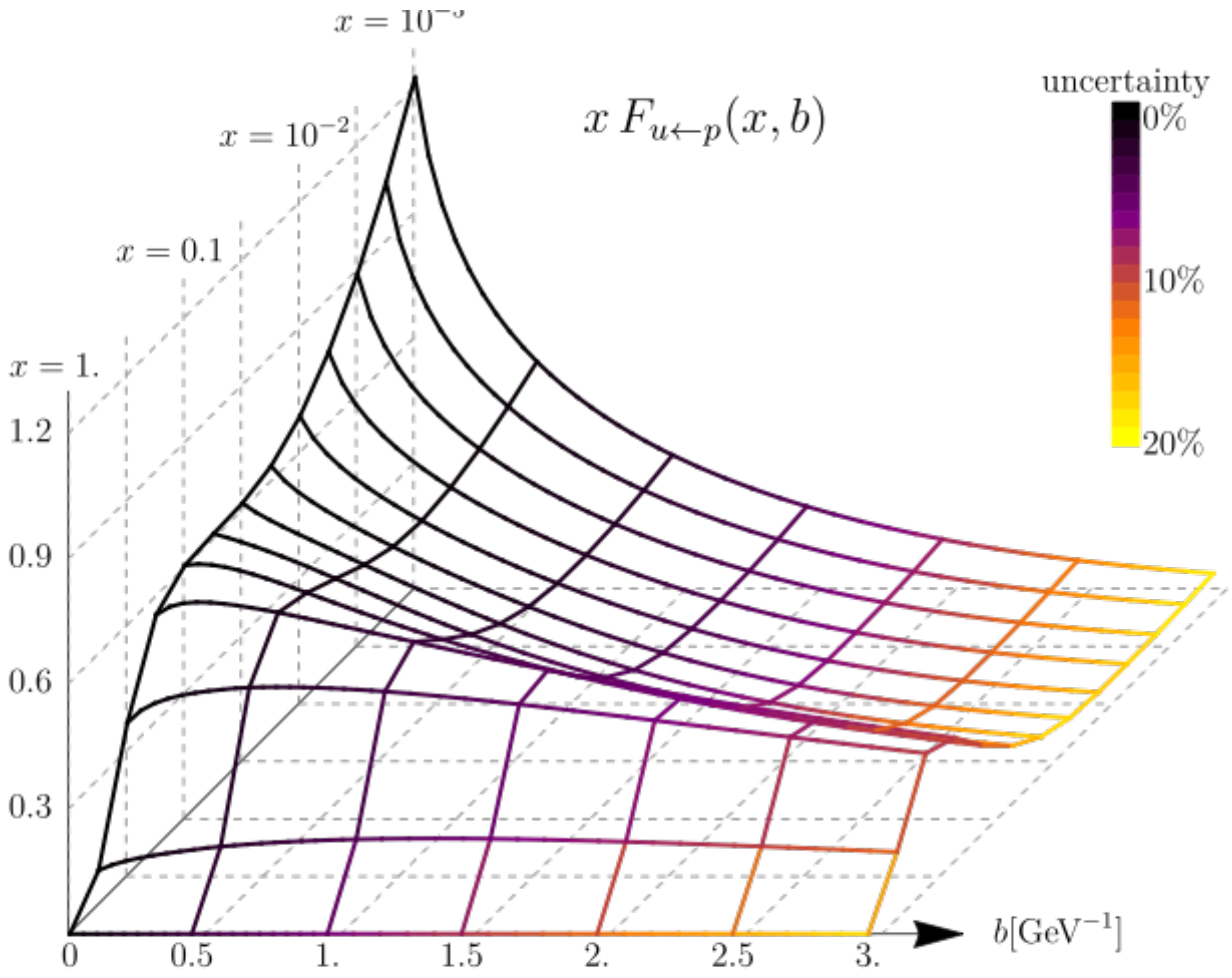

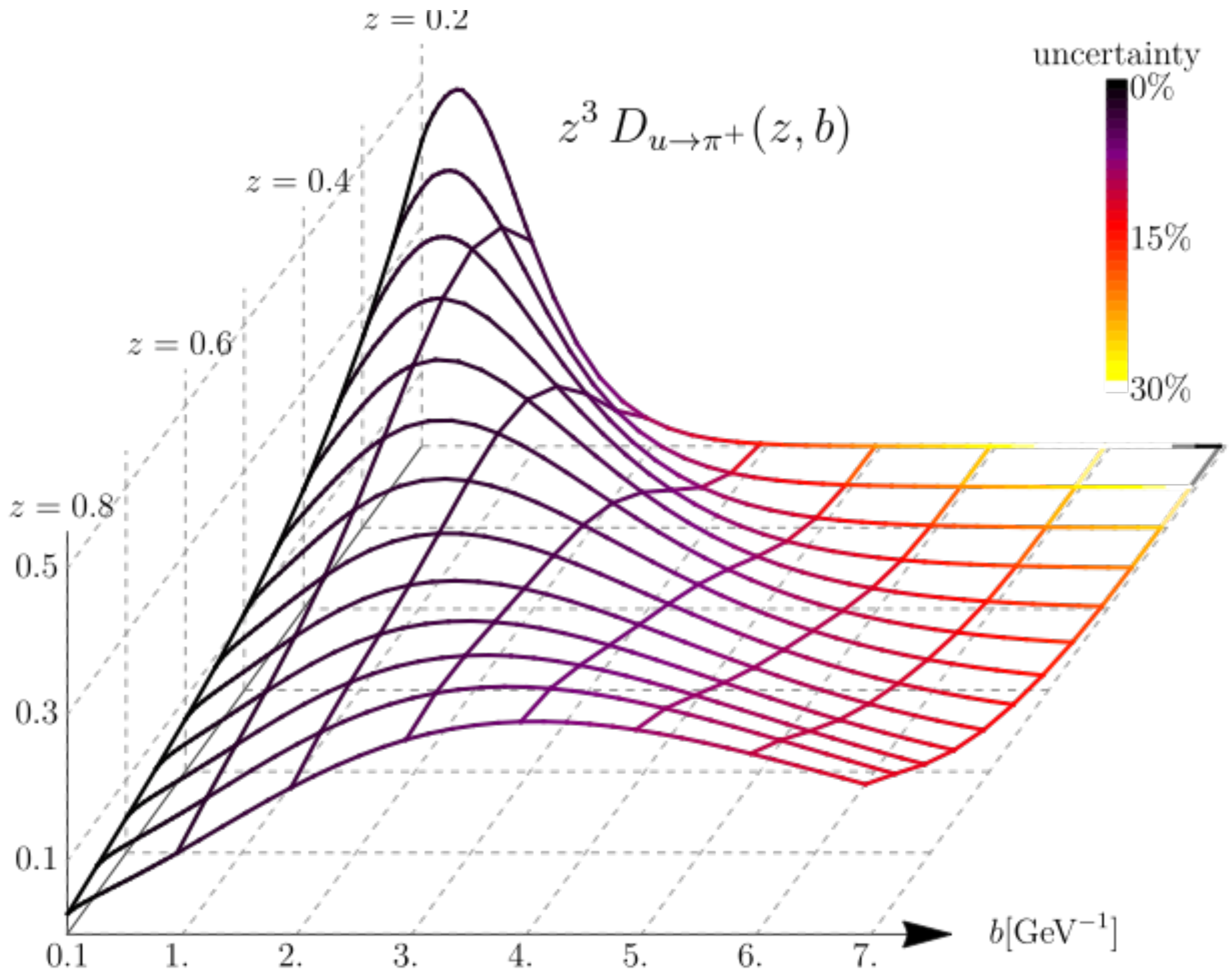

Collins amplitudes: measurement

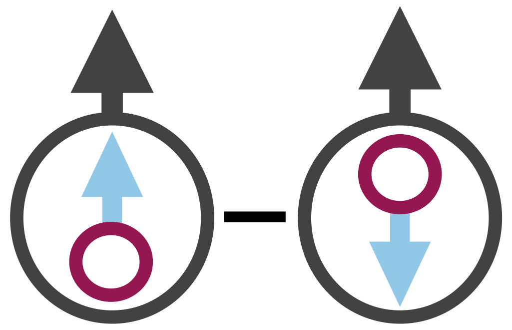

$\mathscr{C}\left[h_{1T}^{q} \times H_1^{\perp,q}\right]$

$$A_{UT} = \frac{1}{\langle|S_T|\rangle} \frac{N^{\uparrow}(\phi,\phi_S) - N^{\downarrow}(\phi,\phi_S)}{N^{\uparrow}(\phi,\phi_S) + N^{\downarrow}(\phi,\phi_S)}$$

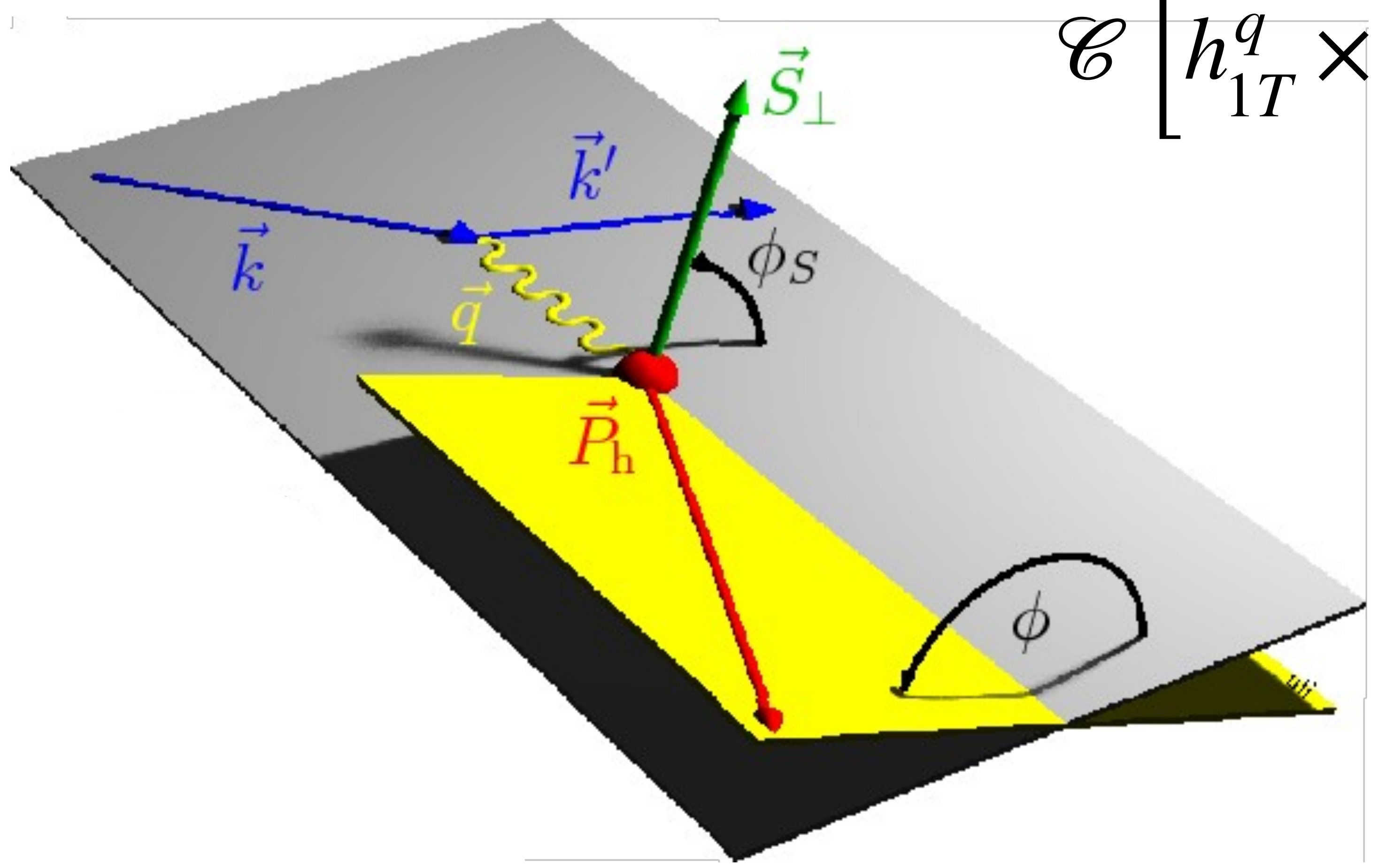

Collins amplitudes: measurement

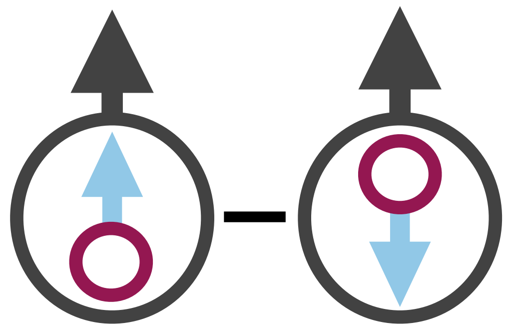

$$\mathscr{C}\left[h_{1T}^{q} \times H_{1}^{\perp,q}\right]$$

$$A_{UT} = \frac{1}{\langle |S_T| \rangle} \frac{N^{\uparrow}(\phi, \phi_S) - N^{\downarrow}(\phi, \phi_S)}{N^{\uparrow}(\phi, \phi_S) + N^{\downarrow}(\phi, \phi_S)}$$

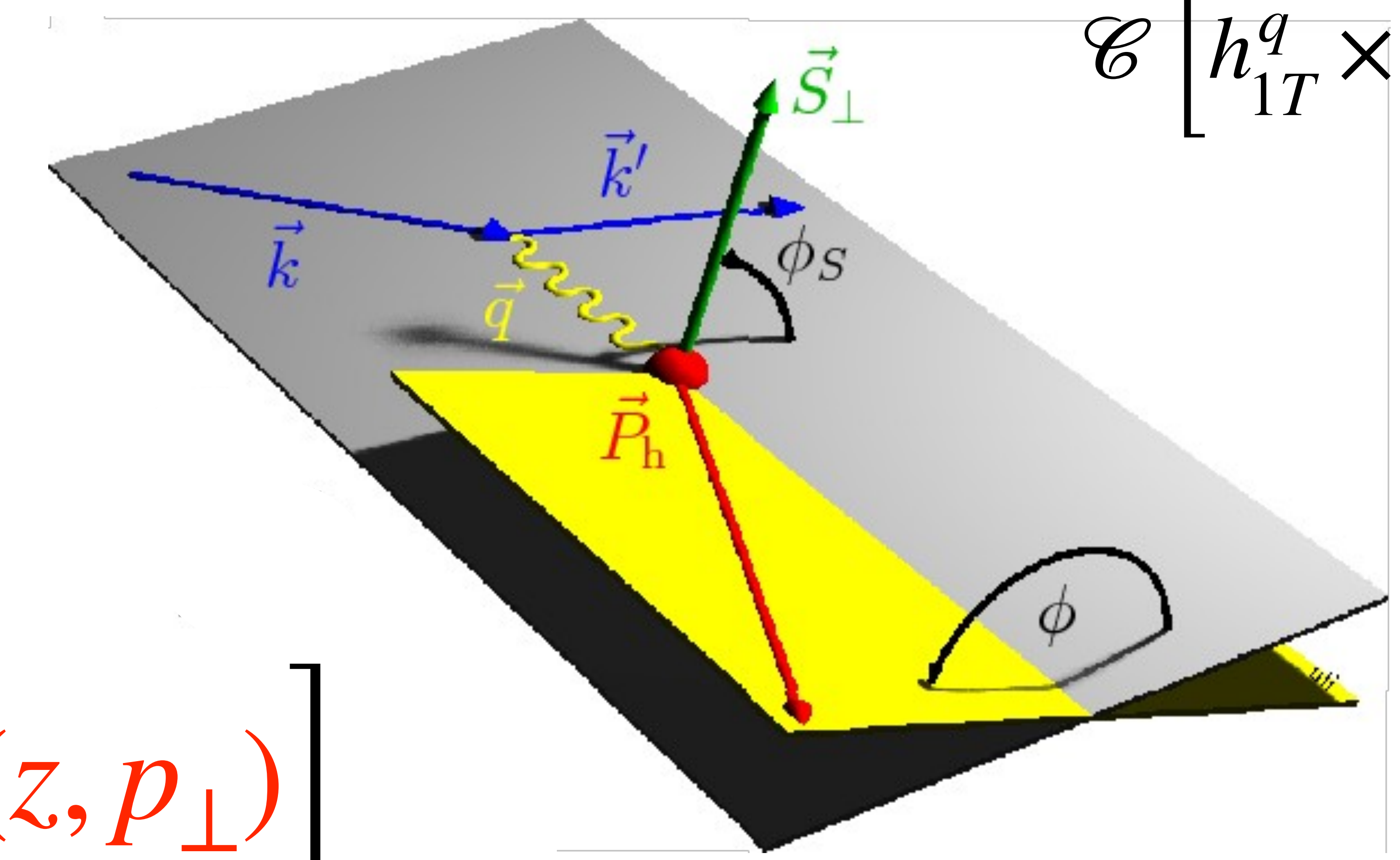

$$\sim \sin(\phi + \phi_S) \sum_q e_q^2 \, C\left[h_{1T}^{q}(x, k_{\perp}) \times H_1^{\perp,q}(z, p_{\perp})\right]$$

Collins amplitudes: measurement

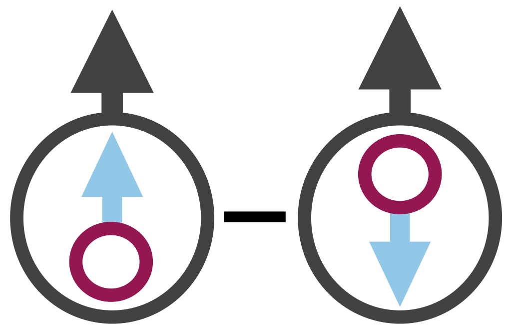

$\mathscr{C}\left[h_{1T}^{q} \times H_{1}^{\perp,q}\right]$

$$A_{UT} = \frac{1}{\langle|S_T|\rangle} \frac{N^{\uparrow}(\phi,\phi_S) - N^{\downarrow}(\phi,\phi_S)}{N^{\uparrow}(\phi,\phi_S) + N^{\downarrow}(\phi,\phi_S)}$$

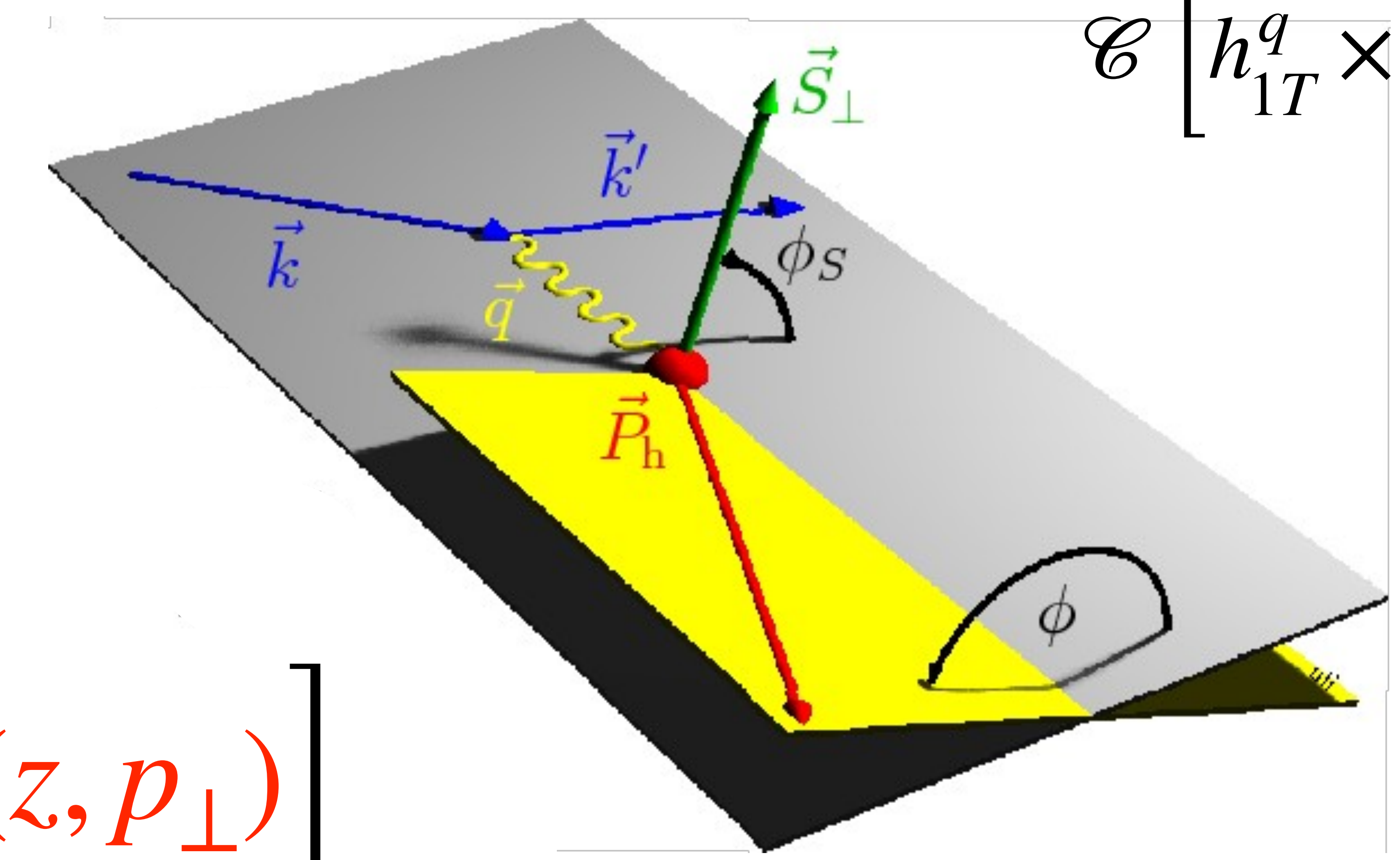

$$\sim \sin(\phi + \phi_S) \sum_q e_q^2 C\left[h_{1T}^{q}(x,k_\perp) \times H_1^{\perp,q}(z,p_\perp)\right]$$

Collins amplitudes: measurement

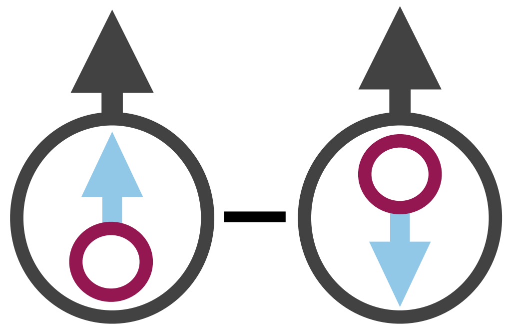

$$\mathscr{C}\left[h_{1T}^{q} \times H_{1}^{\perp,q}\right]$$

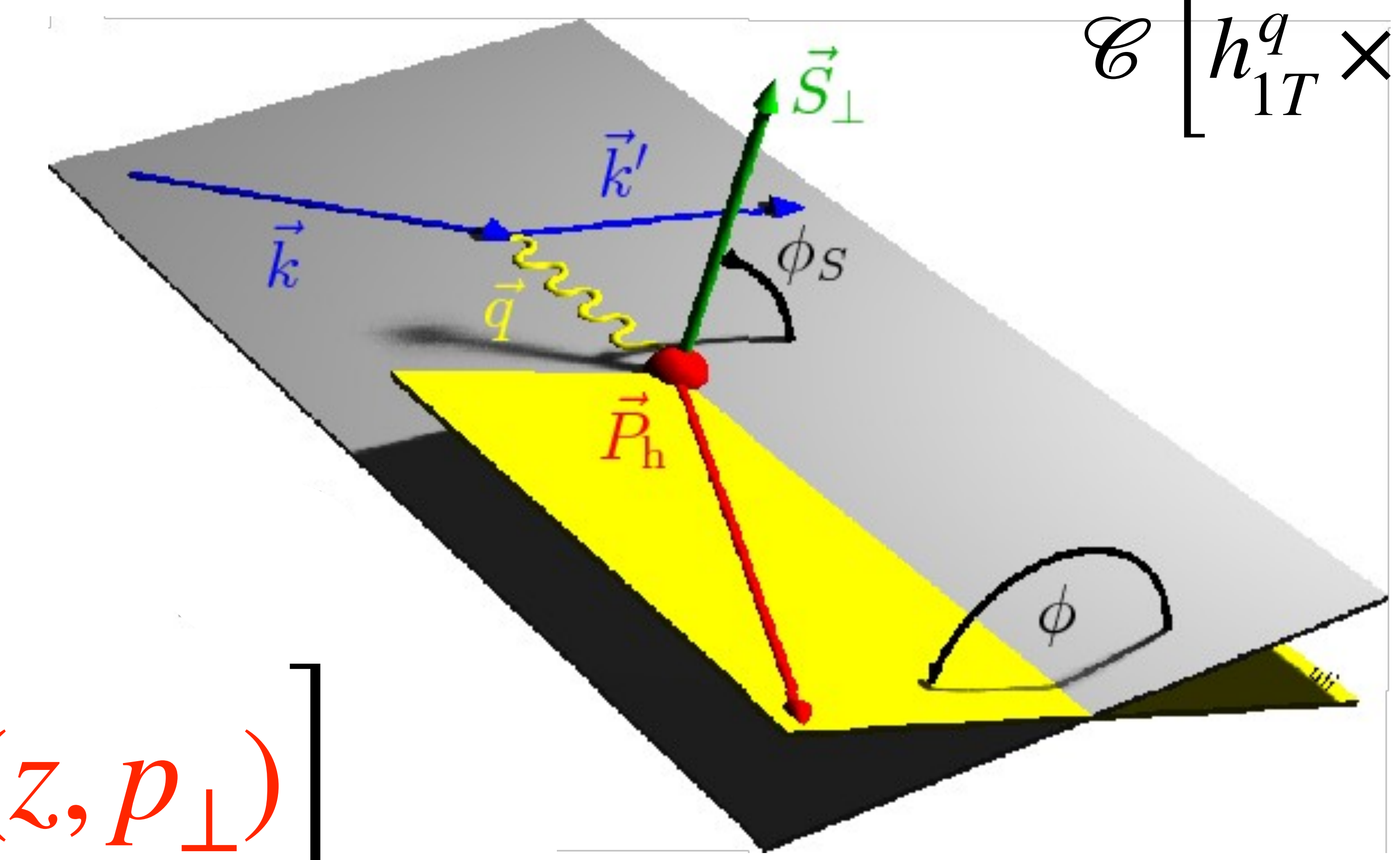

$$A_{UT} = \frac{1}{\langle|S_T|\rangle} \frac{N^{\uparrow}(\phi,\phi_S) - N^{\downarrow}(\phi,\phi_S)}{N^{\uparrow}(\phi,\phi_S) + N^{\downarrow}(\phi,\phi_S)}$$

$$\sim \sin(\phi+\phi_S) \sum_q e_q^2 \, C\left[h_{1T}^{q}(x,k_\perp) \times H_1^{\perp,q}(z,p_\perp)\right]$$

$h_{1T}^{q}(x,k_\perp)$: transversity

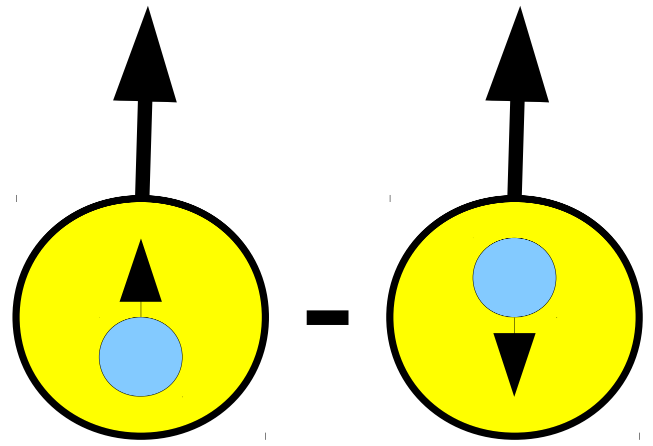

Collins amplitudes: measurement

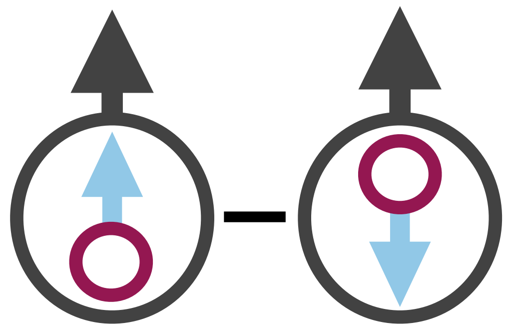

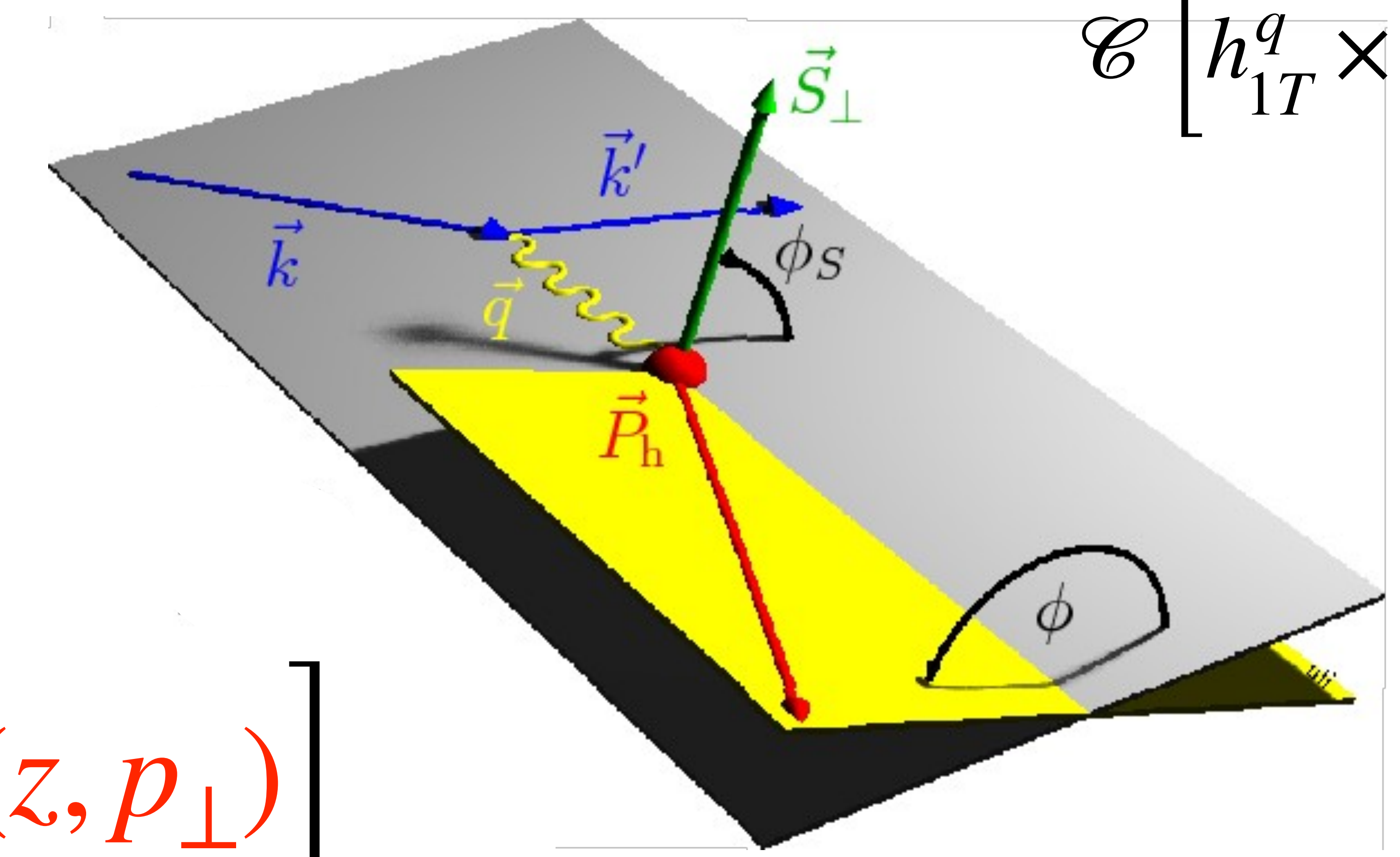

$$A_{UT} = \frac{1}{\langle |S_T| \rangle} \frac{N^\uparrow(\phi,\phi_S) - N^\downarrow(\phi,\phi_S)}{N^\uparrow(\phi,\phi_S) + N^\downarrow(\phi,\phi_S)}$$

$$\sim \sin(\phi+\phi_S) \sum_q e_q^2 C\left[h_{1T}^q(x,k_\perp) \times H_1^{\perp,q}(z,p_\perp)\right]$$

$\mathscr{C}\left[h_{1T}^q \times H_1^{\perp,q}\right]$

$h_{1T}^q(x,k_\perp)$: transversity

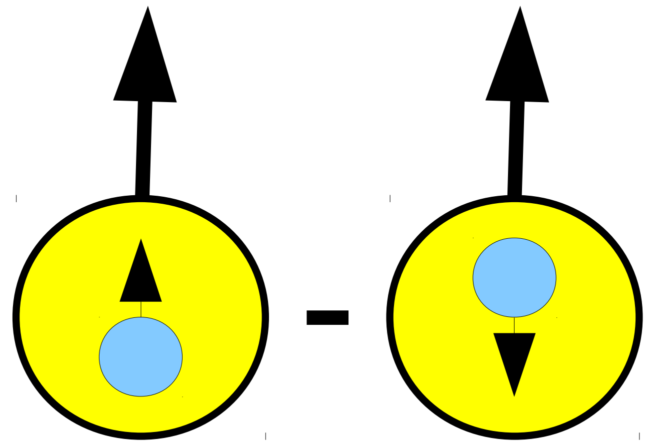

$H_1^{\perp,q}(z,p_\perp)$: Collins fragmentation function

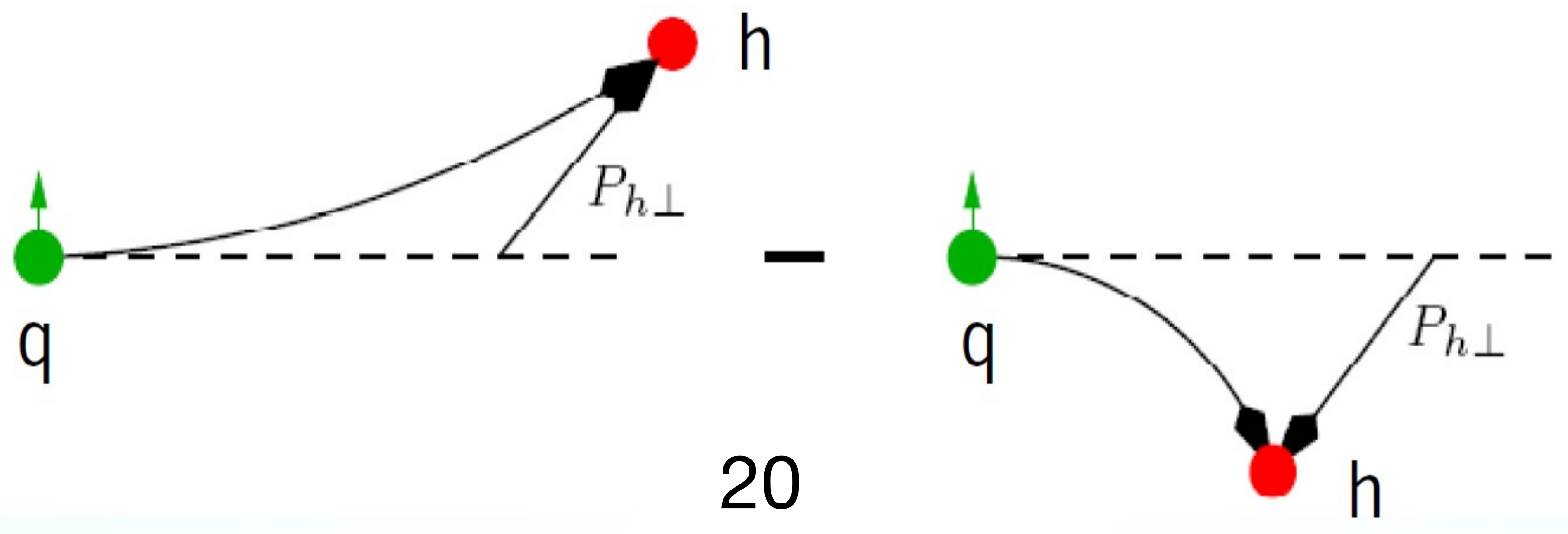

Collins amplitudes

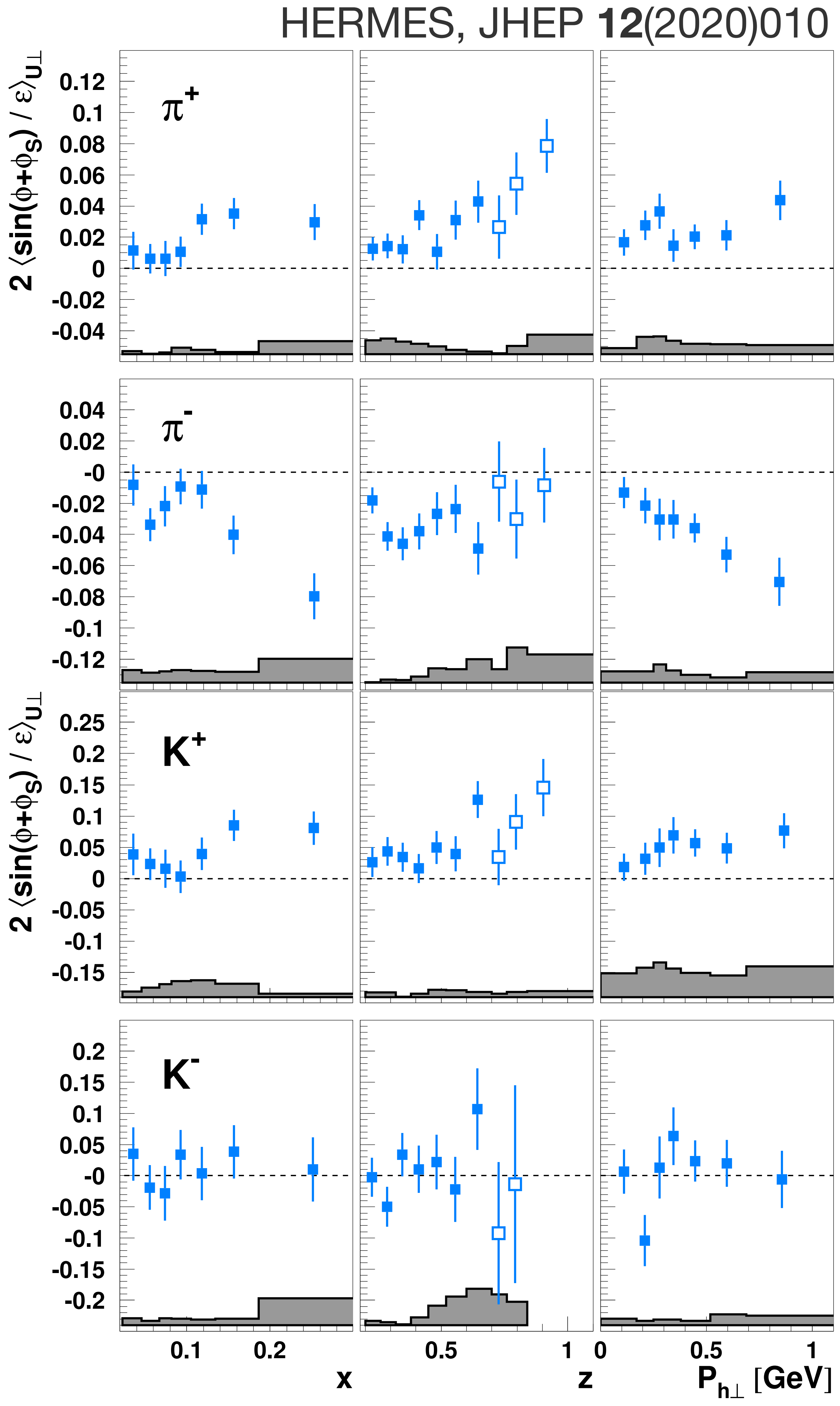

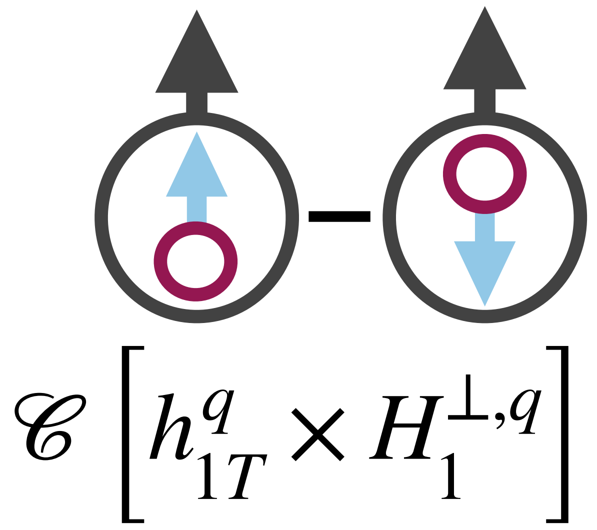

- Oppositely signed amplitudes for π^+ and π^-:

$$H_1^{\perp,u\to\pi^+}\approx -H_1^{\perp,u\to\pi^-}$$

Artru model

X. Artru et al., Z. Phys. C**73** (1997) 527

polarisation component in lepton scattering plane reversed by photoabsorption:

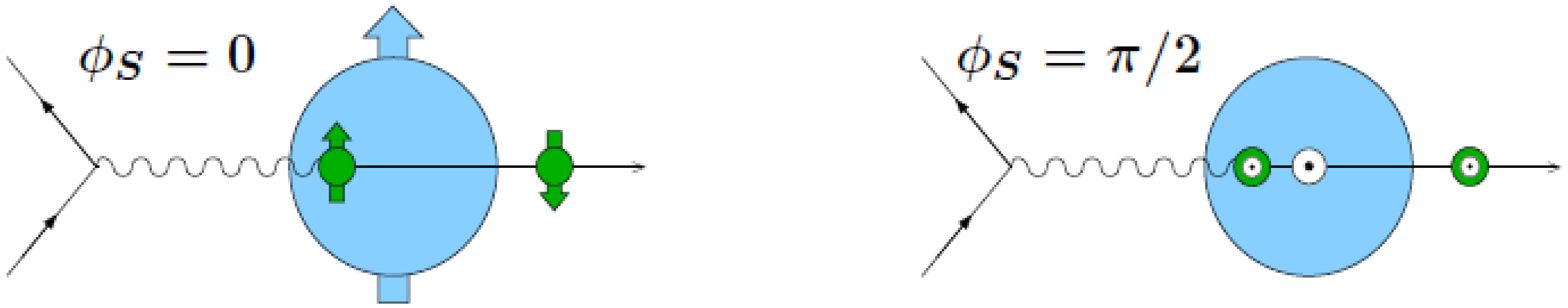

string break, quark-antiquark pair with vacuum numbers:

orbital angular momentum creates transverse momentum:

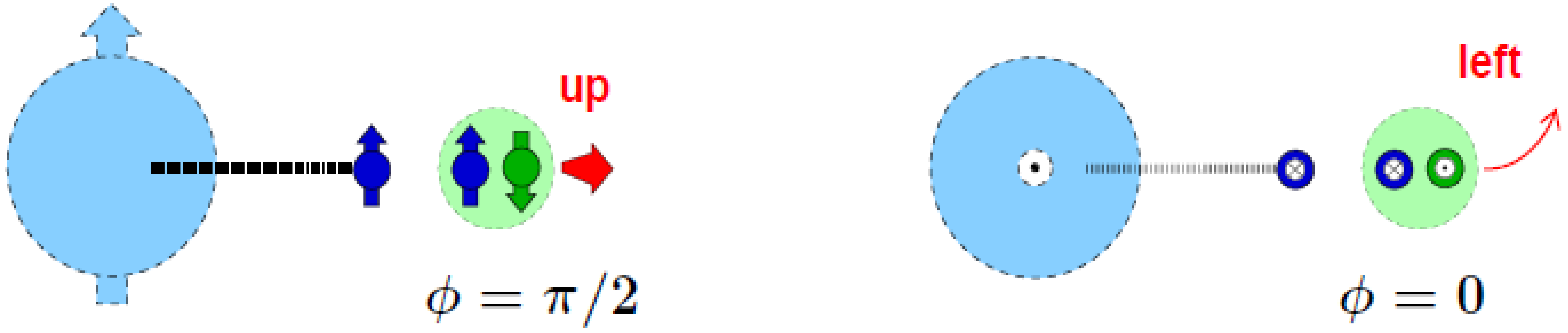

Courtesy U. Elschenbroich

Collins amplitudes

HERMES, JHEP **12**(2020)010

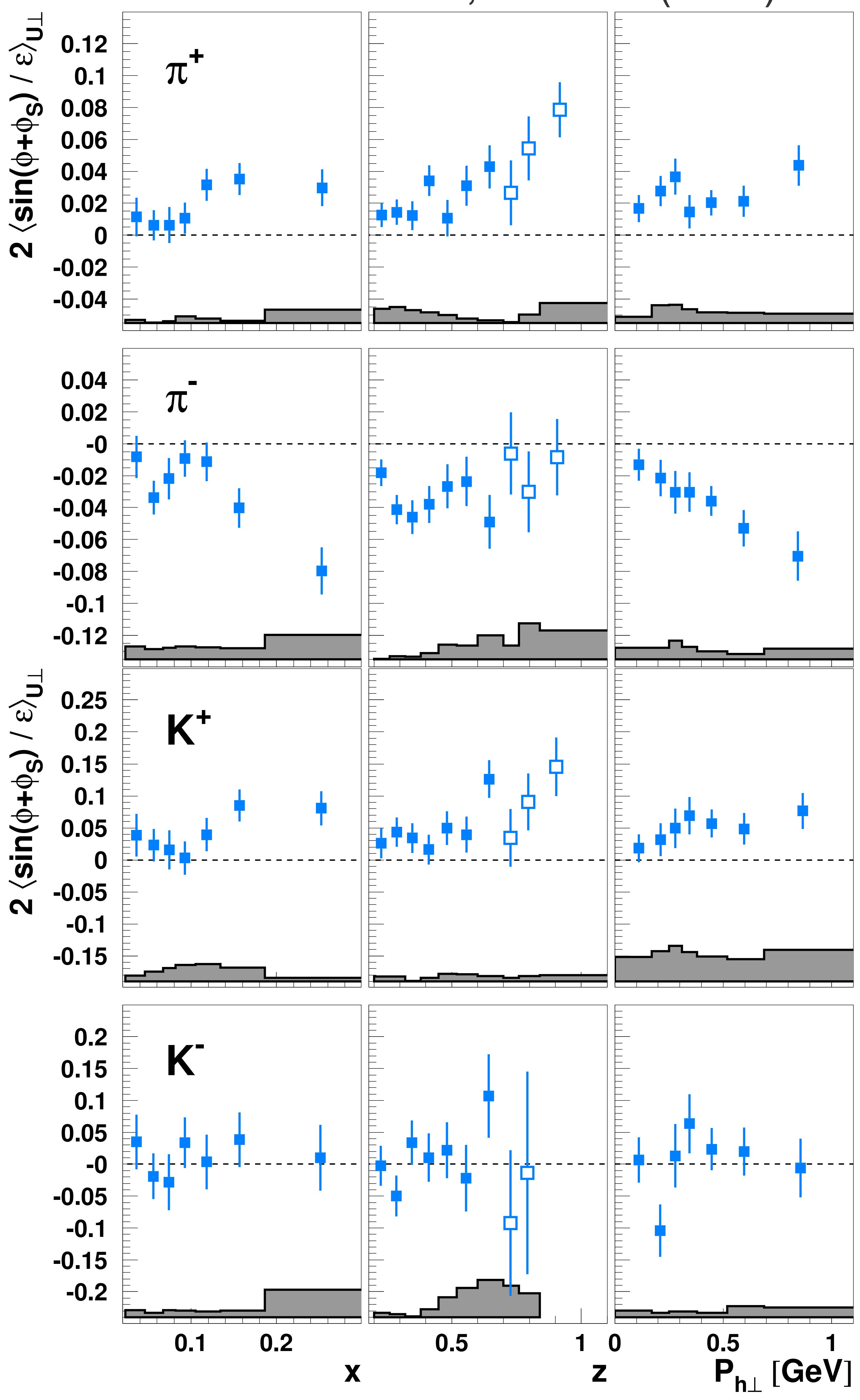

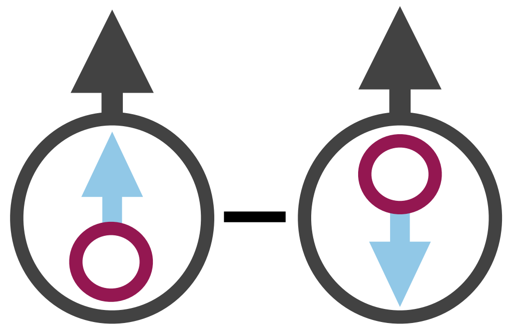

$\mathcal{C}\left[h_{1T}^{q} \times H_1^{\perp,q}\right]$

- Oppositely signed amplitudes for π^+ and π^-:

$$H_1^{\perp,u\to\pi^+} \approx -H_1^{\perp,u\to\pi^-}$$

- Amplitudes for K^+ larger than for π^+:

$$H_1^{\perp,u\to K^+} > H_1^{\perp,u\to\pi^+}$$

Collins amplitudes

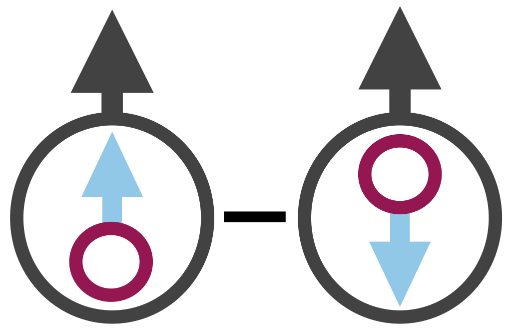

HERMES, JHEP **12**(2020)010

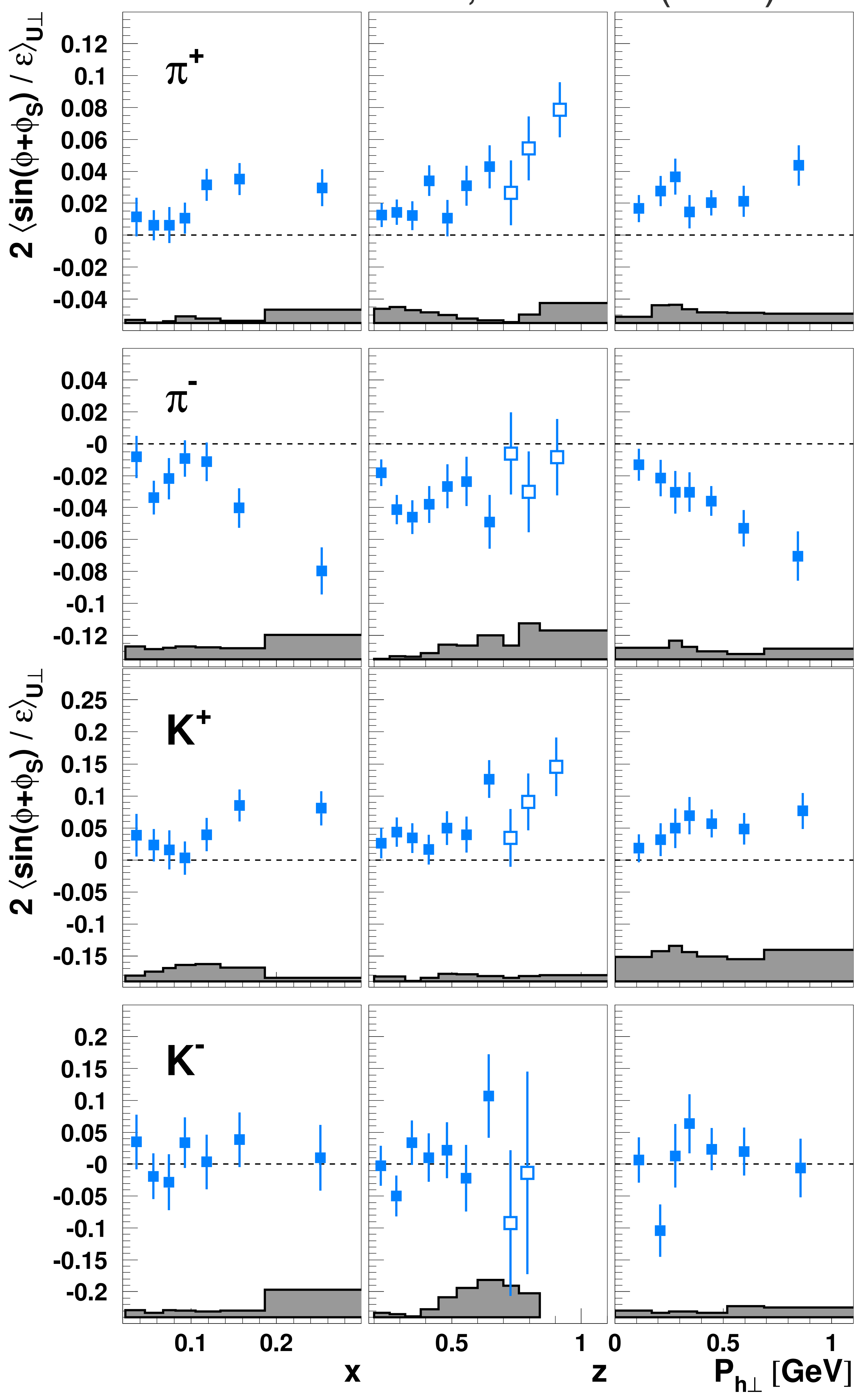

- Oppositely signed amplitudes for π+ and π-:

$$H_1^{\perp,u\to\pi^+} \approx -H_1^{\perp,u\to\pi^-}$$

- Amplitudes for K+ larger than for π+:

$$H_1^{\perp,u\to K^+} > H_1^{\perp,u\to\pi^+}$$

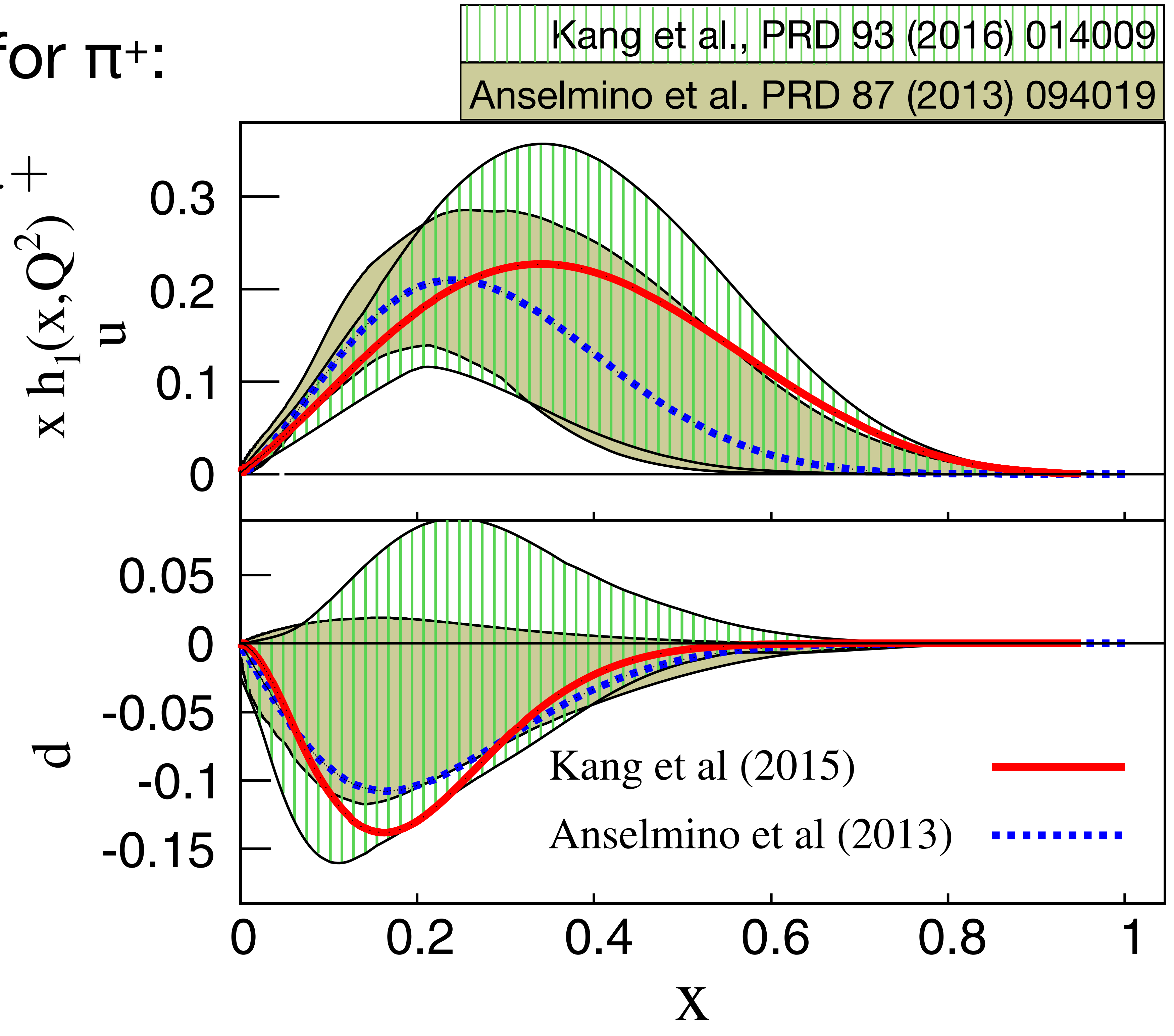

data from Belle, Babar, COMPASS, HERMES, Jefferson Lab Hall A

Sivers amplitudes

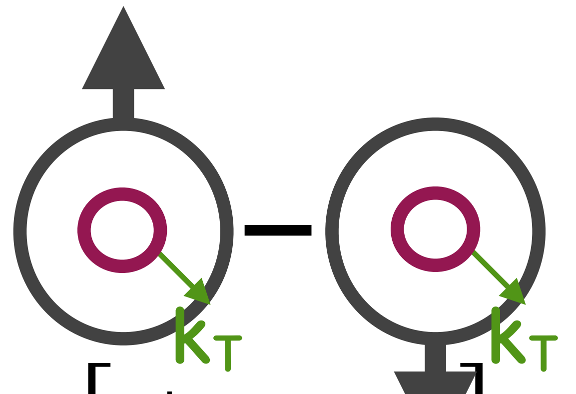

$$\mathscr{C}\left[f_{1T}^{\perp,q} \times D_1\right]$$

- Sivers function:
  - requires non-zero orbital angular momentum
  - final-state interactions ⟶ azimuthal asymmetries

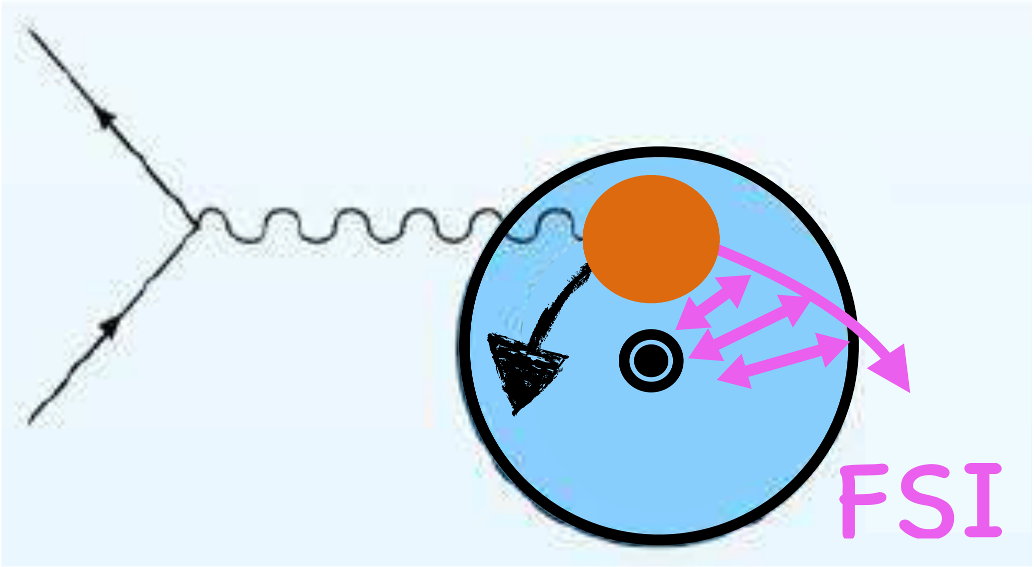

Sivers amplitudes

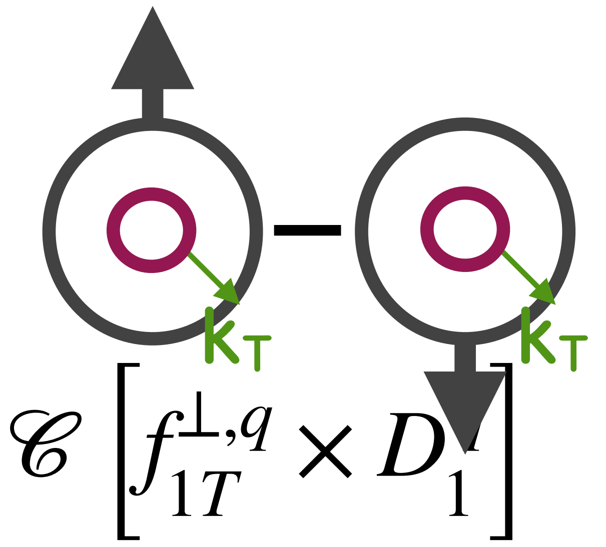

HERMES, JHEP **12**(2020)010

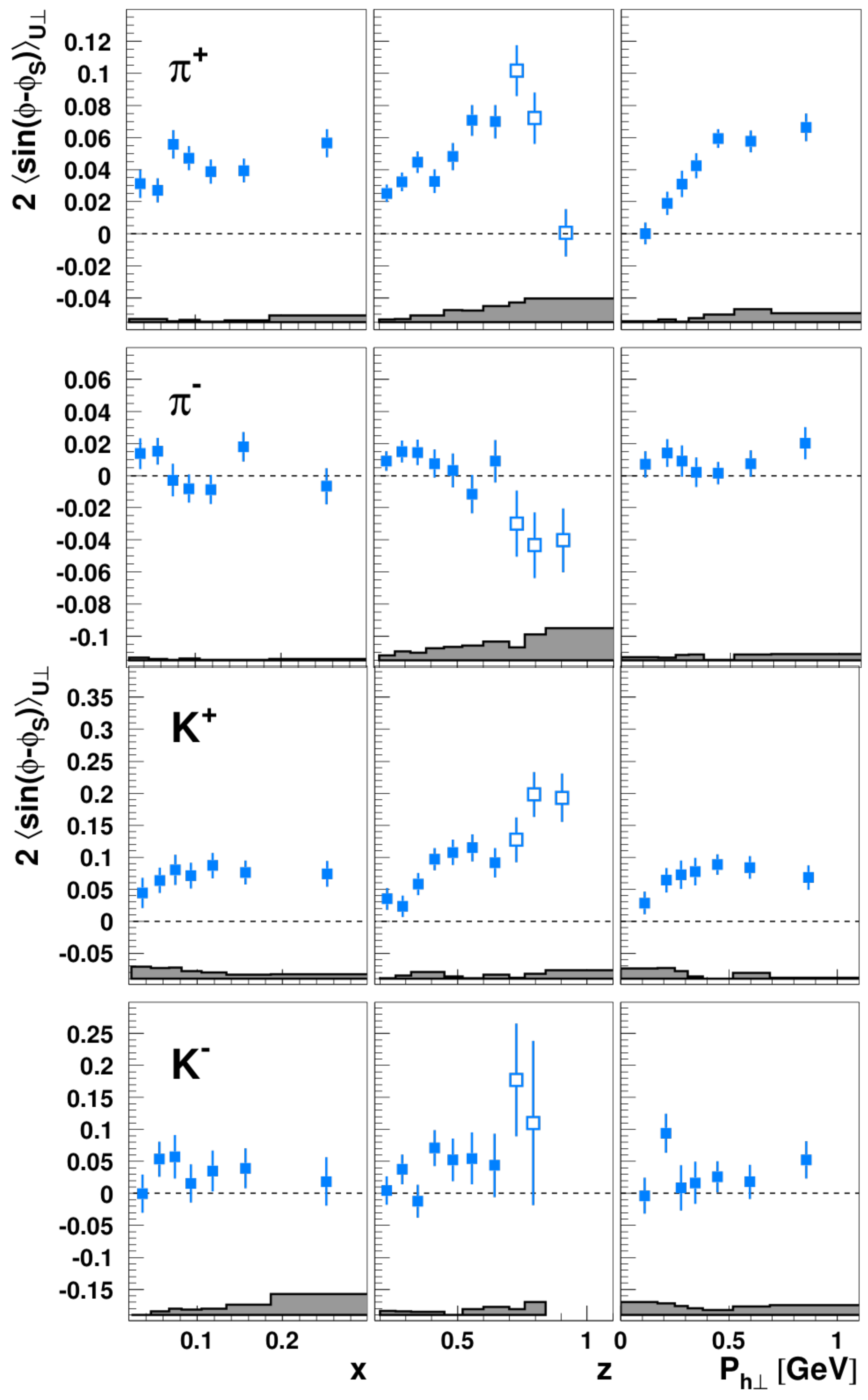

- Sivers function:
  - requires non-zero orbital angular momentum
  - final-state interactions ⟶ azimuthal asymmetries

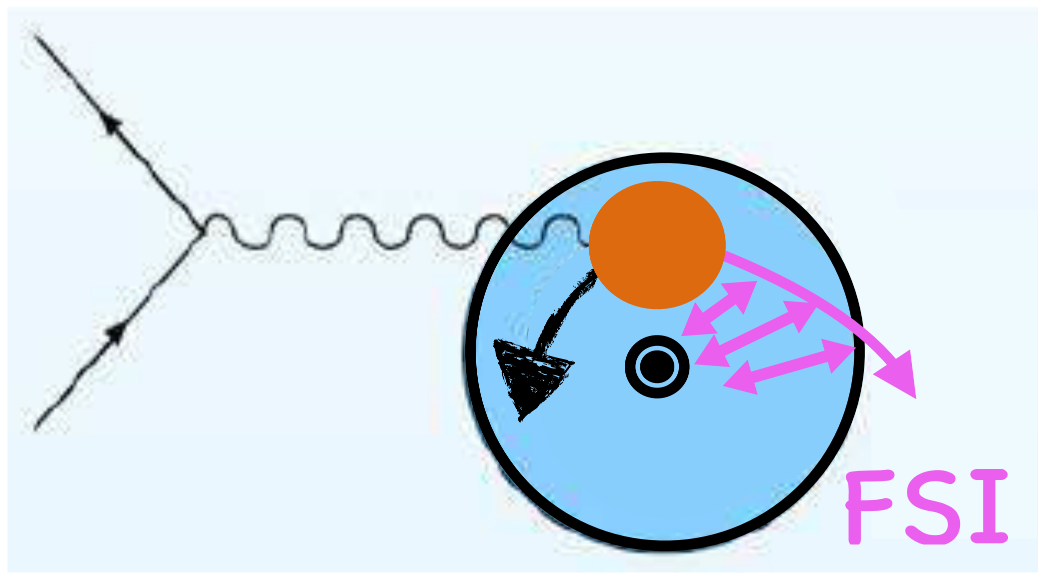

Sivers amplitudes

HERMES, JHEP **12**(2020)010

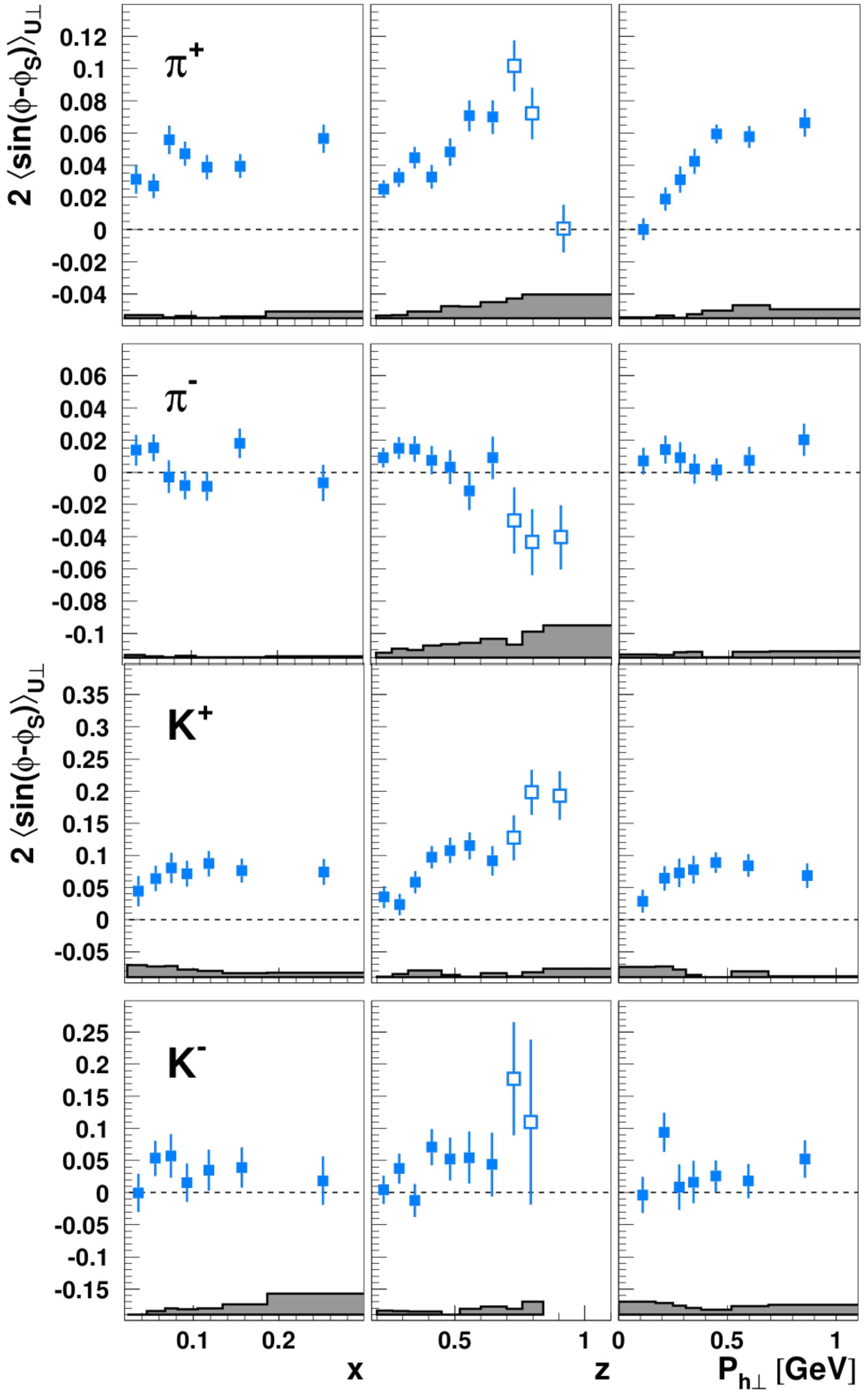

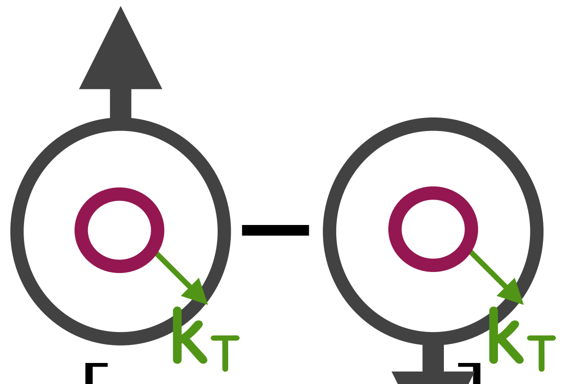

$\mathscr{C}\left[f_{1T}^{\perp,q} \times D_1\right]$

- Sivers function:
  - requires non-zero orbital angular momentum
  - final-state interactions ⟶ azimuthal asymmetries

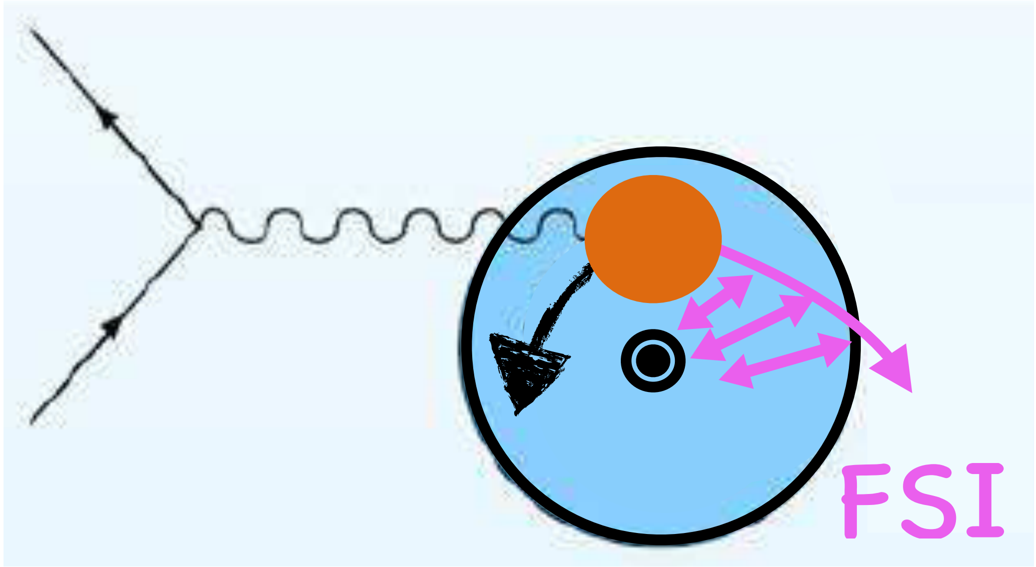

- π^+:
  - positive -> non-zero orbital angular momentum
- π^-:
  - consistent with zero → u and d quark cancelation

Sivers function

M. Anselmino et al., JHEP **04** (2017) 046

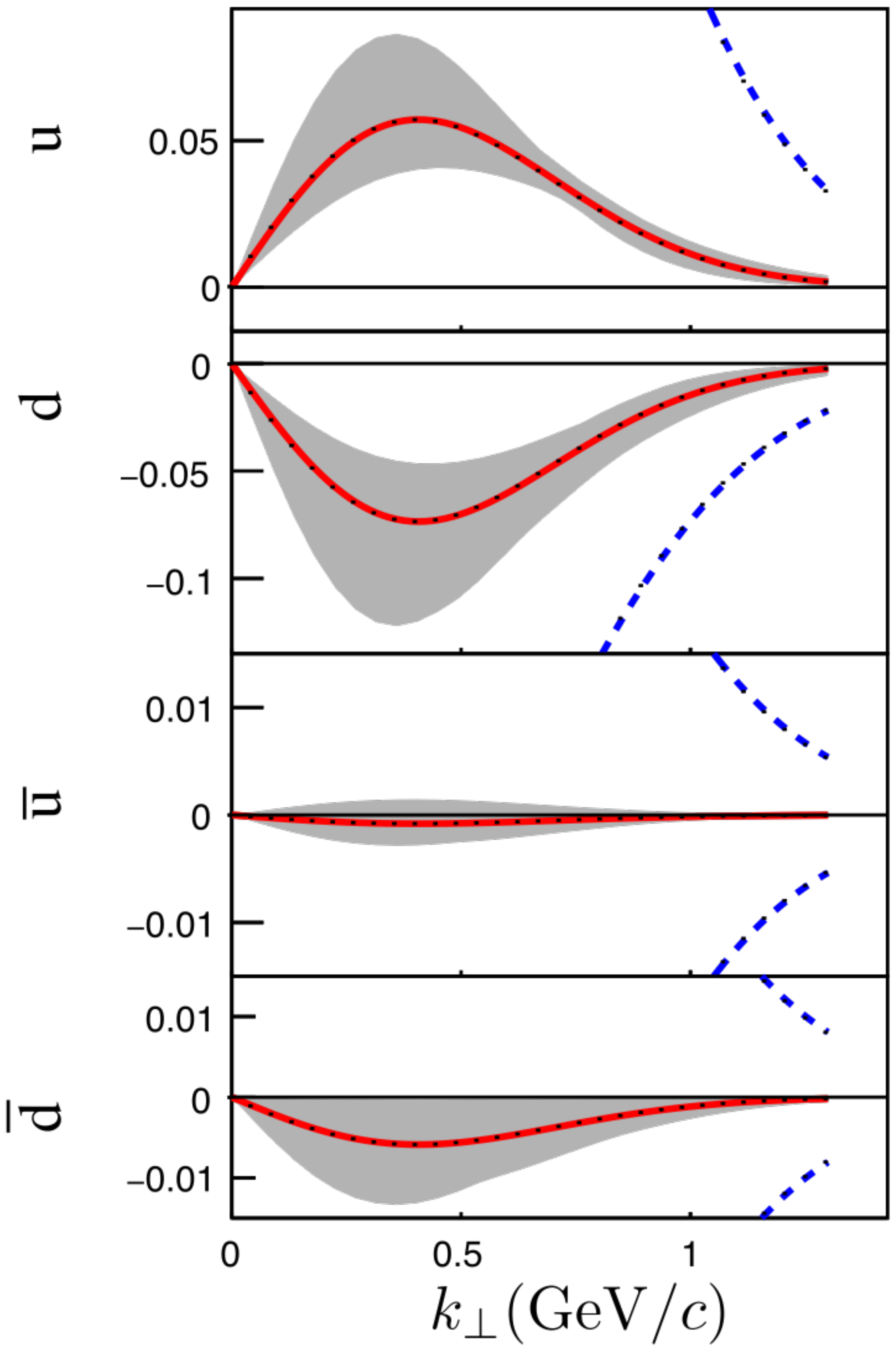

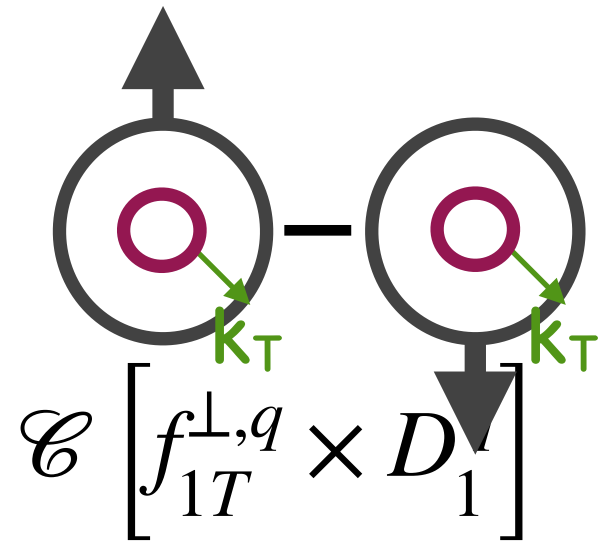

A. Accardi et al., Eur. Phys. J. A **52** (2016) 268

$x\,f_1(x, k_T, S_T)$

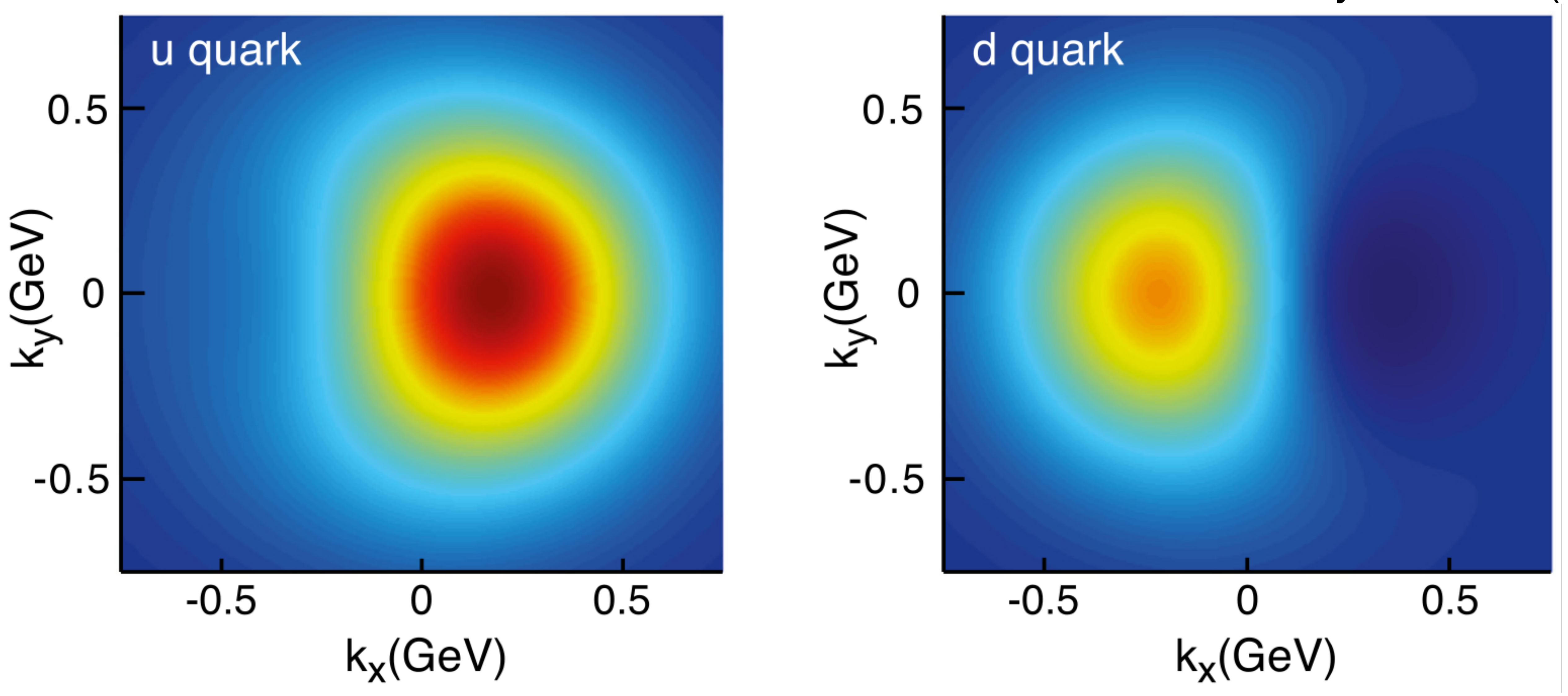

nucleon polarised along $\hat{y}$

Predicted Sivers sign change for SIDIS and Drell-Yan

J. C. Collins, Phys. Lett. B 536 (2002) 43

$$\Phi_{ij}(p,P,S) = \frac{1}{(2\pi)^4}\int d^4\xi\; e^{ip\cdot\xi}\langle P,S|\,\bar{\psi}_j(0)\,U_{[0,\xi]}\,\psi_i(\xi)\,|P,S\rangle$$

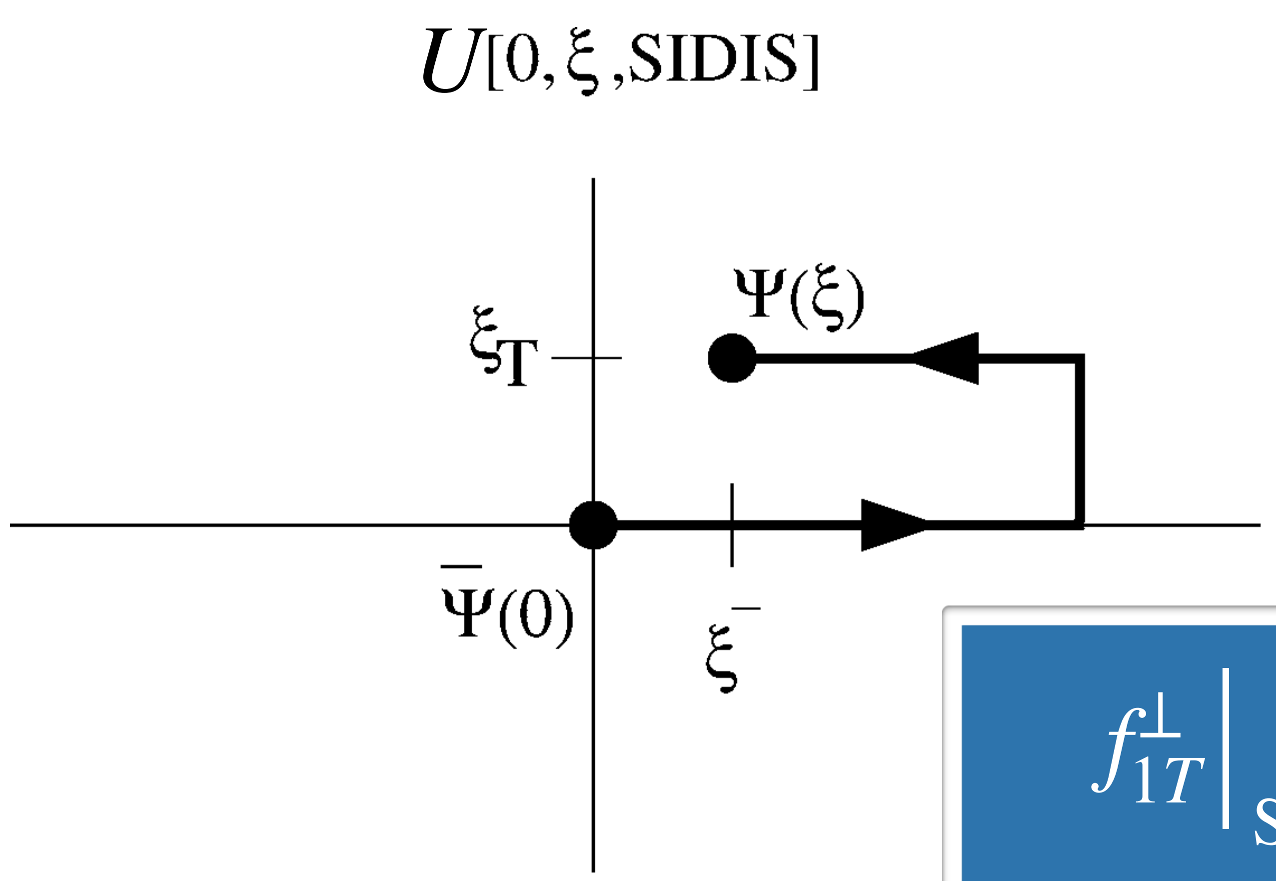

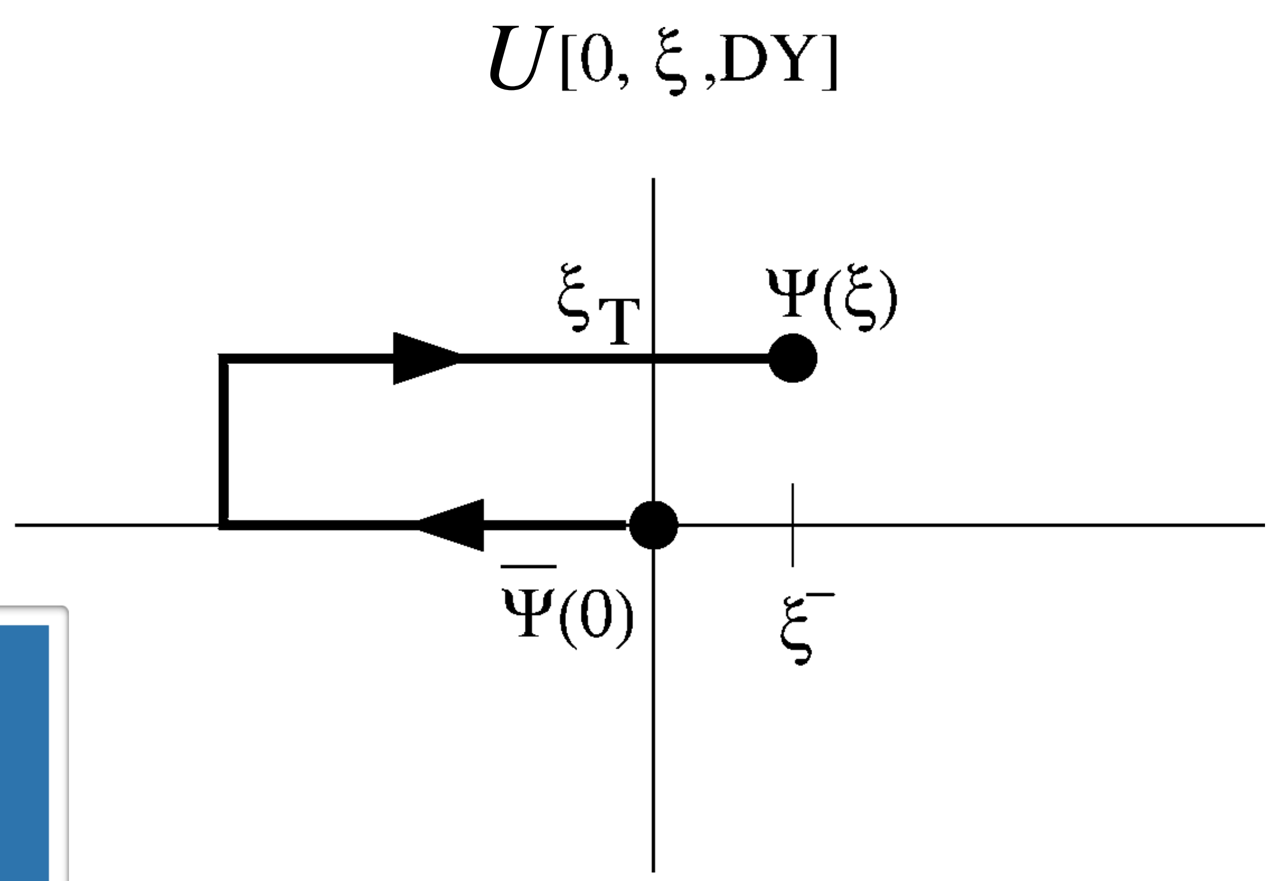

$$f_{1T}^{\perp}\Big|_{\text{SIDIS}} = -f_{1T}^{\perp}\Big|_{\text{DY}}$$

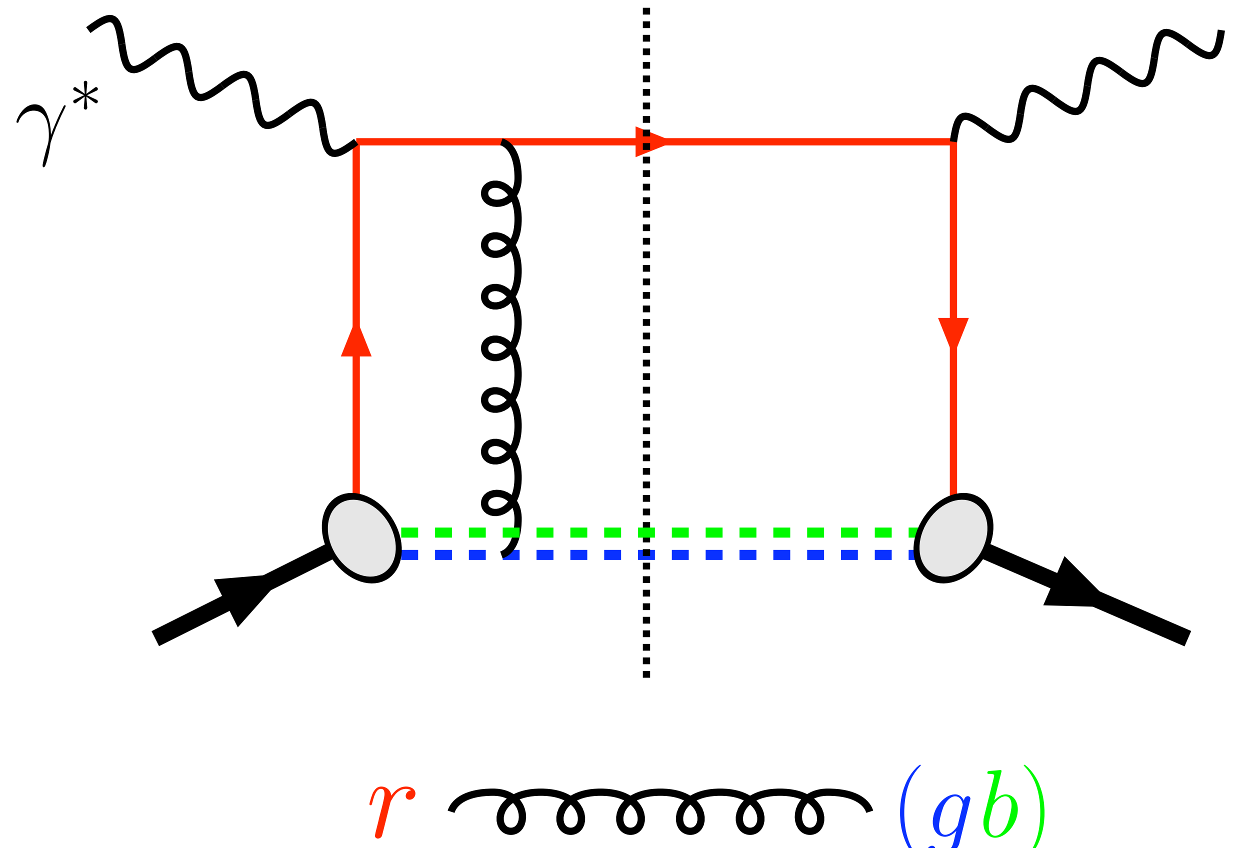

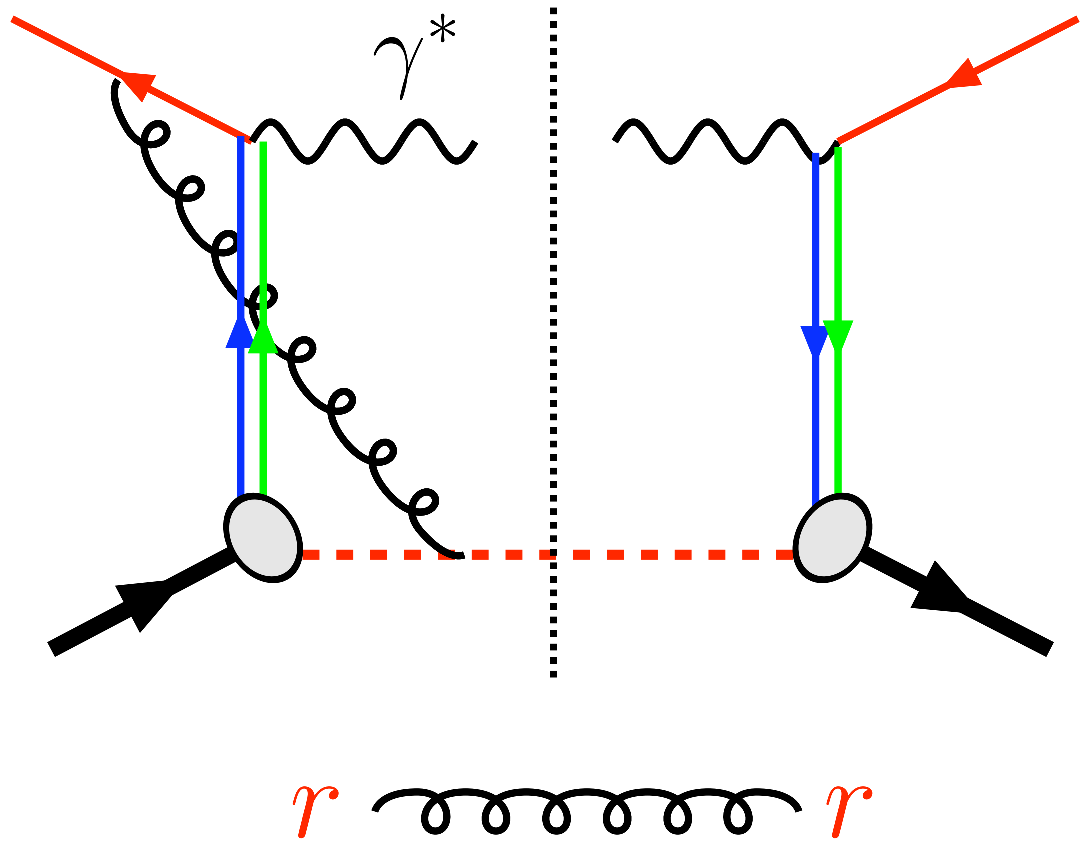

SIDIS

Drell-Yan

Experimental access to Sivers in Drell-Yan

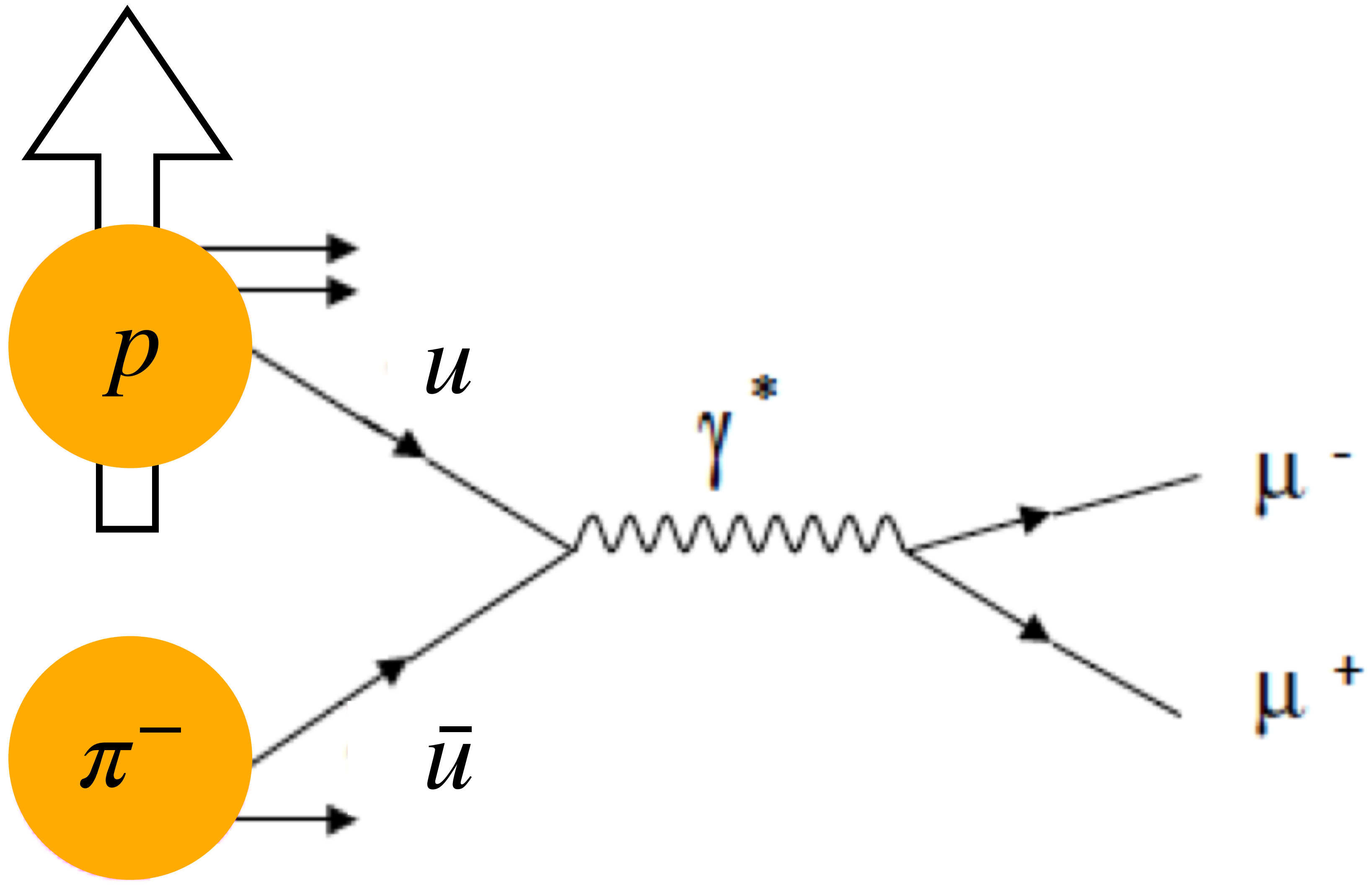

Experimental access to Sivers in Drell-Yan

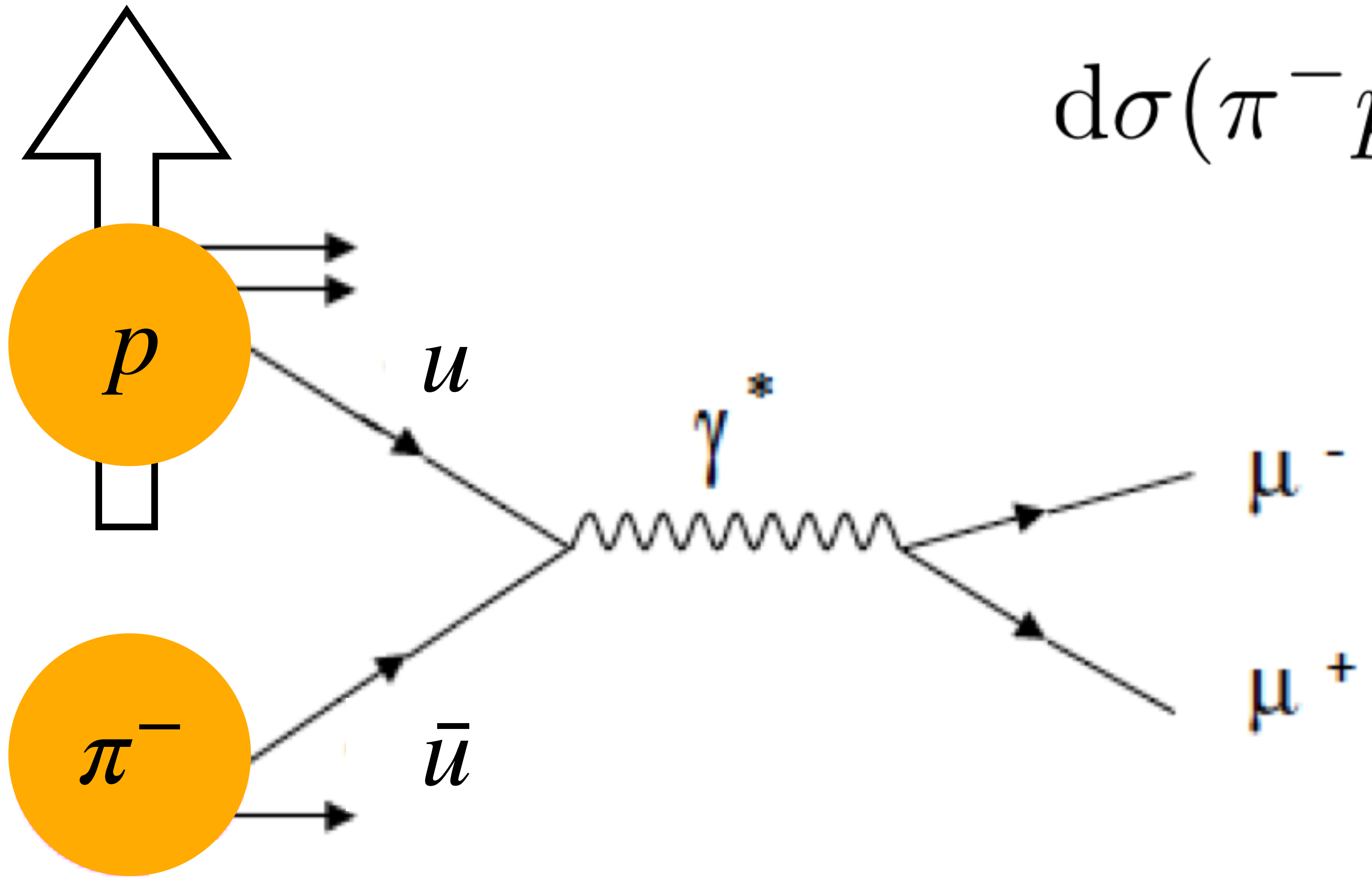

$$\mathrm{d}\sigma(\pi^- p^\uparrow \to \mu^+\mu^- X) \sim 1 + \overline{h}_1^\perp \otimes h_1^\perp \cos(2\phi)$$
$$+|S_T| \;\; \overline{f}_1 \otimes f_{1T}^\perp \sin\phi_S$$
$$+|S_T| \;\; \overline{h}_1^\perp \otimes h_{1T}^\perp \sin(2\phi+\phi_S)$$
$$+|S_T| \;\; \overline{h}_1^\perp \otimes h_{1T} \sin(2\phi-\phi_S)$$

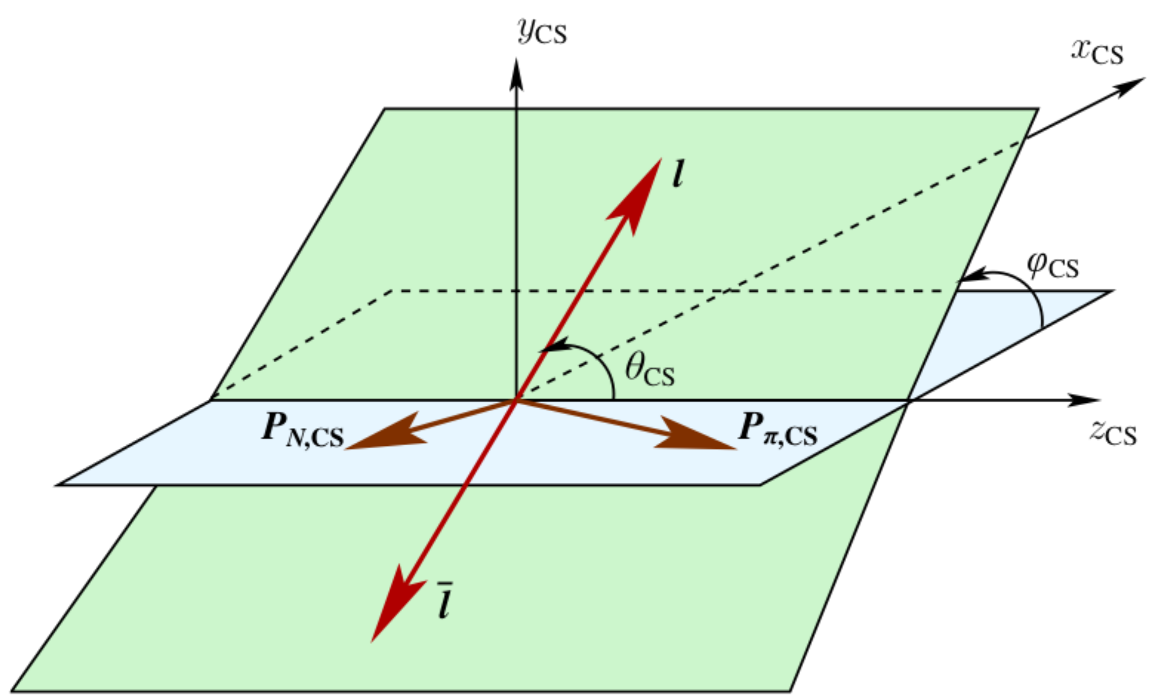

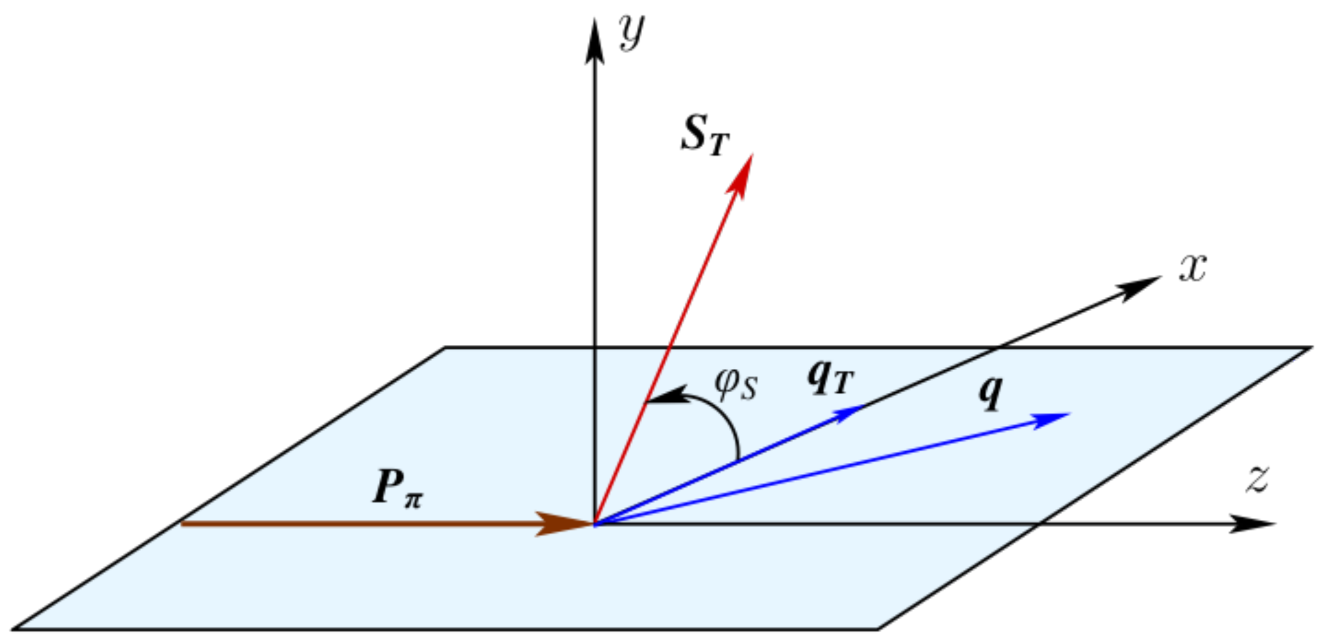

Experimental access to Sivers in Drell-Yan

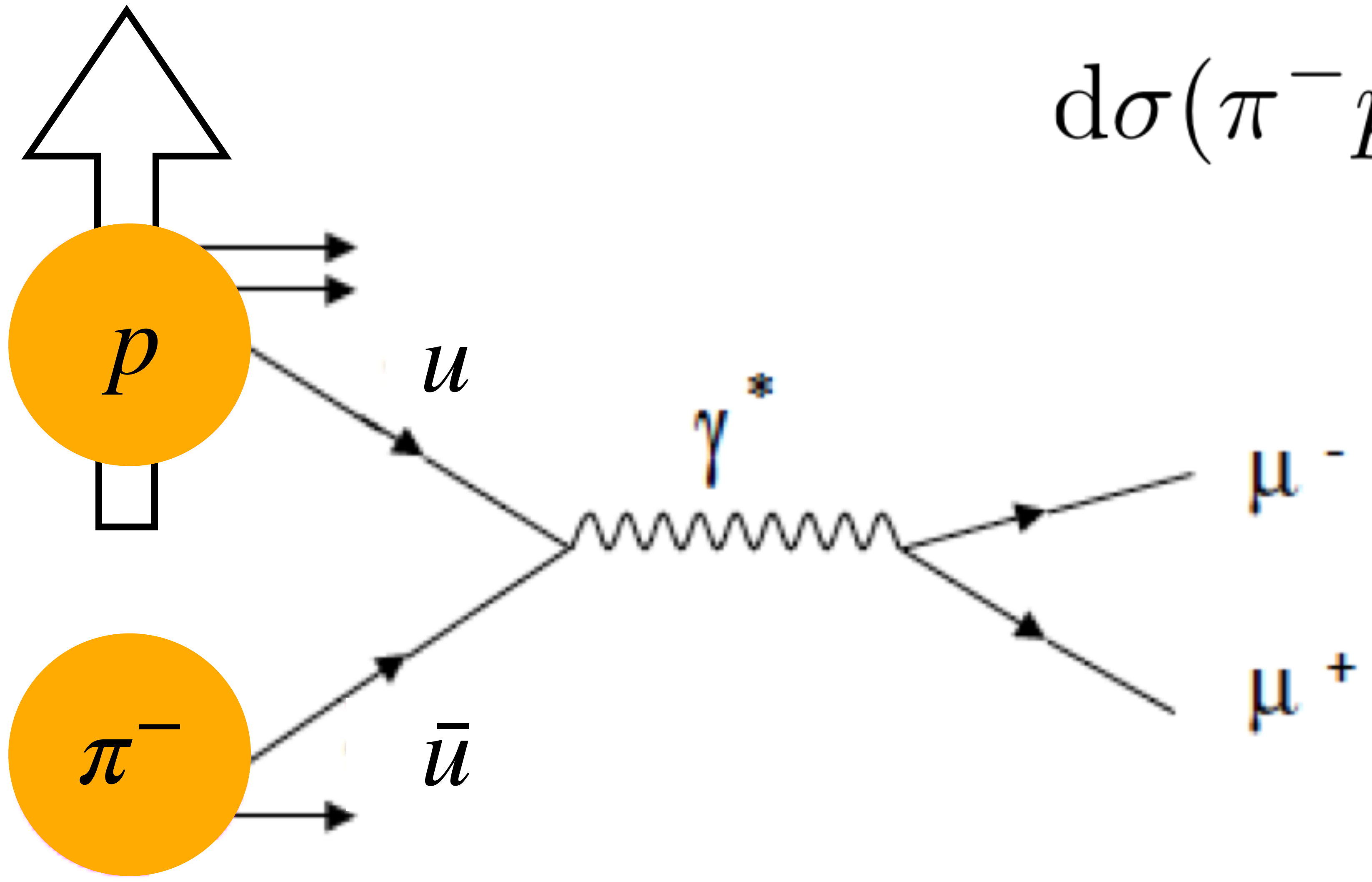

$$\mathrm{d}\sigma(\pi^- p^\uparrow \to \mu^+\mu^- X) \sim 1 + \overline{h}_1^\perp \otimes h_1^\perp \cos(2\phi)$$
$$+|S_T| \;\; \overline{f}_1 \otimes f_{1T}^\perp \sin\phi_S$$
$$+|S_T| \;\; \overline{h}_1^\perp \otimes h_{1T}^\perp \sin(2\phi + \phi_S)$$
$$+|S_T| \;\; \underbrace{\overline{h}_1^\perp}_{\pi^-} \otimes \underbrace{h_{1T}}_{p} \sin(2\phi - \phi_S)$$

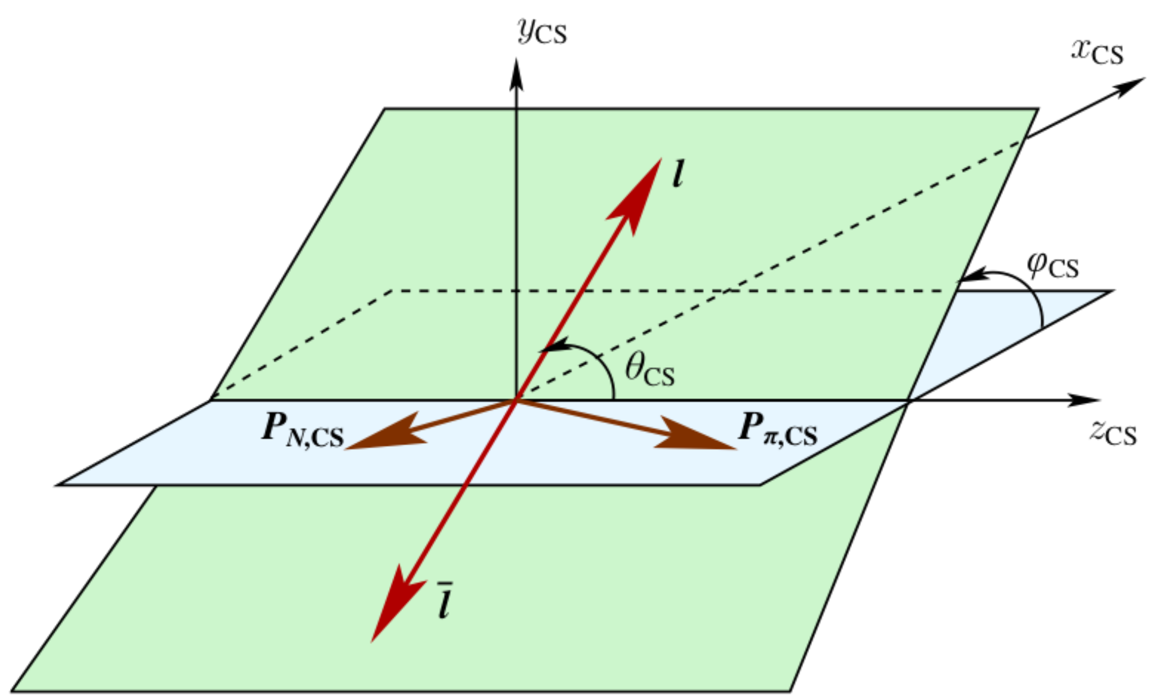

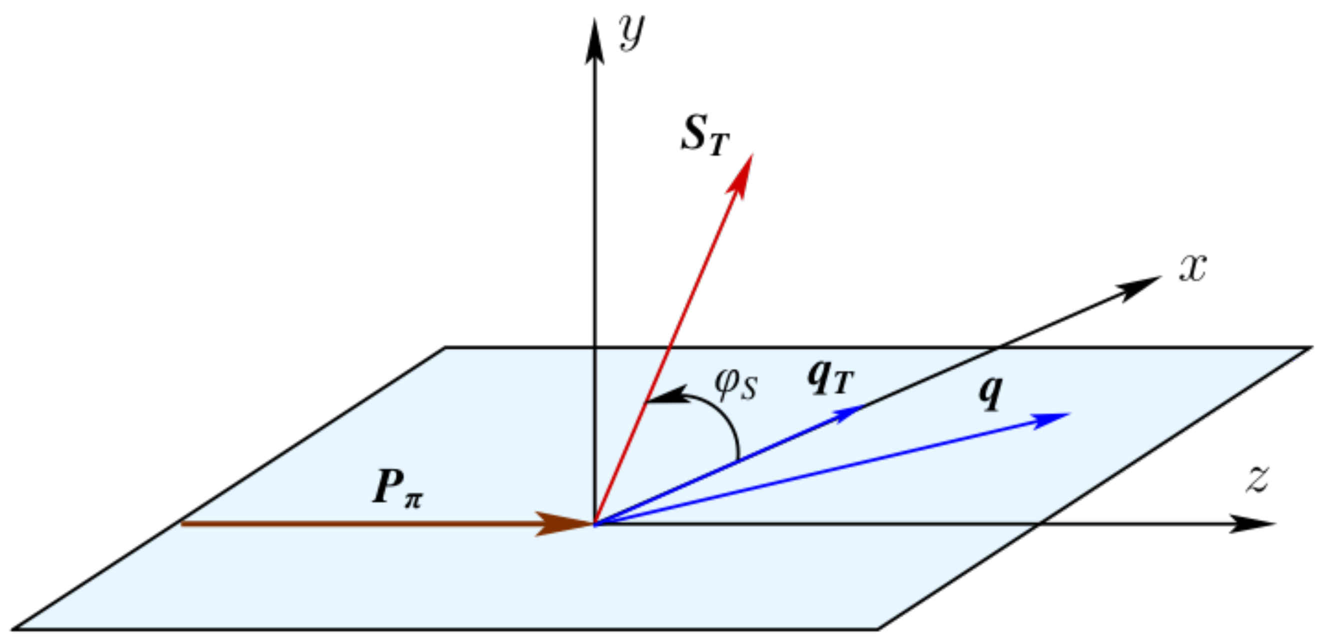

Experimental access to Sivers in Drell-Yan

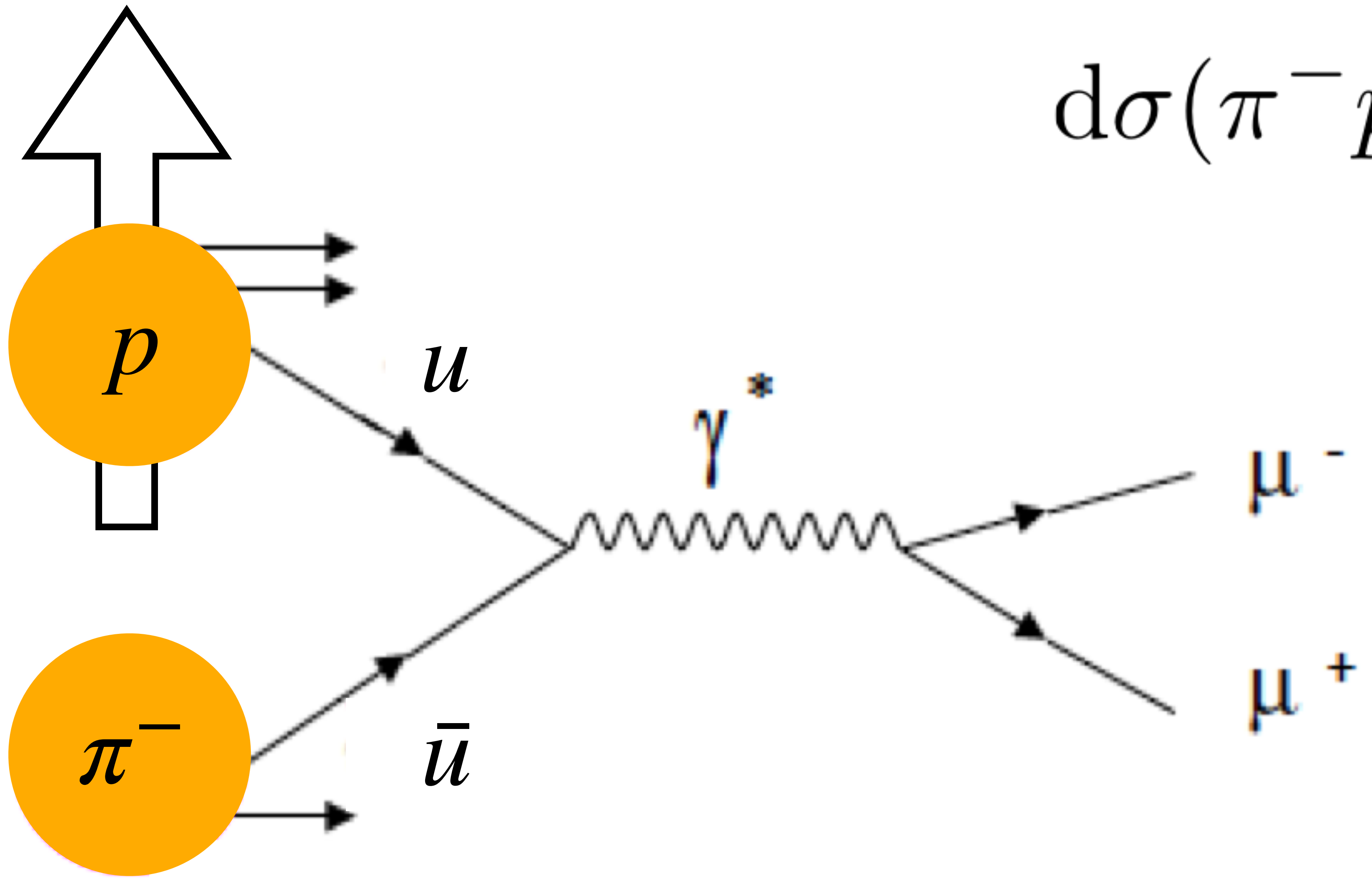

$$\begin{aligned} d\sigma(\pi^- p^\uparrow \to \mu^+\mu^- X) \sim\ & 1 + \overline{h}_1^\perp \otimes h_1^\perp \cos(2\phi) \\ & + |S_T|\ \ \overline{f}_1 \otimes f_{1T}^\perp \sin\phi_S \\ & + |S_T|\ \ \overline{h}_1^\perp \otimes h_{1T}^\perp \sin(2\phi + \phi_S) \\ & + |S_T|\ \ \underbrace{\overline{h}_1^\perp}_{\pi^-} \otimes \underbrace{h_{1T}}_{p} \sin(2\phi - \phi_S) \end{aligned}$$

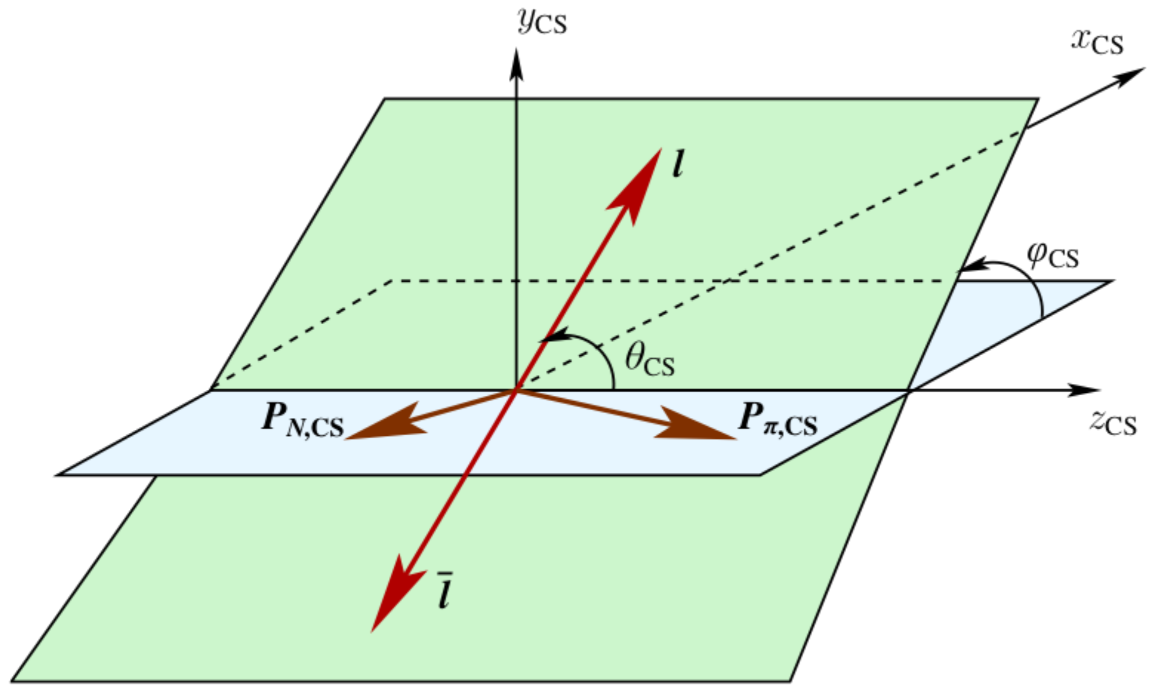

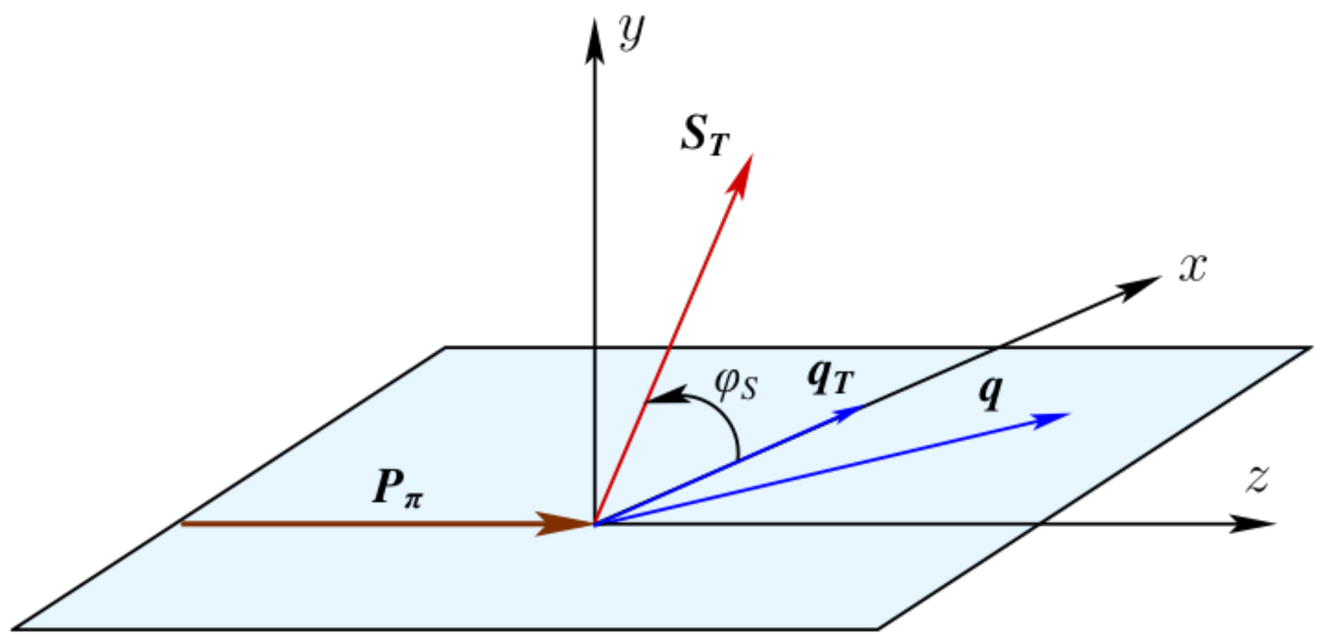

Investigation of the Sivers sign change in $p^{\uparrow}\pi^{-}$ collisions

M. Anselmino et al., JHEP **04** (2017) 046

M. G. Echevarria et al. PRD **89** (2014)074013

P. Sun, F. Yuan, PRD **88** (2013) 114012

COMPASS, PRL **119** (2017) 112002

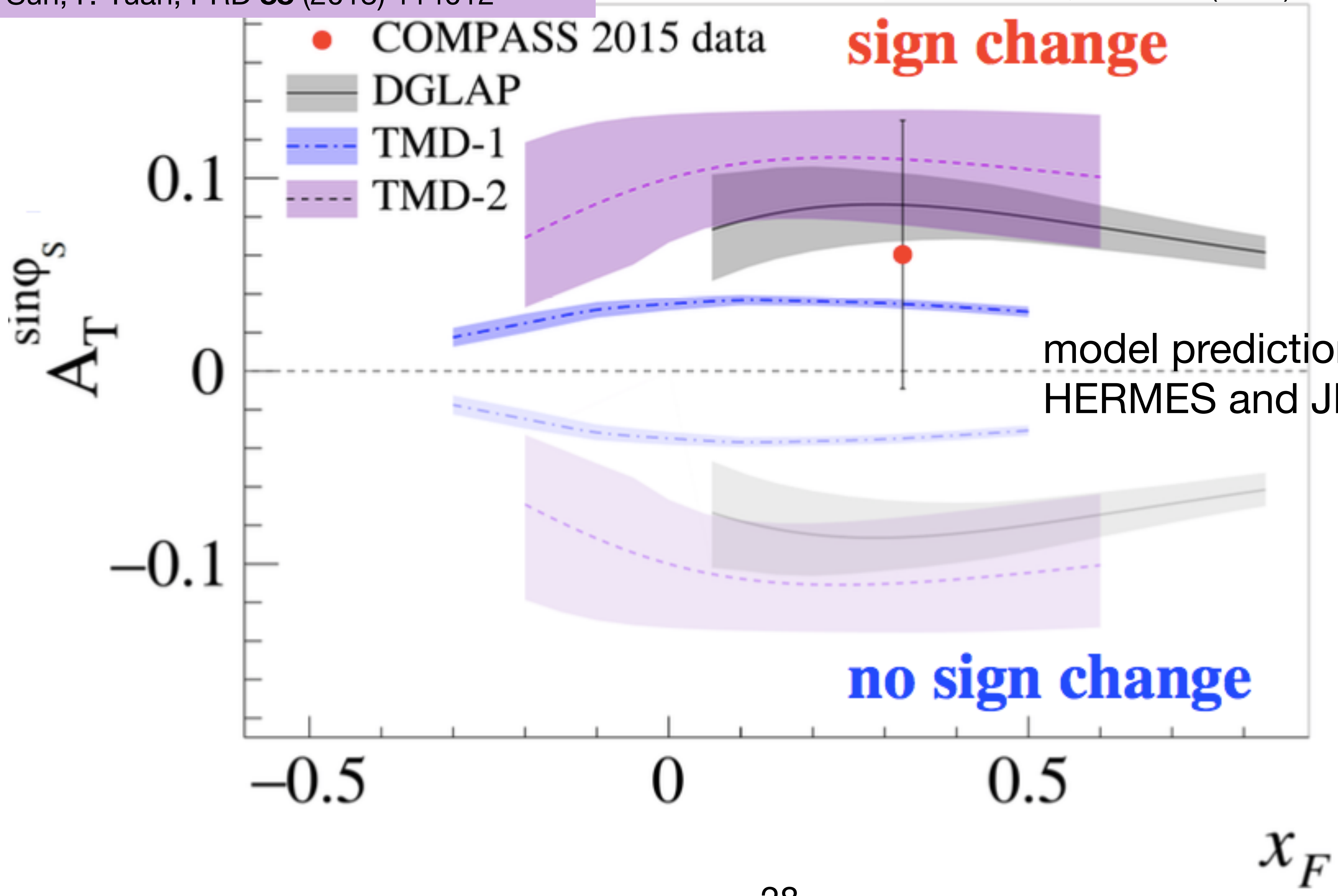

model predictions based on COMPASS, HERMES and JLab semi-inclusive DIS data

Investigation of the Sivers sign change in $p^{\uparrow}p$ collisions

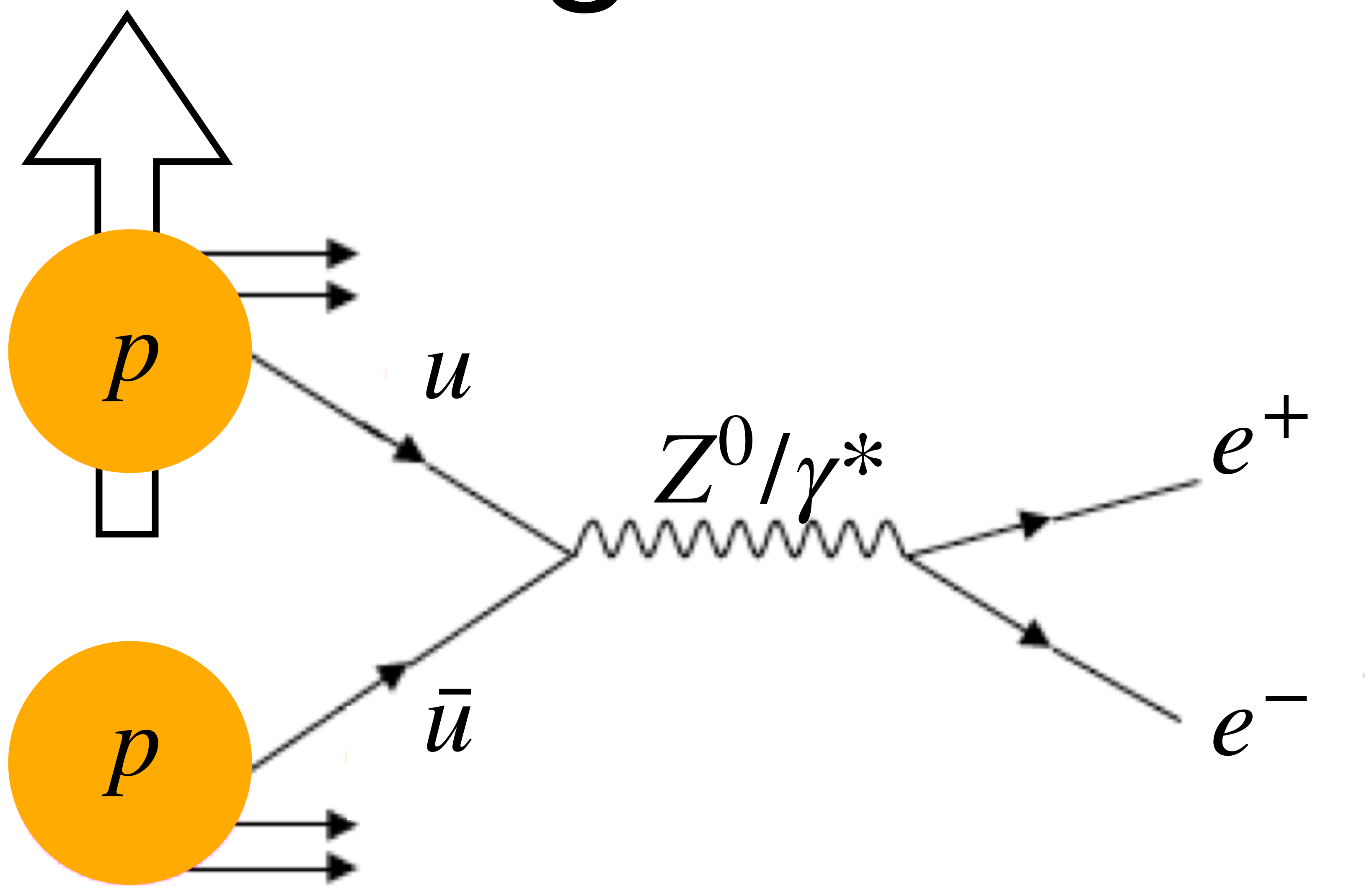

arXiv:2308.15496v1

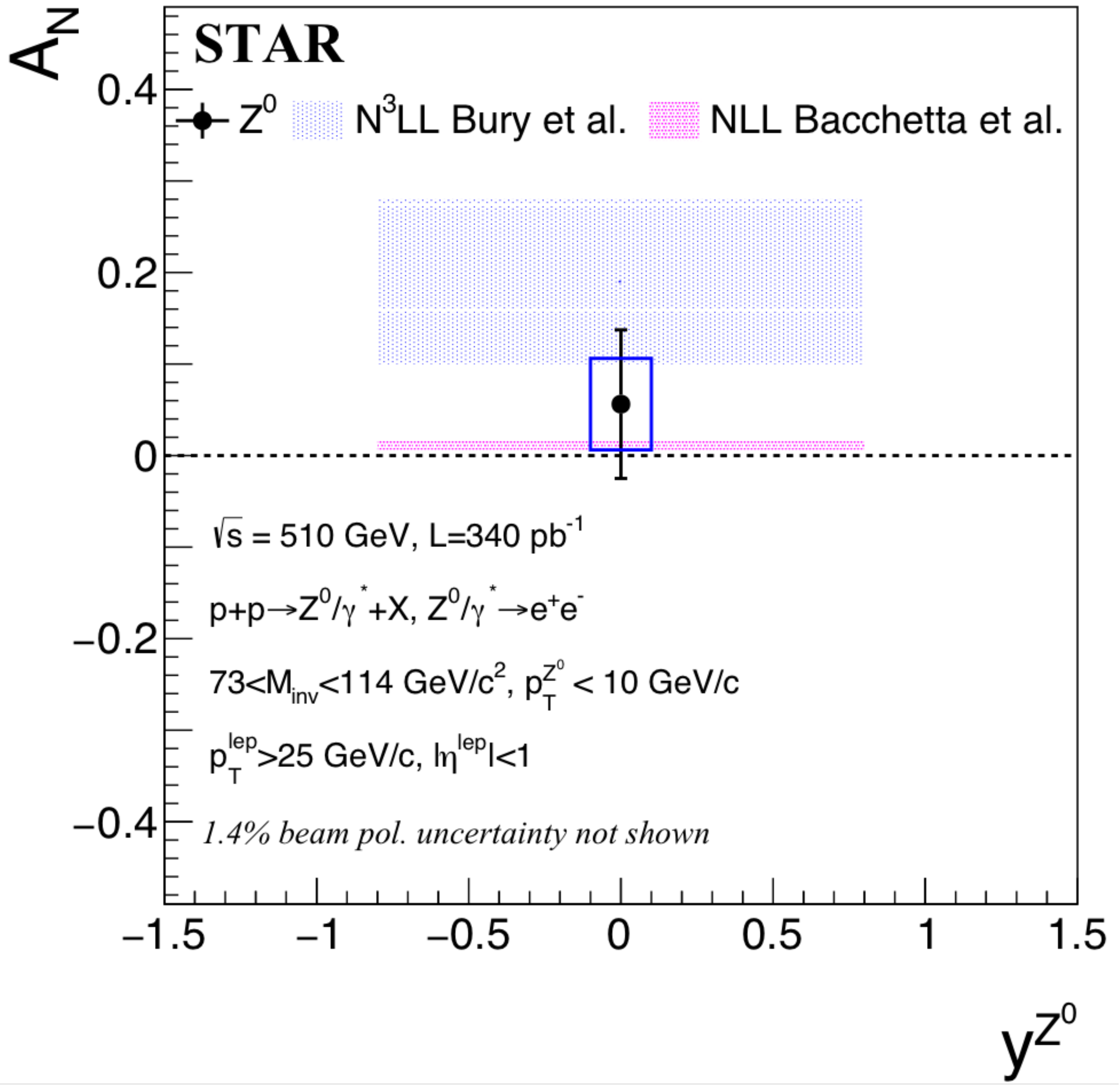

Investigation of the Sivers sign change in $p^{\uparrow}p$ collisions

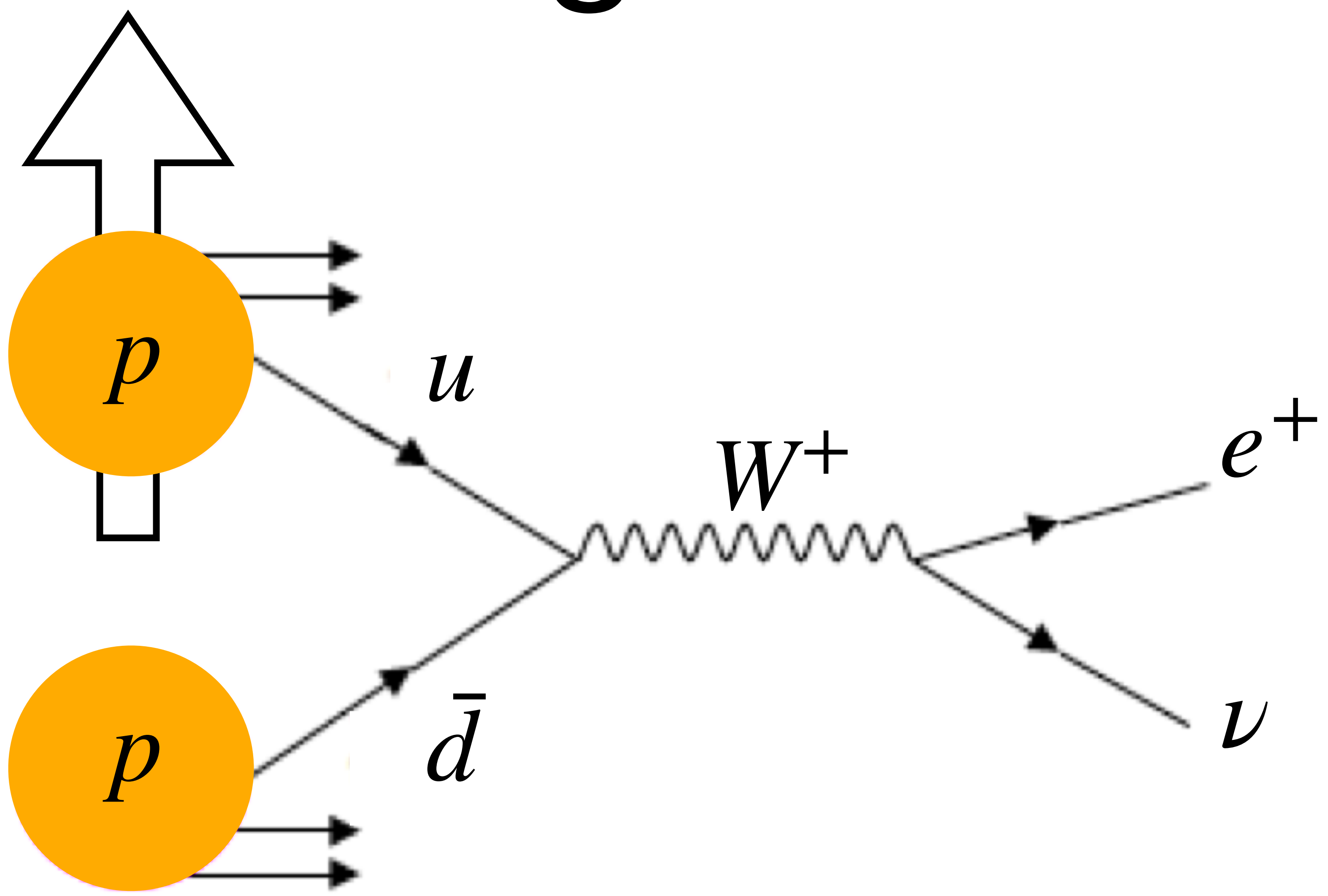

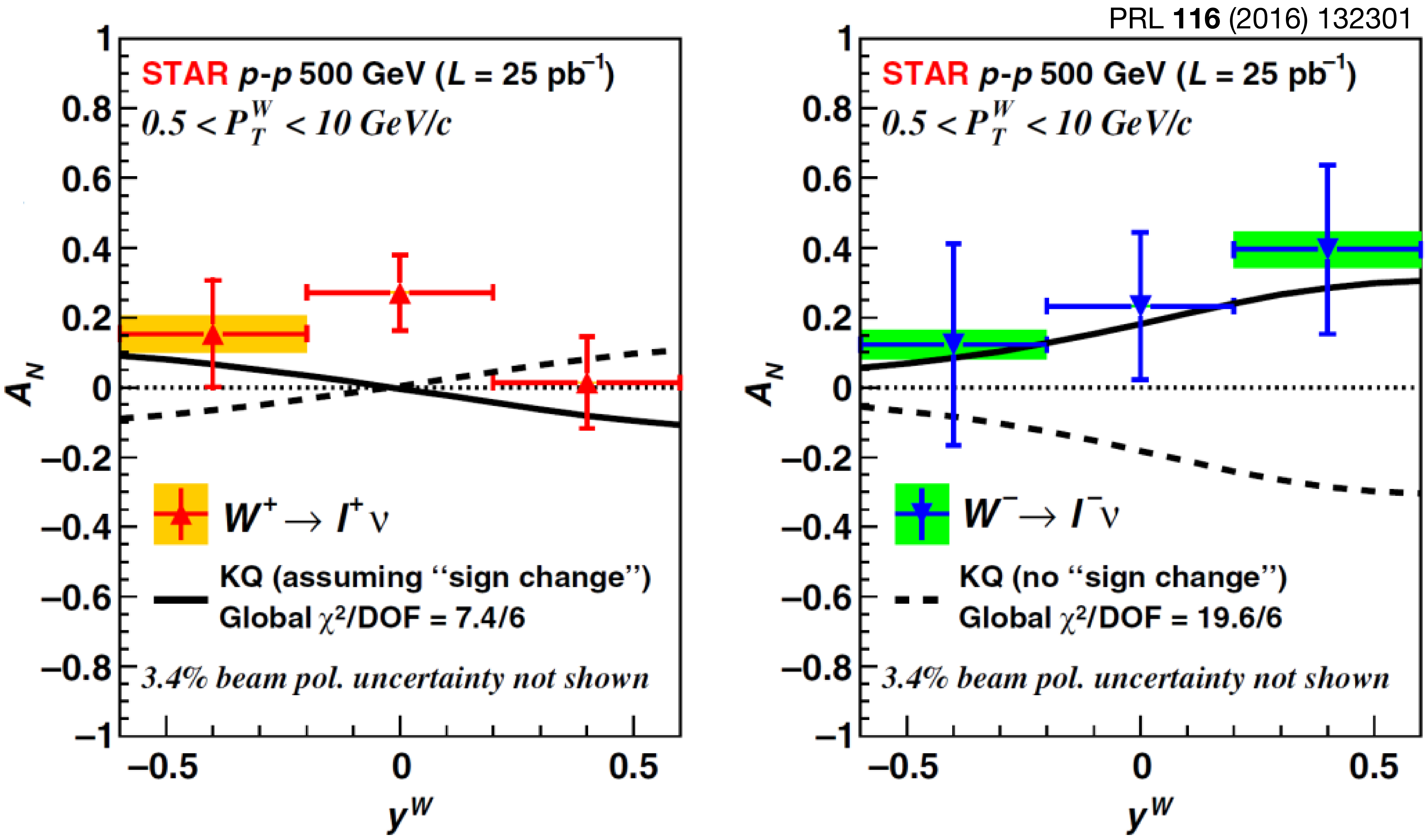

$$x_{1,2} = \frac{Q}{\sqrt{s}} e^{\pm y}$$

Boer-Mulders modulation

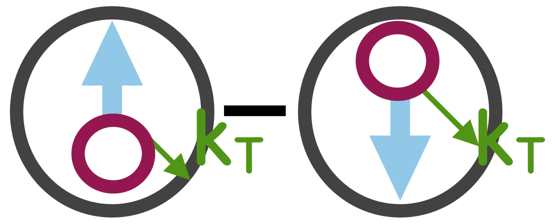

$$\mathscr{C}\left[h_1^{\perp,q} \times H_1^{\perp,q}\right]$$

Boer-Mulders modulation

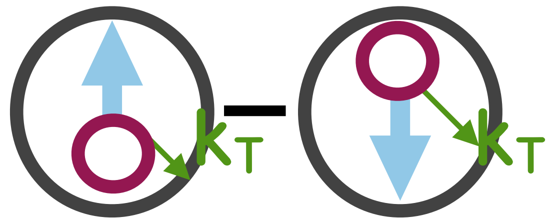

$$\mathscr{C}\left[h_1^{\perp,q}\times H_1^{\perp,q}\right]$$

Boer-Mulders PDF

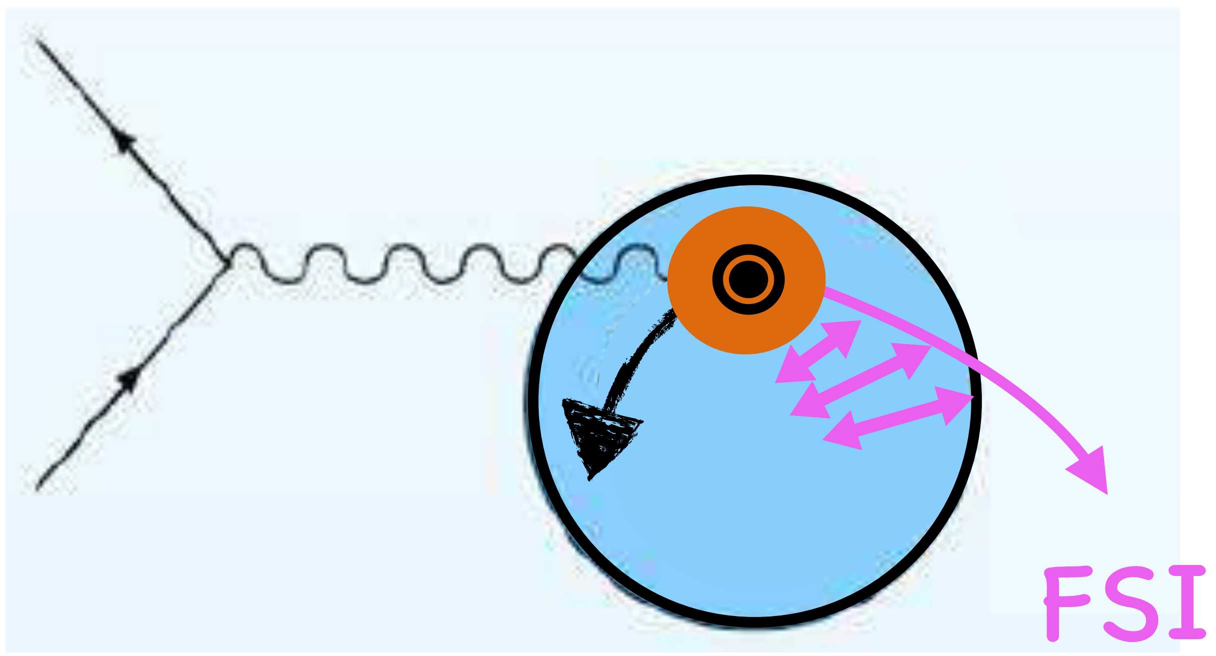

Boer-Mulders modulation

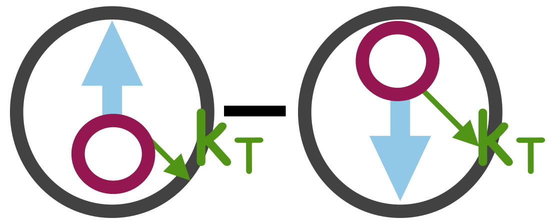

$$\mathscr{C}\left[h_1^{\perp,q} \times H_1^{\perp,q}\right]$$

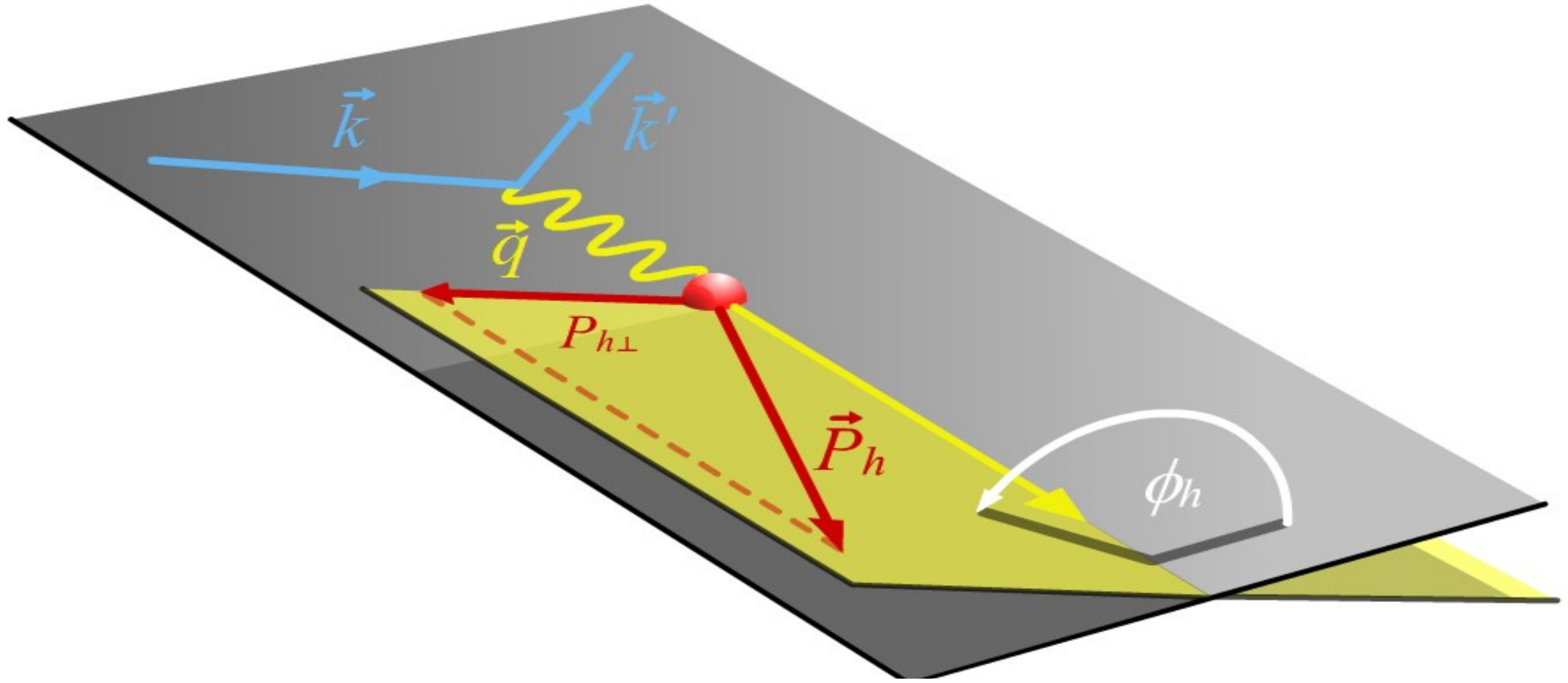

Boer-Mulders PDF

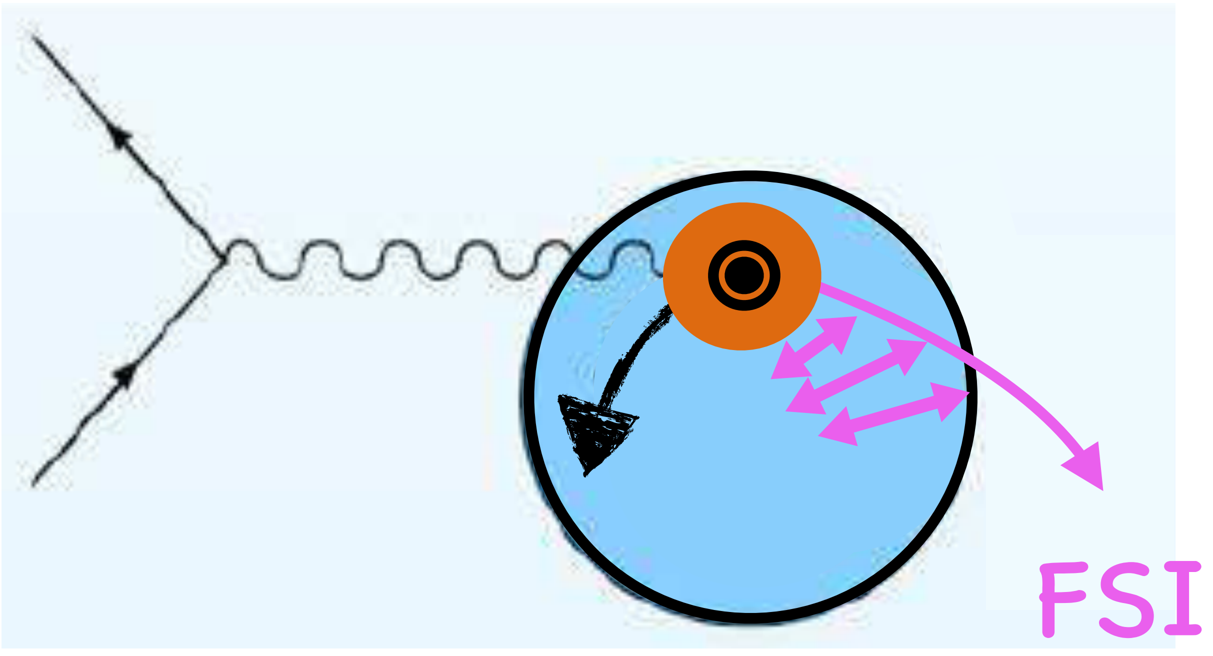

$$\cos(2\phi_h)\sum_q e_q^2\, C\left[h_1^{\perp,q}(x,k_\perp) \times H_1^{\perp,q}(z,p_\perp)\right]$$

Spin-dependence with unpolarised hadrons!

Boer-Mulders modulation

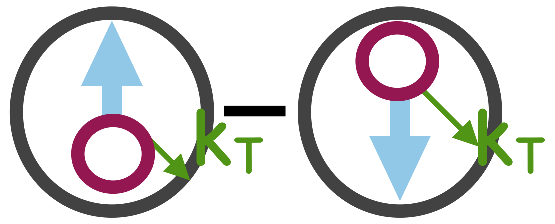

$$\mathscr{C}\left[h_1^{\perp,q} \times H_1^{\perp,q}\right]$$

Measurement in ep: $\langle\cos(2\phi_h)\rangle_{Born}(j)$ $\langle\cos(2\phi_h)\rangle_{meas}(i)$

Boer-Mulders modulation

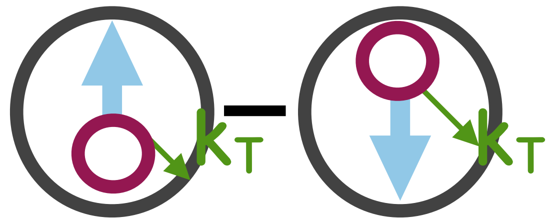

$\mathscr{C}\left[h_1^{\perp,q}\times H_1^{\perp,q}\right]$

Measurement in ep: $\langle\cos(2\phi_h)\rangle_{Born}(j)$ $\langle\cos(2\phi_h)\rangle_{meas}(i)$

- QED radiate effects

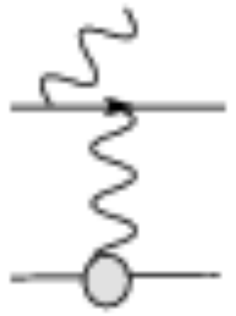

Boer-Mulders modulation

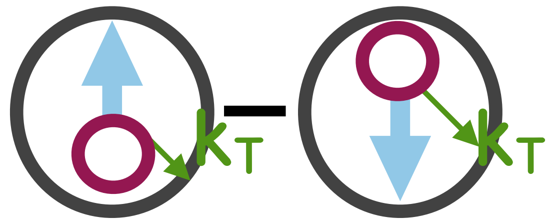

$\mathscr{C}\left[h_1^{\perp,q} \times H_1^{\perp,q}\right]$

Measurement in ep: $\langle\cos(2\phi_h)\rangle_{Born}(j)$ $\langle\cos(2\phi_h)\rangle_{meas}(i)$

- QED radiate effects 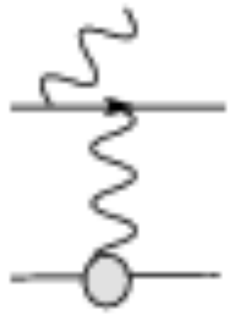
- limited geometric and kinematic acceptance of detector

Boer-Mulders modulation

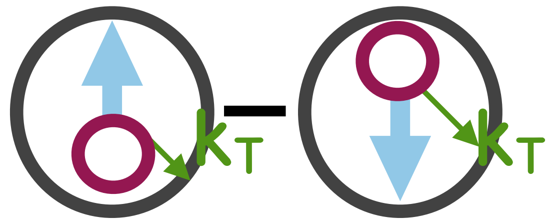

$\mathscr{C}\left[h_1^{\perp,q} \times H_1^{\perp,q}\right]$

Measurement in ep: $\langle\cos(2\phi_h)\rangle_{Born}(j)$ $\langle\cos(2\phi_h)\rangle_{meas}(i)$

- QED radiate effects

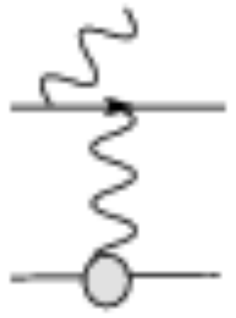

- limited geometric and kinematic acceptance of detector
- limited detector resolution

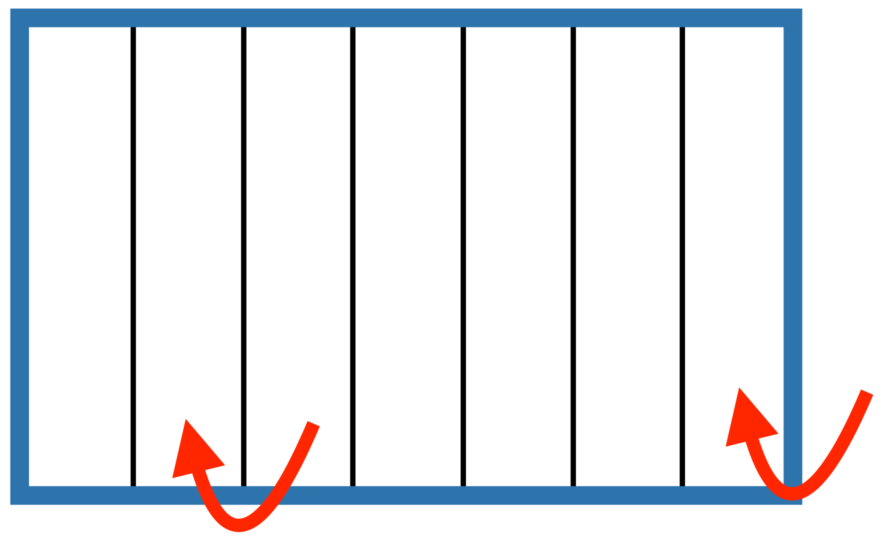

Boer-Mulders modulation

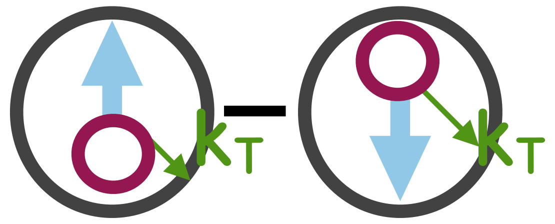

$\mathscr{C}\left[h_1^{\perp,q} \times H_1^{\perp,q}\right]$

Measurement in ep: $\langle\cos(2\phi_h)\rangle_{Born}(j)$ $\langle\cos(2\phi_h)\rangle_{meas}(i)$

- QED radiate effects

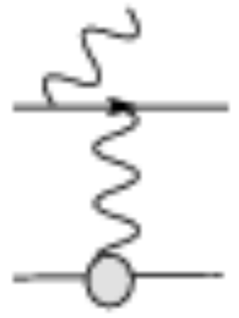

- limited geometric and kinematic acceptance of detector
- limited detector resolution

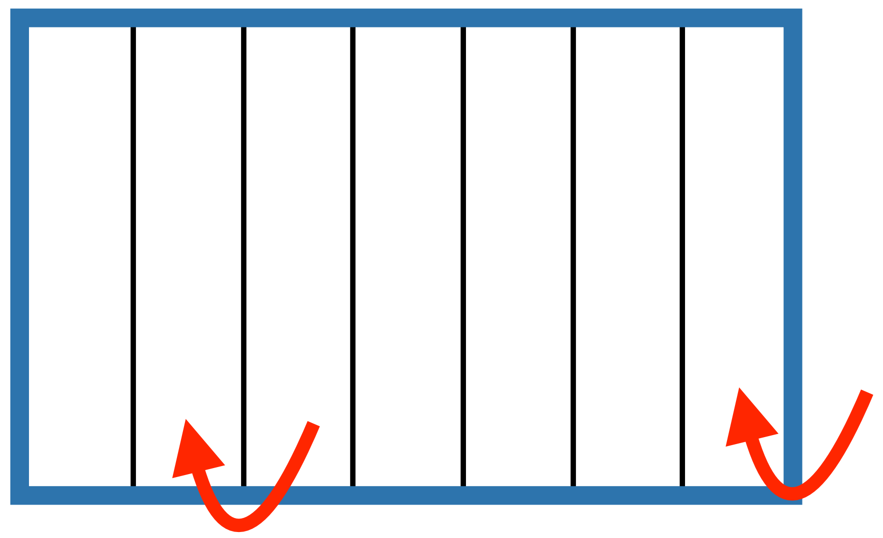

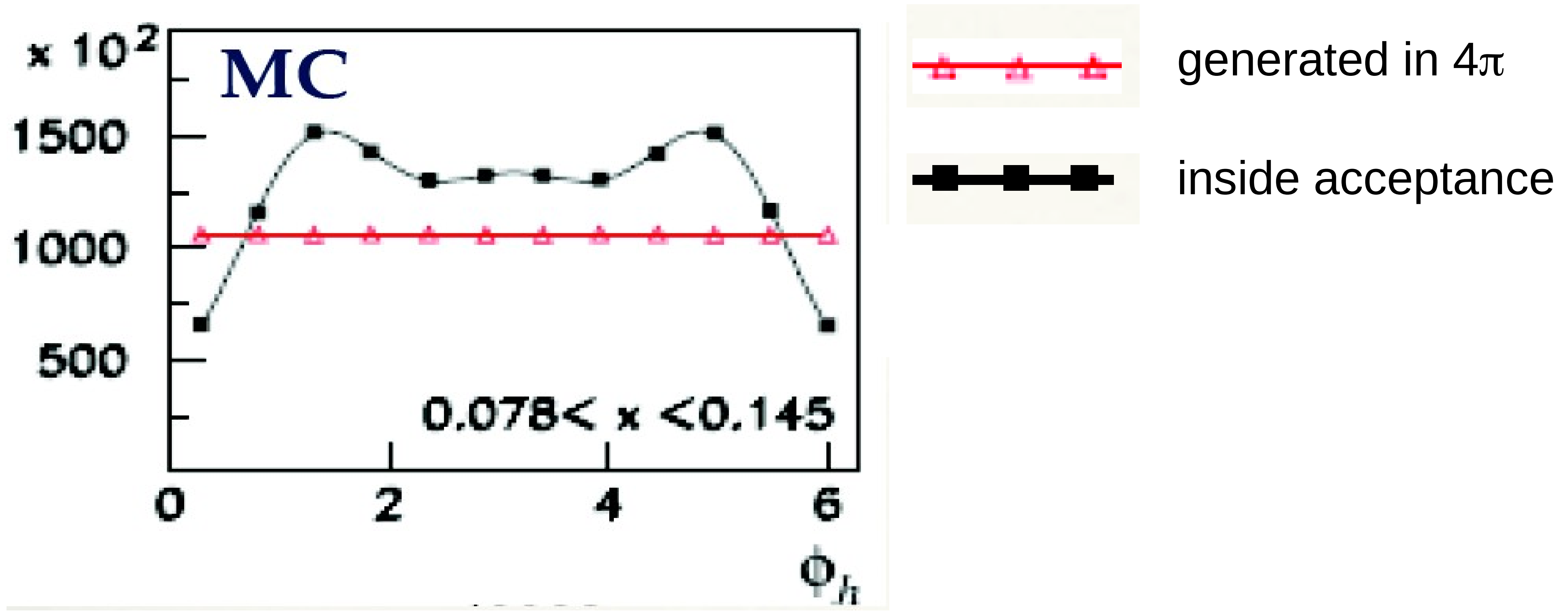

Boer-Mulders modulation

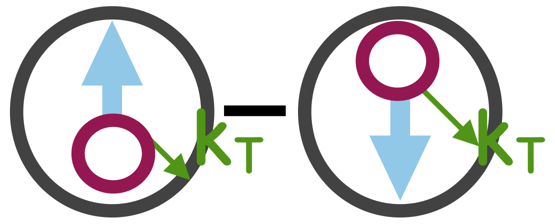

$\mathscr{C}\left[h_1^{\perp,q} \times H_1^{\perp,q}\right]$

Measurement in ep:

Fully differential analysis

Unfolding in 400 x 12 bins

BINNING 400 kinematic bins x 12 ϕ-bins							
Variable	Bin limits						#
x	0.023	0.042	0.078	0.145	0.27	1	5
y	0.3	0.45	0.6	0.7	0.85		4
z	0.2	0.3	0.45	0.6	0.75	1	5
P_{hT}	0.05	0.2	0.35	0.5	0.75		4

tector

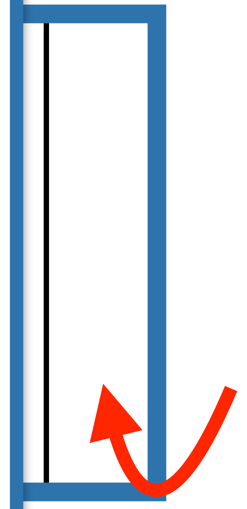

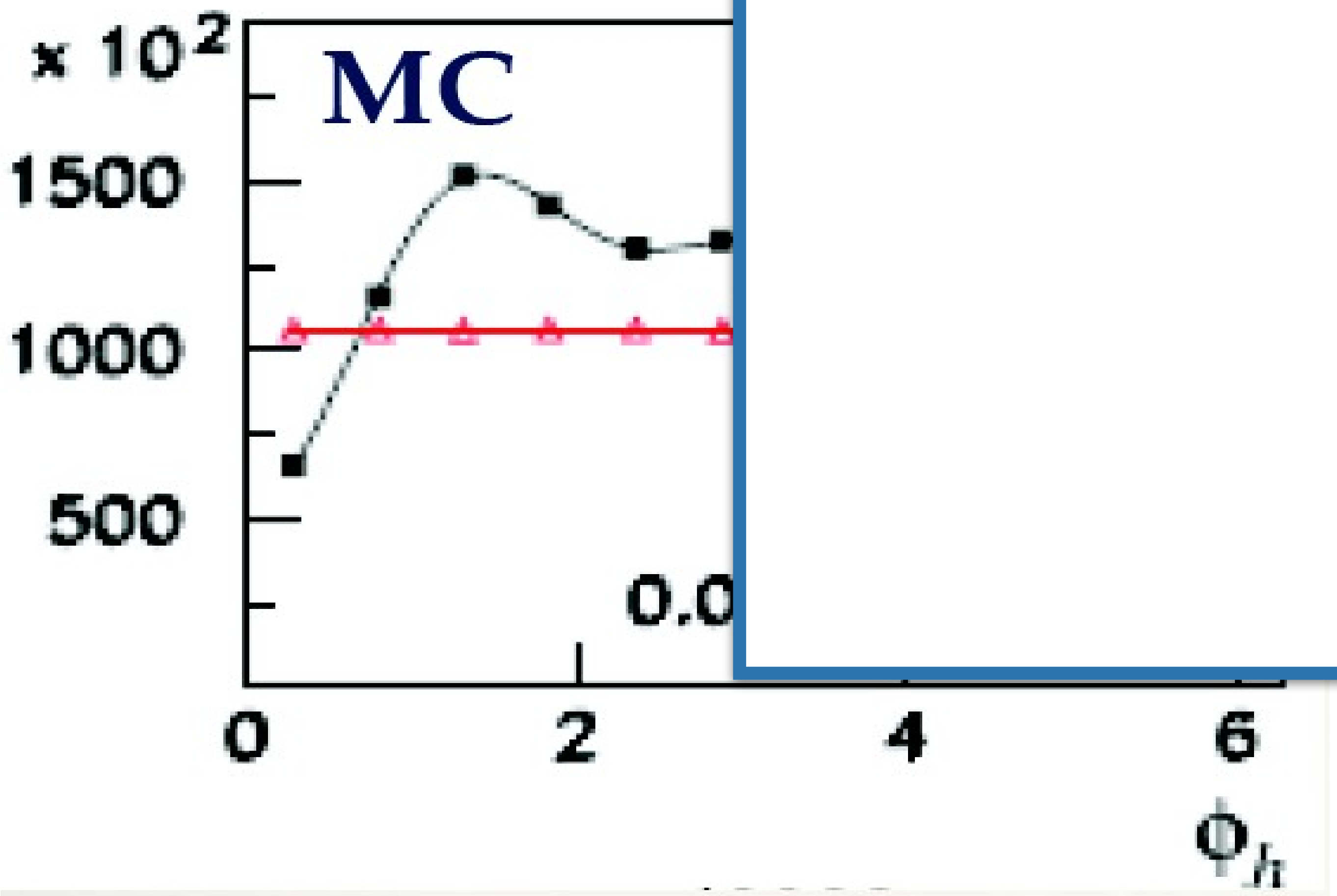

Boer-Mulders asymmetries

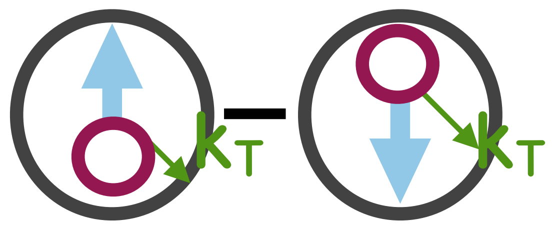

$\mathcal{C}\left[h_1^{\perp,q} \times H_1^{\perp,q}\right]$

A. Airapetian et al., Phys. Rev. D**87** (2013) 012010

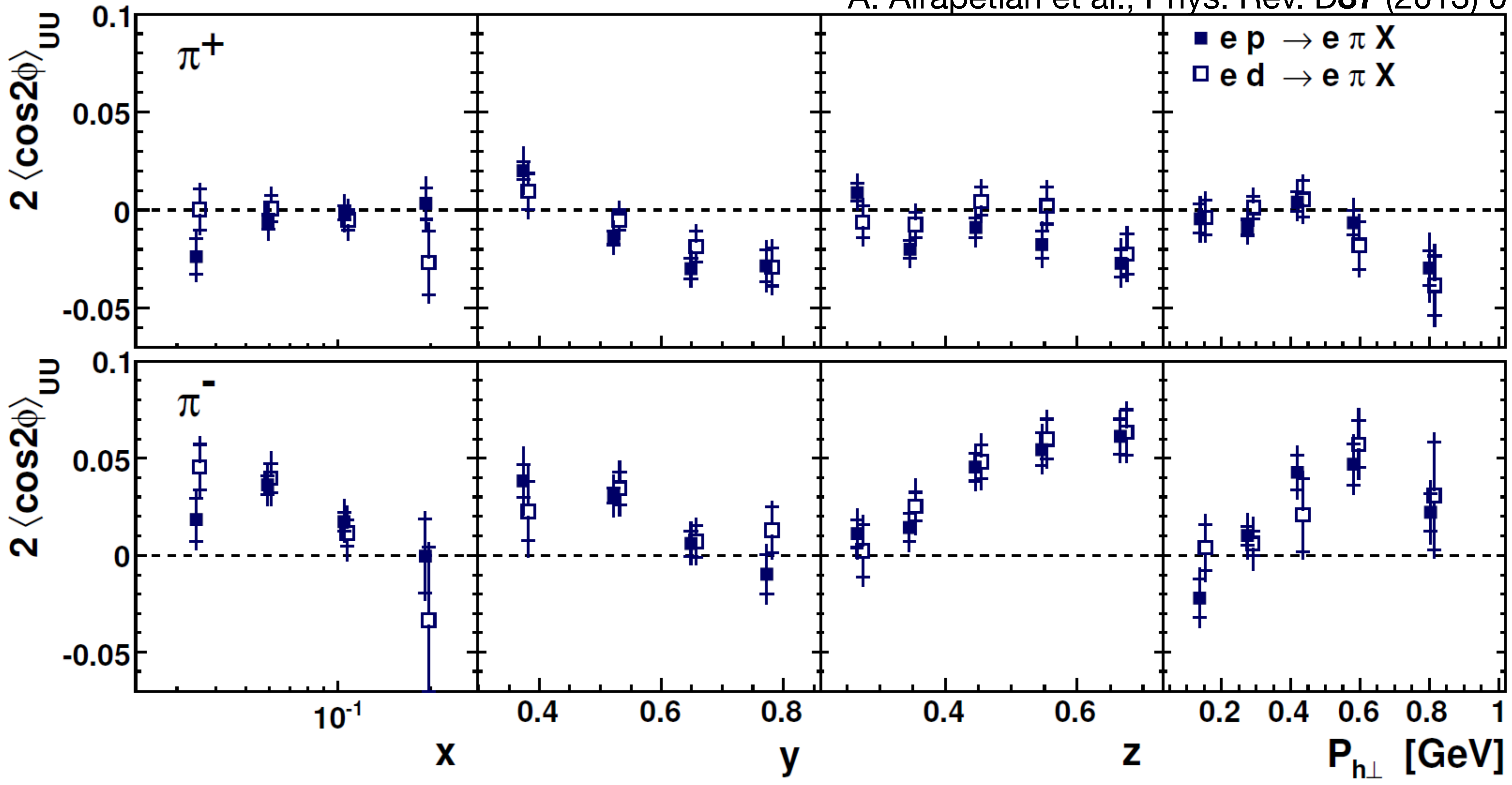

H–D comparison: $h_1^{\perp,u} \approx h_1^{\perp,d}$

Negative for π^+; positive for π^- $\rightarrow H_1^{\perp,fav} \approx -H_1^{\perp,disfav}$

Boer-Mulders asymmetries

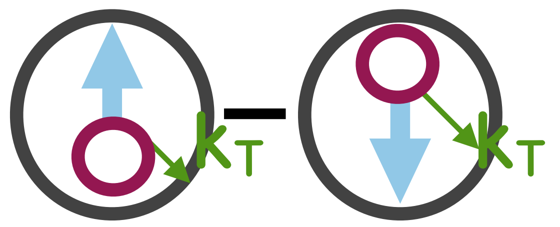

$\mathscr{C}\left[h_1^{\perp,q} \times H_1^{\perp,q}\right]$

A. Airapetian et al., Phys. Rev. D**87** (2013) 012010

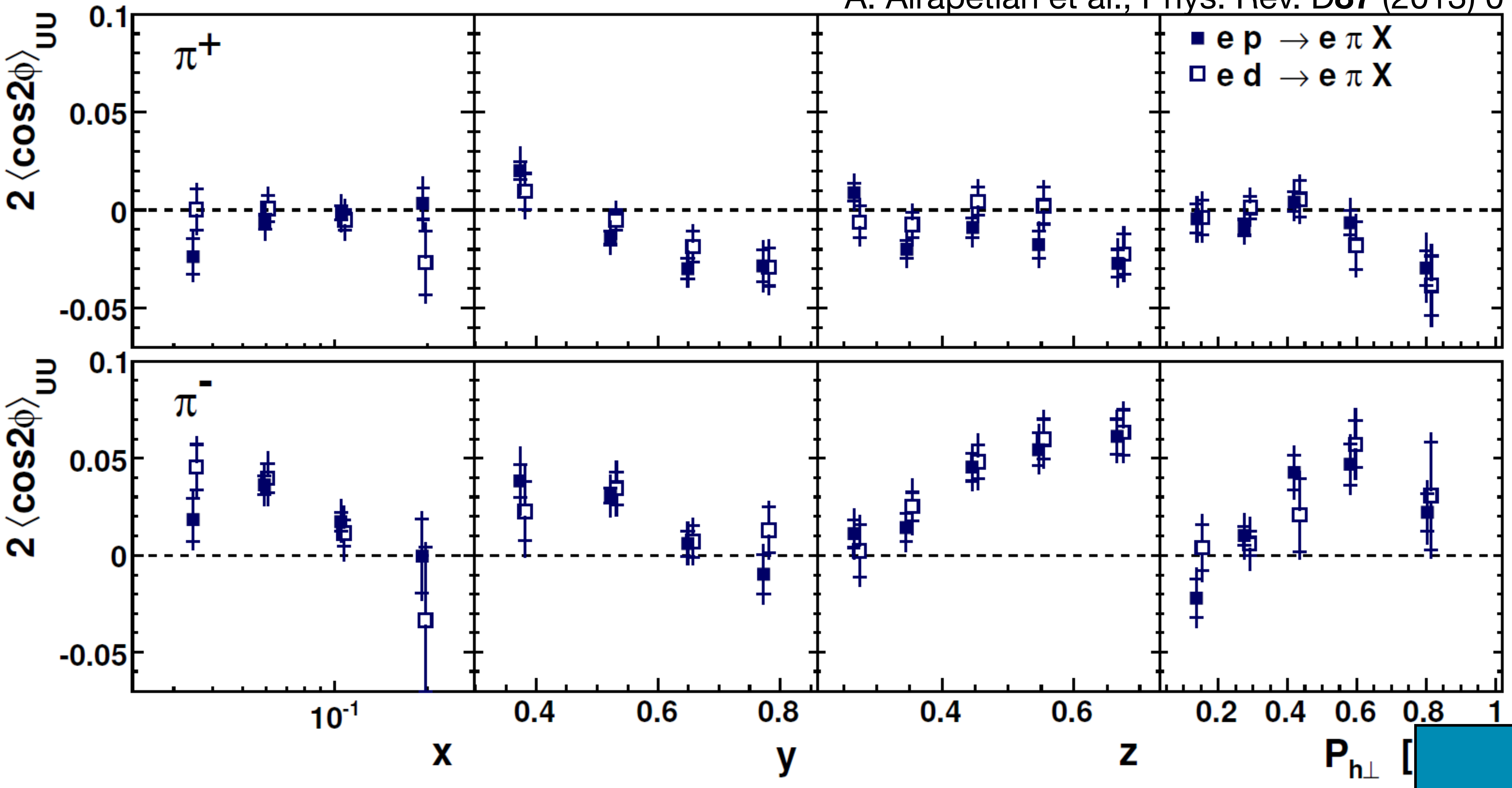

Measurement also possible in Drell Yan.

H–D comparison: $h_1^{\perp,u} \approx h_1^{\perp,d}$

Negative for π^+; positive for π^- $\rightarrow H_1^{\perp,fav} \approx -H_1^{\perp,disfav}$

Gluon TMD PDFs

gluon polarisation

nucleon polarisation	U	circular	linear
U	f_1^g		$h_1^{\perp g}$
L		g_1^g	$h_{1L}^{\perp g}$
T	$f_{1T}^{\perp g}$	g_{1T}^g	h_1^g, $h_{1T}^{\perp g}$

Gluon TMD PDFs

gluon polarisation

nucleon polarisation

	U	circular	linear
U	f_1^g		$h_1^{\perp g}$
L		g_1^g	$h_{1L}^{\perp g}$
T	$f_{1T}^{\perp g}$	g_{1T}^g	h_1^g, $h_{1T}^{\perp g}$

- In contrast to quark TMDs, gluon TMDs are almost unknown

Gluon TMD PDFs

gluon polarisation (columns) / nucleon polarisation (rows)

	U	circular	linear
U	f_1^g		$h_1^{\perp g}$
L		g_1^g	$h_{1L}^{\perp g}$
T	$f_{1T}^{\perp g}$	g_{1T}^g	h_1^g, $h_{1T}^{\perp g}$

- In contrast to quark TMDs, gluon TMDs are almost unknown
- Accessible through production of dijets, high-P_T hadron pairs, quarkonia

Gluon TMD PDFs via $J/\psi J/\psi$ production

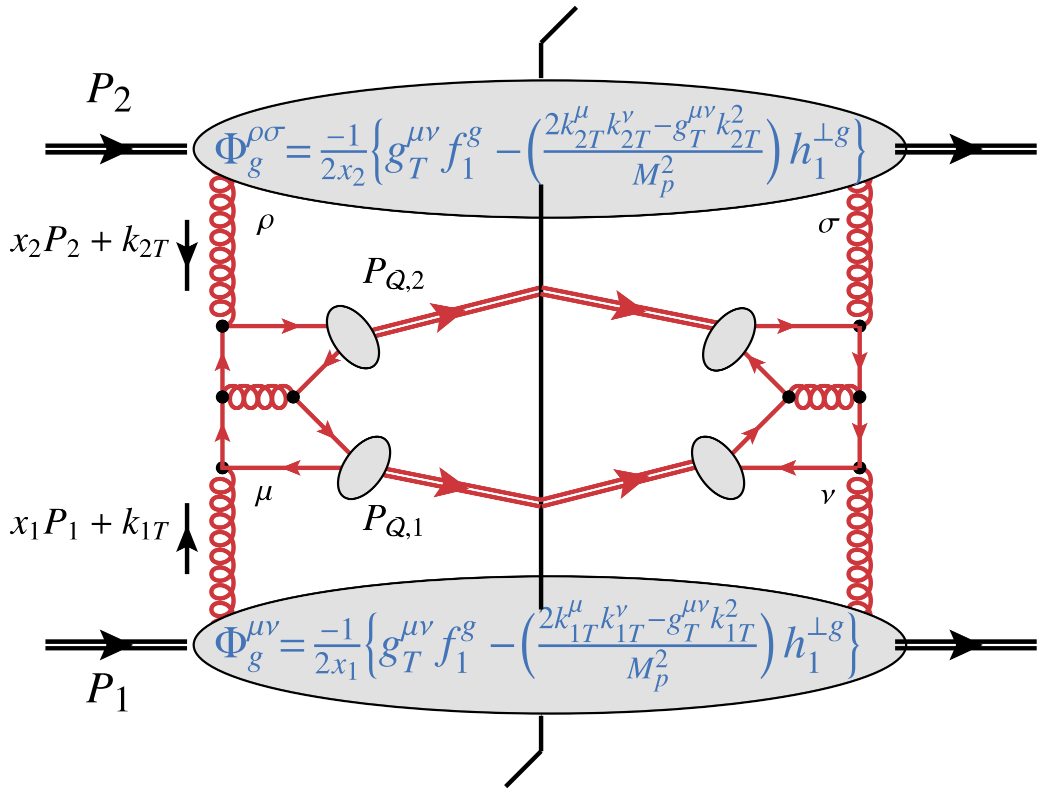

Gluon TMD PDFs via $J/\psi J/\psi$ production

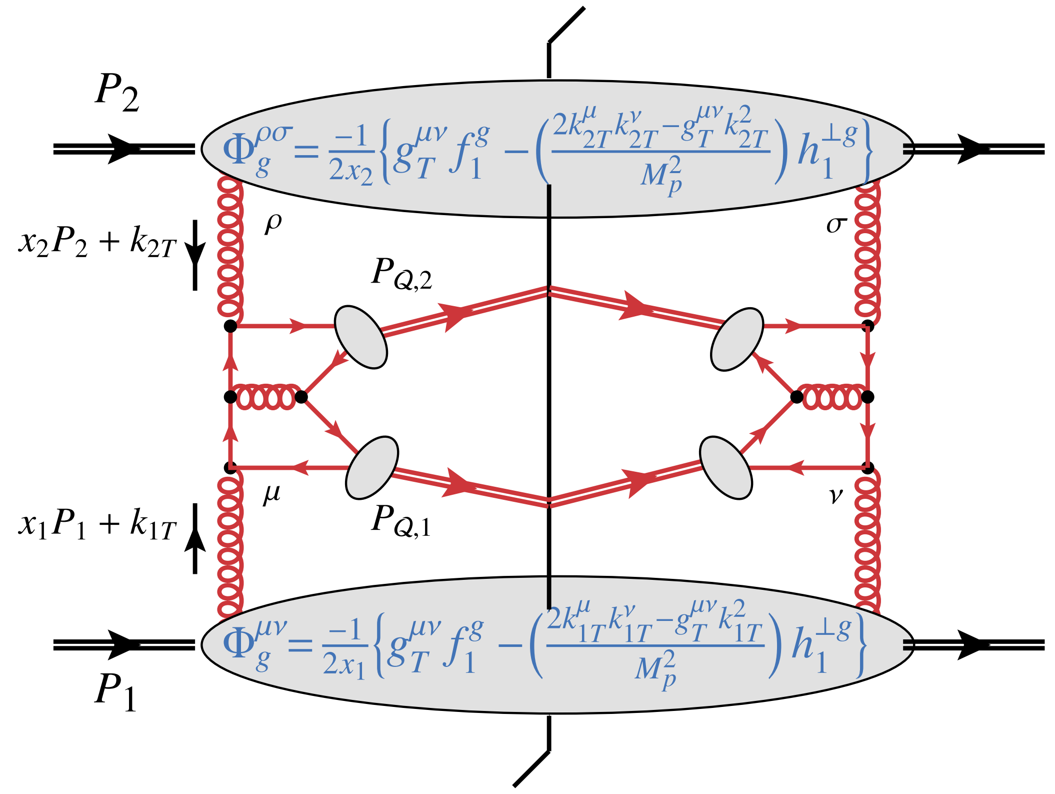

- $J/\psi J/\psi$ production largely dominated by gluon-induced processes

Gluon TMD PDFs via $J/\psi J/\psi$ production

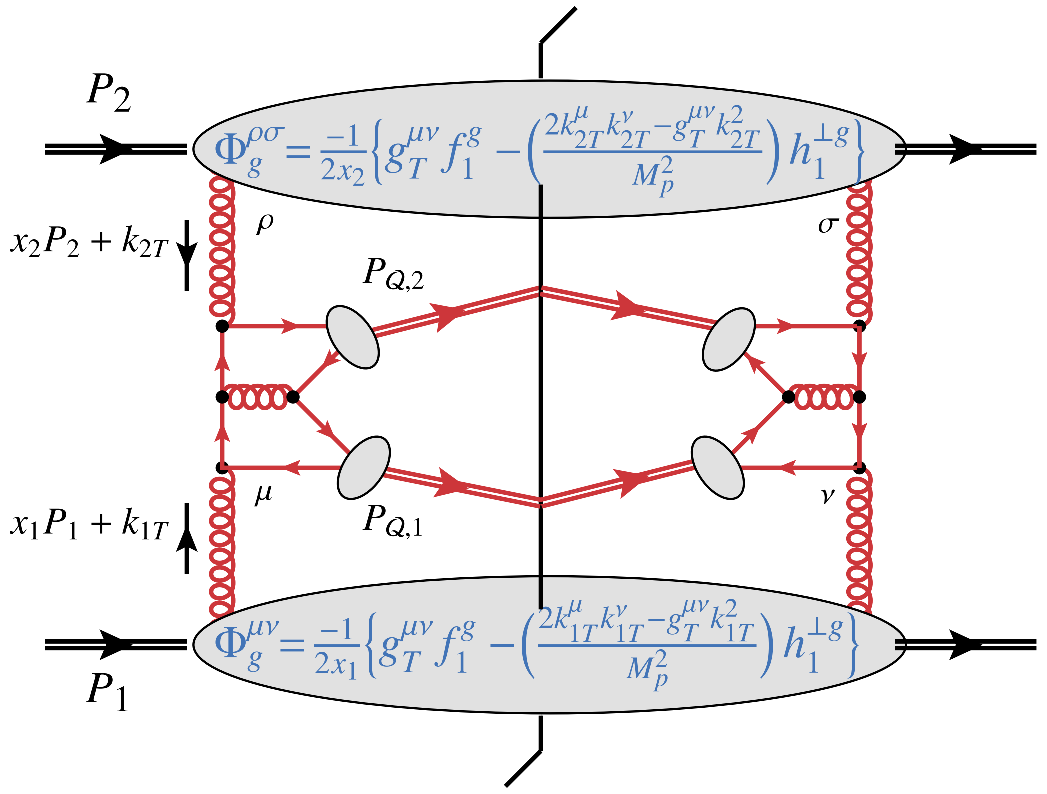

- $J/\psi J/\psi$ production largely dominated by gluon-induced processes

$$\sigma \propto F_1 \mathscr{C}[f_1^g f_1^g] + F_2 \mathscr{C}[w_2 h_1^{g\perp} h_1^{g\perp}] + \left(F_3 \mathscr{C}[w_3 f_1^g h_1^{g\perp}] + F_3' \mathscr{C}[w_3' f_1^g h_1^{g\perp}]\right) \cos\left(2\phi_{CS}\right) + \left(F_4 \mathscr{C}[w_4 h_1^{g\perp} h_1^{g\perp}]\right) \cos\left(4\phi_{CS}\right)$$

Gluon TMD PDFs via $J/\psi J/\psi$ production

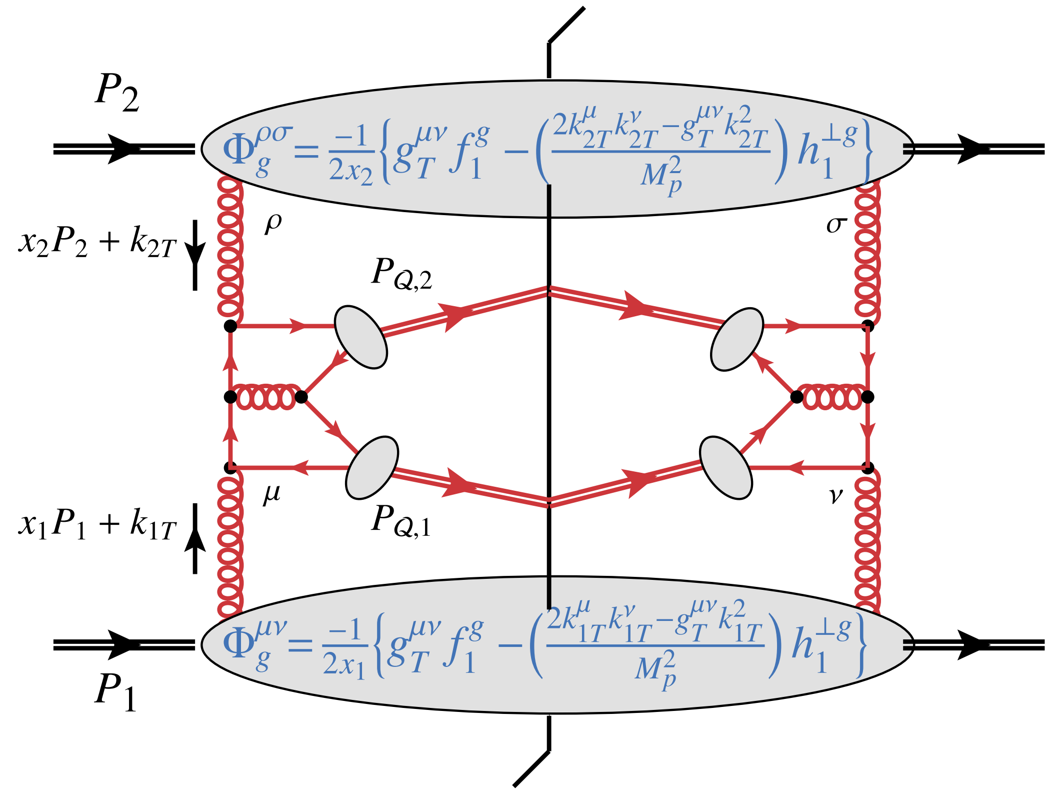

- $J/\psi J/\psi$ production largely dominated by gluon-induced processes

$$\sigma \propto F_1 \mathscr{C}[f_1^g f_1^g] + F_2 \mathscr{C}[w_2 h_1^{g\perp} h_1^{g\perp}] + \left(F_3 \mathscr{C}[w_3 f_1^g h_1^{g\perp}] + F_3' \mathscr{C}[w_3' f_1^g h_1^{g\perp}] \right) \cos(2\phi_{CS}) + \left(F_4 \mathscr{C}[w_4 h_1^{g\perp} h_1^{g\perp}] \right) \cos(4\phi_{CS})$$

Gluon TMD PDFs via $J/\psi J/\psi$ production

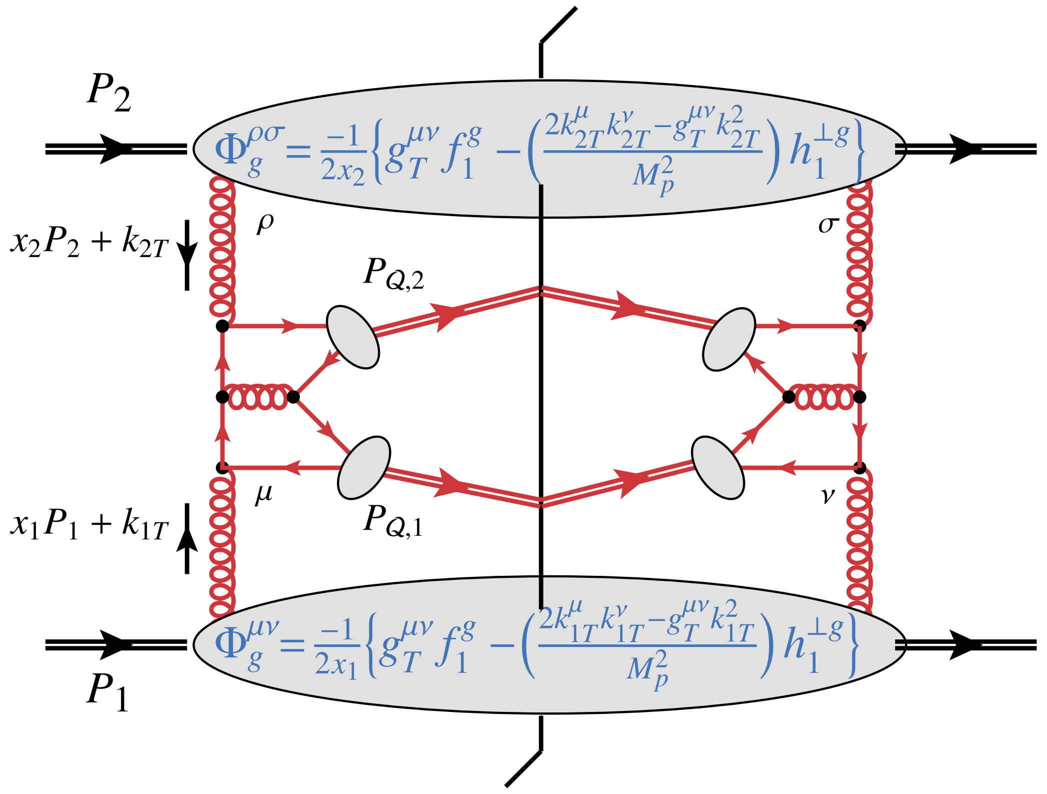

- $J/\psi J/\psi$ production largely dominated by gluon-induced processes

$$\sigma \propto F_1 \mathscr{C}[f_1^g f_1^g] + F_2 \mathscr{C}[w_2 h_1^{g\perp} h_1^{g\perp}] + \left(F_3 \mathscr{C}[w_3 f_1^g h_1^{g\perp}] + F_3' \mathscr{C}[w_3' f_1^g h_1^{g\perp}]\right) \cos\left(2\phi_{CS}\right) + \left(F_4 \mathscr{C}[w_4 h_1^{g\perp} h_1^{g\perp}]\right) \cos\left(4\phi_{CS}\right)$$

Gluon TMD PDFs via $J/\psi J/\psi$ production

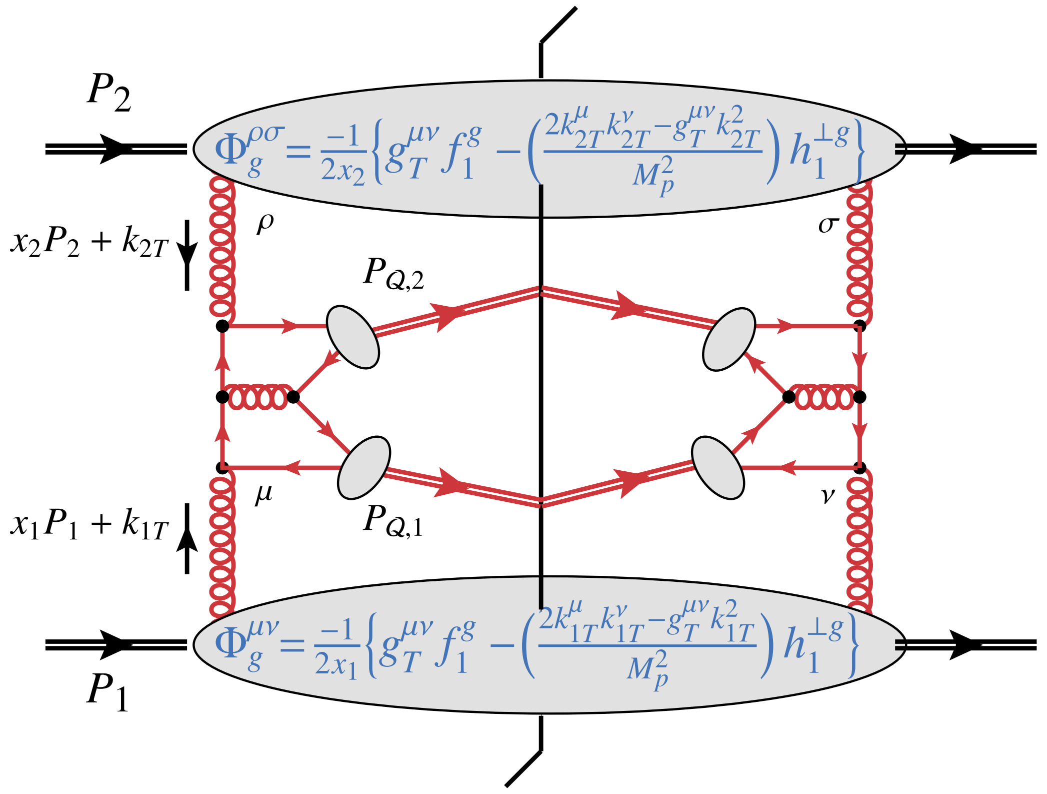

- $J/\psi J/\psi$ production largely dominated by gluon-induced processes

$$\sigma \propto F_1 \mathcal{C}[f_1^g f_1^g] + F_2 \mathcal{C}[w_2 h_1^{g\perp} h_1^{g\perp}] + \left(F_3 \mathcal{C}[w_3 f_1^g h_1^{g\perp}] + F_3' \mathcal{C}[w_3' f_1^g h_1^{g\perp}] \right) \cos(2\phi_{CS}) + \left(F_4 \mathcal{C}[w_4 h_1^{g\perp} h_1^{g\perp}] \right) \cos(4\phi_{CS})$$

Gluon TMD PDFs via $J/\psi J/\psi$ production

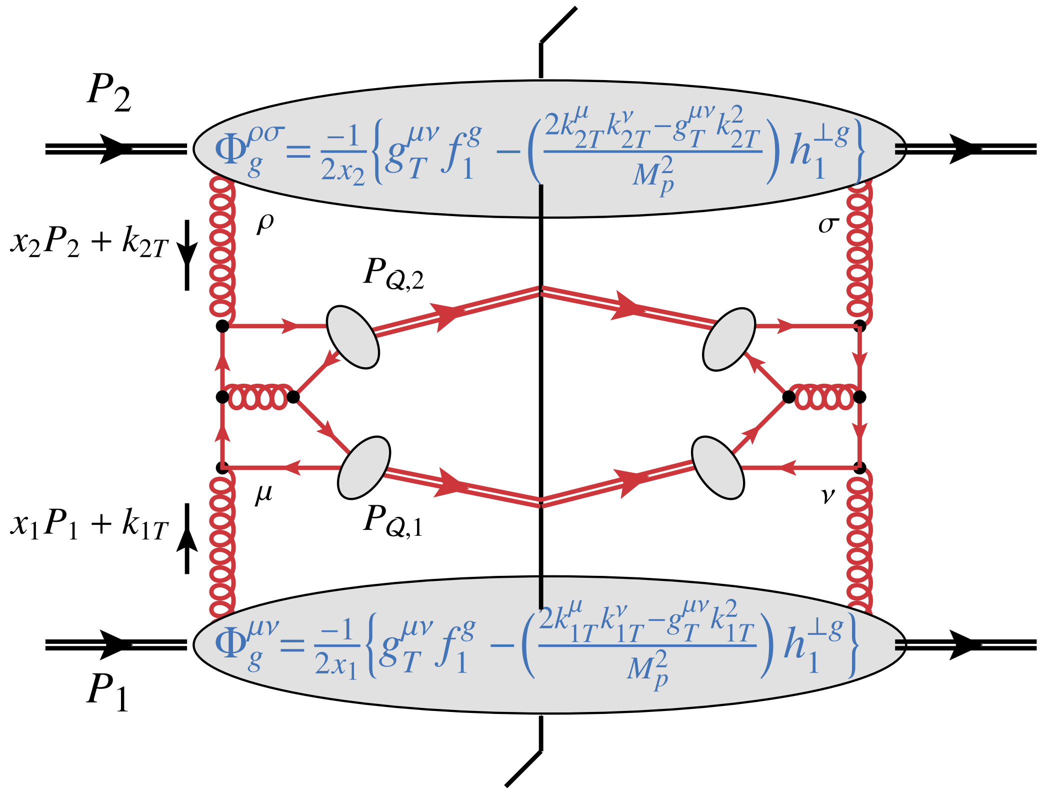

- $J/\psi J/\psi$ production largely dominated by gluon-induced processes

$$\sigma \propto F_1 \mathscr{C}[f_1^g f_1^g] + F_2 \mathscr{C}[w_2 h_1^{g\perp} h_1^{g\perp}] + \left(F_3 \mathscr{C}[w_3 f_1^g h_1^{g\perp}] + F_3' \mathscr{C}[w_3' f_1^g h_1^{g\perp}]\right) \cos(2\phi_{CS}) + \left(F_4 \mathscr{C}[w_4 h_1^{g\perp} h_1^{g\perp}]\right) \cos(4\phi_{CS})$$

- Invariant mass of pair $\rightarrow$ scale variation

Gluon TMD PDFs via $J/\psi J/\psi$ production

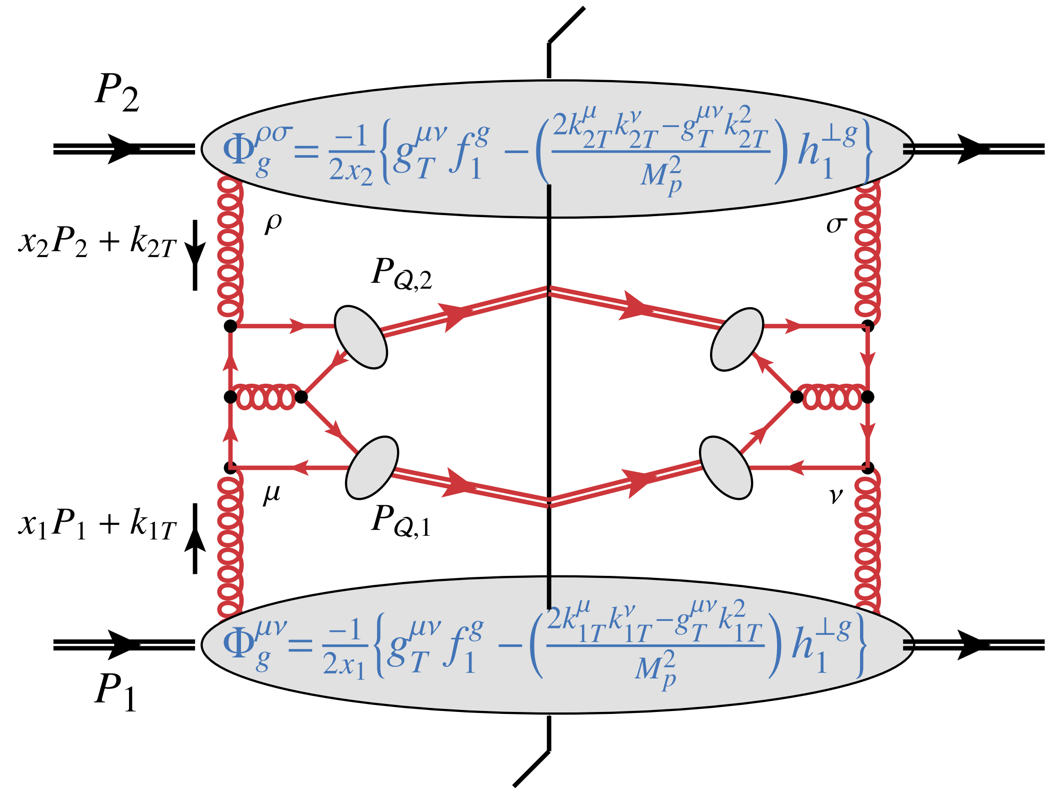

- $J/\psi J/\psi$ production largely dominated by gluon-induced processes

$$\sigma \propto F_1 \mathscr{C}[f_1^g f_1^g] + F_2 \mathscr{C}[w_2 h_1^{g\perp} h_1^{g\perp}] + \left(F_3 \mathscr{C}[w_3 f_1^g h_1^{g\perp}] + F_3' \mathscr{C}[w_3' f_1^g h_1^{g\perp}]\right) \cos(2\phi_{CS}) + \left(F_4 \mathscr{C}[w_4 h_1^{g\perp} h_1^{g\perp}]\right) \cos(4\phi_{CS})$$

- Invariant mass of pair → scale variation
- Need to subtract double-parton-scattering contribution from data

Gluon TMD PDFs via $J/\psi J/\psi$ production

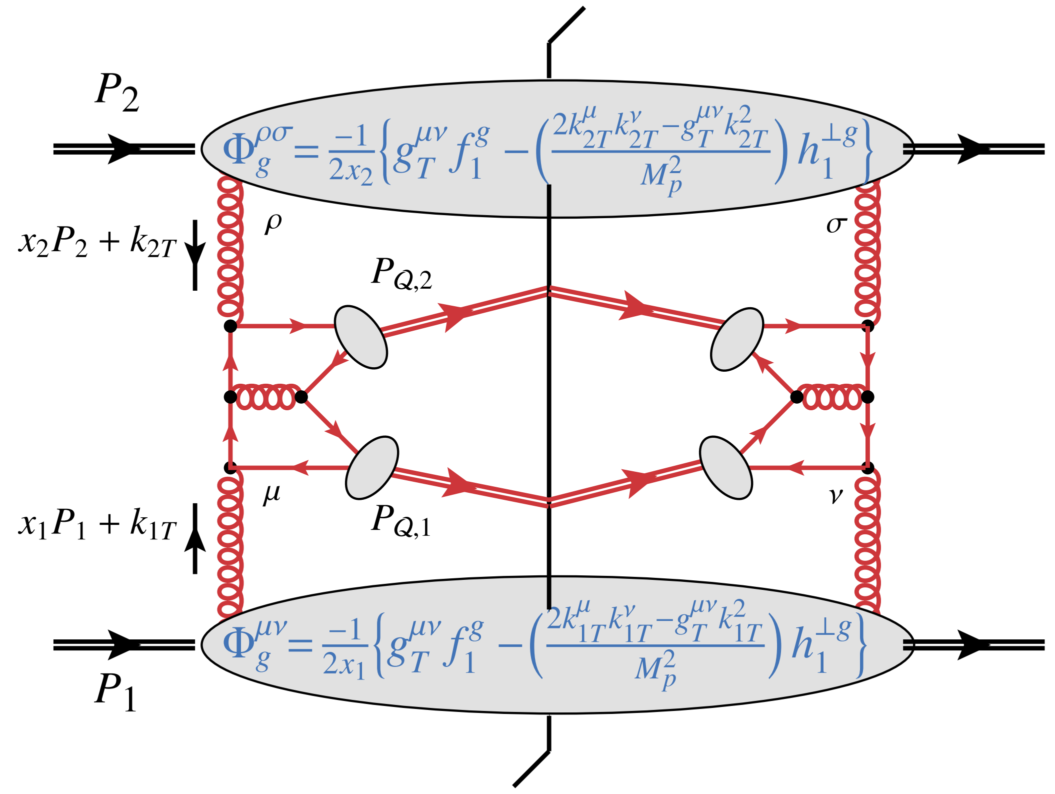

- $J/\psi J/\psi$ production largely dominated by gluon-induced processes

$$\sigma \propto F_1 \mathscr{C}[f_1^g f_1^g] + F_2 \mathscr{C}[w_2 h_1^{g\perp} h_1^{g\perp}] + \left(F_3 \mathscr{C}[w_3 f_1^g h_1^{g\perp}] + F_3' \mathscr{C}[w_3' f_1^g h_1^{g\perp}]\right) \cos(2\phi_{CS}) + \left(F_4 \mathscr{C}[w_4 h_1^{g\perp} h_1^{g\perp}]\right) \cos(4\phi_{CS})$$

- Invariant mass of pair → scale variation
- Need to subtract double-parton-scattering contribution from data

JHEP 03 (2024) 088

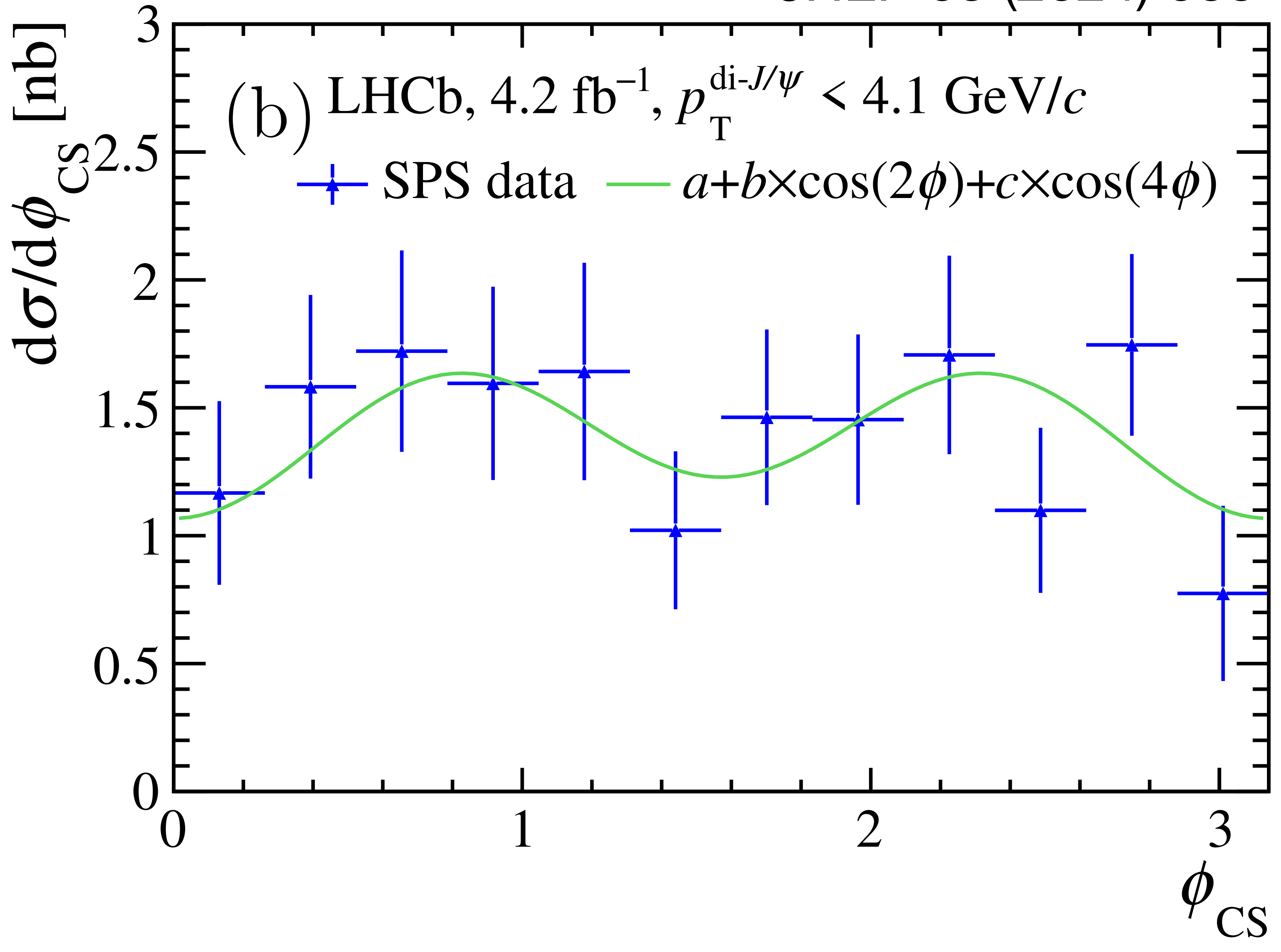

$$p_T^{J/\psi J/\psi} < \frac{\langle M_{J/\psi J/\psi}\rangle}{2},$$

$$\langle M_{J/\psi J/\psi}\rangle = 8.2 \text{ GeV}/c^2$$

Gluon TMD PDFs via $J/\psi J/\psi$ production

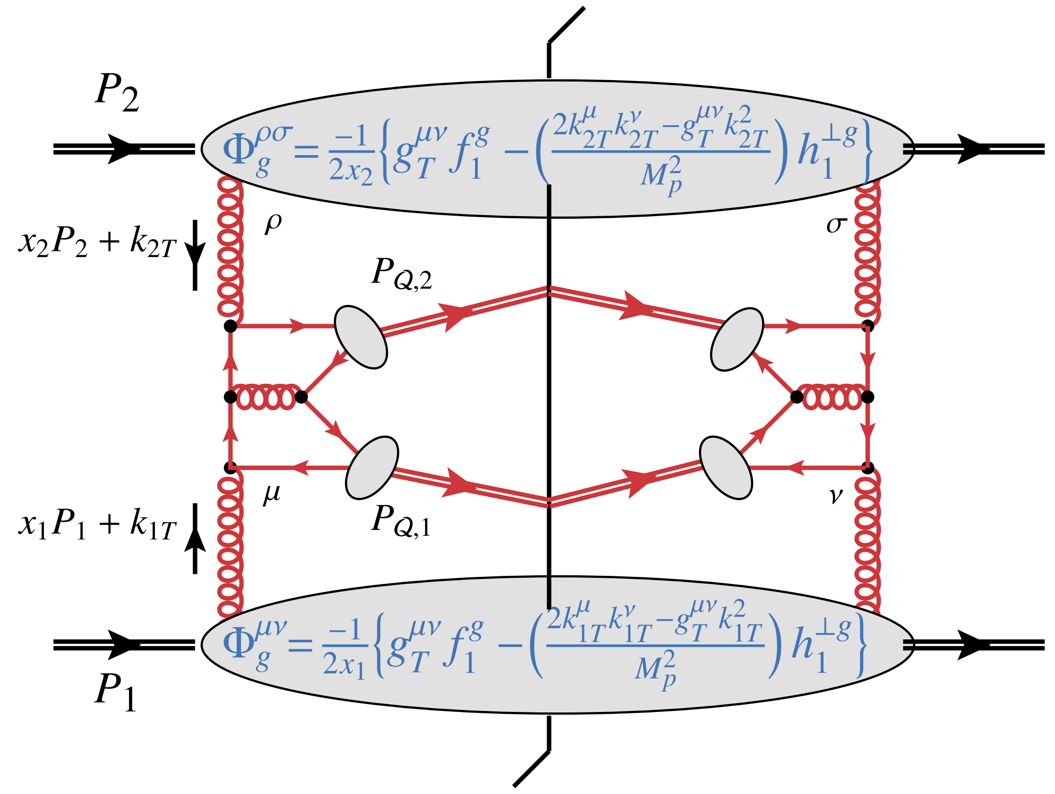

- $J/\psi J/\psi$ production largely dominated by gluon-induced processes

$$\sigma \propto F_1 \mathscr{C}[f_1^g f_1^g] + F_2 \mathscr{C}[w_2 h_1^{g\perp} h_1^{g\perp}] + \left(F_3 \mathscr{C}[w_3 f_1^g h_1^{g\perp}] + F_3' \mathscr{C}[w_3' f_1^g h_1^{g\perp}]\right) \cos(2\phi_{CS}) + \left(F_4 \mathscr{C}[w_4 h_1^{g\perp} h_1^{g\perp}]\right) \cos(4\phi_{CS})$$

- Invariant mass of pair → scale variation
- Need to subtract double-parton-scattering contribution from data

JHEP 03 (2024) 088

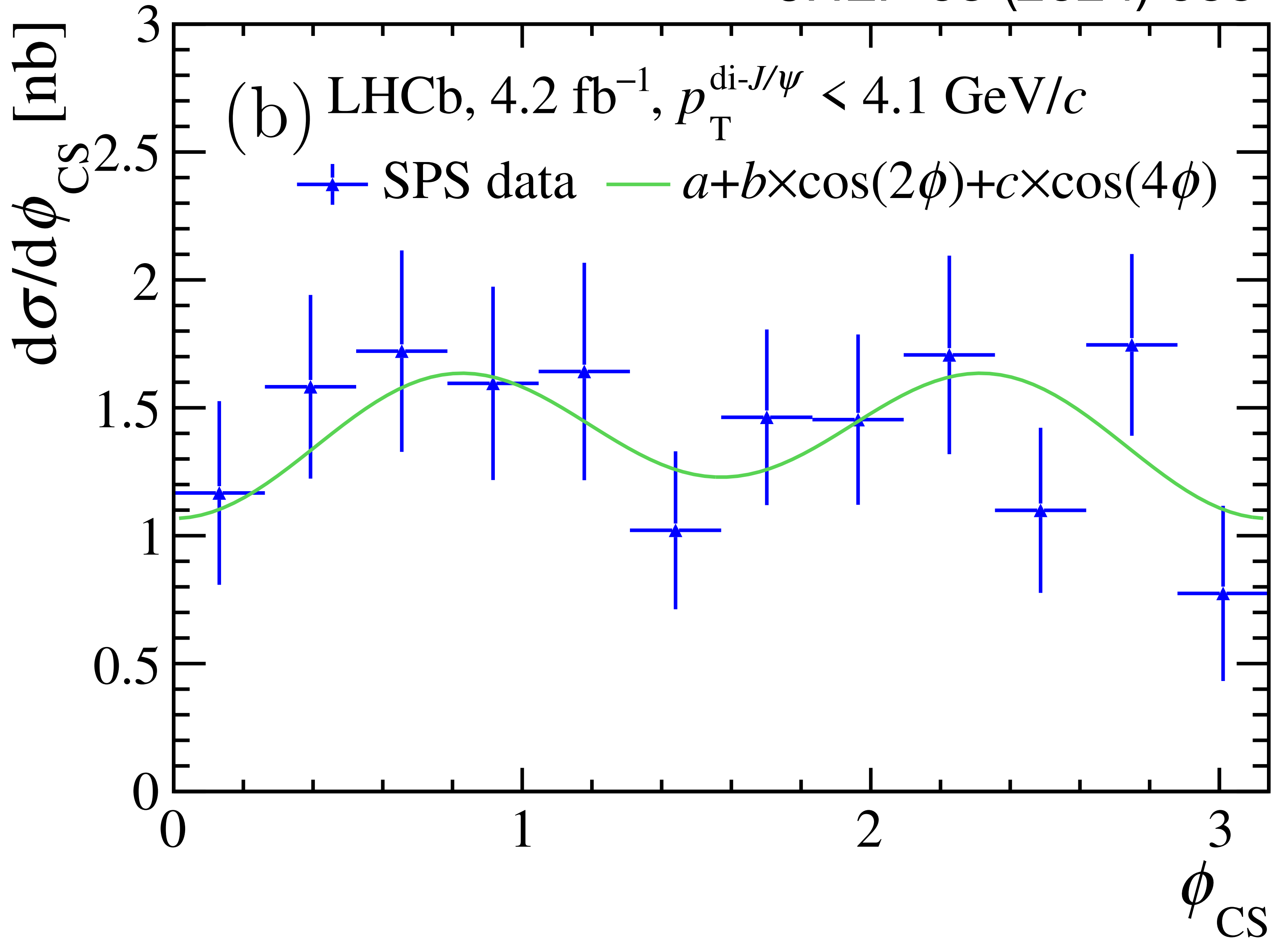

$$p_T^{J/\psi J/\psi} < \frac{\langle M_{J/\psi J/\psi} \rangle}{2},$$

$\langle M_{J/\psi J/\psi} \rangle$ = 8.2 GeV/c^2

$$\langle \cos 2\phi_{CS} \rangle = -0.029 \pm 0.050 \text{ (stat)} \pm 0.009 \text{ (syst)}$$
$$\langle \cos 4\phi_{CS} \rangle = -0.087 \pm 0.052 \text{ (stat)} \pm 0.013 \text{ (syst)}$$

Spin-independent gluon TMDs via $J/\psi J/\psi$ production

JHEP 03 (2024) 088

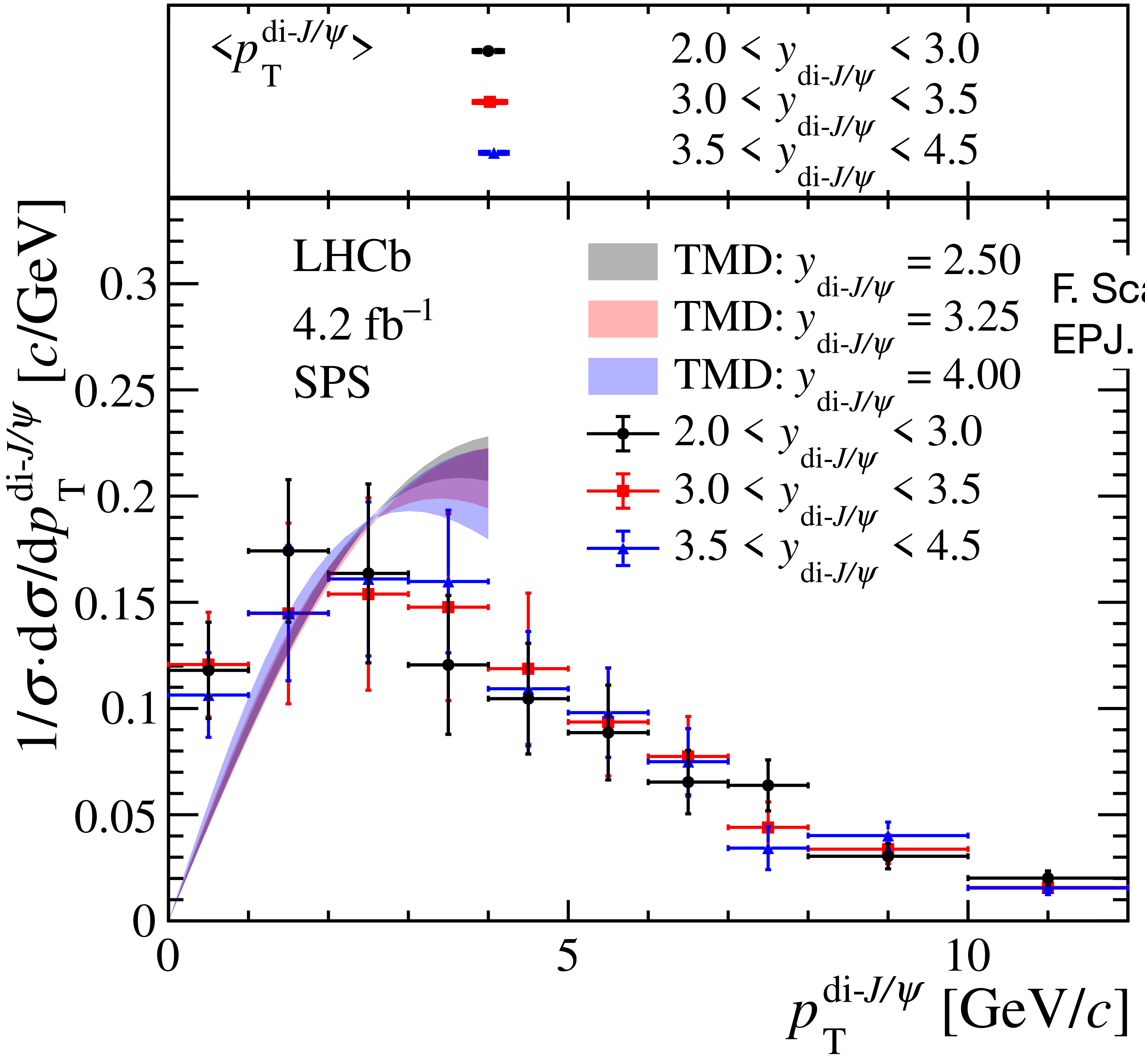

F. Scarpa et al., EPJ. C **80** (2020) 87

JHEP 03 (2024) 088

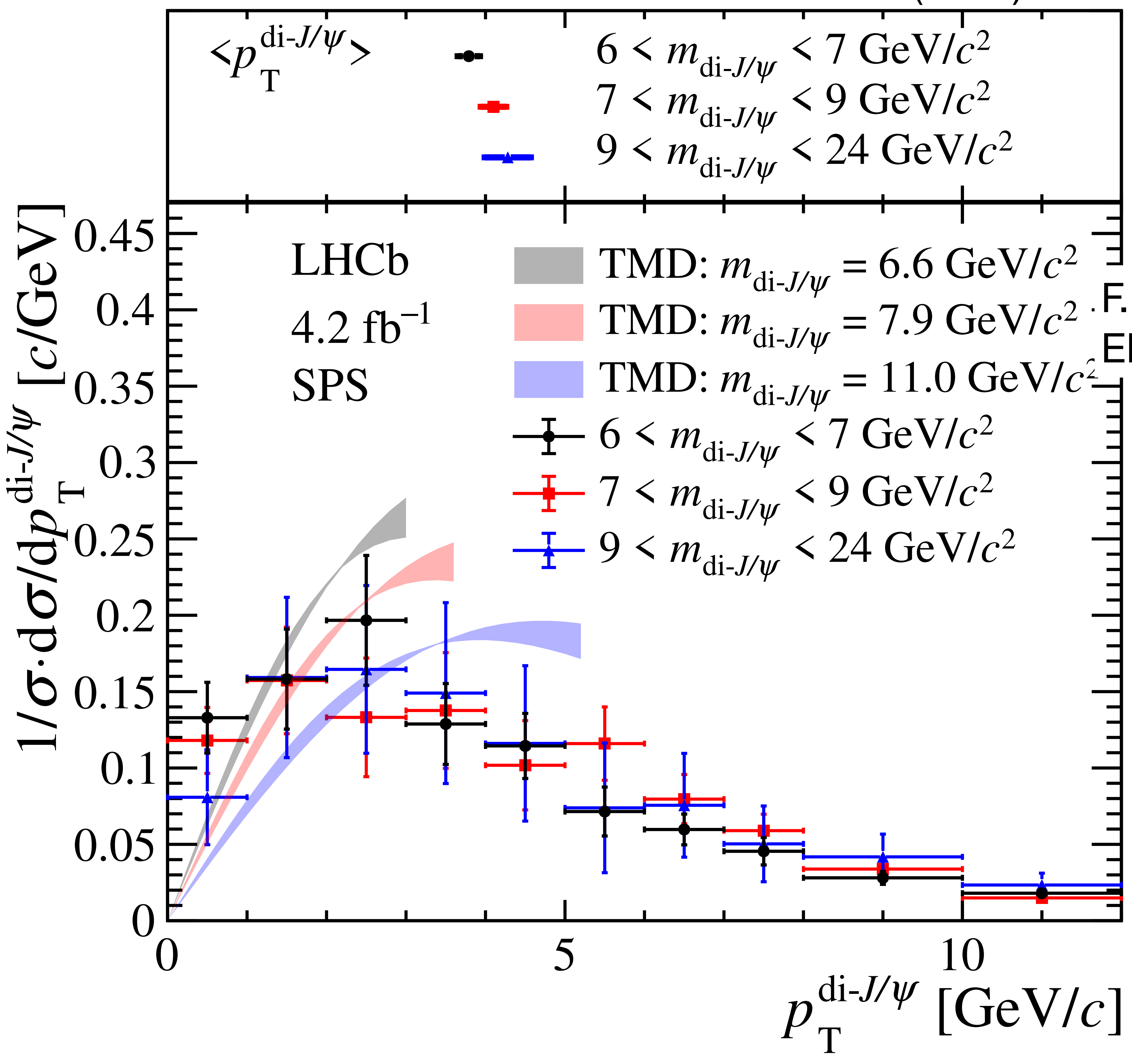

F. Scarpa et al., EPJ. C **80** (2020) 87

Upcoming

AMBER

Apparatus for Meson and Baryon Experimental Research

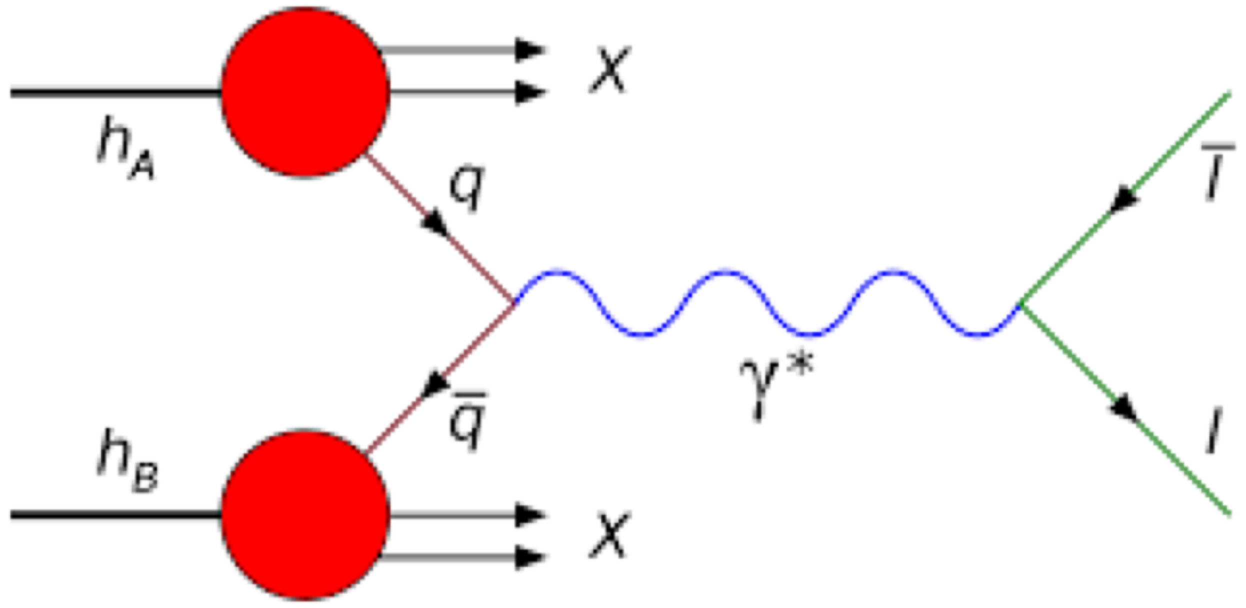

Meson structure

Upcoming

Apparatus for Meson and Baryon Experimental Research

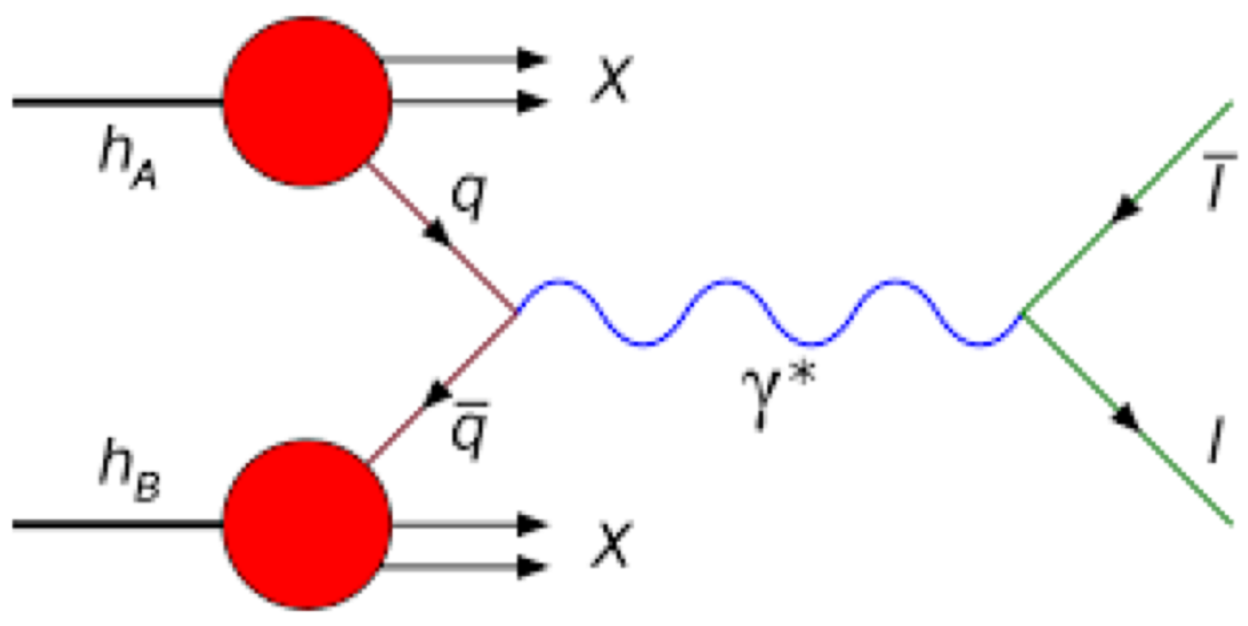

Meson structure

SpinQuest → Sivers function

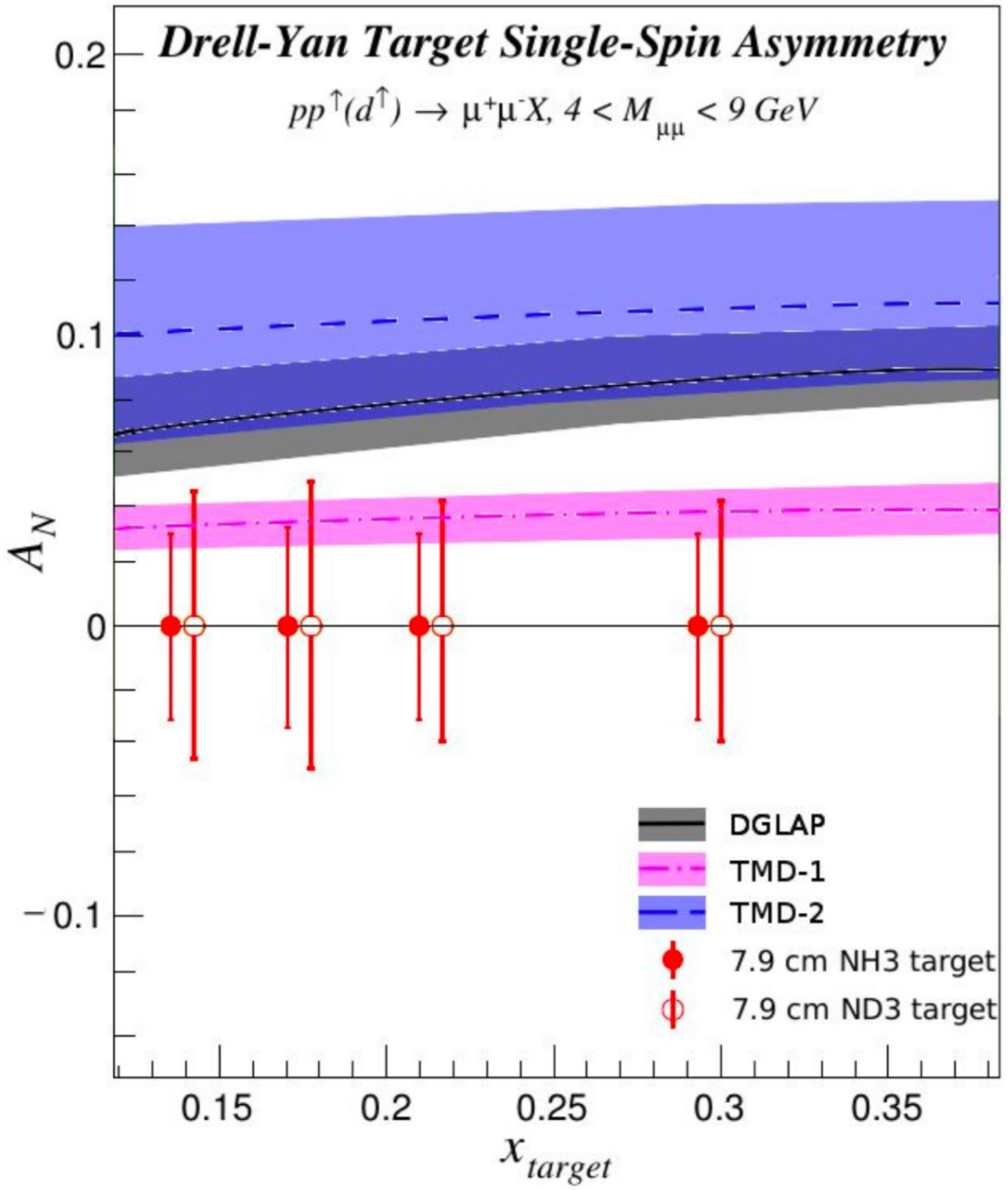

Upcoming

AMBER

Apparatus for Meson and Baryon Experimental Research

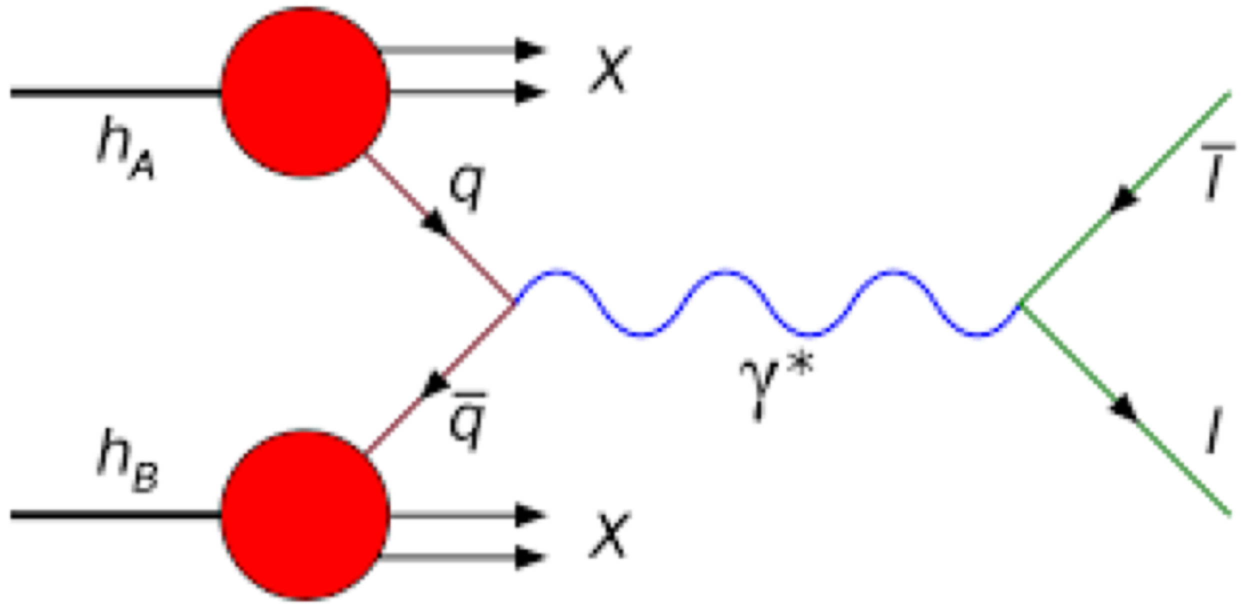

Meson structure

SpinQuest ⟶ Sivers function

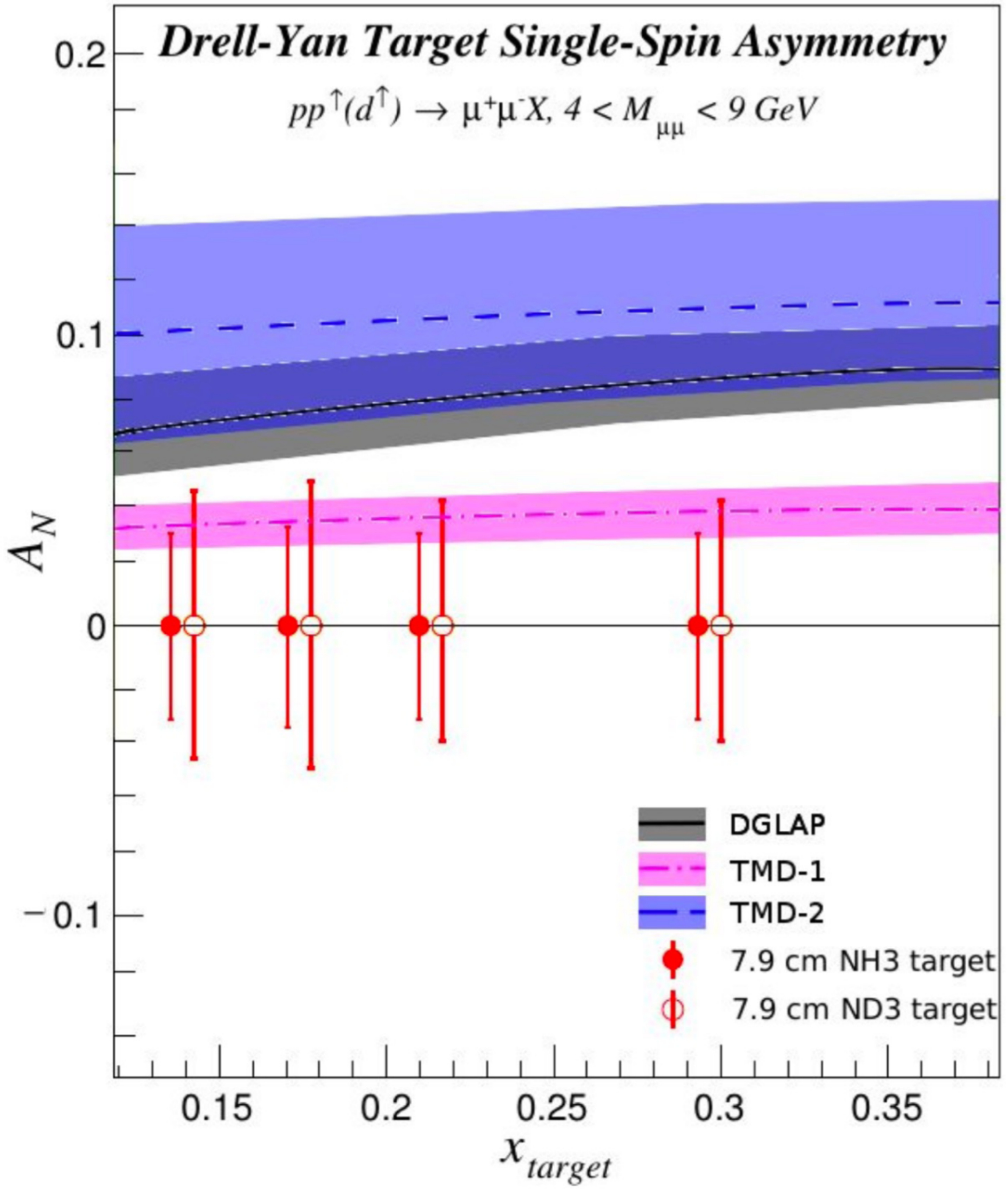

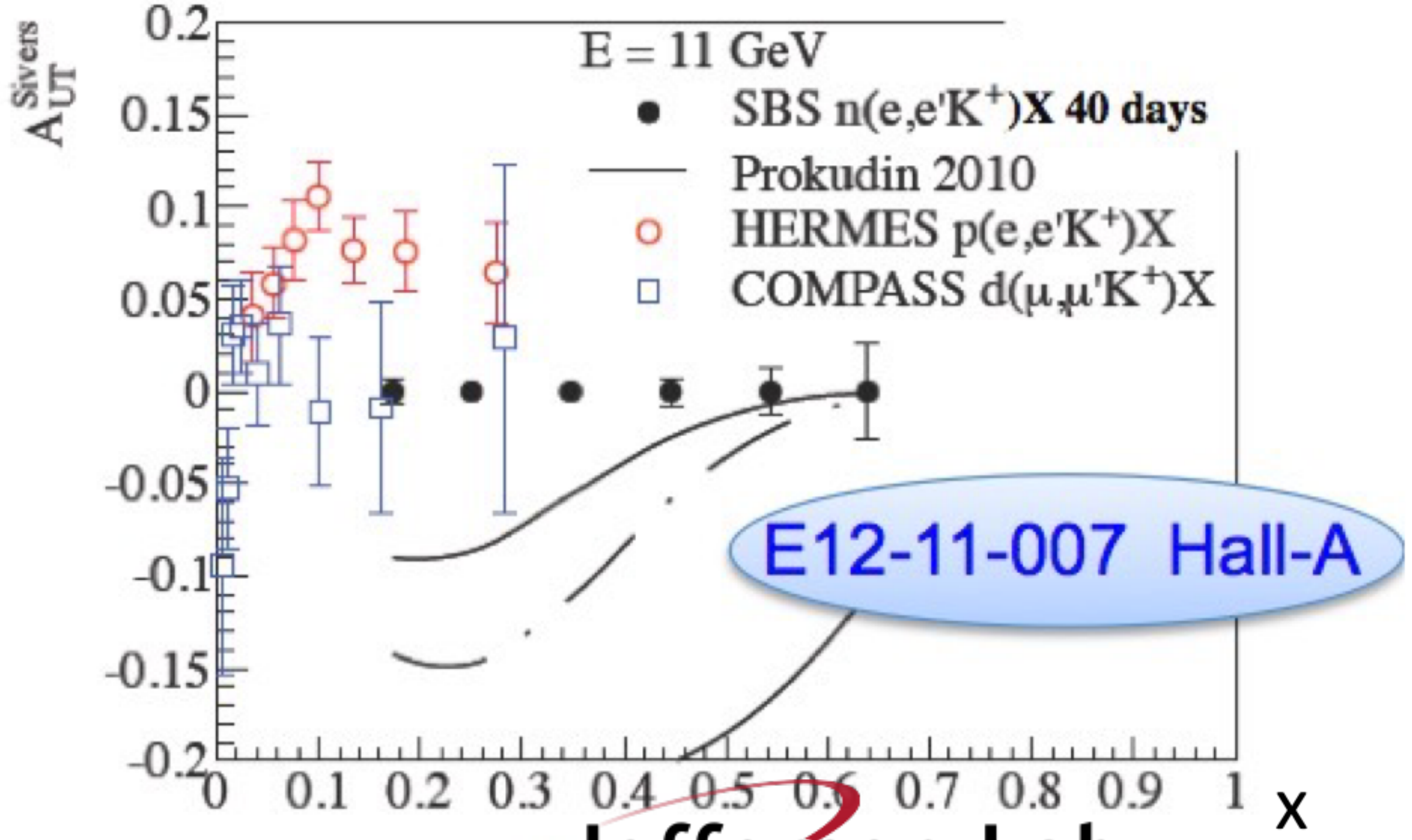

Jefferson Lab

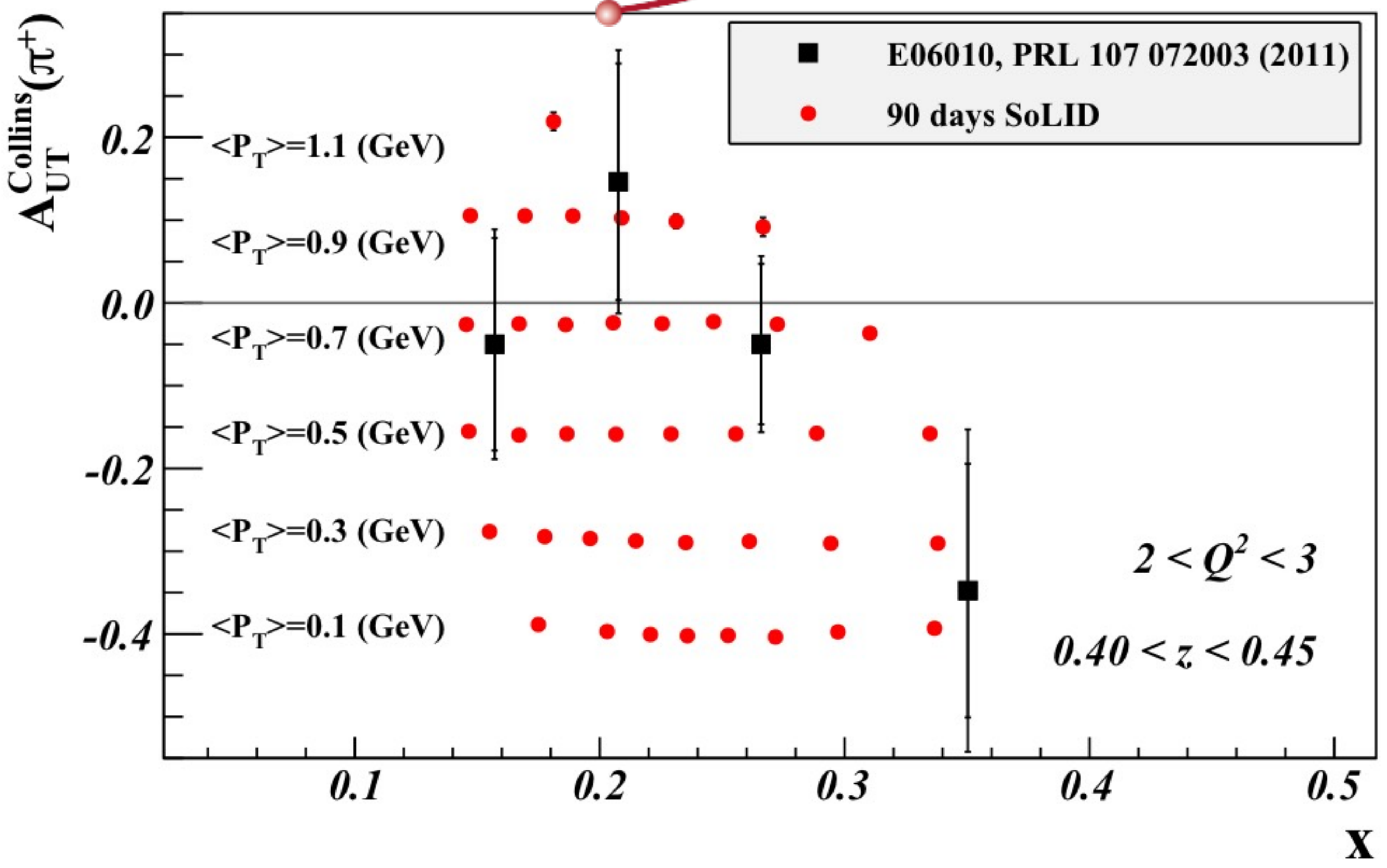

Future

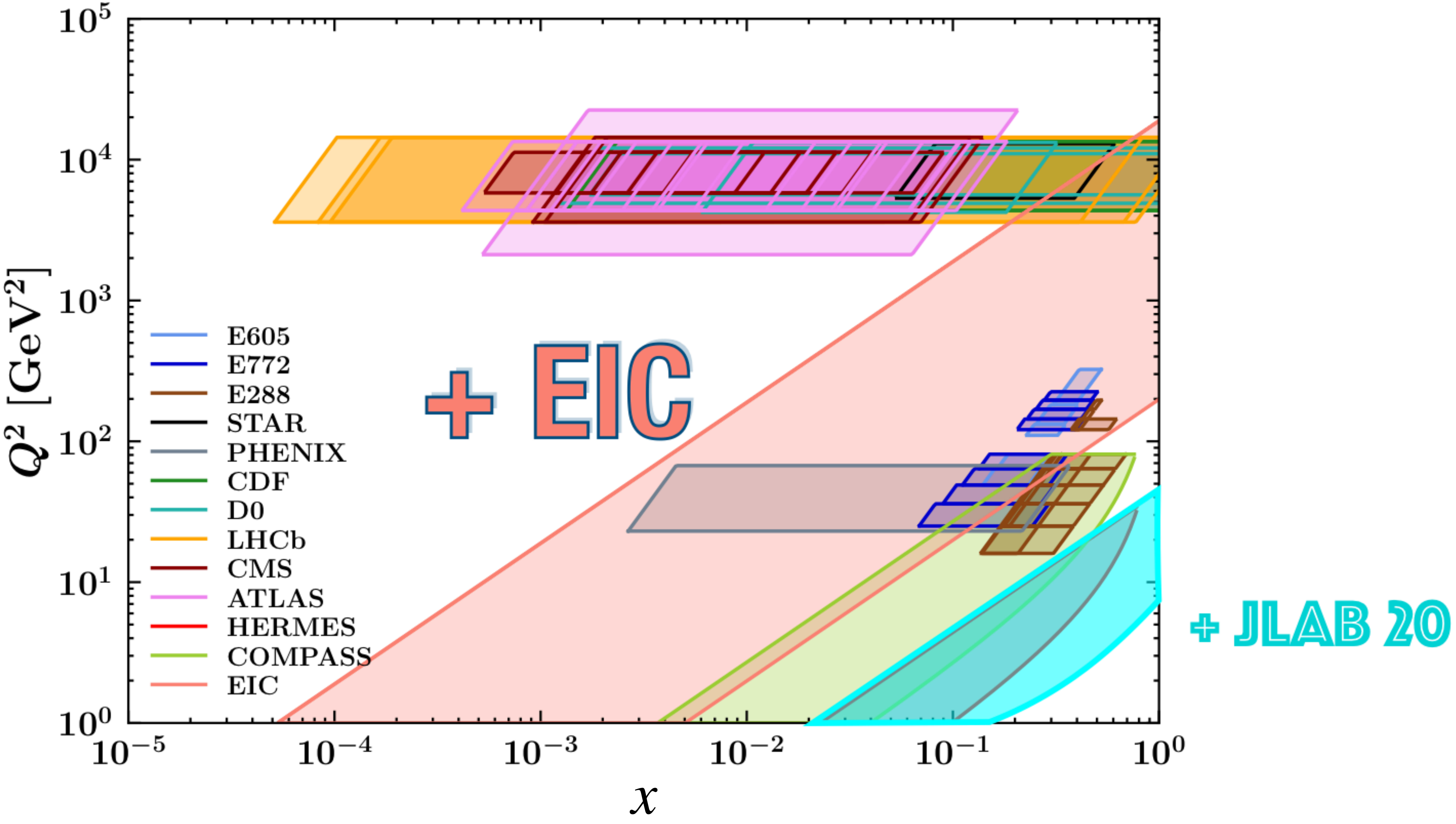

10^5
10^4
10^3
10^2
10^1
10^0
Q^2 [GeV^2]
10^{-5}
10^{-4}
10^{-3}
10^{-2}
10^{-1}
10^0
x
E605
E772
E288
STAR
PHENIX
CDF
D0
LHCb
CMS
ATLAS
HERMES
COMPASS
EIC
+ EIC
+ JLAB 20

Spin-independent TMD PDF: impact of EIC

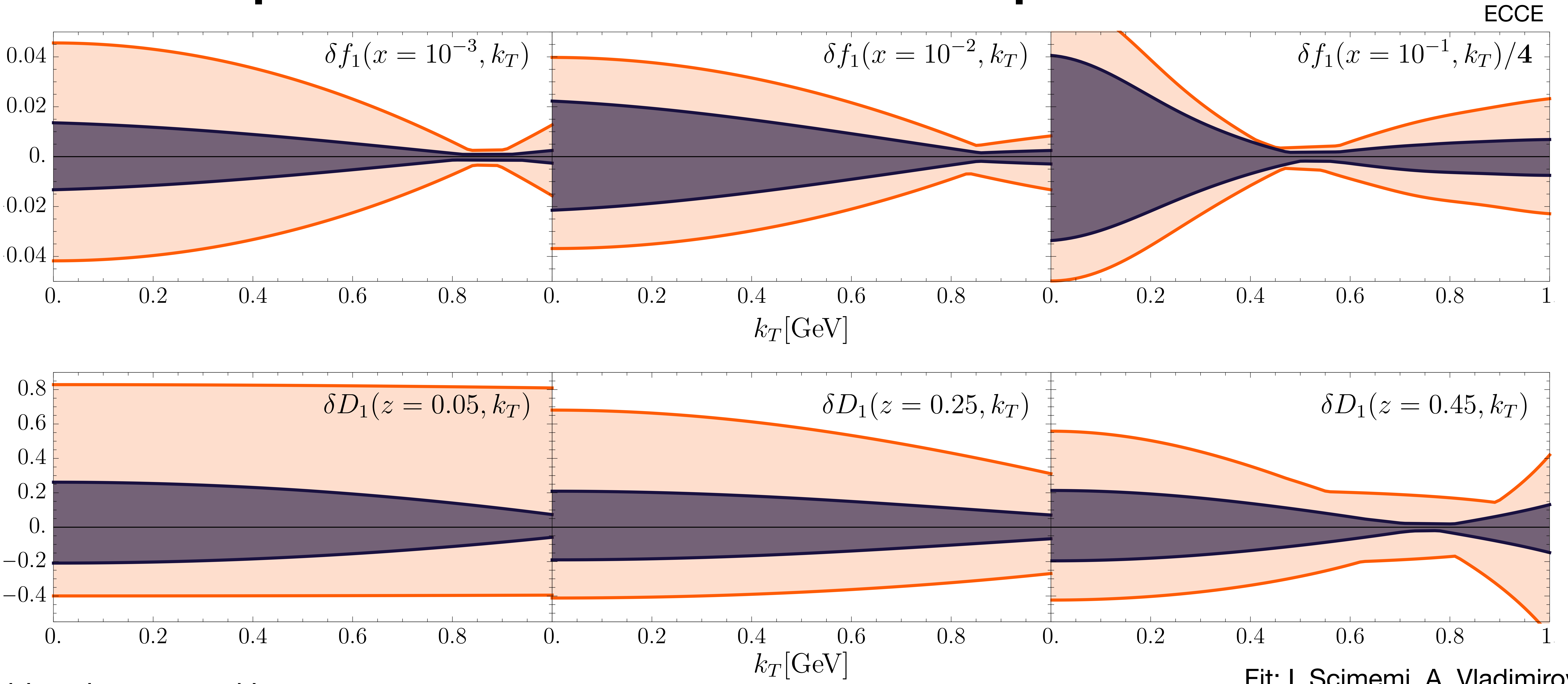

DIS variables via scattered lepton

$$Q^2 > 1\ \text{GeV}^2$$
$$0.01 < y < 0.95$$
$$W^2 > 10\ \text{GeV}^2$$

$5 \times 41\ \text{GeV}^2$
$10 \times 100\ \text{GeV}^2$
$18 \times 100\ \text{GeV}^2$
$18 \times 275\ \text{GeV}^2$

$\mathcal{L} = 10\ \text{fb}^{-1}$ for each collision energy

Fit: I. Scimemi, A. Vladimirov
JHEP, 06:137, 2020

systematic uncertainty= |generated - reconstructed|

Sivers TMD PDF: impact of EIC

Parametrisation from
M. Bury et al., JHEP, 05:151, 2021

Q=2 GeV

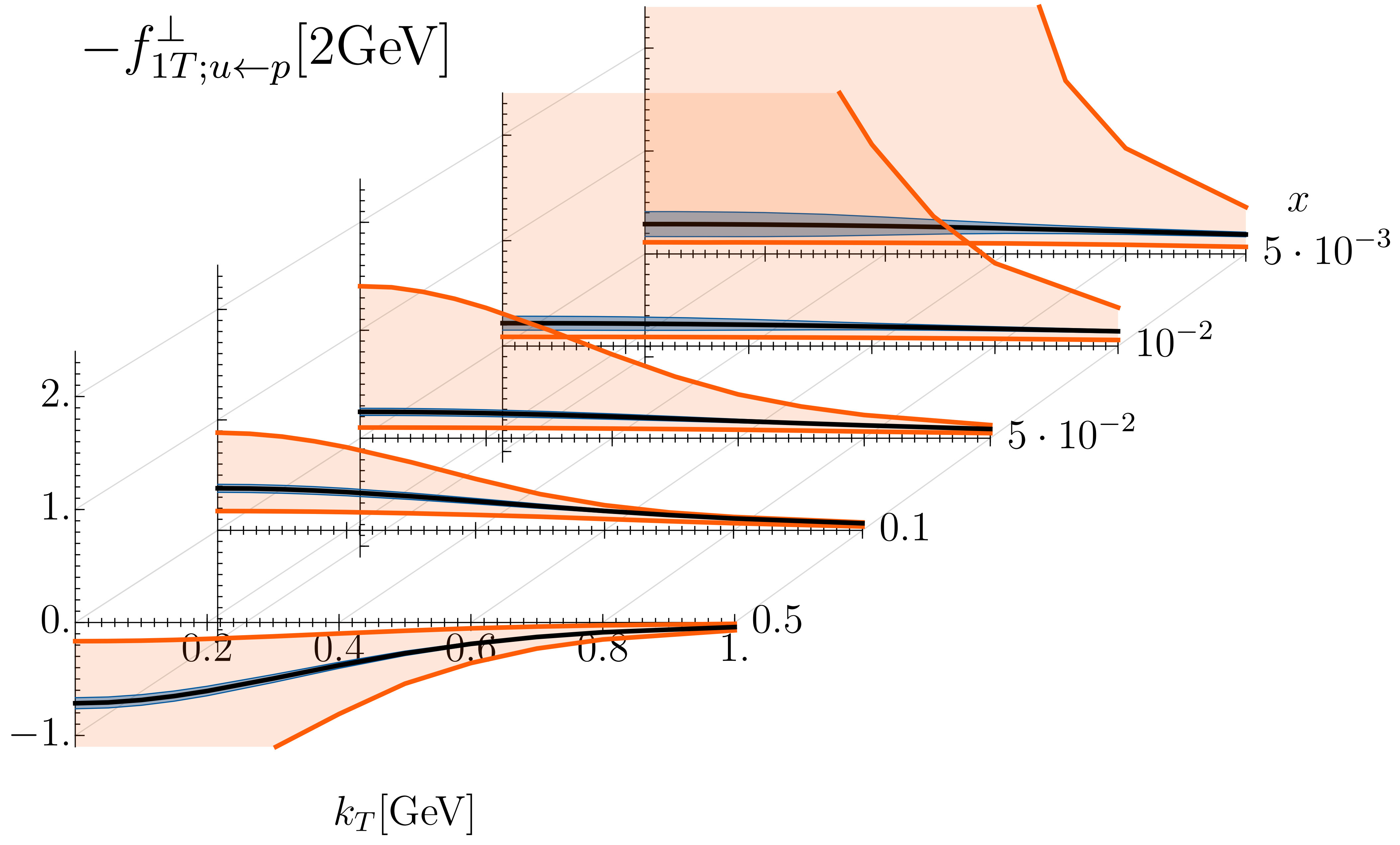

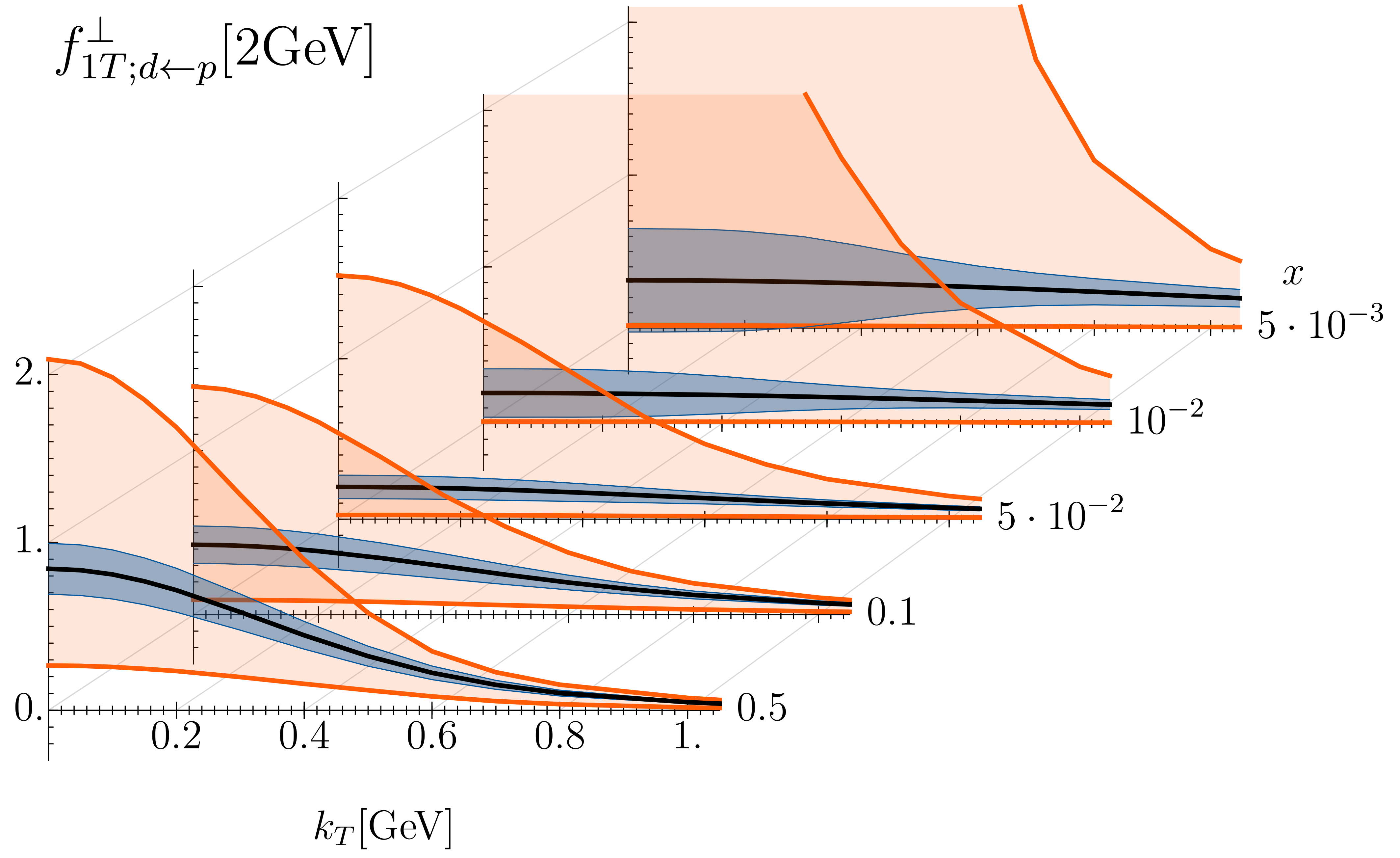

DIS variables via scattered lepton

$Q^2 > 1\ \text{GeV}^2$

$0.01 < y < 0.95$

$W^2 > 10\ \text{GeV}^2$

$5\times 41\ \text{GeV}^2$
$10\times 100\ \text{GeV}^2$
$18\times 100\ \text{GeV}^2$
$18\times 275\ \text{GeV}^2$

$\mathcal{L} = 10\ \text{fb}^{-1}$ for each collision energy

The various dimensions of the nucleon structure

Wigner distributions $W(x, \vec{k}_T, \vec{b}_\perp)$

$\int d^2\vec{b}_\perp$ → transverse-momentum dependent (TMD) parton distribution functions (PDFs)

$\int d^2\vec{k}_T$ → impact-parameter dependent PDFs

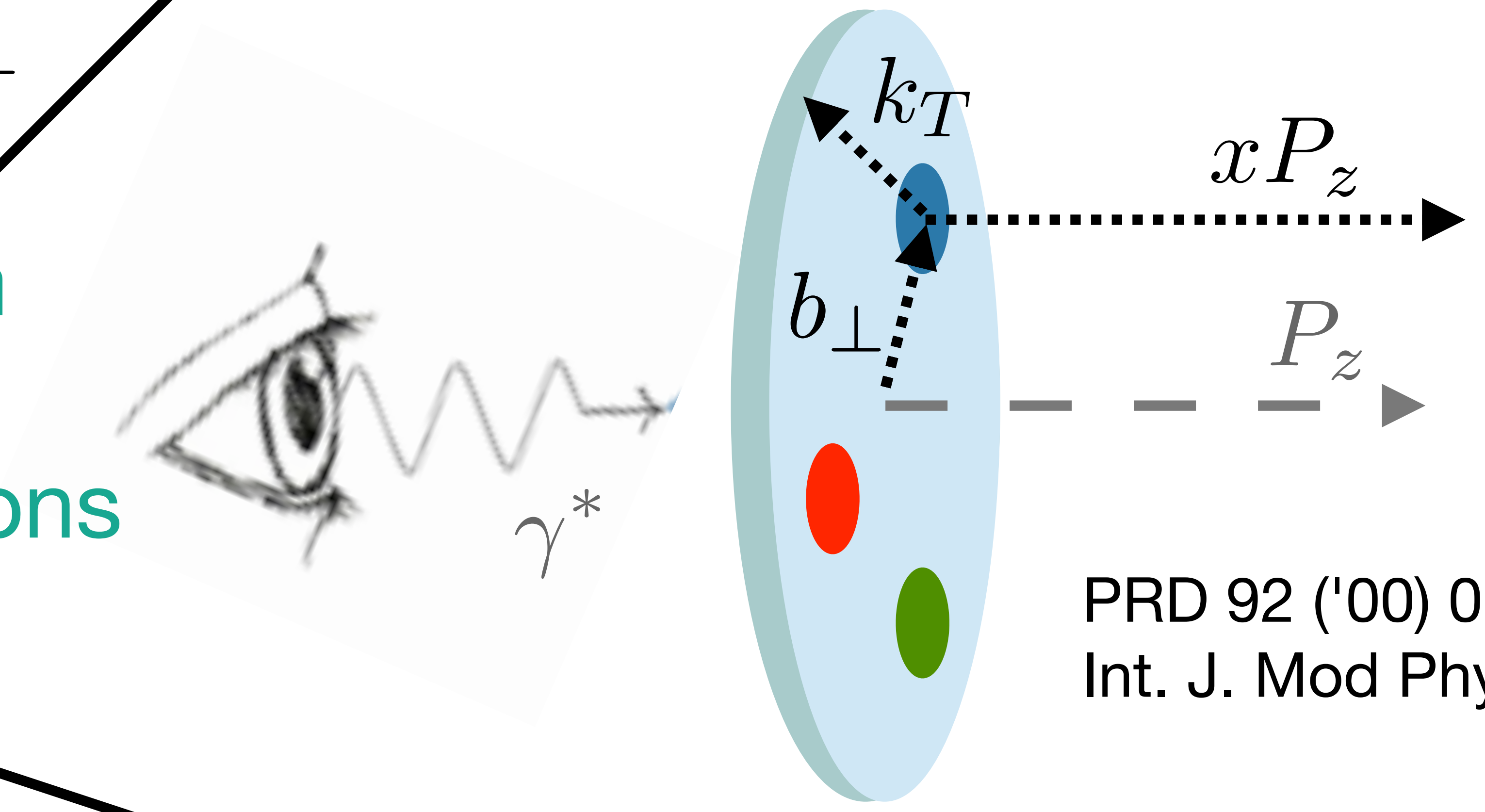

PRD 92 ('00) 071503
Int. J. Mod Phys. A 18 ('03) 173

impact-parameter dependent PDFs → Fourier transform → generalised parton distributions (GPDs)

generalised parton distributions (GPDs) → forward limit → PDFs

transverse-momentum dependent (TMD) parton distribution functions (PDFs) → $\int d^2\vec{k}_T$ → PDFs

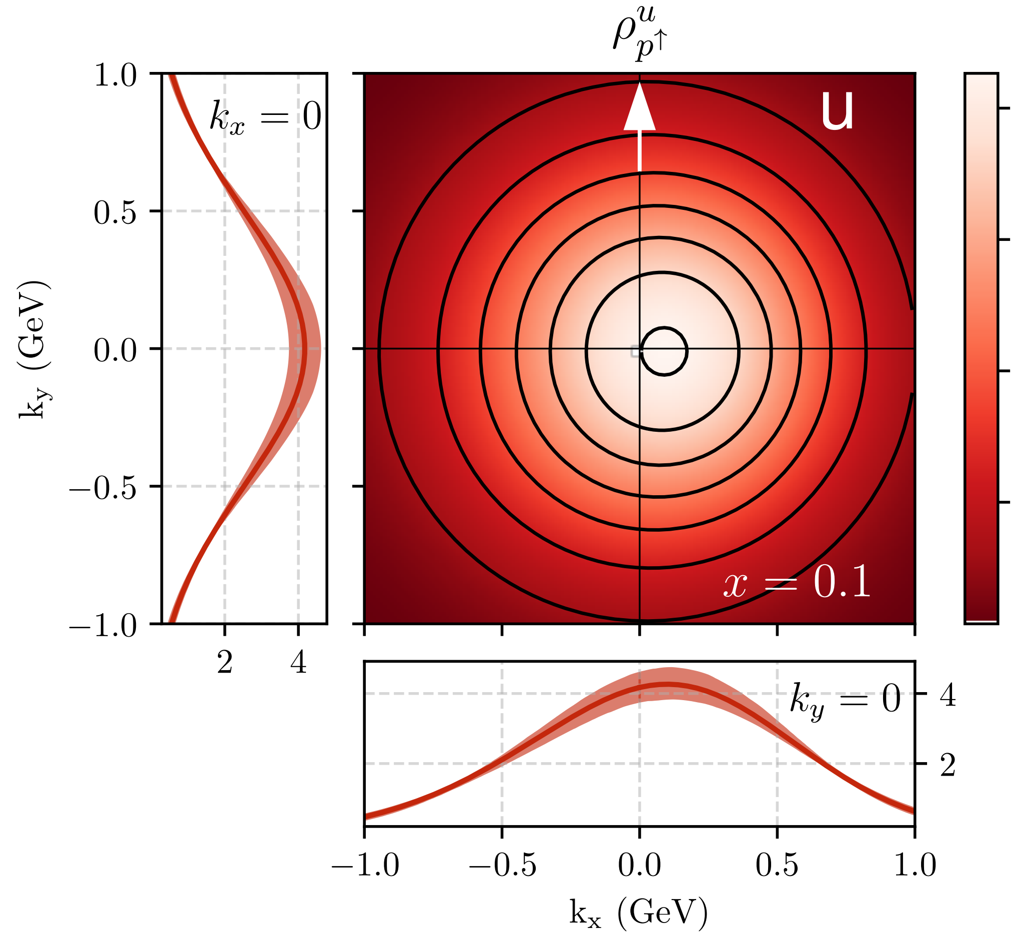

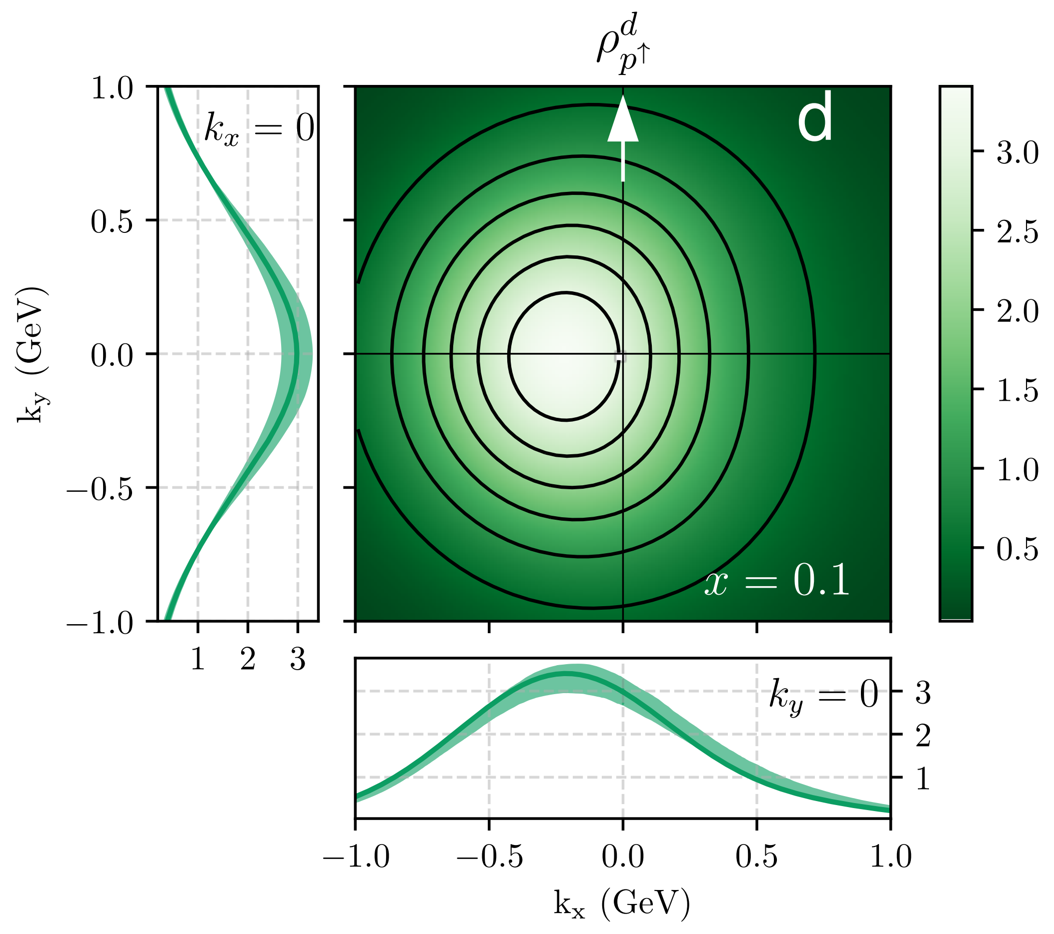

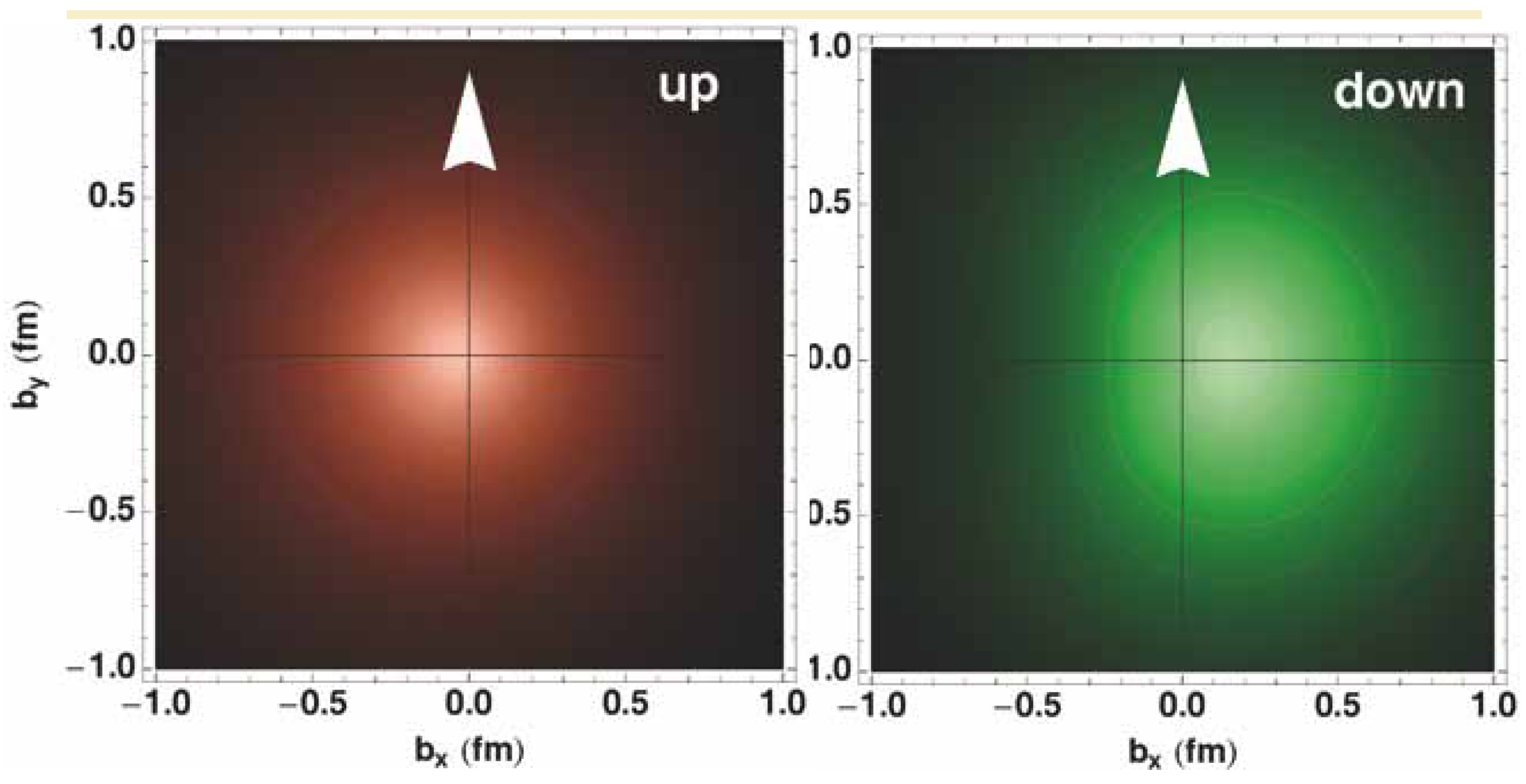

The various dimensions of the nucleon structure

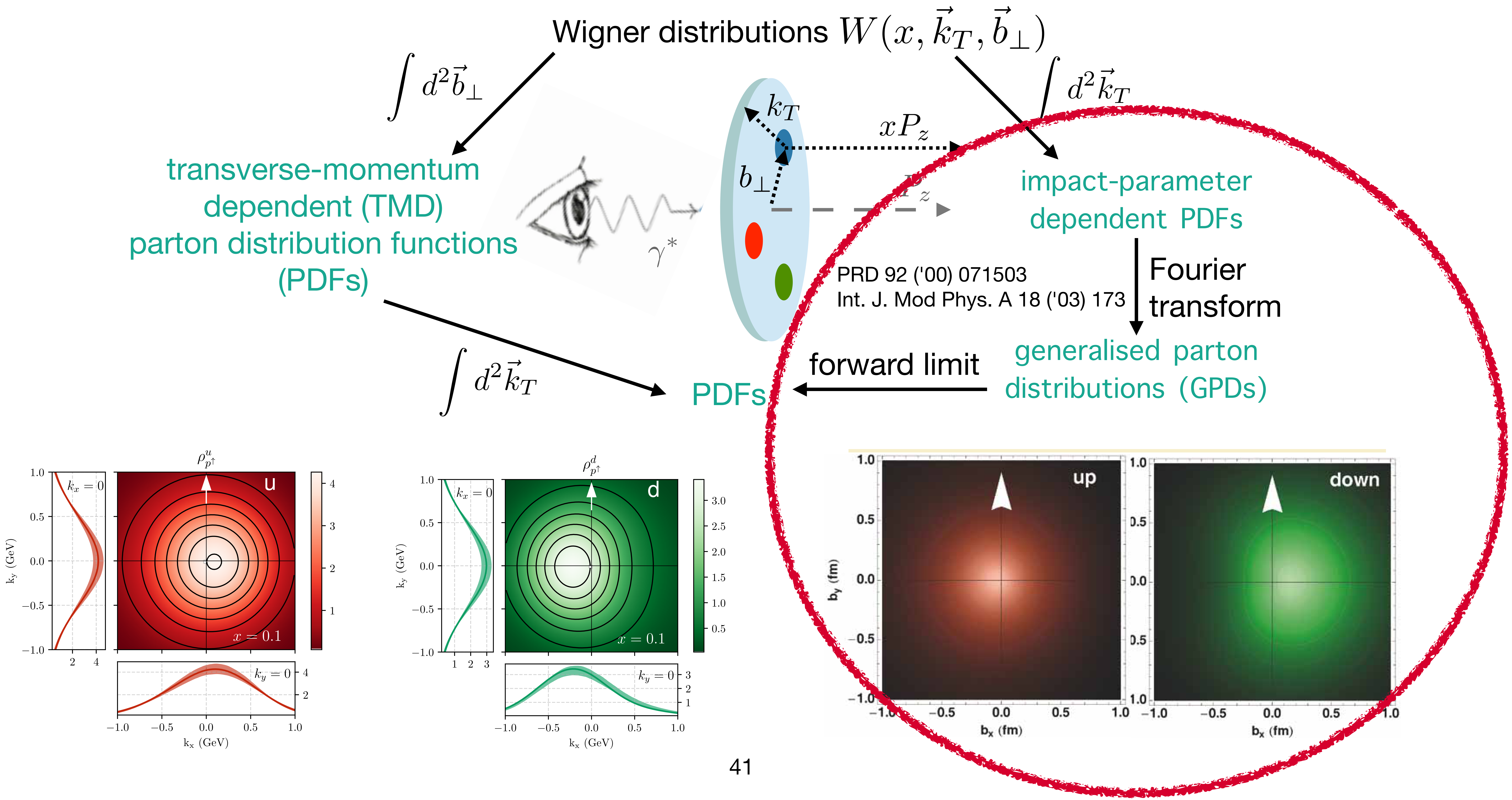

What are generalised parton distributions (GPDs)?

GPDs are probability <u>amplitudes</u>

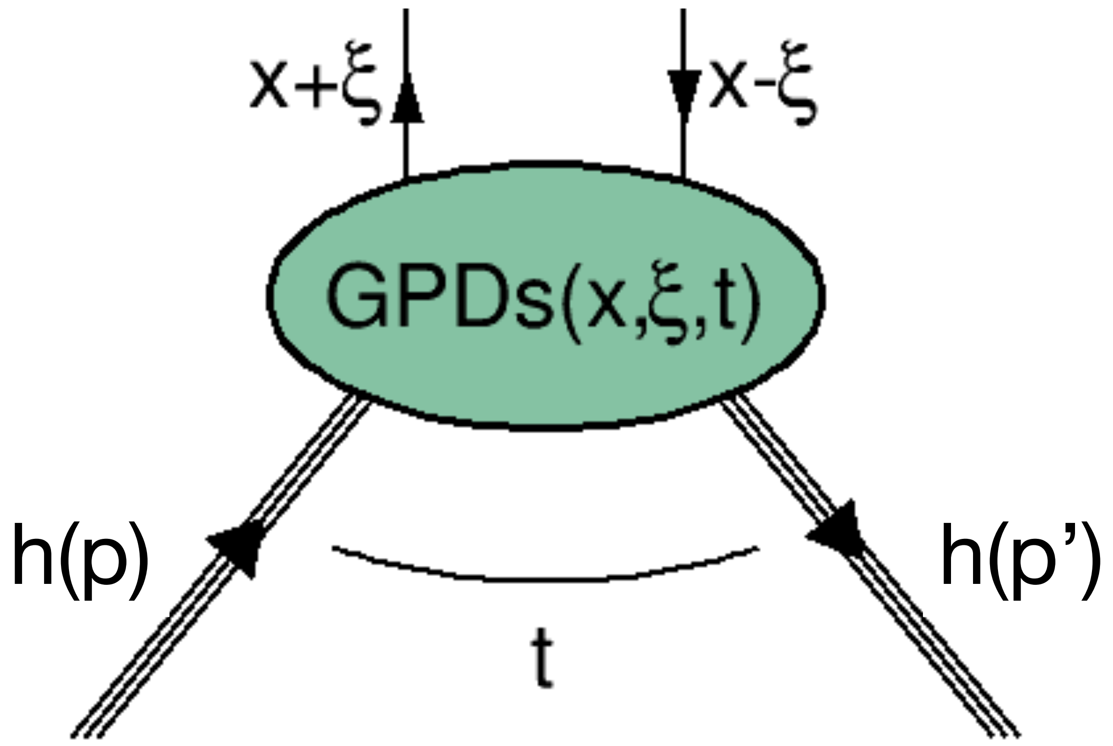

- x=average longitudinal momentum fraction
- 2ξ=longitudinal momentum transfer
- t=squared momentum transfer to hadron

- experimental access to t and ξ
- in general: no experimental access to x

What are generalised parton distributions (GPDs)?

GPDs are probability amplitudes

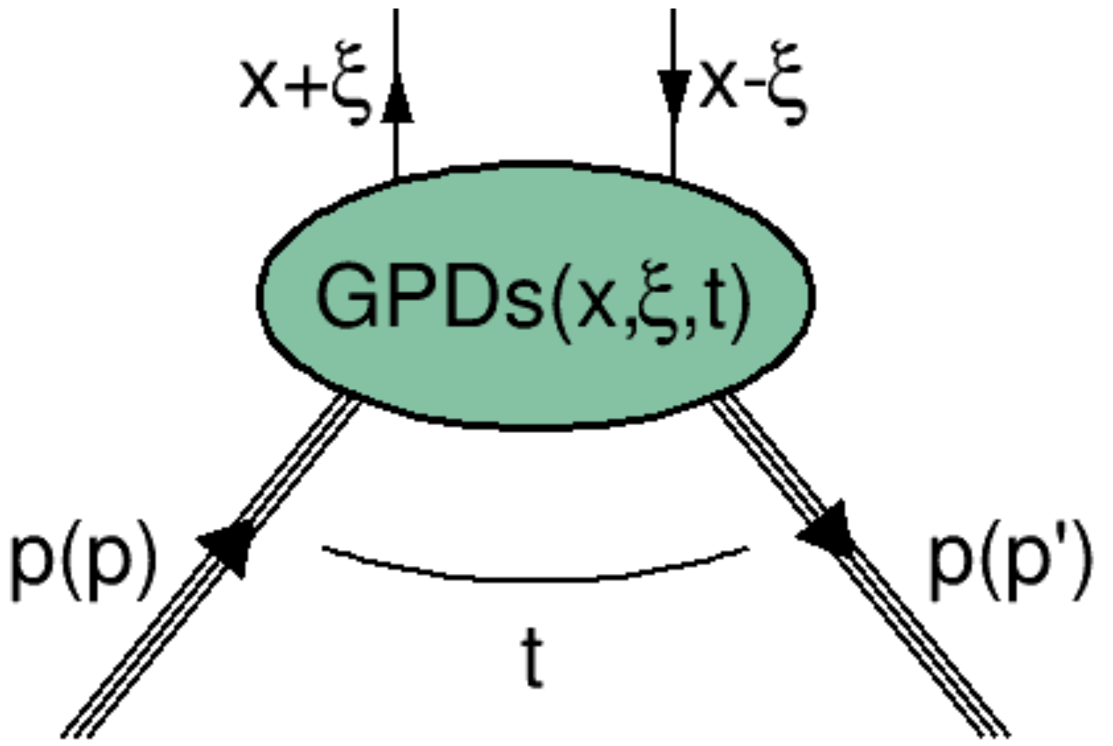

- x=average longitudinal momentum fraction
- 2ξ=longitudinal momentum transfer
- t=squared momentum transfer to hadron

- experimental access to t and ξ
- in general: no experimental access to x

- for spin-1/2 hadron:

Four parton helicity-conserving twist-2 GPDs

$H(x,\xi,t)$	$E(x,\xi,t)$	parton-spin independent
$\tilde{H}(x,\xi,t)$	$\tilde{E}(x,\xi,t)$	parton-spin dependent
proton helicity non flip	proton helicity flip	

Four parton helicity-flip twist-2 GPDs

$H_T(x,\xi,t)$	$E_T(x,\xi,t)$
$\tilde{H}_T(x,\xi,t)$	$\tilde{E}_T(x,\xi,t)$

In the forward limit

forward limit: $\xi = 0,\ t = 0$

for the nucleon:

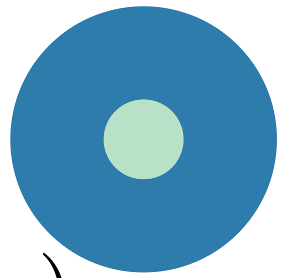

Four parton helicity-conserving twist-2 GPDs

PDFs				
spin-independent PDFs $q(x), g(x)$	← $H(x,\xi,t)$	$E(\cancel{x},\xi,t)$	parton-spin independent
helicity PDFs $\Delta q(x), \Delta g(x)$	← $\tilde{H}(x,\xi,t)$	$\tilde{E}(\cancel{x},\xi,t)$	parton-spin dependent
	proton helicity non flip	proton helicity flip	

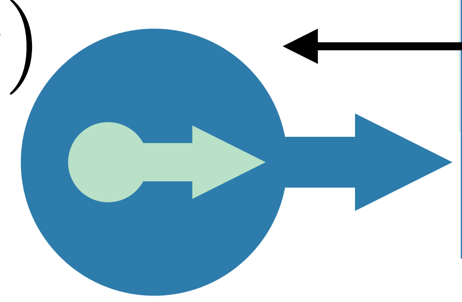

Four parton helicity-flip twist-2 GPDs

PDFs		
transversity PDFs $\delta q(x)$	← $H_T(x,\xi,t)$	$E_T(\cancel{x},\xi,t)$
	$\tilde{H}_T(\cancel{x},\xi,t)$	$\tilde{E}_T(\cancel{x},\xi,t)$

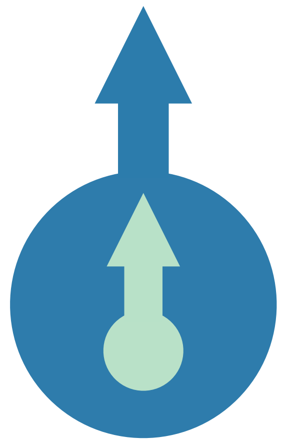

What GPDs tell us about the nucleon

- 3D parton distributions

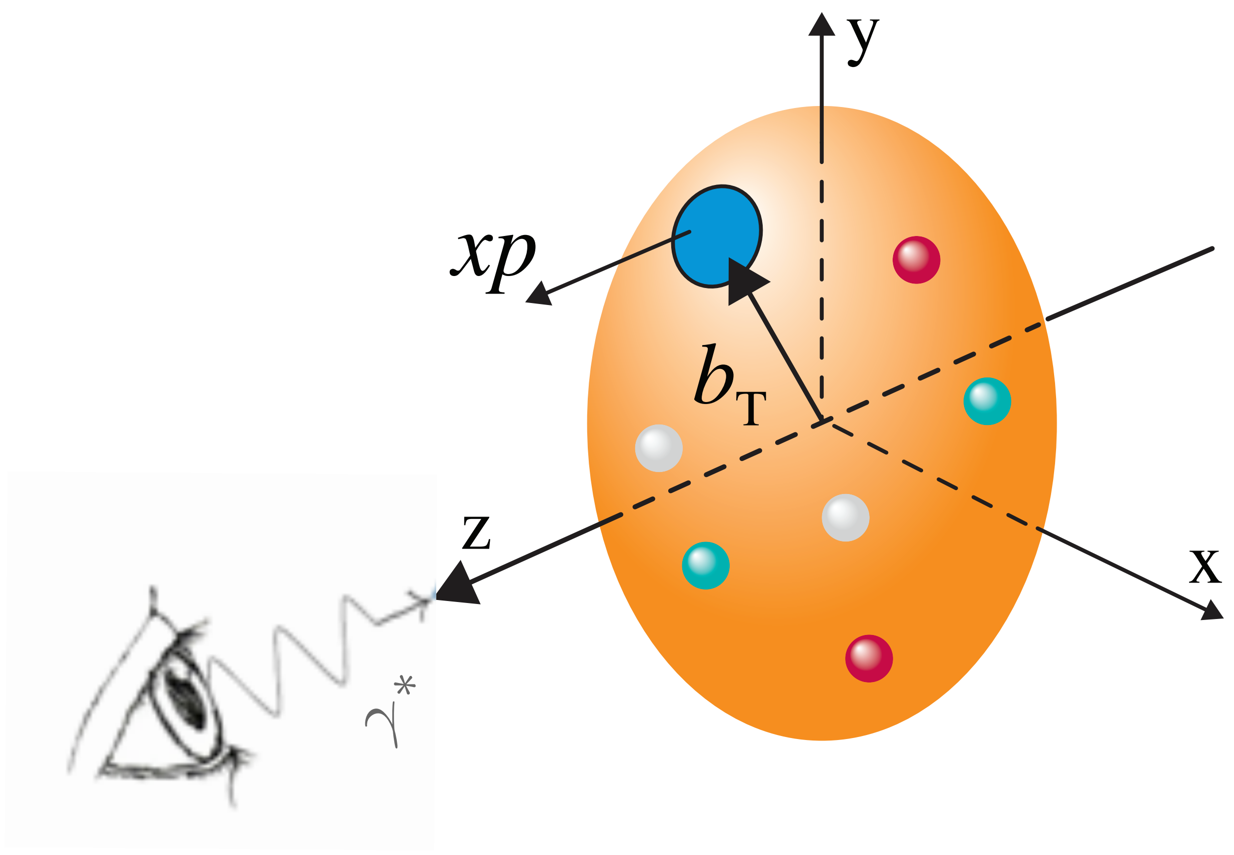

M. Burkardt, PRD **92** ('00) 071503
Int. J. Mod Phys. A **18** ('03) 173

impact-parameter dependent distributions:
probability to find parton (x,b_T)

Fourier
transform for ξ=0

GPDs

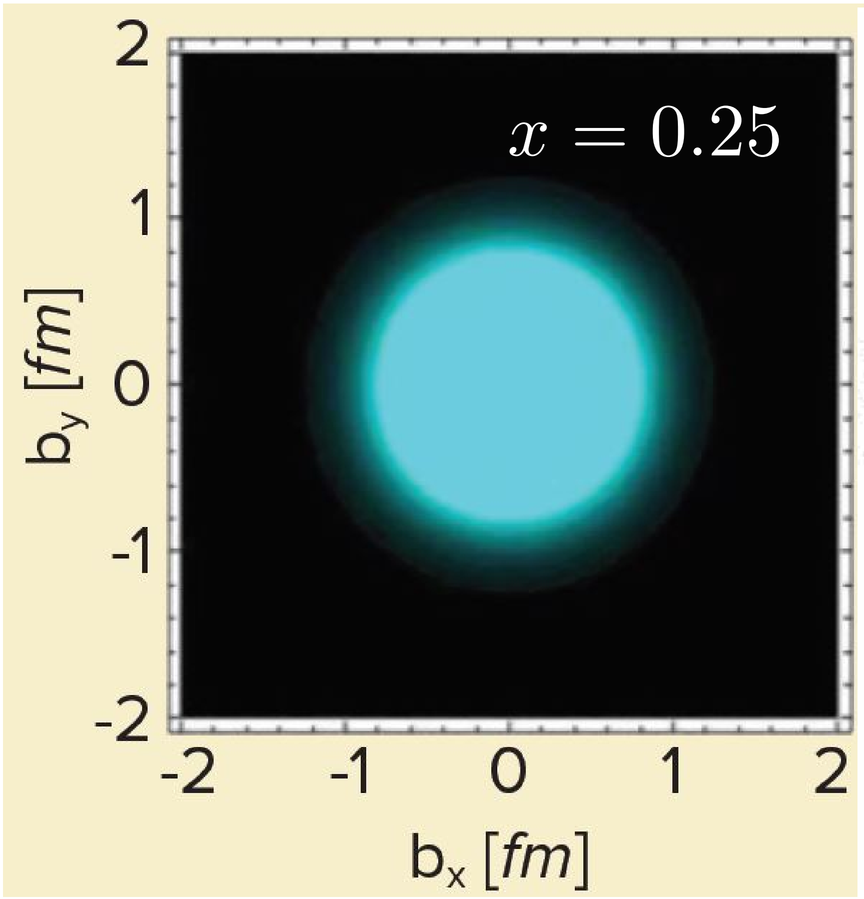

GPD H

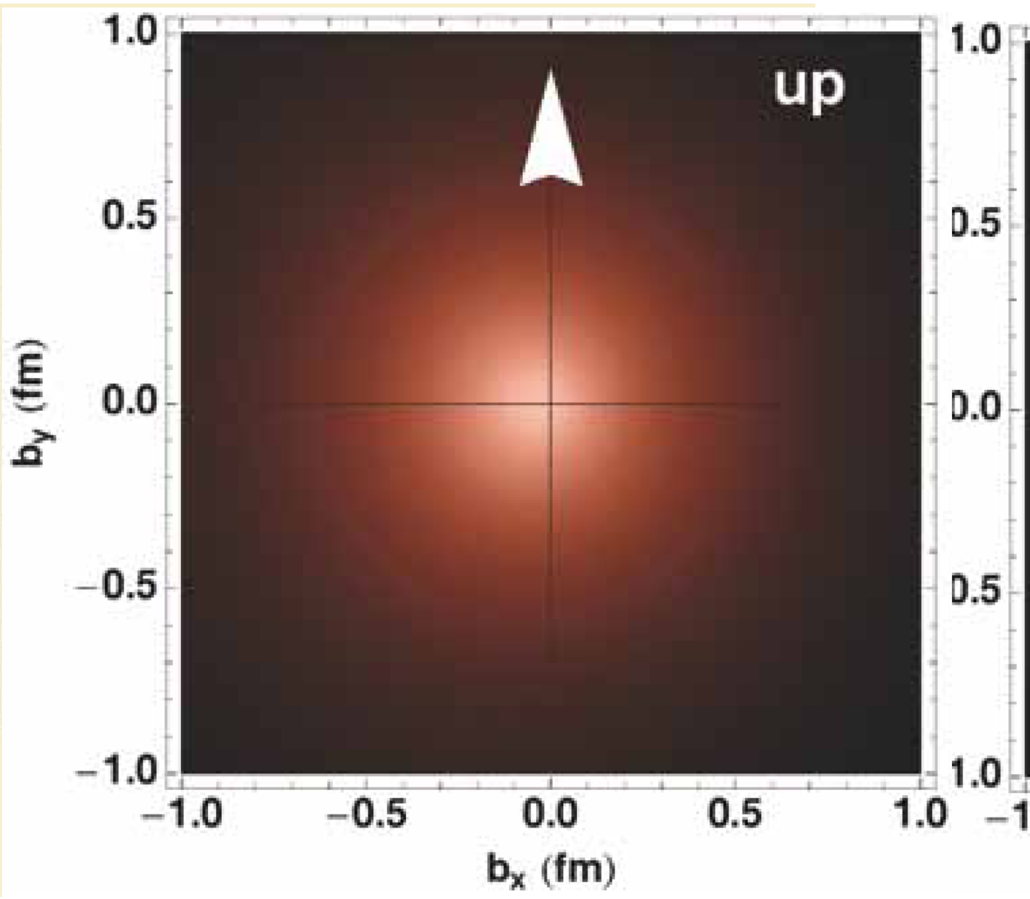

GPDs H+E

What GPDs tell us about the nucleon

- 3D parton distributions

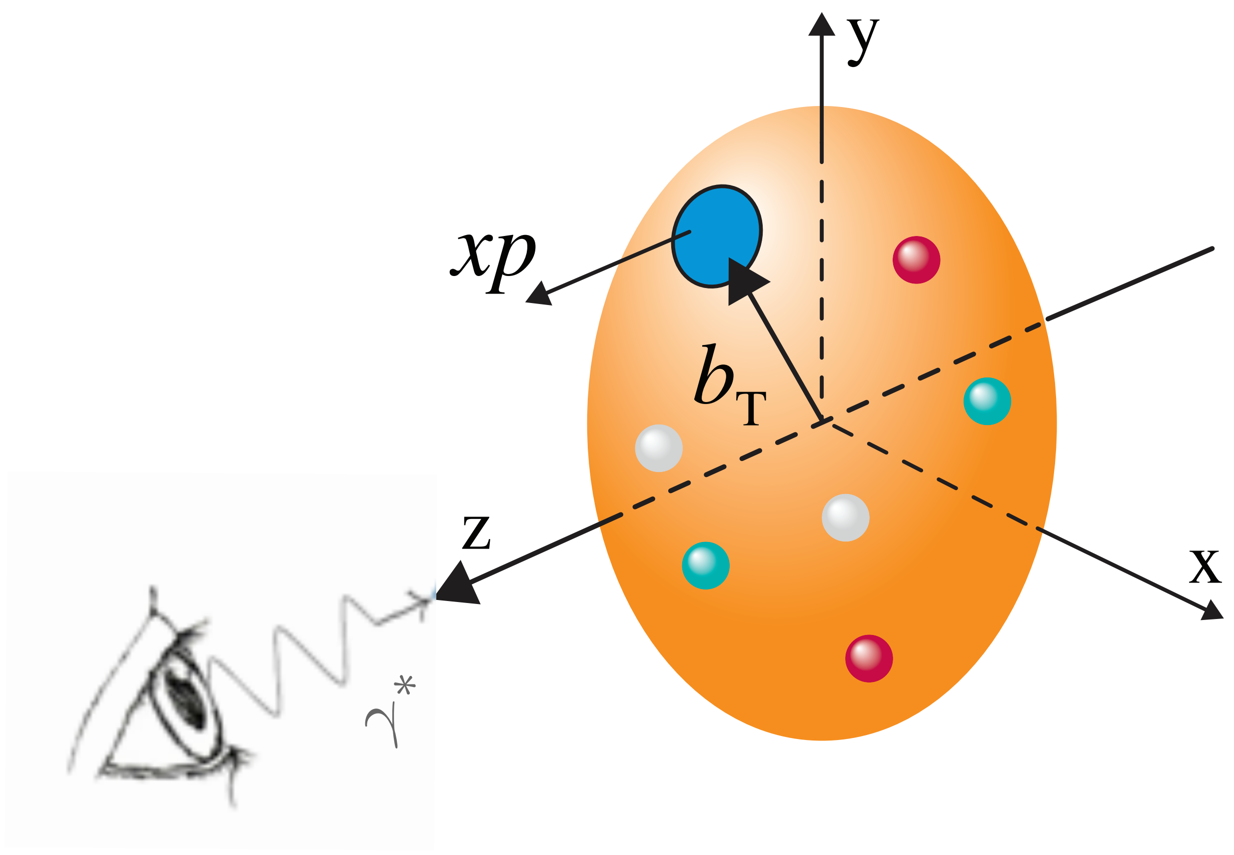

M. Burkardt, PRD **92** ('00) 071503
Int. J. Mod Phys. A **18** ('03) 173

impact-parameter dependent distributions:
probability to find parton (x, b_T)

↑ Fourier transform for $\xi=0$

GPDs

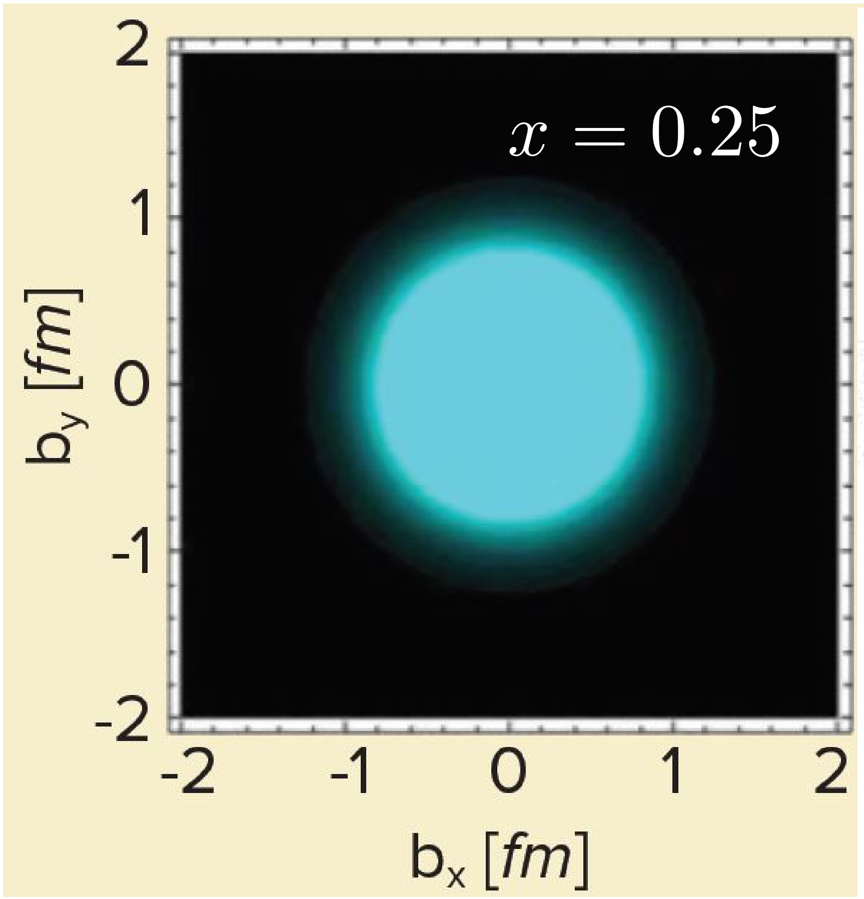

GPD H

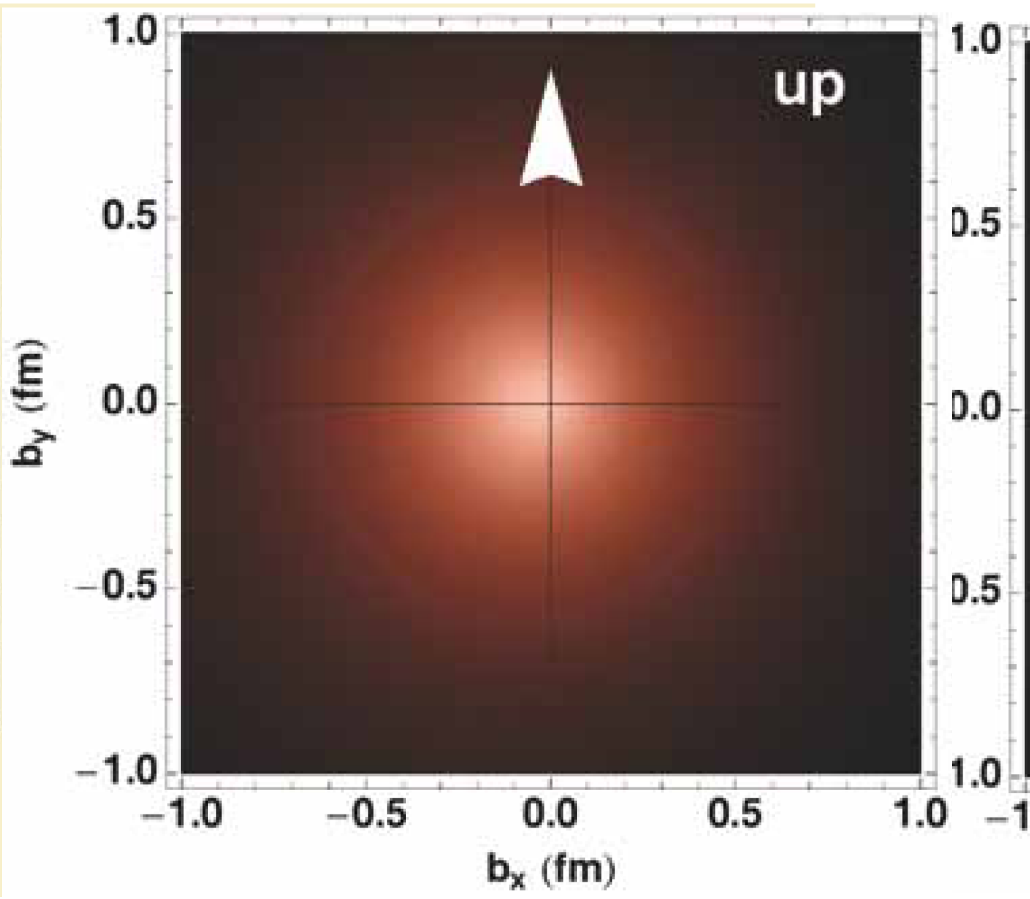

GPDs H+E

- pressure distributions

GPDs

↓ $\int dx\, x$

gravitational form factors

↓ Fourier transform

pressure distributions

What GPDs tell us about the nucleon

- 3D parton distributions

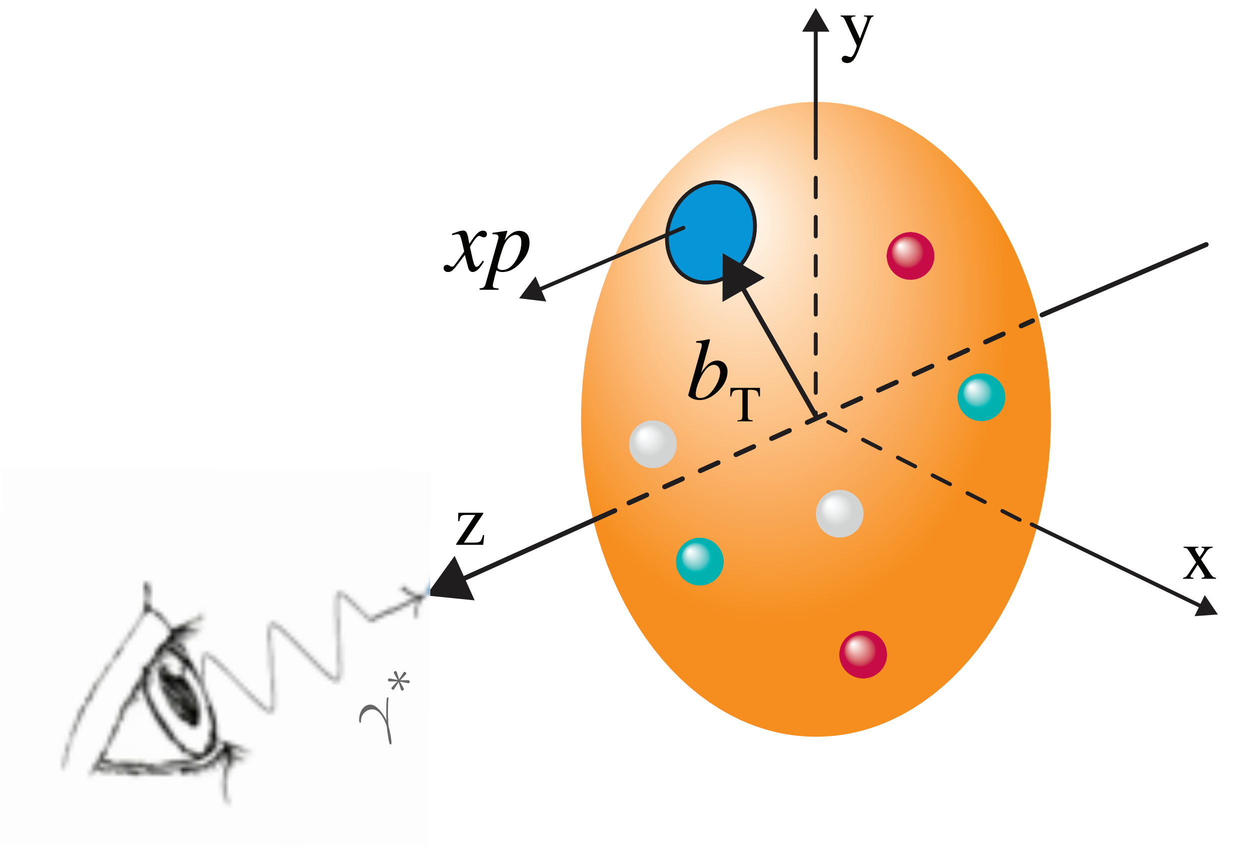

M. Burkardt, PRD **92** ('00) 071503
Int. J. Mod Phys. A **18** ('03) 173

impact-parameter dependent distributions:
probability to find parton (x,b_T)

↑ Fourier transform for ξ=0

GPDs

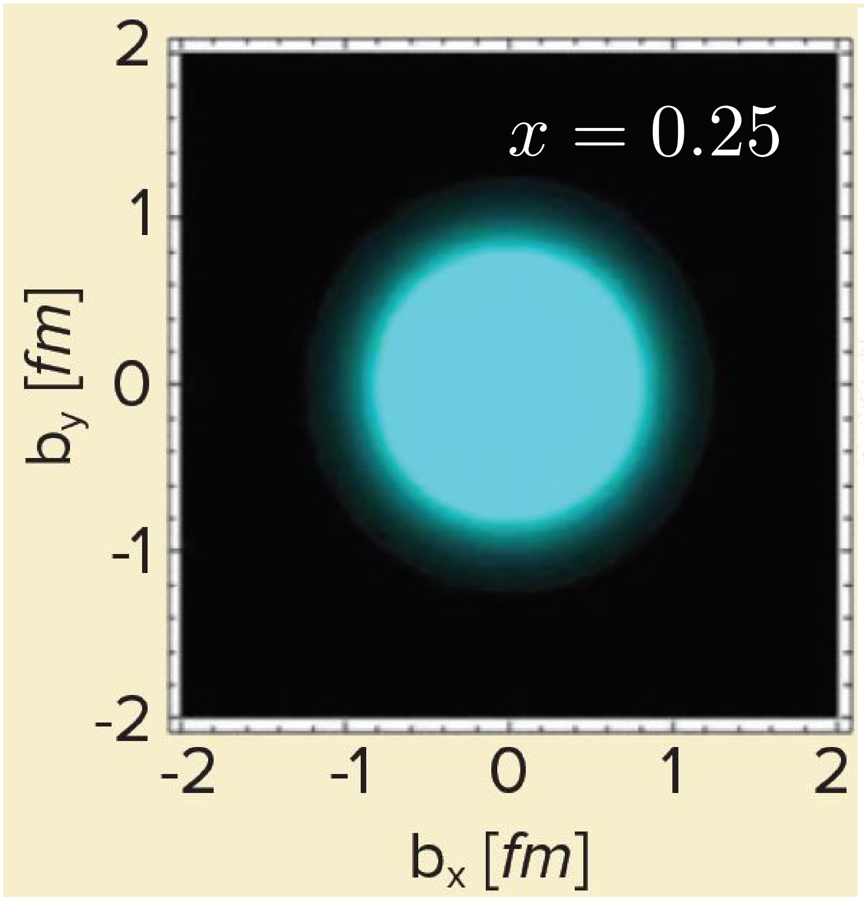

GPD H

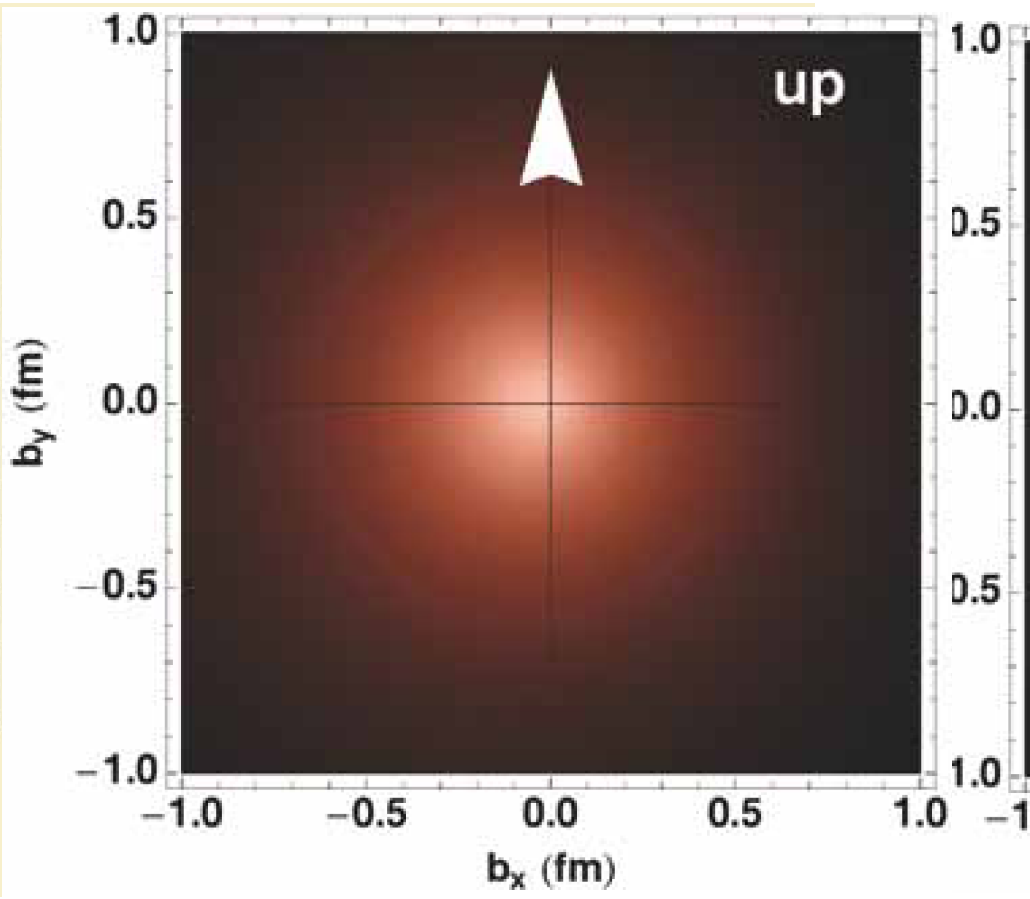

GPDs H+E

- pressure distributions

GPDs

↓ $\int dx\, x$

gravitational form factors

↓ Fourier transform

pressure distributions

radial pressure

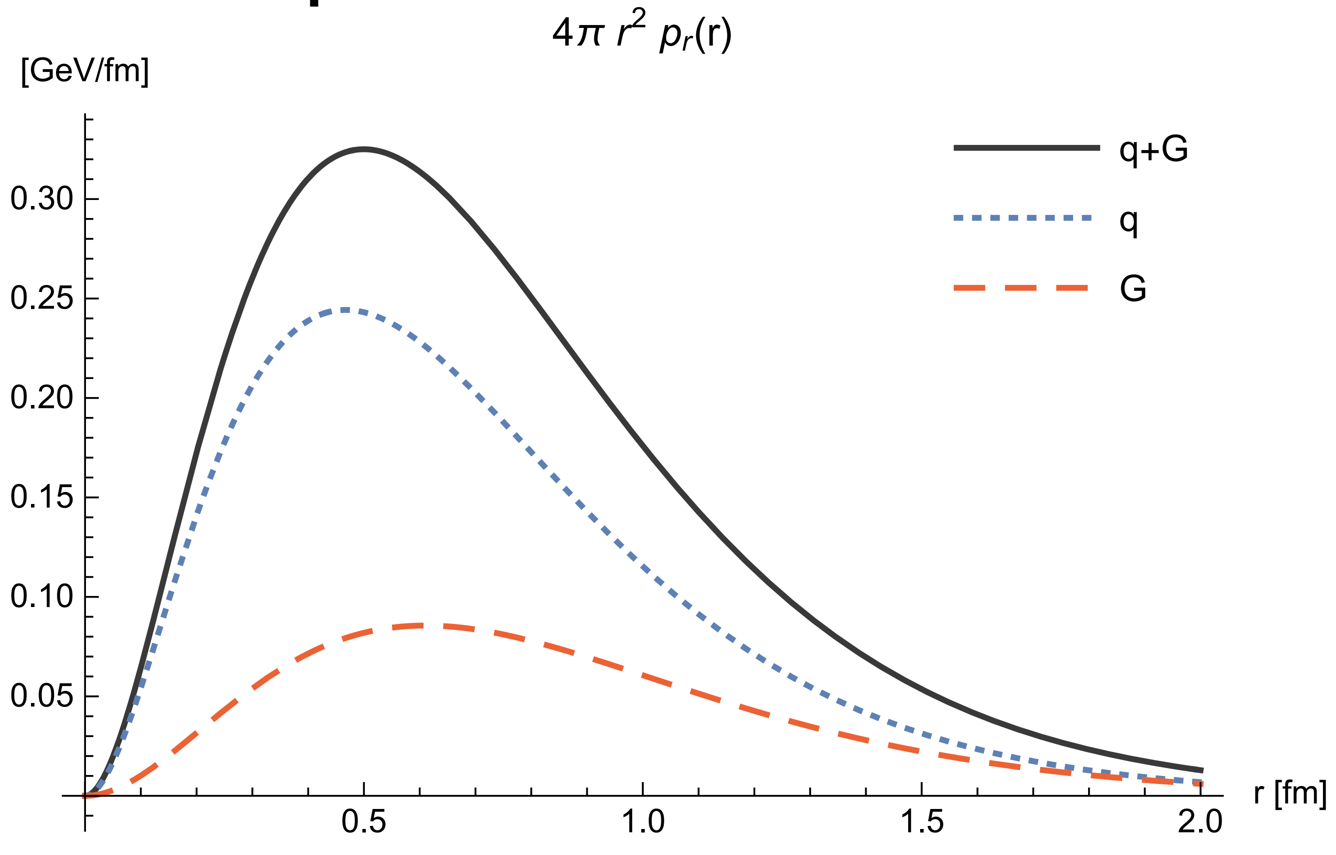

tangential pressure

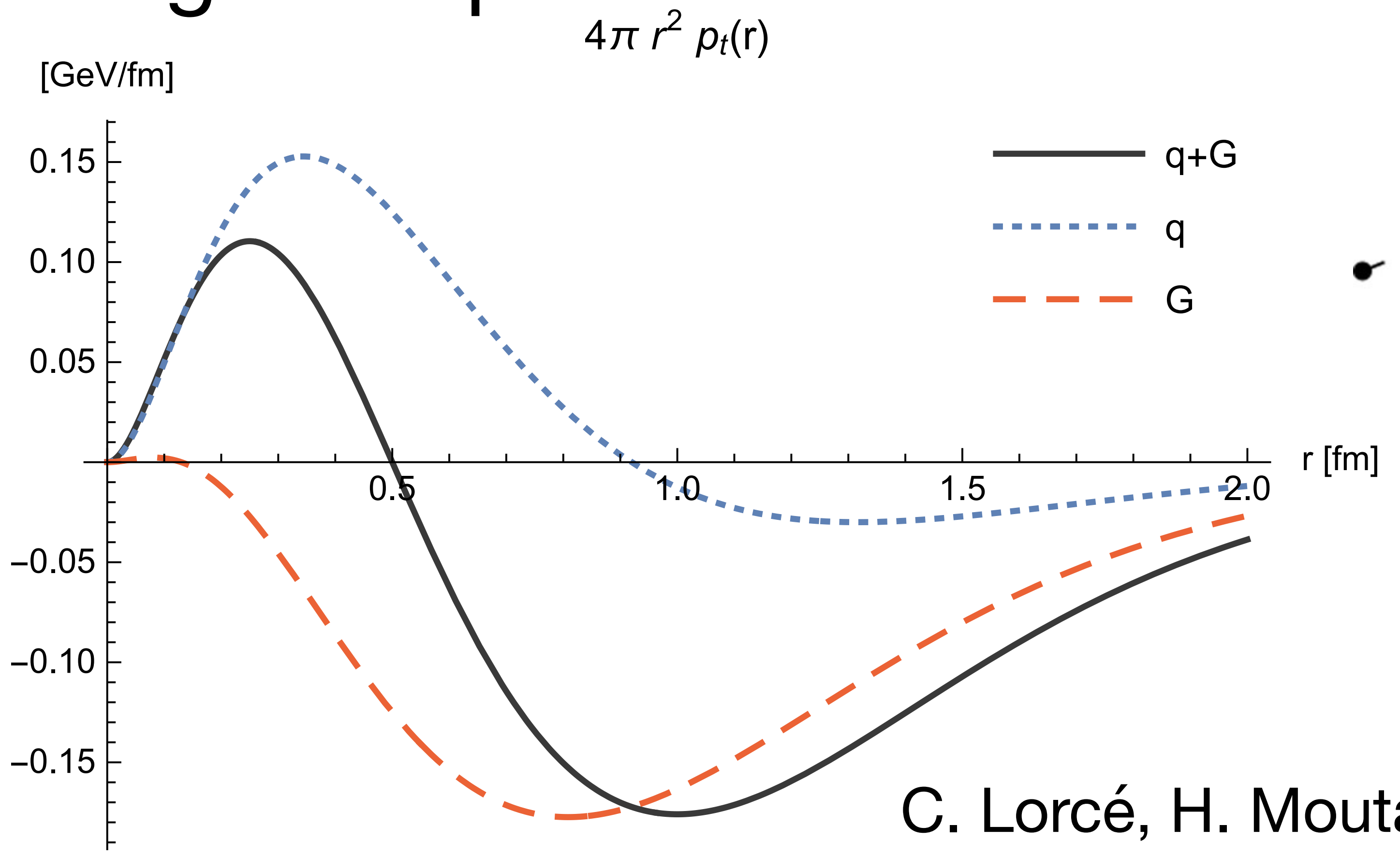

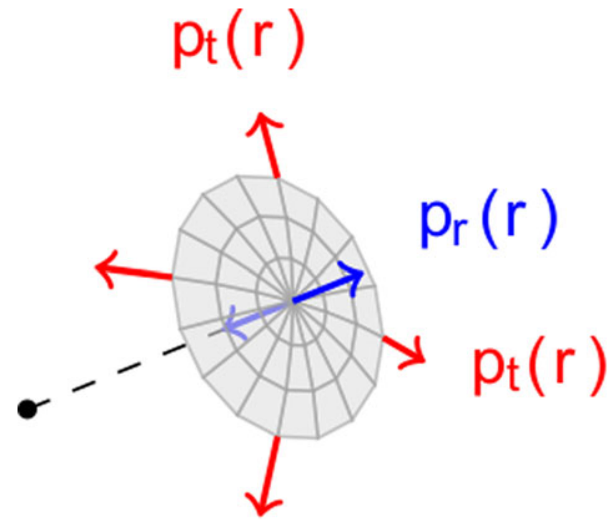

C. Lorcé, H. Moutarde, A. P. Trawiński
Eur. Phys. J. C **79** ('19) 89

… and its spin

longitudinally polarised nucleon

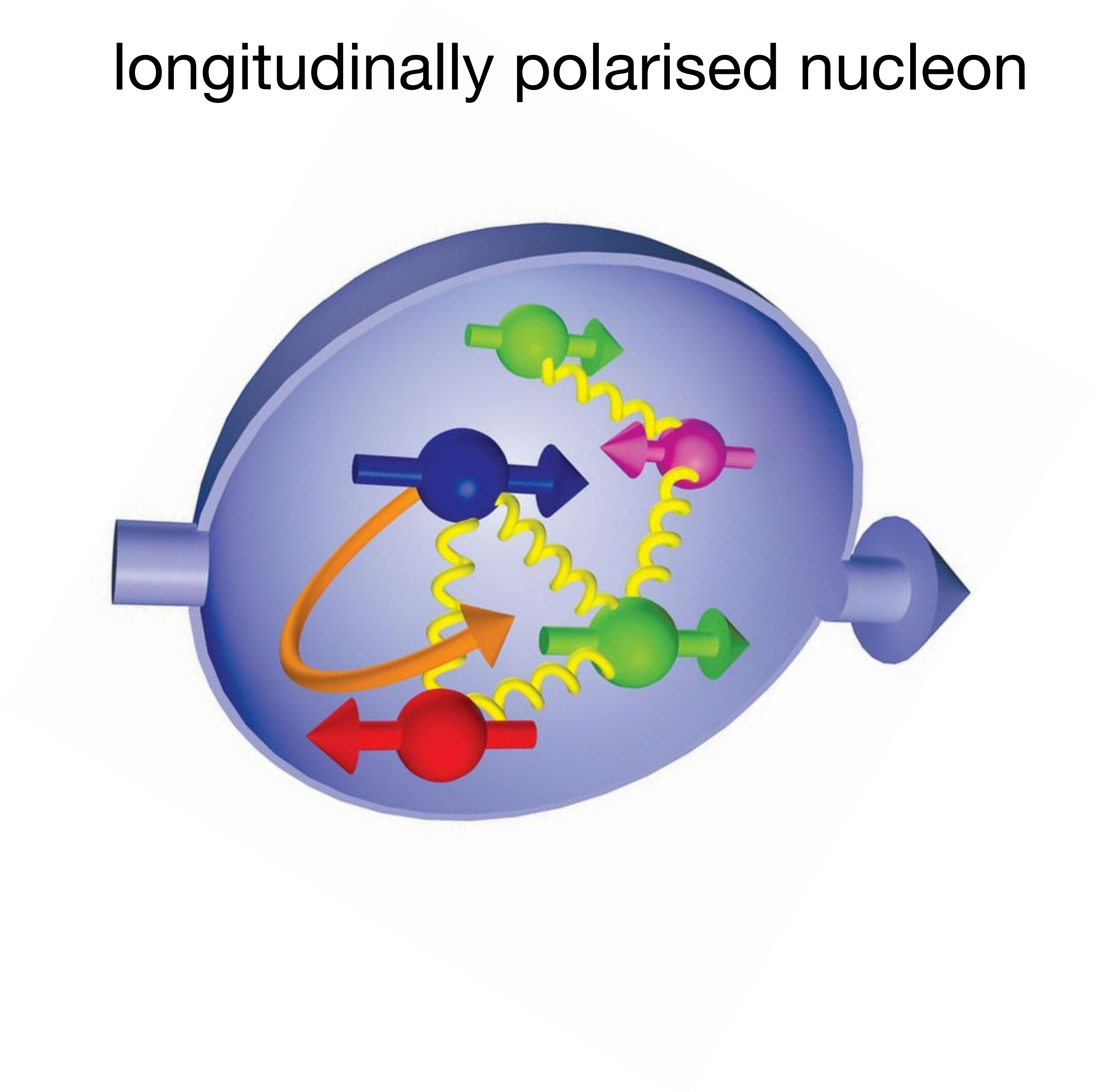

proton spin

$$\frac{1}{2} = \frac{1}{2}\sum_q \Delta q + \sum_q L^q + J^G$$

quark spin — 30%

quark orbital angular momentum — ?

gluon angular momentum — ?

$$J = \lim_{t\to 0} \frac{1}{2}\int_{-1}^{1} dx\, x\, [H(x,\xi,t) + E(x,\xi,t)]$$

X. Ji, Phys. Rev. Lett. 78 (1997) 610

Experimental access to GPDs: electroproduction

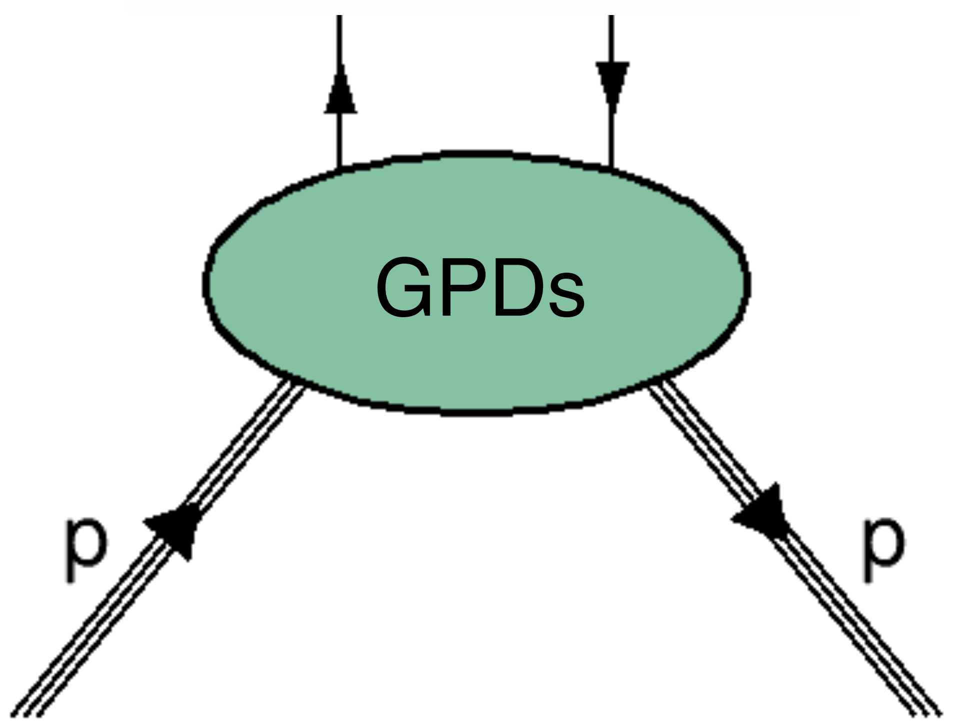

Experimental access to GPDs: electroproduction

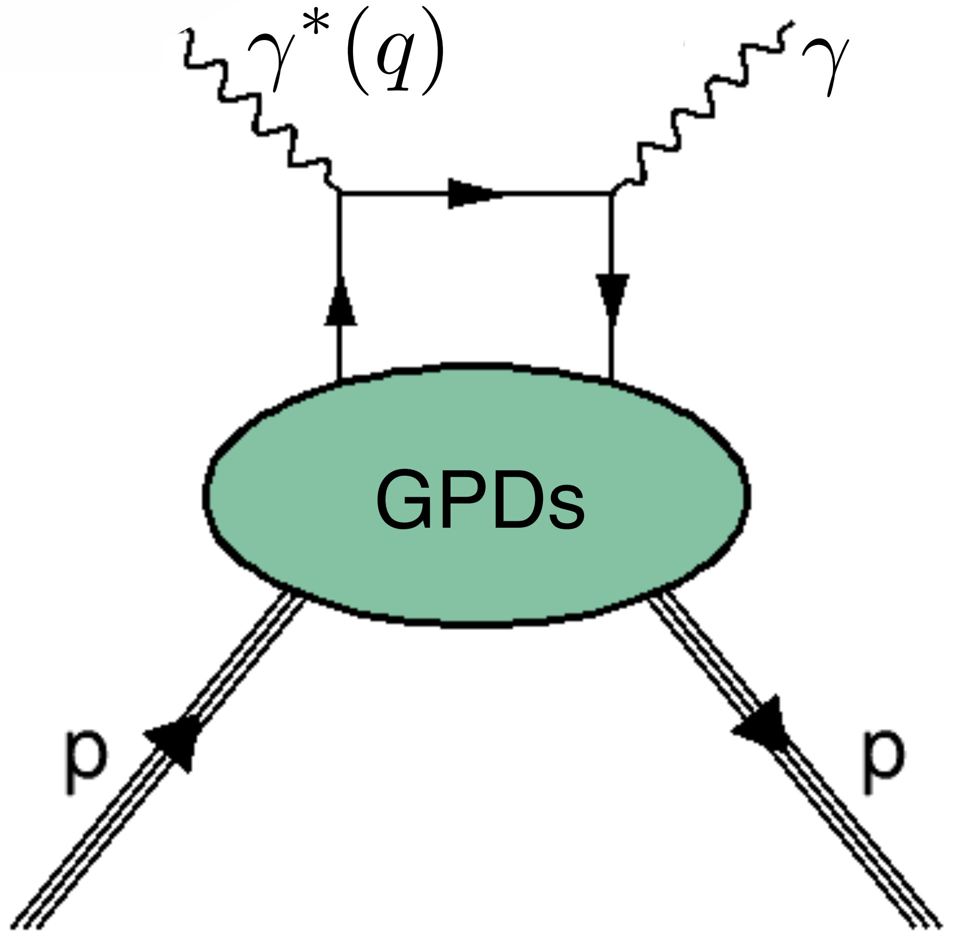

Deeply virtual Compton scattering (DVCS)
Hard scale=large $Q^2=-q^2$

Experimental access to GPDs: electroproduction

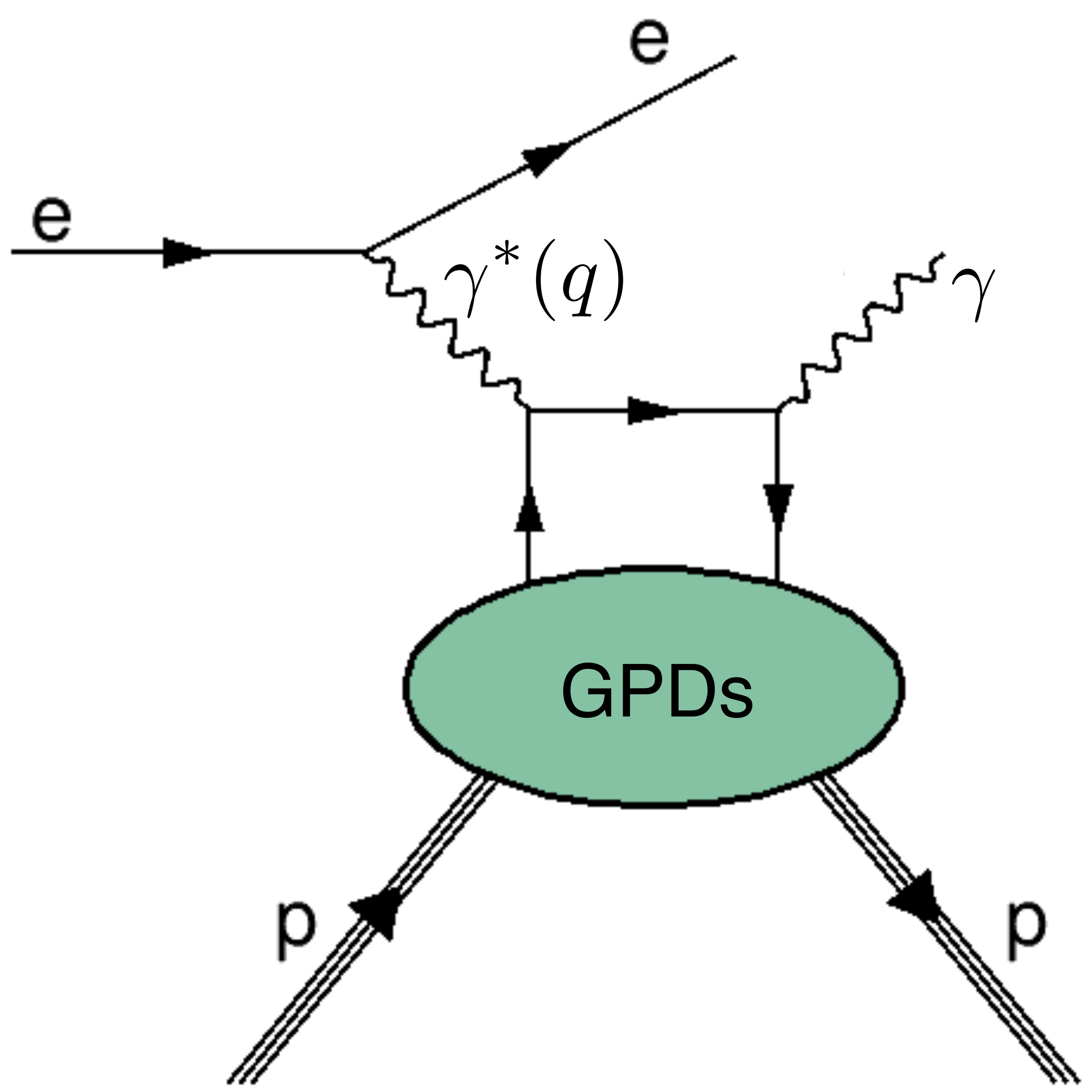

Deeply virtual Compton scattering (DVCS)
Hard scale=large $Q^2=-q^2$

Experimental access to GPDs: electroproduction

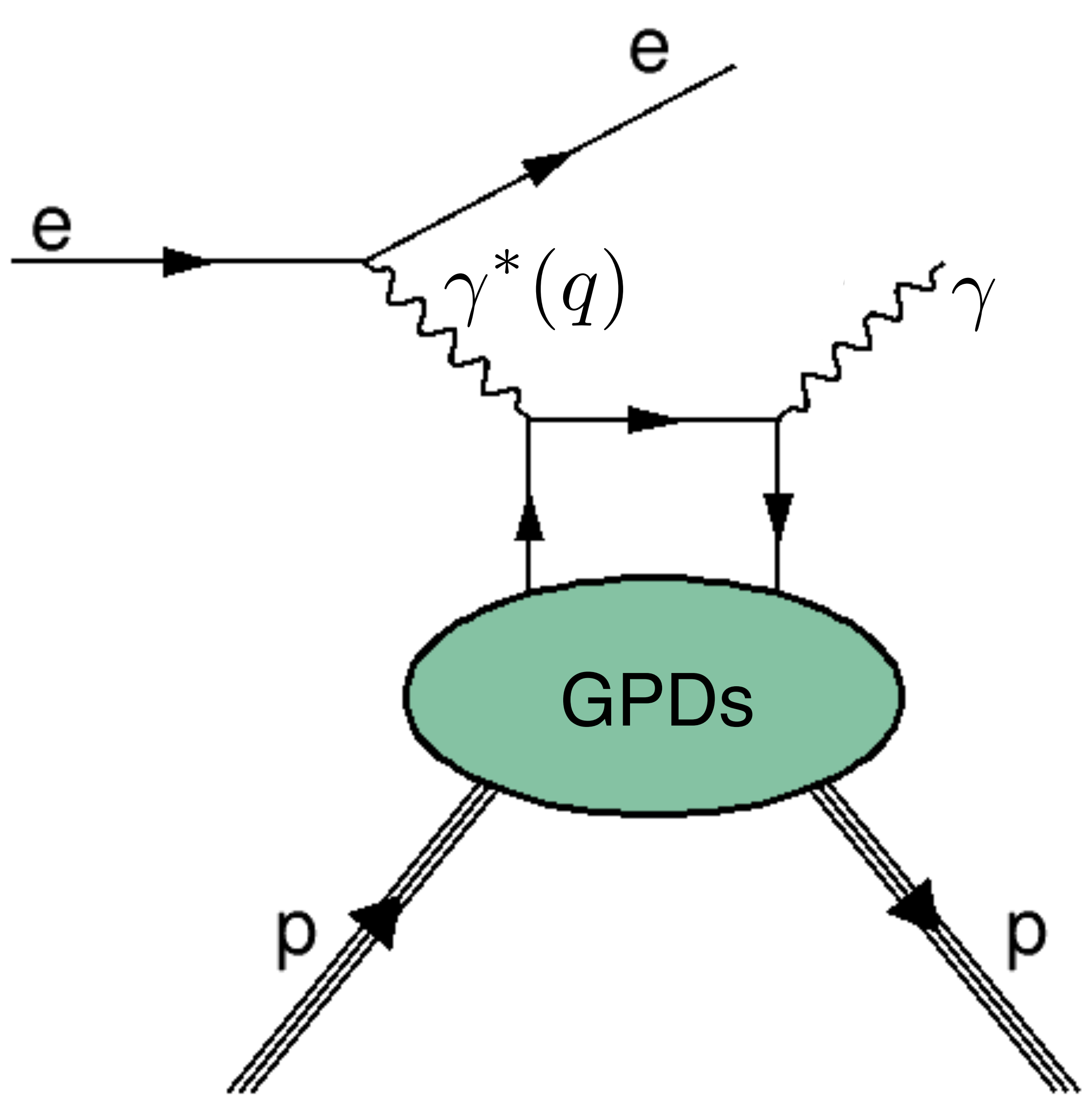

Deeply virtual Compton scattering (DVCS)
Hard scale=large Q^2=-q^2

CLAS – PRC 80 ('09) 035206; PRL 87 ('01) 182002; 100 ('08) 162002

COMPASS – arXiv:1702.06315

JLab Hall A Collaboration – PRL 99 ('07) 242501; PRC 92 ('15) 055202; Nat. Com. **8** ('17) 1408

HERMES – JHEP 10 ('12) 042; PLB 704 ('11) 15; NPB 842 ('11) 265

H1 – PLB 681 ('09) 391; 659 ('07) 796; EPJ C 44 ('05) 1

ZEUS – PLB 573 (2003) 46; JHEP 05 ('09) 108

Experimental access to GPDs: electroproduction

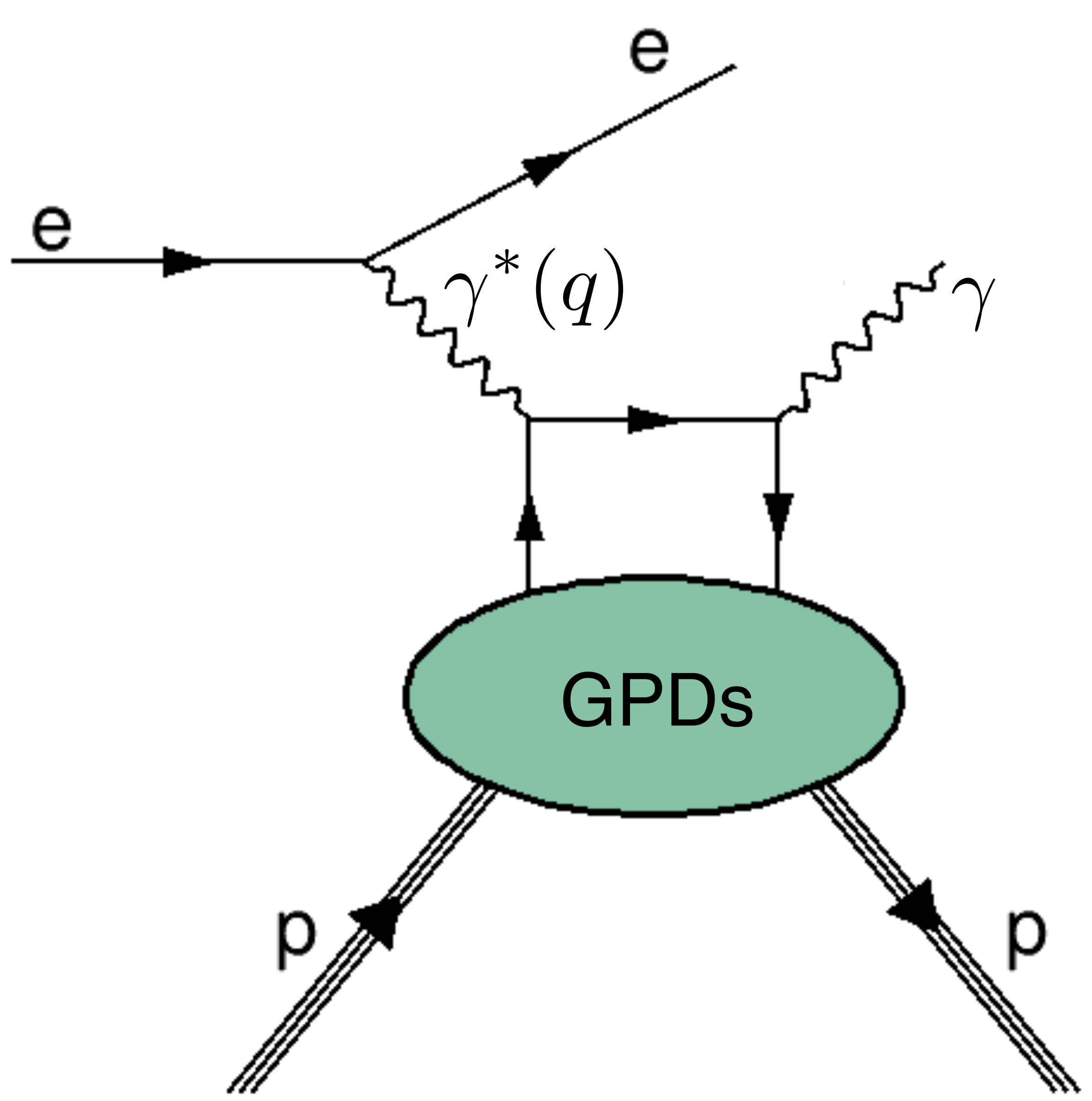

Deeply virtual Compton scattering (DVCS)
Hard scale=large $Q^2=-q^2$

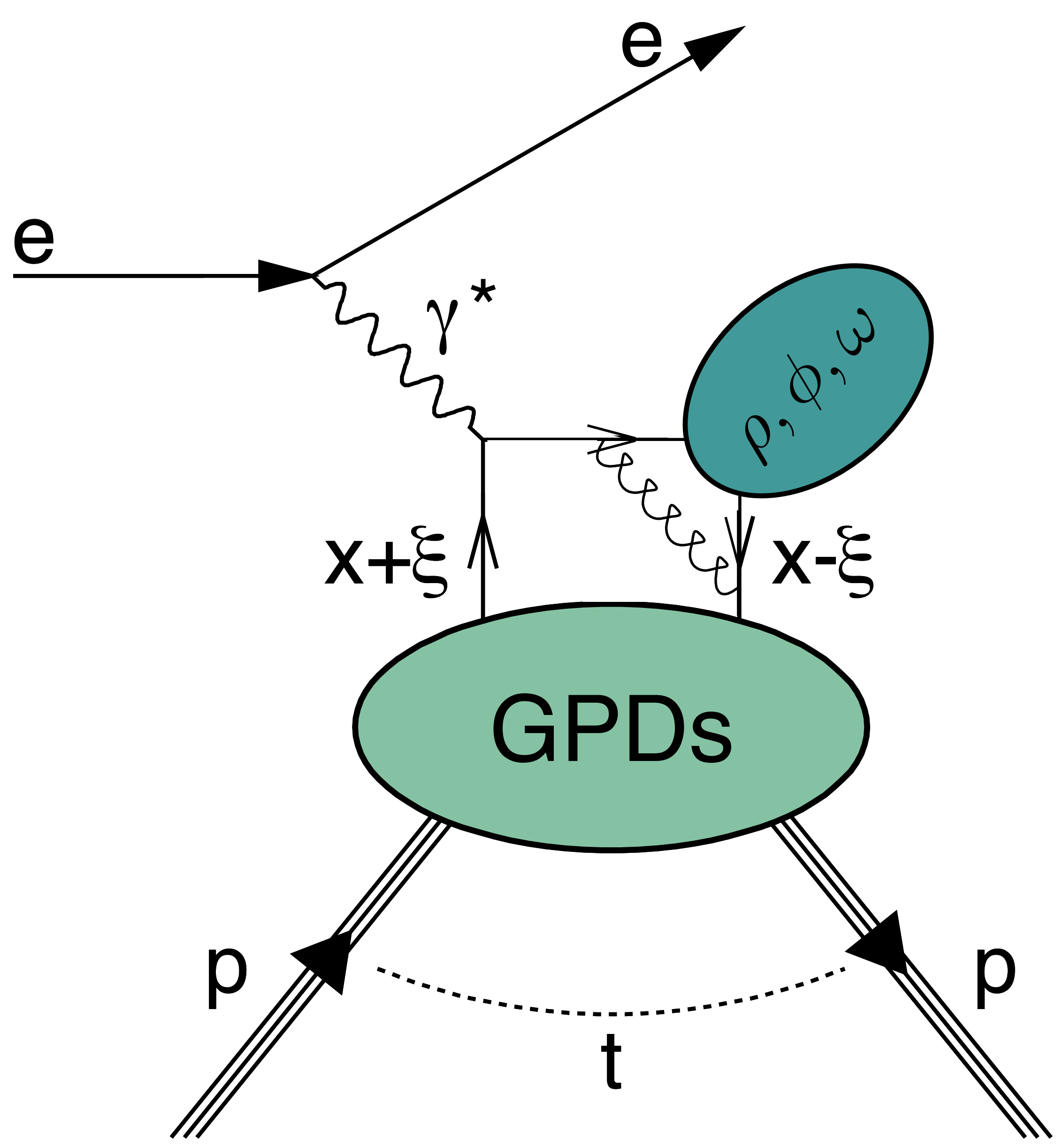

Hard exclusive meson production
Hard scale=large Q^2

CLAS – PRC 80 ('09) 035206; PRL 87 ('01) 182002; 100 ('08) 162002

COMPASS – arXiv:1702.06315

JLab Hall A Collaboration – PRL 99 ('07) 242501; PRC 92 ('15) 055202; Nat. Com. **8** ('17) 1408

HERMES – JHEP 10 ('12) 042; PLB 704 ('11) 15; NPB 842 ('11) 265

H1 – PLB 681 ('09) 391; 659 ('07) 796; EPJ C 44 ('05) 1

ZEUS – PLB 573 (2003) 46; JHEP 05 ('09) 108

Experimental access to GPDs: electroproduction

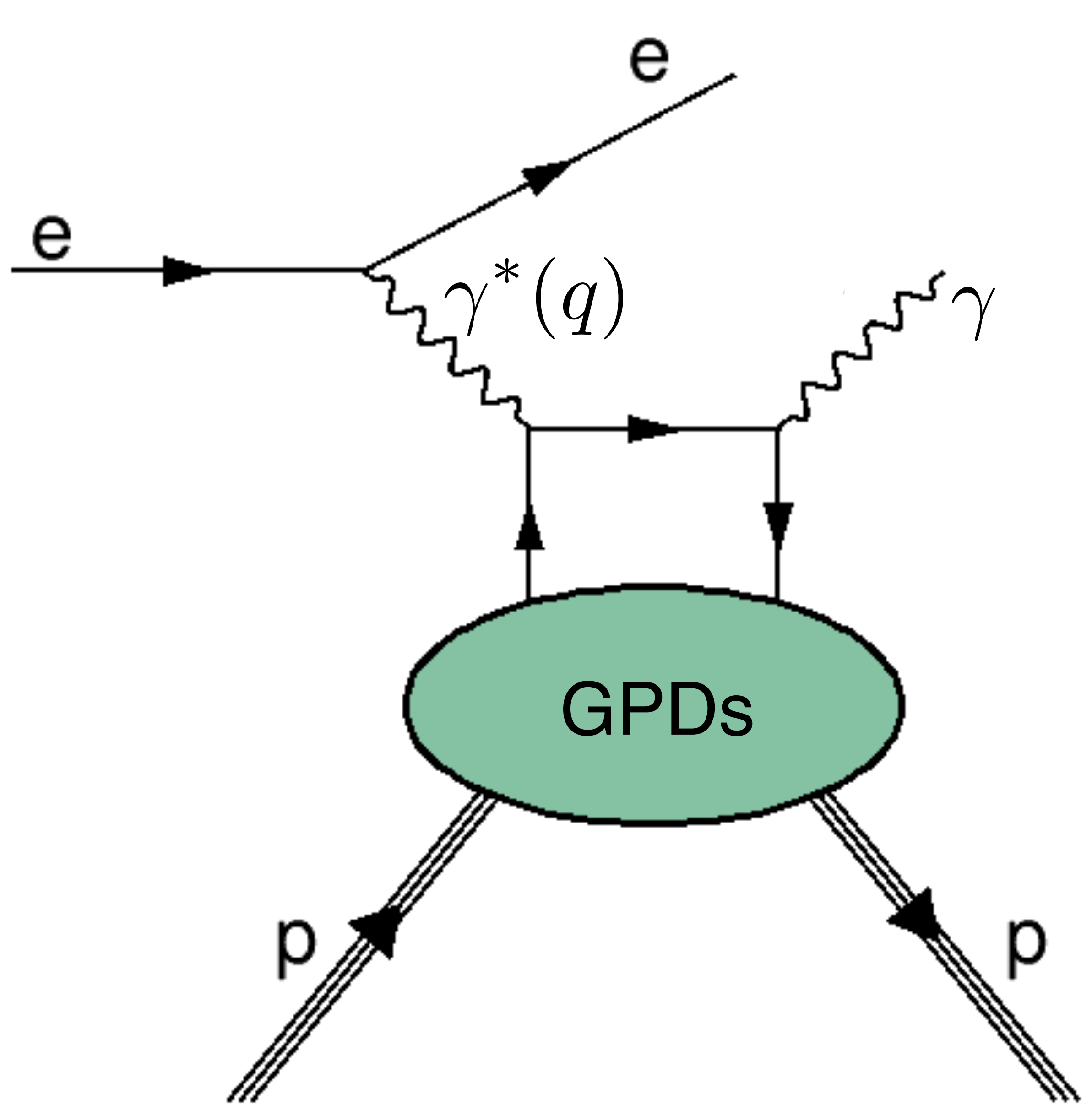

Deeply virtual Compton scattering (DVCS)
Hard scale=large Q^2=-q^2

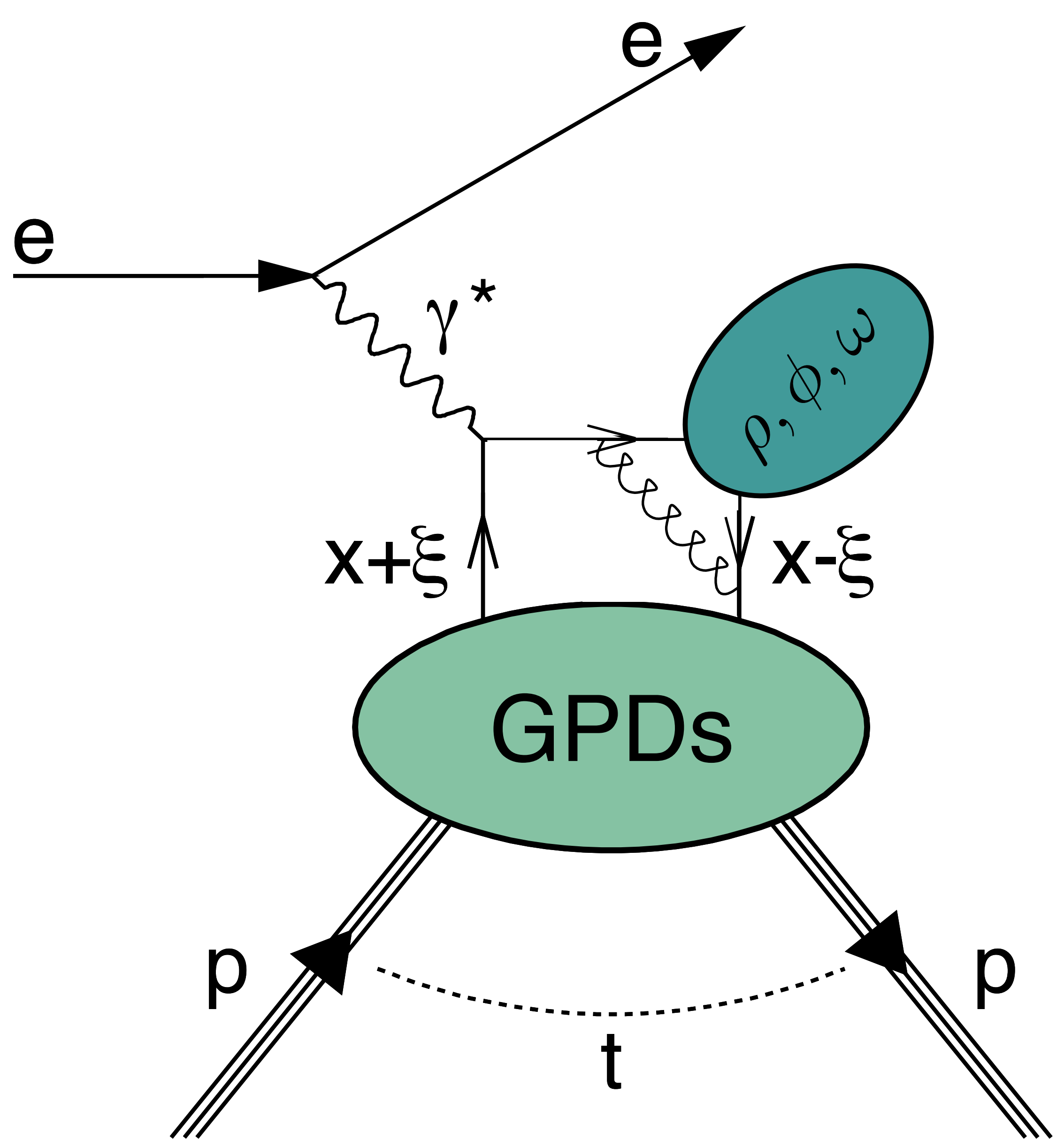

Hard exclusive meson production
Hard scale=large Q^2

CLAS – PRC 80 ('09) 035206; PRL 87 ('01) 182002; 100 ('08) 162002
COMPASS – arXiv:1702.06315
JLab Hall A Collaboration – PRL 99 ('07) 242501; PRC 92 ('15) 055202; Nat. Com. **8** ('17) 1408
HERMES – JHEP 10 ('12) 042; PLB 704 ('11) 15; NPB 842 ('11) 265
H1 – PLB 681 ('09) 391; 659 ('07) 796; EPJ C 44 ('05) 1
ZEUS – PLB 573 (2003) 46; JHEP 05 ('09) 108

CLAS – PRC 95 ('17) 035207; 95 (2017) 035202
COMPASS – PLB 731 ('14) 19; NPB 915 ('17) 454
JLab Hall A Collaboration – PRC 83 ('11) 025201
HERMES – EPJ C 74 ('14) 3110; 75 ('15) 600; 77 ('17) 378

Experimental access to GPDs: electroproduction

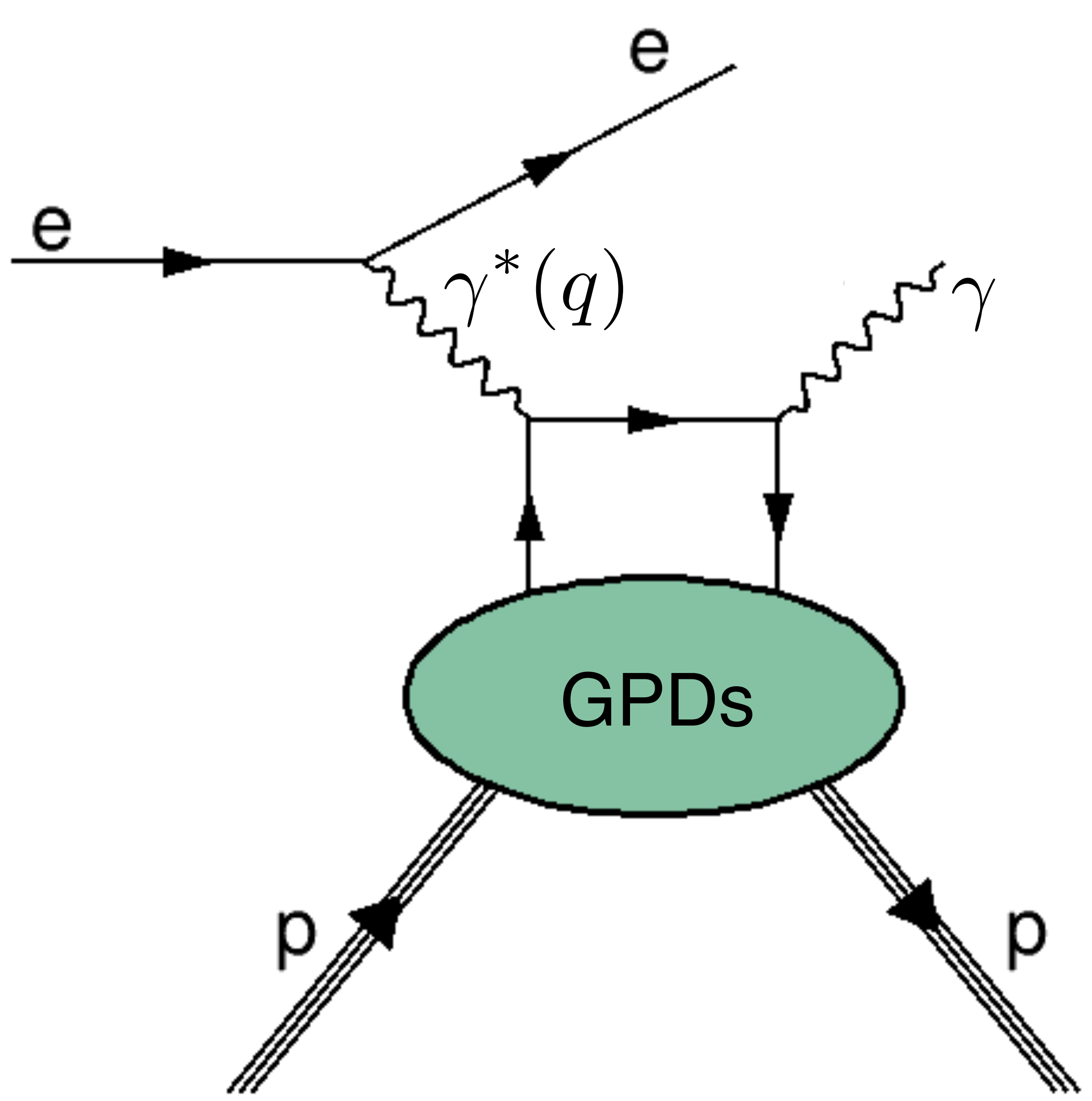

Deeply virtual Compton scattering (DVCS)
Hard scale=large $Q^2=-q^2$

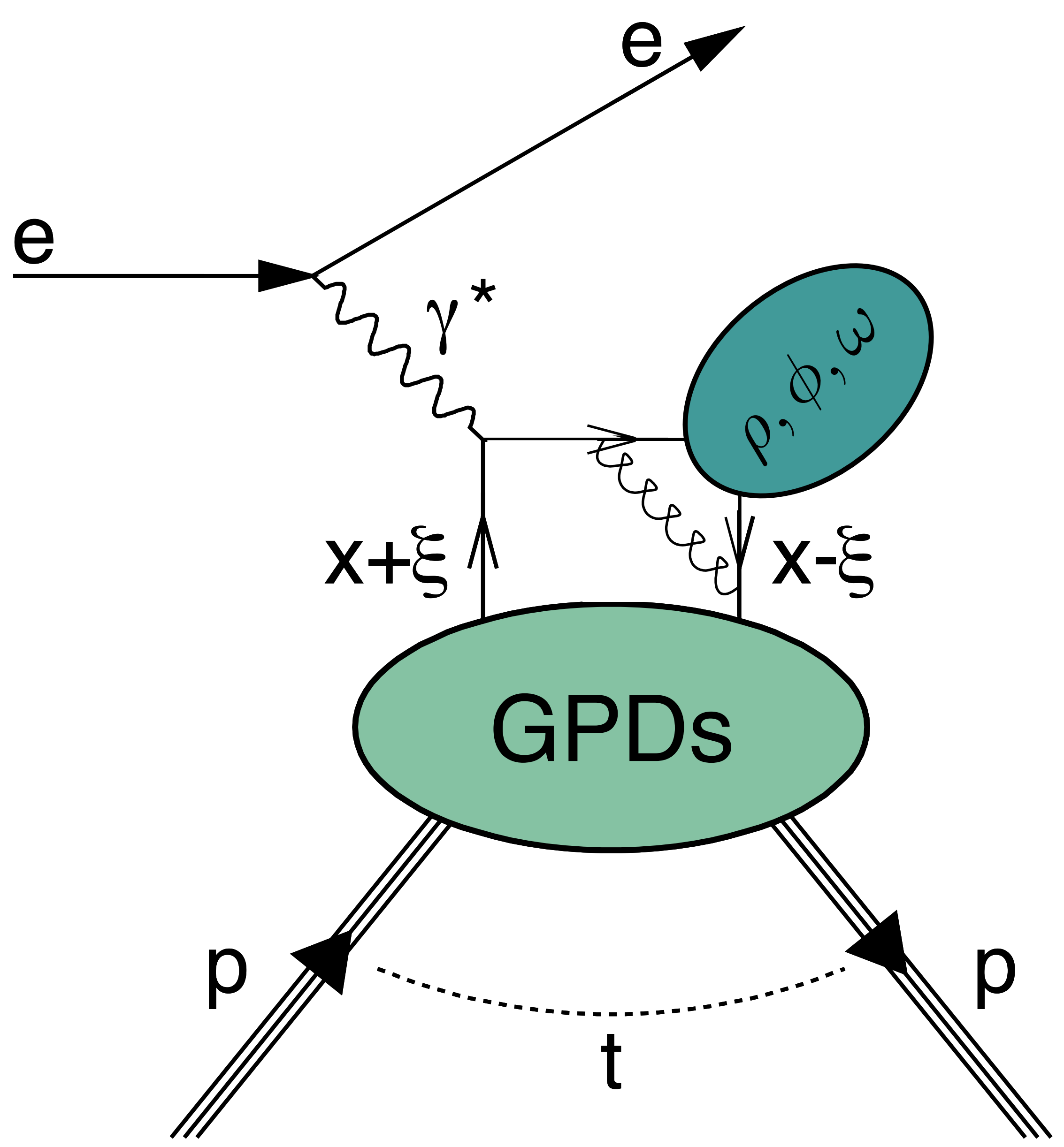

Hard exclusive meson production
Hard scale=large Q^2

CLAS – PRC 80 ('09) 035206; PRL 87 ('01) 182002; 100 ('08) 162002
COMPASS – arXiv:1702.06315
JLab Hall A Collaboration – PRL 99 ('07) 242501; PRC 92 ('15) 055202; Nat. Com. **8** ('17) 1408
HERMES – JHEP 10 ('12) 042; PLB 704 ('11) 15; NPB 842 ('11) 265
H1 – PLB 681 ('09) 391; 659 ('07) 796; EPJ C 44 ('05) 1
ZEUS – PLB 573 (2003) 46; JHEP 05 ('09) 108

CLAS – PRC 95 ('17) 035207; 95 (2017) 035202
COMPASS – PLB 731 ('14) 19; NPB 915 ('17) 454
JLab Hall A Collaboration – PRC 83 ('11) 025201
HERMES – EPJ C 74 ('14) 3110; 75 ('15) 600; 77 ('17) 378

→ fixed target: medium/large x_B , quarks

Experimental access to GPDs: electroproduction

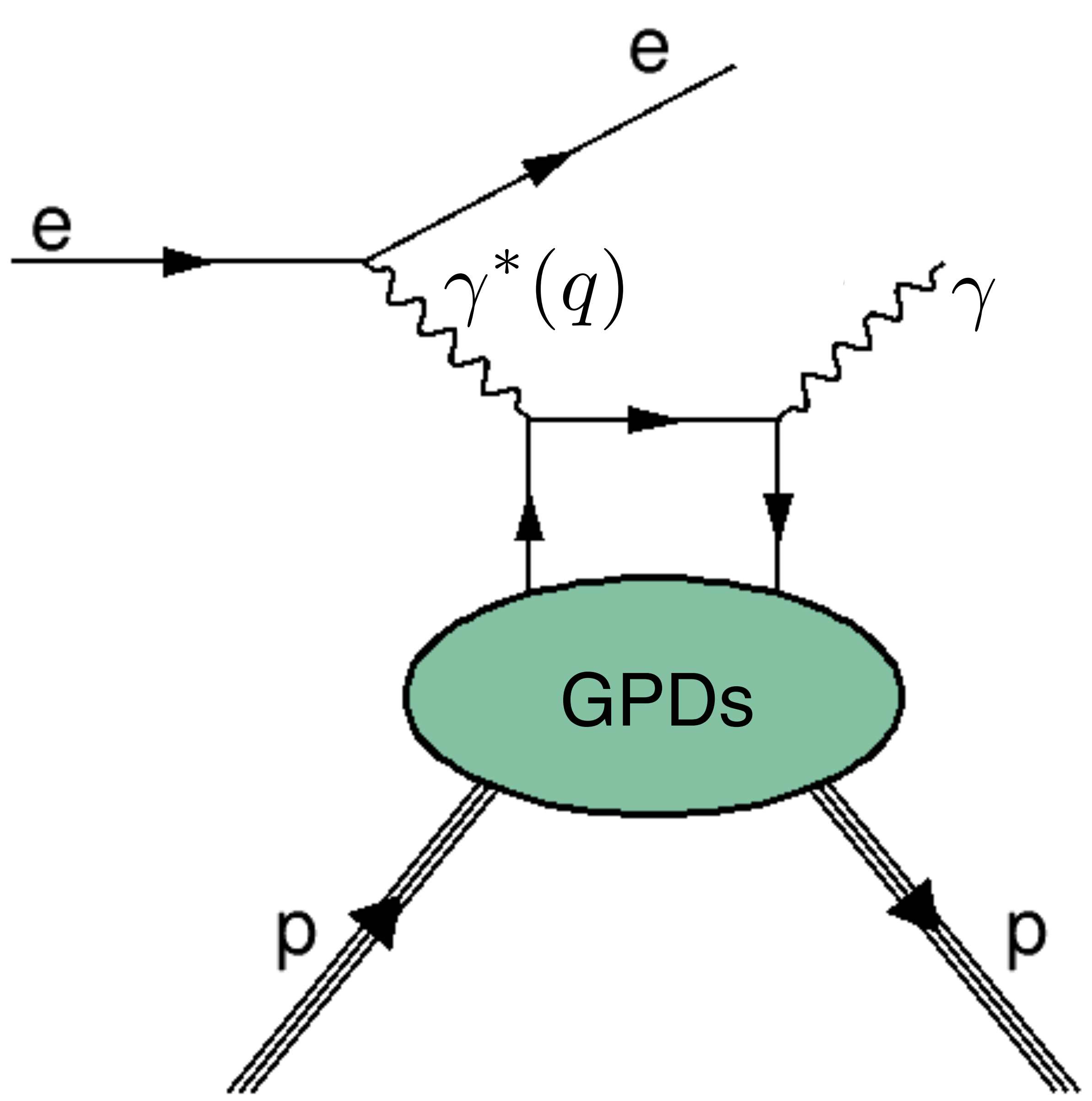

Deeply virtual Compton scattering (DVCS)
Hard scale=large $Q^2=-q^2$

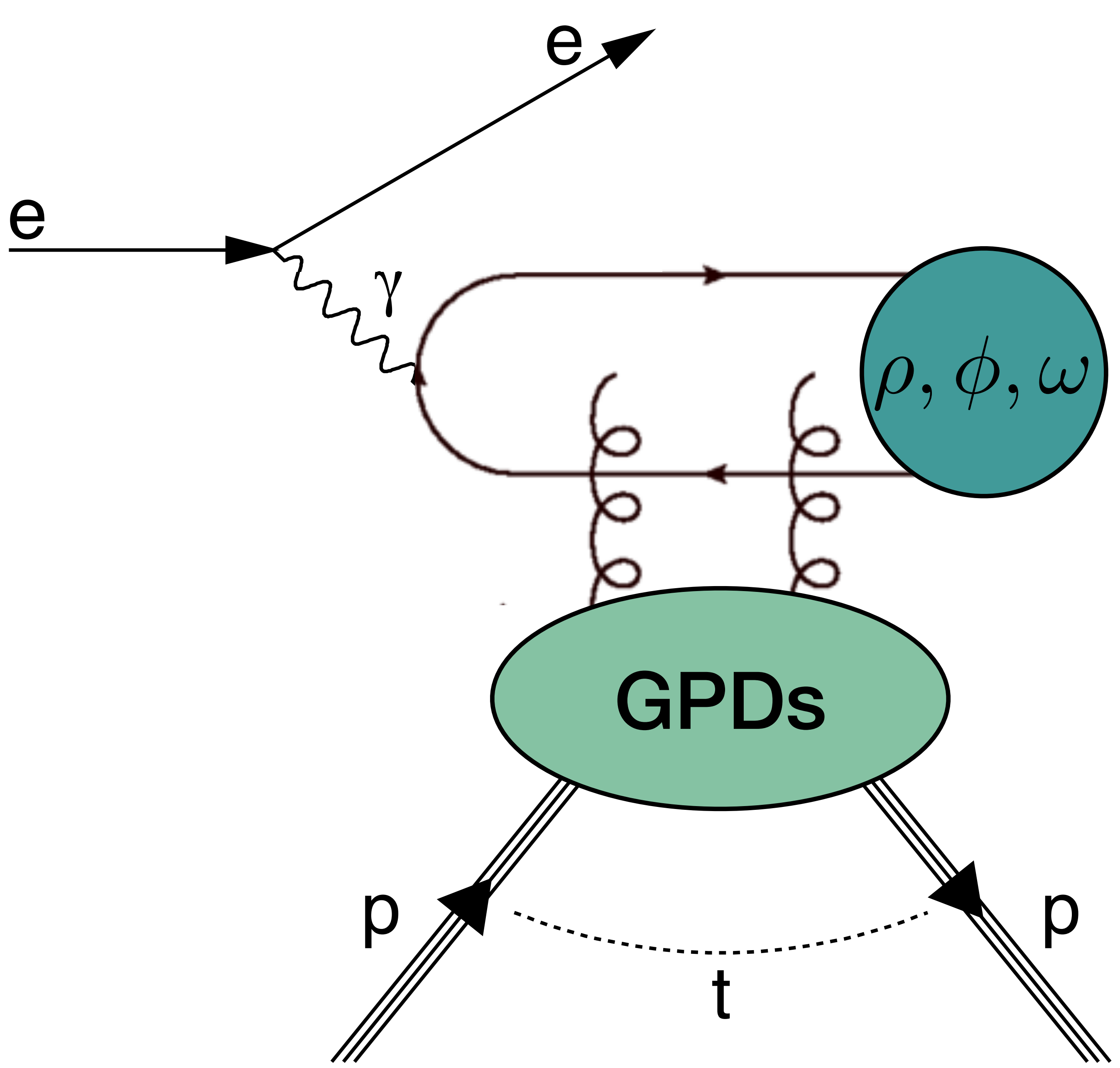

Hard exclusive meson production
Hard scale=large Q^2

CLAS – PRC 80 ('09) 035206; PRL 87 ('01) 182002; 100 ('08) 162002
COMPASS – arXiv:1702.06315
JLab Hall A Collaboration – PRL 99 ('07) 242501; PRC 92 ('15) 055202; Nat. Com. **8** ('17) 1408
HERMES – JHEP 10 ('12) 042; PLB 704 ('11) 15; NPB 842 ('11) 265
H1 – PLB 681 ('09) 391; 659 ('07) 796; EPJ C 44 ('05) 1
ZEUS – PLB 573 (2003) 46; JHEP 05 ('09) 108

CLAS – PRC 95 ('17) 035207; 95 (2017) 035202
COMPASS – PLB 731 ('14) 19; NPB 915 ('17) 454
JLab Hall A Collaboration – PRC 83 ('11) 025201
HERMES – EPJ C 74 ('14) 3110; 75 ('15) 600; 77 ('17) 378
H1 – JHEP 05('10)032; EPJ C 46 ('06) 585
ZEUS – PMC Phys. A1 ('07) 6; NPB 695 ('04) 3

colliders, small x_B, gluons

fixed target: medium/large x_B , quarks

Experimental access to GPDs: photoproduction

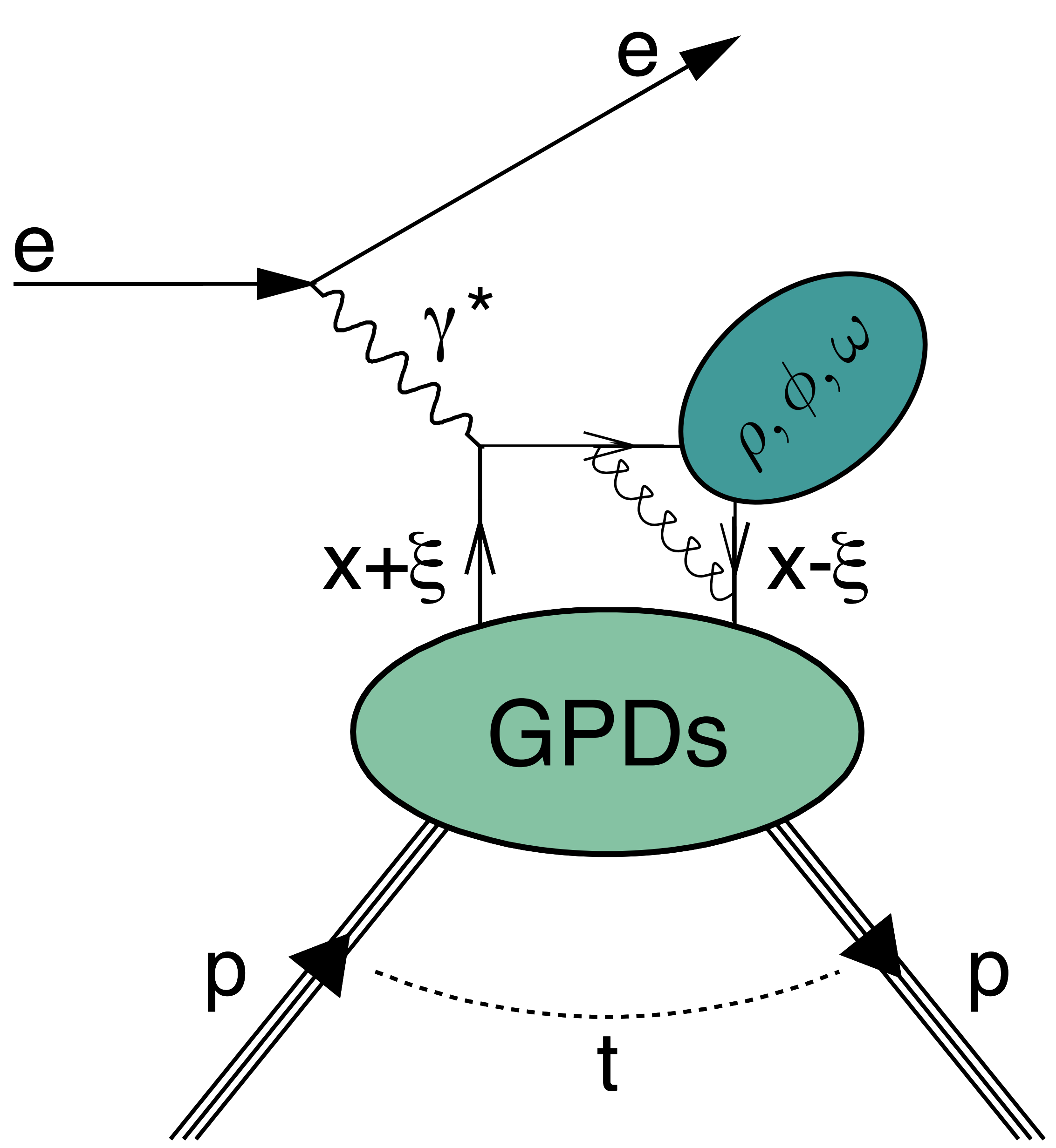

Hard exclusive meson production
Hard scale=large Q^2

CLAS – PRC 95 ('17) 035207; 95 (2017) 035202
COMPASS – PLB 731 ('14) 19; NPB 915 ('17) 454
JLab Hall A Collaboration – PRC 83 ('11) 025201
HERMES – EPJ C 74 ('14) 3110; 75 ('15) 600; 77 ('17) 378
H1 – JHEP 05('10)032; EPJ C 46 ('06) 585
ZEUS – PMC Phys. A1 ('07) 6; NPB 695 ('04) 3

colliders, small x_B, gluons

fixed target: medium/large x_B , quarks

Experimental access to GPDs: photoproduction

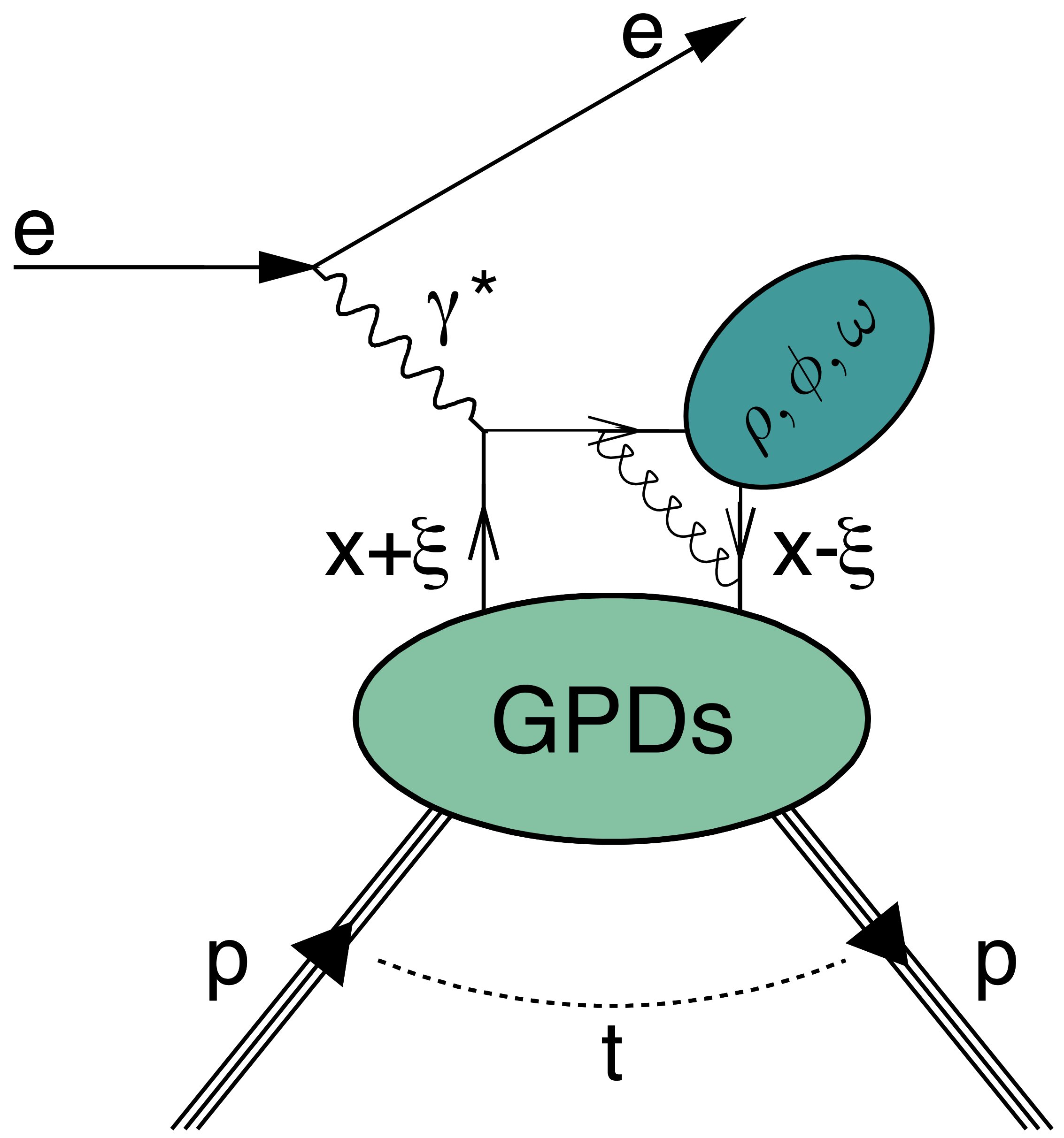

Hard exclusive meson production
Hard scale=large Q^2

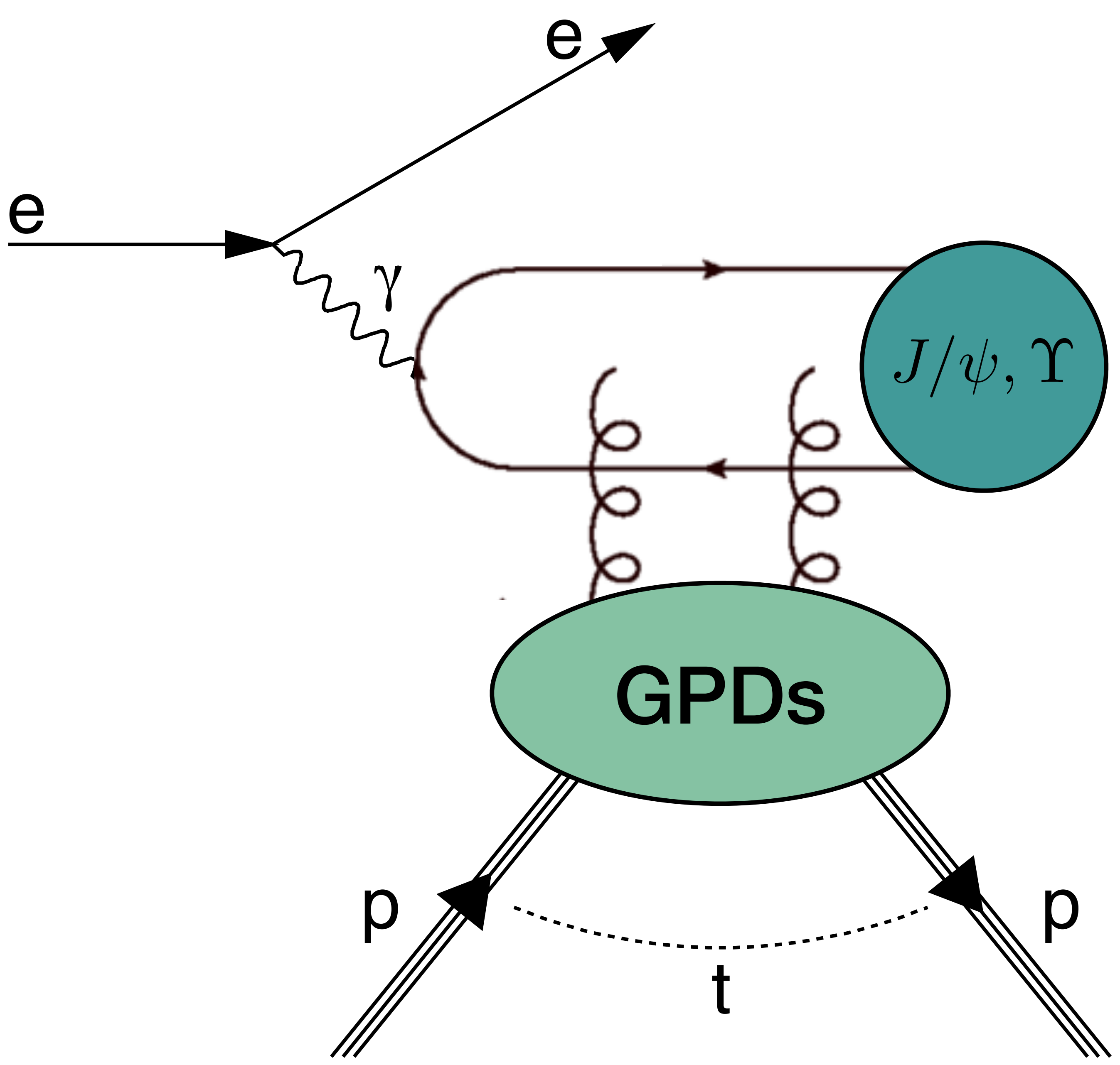

CLAS – PRC 95 ('17) 035207; 95 (2017) 035202
COMPASS – PLB 731 ('14) 19; NPB 915 ('17) 454
JLab Hall A Collaboration – PRC 83 ('11) 025201
HERMES – EPJ C 74 ('14) 3110; 75 ('15) 600; 77 ('17) 378
H1 – JHEP 05('10)032; EPJ C 46 ('06) 585
ZEUS – PMC Phys. A1 ('07) 6; NPB 695 ('04) 3

colliders, small x_B, gluons

fixed target: medium/large x_B , quarks

Experimental access to GPDs: photoproduction

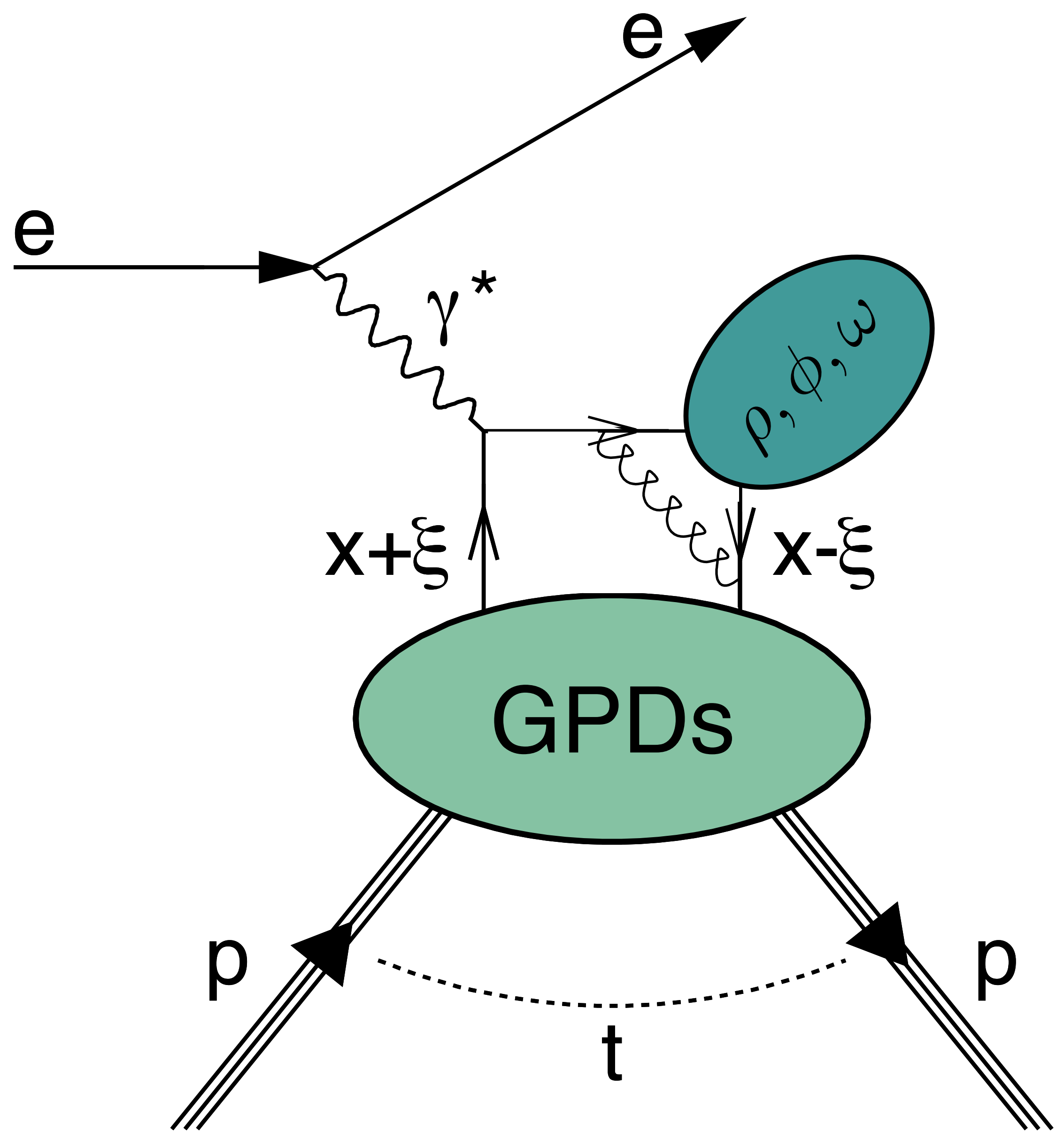

Hard exclusive meson production
Hard scale=large Q^2

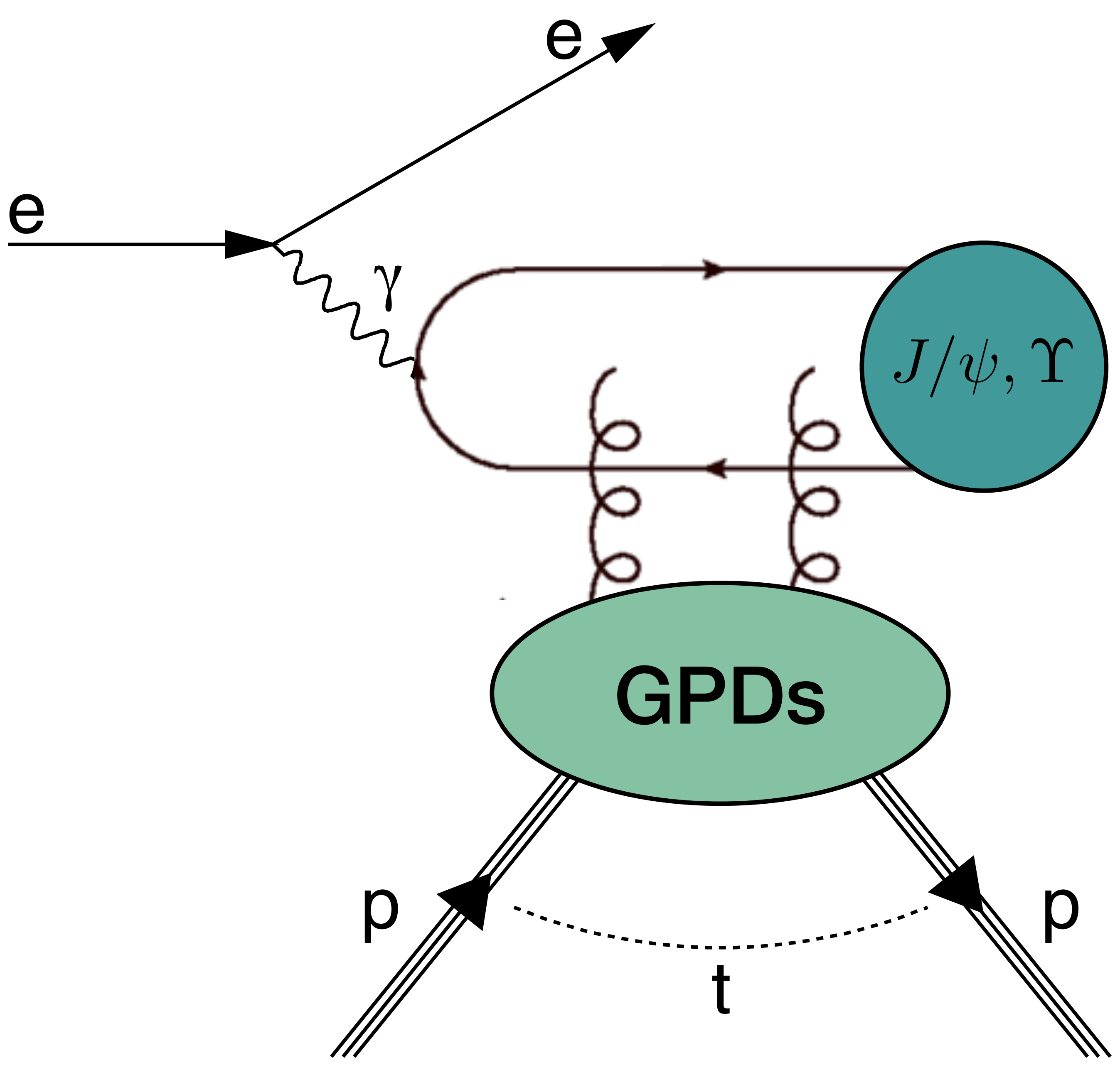

Exclusive meson photoproduction
Hard scale = large charm/bottom-quark mass

CLAS – PRC 95 ('17) 035207; 95 (2017) 035202
COMPASS – PLB 731 ('14) 19; NPB 915 ('17) 454
JLab Hall A Collaboration – PRC 83 ('11) 025201
HERMES – EPJ C 74 ('14) 3110; 75 ('15) 600; 77 ('17) 378
H1 – JHEP 05('10)032; EPJ C 46 ('06) 585
ZEUS – PMC Phys. A1 ('07) 6; NPB 695 ('04) 3

colliders, small x_B, gluons

fixed target: medium/large x_B , quarks

Experimental access to GPDs: photoproduction

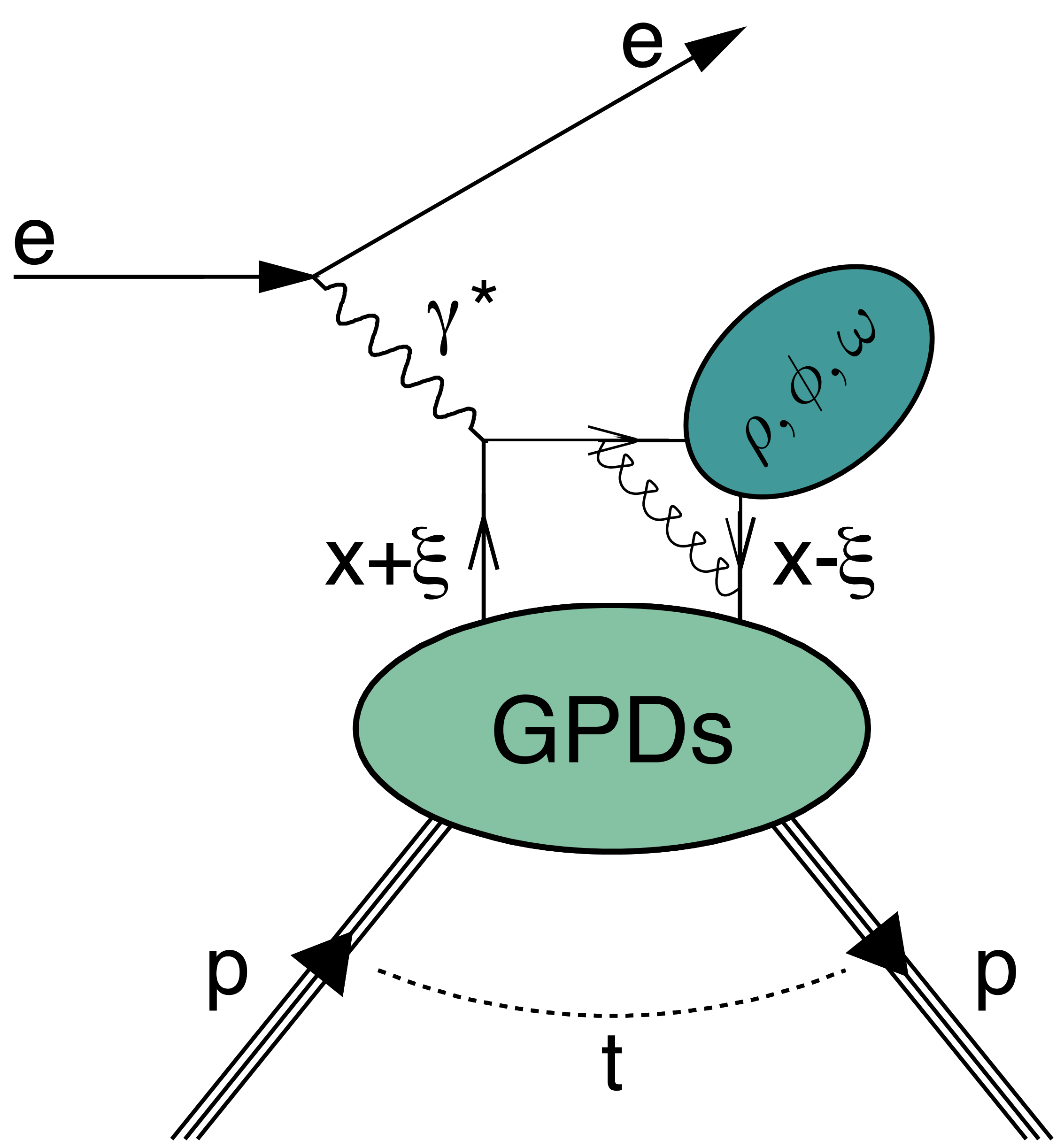

Hard exclusive meson production
Hard scale=large Q^2

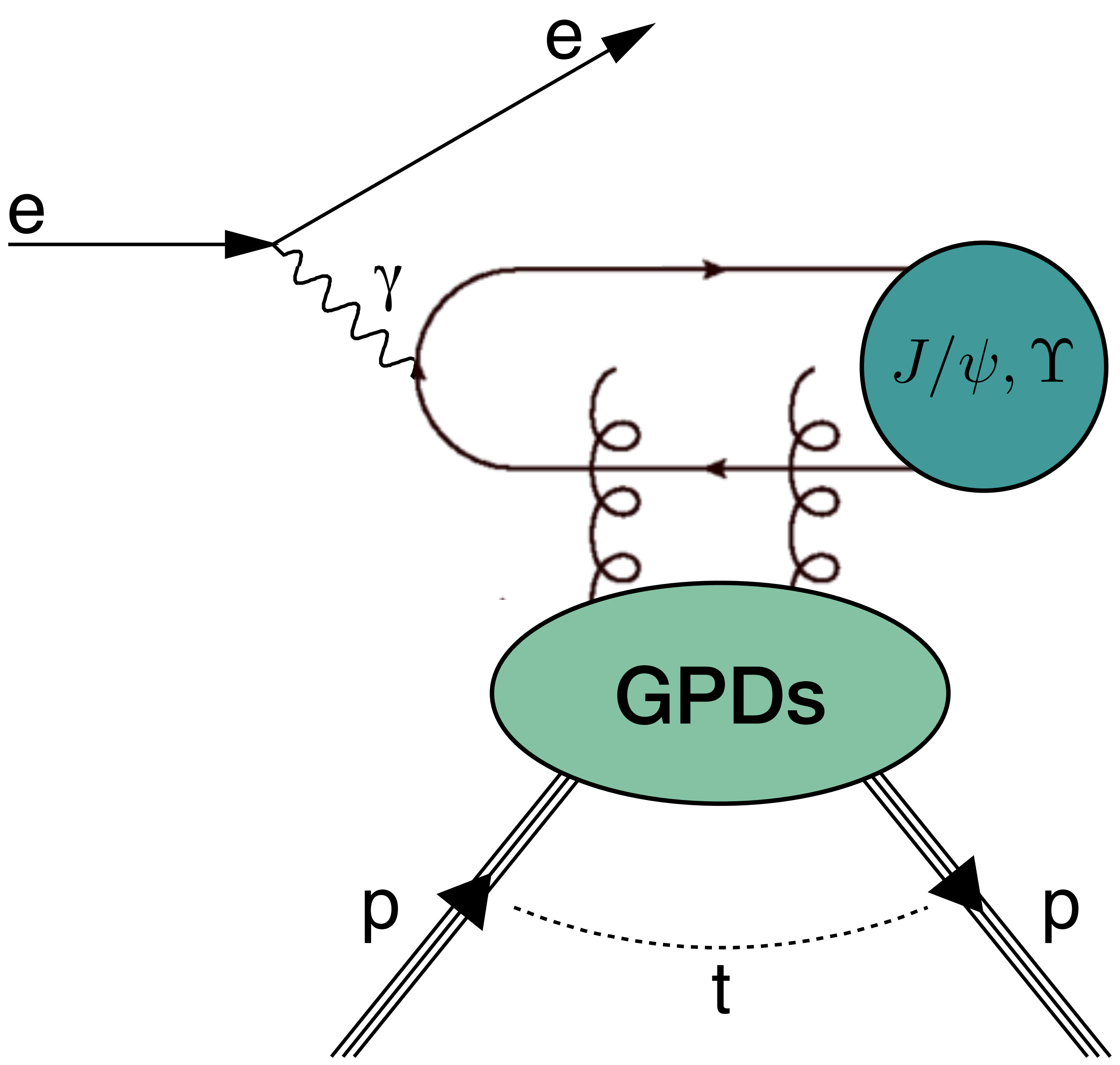

gluons!

Exclusive meson photoproduction
Hard scale = large charm/bottom-quark mass

CLAS – PRC 95 ('17) 035207; 95 (2017) 035202
COMPASS – PLB 731 ('14) 19; NPB 915 ('17) 454
JLab Hall A Collaboration – PRC 83 ('11) 025201
HERMES – EPJ C 74 ('14) 3110; 75 ('15) 600; 77 ('17) 378
H1 – JHEP 05('10)032; EPJ C 46 ('06) 585
ZEUS – PMC Phys. A1 ('07) 6; NPB 695 ('04) 3

colliders, small x_B, gluons

fixed target: medium/large x_B, quarks

Experimental access to GPDs: photoproduction

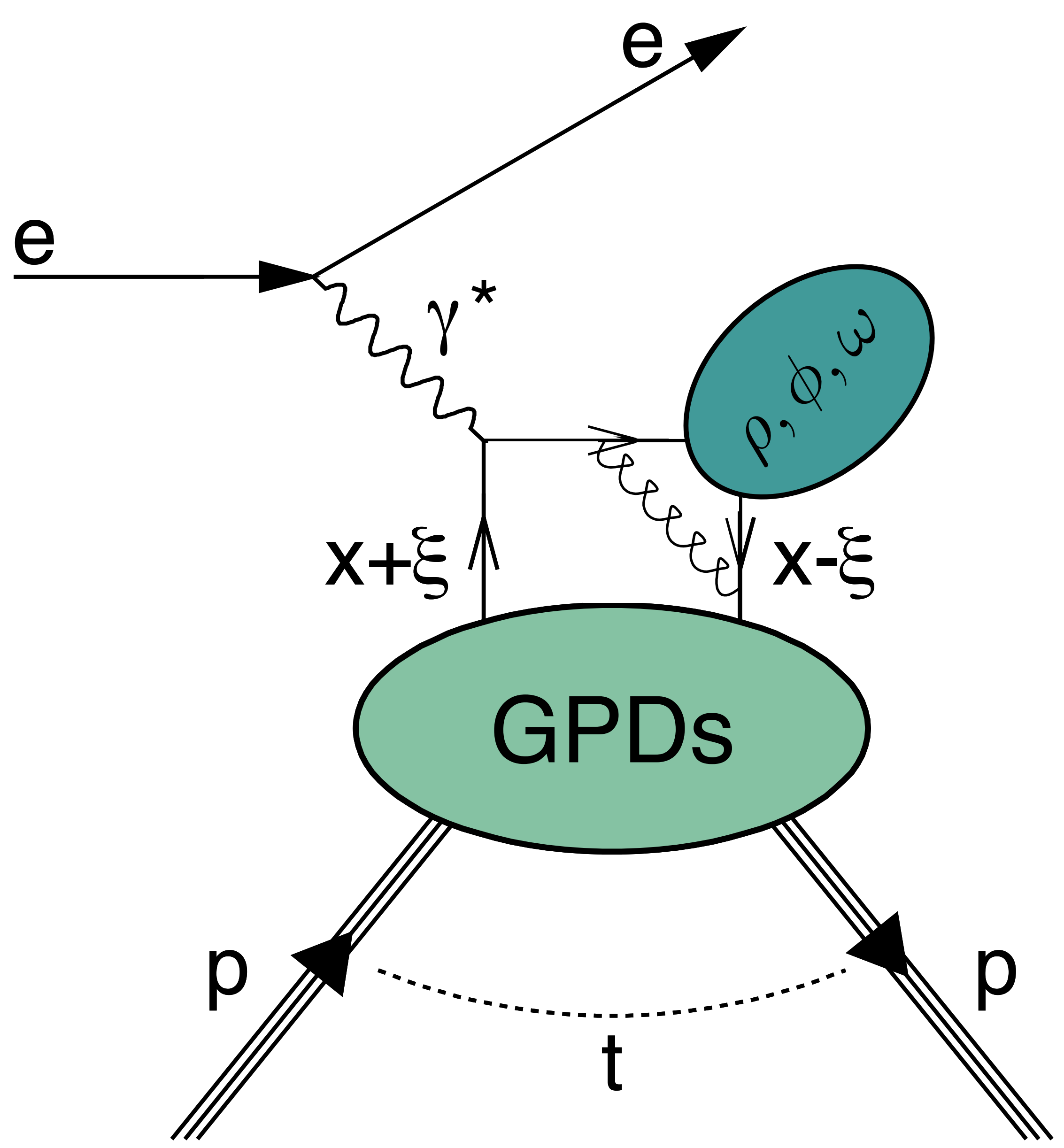

Hard exclusive meson production
Hard scale=large Q^2

CLAS – PRC 95 ('17) 035207; 95 (2017) 035202
COMPASS – PLB 731 ('14) 19; NPB 915 ('17) 454
JLab Hall A Collaboration – PRC 83 ('11) 025201
HERMES – EPJ C 74 ('14) 3110; 75 ('15) 600; 77 ('17) 378
H1 – JHEP 05('10)032; EPJ C 46 ('06) 585
ZEUS – PMC Phys. A1 ('07) 6; NPB 695 ('04) 3

colliders, small x_B, gluons

fixed target: medium/large x_B , quarks

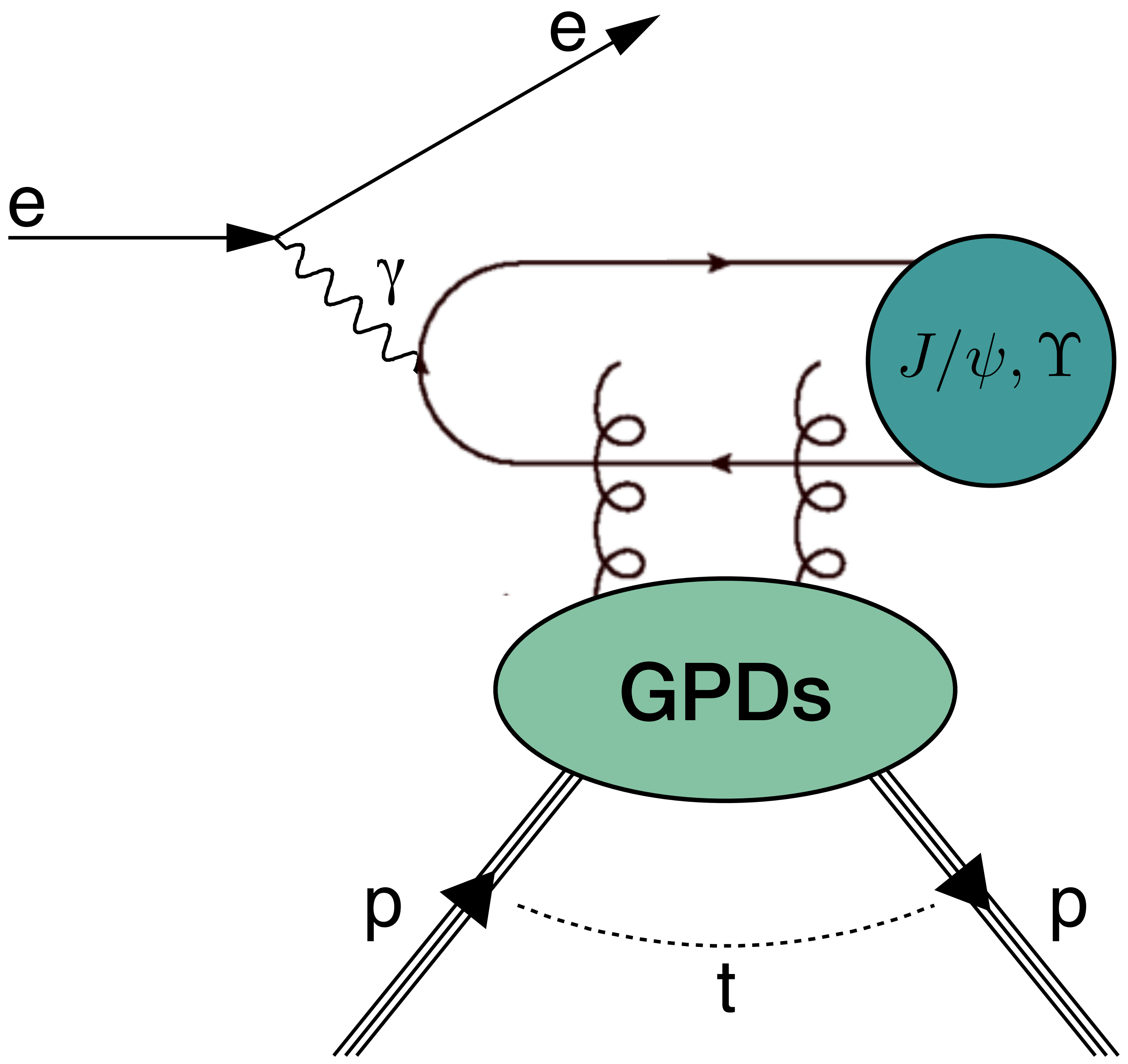

gluons!

Exclusive meson photoproduction
Hard scale = large charm/bottom-quark mass

H1 – EPJ C 46 ('06) 585; 73 ('13) 2466; PLB 541 ('02) 251
ZEUS – Nucl. Phys. B 695 ('04) 3; PLB 680 ('09) 4

$$W_{\gamma p} = [30, 300]\ \text{GeV}$$

down to x_B=10^{-4}

Experiments investigating GPDs

W dependence of exclusive production

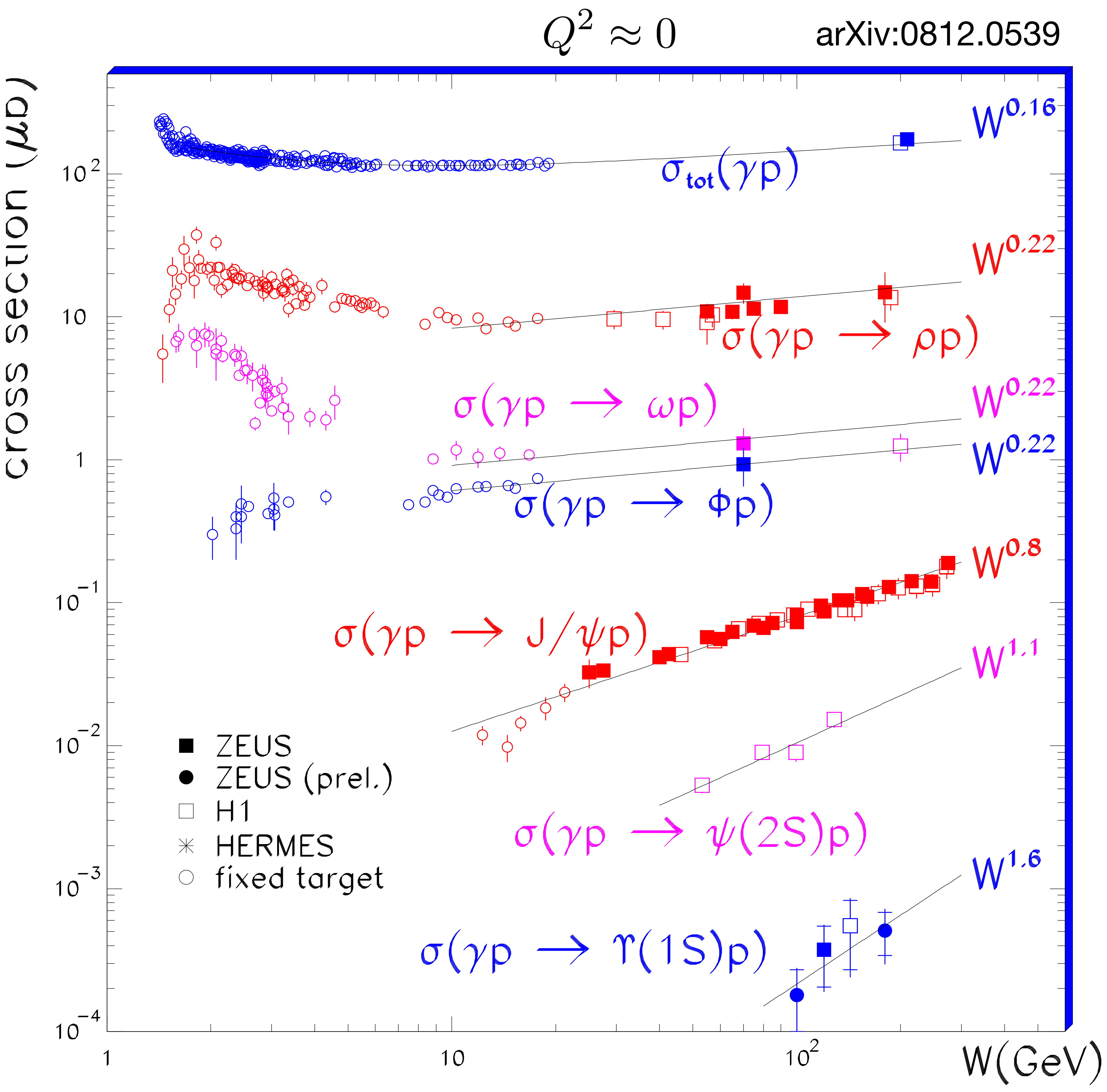

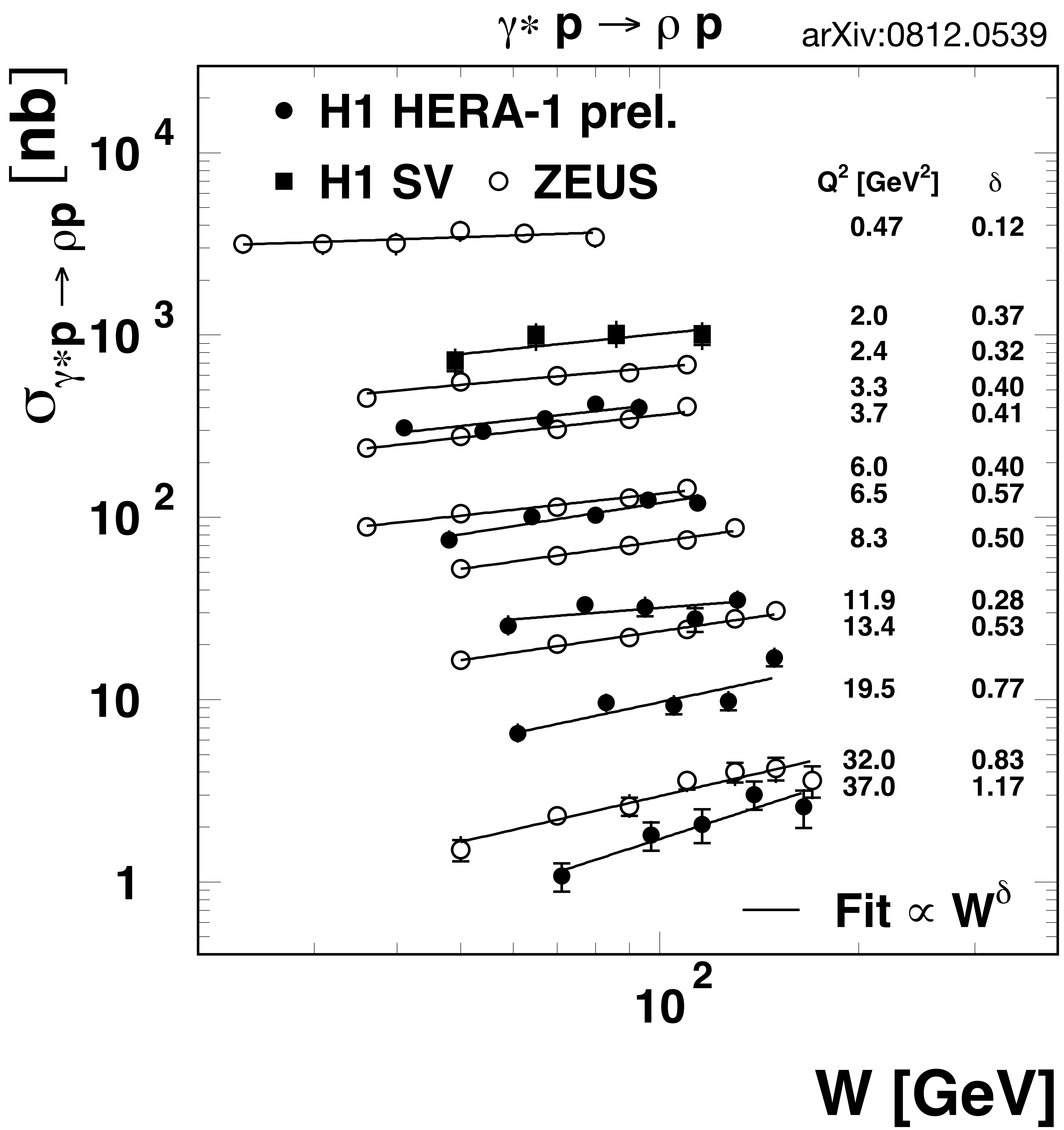

t dependence

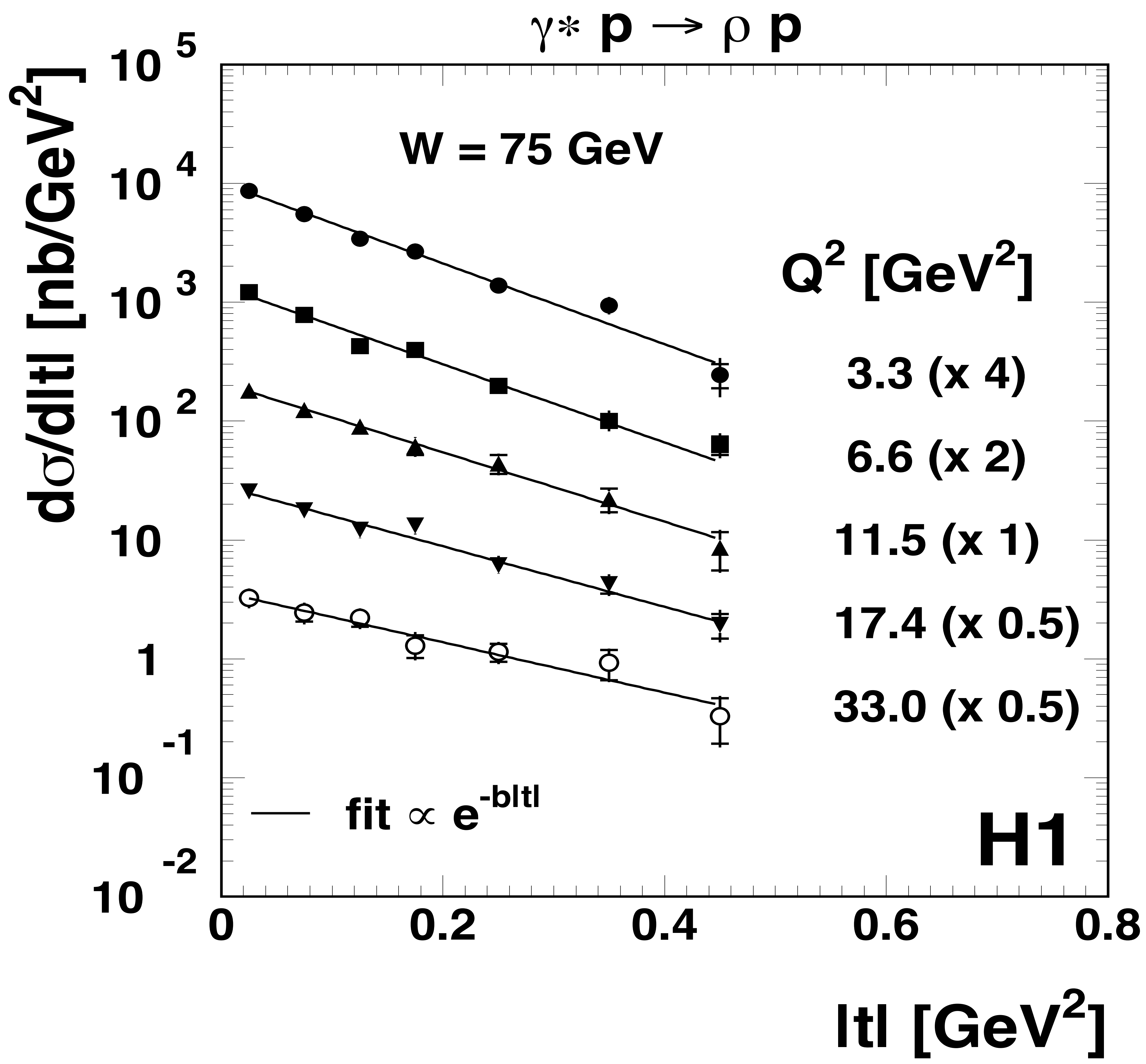

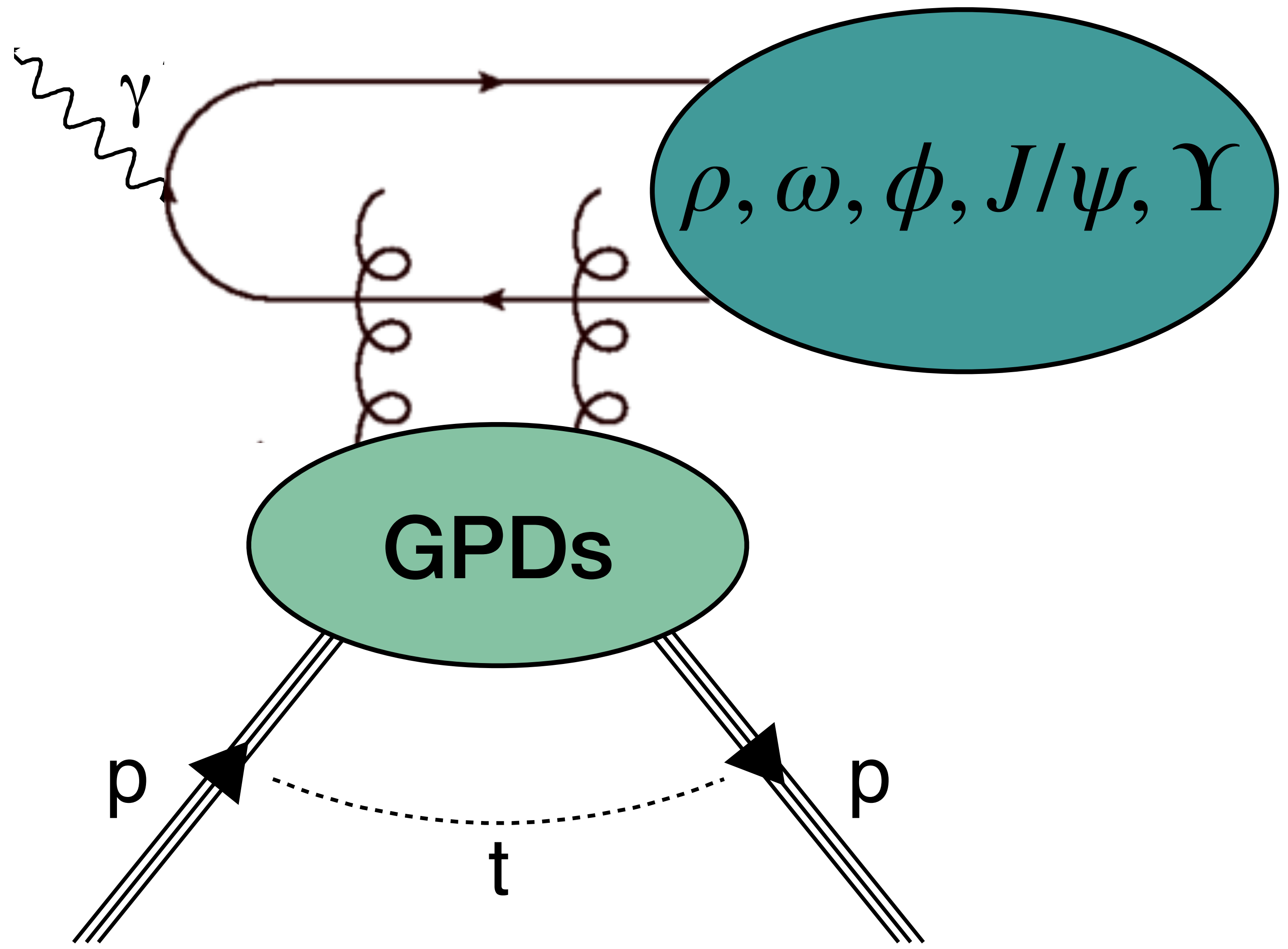

$Q^2+M_V^2$ dependence of b

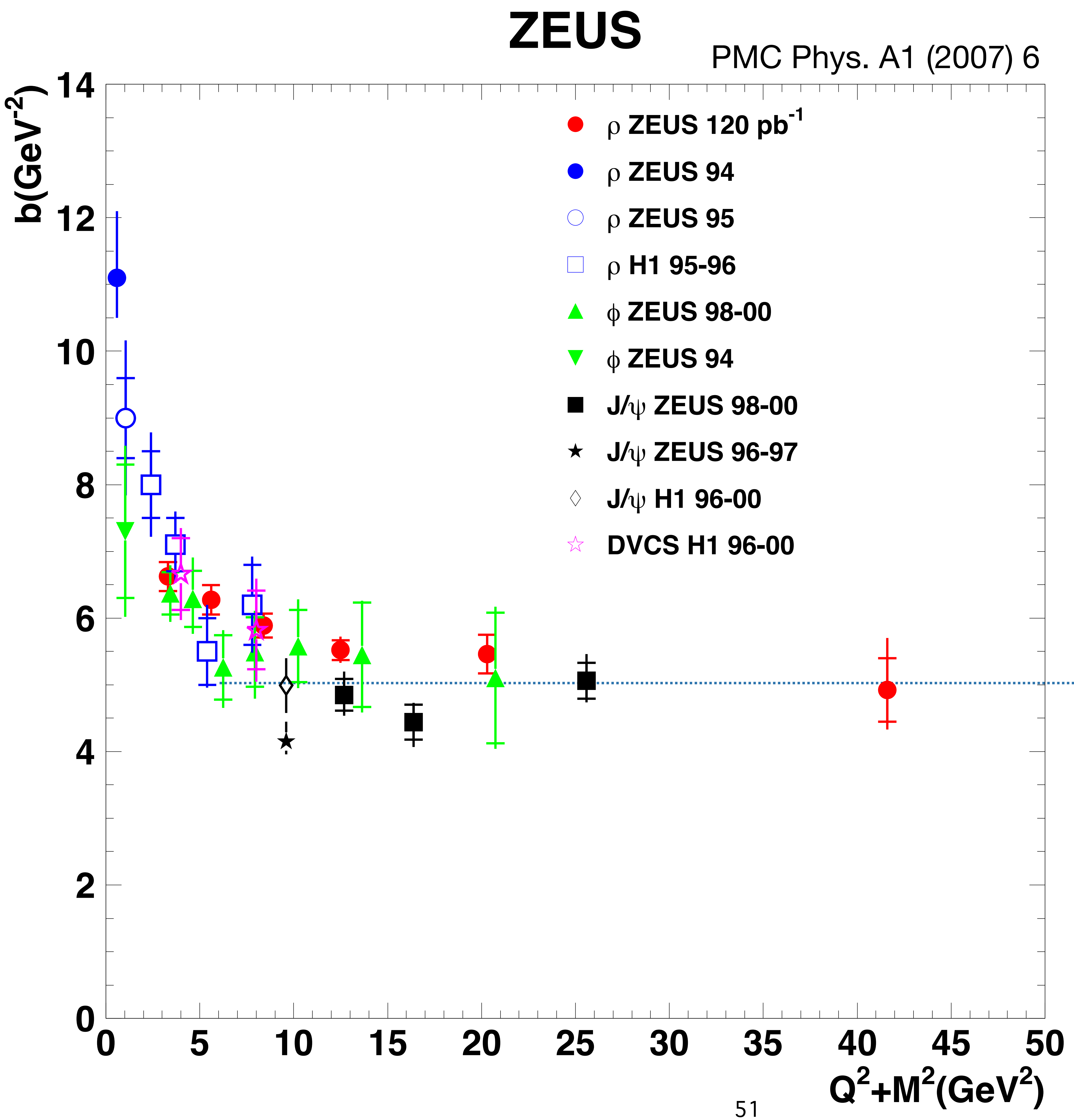

$5\ \mathrm{GeV}^2:\ \langle r\rangle_g \sim 0.6\ \mathrm{fm}$

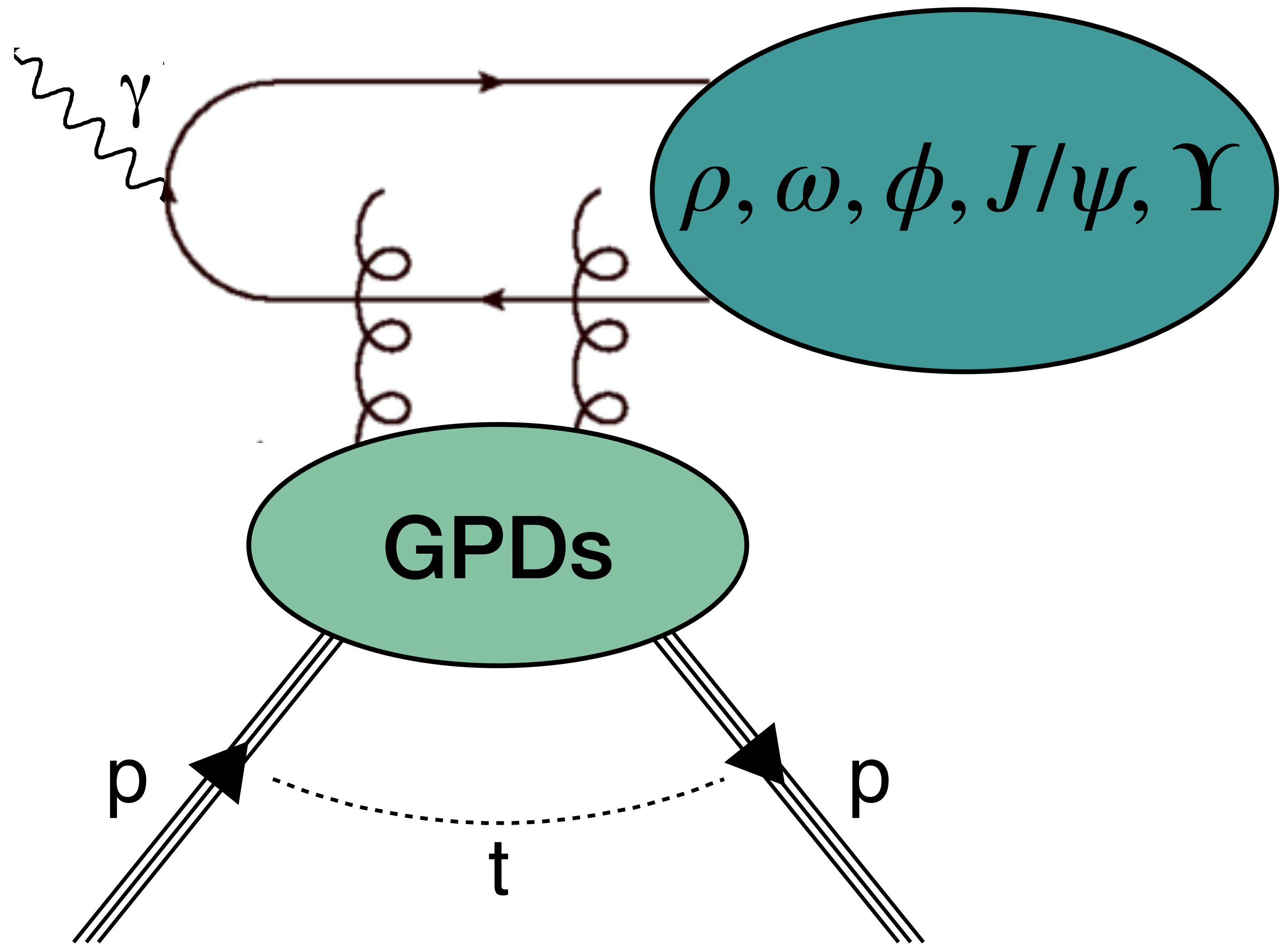

Quark distribution in transverse plane

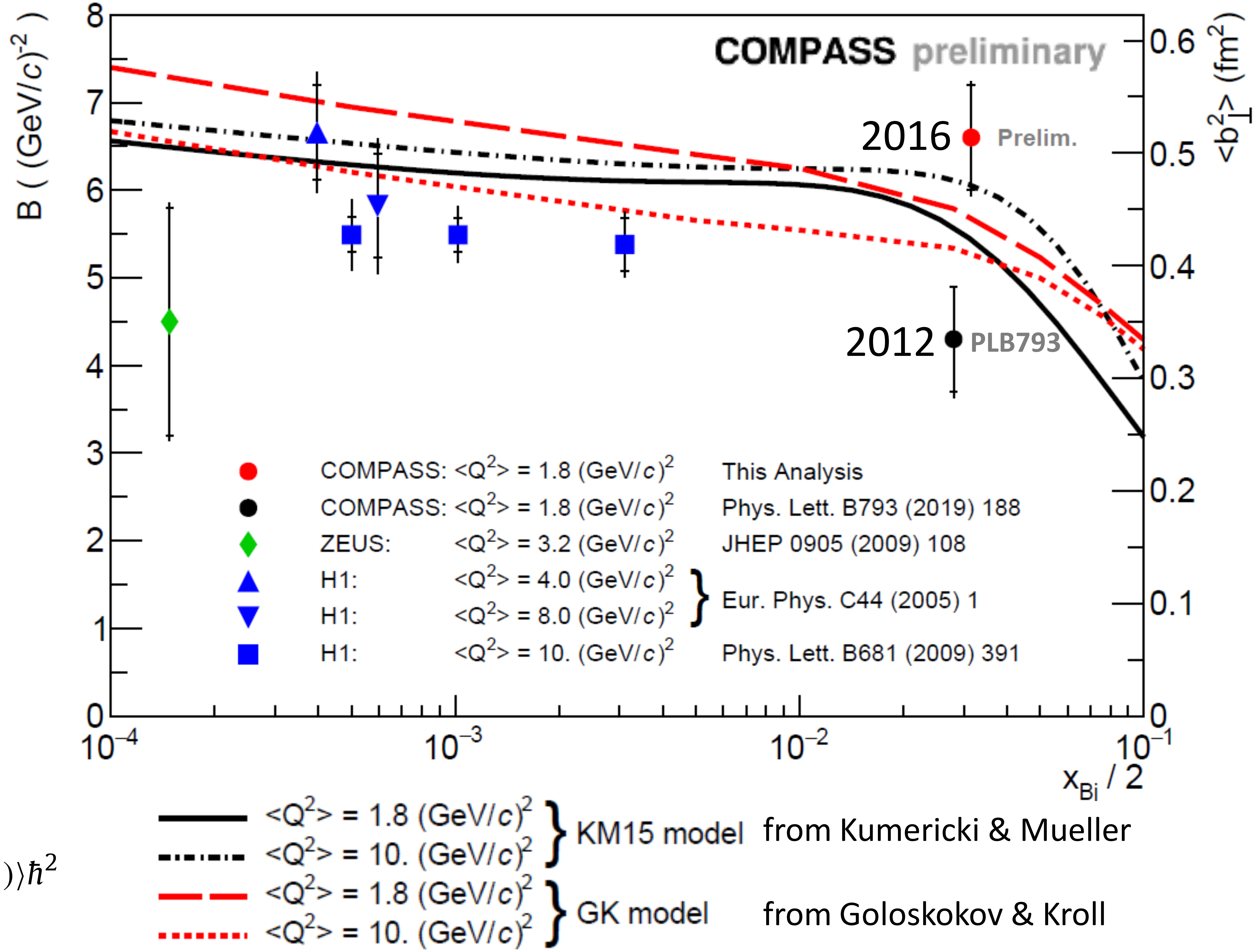

$$\langle r_\perp^2(x_{\mathrm{Bj}})\rangle \approx 2\langle B(x_{\mathrm{Bj}})\rangle \hbar^2$$

Exclusive ρ^0 production on a transversely polarised target

$$e + N \rightarrow e + N + \rho^0$$
$$\rho^0 \rightarrow \pi^+ + \pi^-$$

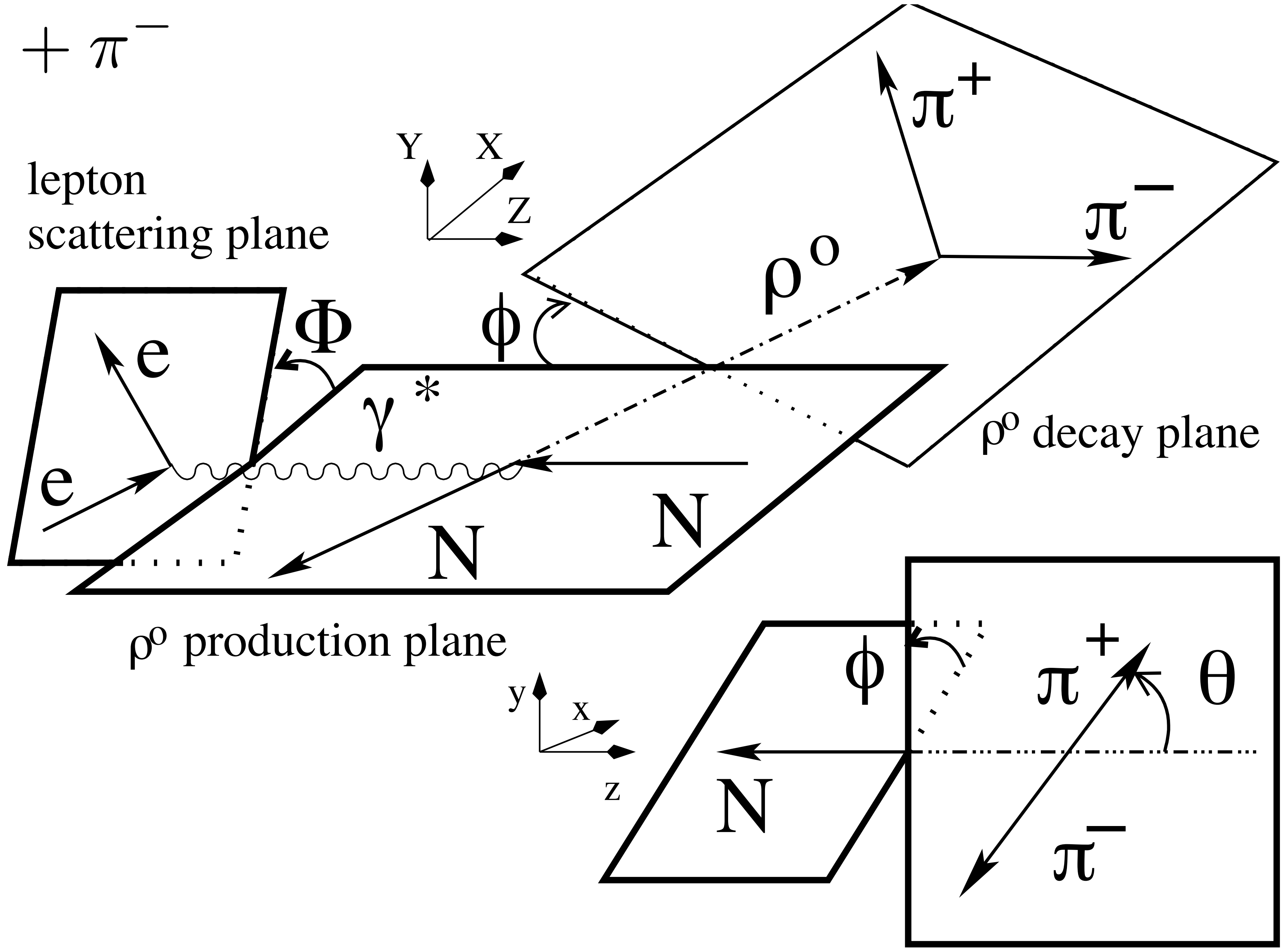

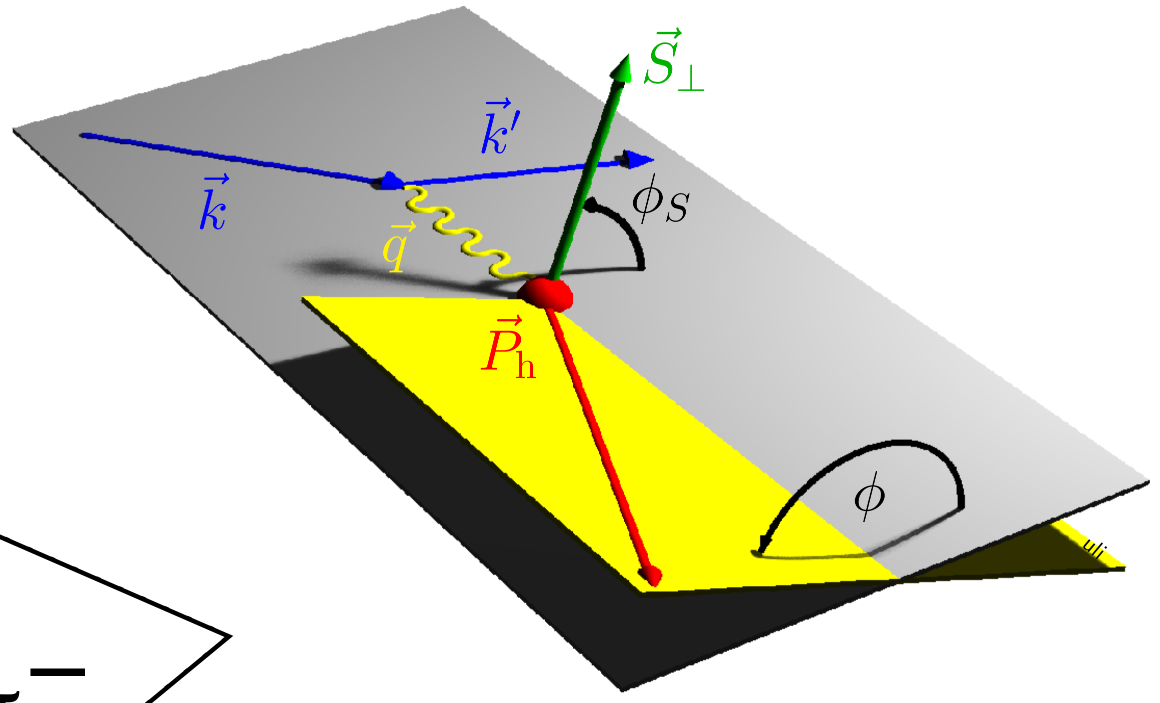

Fit angular distribution of decay pions $\mathcal{W}(\Phi, \phi, \Theta, \phi_S)$ and extract either Spin Density Matrix Elements (SDMEs) or helicity amplitude ratios

Exclusive ρ^0 production on a transversely polarised target

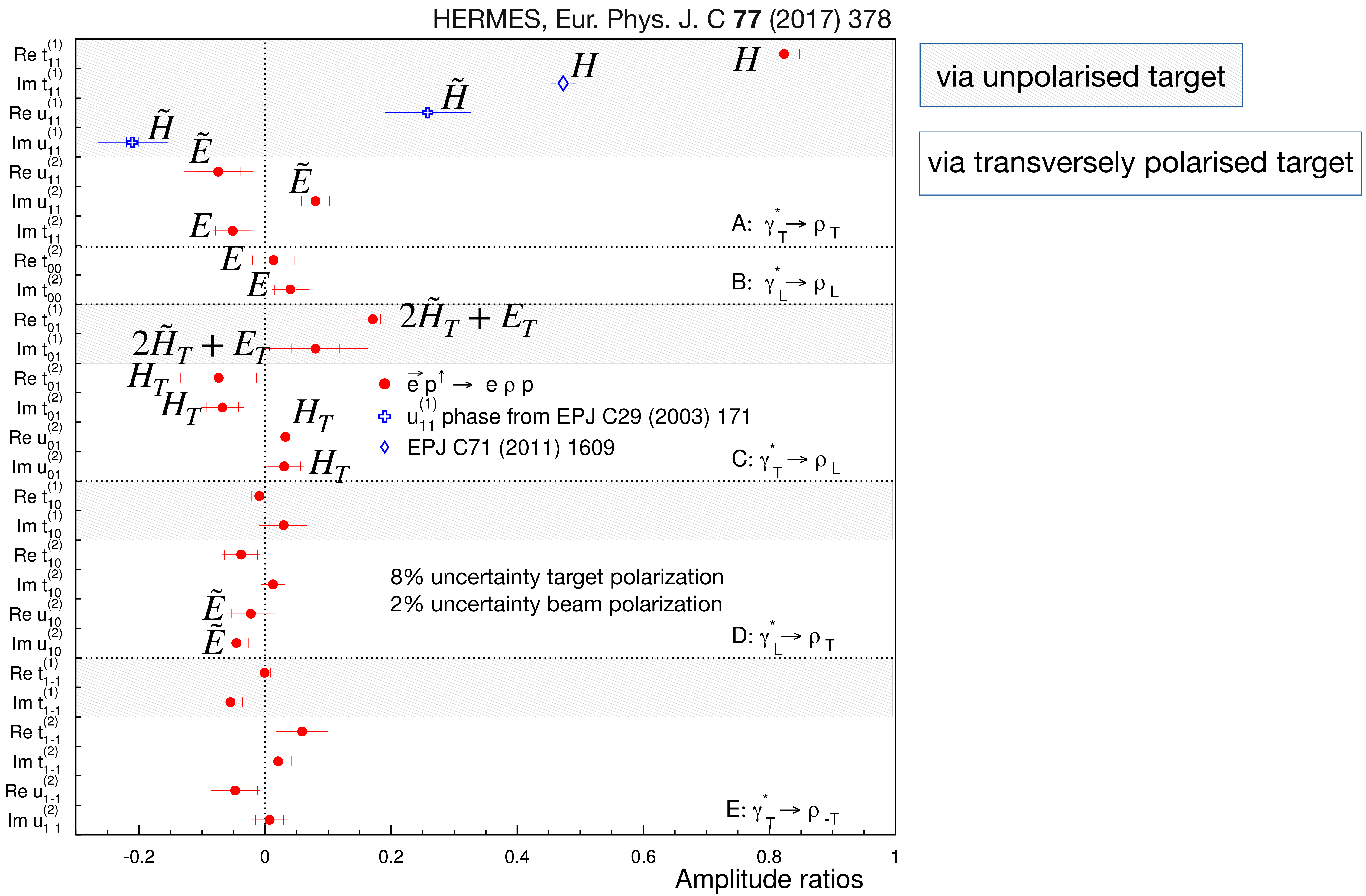

Future: EIC

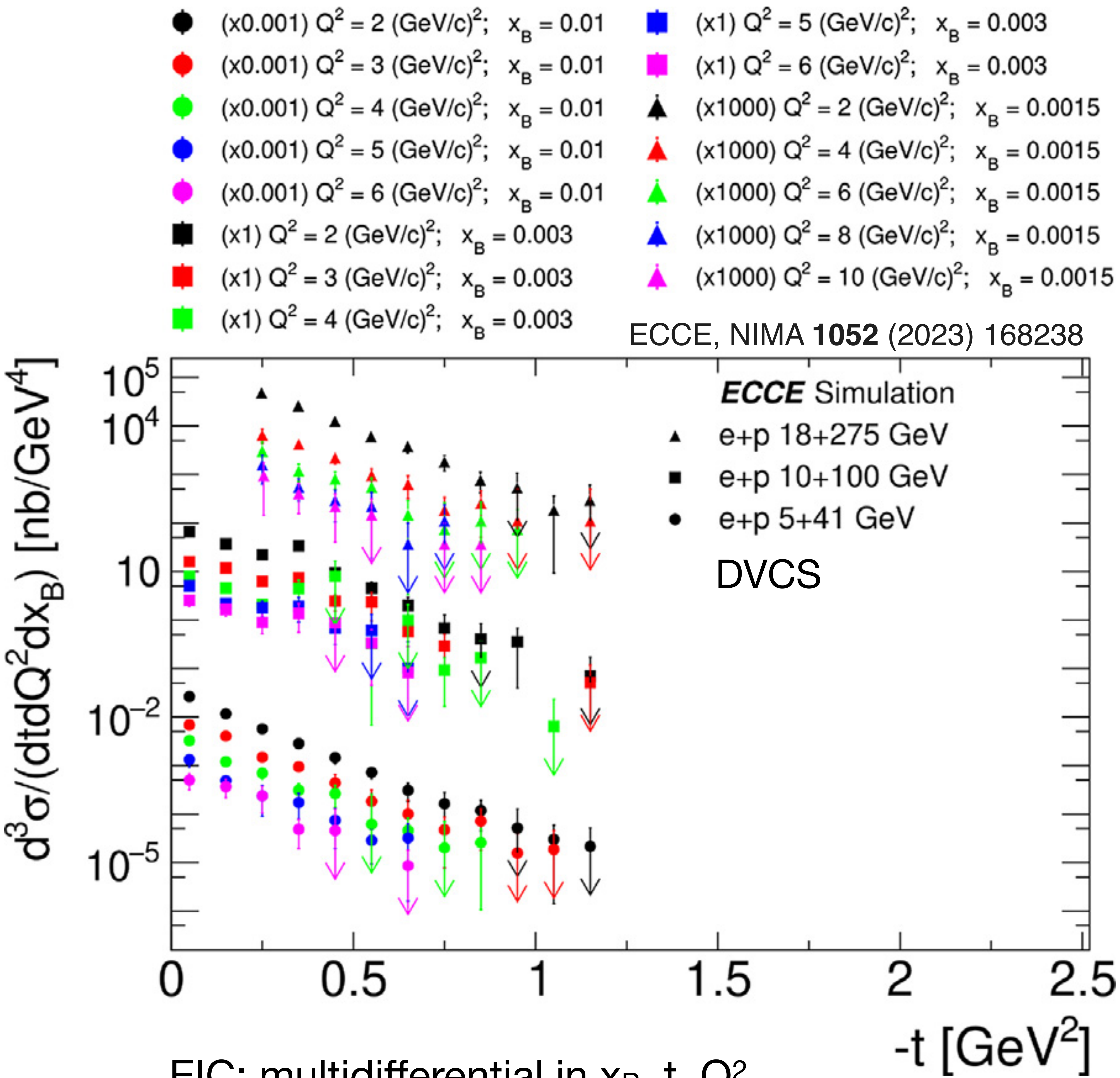

ECCE, NIMA **1052** (2023) 168238

EIC: multidifferential in x_B, t, Q^2
with detection of scattered proton

Experimental access to GPDs: photoproduction

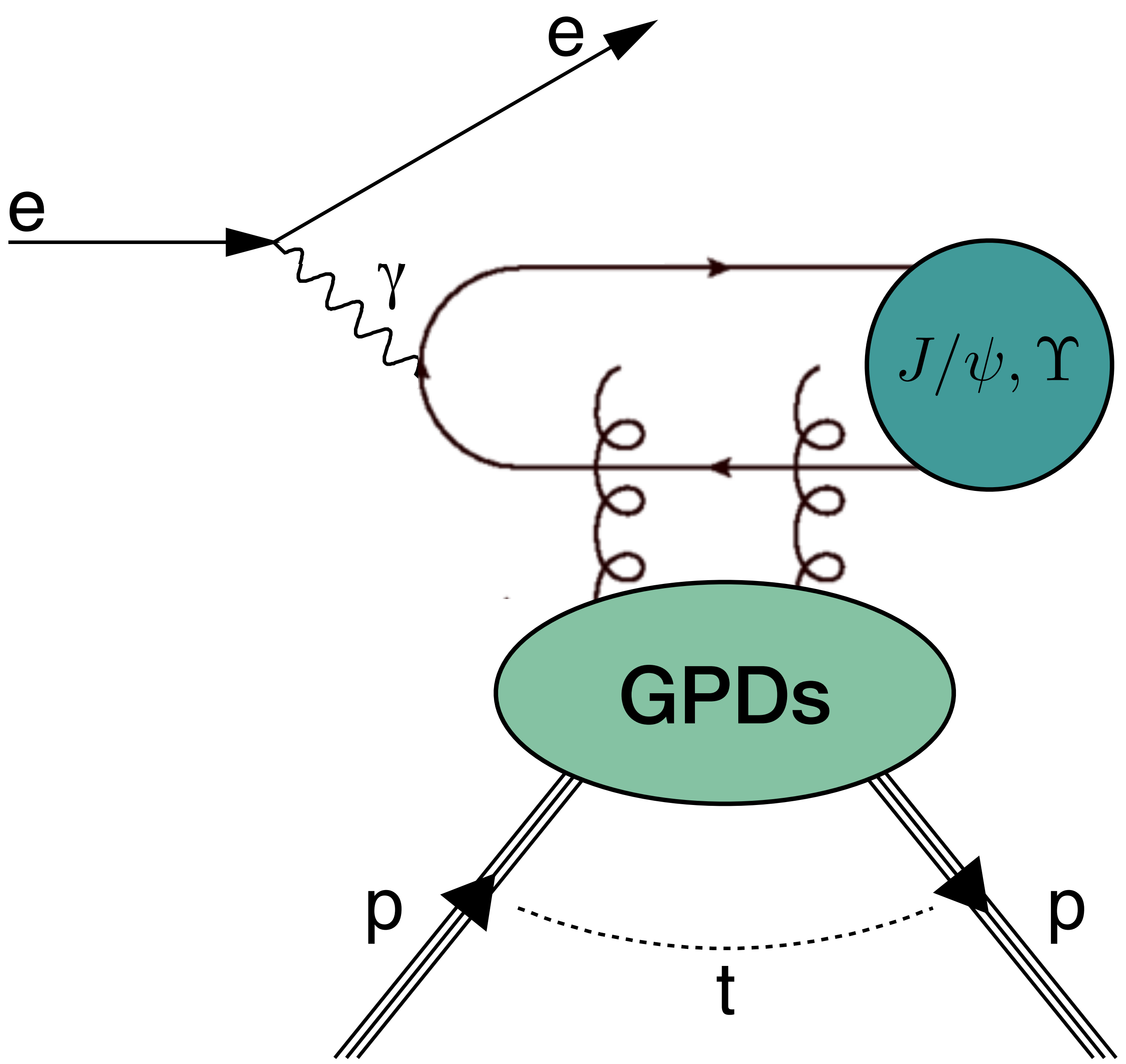

Exclusive meson photoproduction
Hard scale = large charm/bottom-quark mass

H1 – EPJ C 46 ('06) 585; 73 ('13) 2466; PLB 541 ('02) 251
ZEUS – Nucl. Phys. B 695 ('04) 3; PLB 680 ('09) 4

$$W_{\gamma p} = [30, 300]\ \text{GeV}$$

down to $x_B=10^{-4}$

Experimental access to GPDs: photoproduction

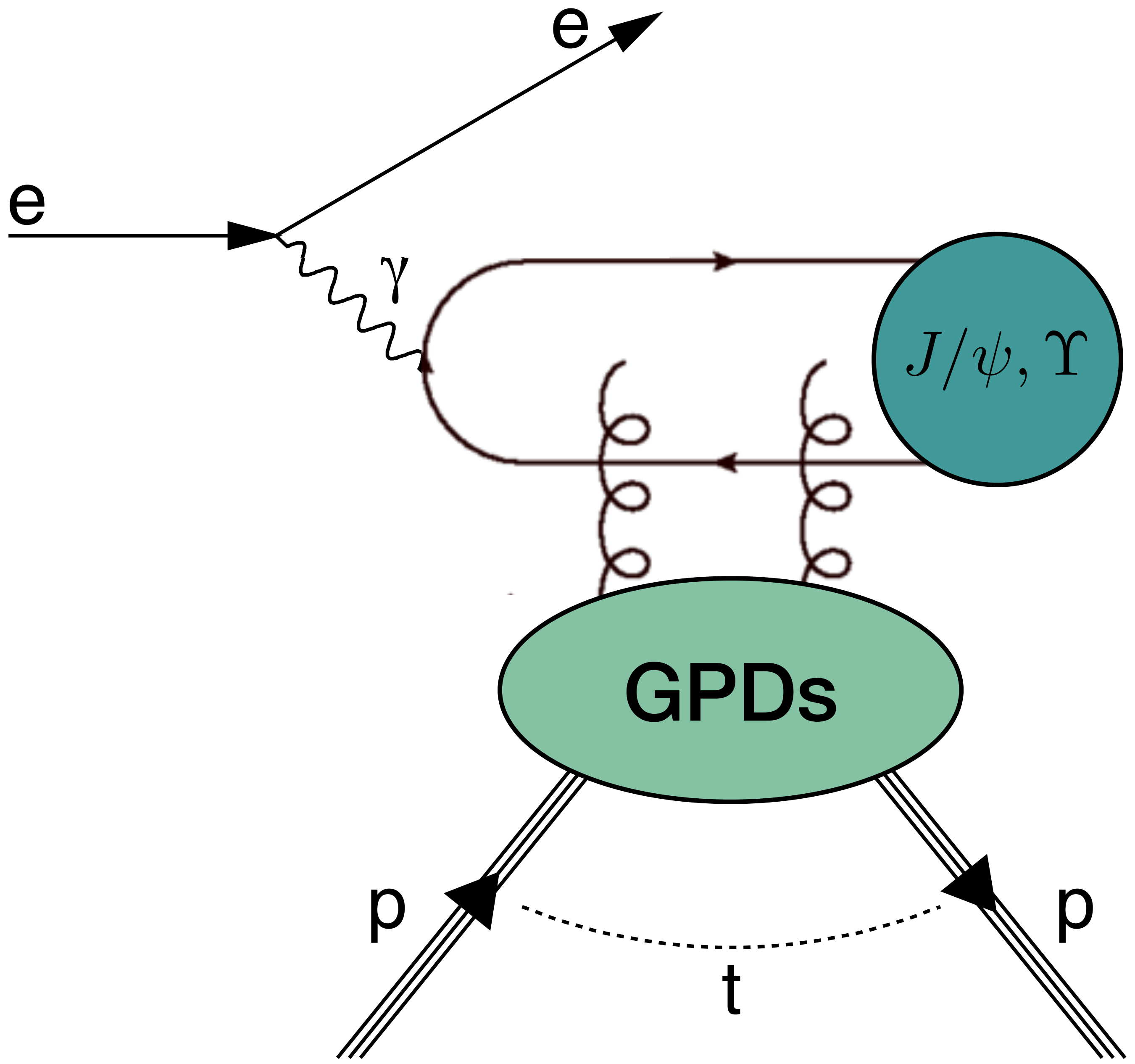

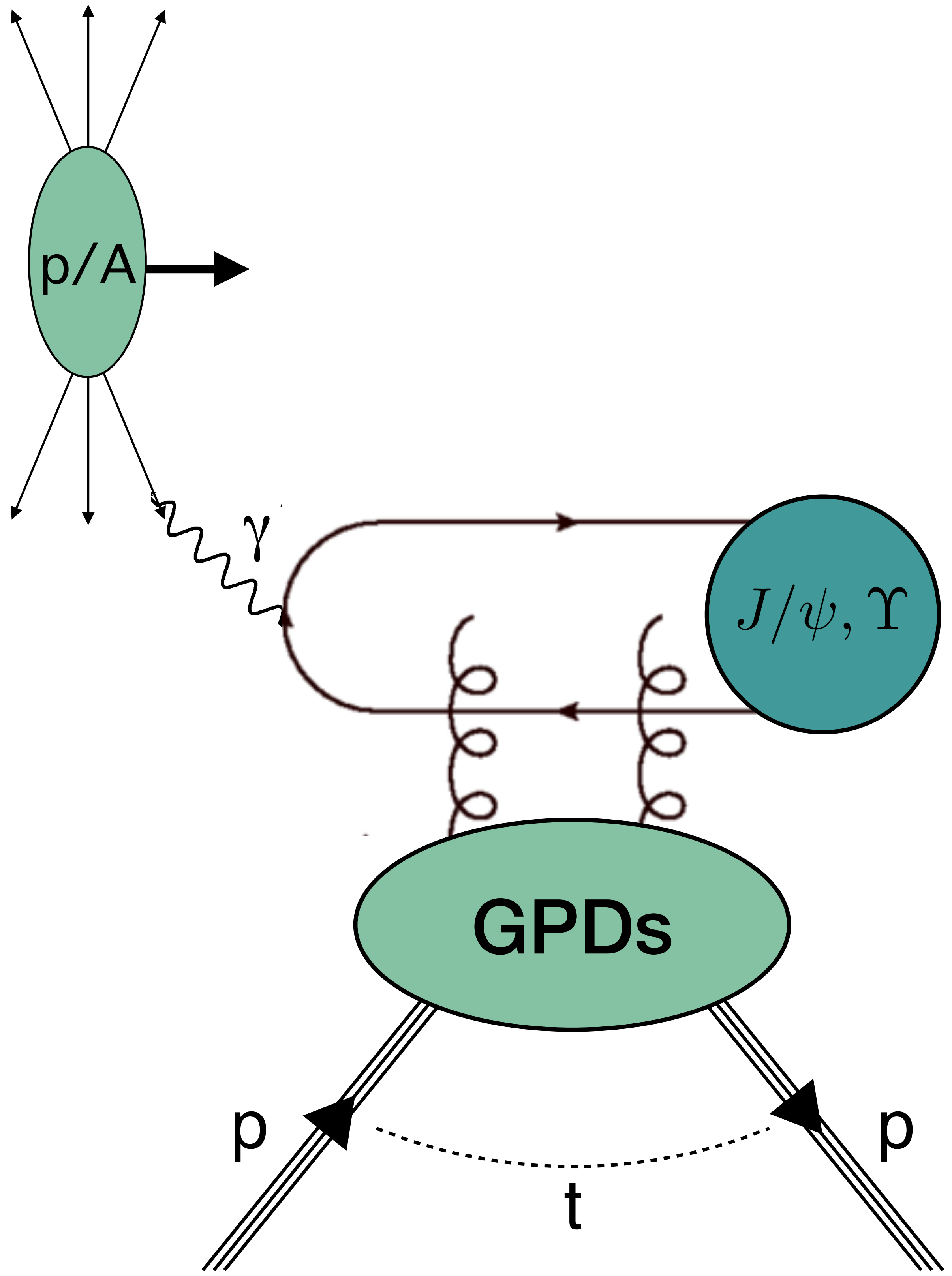

Exclusive meson photoproduction
Hard scale = large charm/bottom-quark mass

H1 – EPJ C 46 ('06) 585; 73 ('13) 2466; PLB 541 ('02) 251
ZEUS – Nucl. Phys. B 695 ('04) 3; PLB 680 ('09) 4

$$W_{\gamma p} = [30, 300] \text{ GeV}$$

down to $x_B=10^{-4}$

Experimental access to GPDs: photoproduction

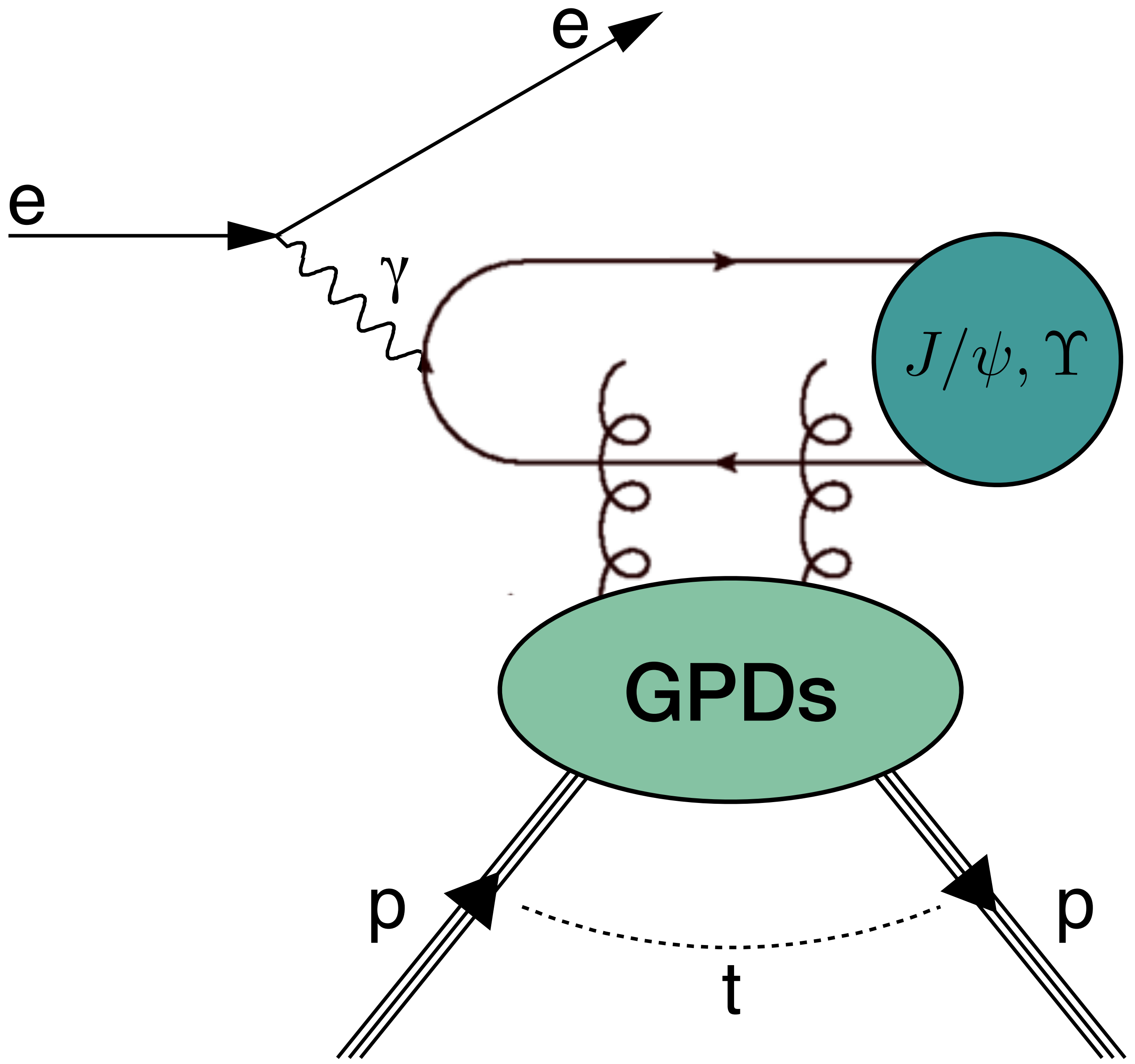

Exclusive meson photoproduction
Hard scale = large charm/bottom-quark mass

H1 – EPJ C 46 ('06) 585; 73 ('13) 2466; PLB 541 ('02) 251
ZEUS – Nucl. Phys. B 695 ('04) 3; PLB 680 ('09) 4

$$W_{\gamma p} = [30, 300]\ \text{GeV}$$

down to $x_B=10^{-4}$

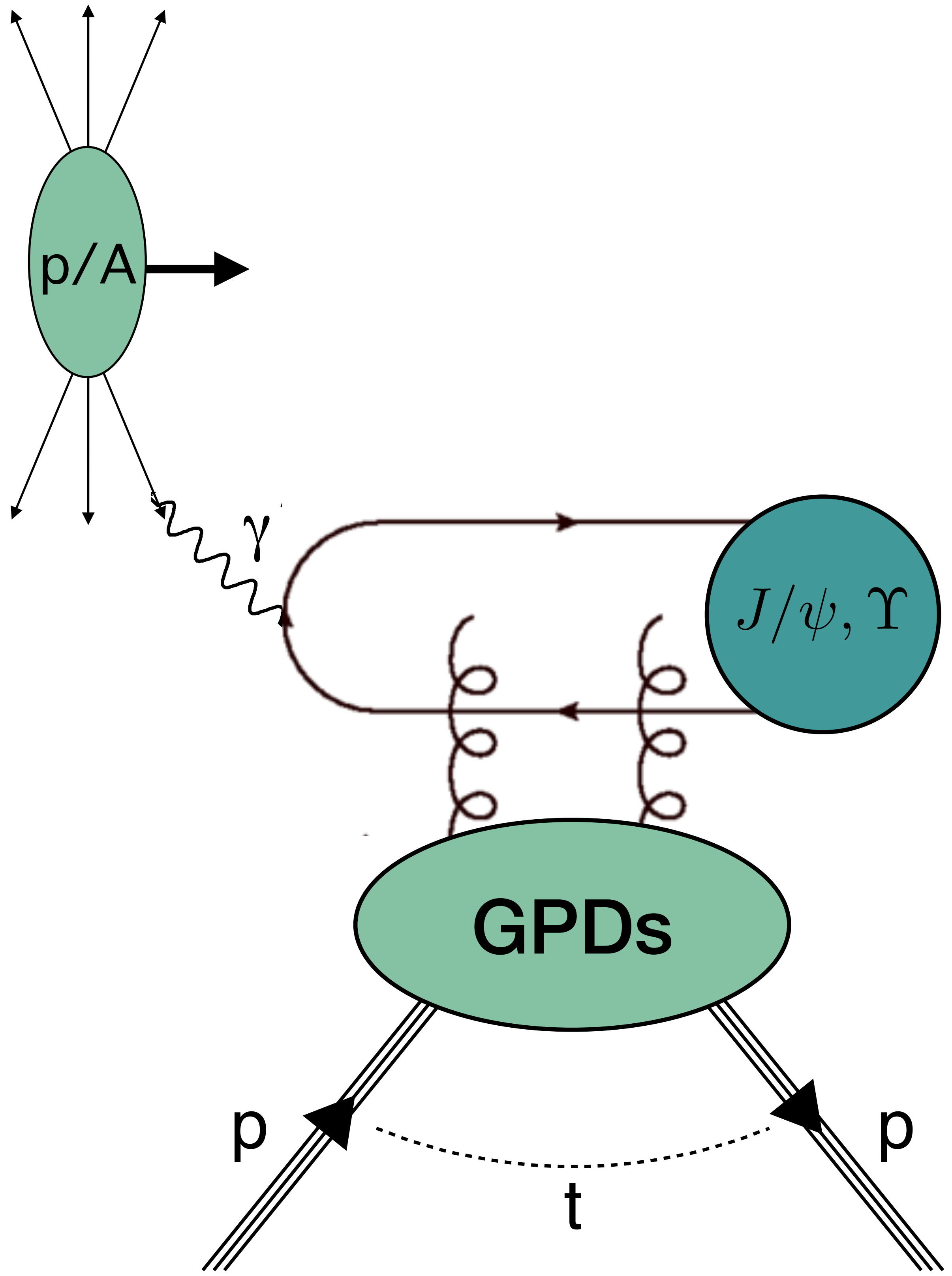

$W_{\gamma N}^{\max} = 34$ GeV

PHENIX: Au-Au – Phys. Lett. B **679** ('09) 321

CDF: p-p̄ – Phys. Rev. Lett. **102** ('09) 242001

CMS, PbPb: Phys. Lett. B **772** ('17) 489

CMS, pPb: Eur. Phys. J. C **79** ('19) 277

ALICE: Pb-Pb – Eur. Phys. J. C **73** ('13) 2617; Phys. Lett. B **718** ('13) 1273; Phys. Lett. B **751** ('15) 358; Phys. Lett. B **798** ('19) 134926.

ALICE: p-Pb – Phys. Rev. Lett. **113** ('14) 232504; Eur. Phys. J. C **79** ('19) 402

LHCb: PbPb – CERN-LHCb-CONF-2018-003

LHCb: pp – J. Phys. G: Nucl. Part. Phys. **40** ('13) 045001; **41** ('14) 055002; JHEP 1509 ('15) 084); JHEP10('18)167

$W_{\gamma p}^{\max} = 1.5$ TeV

down to $x_B=10^{-6}$

Phase-space covered at the LHC

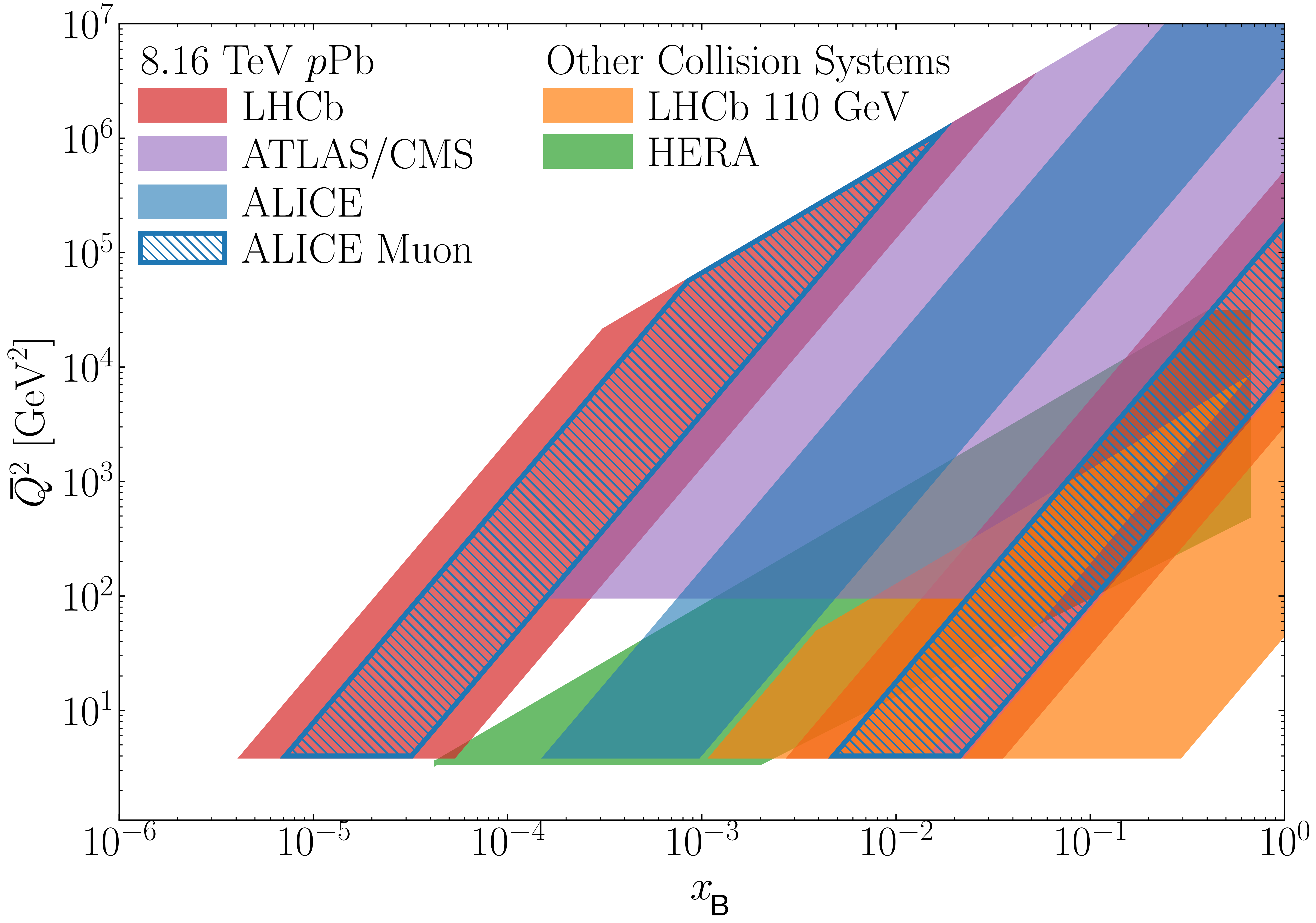

Ultra-peripheral collisions

large–impact-parameter interactions

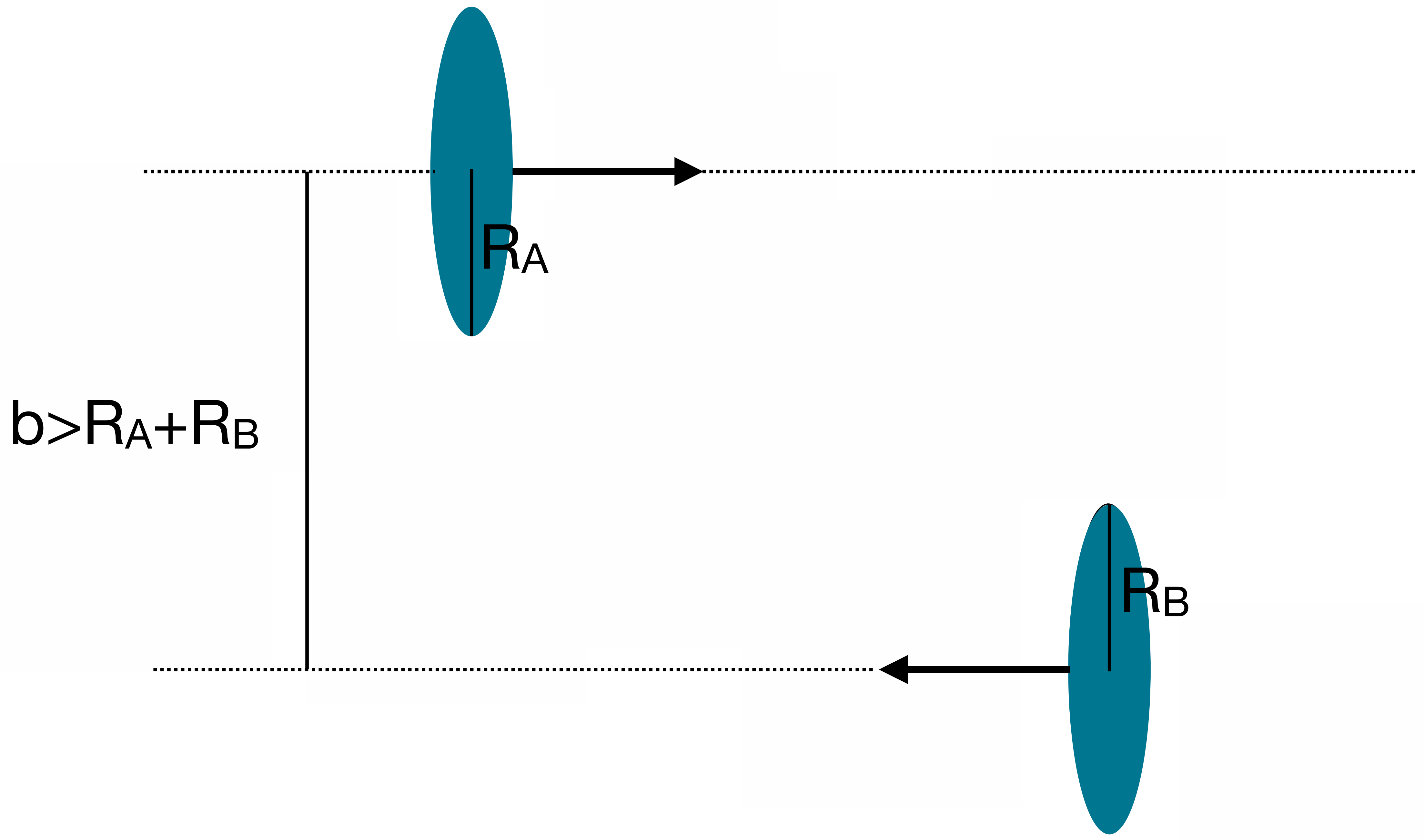

Ultra-peripheral collisions

large–impact-parameter interactions

hadronic interactions strongly suppressed

instead: electromagnetic interactions

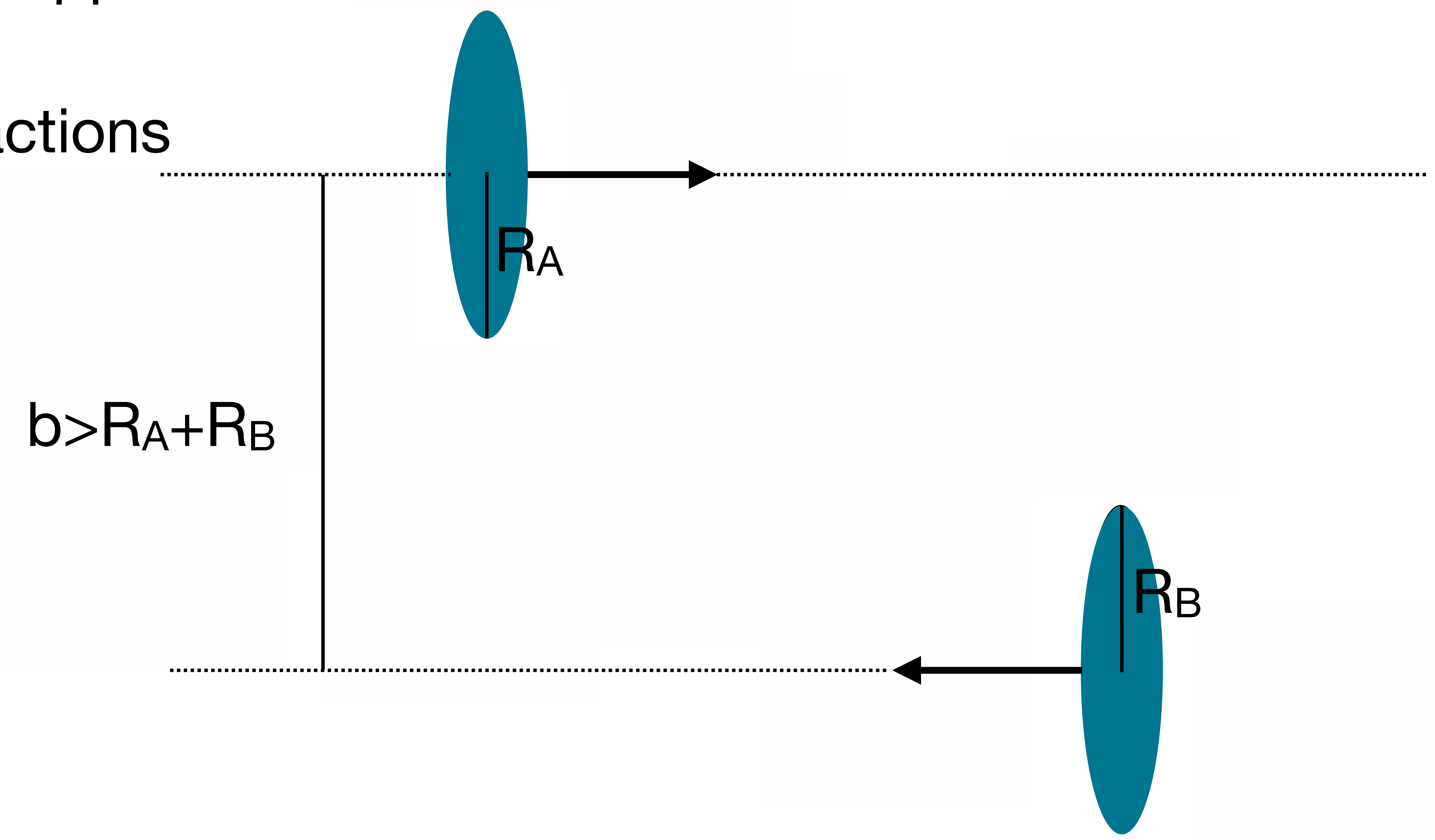

Ultra-peripheral collisions

large–impact-parameter interactions

hadronic interactions strongly suppressed

instead: electromagnetic interactions

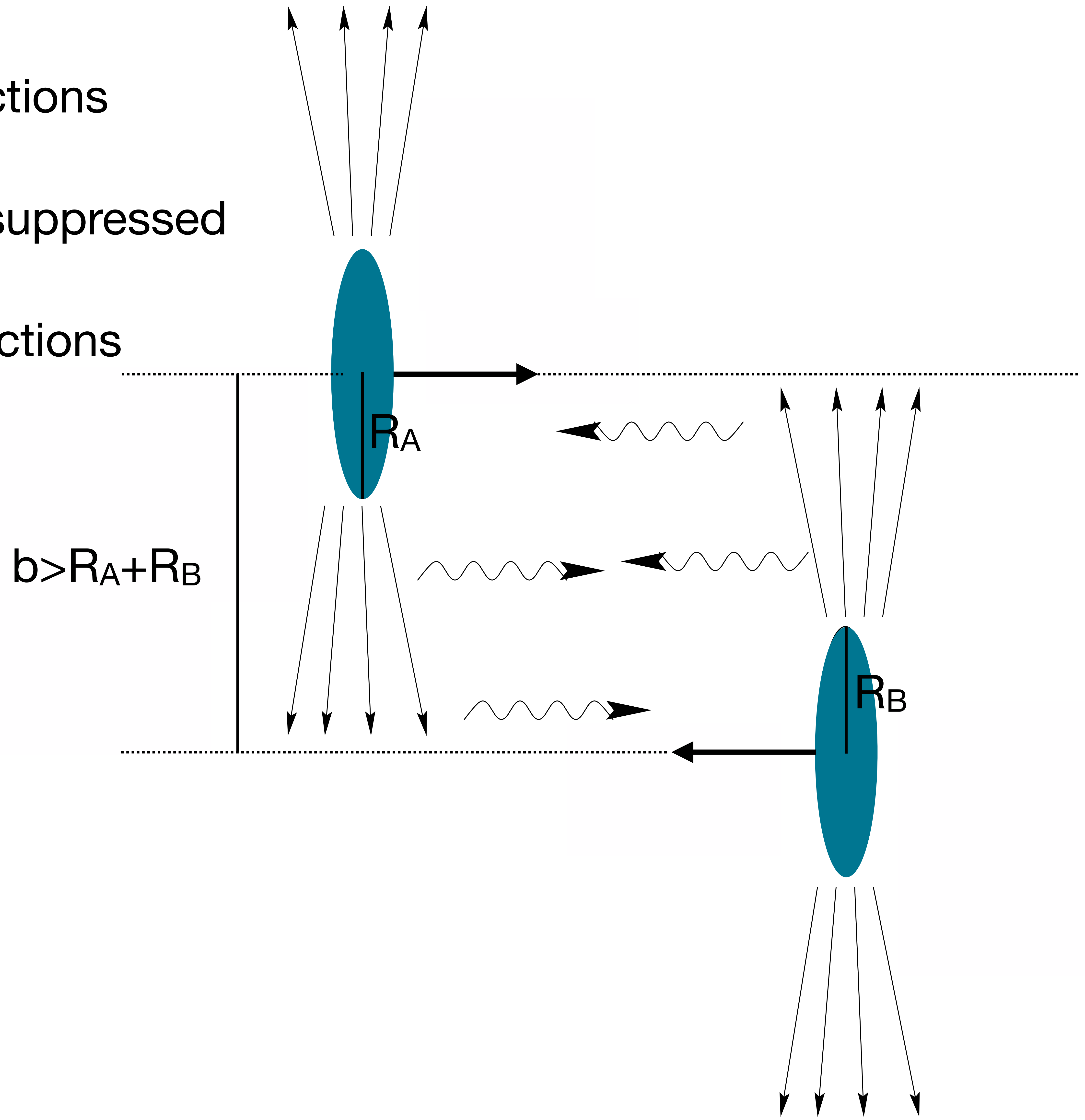

Ultra-peripheral collisions

large–impact-parameter interactions

hadronic interactions strongly suppressed

instead: electromagnetic interactions

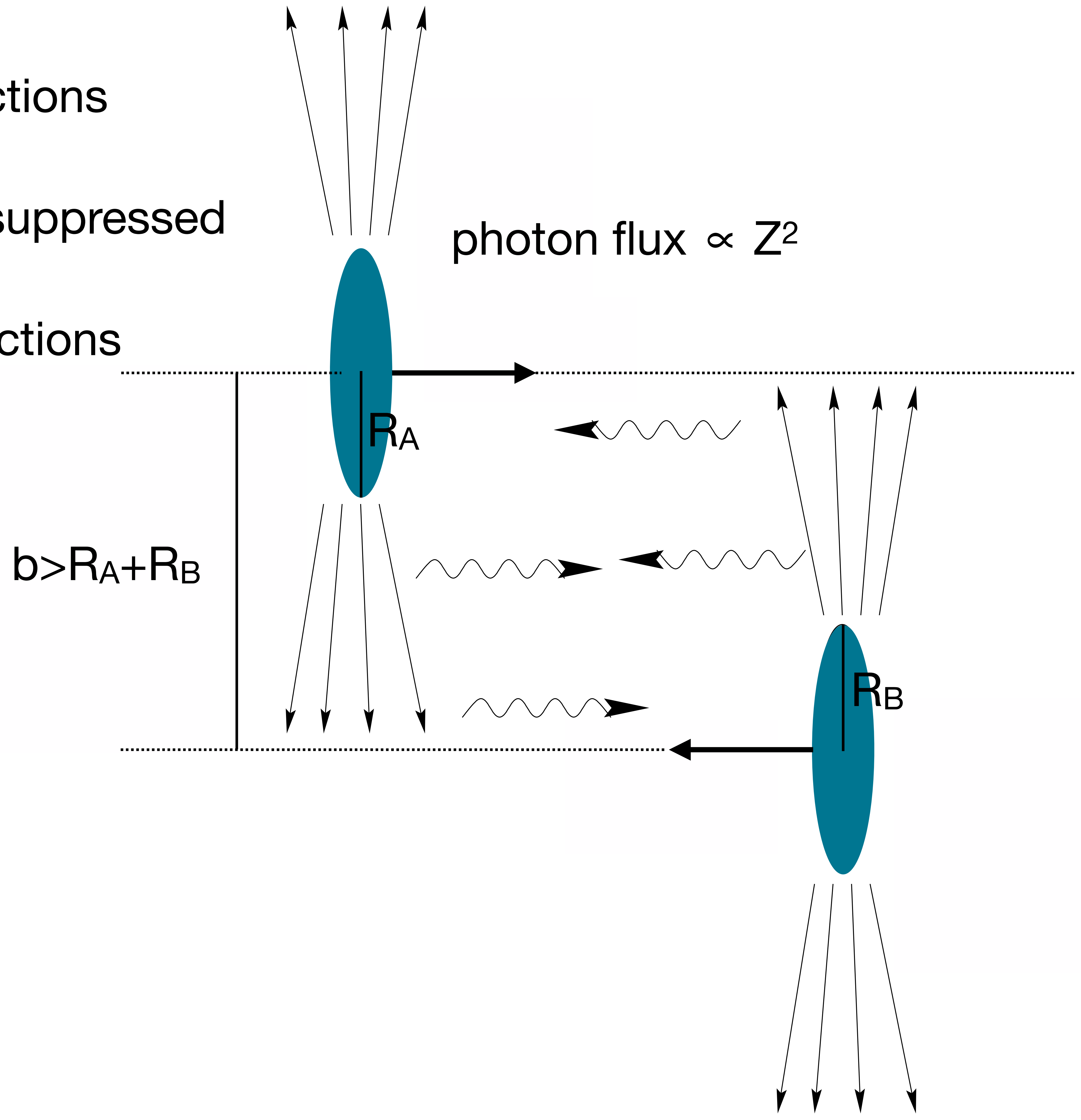

Ultra-peripheral collisions

large–impact-parameter interactions

hadronic interactions strongly suppressed

instead: electromagnetic interactions

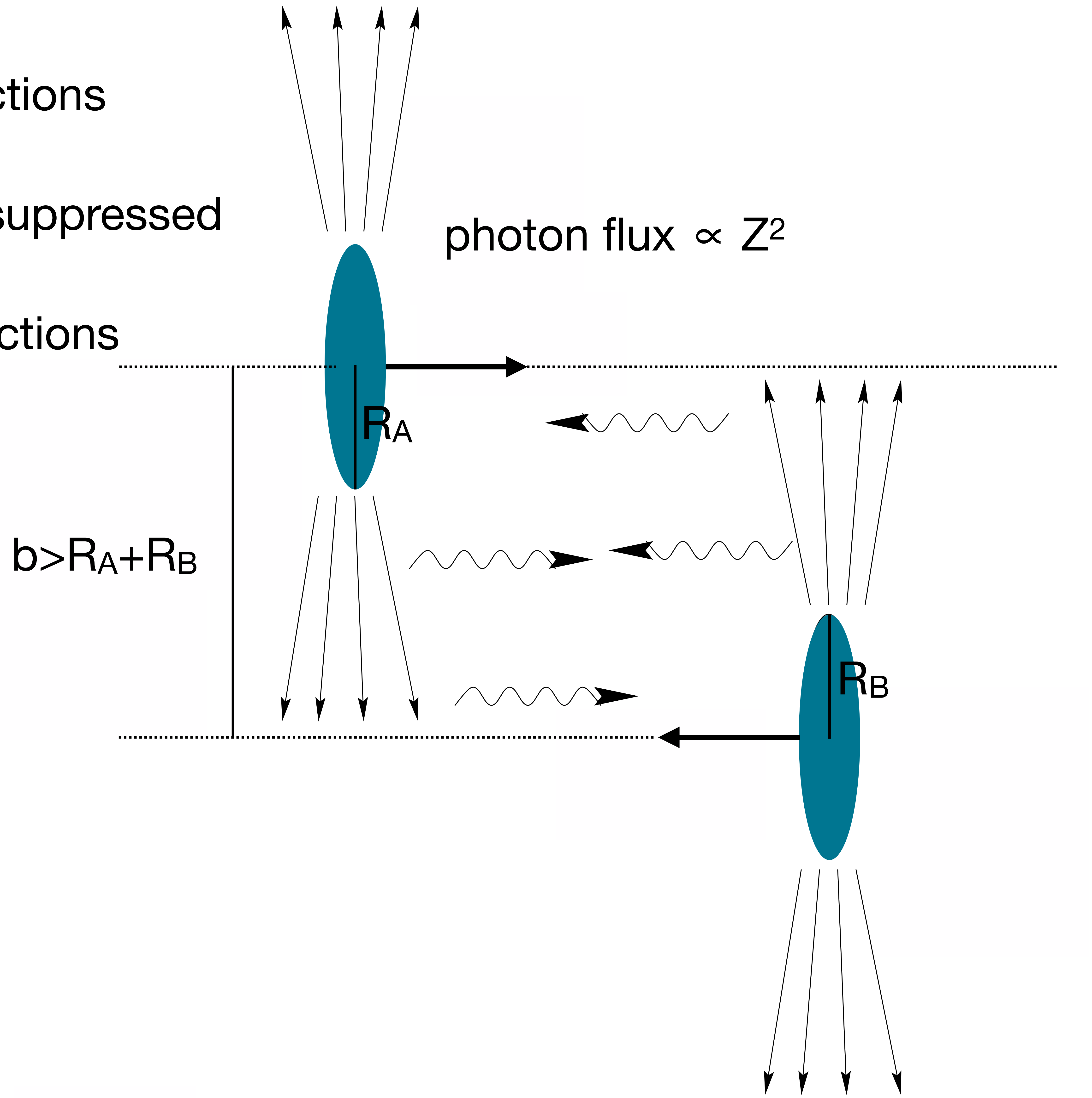

photon virtuality $Q^2 < \left(\frac{\hbar c}{R_A}\right)^2$

→ quasi-real photons

maximum photon energy = $\frac{2\gamma\hbar c}{b_{\mathrm{min}}}$

Ultra-peripheral collisions

large–impact-parameter interactions

hadronic interactions strongly suppressed

instead: electromagnetic interactions

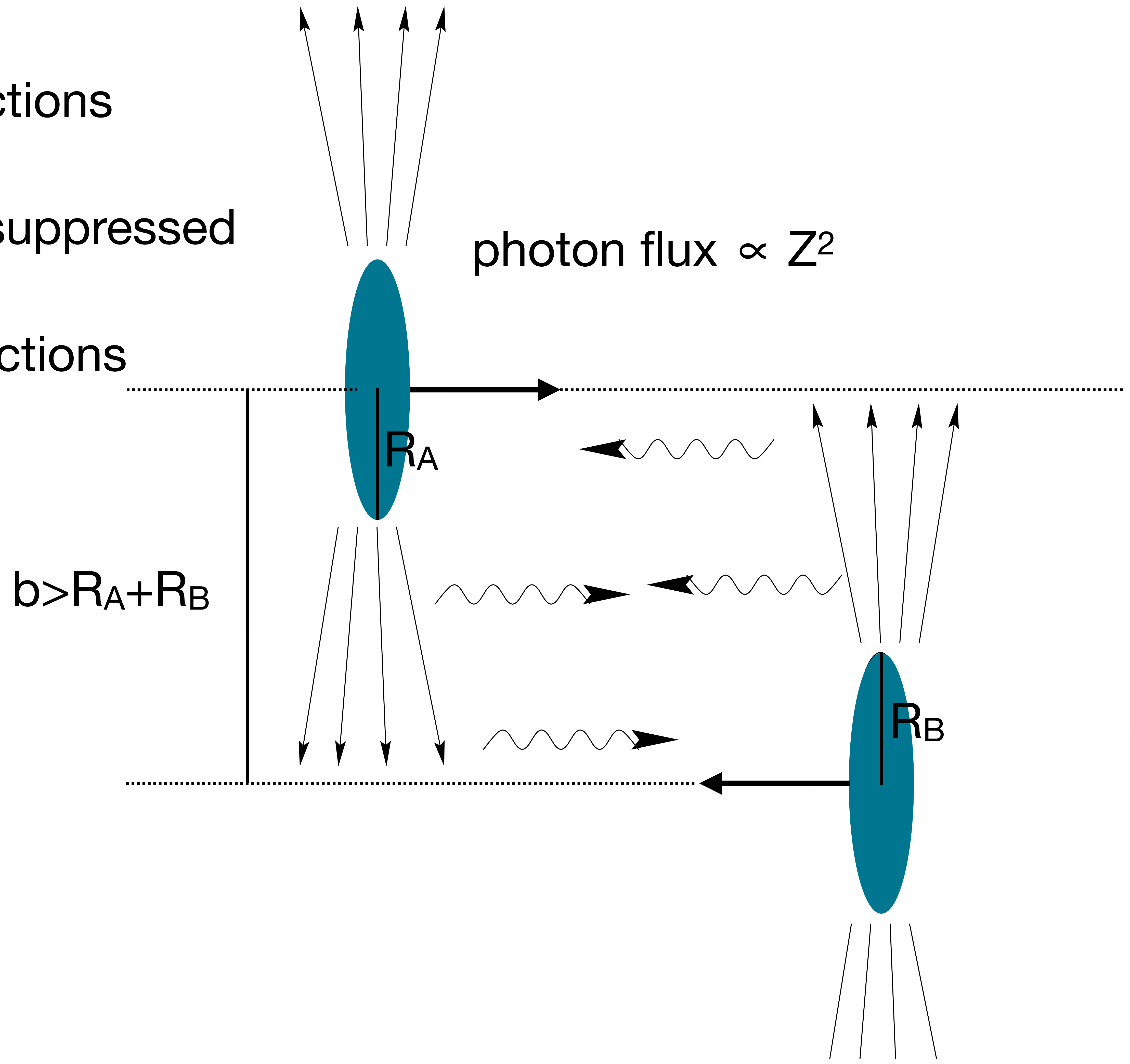

photon virtuality $Q^2 < \left(\frac{\hbar c}{R_A}\right)^2$

→ quasi-real photons

maximum photon energy = $\frac{2\gamma\hbar c}{b_{\mathrm{min}}}$

System	$\sqrt{s_{AB}}$	E_A	E_B	(a) $\gamma_{A\leftrightarrow B}$	(b) $E_{\gamma Max}$	(c) $E^{rest}_{\gamma Max}$	(d) $W^{max}_{\gamma p}$
pPb	5.02 TeV	4 TeV	1.567 TeV	1.43×10^7	28 MeV	0.4 PeV	0.86 TeV
pPb	8.16 TeV	6.5 TeV	2.56 TeV	3.78×10^7	28 MeV	1 PeV	1.4 TeV
pp	13 TeV	6.5 TeV	6.5 TeV	9.6×10^7	116 MeV	11 PeV	4.6 TeV

table: K. Lynch

Measurement of exclusive production at LHCb

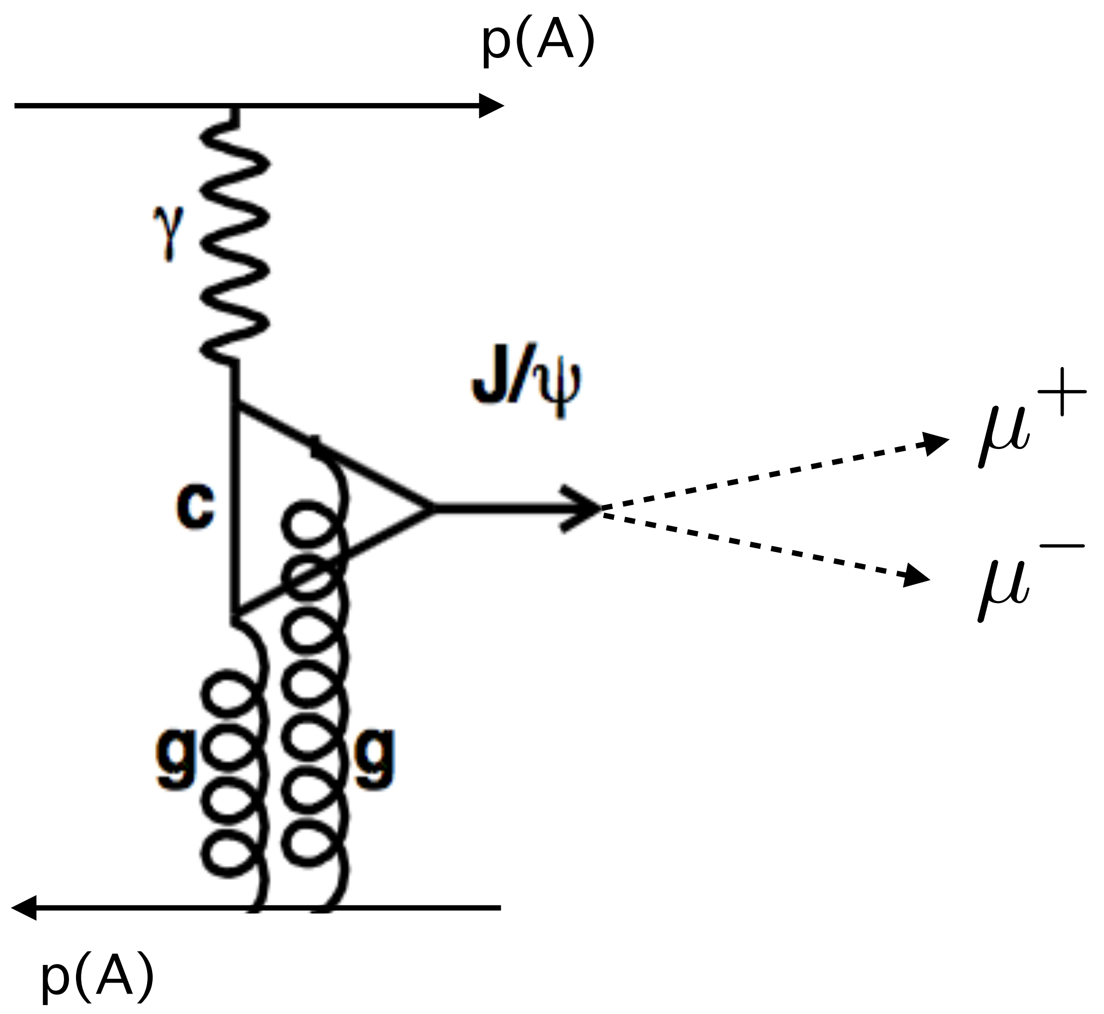

Measurement of exclusive production at LHCb

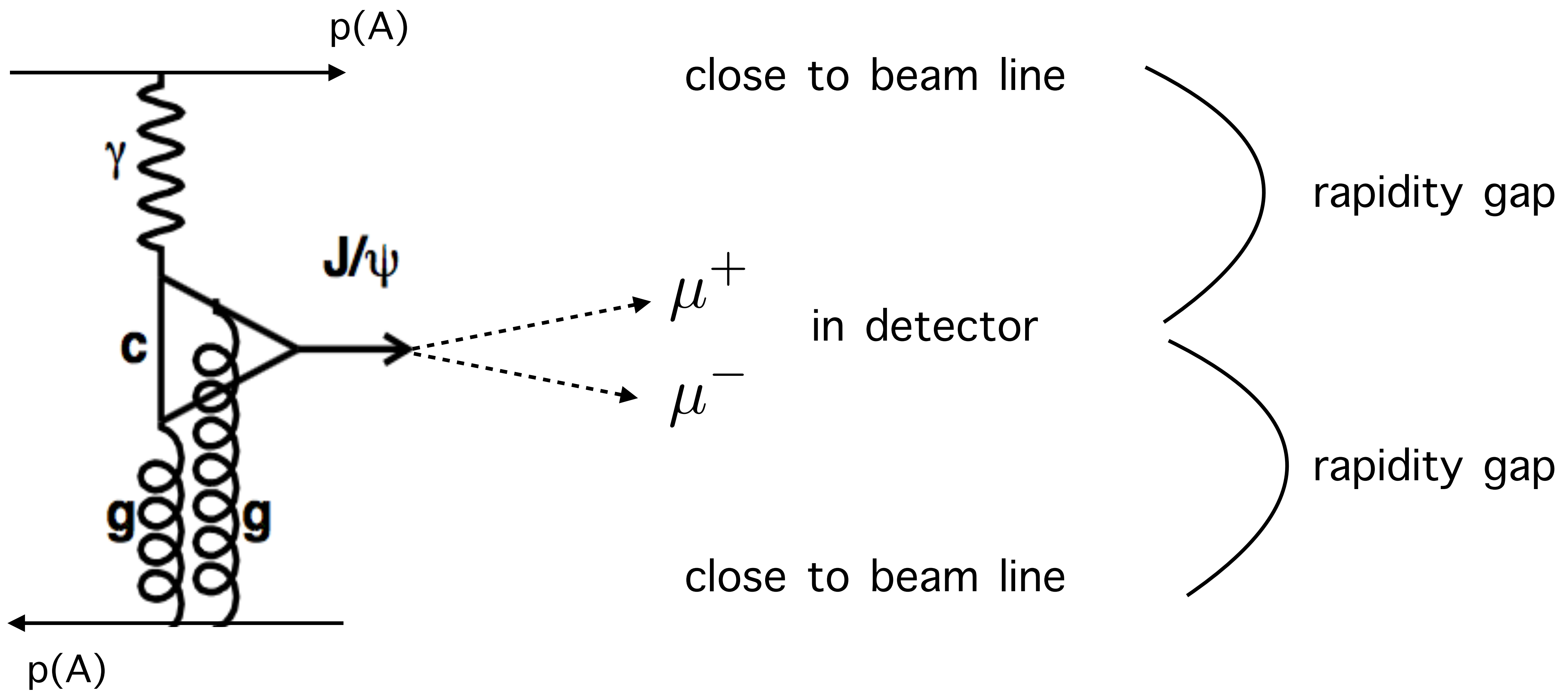

Measurement of exclusive production at LHCb

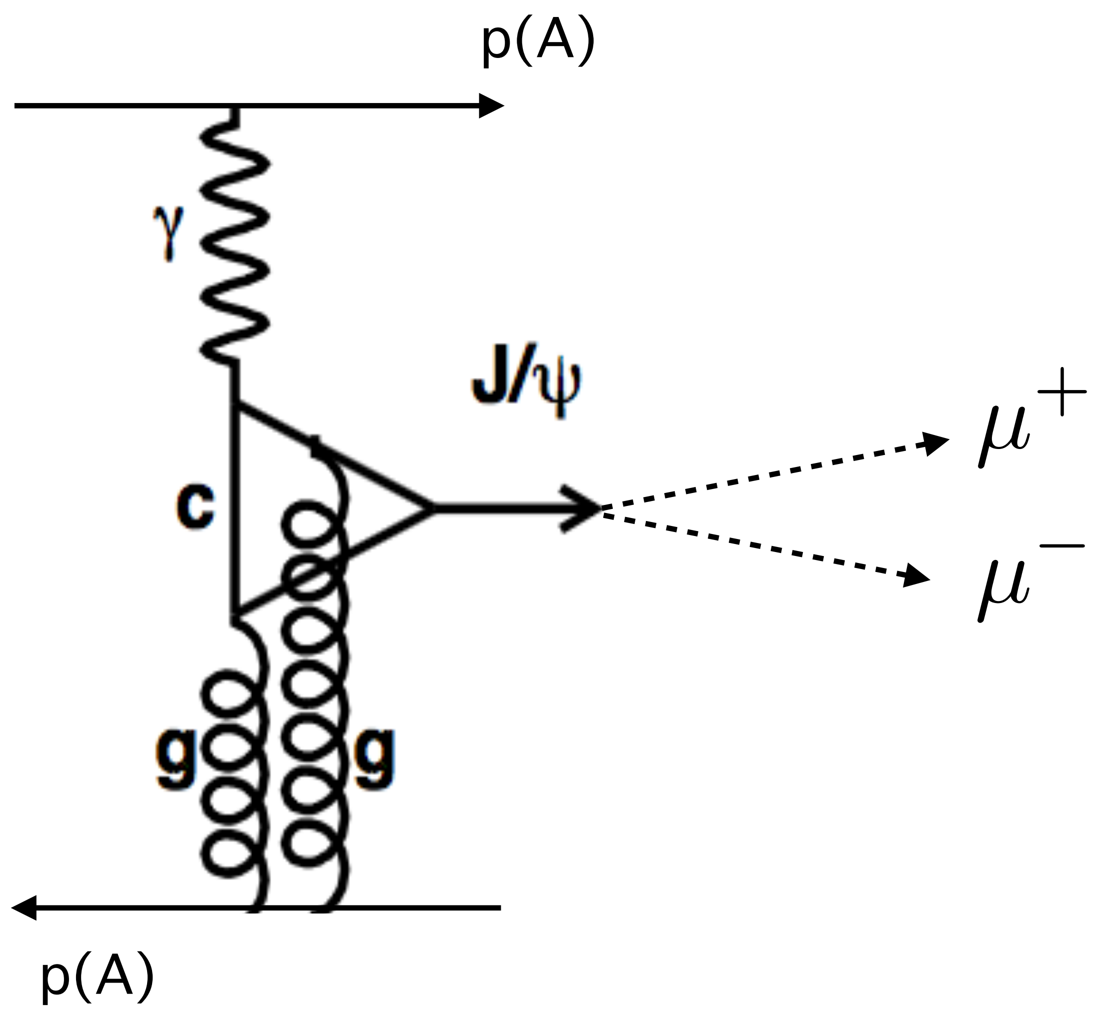

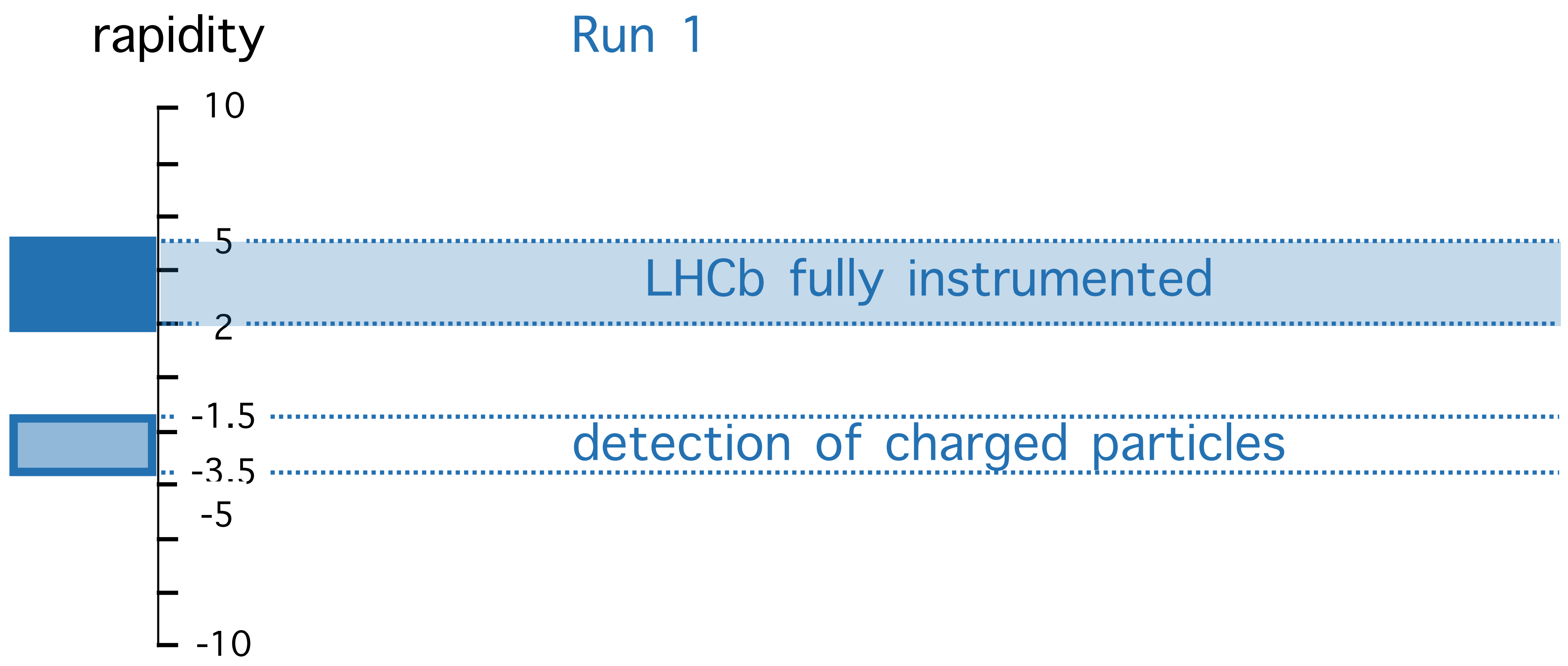

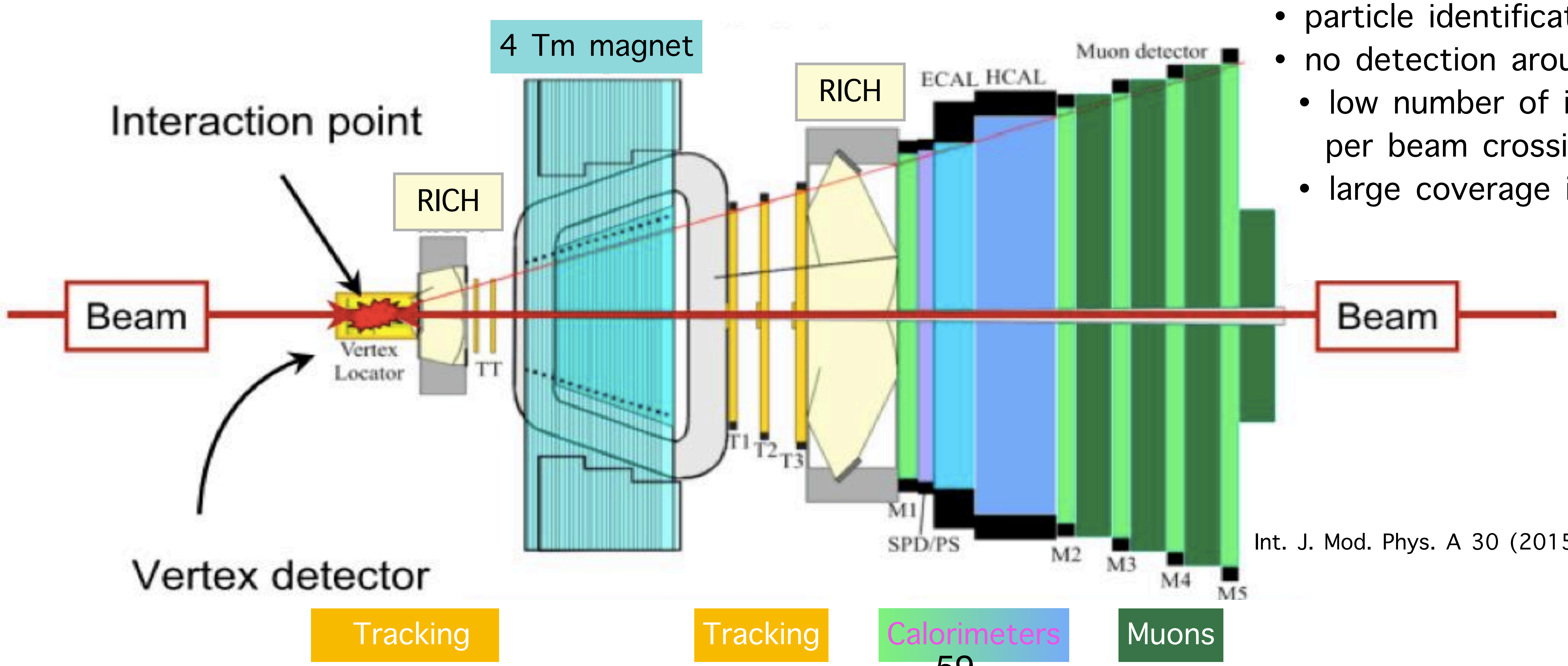

- low p_T threshold: p_T>400 MeV
- particle identification
- no detection around beam line but
  - low number of interactions per beam crossing: 1.1–1.5
  - large coverage in rapidity

Int. J. Mod. Phys. A 30 (2015) 1530022

Measurement of exclusive production at LHCb

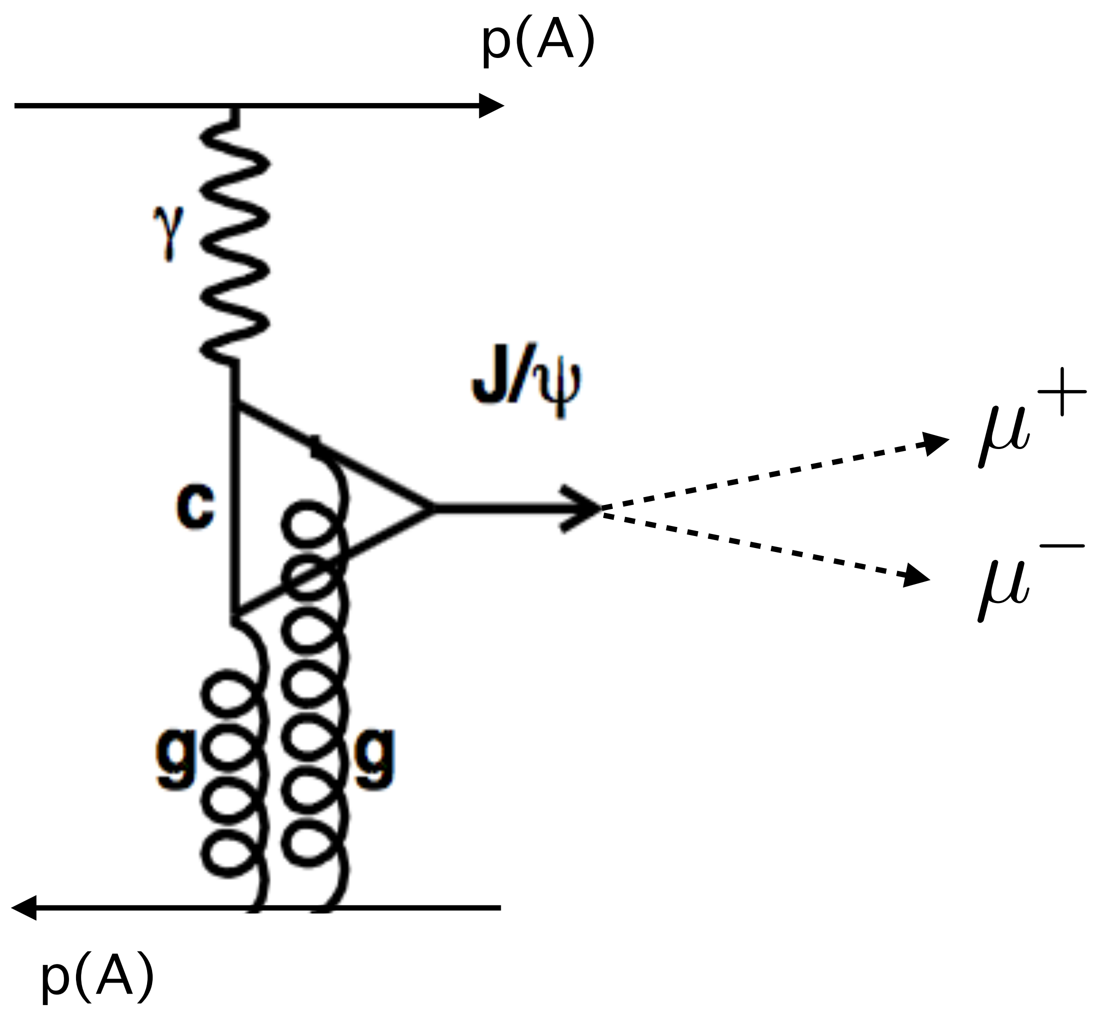

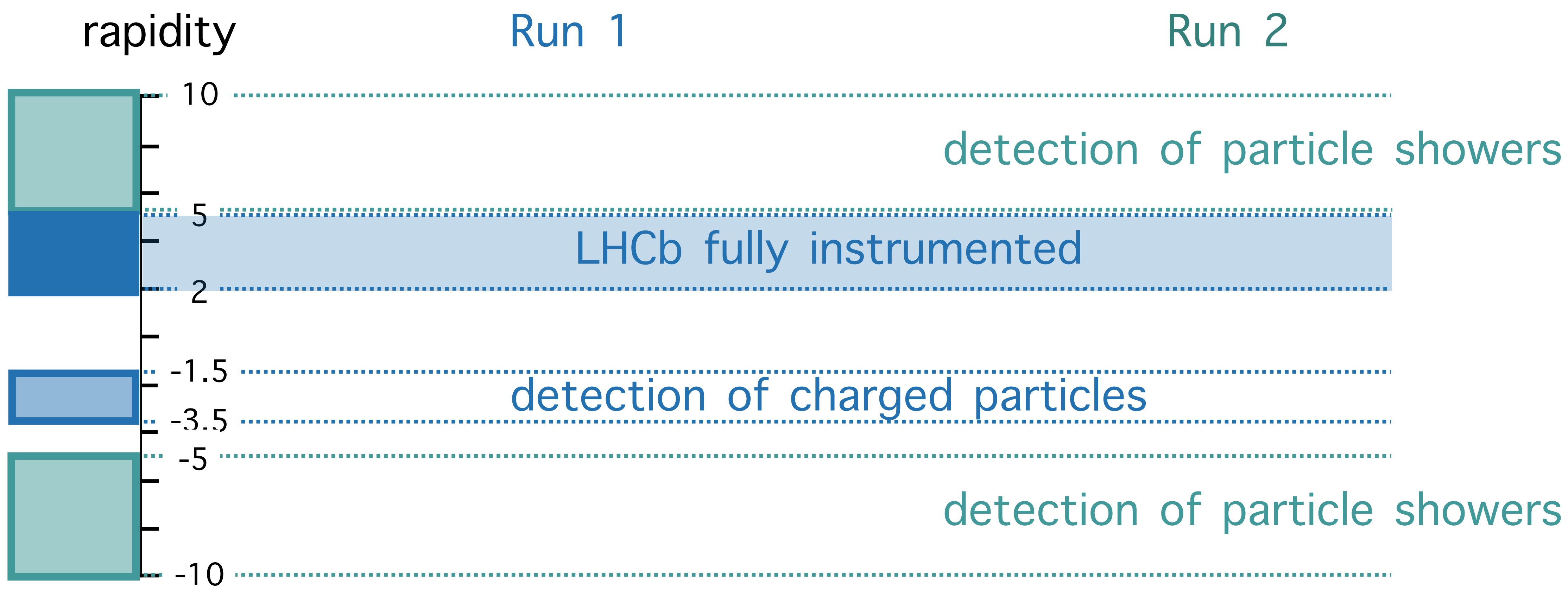

- low p_T threshold: p_T>400 MeV
- particle identification
- no detection around beam line but
  - low number of interactions per beam crossing: 1.1–1.5
  - large coverage in rapidity

Herschel JHEP 10 (2018) 167

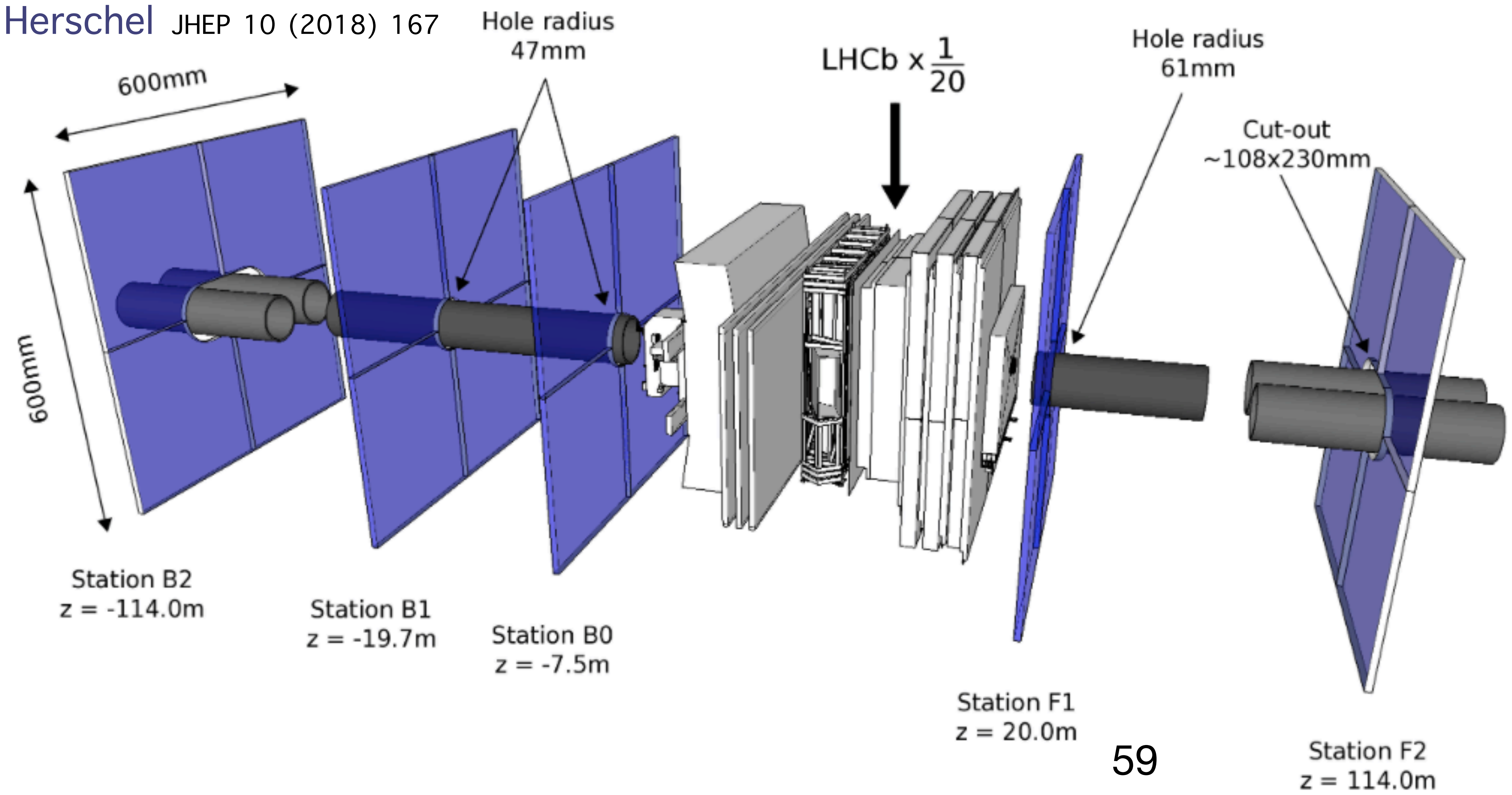

Exclusive single ψ production in pp collisions

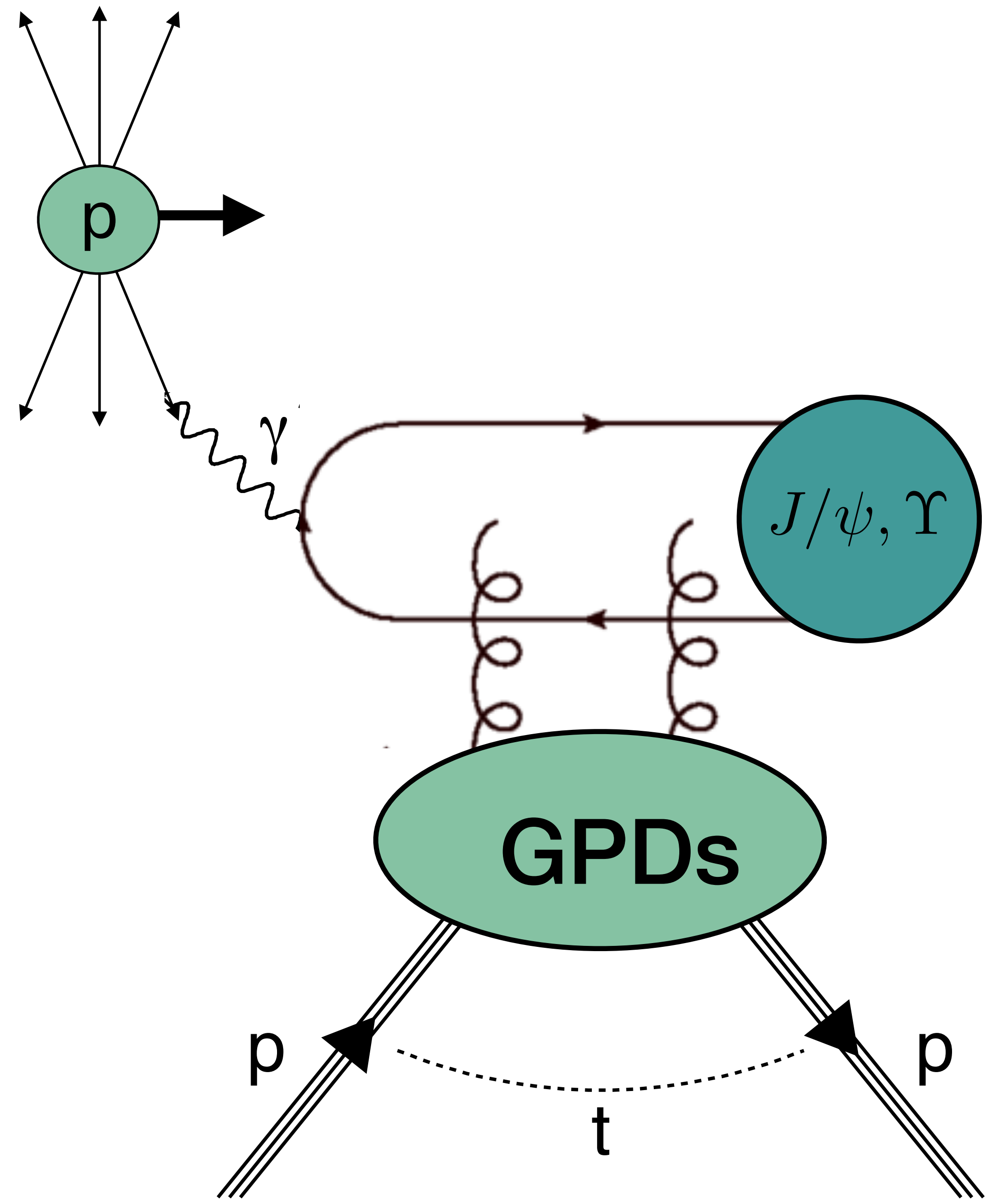

- Exclusive J/ψ and ψ(2S): $\sqrt{s} = 7$ TeV and part of $\sqrt{s} =$13 TeV data (from 2015)

  → x_B down to 2×10^{-6}

- Reconstruction via dimuon decay, with 2<η<4.5.
- No other detector activity.
- Quarkonia J//ψ and ψ(2S): 2<y<4.5 and $p_T^2 < 0.8$ GeV^2

Exclusive single ψ production in pp collisions

- Exclusive J/ψ and ψ(2S): $\sqrt{s} = 7$ TeV and part of $\sqrt{s} = 13$ TeV data (from 2015)

  → x_B down to $2x10^{-6}$
- Reconstruction via dimuon decay, with 2<η<4.5.
- No other detector activity.
- Quarkonia J//ψ and ψ(2S): 2<y<4.5 and p_T^2<0.8 GeV²

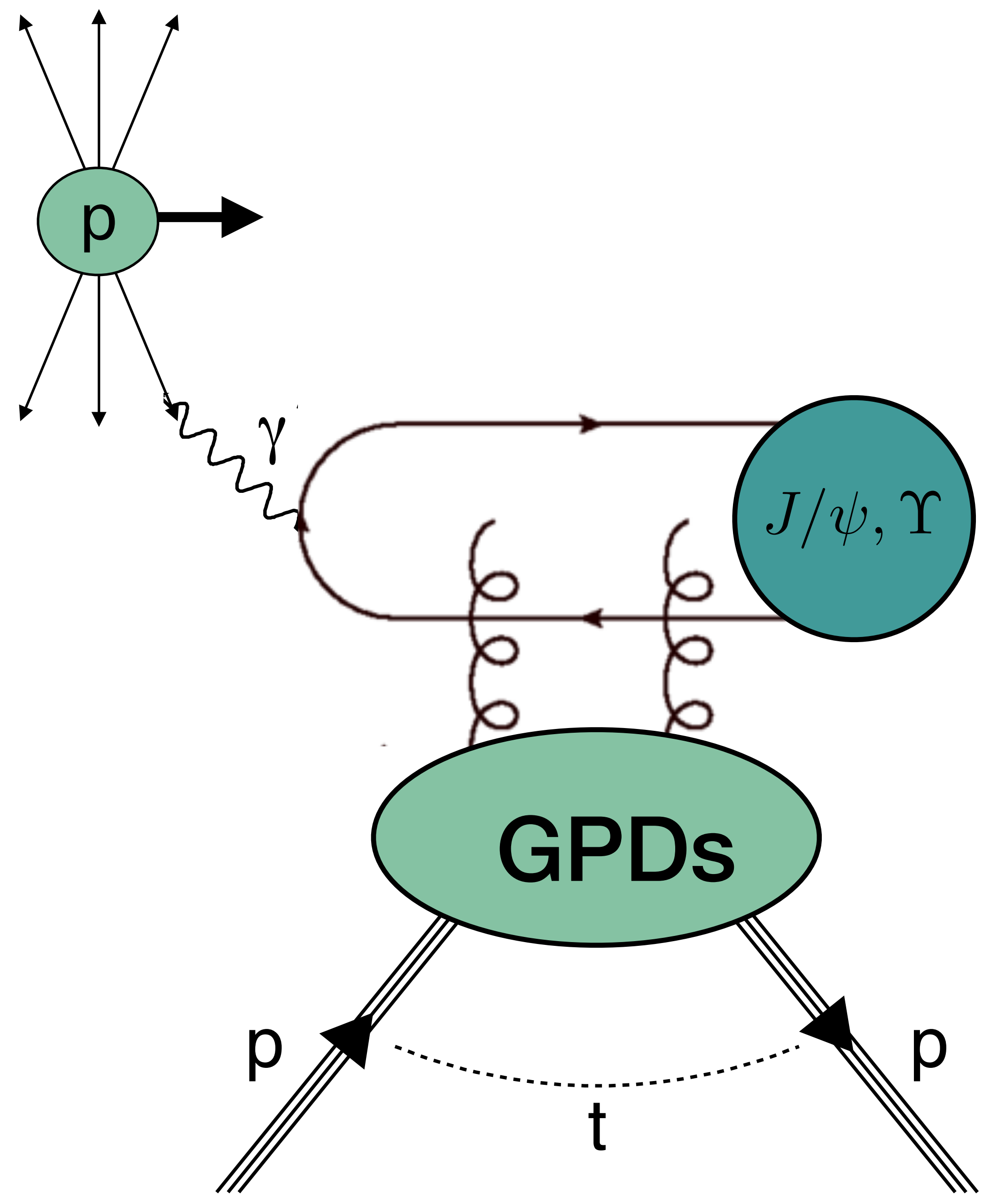

JHEP **10** (2018) 167

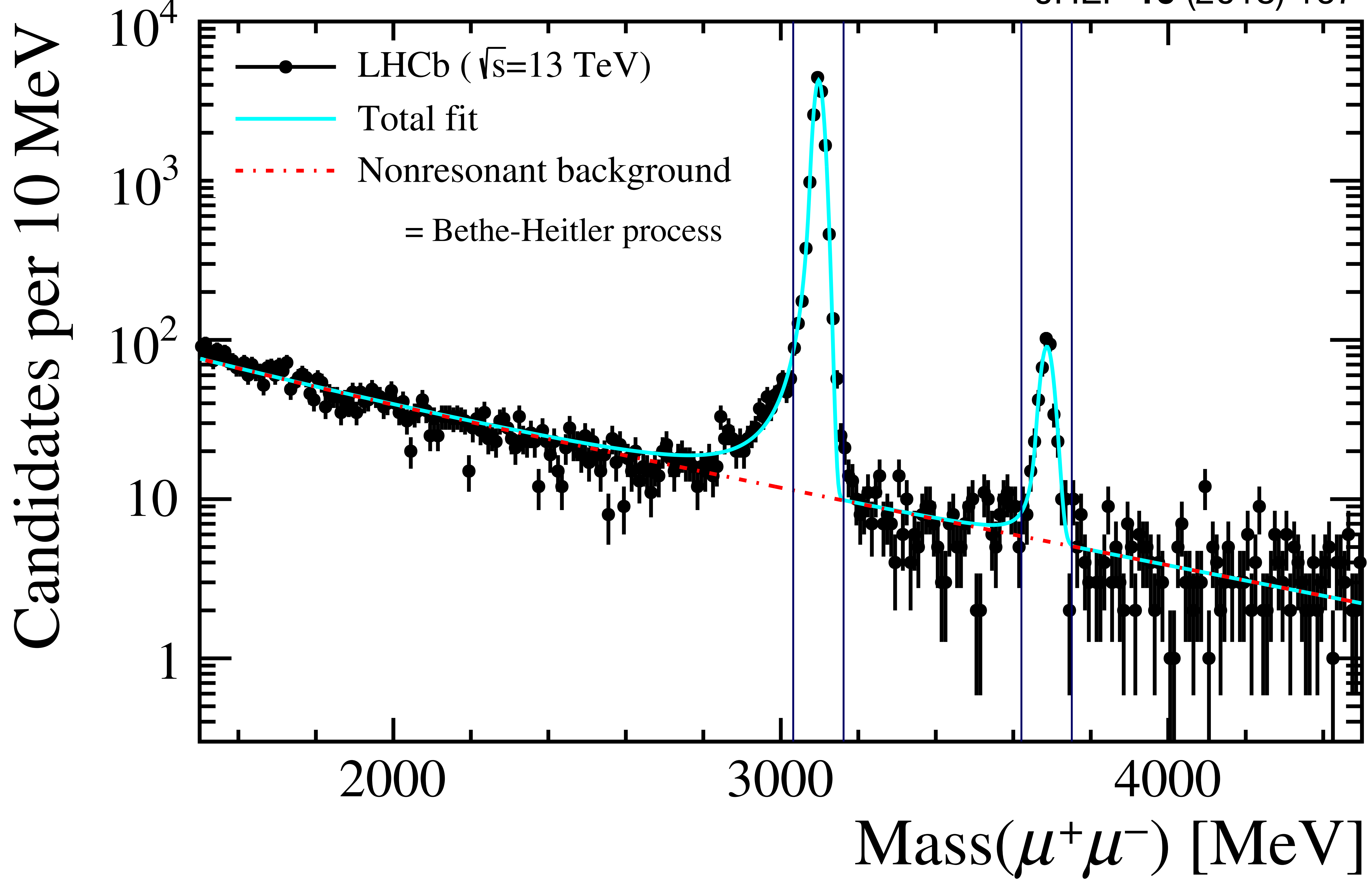

Background: feed down and proton dissociation

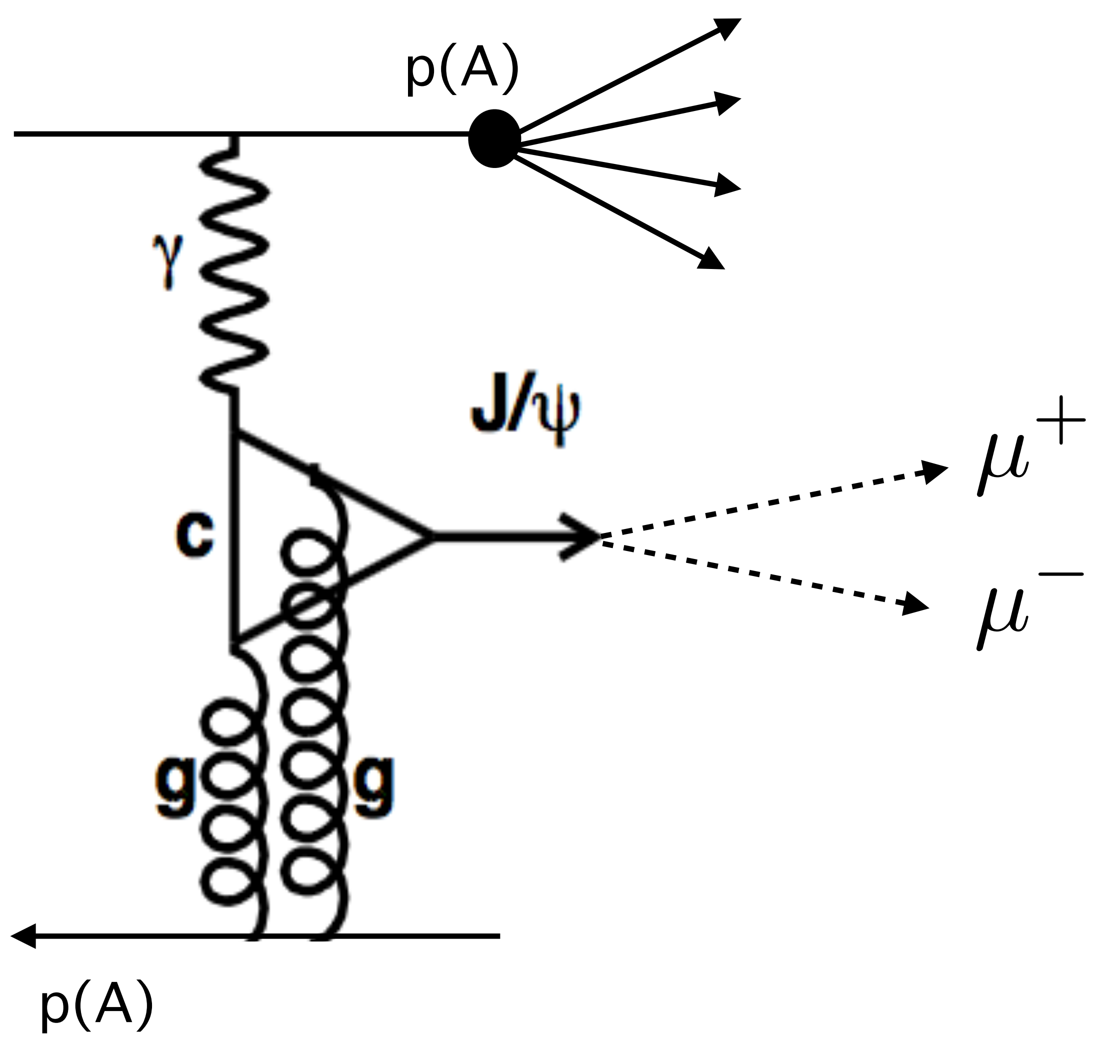

proton/ion dissociation

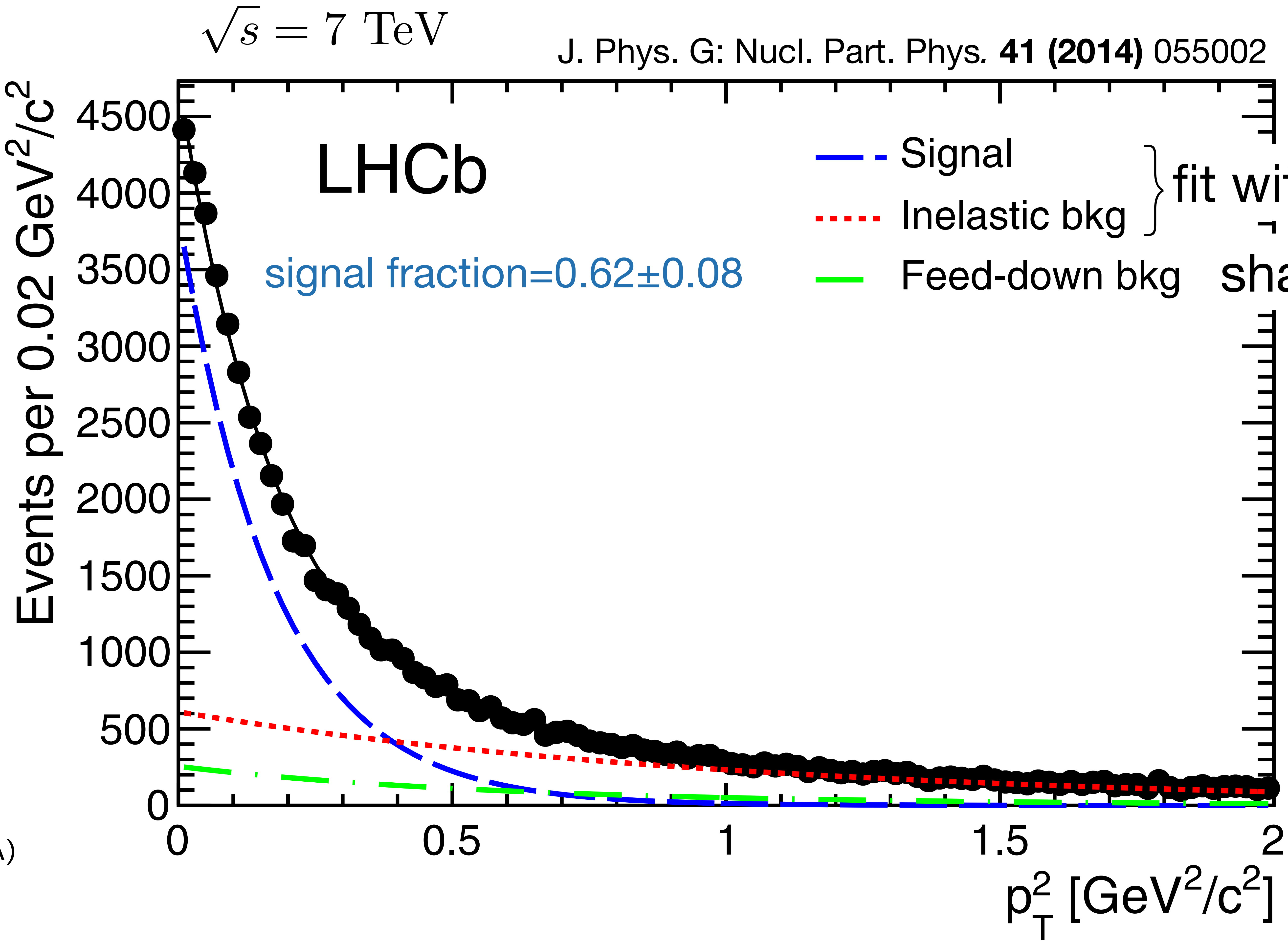

fit with exponential

shape from data

J/ψ feed-down background

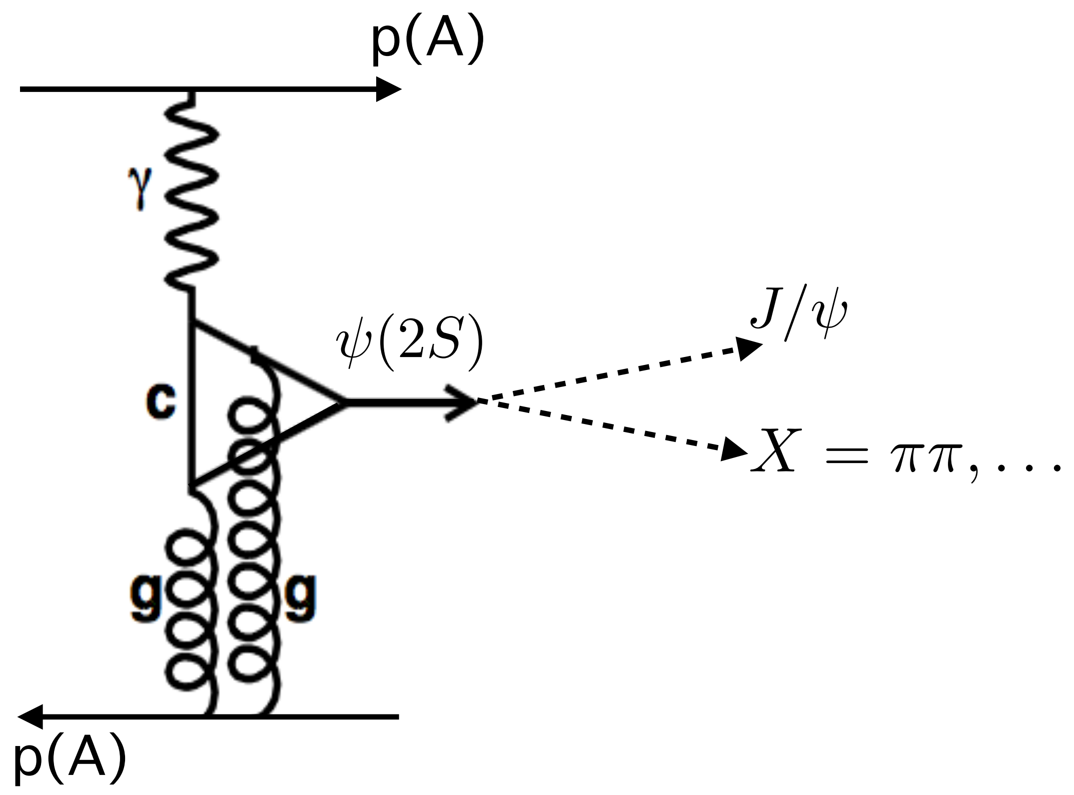

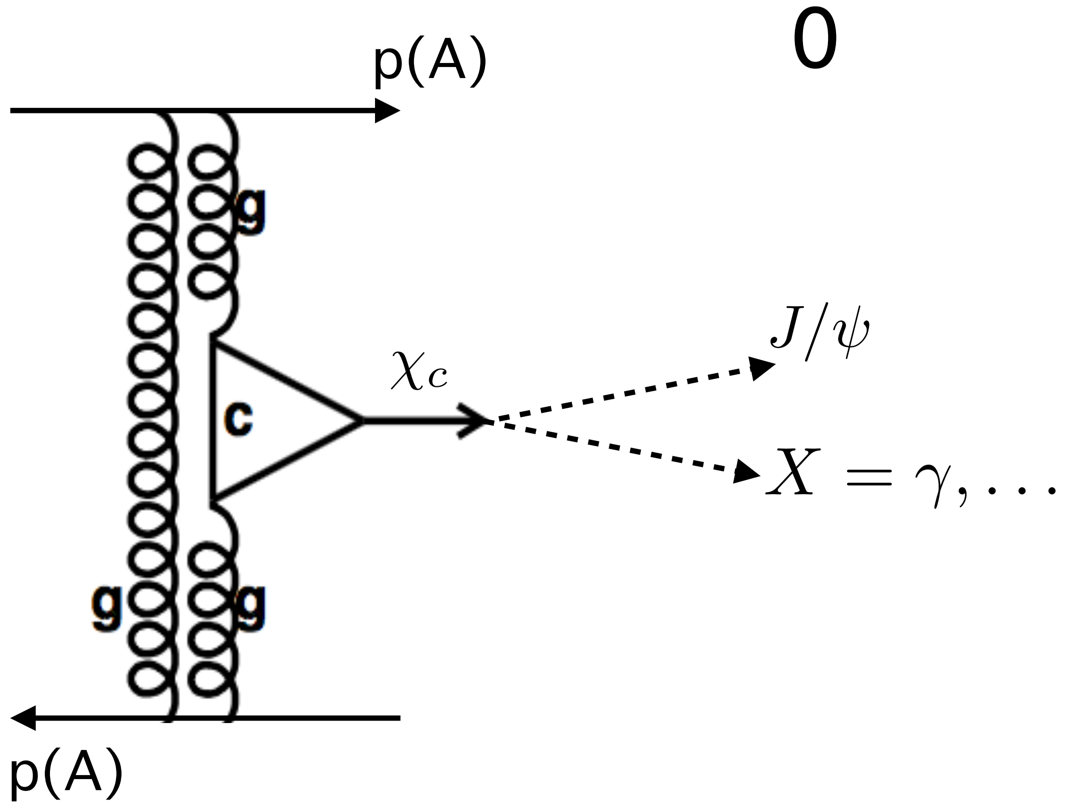

Cross-section calculation

number of events

$$\frac{d\sigma_{\psi\to\mu^+\mu^-}}{dy}(2.0 < \eta_\mu < 4.5) = \frac{\boxed{N}}{\Delta y}$$

Cross-section calculation

signal purity — number of events

$$\frac{d\sigma_{\psi\to\mu^+\mu^-}}{dy}(2.0 < \eta_\mu < 4.5) = \frac{\boxed{\mathcal{P}}\boxed{N}}{\Delta y}$$

Cross-section calculation

signal purity number of events

$$\frac{d\sigma_{\psi\to\mu^+\mu^-}}{dy}(2.0 < \eta_\mu < 4.5) = \frac{\mathcal{P}N}{\epsilon_{\text{rec}} \quad \Delta y}$$

reconstruction efficiency
≈0.3–0.7/0.4–0.6

run1/run2

Cross-section calculation

signal purity number of events

$$\frac{d\sigma_{\psi\to\mu^+\mu^-}}{dy}(2.0 < \eta_\mu < 4.5) = \frac{\mathcal{P} N}{\epsilon_{\text{rec}}\epsilon_{\text{sel}}\Delta y}$$

reconstruction efficiency
≈0.3–0.7/0.4–0.6

selection
efficiency
≈0.87/0.6-0.7

run1/run2

Cross-section calculation

signal purity number of events

$$\frac{d\sigma_{\psi\to\mu^+\mu^-}}{dy}(2.0 < \eta_\mu < 4.5) = \frac{\mathcal{P}N}{\epsilon_{\rm rec}\epsilon_{\rm sel}\Delta y\epsilon_{\rm single}}$$

reconstruction efficiency ≈0.3–0.7/0.4–0.6

selection efficiency ≈0.87/0.6-0.7

single-interaction efficiency≈0.24/0.33

run1/run2

Cross-section calculation

signal purity — number of events

$$\frac{d\sigma_{\psi\to\mu^+\mu^-}}{dy}(2.0 < \eta_\mu < 4.5) = \frac{\mathcal{P}N}{\epsilon_{\rm rec}\epsilon_{\rm sel}\Delta y\,\epsilon_{\rm single}\mathcal{L}_{\rm tot}}$$

luminosity
929 pb^{-1}/204 pb^{-1}

reconstruction efficiency
≈0.3–0.7/0.4–0.6

selection
efficiency
≈0.87/0.6-0.7

single-interaction
efficiency≈0.24/0.33

run1/run2

Cross-section calculation

$$\frac{d\sigma_{\psi\to\mu^+\mu^-}}{dy}(2.0 < \eta_\mu < 4.5) = \frac{\mathcal{P}N}{\epsilon_{\rm rec}\epsilon_{\rm sel}\Delta y\,\epsilon_{\rm single}\mathcal{L}_{\rm tot}}$$

signal purity

number of events

luminosity
929 pb^{-1}/204 pb^{-1}

reconstruction efficiency
≈0.3–0.7/0.4–0.6

selection efficiency
≈0.87/0.6-0.7

single-interaction efficiency≈0.24/0.33

run1/run2

$$\frac{1}{\mathcal{B}(\psi\to\mu^+\mu^-)_{\rm acceptance}}$$

$$\frac{d\sigma_{pp\to p\psi p}}{dy}$$

pp cross section

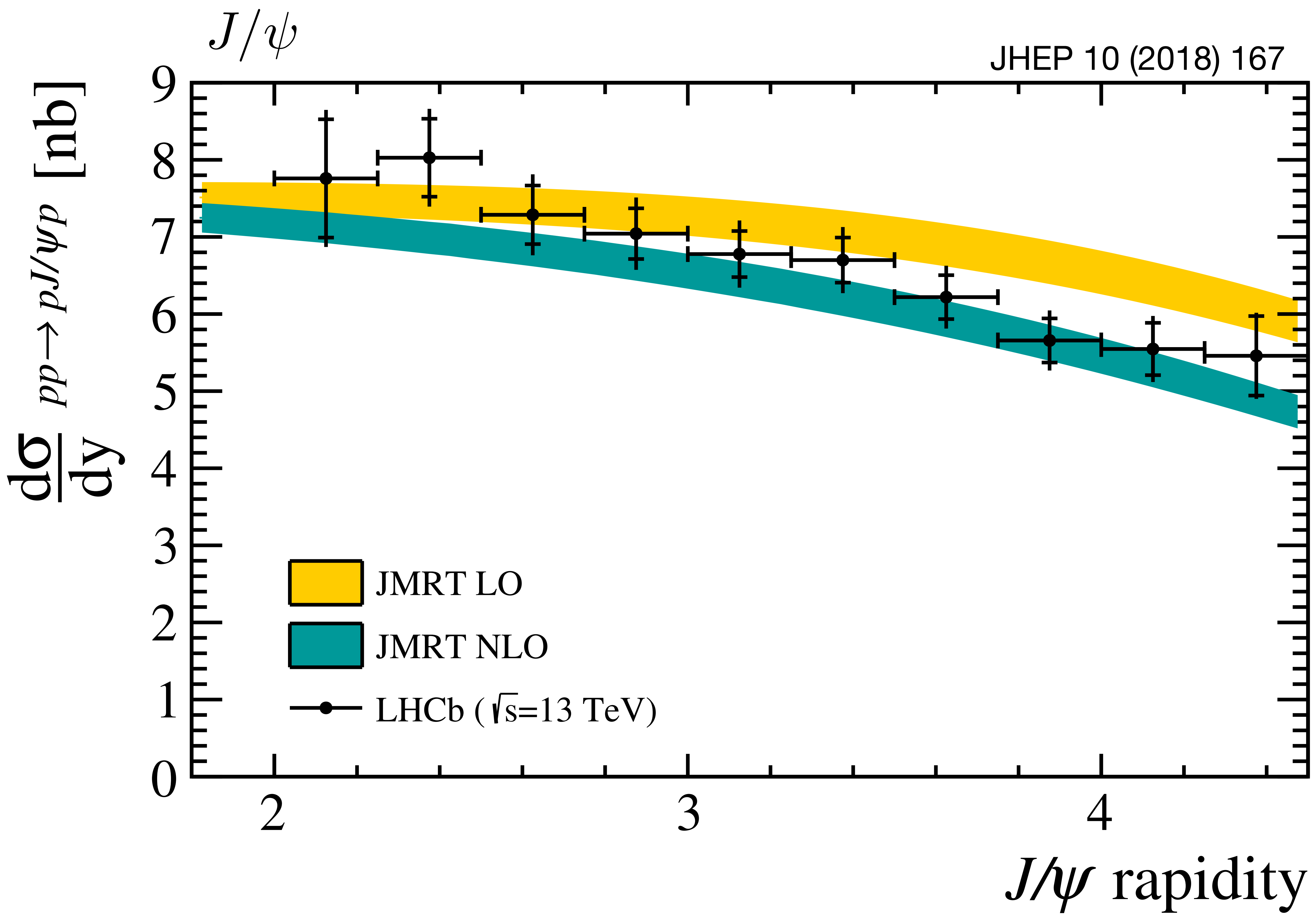

JMRT prediction, based on gluon PDF:

At low x_B, approximate GPD to gluon PDF

$$\left.\frac{d\sigma}{dt}\right|_{t=0} \propto [g(x_B)]^2$$

Z. Phys. C**57** ('93) 89–92;
arXiv:1609.09738

Exclusive single Υ production in pp collisions

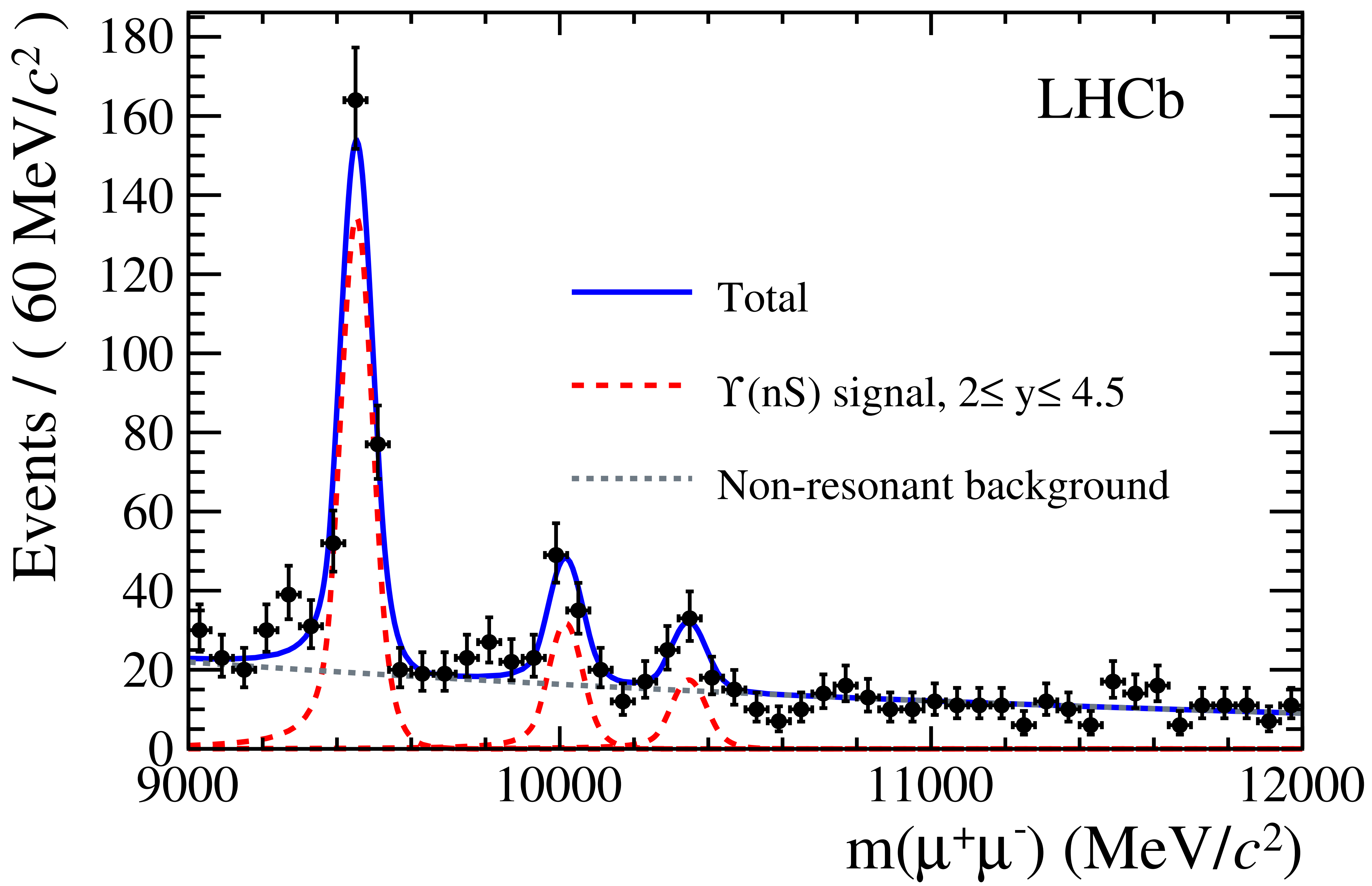

JHEP11(2013)085

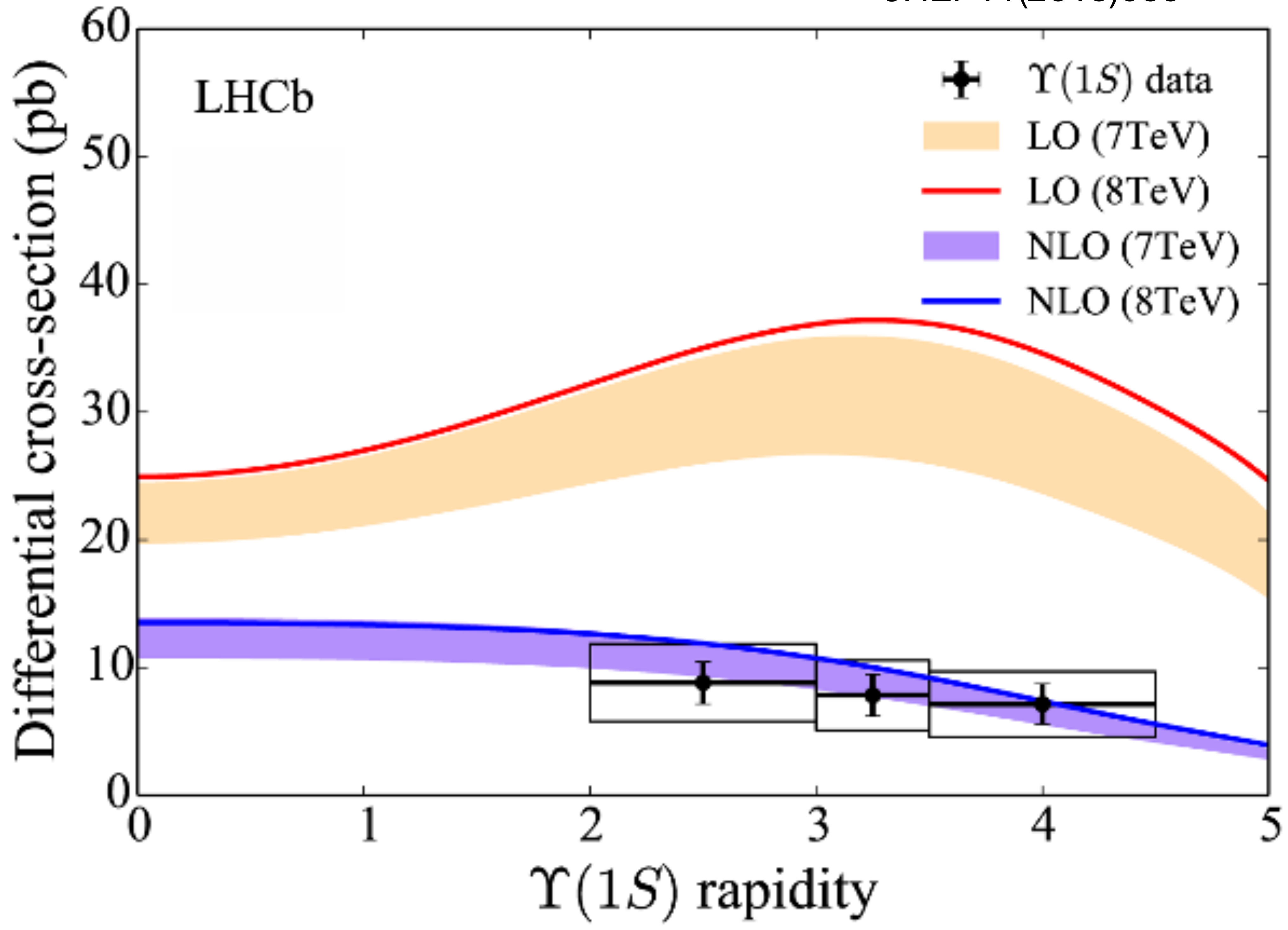

higher Q^2 scale

ALICE: exclusive single-J/ψ production in pPb collisions

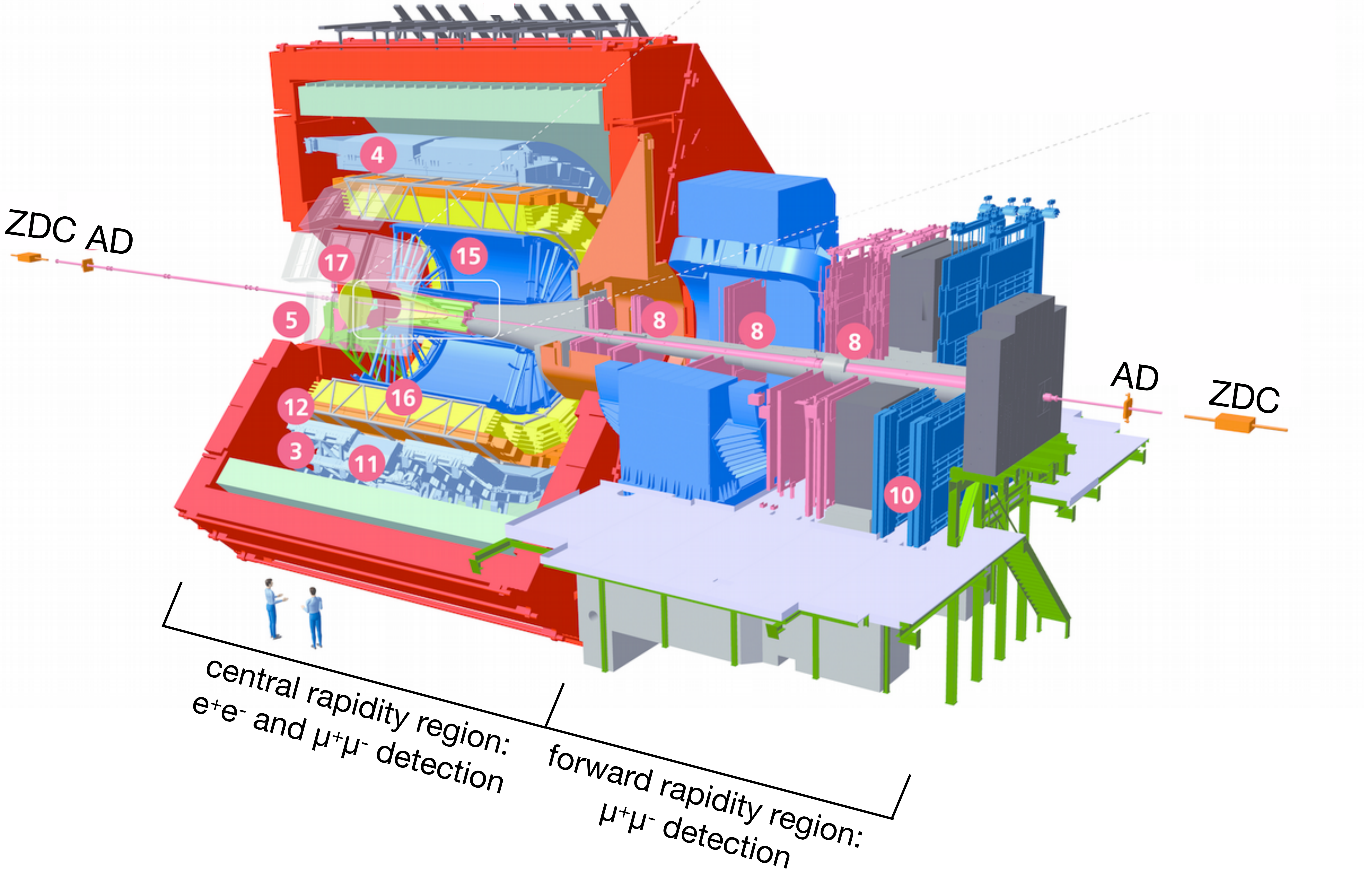

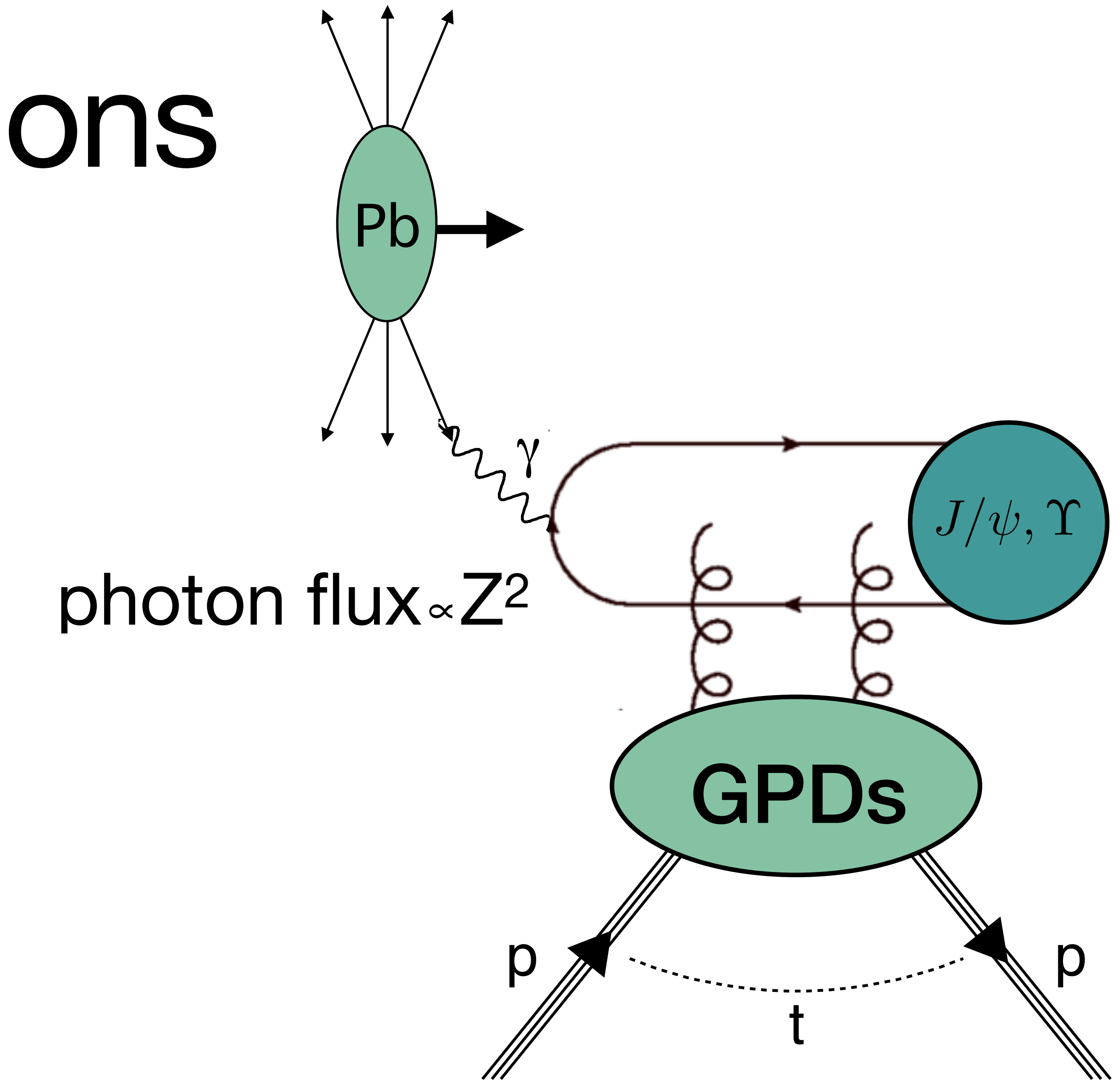

+ Requirement on forward/backward scintillators and far-foward/backward neutron zero-degree calorimeters (ZDCs)

ALICE: exclusive single-J/ψ production in pPb collisions

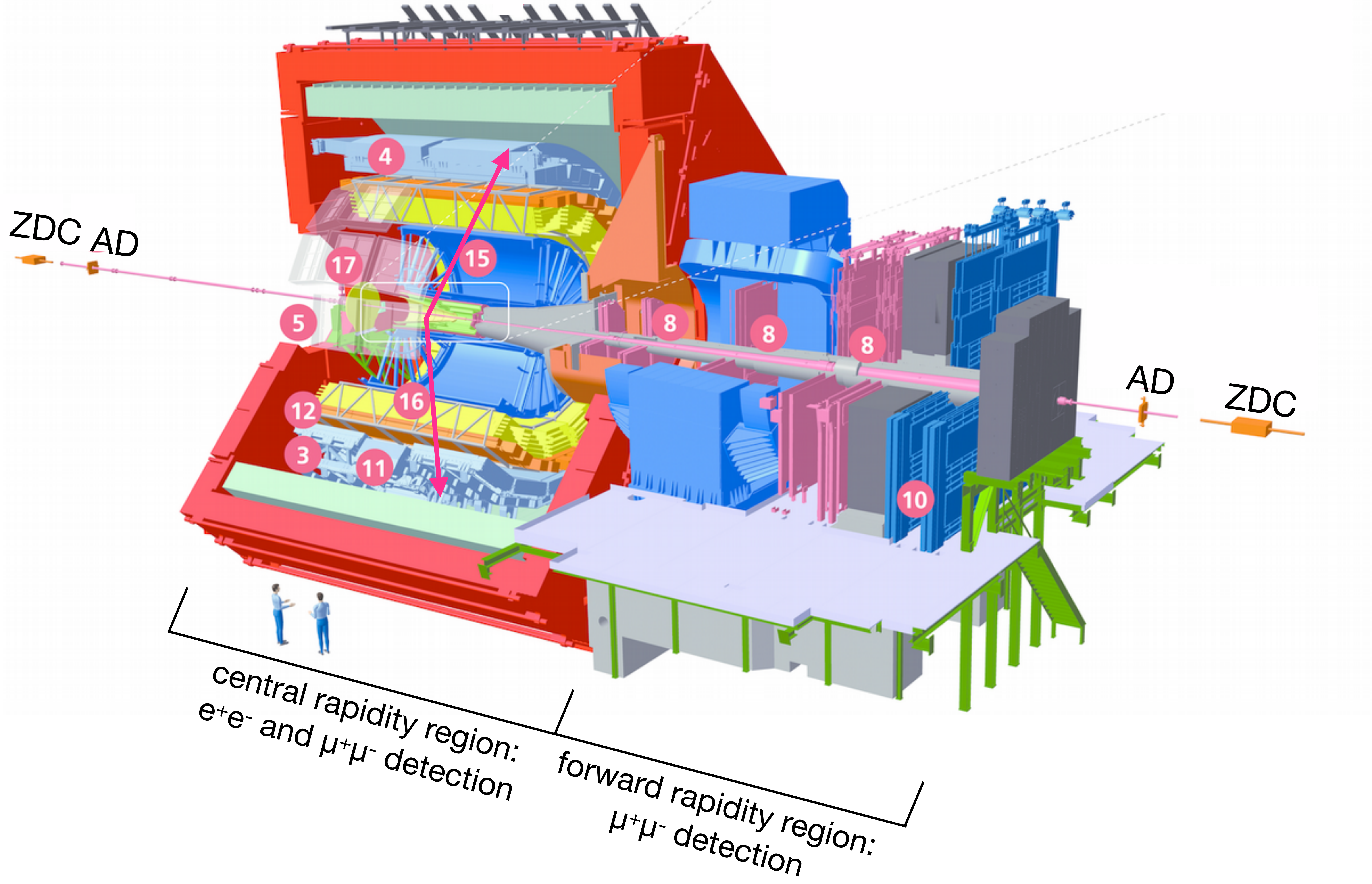

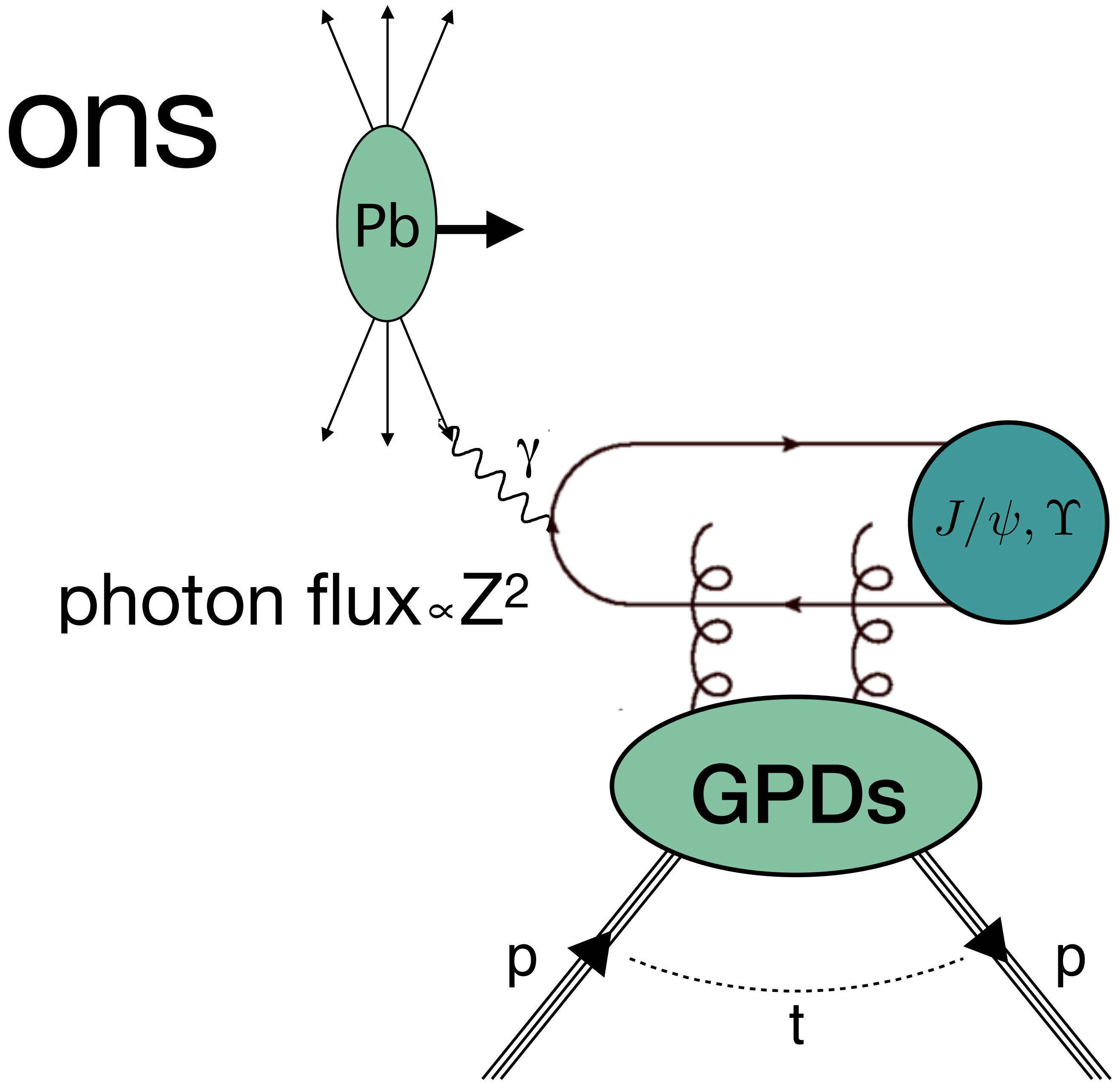

+ Requirement on forward/backward scintillators and far-foward/backward neutron zero-degree calorimeters (ZDCs)

ALICE: exclusive single-J/ψ production in pPb collisions

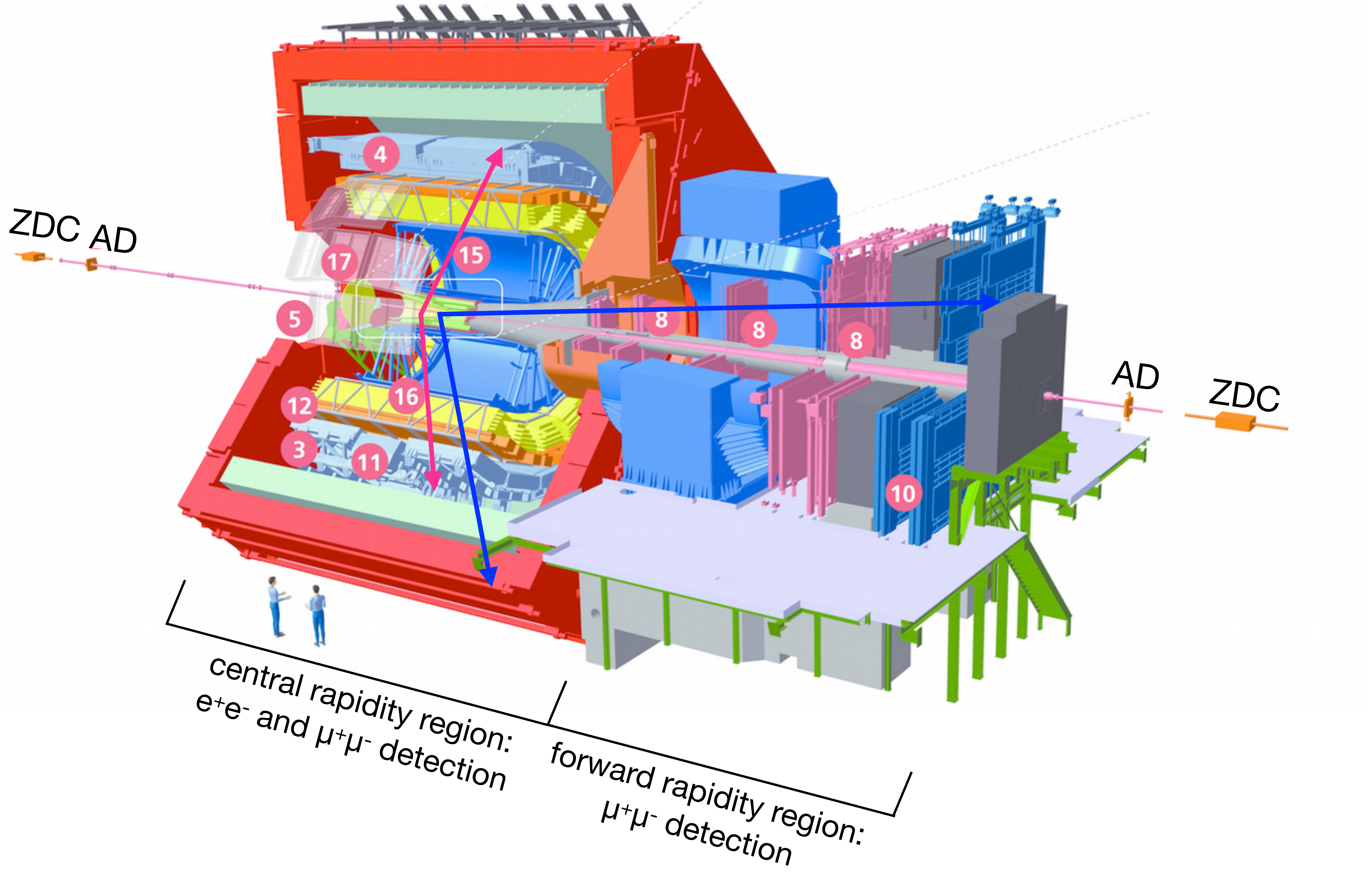

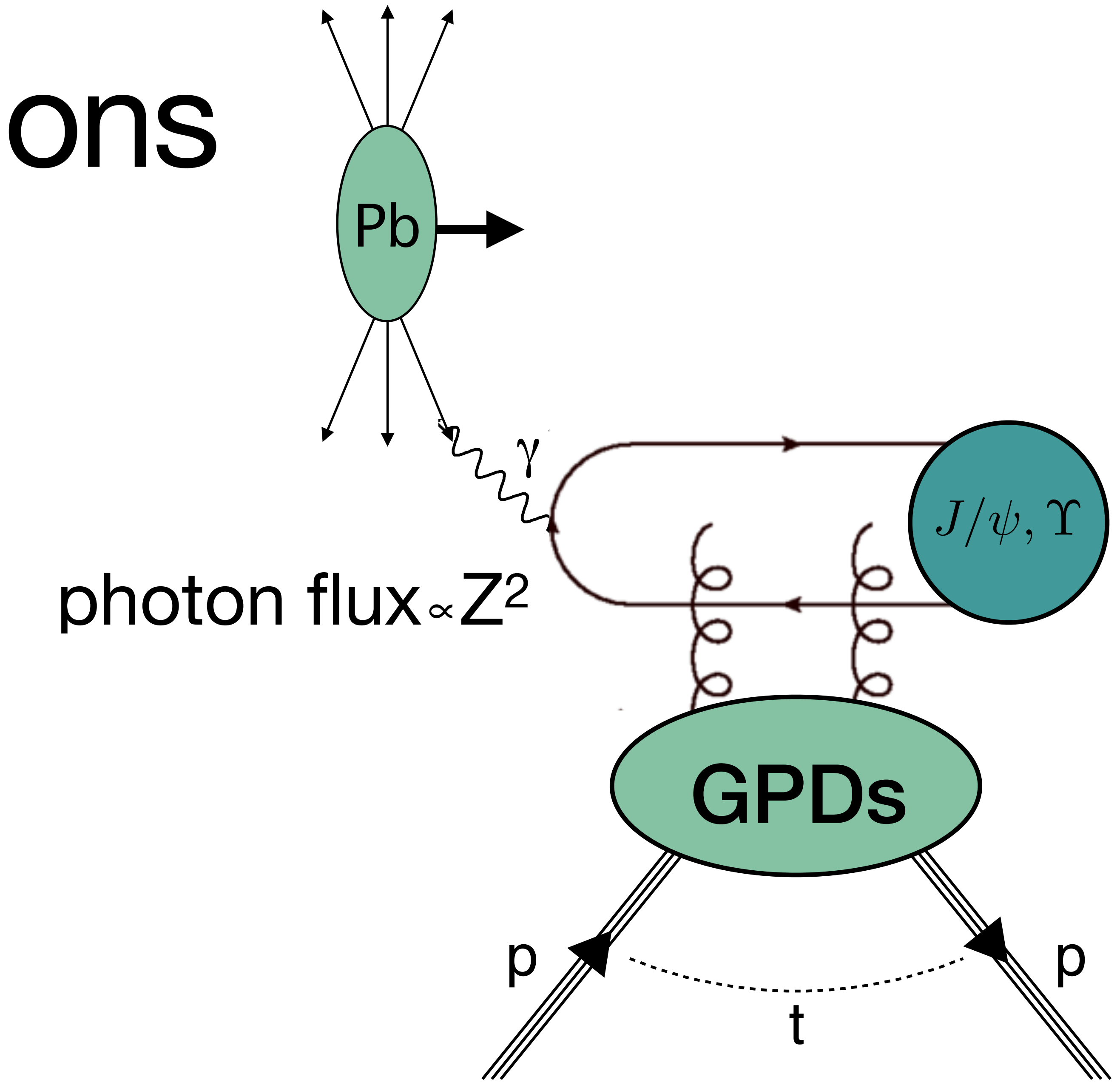

+ Requirement on forward/backward scintillators and far-foward/backward neutron zero-degree calorimeters (ZDCs)

ALICE: exclusive single-J/ψ production in pPb collisions

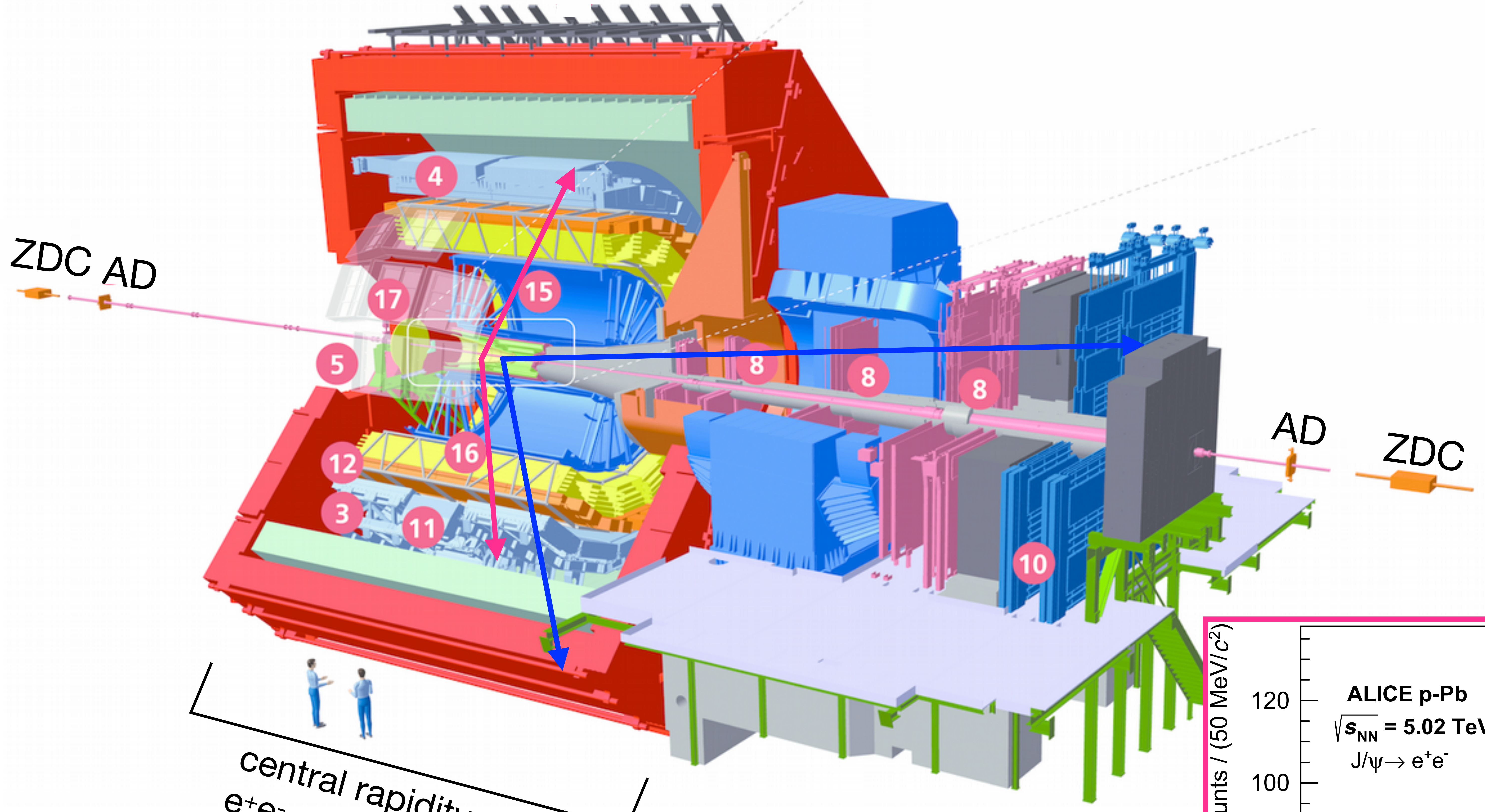

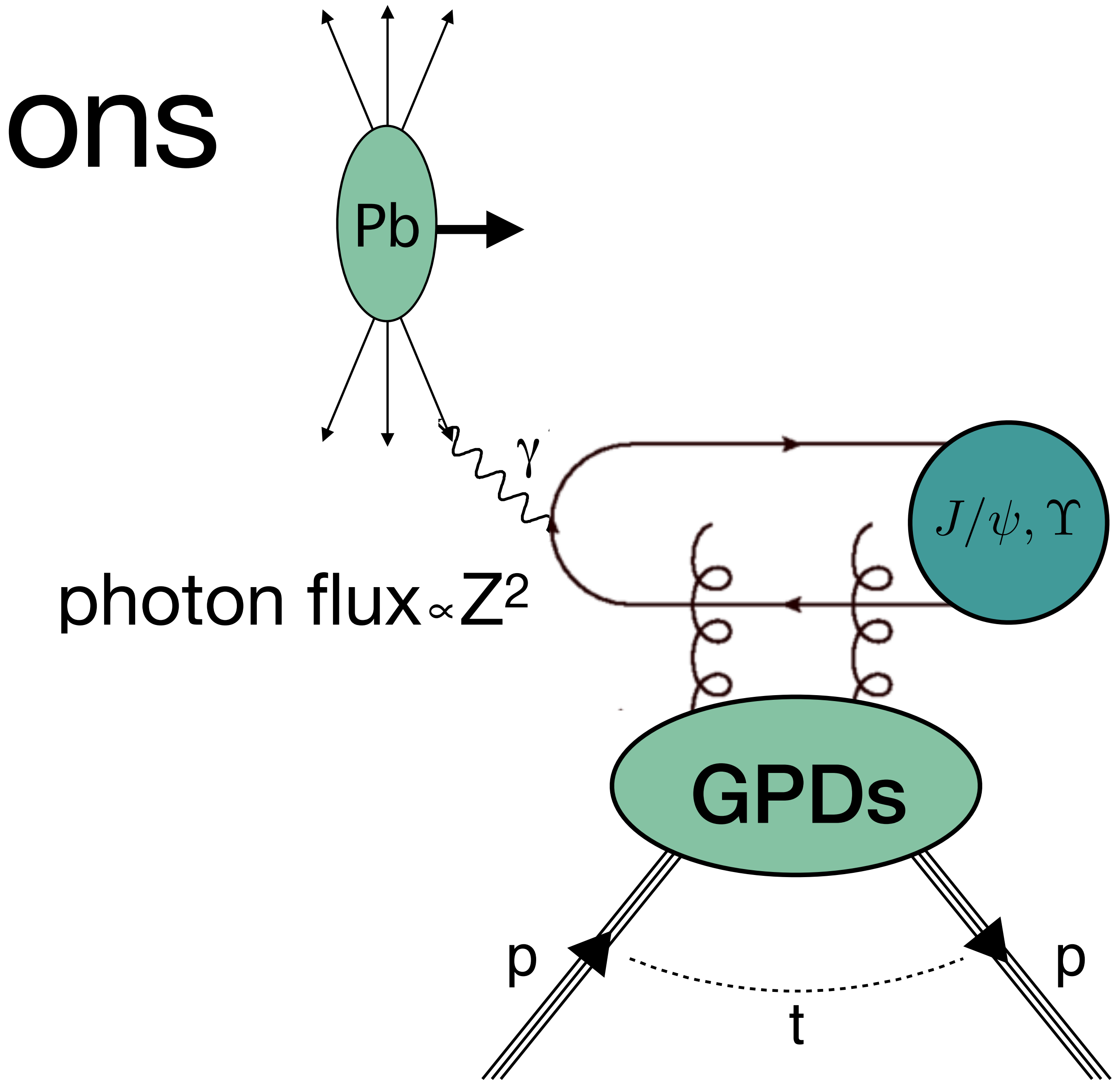

+ Requirement on forward/backward scintillators and far-foward/backward neutron zero-degree calorimeters (ZDCs)

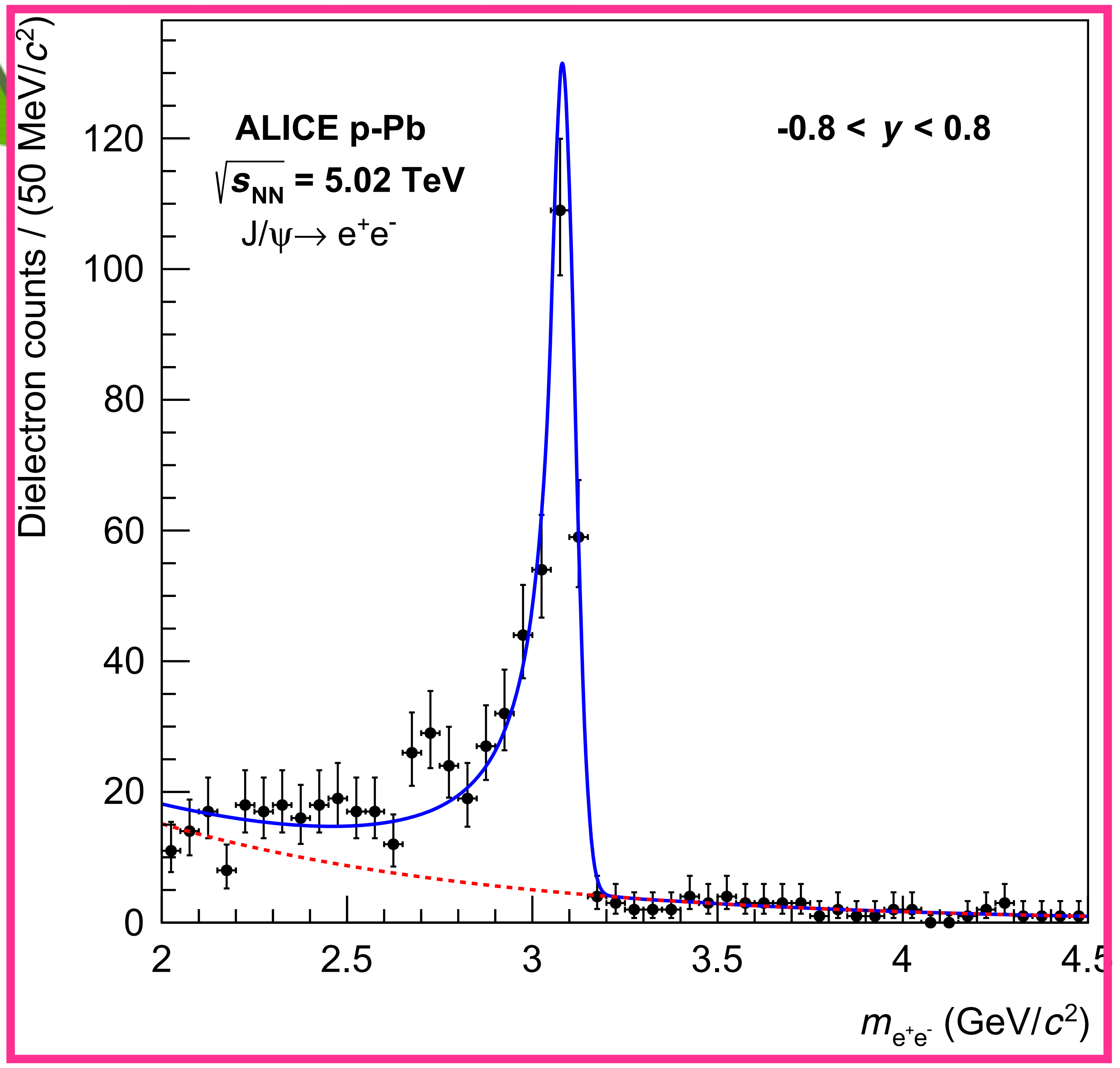

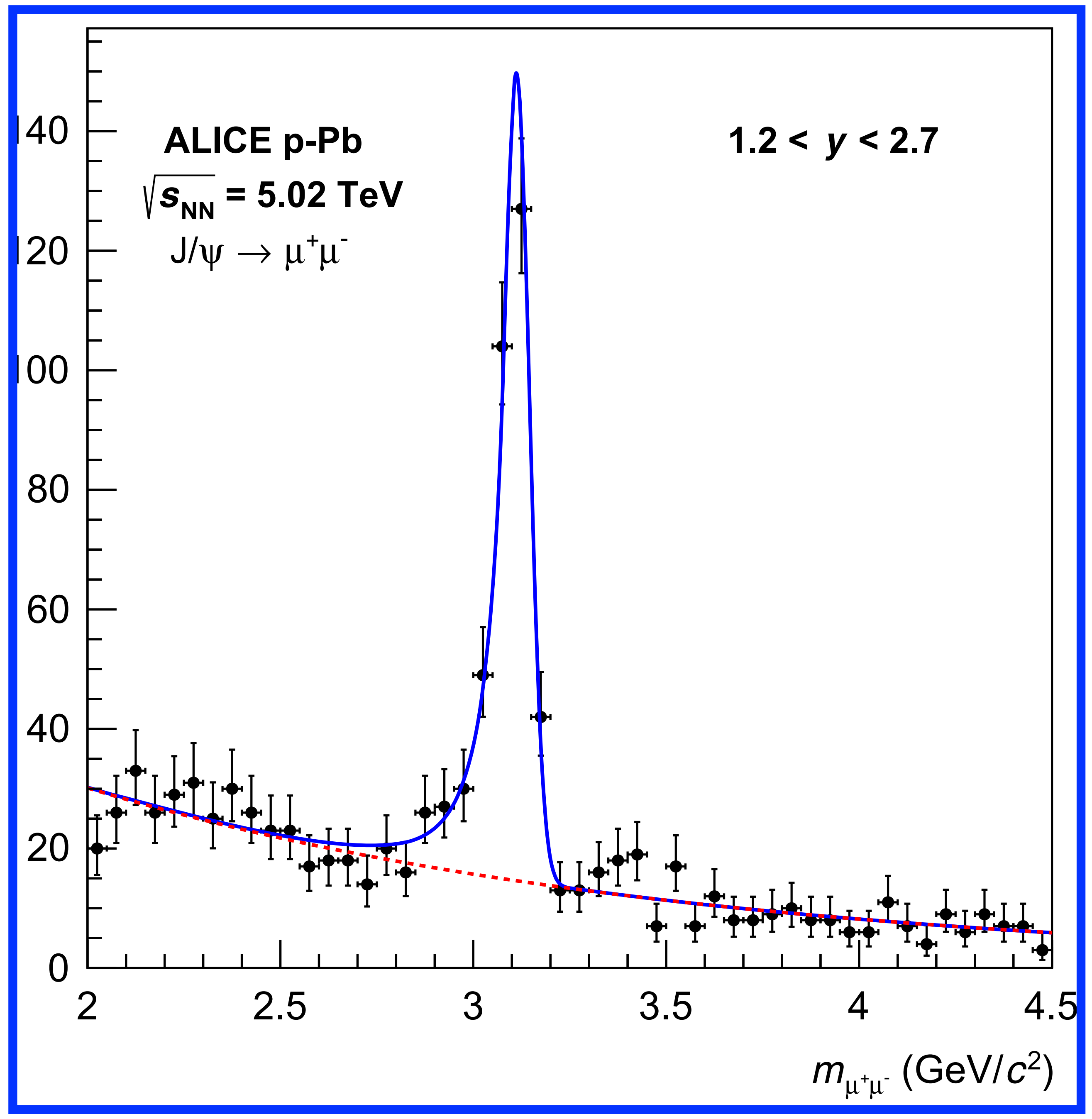

Extraction of the J/ψ photoproduction

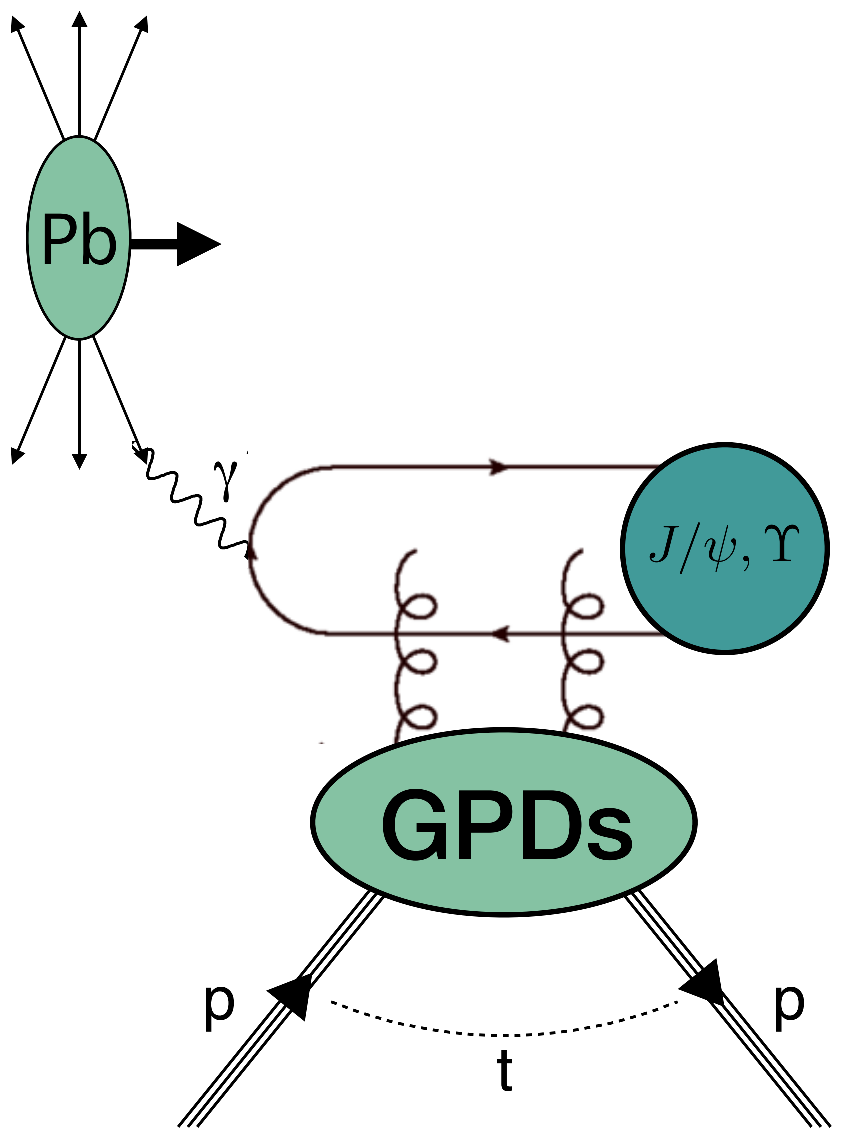

pPb: use Z^2 dependence of photon flux

→ Pb is predominantly photon emitter

Extraction of the J/ψ photoproduction

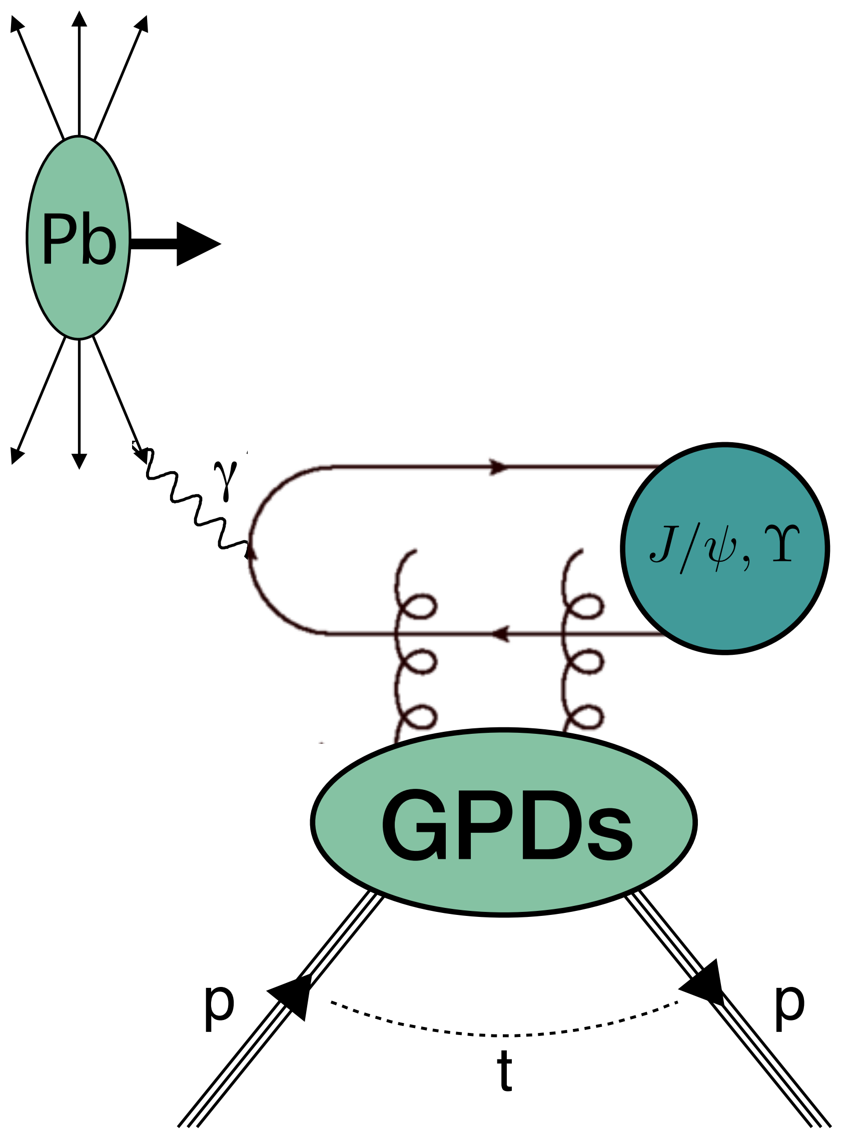

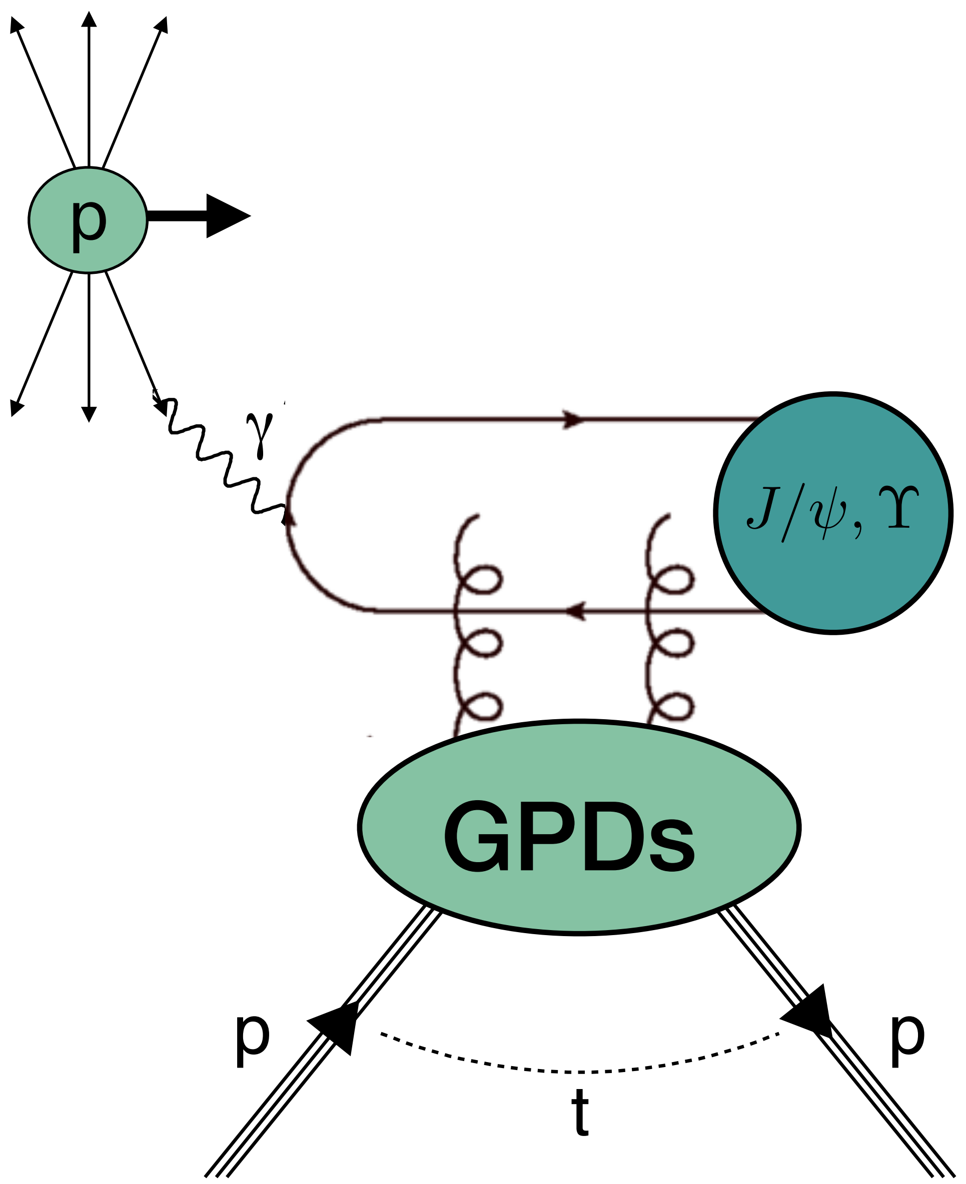

pPb: use Z^2 dependence of photon flux
→ Pb is predominantly photon emitter

pp: ambiguity in ID of photon emitter

Extraction of the J/ψ photoproduction

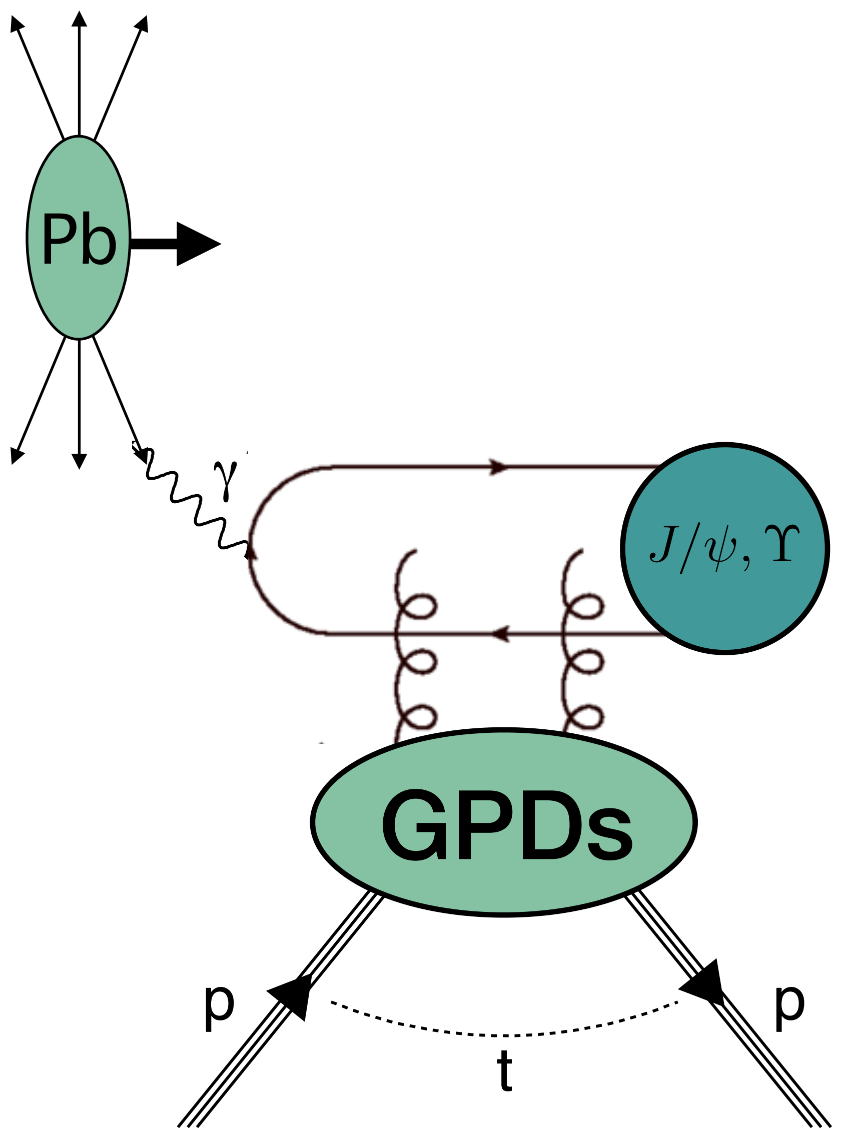

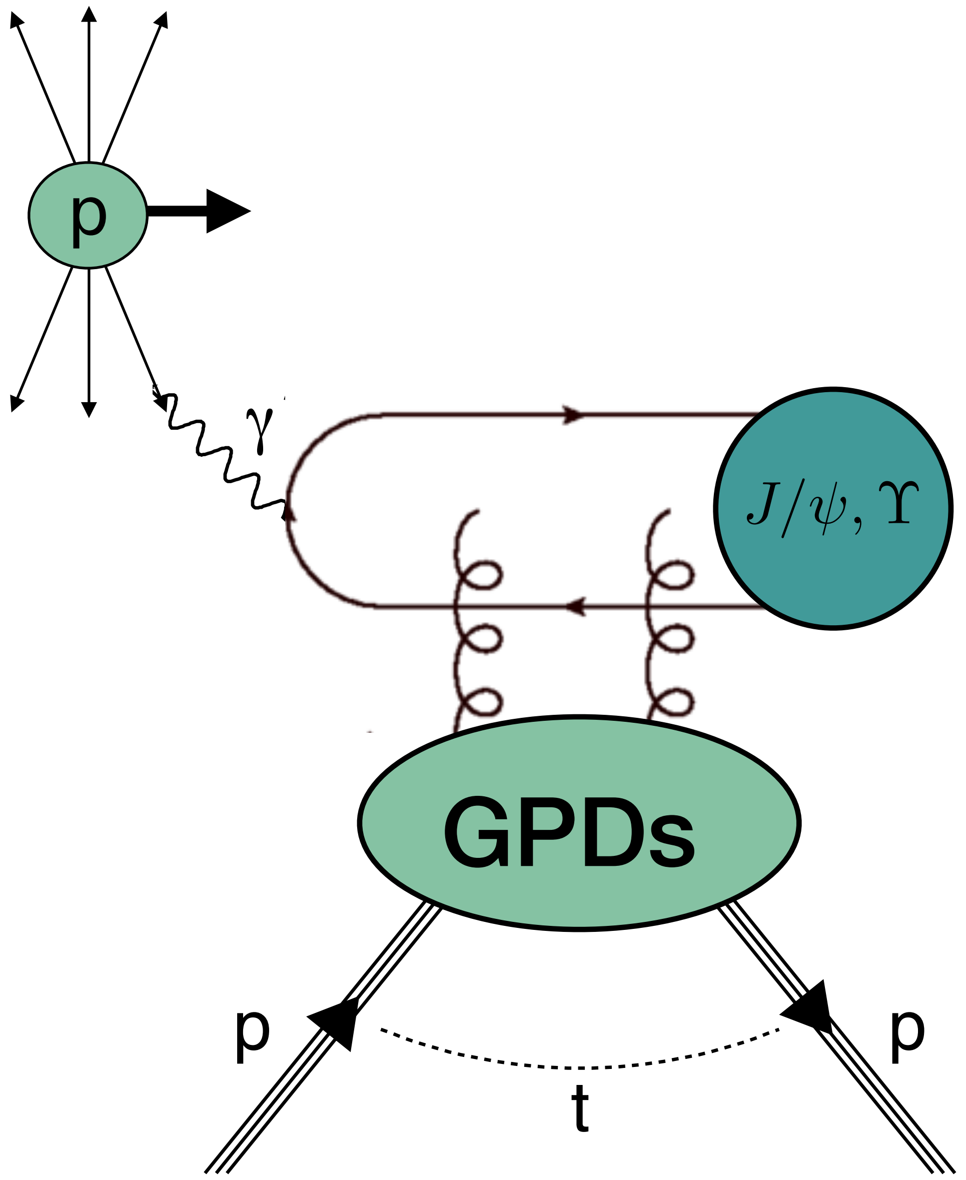

pPb: use Z^2 dependence of photon flux
→ Pb is predominantly photon emitter

pp: ambiguity in ID of photon emitter

- r = gap survival factor
- $k_\pm = \frac{M_\psi}{2} e^{\pm y}$ = photon energy
- $\frac{dn}{dk_\pm}$ = photon flux
- $W_\pm^2 = 2k_\pm\sqrt{s}$ = γp invariant mass

relation pp and γp cross section:

$$\sigma_{pp\to p\psi p} = r(W_+)k_+\frac{\mathrm{d}n}{\mathrm{d}k_+}\sigma_{\gamma p\to\psi p}(W_+) + r(W_-)k_-\frac{\mathrm{d}n}{\mathrm{d}k_-}\sigma_{\gamma p\to\psi p}(W_-)$$

Extraction of the J/ψ photoproduction

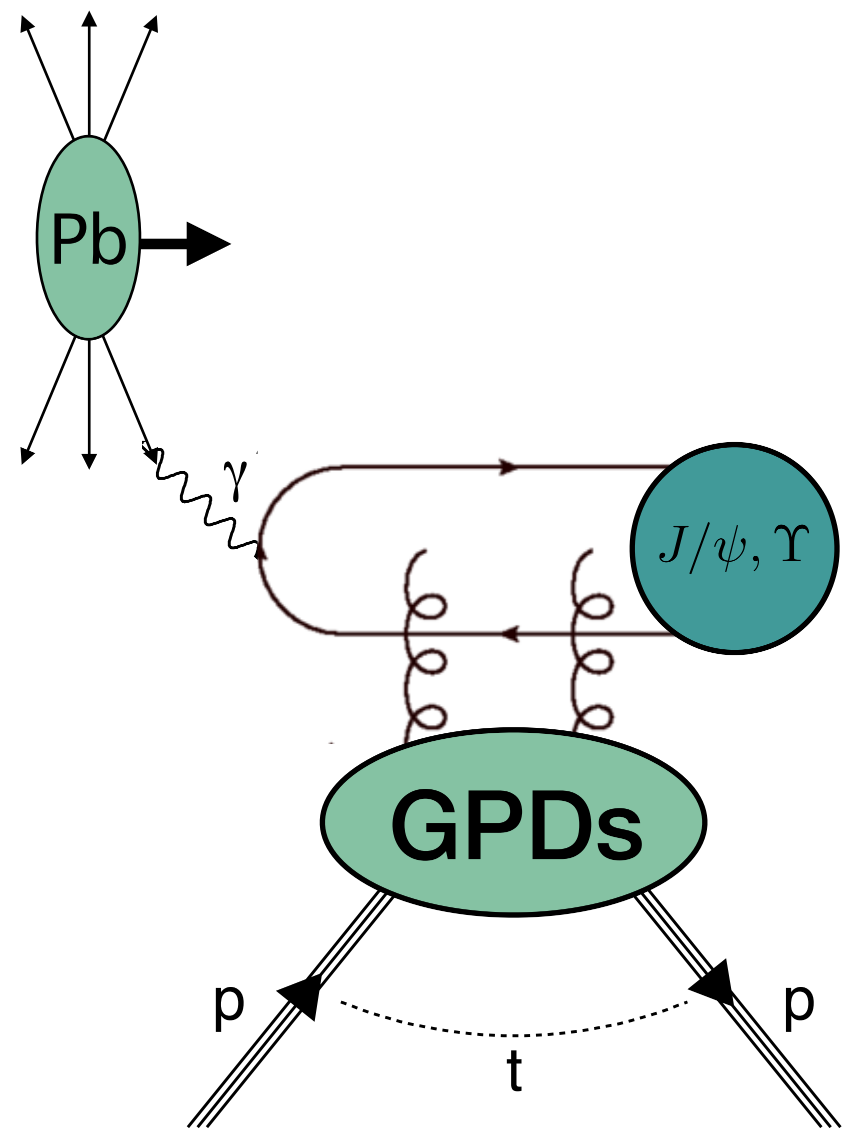

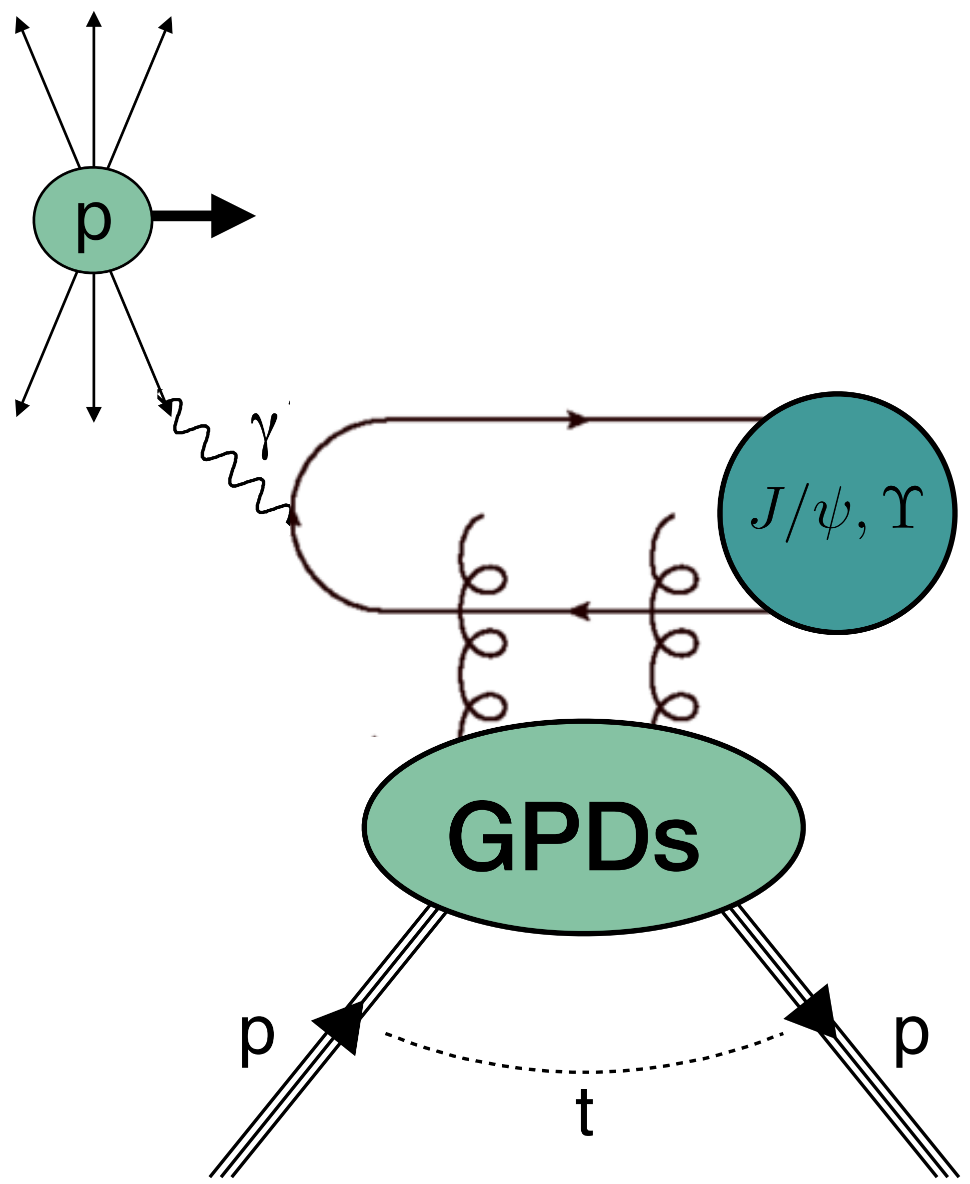

pPb: use Z^2 dependence of photon flux
→ Pb is predominantly photon emitter

pp: ambiguity in ID of photon emitter

- r = gap survival factor
- $k_\pm = \frac{M_\psi}{2} e^{\pm y}$ = photon energy
- $\frac{dn}{dk_\pm}$ = photon flux
- $W_\pm^2 = 2k_\pm \sqrt{s}$ = γp invariant mass

relation pp and γp cross section:

$$\sigma_{pp\to p\psi p} = r(W_+)k_+ \frac{\mathrm{d}n}{\mathrm{d}k_+} \sigma_{\gamma p\to\psi p}(W_+) + r(W_-)k_- \frac{\mathrm{d}n}{\mathrm{d}k_-} \sigma_{\gamma p\to\psi p}(W_-)$$

LHCb used HERA data for low-E_γ (W_-) contribution.

J/ψ photoproduction cross section

Phys. Rev. D **108** ('23) 112004

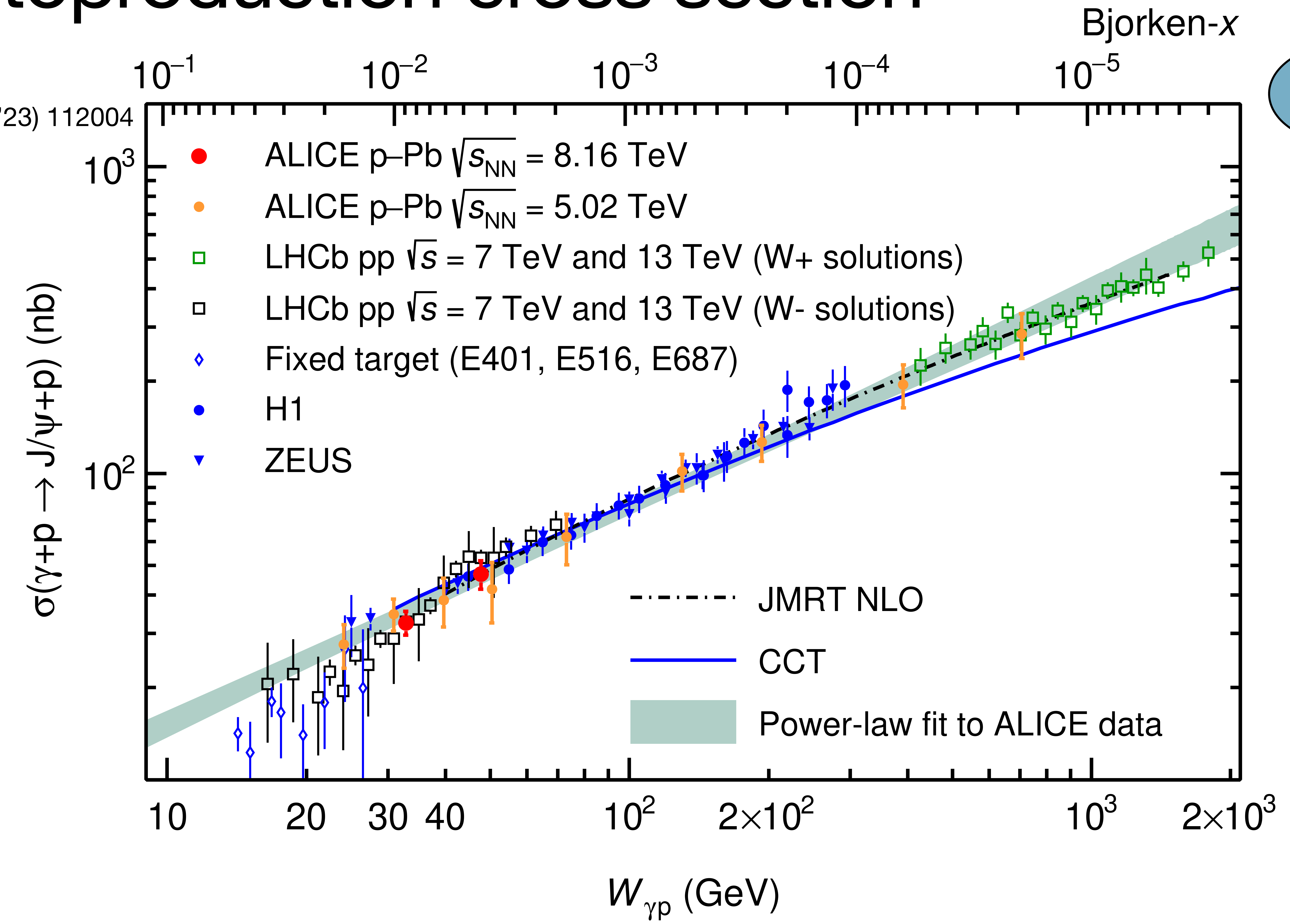

GPD H

J/ψ photoproduction cross section

Phys. Rev. D **108** ('23) 112004

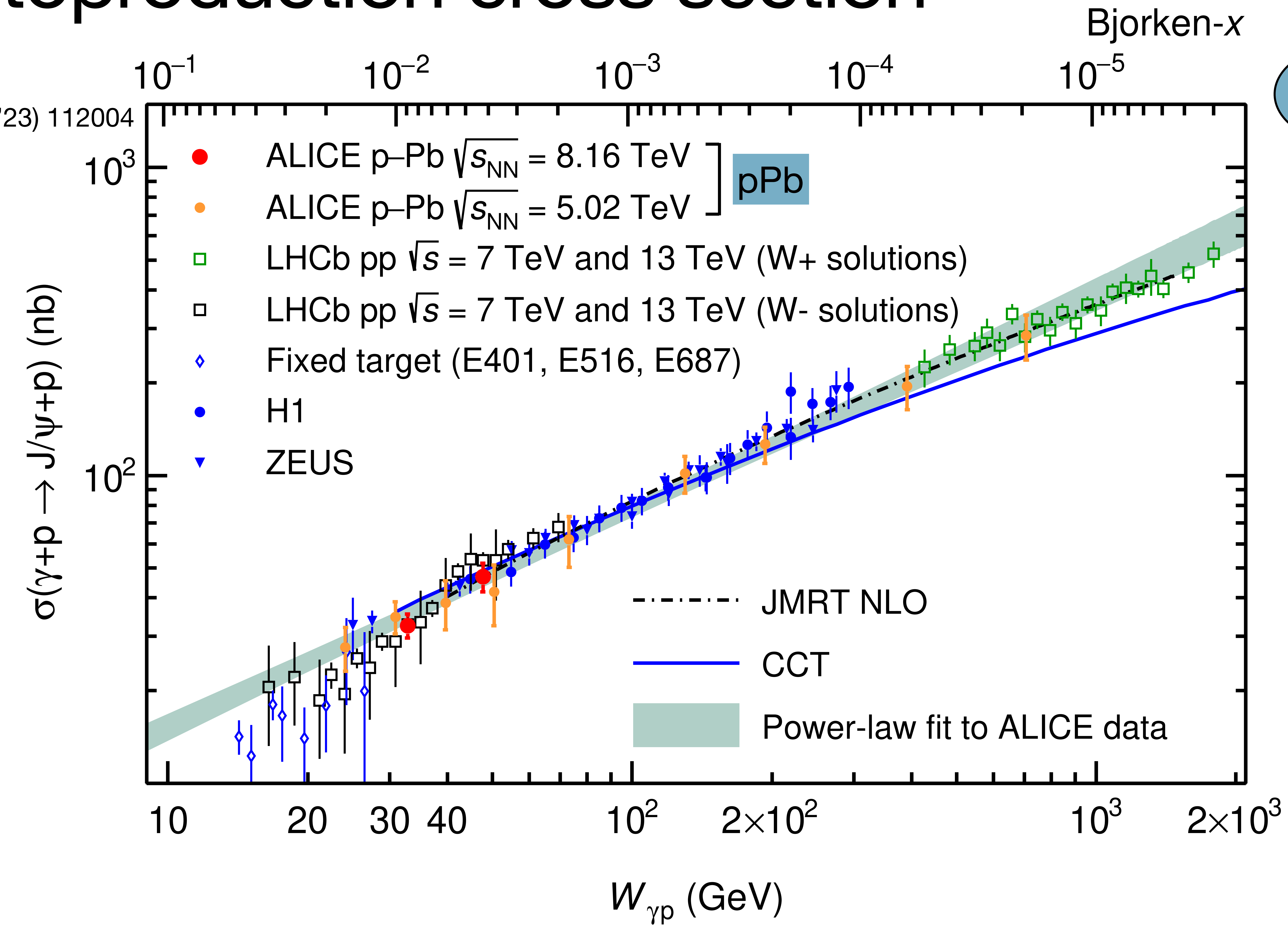

GPD H

J/ψ photoproduction cross section

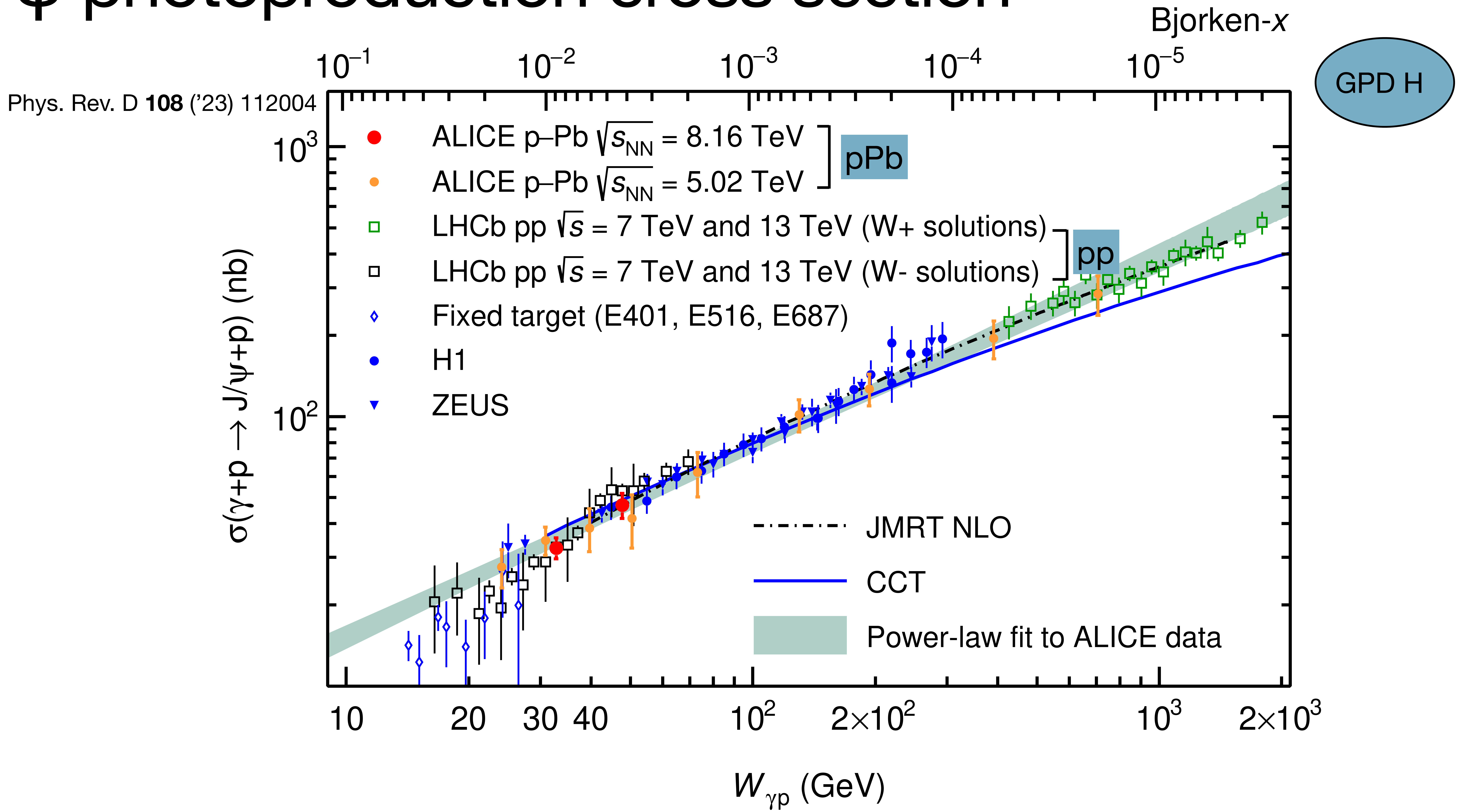

J/ψ photoproduction cross section

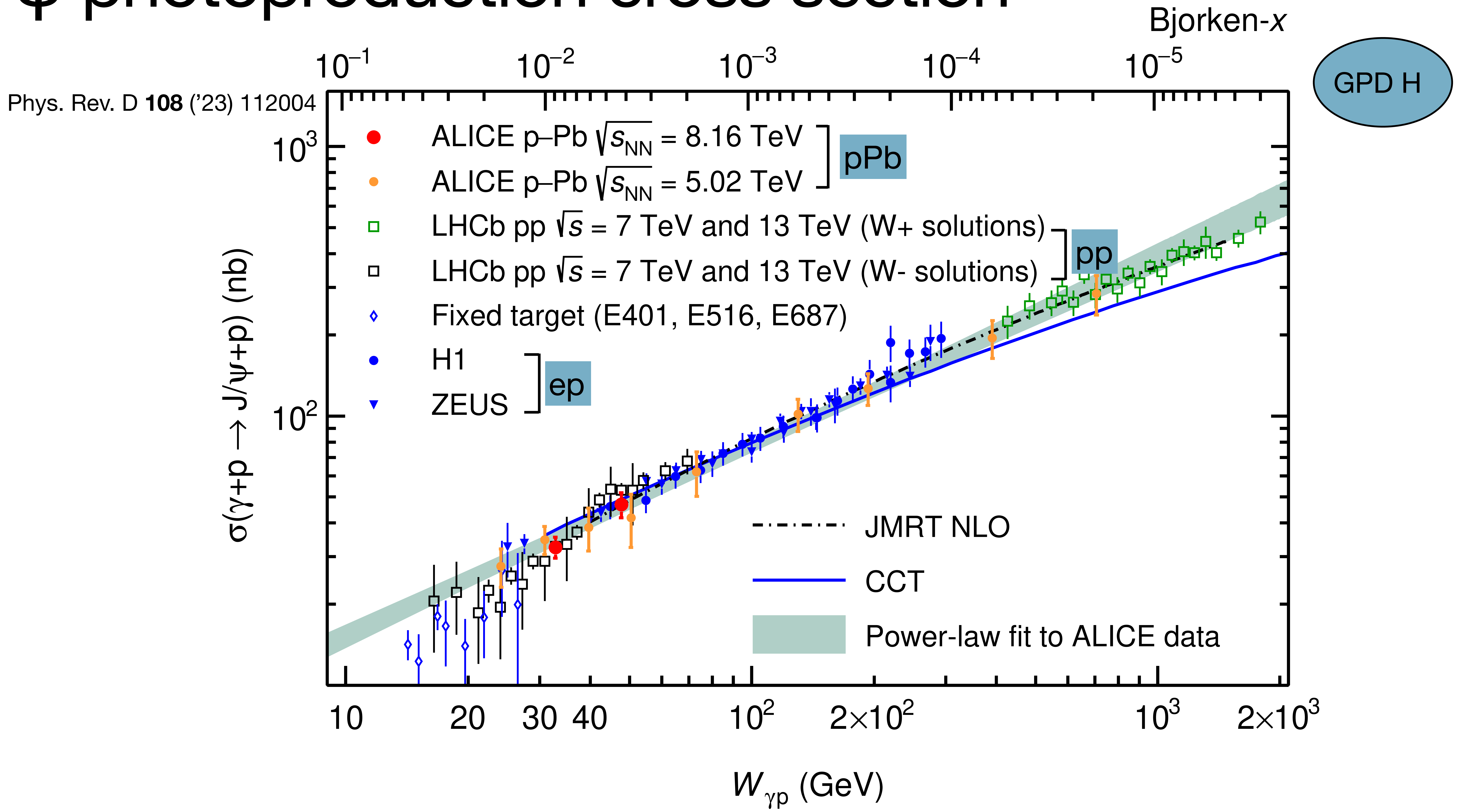

J/ψ photoproduction cross section

Phys. Rev. D **108** ('23) 112004

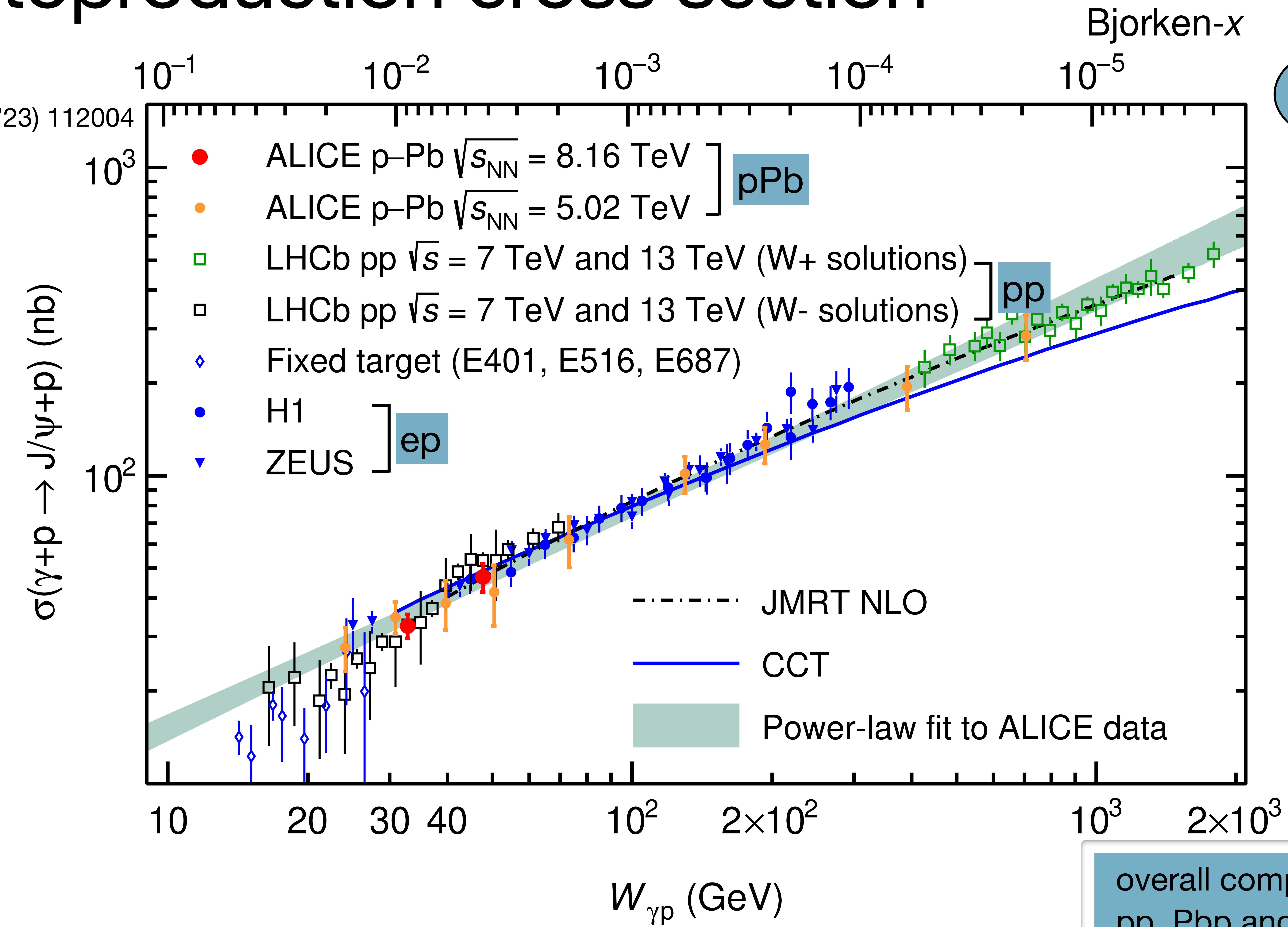

GPD H

overall compatibility between pp, Pbp and ep data: hint of universality of underlying physics

Υ photoproduction cross section

Eur. Phys. J. C **79** (2019) 277
Eur. Phys. J. C **82** (2022) 343

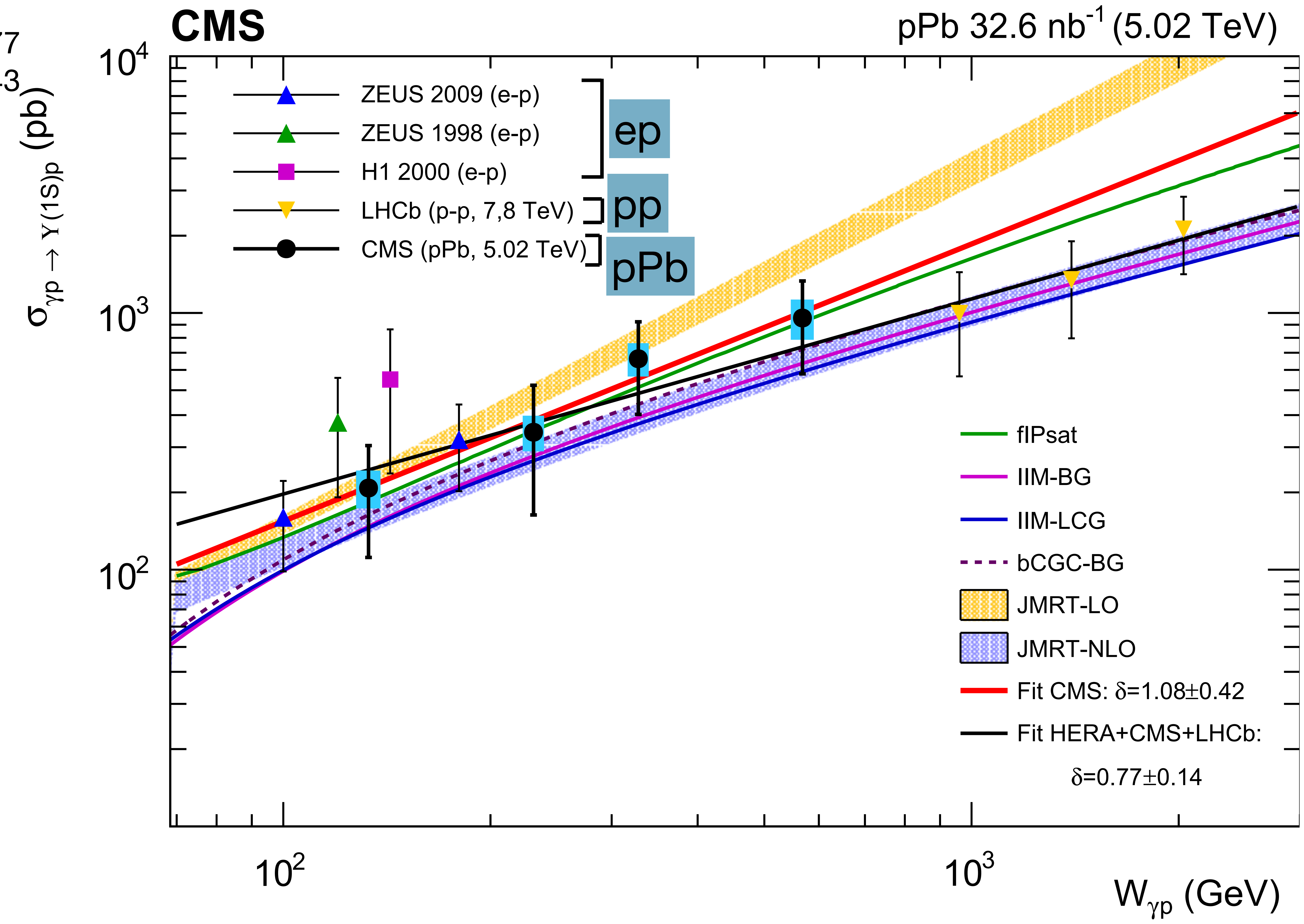

GPD H

overall compatibility between pp, Pbp and ep data: hint of universality of underlying physics

Ultra-peripheral collisions in PbPb

What object are we probing?

Ultra-peripheral collisions in PbPb

What object are we probing?

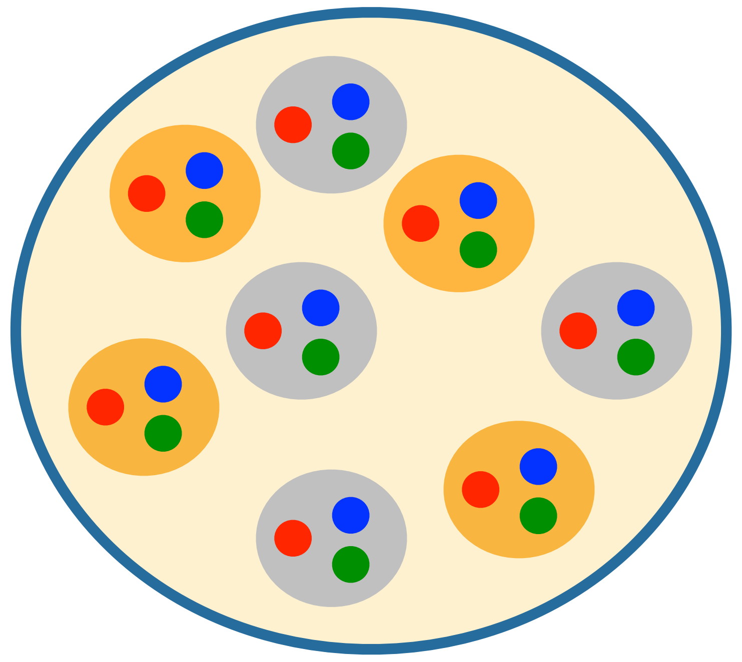

Ultra-peripheral collisions in PbPb

What object are we probing?

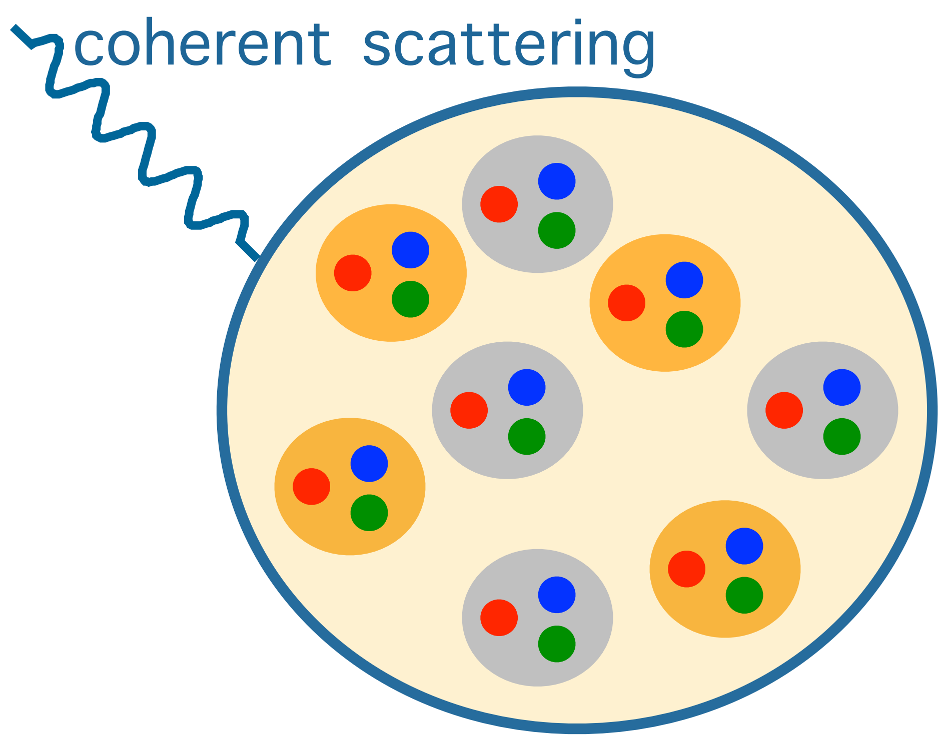

Coherent interaction: interaction with target as a whole.
~ target remains in same quantum state.

Ultra-peripheral collisions in PbPb

What object are we probing?

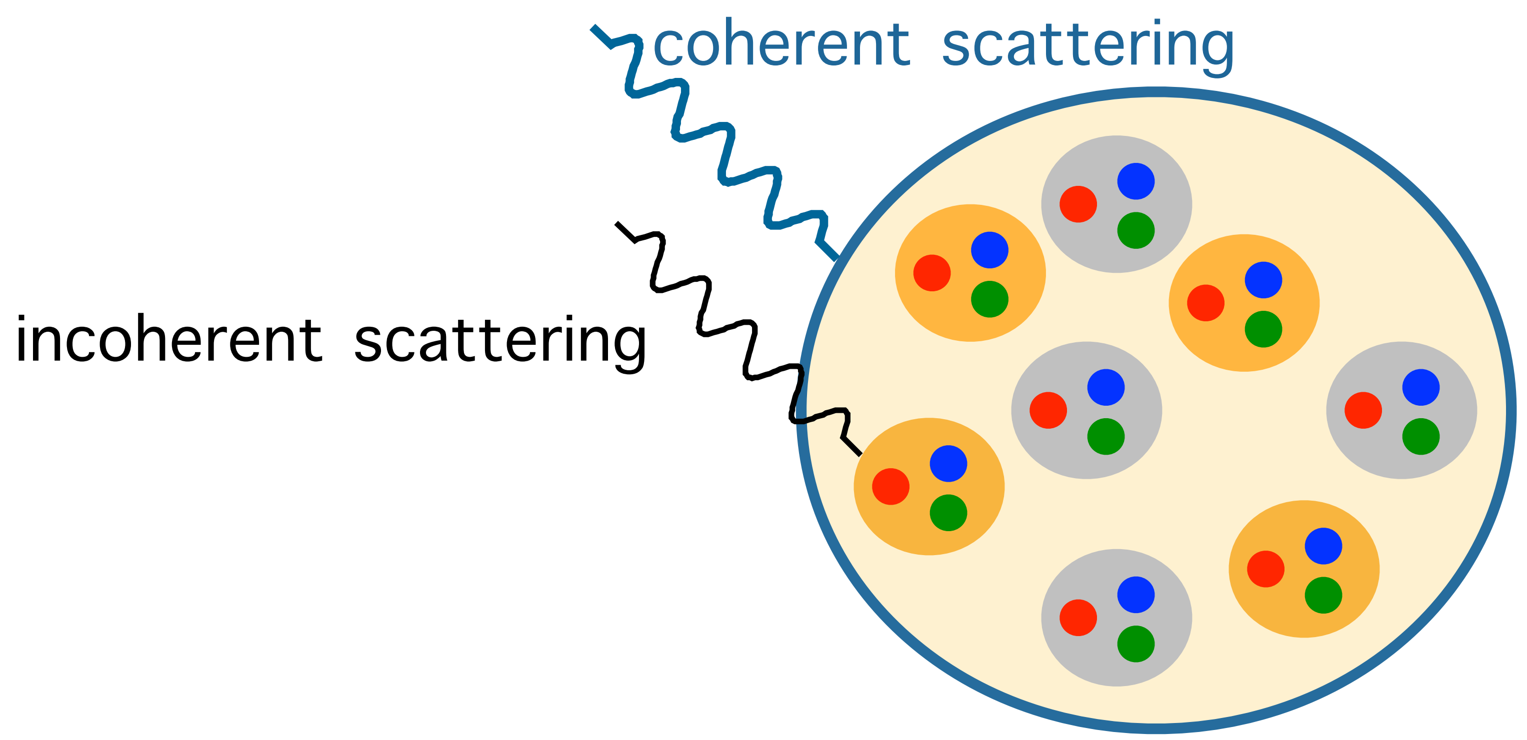

Coherent interaction: interaction with target as a whole.
~ target remains in same quantum state.

Incoherent interaction: interaction with constituents inside target.
~ target does not remain in same quantum state.
Ex.: target dissociation, excitation

Ultra-peripheral collisions in PbPb

What object are we probing?

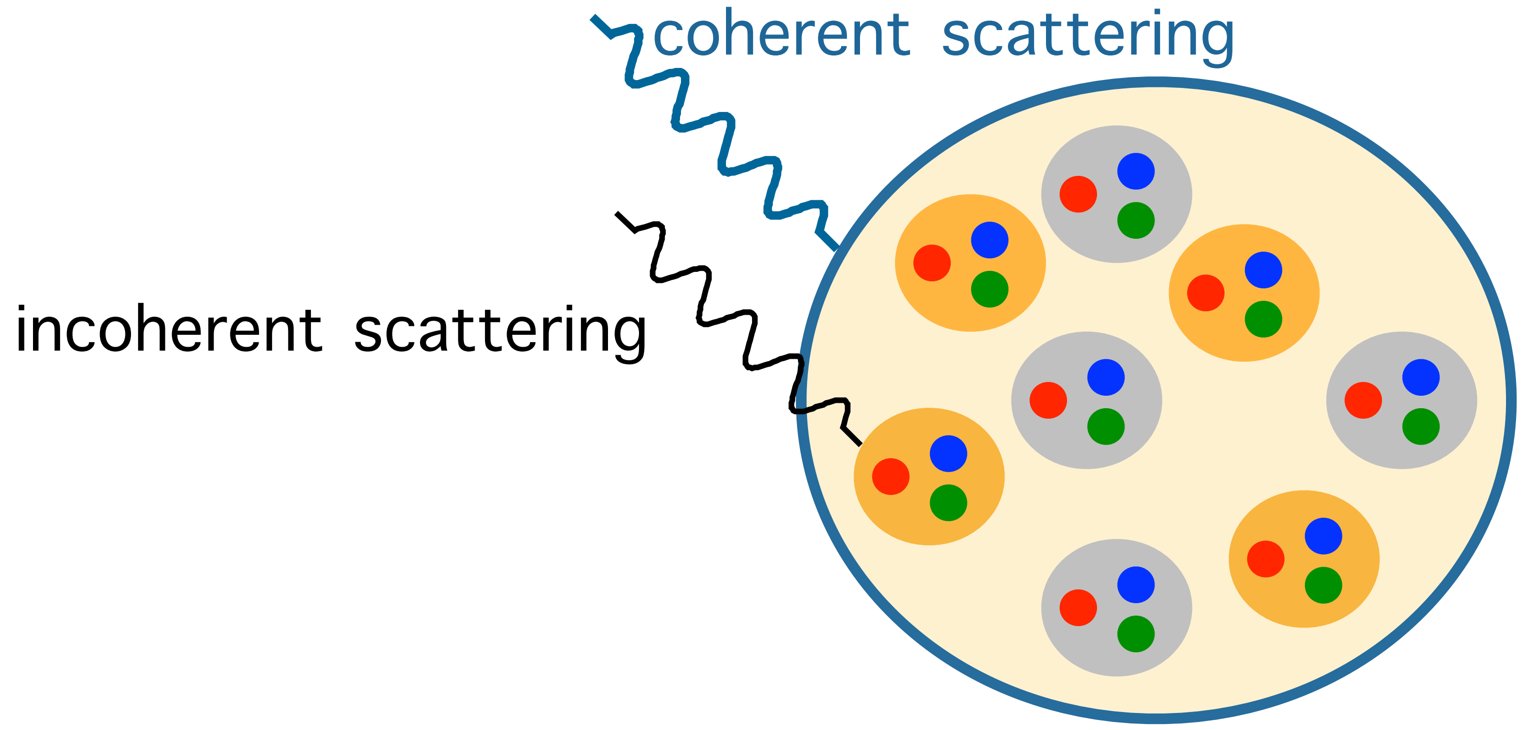

Coherent interaction: interaction with target as a whole.
~ target remains in same quantum state.

Incoherent interaction: interaction with constituents inside target.
~ target does not remain in same quantum state.
Ex.: target dissociation, excitation

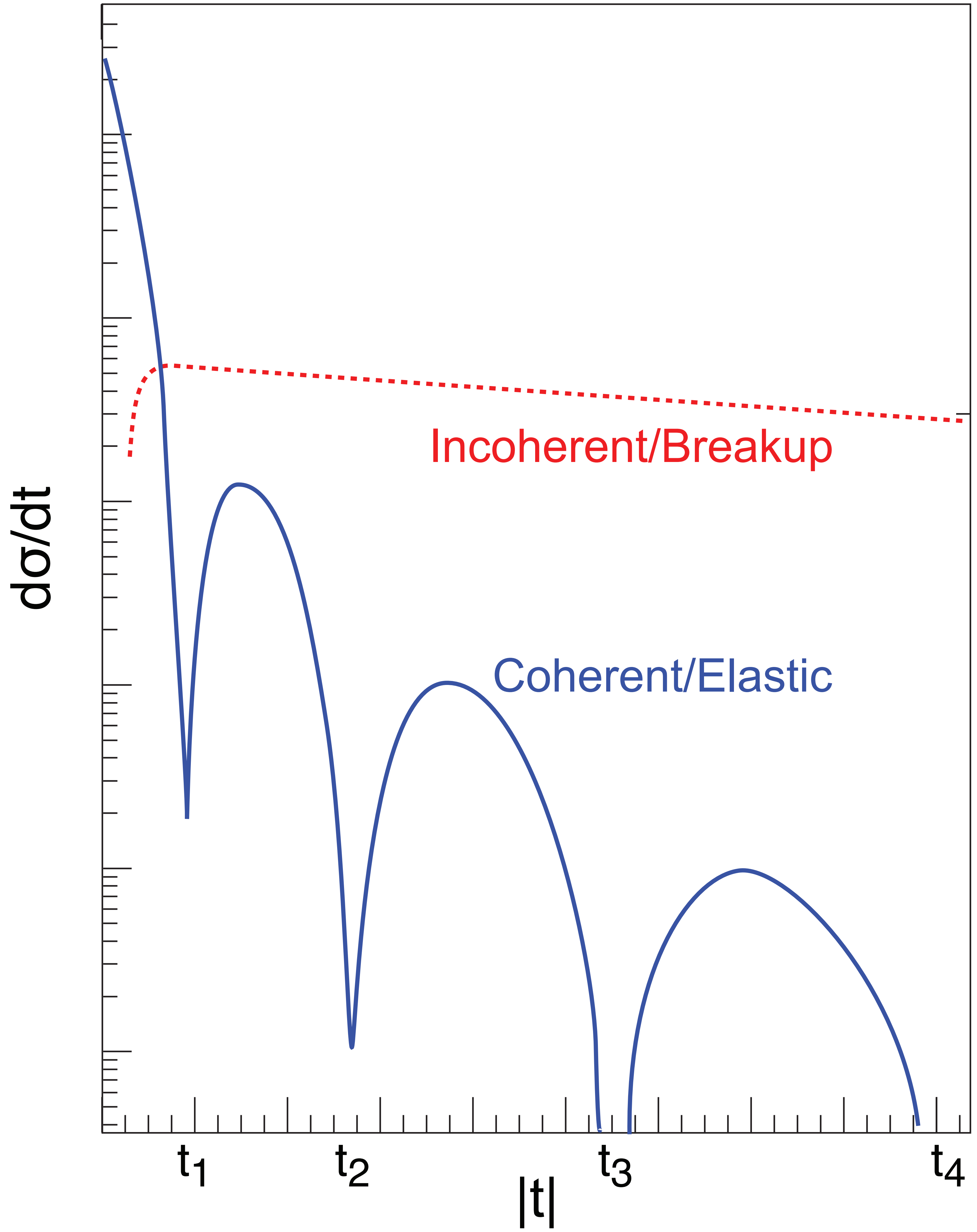

Coherent production

Nuclear GPDs (PDFs at low x_B)

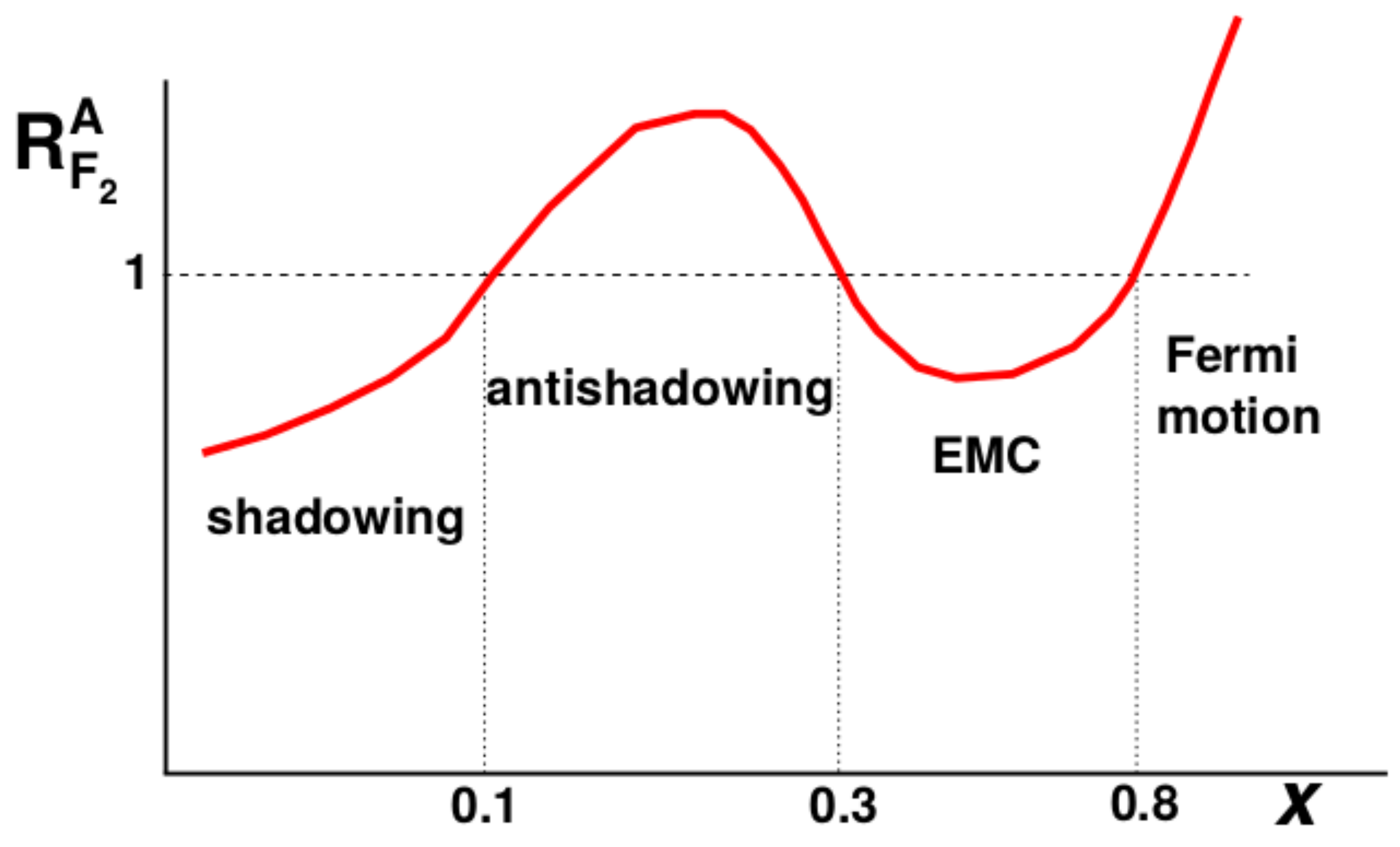

Coherent production

Nuclear GPDs (PDFs at low x_B)

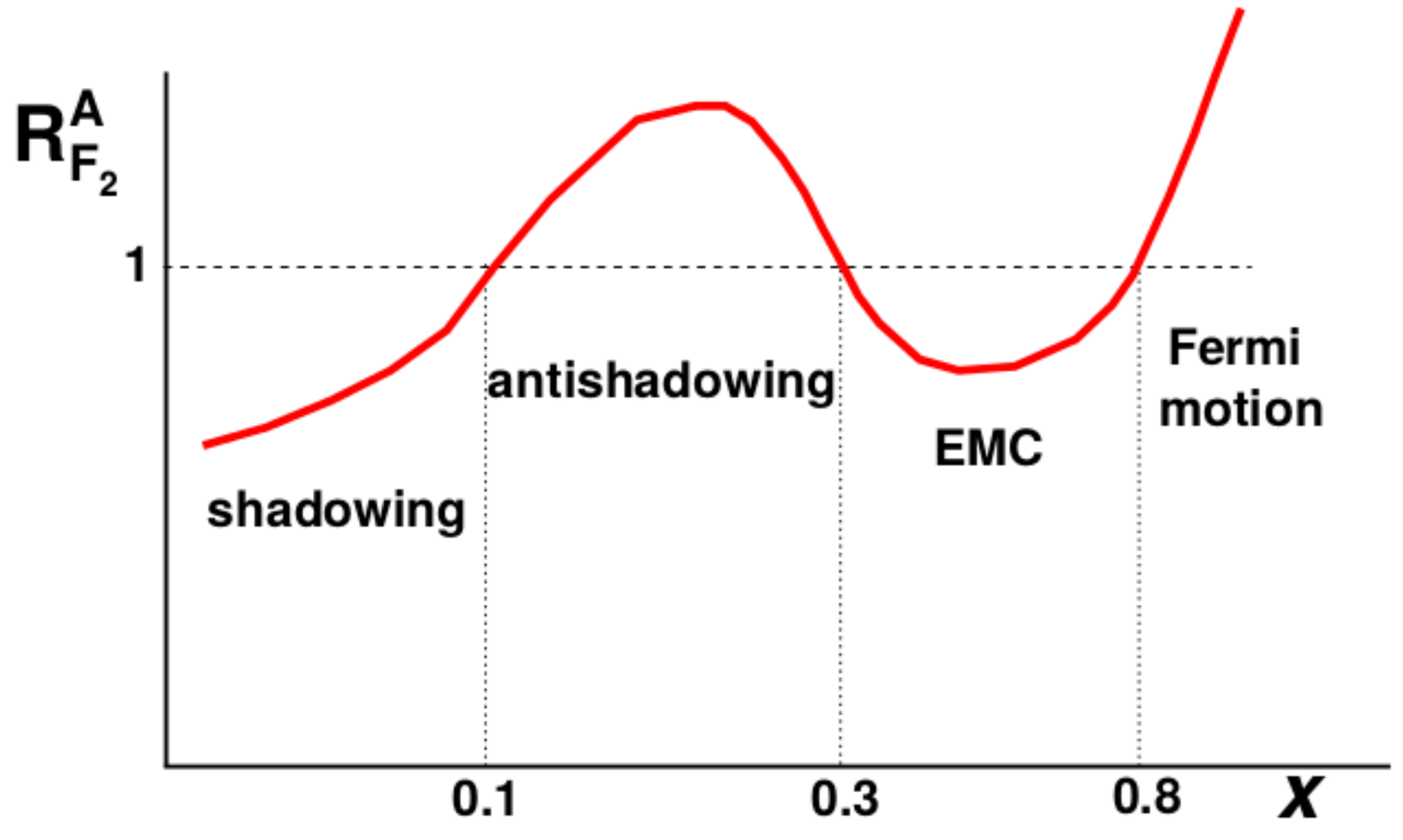

Probing saturation

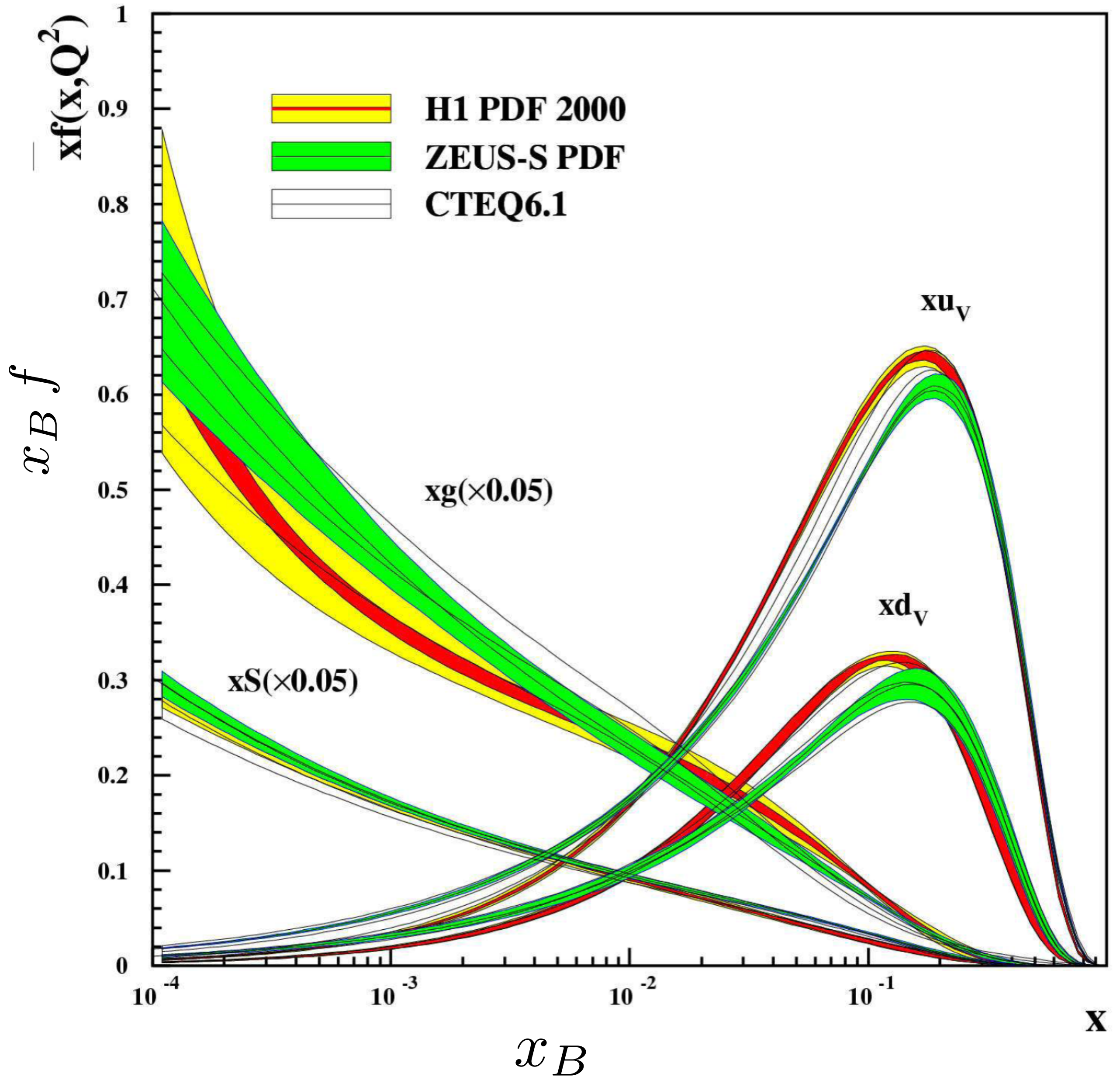

Coherent production

Nuclear GPDs (PDFs at low x_B)

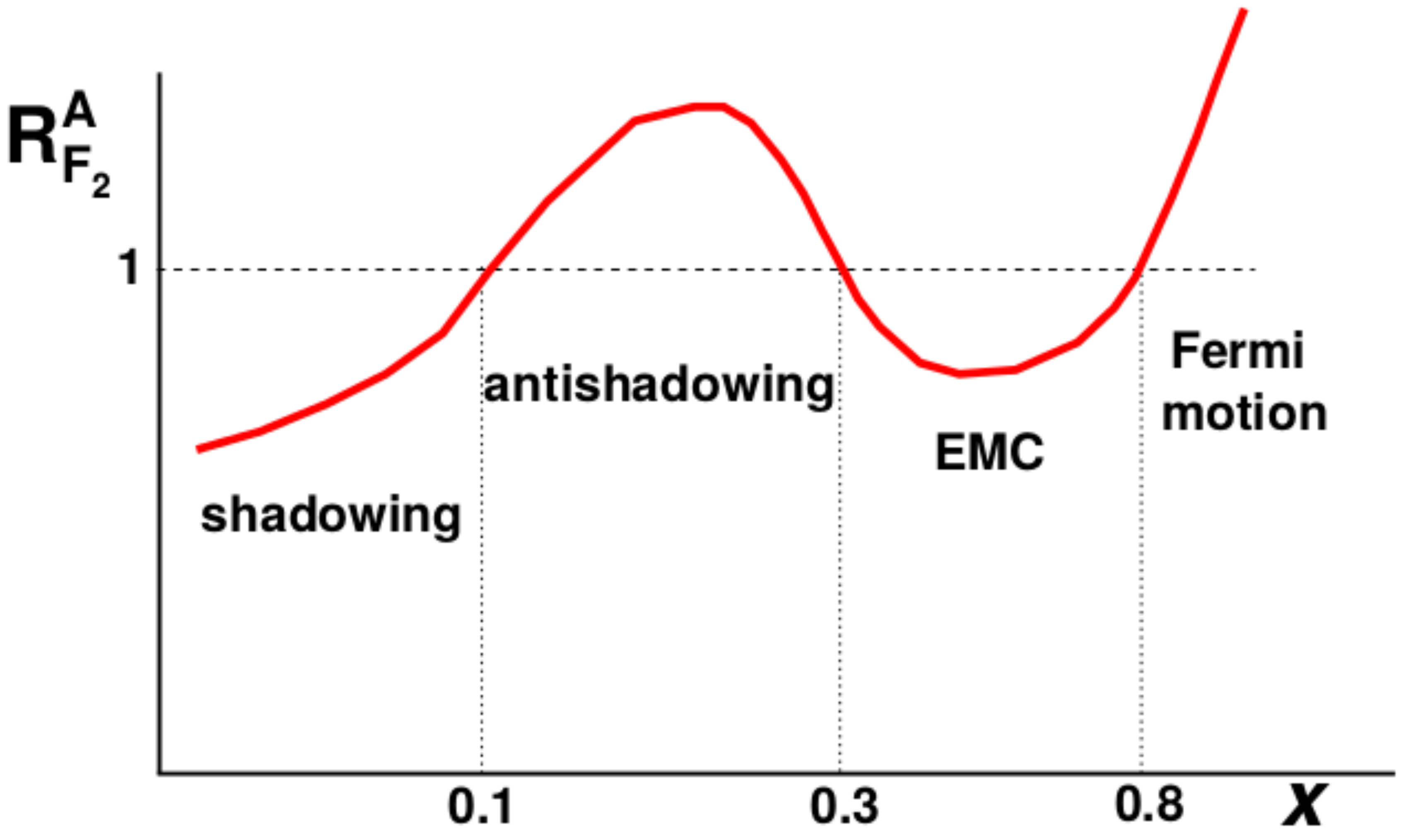

Probing saturation

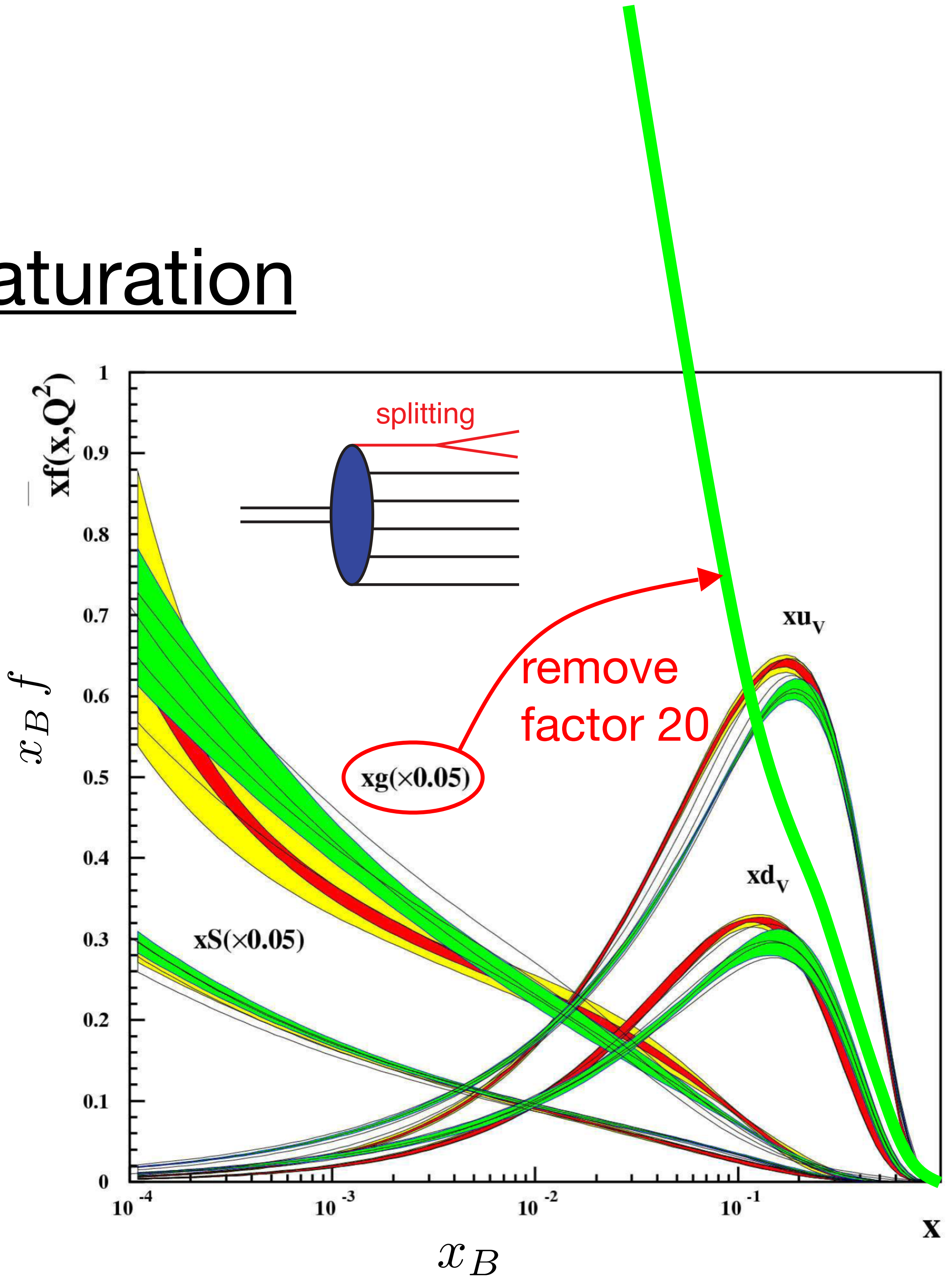

Coherent production

Nuclear GPDs (PDFs at low x_B)

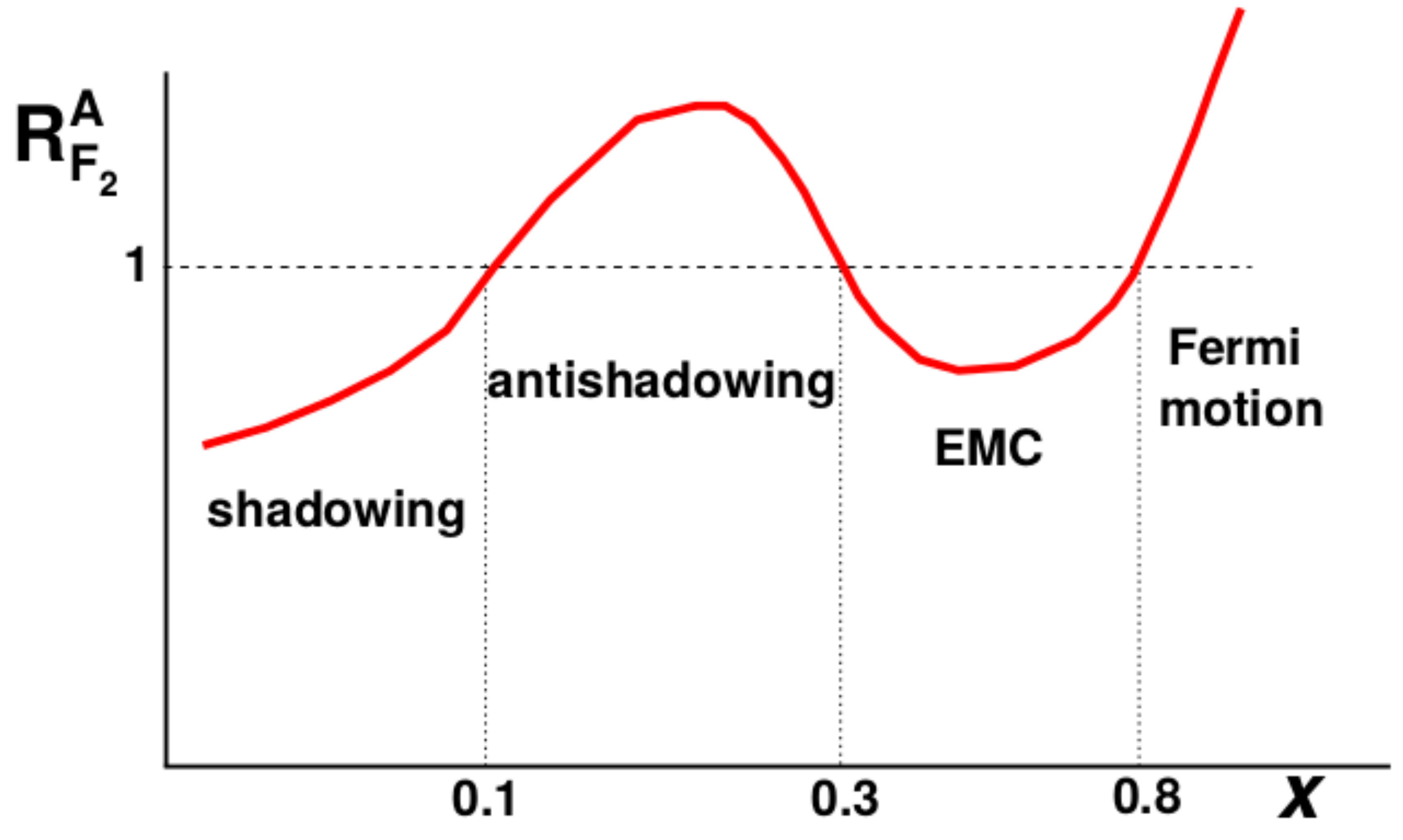

Probing saturation

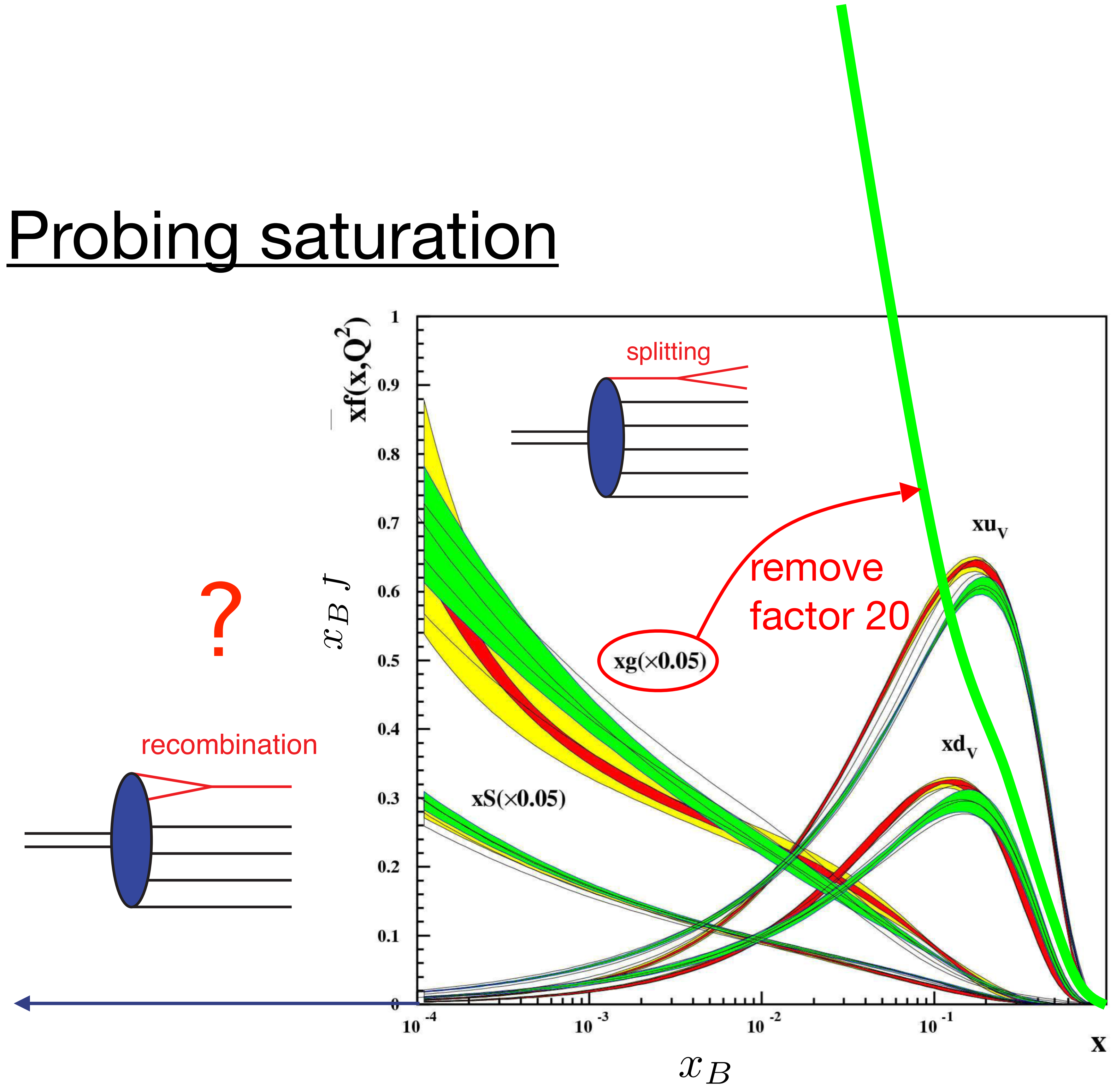

Coherent production

Nuclear GPDs (PDFs at low x_B)

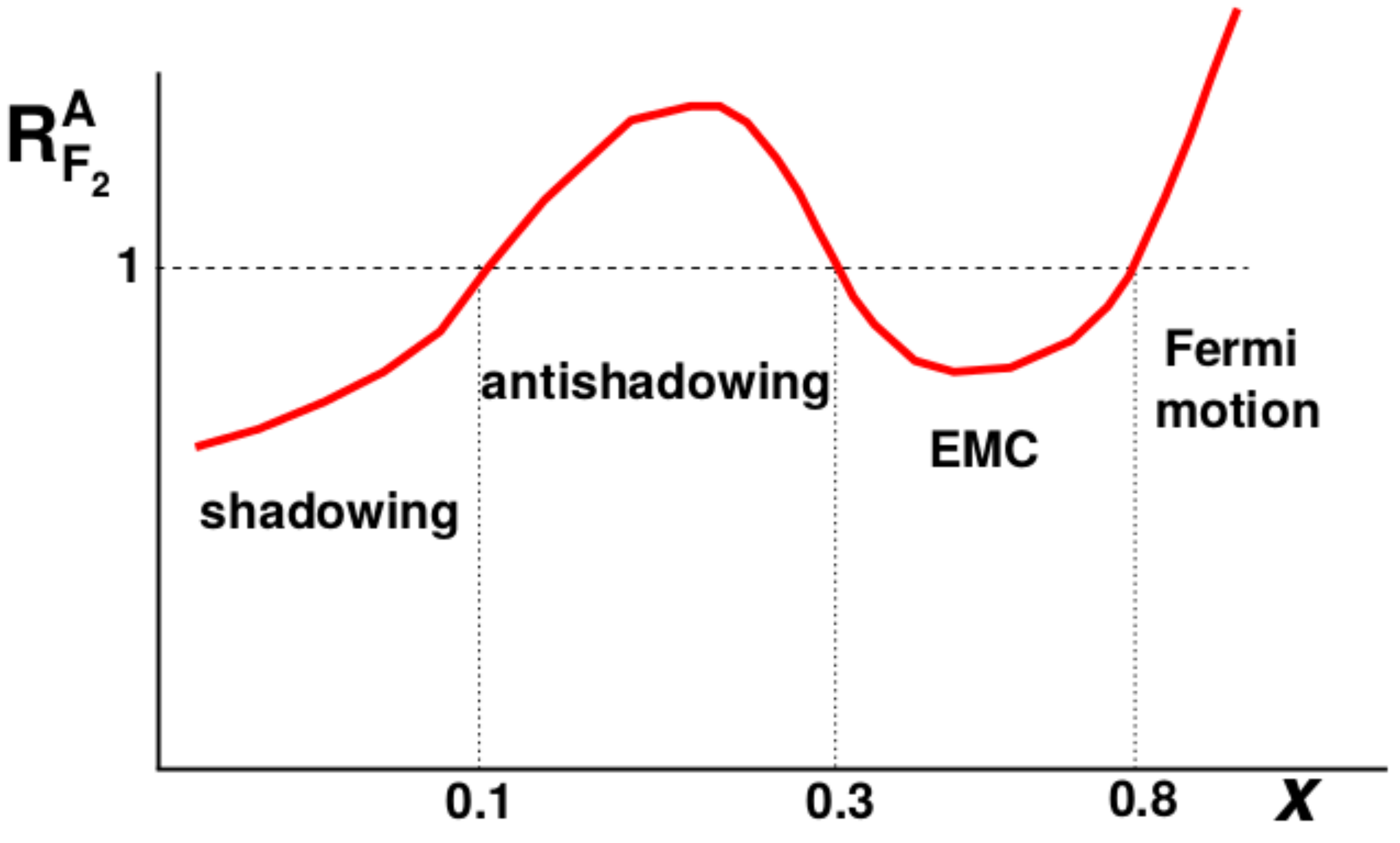

Probing saturation

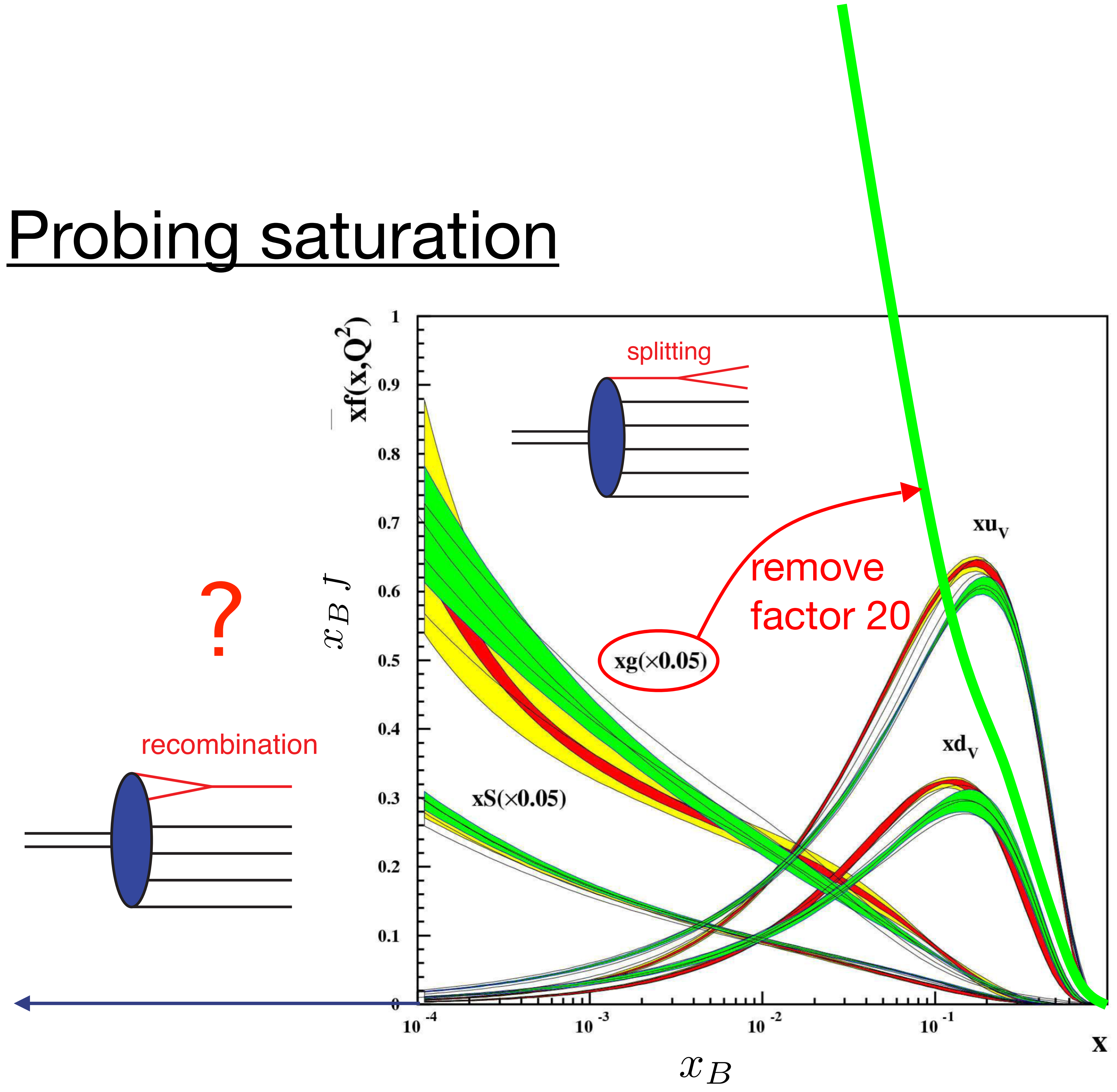

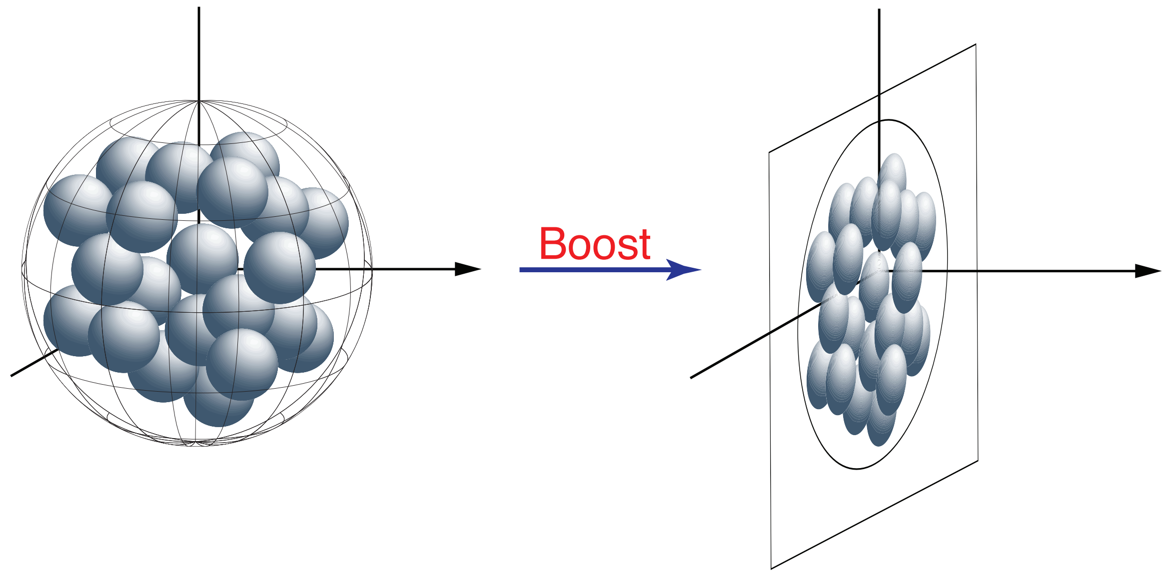

$A^{1/3}$ enhancement
of saturation effect for ions

Coherent photoproduction in PbPb at ALICE

ALICE, Eur. Phys. J. C **81** (2021) 712

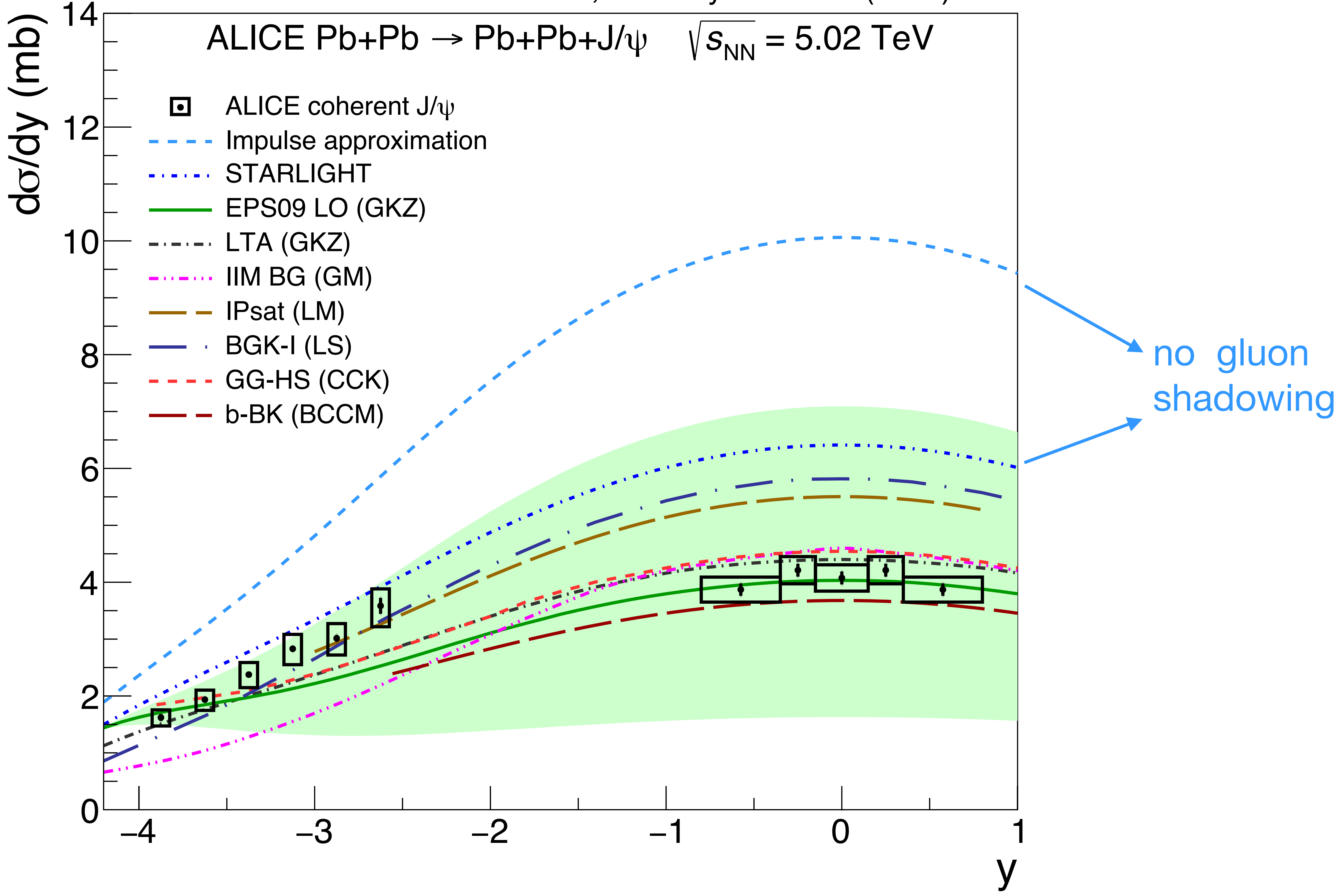

ALICE, Phys. Lett. B **817** (2021) 136280

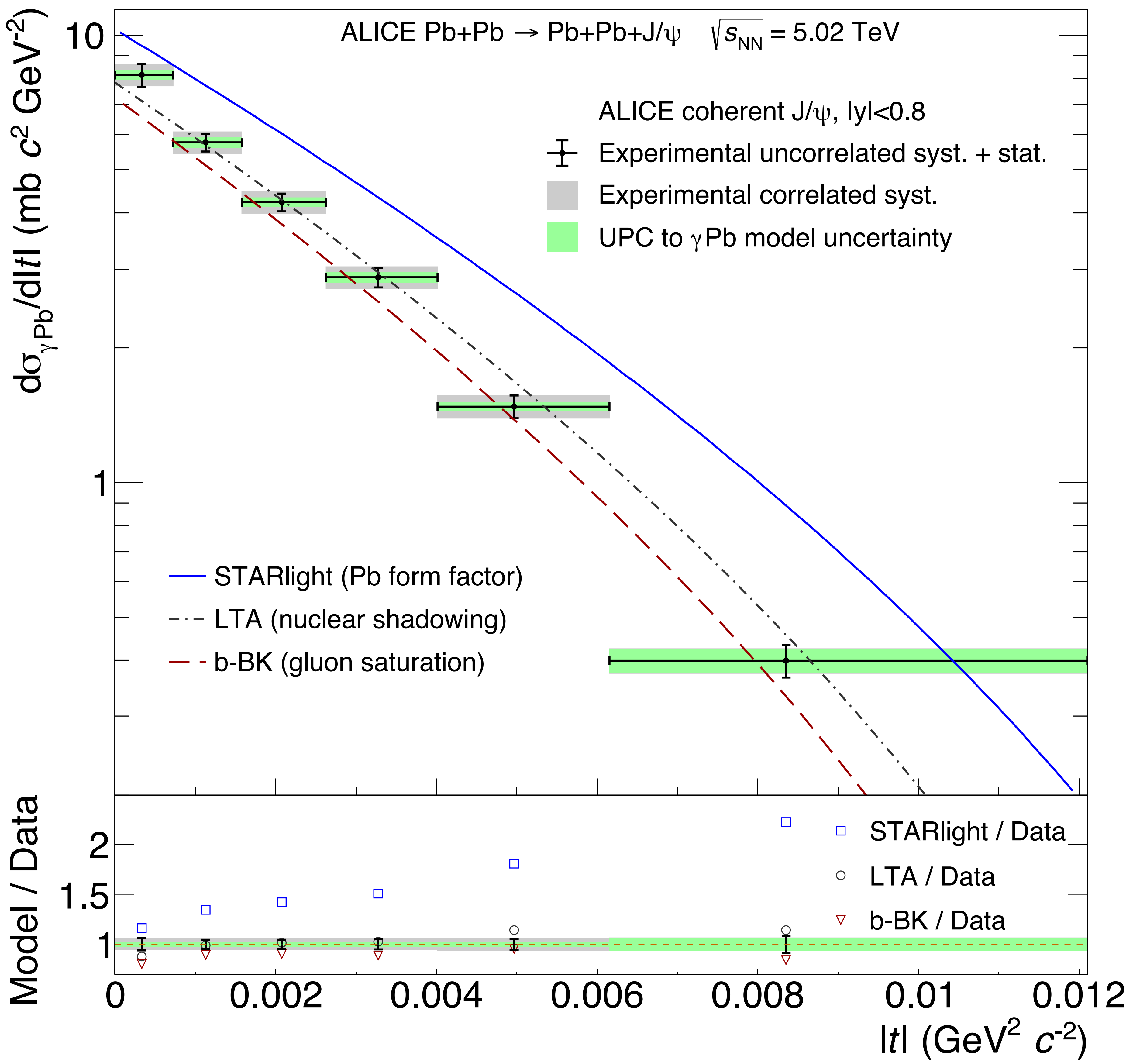

$-4.0<y<-2.5$

$|y|<0.8 \longleftrightarrow 0.3 \times 10^{-3} < x_B < 1.4 \times 10^{-3}$

$0.7 \times 10^{-2} < x_B < 3.3 \times 10^{-2}$ (dominant)

$1.1 \times 10^{-5} < x_B < 5.1 \times 10^{-5}$

Results indicate shadowing in gluon PDF:

$$R_g = \frac{g^{Pb}}{A\, g^p} \approx 0.65 \text{ at } x \approx 10^{-3}$$

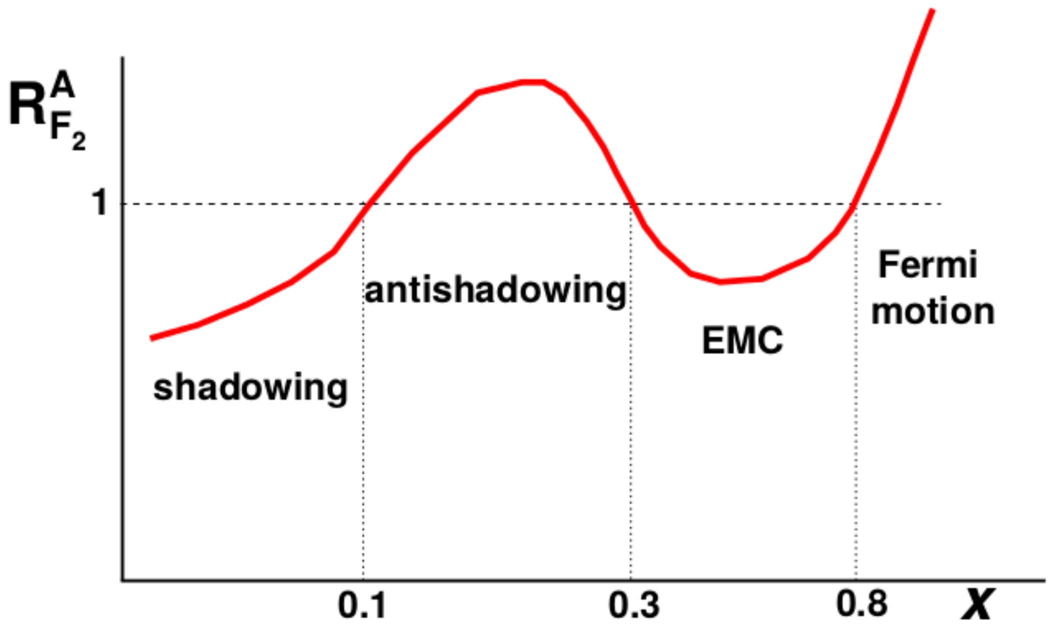

Disentangling the ambiguity on the ID of the γ emitter

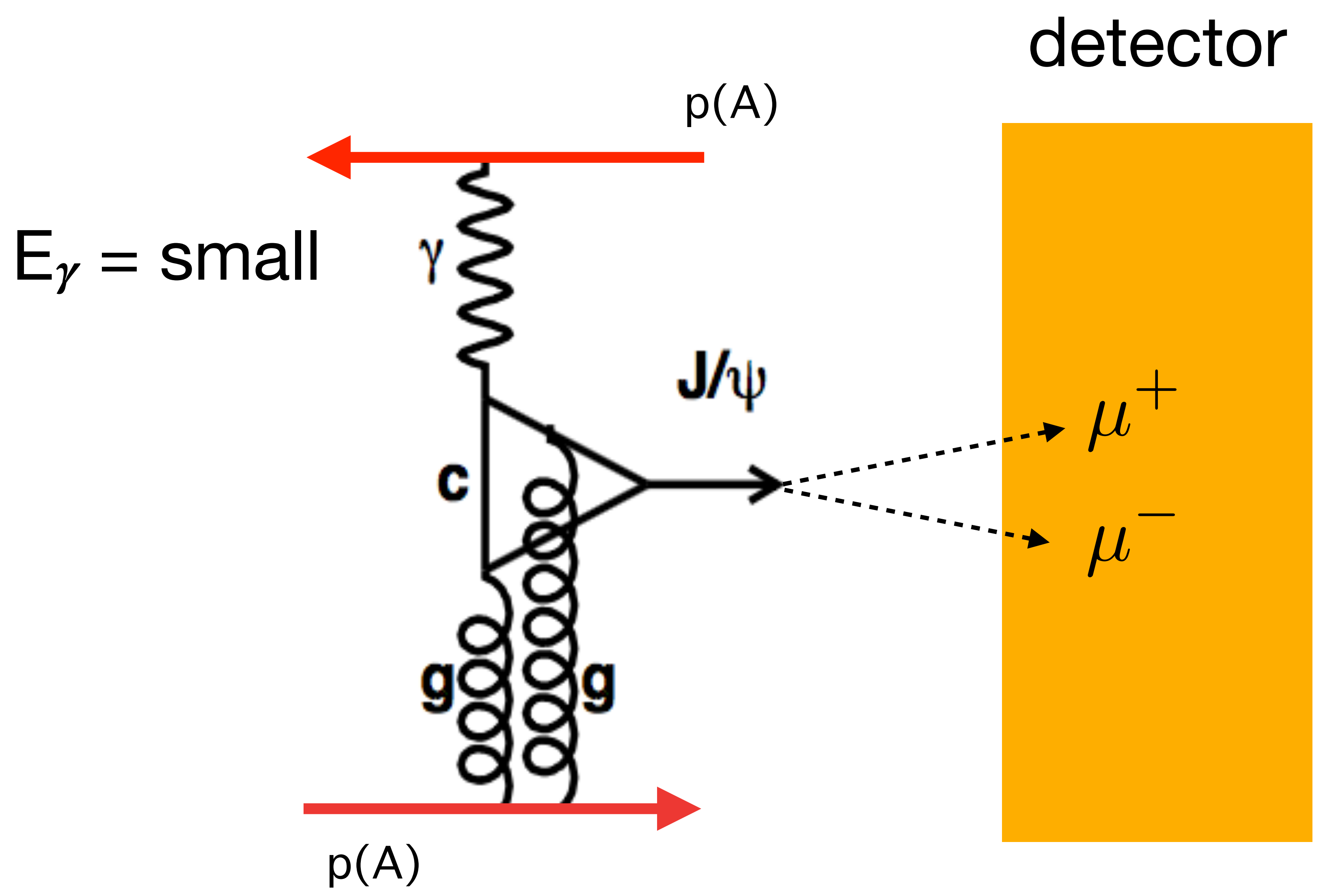

$$E_{\gamma,s} = \frac{M_{J/\psi}}{2} e^{-y}$$

Disentangling the ambiguity on the ID of the γ emitter

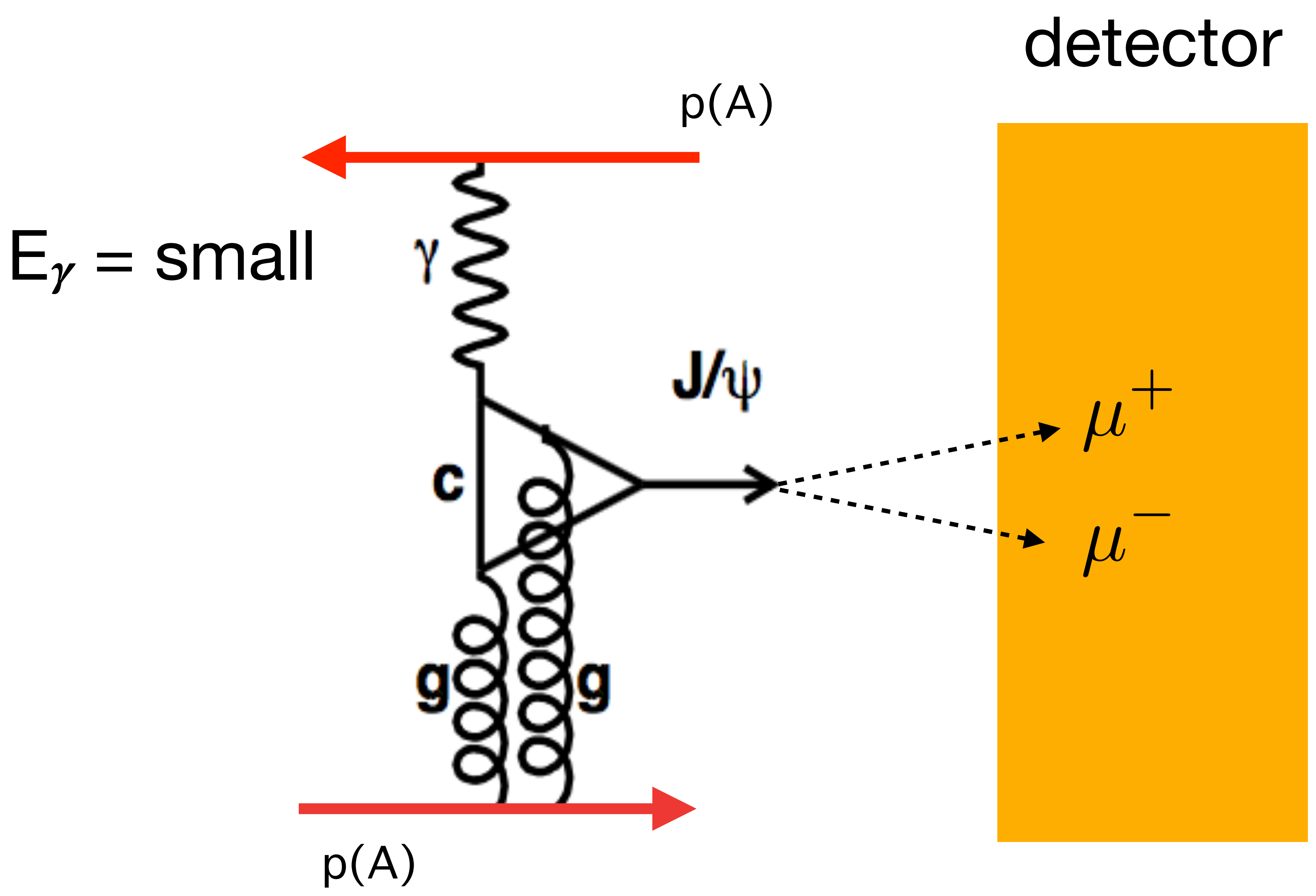

$$E_{\gamma,s} = \frac{M_{J/\psi}}{2} e^{-y}$$

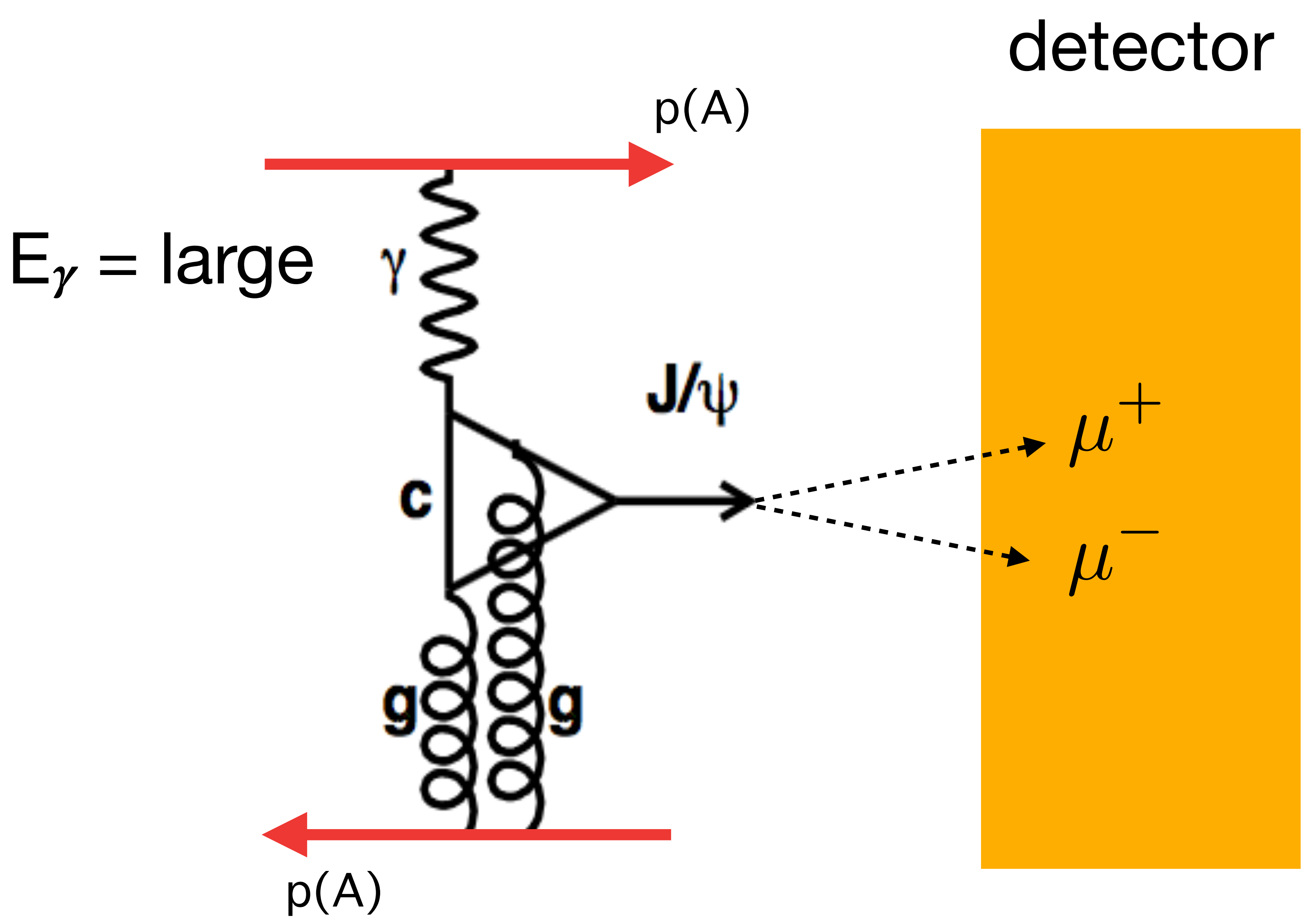

$$E_{\gamma,l} = \frac{M_{J/\psi}}{2} e^{+y}$$

Disentangling the ambiguity on the ID of the γ emitter

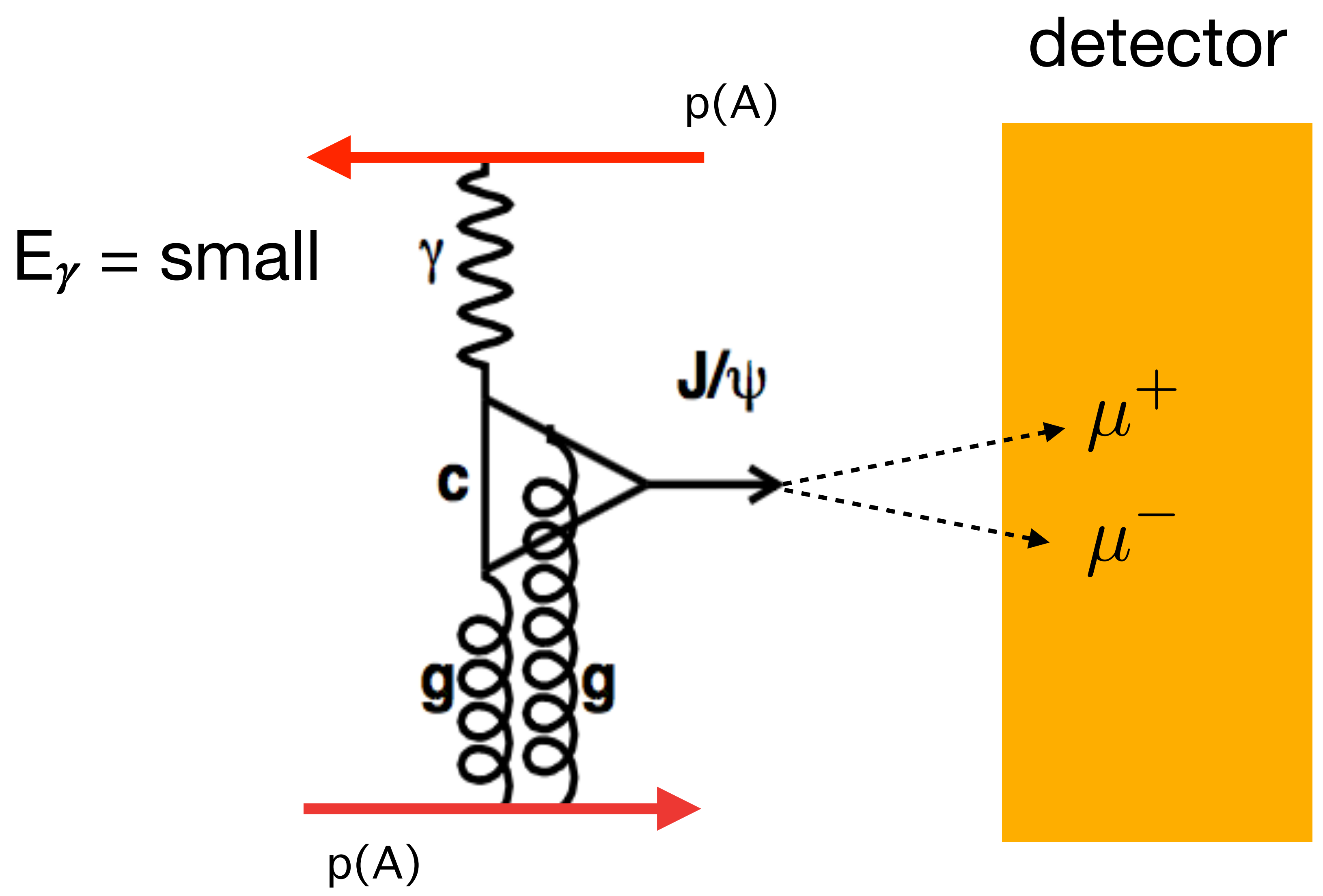

$$E_{\gamma,s} = \frac{M_{J/\psi}}{2} e^{-y}$$

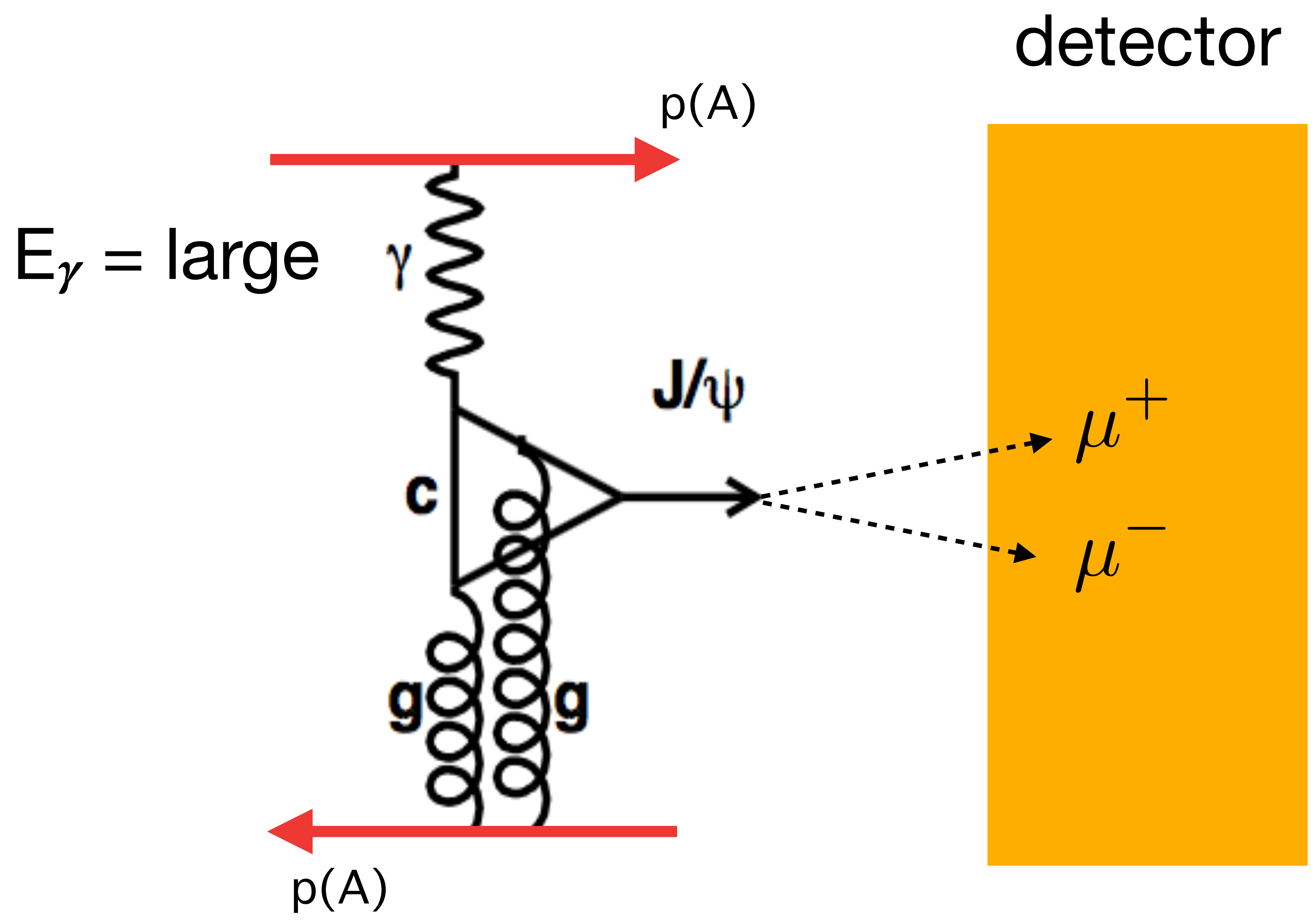

$$E_{\gamma,l} = \frac{M_{J/\psi}}{2} e^{+y}$$

$$\sigma(y) = N_{\gamma/A}(E_{\gamma,s})\,\sigma_{J/\psi}(E_{\gamma,s}) + N_{\gamma/A}(E_{\gamma,l})\,\sigma_{J/\psi}(E_{\gamma,l})$$

Disentangling the ambiguity on the ID of the γ emitter

$$\sigma(y) = N_{\gamma/A}(E_{\gamma,s})\, \sigma_{J/\psi}(E_{\gamma,s}) + N_{\gamma/A}(E_{\gamma,l})\, \sigma_{J/\psi}(E_{\gamma,l})$$

Disentangling the ambiguity on the ID of the γ emitter

$$\sigma(y) = N_{\gamma/A}(E_{\gamma,s})\,\sigma_{J/\psi}(E_{\gamma,s}) + N_{\gamma/A}(E_{\gamma,l})\,\sigma_{J/\psi}(E_{\gamma,l})$$

Photon flux $N_{\gamma/A}(E_\gamma)$ is function of impact parameter:
enhanced for large E_γ at small impact parameter.

Disentangling the ambiguity on the ID of the γ emitter

$$\sigma(y) = N_{\gamma/A}(E_{\gamma,s})\, \sigma_{J/\psi}(E_{\gamma,s}) + N_{\gamma/A}(E_{\gamma,l})\, \sigma_{J/\psi}(E_{\gamma,l})$$

Photon flux $N_{\gamma/A}(E_\gamma)$ is function of impact parameter:
enhanced for large E_γ at small impact parameter.

Small impact parameter, b ⟶ higher probability for exciting ($\propto 1/b^2$) ⟶ higher probability to emit neutrons.

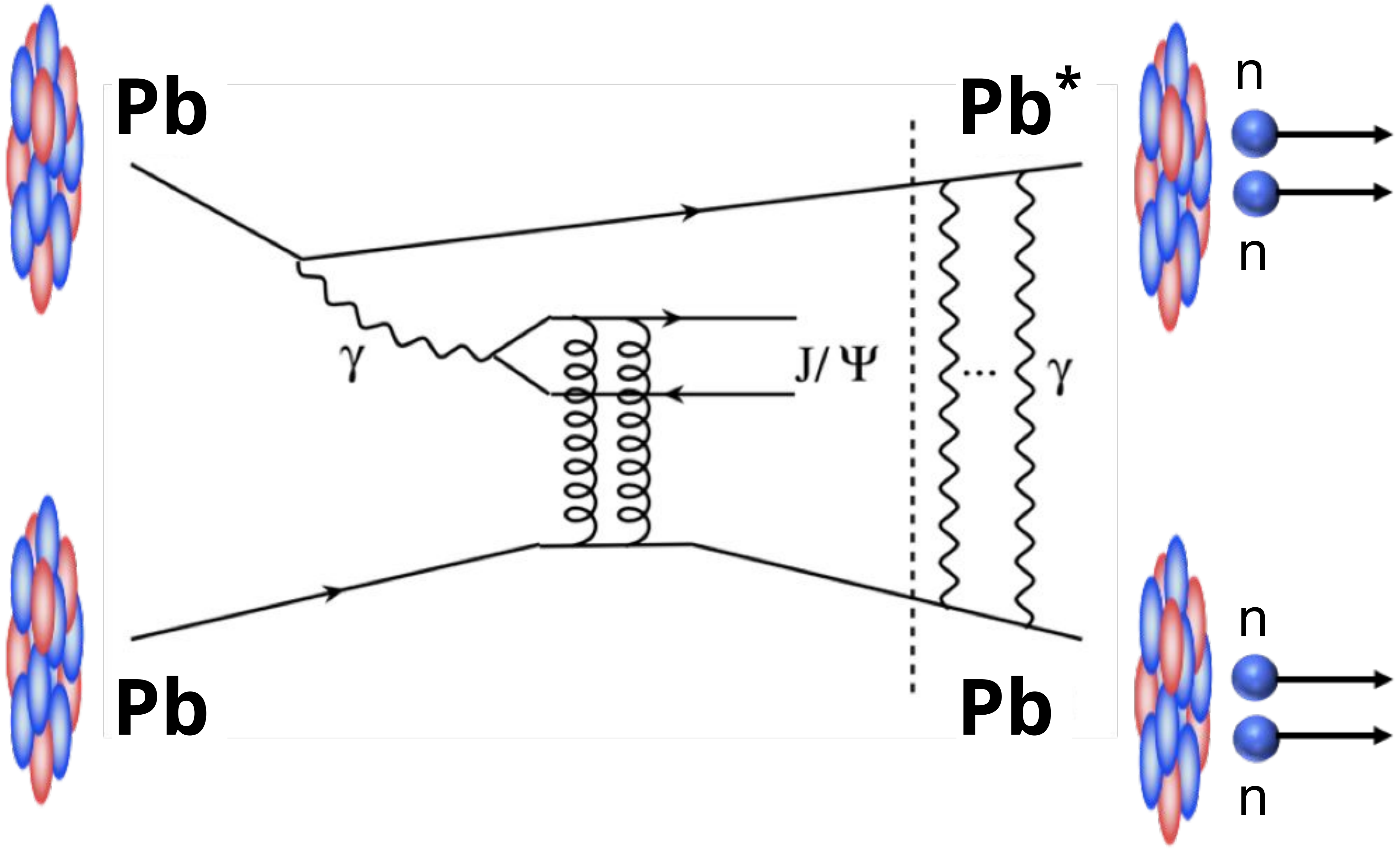

Picture from André Ståhl

Disentangling the ambiguity on the ID of the γ emitter

$$\sigma(y) = N_{\gamma/A}(E_{\gamma,s})\,\sigma_{J/\psi}(E_{\gamma,s}) + N_{\gamma/A}(E_{\gamma,l})\,\sigma_{J/\psi}(E_{\gamma,l})$$

Photon flux $N_{\gamma/A}(E_\gamma)$ is function of impact parameter:
enhanced for large E_γ at small impact parameter.

Small impact parameter, b ⟶ higher probability for exciting ($\propto 1/b^2$) ⟶ higher probability to emit neutrons.

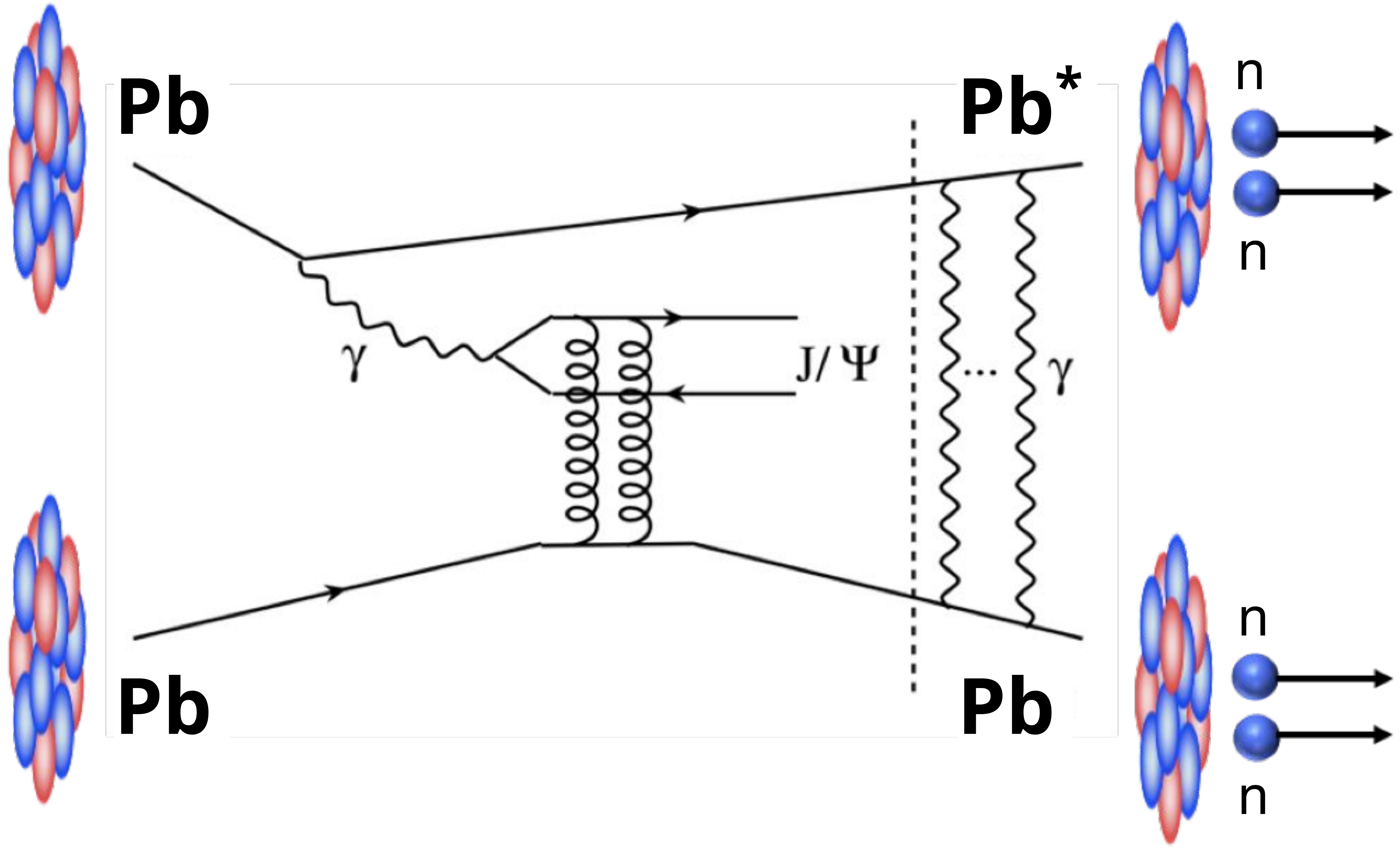

⟶ Make measurement with possibility to detect neutrons

Picture from André Ståhl

CMS central detector and the (far-)forward region

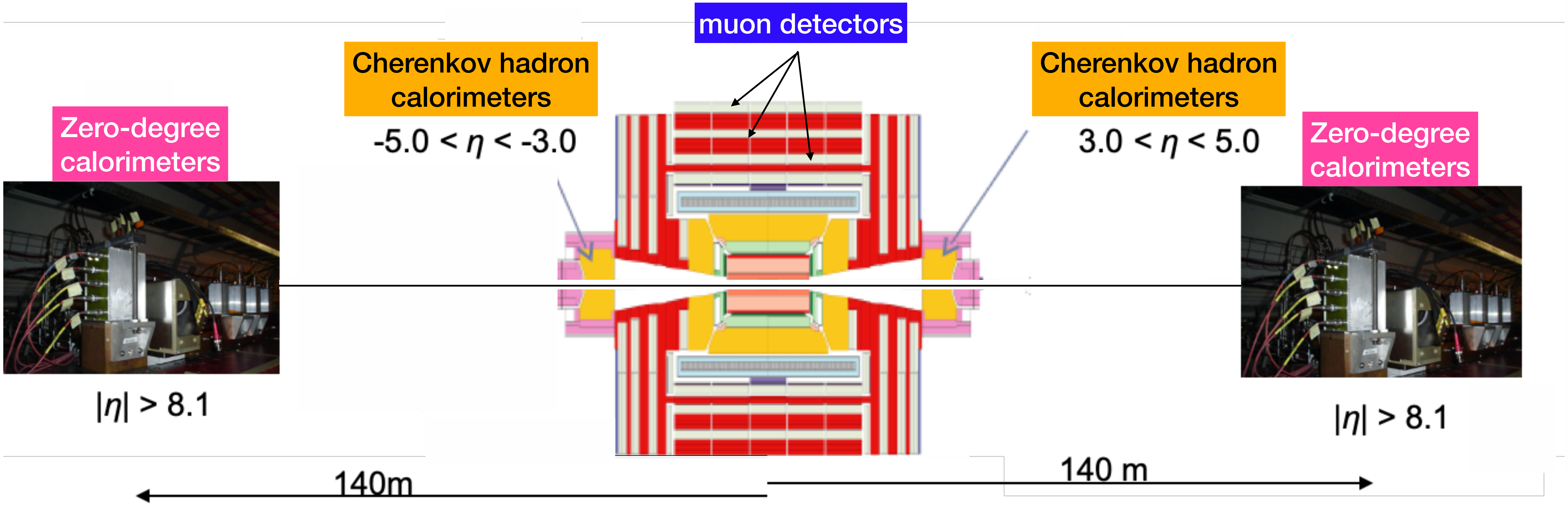

CMS central detector and the (far-)forward region

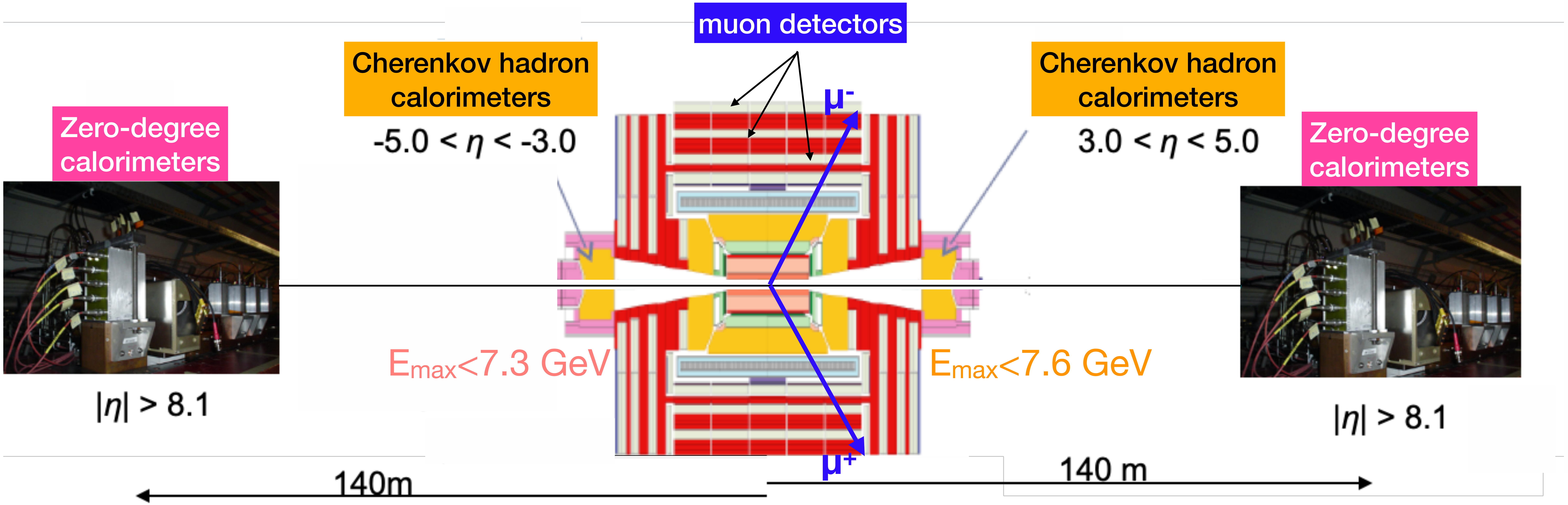

$$1.6 < |y_{\mu^+\mu^-}| < 2.4$$

CMS central detector and the (far-)forward region

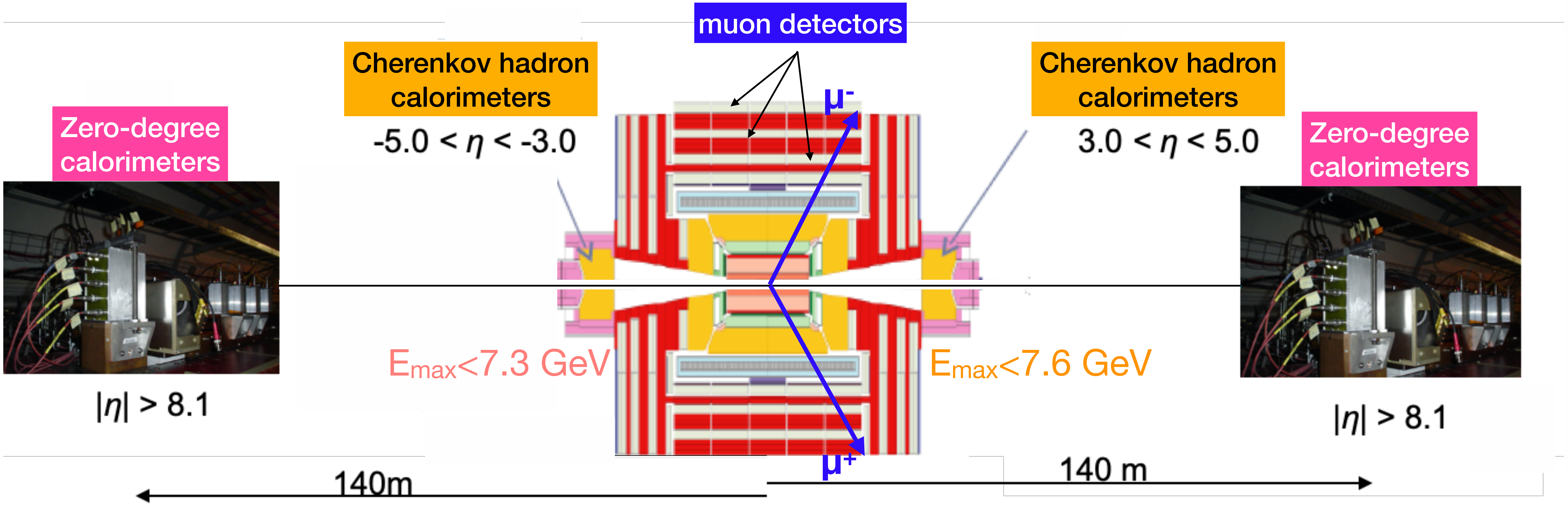

$$1.6 < |y_{\mu^+\mu^-}| < 2.4$$

0 neutrons
≥1 neutron

0 neutrons
≥1 neutron

0n0n
0nXn
XnXn

Disentangling the ambiguity on the ID of the γ emitter

$$\sigma^{0n0n}(y) = N^{0n0n}_{\gamma/A}(E_{\gamma,s})\ \sigma_{J/\psi}(E_{\gamma,s}) + N^{0n0n}_{\gamma/A}(E_{\gamma,l})\ \sigma_{J/\psi}(E_{\gamma,l})$$

$$\sigma^{0nXn}(y) = N^{0nXn}_{\gamma/A}(E_{\gamma,s})\ \sigma_{J/\psi}(E_{\gamma,s}) + N^{0nXn}_{\gamma/A}(E_{\gamma,l})\ \sigma_{J/\psi}(E_{\gamma,l})$$

$$\sigma^{XnXn}(y) = N^{XnXn}_{\gamma/A}(E_{\gamma,s})\ \sigma_{J/\psi}(E_{\gamma,s}) + N^{XnXn}_{\gamma/A}(E_{\gamma,l})\ \sigma_{J/\psi}(E_{\gamma,l})$$

measured

Disentangling the ambiguity on the ID of the γ emitter

$$\sigma^{0n0n}(y) = N^{0n0n}_{\gamma/A}(E_{\gamma,s})\,\sigma_{J/\psi}(E_{\gamma,s}) + N^{0n0n}_{\gamma/A}(E_{\gamma,l})\,\sigma_{J/\psi}(E_{\gamma,l})$$

$$\sigma^{0nXn}(y) = N^{0nXn}_{\gamma/A}(E_{\gamma,s})\,\sigma_{J/\psi}(E_{\gamma,s}) + N^{0nXn}_{\gamma/A}(E_{\gamma,l})\,\sigma_{J/\psi}(E_{\gamma,l})$$

$$\sigma^{XnXn}(y) = N^{XnXn}_{\gamma/A}(E_{\gamma,s})\,\sigma_{J/\psi}(E_{\gamma,s}) + N^{XnXn}_{\gamma/A}(E_{\gamma,l})\,\sigma_{J/\psi}(E_{\gamma,l})$$

measured

computed (StarLight)

computed (StarLight)

Disentangling the ambiguity on the ID of the γ emitter

$$\sigma^{0n0n}(y) = N^{0n0n}_{\gamma/A}(E_{\gamma,s})\,\sigma_{J/\psi}(E_{\gamma,s}) + N^{0n0n}_{\gamma/A}(E_{\gamma,l})\,\sigma_{J/\psi}(E_{\gamma,l})$$

$$\sigma^{0nXn}(y) = N^{0nXn}_{\gamma/A}(E_{\gamma,s})\,\sigma_{J/\psi}(E_{\gamma,s}) + N^{0nXn}_{\gamma/A}(E_{\gamma,l})\,\sigma_{J/\psi}(E_{\gamma,l})$$

$$\sigma^{XnXn}(y) = N^{XnXn}_{\gamma/A}(E_{\gamma,s})\,\sigma_{J/\psi}(E_{\gamma,s}) + N^{XnXn}_{\gamma/A}(E_{\gamma,l})\,\sigma_{J/\psi}(E_{\gamma,l})$$

measured | computed (StarLight) | extracted | computed (StarLight) | extracted

CMS: γPb cross section, energy dependence

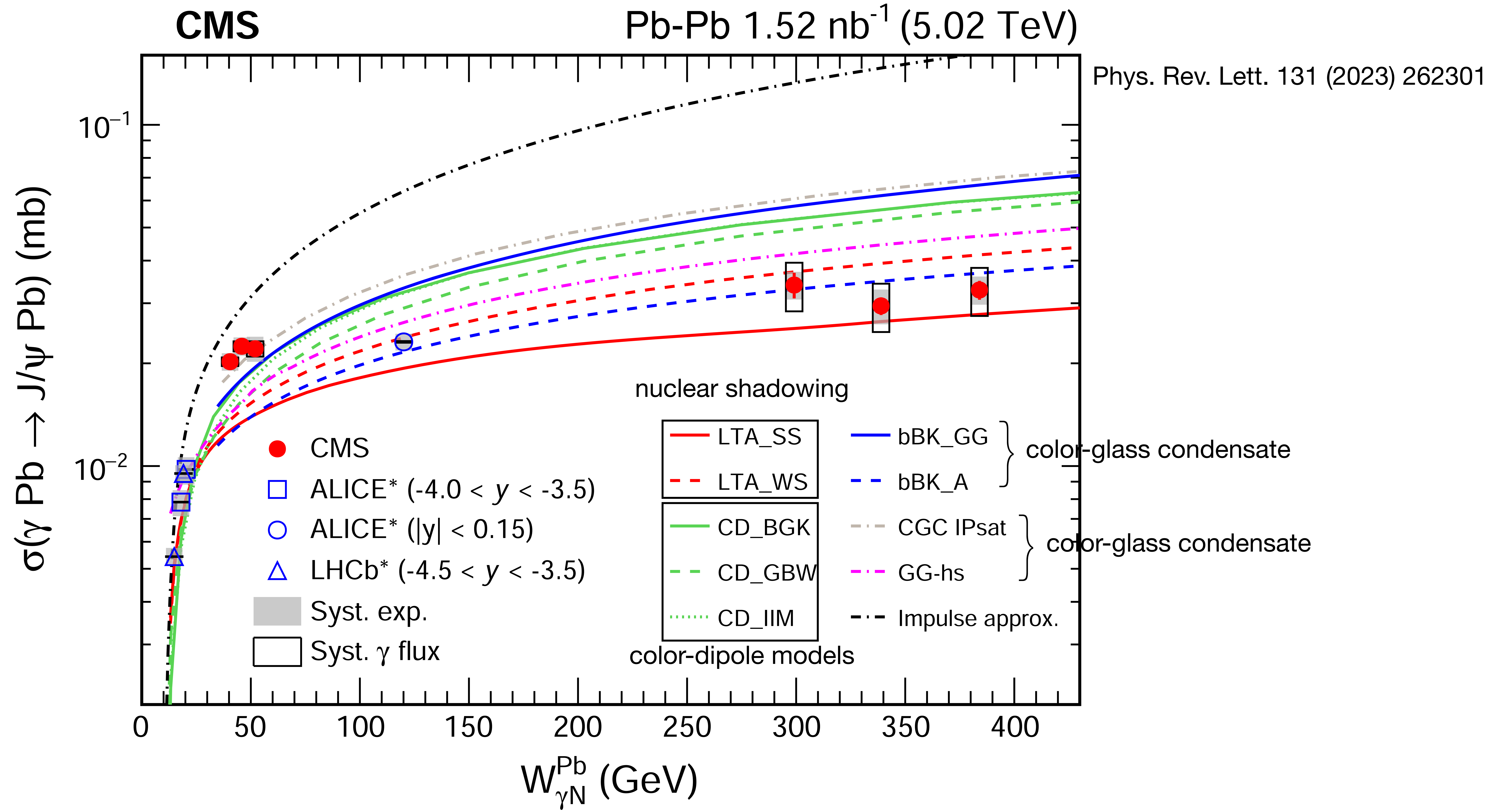

Incoherent production

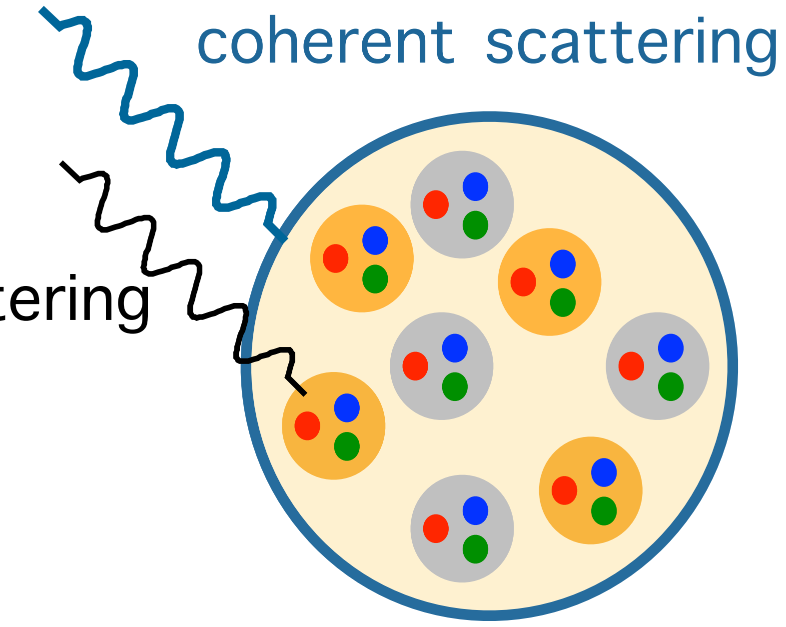

$$\sigma_{\text{tot}} \sim \langle |A|^2 \rangle$$

average cross sections

$$\sigma_{\text{coh}} \sim |\langle A \rangle|^2$$

average amplitude over target configurations:
probes average distributions

$$\sigma_{\text{incoh}} \sim \sum_{f \neq i} |\langle f|A|i\rangle|^2$$

$$= \sum_f \langle i|A|f\rangle^\dagger \langle f|A|i\rangle - \langle i|A|i\rangle^\dagger \langle i|A|i\rangle$$

$$= \left(\langle |A|^2 \rangle - |\langle A \rangle|^2 \right)$$

Incoherent
= difference between both:
probes event-by-event fluctuations

Incoherent production

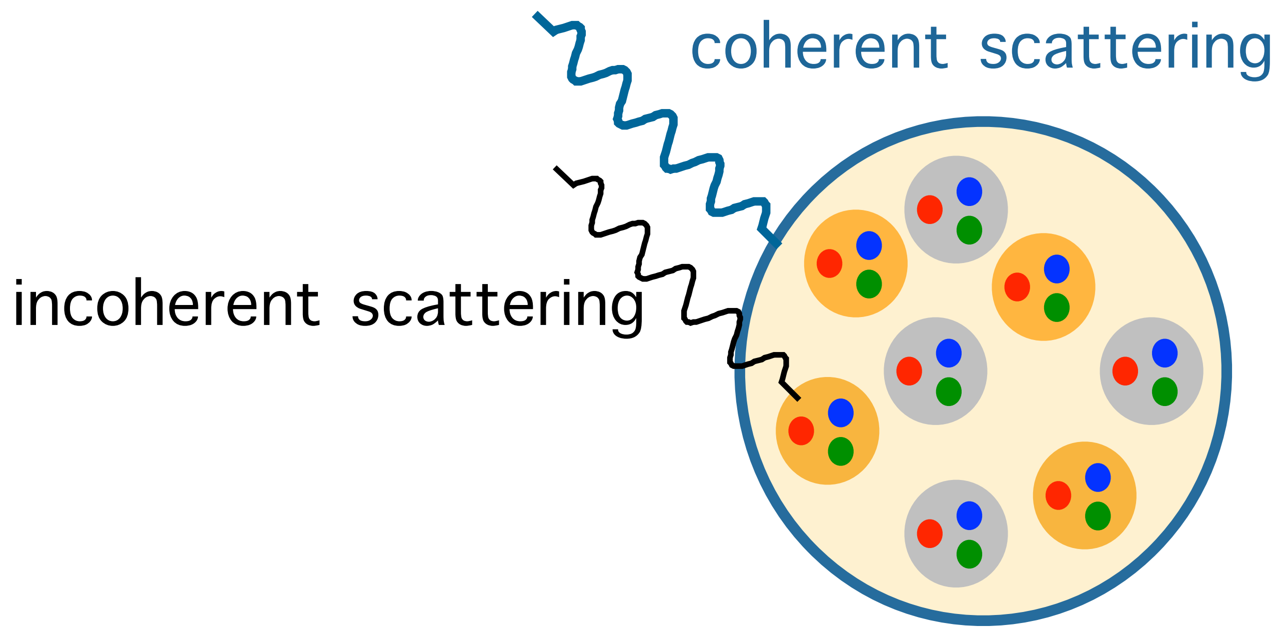

$$\sigma_{\rm tot} \sim \langle |A|^2 \rangle$$

average cross sections

$$\sigma_{\rm coh} \sim |\langle A \rangle|^2$$

average amplitude over target configurations:
probes average distributions

$$\sigma_{\rm incoh} \sim \sum_{f \neq i} |\langle f|A|i\rangle|^2$$

$$= \sum_f \langle i|A|f\rangle^\dagger \langle f|A|i\rangle - \langle i|A|i\rangle^\dagger \langle i|A|i\rangle$$

$$= \left(\langle |A|^2 \rangle - |\langle A \rangle|^2 \right)$$

Incoherent
= difference between both:
probes event-by-event fluctuations

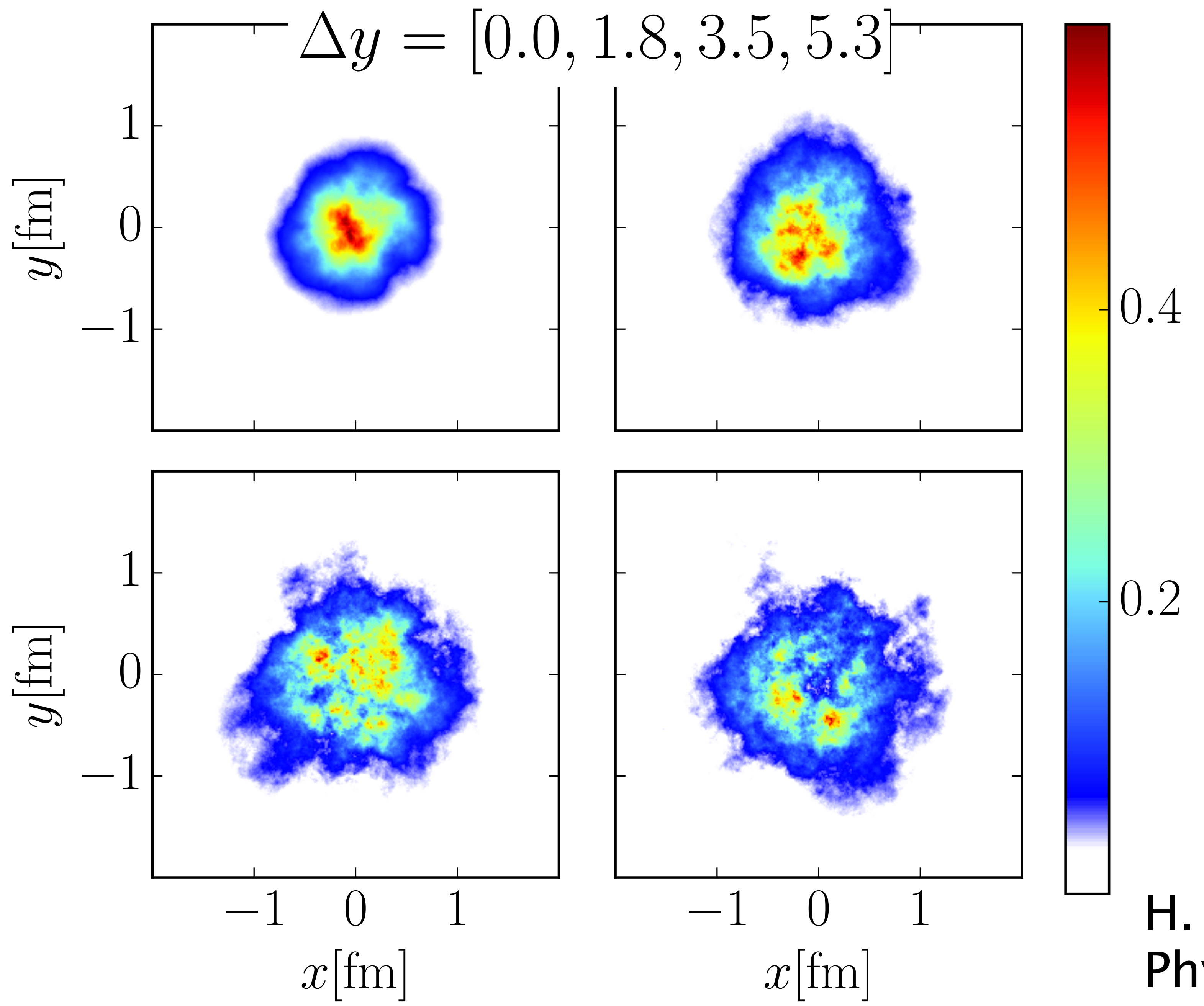

H. Mäntysaari and B. Schenke.
Phys. Rev. D 98, 034013 (2018)

Dissociative production measured by ALICE

pPb

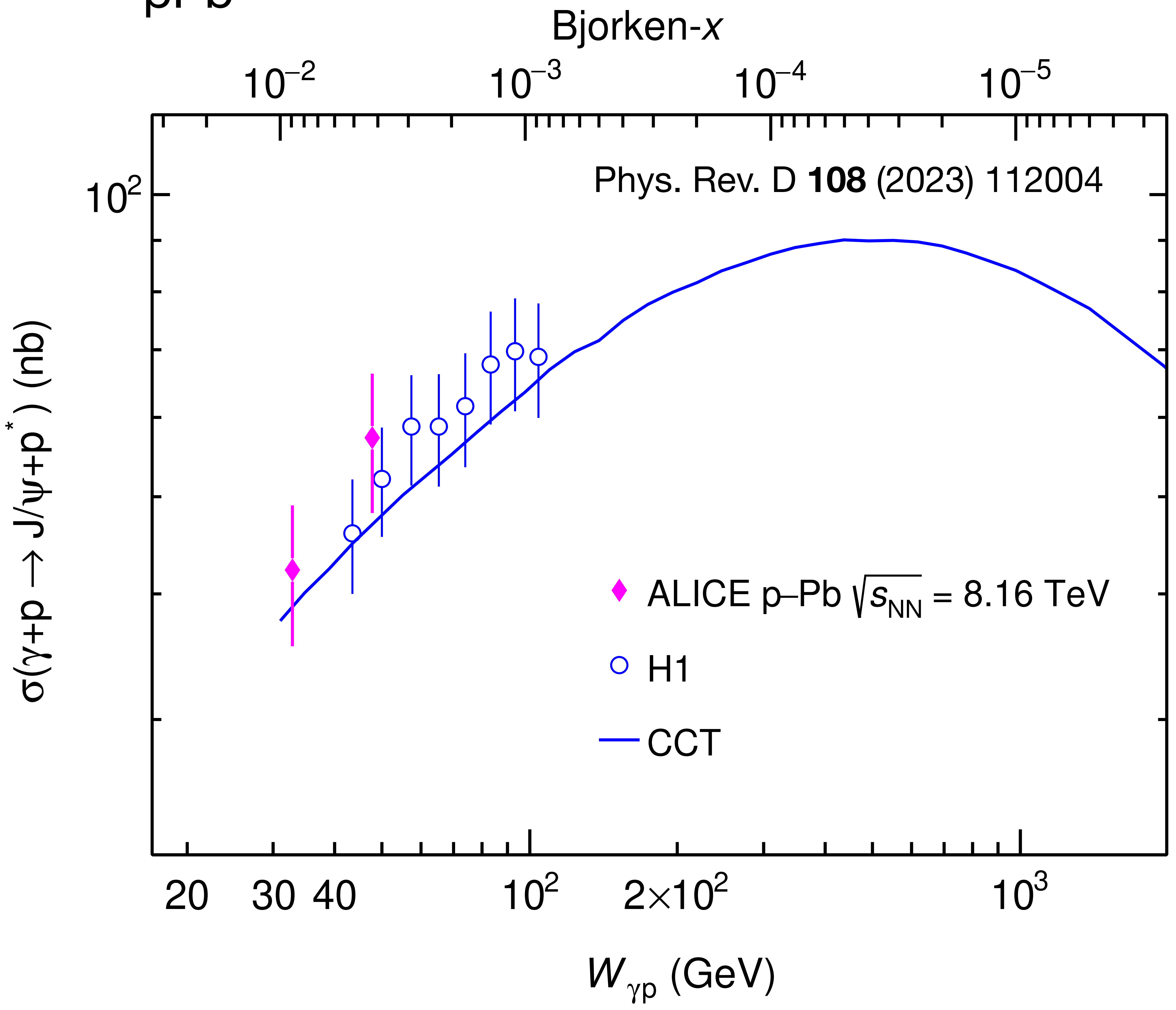

PbPb